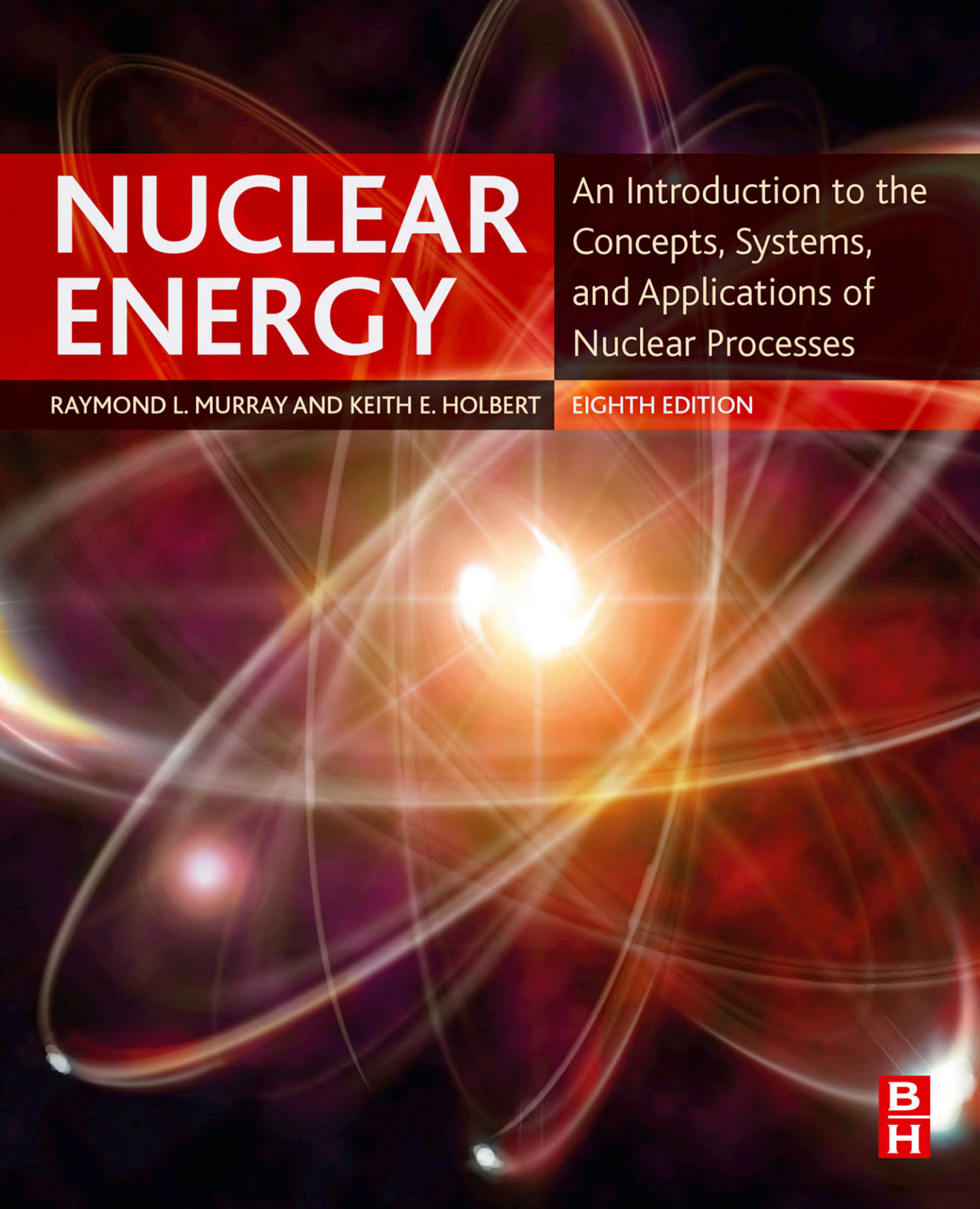
NUCLEAR ENERGY
An Introduction to the Concepts, Systems, and Applications of Nuclear Processes
RAYMOND L. MURRAY AND KEITH E. HOLBERT
EIGHTH EDITION
BH

Nuclear Energy

Eighth Edition

Nuclear Energy

An Introduction to the Concepts, Systems, and Applications of Nuclear Processes

Eighth Edition

Raymond L. Murray

Keith E. Holbert

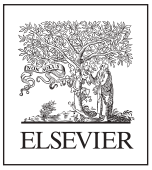

Butterworth-Heinemann
An imprint of Elsevier

Butterworth-Heinemann is an imprint of Elsevier
The Boulevard, Langford Lane, Kidlington, Oxford OX5 1GB, United Kingdom
50 Hampshire Street, 5th Floor, Cambridge, MA 02139, United States

Notices
Knowledge and best practice in this field are constantly changing. As new research and experience broaden our understanding, changes in research methods, professional practices, or medical treatment may become necessary.

Practitioners and researchers must always rely on their own experience and knowledge in evaluating and using any information, methods, compounds, or experiments described herein. In using such information or methods they should be mindful of their own safety and the safety of others, including parties for whom they have a professional responsibility.

To the fullest extent of the law, neither the Publisher nor the authors, contributors, or editors, assume any liability for any injury and/or damage to persons or property as a matter of products liability, negligence or otherwise, or from any use or operation of any methods, products, instructions, or ideas contained in the material herein.

Library of Congress Cataloging-in-Publication Data
A catalog record for this book is available from the Library of Congress

British Library Cataloguing-in-Publication Data
A catalogue record for this book is available from the British Library

ISBN: 978-0-12-812881-7

Publisher: Katey Birtcher
Sr. Acquisitions Editor: Steve Merken
Sr. Content Development Specialist: Nate McFadden
Production Project Manager: Punithavathy Govindaradjane
Cover Designer: Mark Rogers

Typeset by SPi Global, India

About the Authors

Raymond L. Murray (Ph.D., University of Tennessee, 1950) was a long-time faculty member in the Department of Nuclear Engineering of North Carolina State University. Professor Murray studied under J. Robert Oppenheimer at the University of California at Berkeley. In the Manhattan Project of World War II, he contributed to the uranium isotope separation process at Berkeley and Oak Ridge. In the early 1950s, he helped found the first university nuclear engineering program and the first university nuclear reactor. During his 30 years of teaching and research in reactor analysis at North Carolina State, he taught many of our leaders in universities and industries throughout the world. He was the author of textbooks in physics and nuclear technology and the recipient of a number of awards, including the Eugene P. Wigner Reactor Physicist Award of the American Nuclear Society in 1994. He was a Fellow of the American Physical Society, a Fellow of the American Nuclear Society, and a member of several honorary, scientific, and engineering societies. After retirement from the university, Dr. Murray was a consultant on criticality for the Three Mile Island Recovery Program, served as chairperson of the North Carolina Radiation Protection Commission, and served as chairperson of the North Carolina Low-Level Radioactive Waste Management Authority. He provided an annual lecture at MIT for the Institute of Nuclear Power Operations.

Keith E. Holbert (Ph.D., University of Tennessee, 1989) is presently an Associate Professor in the School of Electrical, Computer, and Energy Engineering at Arizona State University. His research expertise is in the area of instrumentation and system diagnostics, including radiation effects on sensors. Dr. Holbert has performed tests on safety-related systems in more than a dozen nuclear power plants in the United States. He has published more than 200 journal and conference papers and two textbooks, and holds two patents. Dr. Holbert is a registered professional (nuclear) engineer. He is a member of the American Nuclear Society and a Senior Member of the IEEE. As the founding Director of the Nuclear Power Generation Program at ASU, Professor Holbert teaches undergraduate and graduate engineering courses on electric power generation (from all forms of energy), nuclear reactor theory and design, nuclear power plant controls and diagnostics, reactor safety analysis, and health physics and radiation measurements. Dr. Holbert has been the recipient of multiple teaching awards. Keith is a Christian, who ascribes to the doctrine that God has entrusted humanity with good stewardship of His creation.

Preface

Professor Raymond L. Murray (1920–2011) authored six editions of this textbook until his death. Standing on the shoulders of his work, I have humbly attempted to expand the coverage and depth of the material while keeping with its original intent. As stated in the preface to the first edition (1975), this book "is designed for use by anyone who wishes to know about the role of nuclear energy in our society or to learn nuclear concepts for use in professional work." The continued hope is that this book will benefit both (future) nuclear professionals and interested members of the public.

By many accounts, humanity stands at a crossroads, with self-inflicted stresses due to population growth and anthropogenic climate change. Simultaneously, the quality of life is enhanced through the availability of affordable energy sources. Trends show electricity being increasingly tapped as the end-use energy form. Concomitantly, Internet-connected devices are consuming larger amounts of power while on standby. Another challenge is the competitive collaboration between two critical resources—the energy-water nexus.

In the United States, natural gas has become the favored choice for new electric generating stations due to its lower costs. However, external costs due to climate change are unaccounted for in a consumer's electric utility bills. Data in Chapter 24 reveal that the lifecycle greenhouse gas emissions from nuclear power plants are as small as those from renewable energy power facilities. Nuclear reactors have the potential to combat climate change. Future generations may justifiably criticize present generations for not being willing to pay the full price for energy utilization.

Besides nuclear power generation, associated technologies are utilized in a variety of applications, including nuclear medicine and smoke detectors. Furthermore, since the terrorist attacks of 2001, radiation detectors have been installed at ports of entry worldwide to intercept illicit shipments of nuclear materials.

Like politics and religion, the subject of nuclear energy can generate heated debate. Hence, one purpose of this book must be to bring factual information to the discussion. Topics that seem to generate the most concern inevitably include the persistent nuclear waste issue, nuclear power plant safety, radiation, and atomic weapons. Therefore, the authors are compelled to devote coverage to these (sometimes controversial) areas.

While the overall organization of the eighth edition has not changed, the material coverage and nuclear data have been updated and expanded. In addition, there is a significant increase in the number of examples and exercises because student learning is enhanced by performing calculations and analyses on nuclear quantities. The exercises are solvable by a handheld calculator or spreadsheet software, with many answers given in Appendix B. In addition, MATLAB programs and Excel workbooks for the solution of computer exercises in the text can be downloaded from https://www.elsevier.com/books/nuclear-energy/murray/978-0-12-812881-7. Sincere thanks are extended to Cliff Gold for creating most of the Excel versions of the programs.

This eighth edition of the textbook benefitted significantly from the meticulous reading of the seventh edition by Professors Toyohiko Yano, Hiroshi Sekimoto, and Hitoshi Kato, who translated the text into Japanese. My wife, Cecilia, must also be acknowledged for her rendering of many of the diagrams as well as her thorough proofreading of the text. The author welcomes any constructive comments and corrections to the text (holbert@asu.edu).

Keith E. Holbert
Tempe, Arizona, 2018

PART

BASIC CONCEPTS

I

In the study of the practical applications of nuclear energy, we must consider the properties of individual particles of matter—their "microscopic" features—as well as the character of matter in its ordinary form, a "macroscopic" (large-scale) view. Examples of the small-scale properties are masses of atoms and nuclear particles, their effective sizes for interaction with each other, and the number of particles in a certain volume. The combined behavior of large numbers of individual particles is expressed in terms of properties such as mass density, charge density, electrical conductivity, thermal conductivity, and elastic constants. We continually seek consistency between the microscopic and macroscopic views.

Because all processes involve the interactions of particles, it is necessary to develop a background understanding of the basic physical facts and principles that govern such interactions. In Part I, we shall examine the concept of energy, describe the models of atomic and nuclear structure, discuss radioactivity and nuclear reactions in general, review the ways radiation interacts with matter, and concentrate on two important nuclear processes: fission and fusion.

CHAPTER

ENERGY 1

CHAPTER OUTLINE

Our material world is composed of many substances distinguished by their chemical, mechanical, and electrical properties. They are found in nature in various physical states: the familiar solid, liquid, and gas along with ionic plasma. However, the apparent diversity of kinds and forms of material is reduced by the knowledge that there are only about 90 naturally occurring chemical elements and that the chemical and physical features of substances depend merely on the strength of force bonds between atoms.

In turn, the distinctions between the elements of nature arise from the number and arrangement of basic particles: electrons, protons, and neutrons. At both the atomic and nuclear levels, internal forces and energy determine the structure of elements.

1.1 FORCES AND ENERGY

A limited number of basic forces exist: gravitational, electromagnetic, and strong and weak nuclear. Associated with each of these is the ability to do work. Thus, energy in different forms may be stored, released, transformed, transferred, and "used" in both natural processes and man-made devices. It is often convenient to view nature in terms of only two basic entities: particles and energy. Even this distinction can be removed because we know that matter can be converted into energy and vice versa.

Let us review some principles of physics needed for the study of the release of nuclear energy and its conversion into thermal and electrical forms. We recall that if a constant force F is applied to an object to move it a distance s, the amount of work W done is the product $W = Fs$. As a simple example, we pick

Nuclear Energy. https://doi.org/10.1016/B978-0-12-812881-7.00001-0

up a book from the floor and place it on a table. Our muscles provide the means to lift against the force of gravity on the book. We have done work on the object, which now possesses stored energy (potential energy) because it could do work if allowed to fall back to the original level. Now, a force F acting on a mass m provides an acceleration a, given by Newton's law $F = ma$. Starting from rest, the object gains a speed v, and at any instant has energy of motion (kinetic energy) in the amount

$$E_K = \frac{1}{2}mv^2 \tag{1.1}$$

For objects falling under the force of gravity, we find that the potential energy diminishes as the kinetic energy increases, but the sum of the two energy types remains constant. This is an example of the principle of conservation of energy. Let us apply this principle to a practical situation and perform some illustrative calculations.

As we know, falling water provides one primary source for generating electrical energy. In a hydroelectric plant, river water is collected by a dam and allowed to fall through a considerable height h, known as the head. The potential energy of water is thus converted into kinetic energy. The water is directed to strike the blades of a hydraulic turbine, which turns an electric generator.

The potential energy of a mass m located at the top of a dam is $E_P = Fh$, being the work done to place it there. The force is the weight $F = mg$, where g is the acceleration of gravity. Thus, the potential energy is

$$E_P = mgh \tag{1.2}$$

EXAMPLE 1.1

Find the velocity of water descending through a dam with a 50 m head. Ignoring friction, the initial potential energy would appear at the bottom in kinetic form, that is, $E_K = E_P$. Using gravitational acceleration at the Earth's surface $g_0 = 9.81\,\text{m/s}^2$, the water speed at the turbine inlet would be

$$v = \sqrt{\frac{2E_K}{m}} = \sqrt{\frac{2E_P}{m}} = \sqrt{\frac{2mg_0h}{m}} = \sqrt{2(9.81\,\text{m/s}^2)(50\,\text{m})} = 31.3\,\text{m/s}$$

Energy takes on various forms, classified according to the type of force that is acting. The water in the hydroelectric plant experiences the force of gravity, and thus gravitational energy is involved. It is transformed into mechanical energy of rotation in the turbine, which is then converted to electrical energy by the generator. At the terminals of the generator, there is an electrical potential difference, which provides the force to move charged particles (electrons) through the network of the electrical supply system. The electrical energy may then be converted into mechanical energy as in motors, into light energy as in light bulbs, into thermal energy as in electrically heated homes, or into chemical energy as in a storage battery.

The automobile also provides familiar examples of energy transformations. The burning of gasoline releases the chemical energy of the fuel in the form of heat, part of which is converted to energy of motion of mechanical parts while the rest is transferred to the atmosphere and highway. The vehicle's alternator provides electricity for control and lighting. In each of these examples, energy is changed from one form to another but is not destroyed. Two laws, the first and second laws of thermodynamics,

govern the conversion of heat to other forms of energy. The first law states that energy is conserved; the second specifies inherent limits on the efficiency of the energy conversion.

Energy can be classified according to the primary source. We have already noted two sources of energy: falling water and the burning of the chemical fuel gasoline, which is derived from petroleum, one of the main fossil fuels. To these we can add solar energy; the energy from winds, tides, or sea motion; and heat from within the Earth. Finally, we have energy from nuclear reactions (i.e., the "burning" of nuclear fuel).

1.2 UNITS OF MEASURE

For many purposes, we use the metric system of units, more precisely designated as SI or Système Internationale. In this system (Taylor and Thompson, 2008), the base units are the kilogram (kg) for mass, the meter (m) for length, the second (s) for time, the mole (mol) for amount of substance, the ampere (A) for electric current, the kelvin (K) for thermodynamic temperature, and the candela (cd) for luminous intensity. Table 1.1 summarizes these SI base units and important derived quantities. In addition, the liter (L) and metric ton (tonne) are in common use ($1\,\mathrm{L} = 10^{-3}\ \mathrm{m}^3$; $1\,\text{tonne} = 1000\,\mathrm{kg}$). However, for understanding earlier literature, one requires knowledge of other systems. The transition

Table 1.1 SI Base and Derived Quantities and Units

Quantity	Unit	Unit Symbol	Unit Dimension(s)
Length	meter	m	
Mass	kilogram	kg	
Time	second	s	
Electric current	ampere	A	
Thermodynamic temperature	kelvin	K	
Amount of substance	mole	mol	
Luminous intensity	candela	cd	
Frequency	hertz	Hz	1/s
Force	newton	N	$\mathrm{kg\,m/s^2 = J/m}$
Pressure	pascal	Pa	$\mathrm{N/m^2 = kg/(m\,s^2)}$
Energy, work, heat	joule	J	$\mathrm{N\,m = kg\,m^2/s^2}$
Power	watt	W	$\mathrm{J/s = kg\,m^2/s^3}$
Electric charge	coulomb	C	A s
Electric potential	volt	V	$\mathrm{J/C = W/A = kg\,m^2/(s^3\ A)}$
Electric capacitance	farad	F	$\mathrm{C/V = C^2/J}$
Magnetic flux	weber	Wb	V s
Magnetic flux density	tesla	T	$\mathrm{Wb/m^2}$
Absorbed dose	gray	Gy	J/kg
Dose equivalent	sievert	Sv	J/kg
Activity	becquerel	Bq	1/s

in the United States from British units to SI units has been much slower than expected. To ease understanding by the typical reader, a dual display of numbers and their units is frequently given in this book. Familiar and widely used units such as the centimeter, the barn, the curie, and the rem are retained. Table A.3 in Appendix A lists useful conversions from British units to SI units.

In dealing with forces and energy at the level of molecules, atoms, and nuclei, it is conventional to use another energy unit, the *electronvolt* (eV). Its origin is electrical in character, being the amount of kinetic energy that would be imparted to an electron (charge 1.602×10^{-19} C) if it were accelerated through a potential difference of 1 V. Because the work done on 1 C would be 1 J, we see that $1\,\text{eV} = 1.602 \times 10^{-19}$ J. The unit is of convenient size for describing atomic reactions. For instance, to remove the one electron from the hydrogen atom requires 13.6 eV of energy. However, when dealing with nuclear forces, which are very much larger than atomic forces, it is preferable to use the mega-electronvolt unit (MeV). To separate the neutron from the proton in the nucleus of heavy hydrogen, for example, requires an energy of about 2.2 MeV (i.e., 2.2×10^6 eV).

1.3 THERMAL ENERGY

Of special importance to us is thermal energy as the form most readily available from the sun, from burning of ordinary fuels, and from the nuclear fission process. First, we recall that a simple definition of the temperature of a substance is the number read from a measuring device such as a thermometer in intimate contact with the material. If energy is supplied, the temperature rises (e.g., energy from the sun warms the air during the day). Each material responds to the supply of energy according to its internal molecular or atomic structure, characterized on a macroscopic scale by the specific heat c_p. If an amount of thermal energy Q is added to the material mass without a change of state, a temperature rise, ΔT, is induced in accordance with

$$Q = mc_p \Delta T \tag{1.3}$$

EXAMPLE 1.2

At constant pressure, the specific heat for water at 15°C and 1 atm is $c_p = 4.186$ J/(g °C). Thus, it requires 4.186 joules (J) of energy to raise the temperature of 1 g of water by 1 degree Celsius (1°C).

From our modern knowledge of the atomic nature of matter, we readily appreciate the idea that energy supplied to a material increases the motion of the individual particles of the substance. Temperature can thus be related to the average kinetic energy of the atoms. For example, in a gas such as air, the average energy of translational motion of the molecules $\overline{E}$ is directly proportional to the absolute temperature T, through the relation

$$\overline{E} = \frac{3}{2}kT \tag{1.4}$$

where k is Boltzmann's constant, 1.38×10^{-23} J/K (Recall that the Kelvin scale has the same spacing of degrees as does the Celsius scale, but its zero is at −273.15°C.)

EXAMPLE 1.3

To gain an appreciation of molecules in motion, let us find the typical speed of oxygen molecules at room temperature 20° C, or 293 K. The molecular weight of O_2 is 32, and because one unit of atomic weight corresponds to 1.66×10^{-27} kg, the mass of the oxygen molecule is 5.30×10^{-26} kg. Now

$$\overline{E} = \frac{3}{2}kT = \frac{3}{2}(1.38 \times 10^{-23}\,\text{J/K})(293\,\text{K}) = 6.07 \times 10^{-21}\,\text{J}$$

and thus from Eq. (1.1), the speed is

$$v = \sqrt{2\overline{E}/m} = \sqrt{2(6.07 \times 10^{-21}\,\text{J})/(5.30 \times 10^{-26}\,\text{kg})} = 479\,\text{m/s}$$

Closely related to energy is the physical entity *power*, P, which is the rate at which work is done. Hence, the power may be expressed in terms of the time derivative of energy

$$P = \frac{d}{dt}E \tag{1.5}$$

For a constant power, the energy is simply the product of the power and the time period, T, that is, $E = PT$.

EXAMPLE 1.4

To illustrate, let the mass flow rate $\dot{m}$ of water in the hydropower plant of Example 1.1 be 2×10^6 kg/s. As power is the time rate of change of energy, the power available is

$$P = \frac{d}{dt}E_P = \dot{m}gh = (2 \times 10^6\,\text{kg/s})(9.81\,\text{m/s}^2)(50\,\text{m}) = 9.81 \times 10^8\,\text{J/s}$$

For convenience, the unit joule per second is called the watt (W). This hydroelectric plant thus involves 9.8×10^8 W. We can conveniently express this in kilowatts ($1\,\text{kW} = 10^3\,\text{W}$) or megawatts ($1\,\text{MW} = 10^6\,\text{W}$). Such multiples of units are used because of the enormous range of magnitudes of quantities in nature, from the submicroscopic to the astronomical. Table 1.2 gives the standard set of prefixes for the system of units.

Table 1.2 Prefixes for Numbers and Abbreviations

yotta	Y	10^{24}	deci	d	10^{-1}
zetta	Z	10^{21}	centi	c	10^{-2}
exa	E	10^{18}	milli	m	10^{-3}
peta	P	10^{15}	micro	μ	10^{-6}
tera	T	10^{12}	nano	n	10^{-9}
giga	G	10^{9}	pico	p	10^{-12}
mega	M	10^{6}	femto	f	10^{-15}
kilo	k	10^{3}	atto	a	10^{-18}
hecto	h	10^{2}	zepto	z	10^{-21}
deca	da	10^{1}	yocto	y	10^{-24}

1.4 RADIANT ENERGY

Another form of energy is electromagnetic or radiant energy. We recall that this energy may be released by heating of solids, as in the wire of an incandescent light bulb; by electrical oscillations, as in radio or television transmitters; or by atomic interactions, as in the sun. The radiation can be viewed in either of two ways—as a wave or as a particle—depending on the process under study. In the wave view, it is a combination of electric and magnetic vibrations moving through space. In the particle view, it is a compact moving uncharged object, the photon, which is a bundle of pure energy having mass only by virtue of its motion. Regardless of its origin, all radiation can be characterized by its frequency, which is related to speed and wavelength. Letting c be the speed of light, λ its wavelength, and ν its frequency, we have[1]

$$c = \lambda\nu \tag{1.6}$$

Fig. 1.1 presents the electromagnetic spectrum comparing the frequencies and wavelengths of the various constituents such as visible light from 380 to 760 nm; however, the boundaries and ranges of the components are not fixed. Of particular interest are the ionizing wavelengths, which begin within the ultraviolet (UV) region (~10 eV). In Section 10.4, we surmise that this is the reason some UV rays cause skin cancer. X-rays and gamma rays are electromagnetic radiation arising from the interactions of atomic and nuclear particles, respectively. They have energies and frequencies much higher than those of optical light.

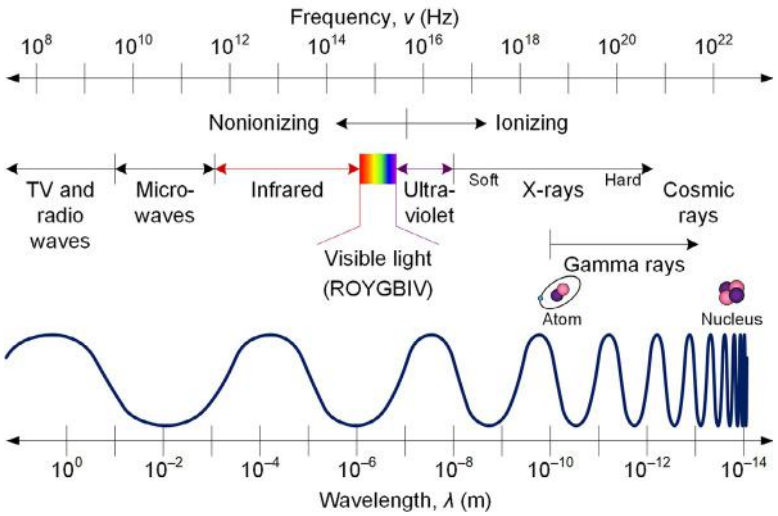

FIG. 1.1

Electromagnetic spectrum (ROYGBIV: red, orange, yellow, green, blue, indigo, violet).

[1]We need both Roman and Greek characters, identifying the latter by name the first time they are used, thus λ (lambda) and ν (nu). The Greek alphabet is compiled in Table A.1 for reference. The reader must be alert to symbols used for more than one quantity.

EXAMPLE 1.5

Find the frequency of an ultraviolet photon of wavelength 280 nm. The speed of light in a vacuum is $c = 3 \times 10^8$ m/s; thus this UV light frequency is

$$\nu = \frac{c}{\lambda} = \frac{3.00 \times 10^8 \text{ m/s}}{(280 \text{ nm})(10^{-9} \text{ m/nm})} = 1.07 \times 10^{15} \text{ Hz}$$

To appreciate the relationship of states of matter, atomic and nuclear interactions, and energy, let us visualize an experiment in which we supply energy to a sample of water from a source of energy that is as large and as sophisticated as we wish. Thus, we increase the degree of internal motion and eventually dissociate the material into its most elementary components. Suppose in Fig. 1.2 that the water is initially ice at nearly absolute zero temperature, where water (H_2O) molecules are essentially at rest. As we add thermal energy to increase the temperature to 0°C (32°F), molecular movement increases to the point at which the ice melts to become liquid water, which can flow rather freely. To cause a change from the solid state to the liquid state, a definite amount of energy—termed the *heat of fusion*—is required. In the case of water, this latent heat is 334 J/g. For the temperature range within which water is liquid, thermal agitation of the molecules permits some evaporation from the surface. At the boiling point, 100°C (212°F) at atmospheric pressure, the liquid turns into the gaseous form as steam. Again, energy is required to cause the change of state, with a *heat of vaporization* of 2258 J/g. Further heating by use of special high temperature equipment causes dissociation of water into atoms of hydrogen (H) and oxygen (O). By electrical means, electrons can be removed from hydrogen and oxygen atoms, leaving a mixture of charged ions and electrons. Through nuclear bombardment, the oxygen nucleus can be broken into smaller nuclei, and for temperatures in the billions of degrees, the material can be decomposed into an assembly of electrons, protons, and neutrons.

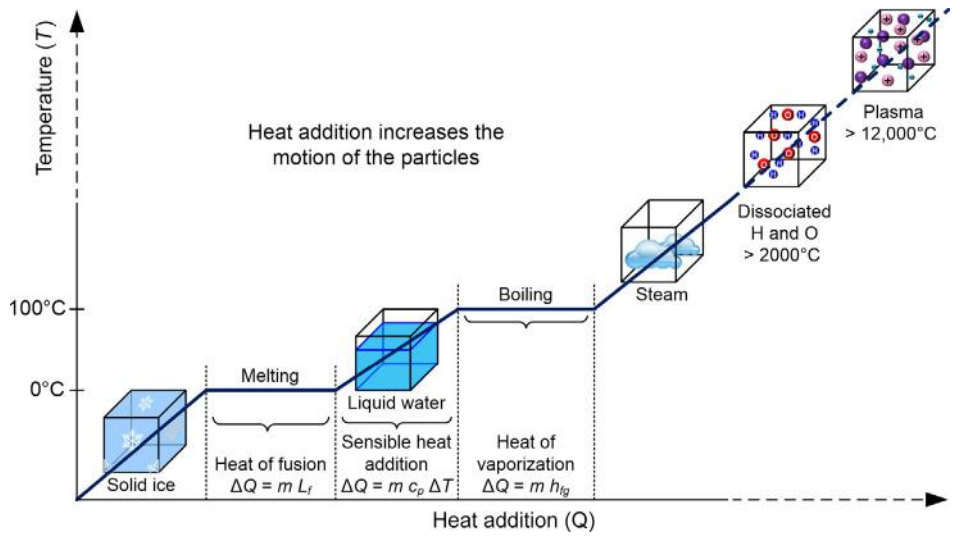

FIG. 1.2

Effect of energy added to water.

1.5 THE EQUIVALENCE OF MATTER AND ENERGY

The connection between energy and matter is provided by Einstein's (1905a) theory of special relativity. It predicts that the mass of any object increases with its speed. Letting the mass when the object is stationary be m_0, the *rest mass*; letting m be the mass when it is at speed v; and noting that the speed of light in a vacuum is c, then the *relativistic mass* is

$$m = \frac{m_0}{\sqrt{1-(v/c)^2}} \tag{1.7}$$

For motion at low speed (e.g., 500 m/s), the relativistic mass is almost identical to the rest mass because v/c and its square are very small. Although the theory has the status of natural law, its rigor is not required except for particle motion at high speed (i.e., when v is at least several percent of c). The relation shows that a material object can have a speed no higher than c.

The implication of Einstein's (1905b) formula is that any object has a rest mass energy

$$E_0 = m_0 c^2 \tag{1.8}$$

when motionless, and a total energy

$$E_T = mc^2 \tag{1.9}$$

The difference being E_K the kinetic energy, that is

$$E_T = E_0 + E_K \tag{1.10}$$

The kinetic energy imparted to a particle by the application of force according to Einstein is

$$E_K = (m - m_0)\, c^2 \tag{1.11}$$

For low speeds, $v \ll c$, E_K is approximately $\frac{1}{2} m_0 v^2$, the classical relation (see Exercises 1.7 and 1.18).

EXAMPLE 1.6

Let us compute the rest energy for an electron of mass 9.109×10^{-31} kg

$$\begin{aligned} E_0 = m_0 c^2 &= (9.109 \times 10^{-31}\,\text{kg})(2.998 \times 10^8\,\text{m/s})^2 = 8.19 \times 10^{-14}\,\text{J} \\ &= (8.19 \times 10^{-14}\,\text{J})/(1.602 \times 10^{-13}\,\text{J/MeV}) = 0.511\,\text{MeV} \end{aligned}$$

For one unit of atomic mass, 1.66×10^{-27} kg, which is close to the mass of a hydrogen atom, the corresponding energy is 931.5 MeV (see Exercise 1.14).

Thus we see that matter and energy are equivalent, with the factor c^2 relating the amounts of each. This suggests that matter can be converted into energy and that energy can be converted into matter. Although Einstein's relationship is completely general, it is especially important in calculating the release of energy by nuclear means. We find that *the energy yield from a kilogram of nuclear fuel is more than a million times that from chemical fuel*. To prove this startling statement, we first find

the result of the complete transformation of 1 kg of matter into energy, namely, $(1\,\text{kg})(3.0\times 10^8\,\text{m/s})^2 = 9\times 10^{16}\,\text{J}$. The nuclear fission process, as one method of converting mass into energy, is relatively inefficient, because the burning of 1 kg of uranium involves the conversion of only 0.87 g of matter into energy. This corresponds to approximately $7.8\times 10^{13}\,\text{J/kg}$ of the uranium consumed. The enormous magnitude of this energy release can be appreciated only by comparison with the heat of combustion of a familiar fuel such as gasoline, $5\times 10^7\,\text{J/kg}$. The ratio of these numbers, 1.5×10^6, reveals the tremendous difference between nuclear and chemical energies.

Calculations involving Einstein's theory of relativity are readily accomplished using a program ALBERT, described in Computer Exercise 1.A.

1.6 ENERGY AND THE WORLD

All the activities of human civilization depend on energy, as we realize when we consider the dimensions of the world's energy problem. The efficient production of food requires machines, fertilizer, and water, each making use of energy in a different way. Energy is vital to transportation, protection against the weather, and the manufacturing of all goods. An adequate long-term supply of energy is therefore essential for humanity's survival. The world energy problem has many dimensions: the increasing cost to acquire fuels as they become more scarce; the potential for global climate change resulting from burning fossil fuels; the effects on safety and health of the byproducts of energy consumption; the inequitable distribution of energy resources among regions and nations; and the discrepancies between current energy use and human expectations throughout the world. The global energy situation is a complex subject to which we devote further discussion in Chapter 24, within the context of future directions and trends for nuclear energy.

1.7 SUMMARY

Associated with each basic type of force is an energy, which may be transformed to another form for practical use. The addition of thermal energy to a substance causes an increase in temperature, the measure of particle motion. Electromagnetic radiation arising from electrical devices, atoms, or nuclei may be considered to be composed of waves or of photons. Matter can be converted into energy and vice versa, according to Einstein's formula $E = mc^2$. The energy of nuclear fission is millions of times larger than that from chemical reactions. Energy is fundamental to all human endeavors and, indeed, survival.

1.8 EXERCISES

1.1 Find the kinetic energy of a 75-kg basketball player as he moves down the floor at 8 m/s.

1.2 Recalling the conversion formulas for temperature,

$$C = \frac{5}{9}(F-32) \qquad F = \frac{9}{5}C + 32$$

where C and F are degrees in the Celsius and Fahrenheit systems, convert each of the following: (a) 68°F, (b) 500°F, (c) −273°C, (d) 1000°C, (e) −40°C, (f) 212°F.

1.3 If the specific heat of iron is 450 J/(kg °C), how much energy is required to bring 0.5 kg of iron from 0°C to 100°C?

1.4 Find the speed corresponding to the average energy of nitrogen gas molecules (N_2, 28 units of atomic weight) at room temperature.

1.5 Find the power in kilowatts of an automobile rated at 200 hp. In a drive for 4 h at average speed 45 mph, how many kWh of energy are required?

1.6 Find the frequencies of (a) gamma-ray and (b) X-ray photons of wavelengths 1.5 pm and 0.10 nm, respectively.

1.7 (a) For very small velocities compared with the velocity of light, show that the relativistic formula for kinetic energy is $\frac{1}{2} m_0 v^2$. *Hint:* Use the binomial expansion $(1+x)^n = 1+nx+\ldots$ (b) Find the approximate relativistic mass increase of a car with rest mass 1000 kg moving at 20 m/s.

1.8 Noting that the electronvolt is 1.60×10^{-19} J, how many joules are released in the fission of one uranium nucleus, which yields 190 MeV?

1.9 Applying Einstein's formula for the equivalence of mass and energy, $E = mc^2$, how many kilograms of matter are converted into energy in Exercise 1.8?

1.10 If the atom of uranium-235 has mass of (235) (1.66×10^{-27}) kg, what amount of equivalent energy does it have?

1.11 Using the results of Exercises 1.8–1.10, what fraction of the mass of a U-235 nucleus is converted into energy when fission takes place?

1.12 Show that to obtain a power of 1 W from fission of uranium, it is necessary to cause 3.3×10^{10} fission events per second. Assume that each fission releases 190 MeV of useful energy.

1.13 Using the rest mass of each, compute the rest mass energy in MeV for (a) a proton and (b) a neutron. Compare to values given in Table A.2.

1.14 Using the mass of $1.6605389 \times 10^{-27}$ kg for one atomic unit, calculate the equivalent energy (in MeV) to five significant digits.

1.15 (a) If the fractional mass increase caused by relativity is $\Delta E/E_0$, show that

$$v/c = \sqrt{1 - (1 + \Delta E/E_0)^{-2}}$$

(b) At what fraction of the speed of light does a particle have a mass that is 1% higher than the rest mass? 10%? 100%?

1.16 The heat of combustion of hydrogen by the reaction $2H + O = H_2O$ is quoted as 34.18 kilogram-calories per gram of hydrogen. (a) Find how many Btu per pound this is with the conversions 1 Btu = 0.252 kcal, 1 lb. = 454 g. (b) Find how many joules per gram this is noting 1 cal = 4.184 J. (c) Calculate the heat of combustion in eV per H_2 molecule. *Note:* Recall the number of particles per gram of molecular weight, Avogadro's number, $N_A = 6.022 \times 10^{23}$.

1.17 Derive an analytical expression for finding the velocity of a relativistic particle given its kinetic energy and rest mass.

1.18 Graph the percentage error in the kinetic energy computed from the classic mechanics expression as compared to the full relativistic formula as a function of the fraction of the speed of light (v/c).

1.9 COMPUTER EXERCISE

1.A Properties of particles moving at high velocities are related in a complicated way, according to Einstein's theory of special relativity. To obtain answers easily, the program ALBERT (after Dr. Einstein) can be used to treat the following quantities: velocity, momentum, total energy, kinetic energy, and ratio of mass to rest mass. Given one of these for a selected particle, ALBERT calculates the others. Test the program with various inputs, including (a) an electron with velocity $0.5\,c$, (b) a proton with 1000 MeV total energy, (c) a neutron with 0.025 eV kinetic energy, (d) deuteron with $m/m_0 = 1.01$, and (e) alpha with momentum 10^{-19} kg m/s.

REFERENCES

Einstein, A., 1905a. Zur elektrodynamik bewegter körper (On the electrodynamics of moving bodies). Ann. Phys. 322 (10), 891–921.

Einstein, A., 1905b. Ist die trägheit eines körpers von seinem energieinhalt abhängig? (Does the inertia of a body depend upon its energy content?). Ann. Phys. 323 (13), 639–641.

Taylor, B.N., Thompson, A. (Eds.), 2008. The International System of Units (SI). National Institute of Standards and Technology (NIST), SP 330.

CHAPTER

ATOMS AND NUCLEI

2

CHAPTER OUTLINE

A complete understanding of the microscopic structure of matter and the exact nature of the forces acting on that matter have yet to be realized. However, excellent models have been developed to predict behavior to an adequate degree of accuracy for most practical purposes. These models are descriptive or mathematical, often based on analogy with large-scale processes, on experimental data, or on advanced theory.

2.1 ATOMIC THEORY

The most elementary concept is that matter is composed of individual particles—atoms—that retain their identity as elements in ordinary physical and chemical interactions. Thus, a collection of helium atoms that forms a gas has a total weight that is the sum of the weights of the individual atoms. In addition, when two elements combine to form a compound (e.g., if carbon atoms combine with oxygen atoms to form carbon monoxide molecules), the total weight of the new substance is the sum of the weights of the original elements.

There are more than 100 known elements, most of which are found in nature, although some are artificially produced. Each is given a specific *atomic number* in the periodic table of the elements; examples are hydrogen (H) 1, helium (He) 2, oxygen (O) 8, and uranium (U) 92. The symbol Z is assigned to that atomic number, which is the number of protons in the nucleus. Z also equals the number of electrons in the neutral atom and determines its chemical properties. Fig. 2.1 shows the periodic table.

Nuclear Energy. https://doi.org/10.1016/B978-0-12-812881-7.00002-2

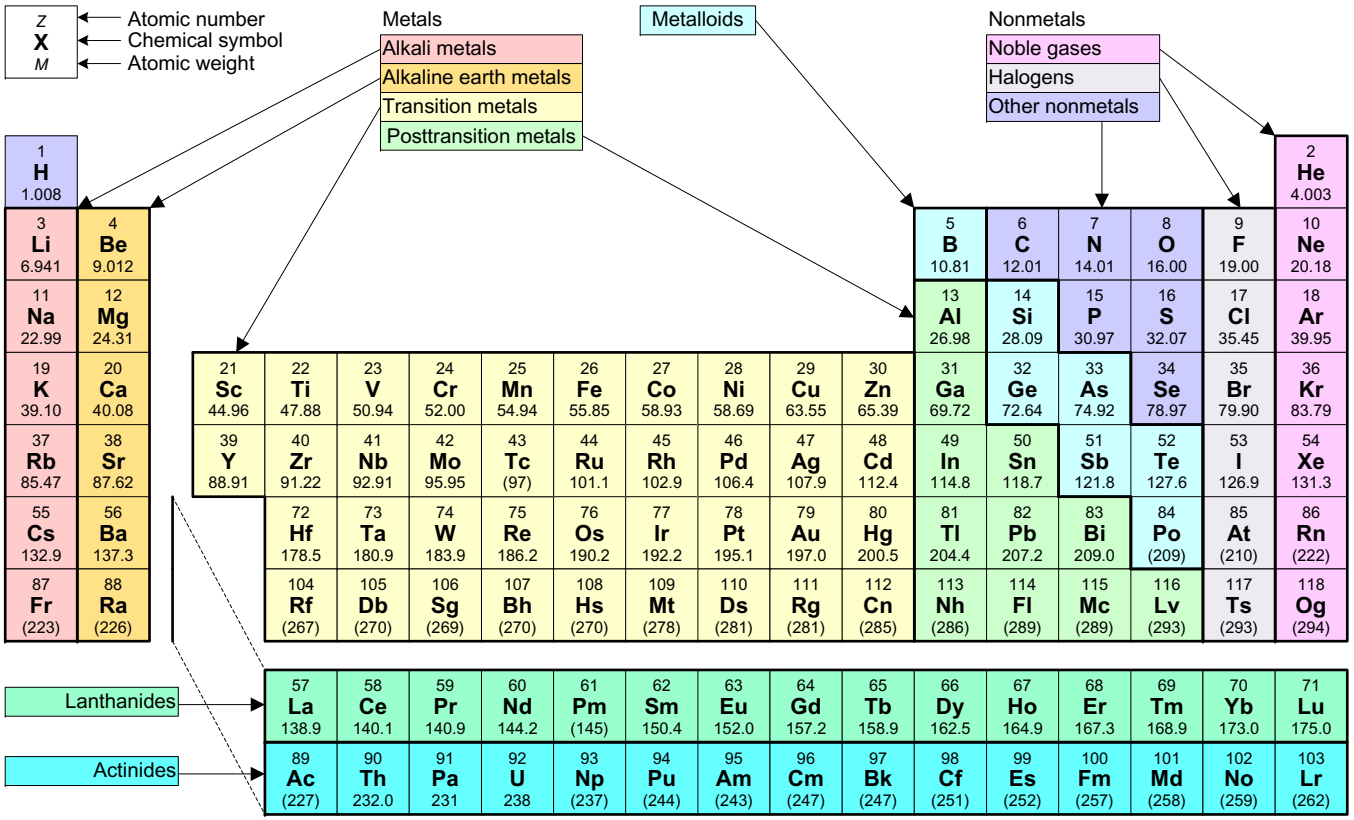

FIG. 2.1

Periodic table of the elements.

Generally, the further down an element is listed in the periodic table, the heavier its atoms. The *atomic weight M* is the weight in grams of a definite number of atoms, 6.022×10^{23}, which is Avogadro's number, N_A. Although we often use the terms atomic weight and atomic mass interchangeably, atomic mass describes the mass of a single atom of a particular isotope, whereas atomic weight provides a weighted average mass for an element based on the abundance of its constituent isotopes. For the elements just mentioned, the values of M are approximately H, 1.008; He, 4.003; O, 16.00; and U, 238.0. Atomic weight is expressed using grams/mol or atomic mass units (u) while atomic mass is quantified using atomic mass units (u). Accurate values of atomic weights of all the elements are given in Table A.4 in Appendix A.

If an element has a nonnatural abundance of its isotopes (i.e., the elemental material is either *enriched* or *depleted*), then it is necessary to compute the atomic weight of the element M from the weighted sum of all the atomic masses of the isotopes M_j rather than use the tabulated M value found in a reference. In such cases, the isotopic abundance may be expressed either as an atom abundance or fraction γ_j, or as a weight or mass fraction ω_j. This distinction leads to two formulas for determining the elemental atomic weight:

$$M = \sum \gamma_j M_j$$
$$\frac{1}{M} = \sum \frac{\omega_j}{M_j} \tag{2.1}$$

We can easily find the number of atoms per cubic centimeter in a substance if its density ρ (rho) in grams per cubic centimeter is known. This procedure can be expressed as a convenient formula for finding N, the atomic number density for any material

$$N = \frac{\rho N_A}{M} \tag{2.2}$$

The relationship holds for compounds as well, if M is taken as the molecular weight.

EXAMPLE 2.1

Using the density and atomic weight for natural uranium given in Table A.4, we find a uranium atom density of

$$N_U = \frac{\rho_U N_A}{M_U} = \frac{(18.95\,\text{g/cm}^3)(6.022 \times 10^{23}\,\text{atoms/mol})}{238.03\,\text{g/mol}} = 4.79 \times 10^{22}\,\frac{\text{atoms}}{\text{cm}^3}$$

EXAMPLE 2.2

For a compound such as water, H_2O, the molecular weight is first found,

$$M_{H_2O} = 2M_H + M_O = (2)(1.008) + 15.999 = 18.015\,\text{g/mol}$$

Using the customary water density of $\rho = 1.0\,\text{g/cm}^3$, the molecular density is

$$N_{H_2O} = \frac{\rho_{H_2O} N_A}{M_{H_2O}} = \frac{(1.0\,\text{g/cm}^3)(6.022 \times 10^{23}\,\text{atoms/mol})}{18.015\,\text{g/mol}} = 3.34 \times 10^{22}\,\frac{\text{molecules}}{\text{cm}^3}$$

With two atoms of hydrogen for every water molecule, the hydrogen atomic density is twice the molecular density of water, that is, $N_H = 2N_{H_2O} = 6.68 \times 10^{22}$ atoms/cm^3; whereas the oxygen density is numerically equivalent to the water concentration, $N_O = N_{H_2O}$.

2.2 GASES

Substances in the gaseous state are described approximately by the perfect or ideal gas law, relating pressure p, volume V, and absolute temperature T,

$$pV = nkT \tag{2.3}$$

where n is the number of particles and k is the Boltzmann constant. An increase in the temperature of the gas as a result of heating causes greater molecular motion, which results in an increase of particle bombardment of a container wall and thus of pressure on the wall.

The gas particles, each of mass m, have a variety of speeds v in accord with Maxwell's gas theory, as shown in Fig. 2.2. Boltzmann's formula for the number of molecules per unit speed is

$$n(v) = \frac{n_0 4\pi v^2}{(2\pi kT/m)^{3/2}} \exp\left(-mv^2/2kT\right) \tag{2.4}$$

where n_0 is the total number of molecules. The most probable speed, at the peak of this Maxwell-Boltzmann distribution, depends on temperature according to the relation (see Exercise 2.16)

$$v_p = \sqrt{2kT/m} \tag{2.5}$$

while the average speed is

$$\bar{v} = \sqrt{\frac{8kT}{\pi m}} = \frac{2}{\sqrt{\pi}} v_p \tag{2.6}$$

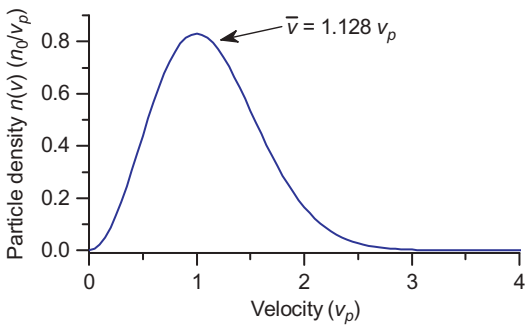

FIG. 2.2

Maxwellian distribution of molecular speeds.

EXAMPLE 2.3

At an ambient temperature of 20°C (or 293 K), the most probable particle speed corresponds to a kinetic energy of

$$E = kT = \left(8.62 \times 10^{-5}\,\text{eV/K}\right)(20 + 273\,\text{K}) = 0.0253\,\text{eV}$$

in which the Boltzmann constant k is obtained from Table A.2.

The kinetic theory of gases provides a basis for calculating properties such as the specific heat. Recalling from Section 1.3 that the average energy of gas molecules is proportional to the temperature, $\overline{E} = \frac{3}{2}kT$, we can deduce, as in Exercise 2.4, that the specific heat of a gas consisting only of single atoms (monoatomic) is $c_V = \frac{3}{2}k/m$, in which m is the mass of one atom. Thus, we see an intimate relationship between mechanical and thermal properties of materials.

2.3 THE ATOM AND LIGHT

Until the 20th century, the internal structure of atoms was unknown, but it was believed that electric charge and mass were uniform. Rutherford supervised some crucial experiments in which gold atoms were bombarded by charged particles (Geiger and Marsden, 1909). He deduced (Rutherford, 1911) that most of the mass and positive charge of an atom were concentrated in a *nucleus* of radius only approximately 10^{-5} times that of the atom, and thereby occupying a volume of approximately 10^{-15} times that of the atom (see Exercises 2.2 and 2.12). The new view of atoms paved the way for Bohr to find an explanation for the production of light.

It is well known that the color of a heated solid or gas changes as the temperature is increased, tending to go from the red end of the visible region toward the blue end (i.e., from long wavelengths to short wavelengths). The measured distribution of light among the different wavelengths at a certain temperature can be explained by the assumption that light is in the form of *photons*. These are absorbed and emitted with definite amounts of energy E that are proportional to the frequency ν, according to

$$E = h\nu \tag{2.7}$$

where h is the Planck constant, $6.63 \times 10^{-34}\,\text{J s}$.

EXAMPLE 2.4

The energy corresponding to a 280-nm ultraviolet light of frequency of $1.07 \times 10^{15}\,\text{Hz}$ (from Example 1.5) is

$$E = h\nu = \left(6.63 \times 10^{-34}\,\text{J s}\right)\left(1.07 \times 10^{15}/\text{s}\right) = 7.09 \times 10^{-19}\,\text{J}$$

This is a very minute amount of energy (also see Exercise 2.6).

Danish physicist Niels Bohr (1913) first explained the emission and absorption of light from incandescent hydrogen gas with a novel model of the hydrogen atom. He assumed that the atom consists of a single electron moving at constant speed v in a circular orbit about a nucleus—the proton—as shown in Fig. 2.3. Each particle has an electric charge e of 1.6×10^{-19} coulombs (C), but the positively charged

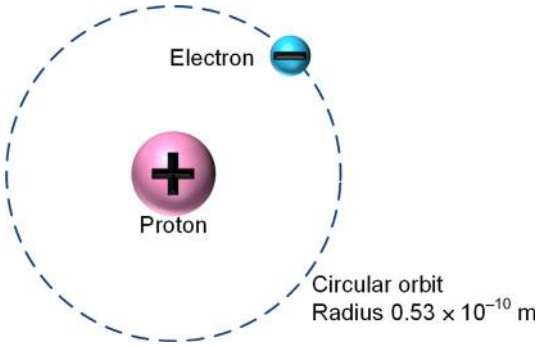

FIG. 2.3

Hydrogen atom.

proton has a mass that is 1836 times that of the negatively charged electron. The radius R_n of the orbit is set by the equality of electrostatic force, attracting the two charges toward each other, to centripetal force, required to keep the electron on a circular path, that is,

$$\frac{e^2}{4\pi\varepsilon_0 R_n^2} = \frac{m_e v^2}{R_n} \tag{2.8}$$

where m_e is the electron rest mass and ε_0 is the electric constant (or permittivity of free space). If sufficient energy is supplied to the hydrogen atom from the outside, the electron is caused to jump to a larger orbit of definite radius. At some later time, the electron falls back spontaneously to the original orbit, and energy is released in the form of a photon of light. The photon energy $h\nu$ is equal to the difference between energies in the two orbits. The smallest orbit has a radius $R_1 = 0.529 \times 10^{-10}$ m, whereas the others have radii increasing as the square of integers, n, which are called principal *quantum numbers*. Thus if n is 1, 2, 3, …, 7, the radius of the n-th orbit is

$$R_n = n^2 R_1 \tag{2.9}$$

Fig. 2.4 shows the allowed electron orbits in hydrogen. The energy of the atom system when the electron is in the first orbit is $E_1 = -13.6$ eV (Exercise 2.23), in which the negative sign means that energy must be supplied to remove the electron to a great distance and leave the hydrogen as a positive ion. The total potential and kinetic energy when the electron is in the n-th orbit is

$$E_n = \frac{E_1}{n^2} = \frac{-m_e e^4}{8\varepsilon_0^2 h^2 n^2} \tag{2.10}$$

The various discrete levels are shown in Fig. 2.5. The electron transitions for the Lyman, Balmer, and Paschen series result, respectively, in the emission of ultraviolet, visible (for the first four lines), and infrared light. For the heavier atoms, the photon emanations are termed characteristic X-rays with energies from 0.02 to 116 keV (Bearden, 1967).

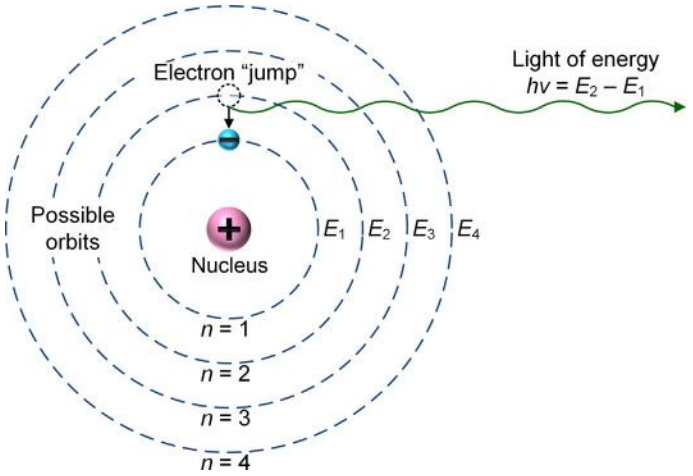

FIG. 2.4

Electron orbits in hydrogen (Bohr theory).

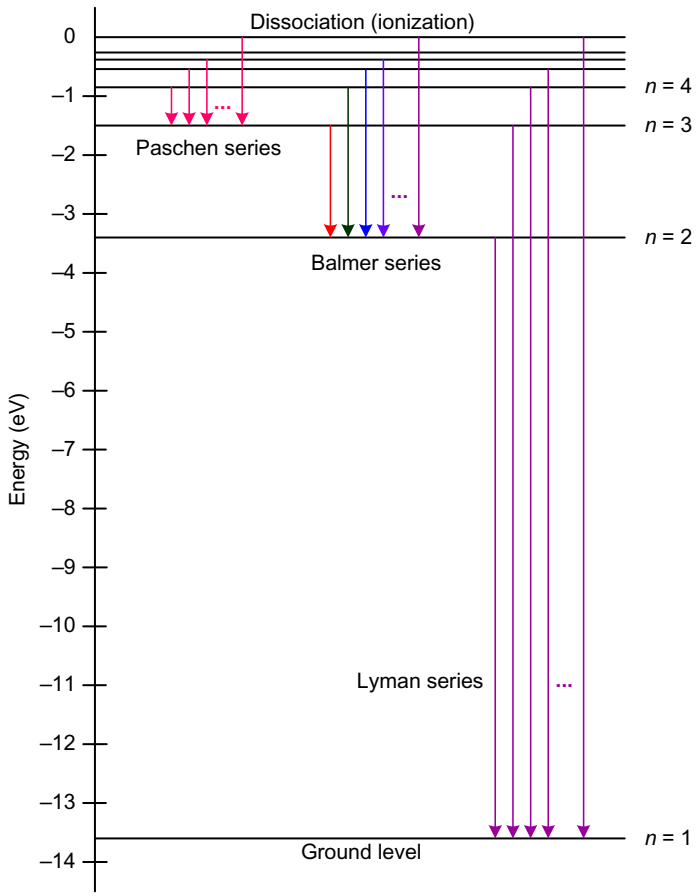

FIG. 2.5

Electron energy levels and transitions in the hydrogen atom.

EXAMPLE 2.5

The energy of an emitted photon based on a transition in the hydrogen atom from the $n=3$ to $n=2$ orbit (i.e., the first Balmer series line) is found using Eq. (2.10)

$$E=E_3-E_2=\frac{E_1}{3^2}-\frac{E_1}{2^2}=(-13.6\text{eV})\left(\frac{1}{9}-\frac{1}{4}\right)=1.89\text{eV}$$

This is an optical emission of red color.

The electronic structure of the other elements is described by the shell model, in which a limited number of electrons can occupy a given orbit or shell. The atomic number Z is unique for each chemical element and represents both the number of positive charges in the central massive nucleus of the atom and the number of electrons in orbits around the nucleus. The maximum allowed number of electrons in each orbit as Z increases is $2n^2$, so for the first three shells: 2, 8, and 18 electrons. The number of electrons in the outermost, or valence, shell determines the chemical behavior of elements. For example, oxygen with $Z=8$ has two electrons in the inner shell, six in the outer. Thus, oxygen has an affinity for elements with two electrons in the valence shell. The formation of molecules from atoms by electron sharing is illustrated by Fig. 2.6, which shows the water molecule.

The Bohr model of atoms is useful for visualization, but quantum mechanics provides a more rigorous view. There, the location of the electron in the H atom is described by a probability expression. A key feature of quantum mechanics is Heisenberg's uncertainty principle. It states that the precise values of both a particle's position and momentum cannot be known.

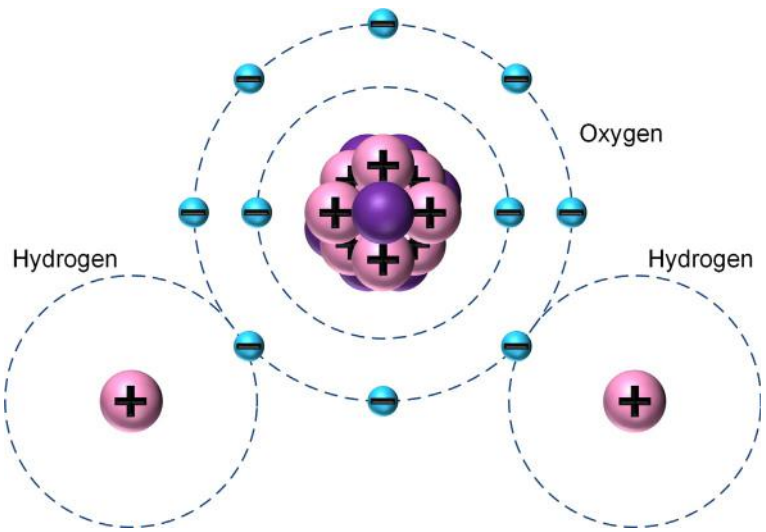

FIG. 2.6

Water molecule with shared electrons.

2.4 LASER BEAMS

Ordinary light, as in the visible range, is a mixture of many frequencies, directions, and phases. In contrast, light from a *laser* (**l**ight **a**mplified by **s**timulated **e**mission of **r**adiation) consists of a direct beam of one color and with the waves in synchronization. The device consists of a tube of material to which energy is supplied, exciting the atoms to higher energy states. A photon of a certain frequency is introduced. It strikes an excited atom, causing it to fall back to the ground state and in so doing emit another photon of the same frequency. The two photons strike other atoms, producing four identical photons, and so on. The ends of the laser are partially reflecting, which causes the light to be trapped and to build up inside by a combination of reflection and stimulation. An avalanche of photons is produced that makes a very intense beam. Light moving in directions other than the long axis of the laser is lost through the sides, so that the beam that escapes from the end proceeds in only one direction. The reflection between the two end mirrors assures a coherent beam (i.e., the waves are in phase).

Lasers can be constructed from several materials. The original laser (Maiman, 1960) was the crystalline gem ruby. Others use gases such as a helium-neon mixture, liquids with dye in them, or semiconductors. The external supply of energy can be chemical reactions, a discharge produced by accelerated electrons, energetic particles from nuclear reactions, or another laser. Some lasers operate continuously, whereas others produce pulses of energy as short as a fraction of a nanosecond (10^{-9} s) with a power of a terawatt (10^{12} W). Because of the high intensity, laser light, if viewed directly, can be hazardous to the eyes.

Lasers are widely used where an intense, well-directed beam is required, as in metal cutting and welding, eye surgery and other medical applications, and accurate surveying and range finding. Newer applications include digital optical disc data storage (e.g., Blu-ray discs), holograms (three-dimensional images), powering signals in optical-fiber communication networks, and lidar (light detection and ranging) that employs laser light rather than radio waves utilized by radar. In later chapters, we will describe some nuclear applications: isotope separation (Section 15.5) and thermonuclear fusion (Section 26.4).

2.5 NUCLEAR STRUCTURE

Most elements are composed of atoms of different mass, called *isotopes*. For instance, hydrogen has three isotopes of weights in proportion 1, 2, and 3—ordinary hydrogen (protium), heavy hydrogen (deuterium), and tritium. Each has atomic number $Z = 1$ and the same chemical properties, but they differ in the composition of the central nucleus, where most of the mass resides. The nucleus of ordinary hydrogen is the positively charged proton; the *deuteron* consists of a proton plus a neutron; and the *triton* contains a proton plus two neutrons. The *neutron* is a neutral particle of mass very close to that of the proton. To distinguish isotopes, we identify the *atomic mass number* A as the total number of nucleons, which are the heavy particles in the nucleus. The atomic weight, a real number, is approximated by the mass number, which is an integer, $M \cong A$. The complete shorthand notation for an isotope is given by the chemical symbol X with leading superscript A and subscript Z values, that is, ${}^{A}_{Z}\mathrm{X}$. Fig. 2.7 shows the nuclear and atomic structure of the three hydrogen isotopes (i.e., ${}^{1}_{1}\mathrm{H}$, ${}^{2}_{1}\mathrm{H}$, and ${}^{3}_{1}\mathrm{H}$). Each has one electron in the outer shell, in accord with the Bohr theory described earlier.

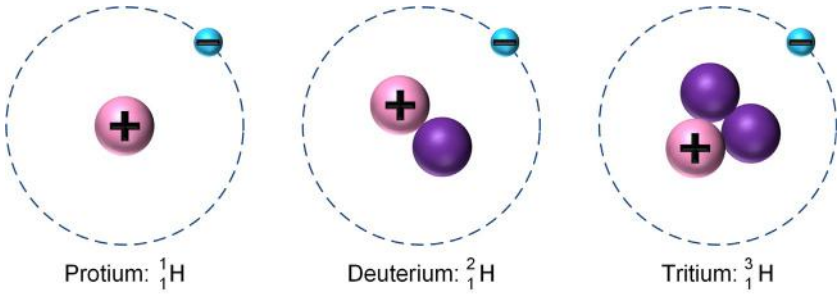

FIG. 2.7

Isotopes of hydrogen.

The structure of some of the lighter elements and isotopes is shown in Fig. 2.8. In each case, the atom is neutral because the negative charge of the Z electrons in the outside shell balances the positive charge of the Z protons in the nucleus. The symbols for the isotopes shown in Fig. 2.8 are:

$$^{1}_{1}H,\ ^{4}_{2}He,\ ^{6}_{3}Li,\ ^{7}_{3}Li,\ ^{9}_{4}Be,\ ^{16}_{8}O,\ ^{23}_{11}Na$$

In addition to the atomic number Z and the mass number A, we often need to write the neutron number N, which is, of course, $N = A - Z$. For the set of isotopes just listed, N is 0, 2, 3, 4, 5, 8, and 12, respectively. Nuclides with an identical number of neutrons are termed isotones while isobars are isotopes of different elements but having the same atomic mass number.

When we study nuclear reactions, it is convenient to let the neutron be represented by the symbol $^{1}_{0}n$, implying a mass comparable to that of hydrogen, $^{1}_{1}H$, but with no electronic charge, $Z = 0$. Similarly, the electron is represented by $^{0}_{-1}e$, suggesting nearly zero mass in comparison with that of hydrogen, but with negative charge. An identification of isotopes frequently used in qualitative discussion consists of the element name and its A value, thus sodium-23 and uranium-235, or even more simply Na-23 or ^{23}Na and U-235 or ^{235}U. Prohibited from referring to U-235 and Pu-239, Manhattan Project scientists represented them in shorthand (still in use today) as simply "25" and "49," respectively, using the last digits of Z and A.

2.6 SIZES AND MASSES OF NUCLEI

The dimensions of nuclei are found to be very much smaller than those of atoms. Whereas the hydrogen atom has a radius of approximately 5×10^{-9} cm, its nucleus has a radius of only approximately 10^{-13} cm. Because the proton mass is much larger than the electron mass, the nucleus is extremely dense. The nuclei of other isotopes may be viewed as closely packed particles of matter—neutrons and protons—forming a sphere whose volume, $\frac{4}{3}\pi R^3$, depends on A, the number of nucleons. A useful rule of thumb to calculate radii of nuclei is (Krane, 1988)

$$R\,[\text{cm}] = 1.25 \times 10^{-13} A^{1/3} \tag{2.11}$$

Because A ranges from 1 to approximately 250, we see that all nuclei are smaller than 10^{-12} cm. The radius of an entire atom is much larger, on the order of 10^{-8} cm.

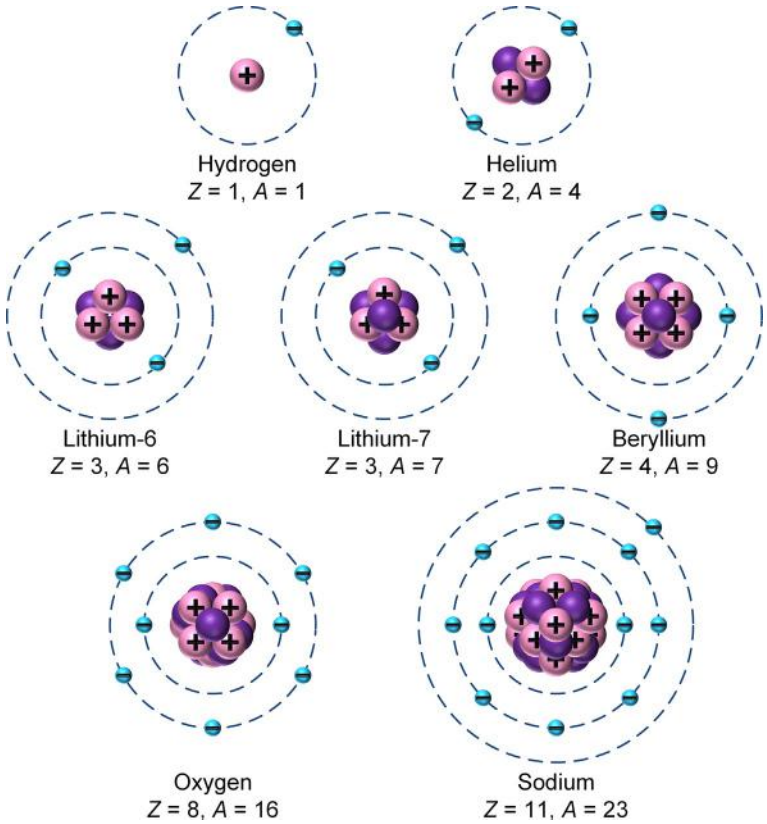

FIG. 2.8

Atomic and nuclear structure.

The masses of atoms, labeled M, are compared on a scale in which an isotope of carbon ${}^{12}_{6}\mathrm{C}$ has a mass of exactly 12. For ${}^{1}_{1}\mathrm{H}$, the atomic mass is $M_{\mathrm{H\text{-}1}} = 1.007825$, for ${}^{2}_{1}\mathrm{H}$, $M_{\mathrm{H\text{-}2}} = 2.014102$, and so on. The atomic mass of the proton is 1.007276, of the neutron 1.008665, the difference being only about 0.1%. The mass of the electron on this scale is 0.000549. A list of atomic masses appears in Table A.5.

EXAMPLE 2.6

Use the isotopic abundances and atomic masses of ${}^{1}\mathrm{H}$ and ${}^{2}\mathrm{H}$ to determine the atomic weight of hydrogen. Employing the first expression of Eq. (2.1) and data from Table A.5 yields

$$\begin{aligned} M_{\mathrm{H}} &= \gamma_{\mathrm{H}-1} M_{\mathrm{H}-1} + \gamma_{\mathrm{H}-2} M_{\mathrm{H}-2} \\ &= (0.99984426)(1.007825) + (0.00015574)(2.014102) = 1.0080 \end{aligned}$$

This result is identical to the atomic weight for hydrogen given in Table A.4.

The atomic mass unit (amu or formally "u"), as one-twelfth the mass of ${}^{12}_{6}\mathrm{C}$, corresponds to an actual mass of 1.660539×10^{-24} g. To verify this, merely divide 1 g by Avogadro's number 6.022141×10^{23}. We can calculate the actual masses of atoms and nuclei by multiplying their mass in atomic mass units by the mass of 1 amu.

EXAMPLE 2.7

The rest mass of the neutron is

$$(1.008665\,\text{amu})\left(1.660539 \times 10^{-24}\,\text{g/amu}\right) = 1.674928 \times 10^{-24}\,\text{g}$$

By use of Einstein's $E = mc^2$ with constants in Table A.2, we found in Exercise 1.14 that 1 amu = 931.494 MeV ($\cong$931.5 MeV). This mass-energy equivalence factor will prove useful.

2.7 BINDING ENERGY

The force of electrostatic repulsion between like charges, which varies inversely as the square of their separation, would be expected to be so large that nuclei could not be formed. The fact that they do exist is evidence that there is an even larger force of attraction. The strong nuclear force is of very short range, as we can deduce from the preceding rule of thumb. As shown in Exercise 2.10, the radius of a nucleon is approximately 1.25×10^{-13} cm; the distance of separation of centers is about twice that. The strong nuclear force acts only when the nucleons are very close to each other and binds them into a compact structure. Associated with the net force is a potential energy of binding.

To disrupt a nucleus and separate it into its component nucleons, energy must be supplied from the outside. Recalling Einstein's relation between mass and energy, this is the same as saying that a given nucleus is lighter than the sum of its separate nucleons, the difference being the mass defect. Let the mass of an atom, including nucleus and external electrons, be M, and let m_n and M_H be the respective masses of the neutron and the proton plus matching electron. Then the *mass defect* is

$$\Delta m = \underbrace{Nm_\mathrm{n} + ZM_\mathrm{H}}_{\substack{\text{total mass of} \\ \text{separate particles}}} - M \tag{2.12}$$

Neglected in this relation is a small energy of atomic or chemical binding. The corresponding nuclear *binding energy* is simply

$$BE = \Delta m\, c^2 \tag{2.13}$$

If the binding energy per nucleon (BE/A) can be increased, then energy will be liberated in the process. The BE/A curve shown in Fig. 2.9 reveals a maximum around ${}^{56}\mathrm{Fe}$, but ${}^{62}\mathrm{Ni}$ is the most bound nucleus. The release of binding energy is exploited in both nuclear fission and fusion.

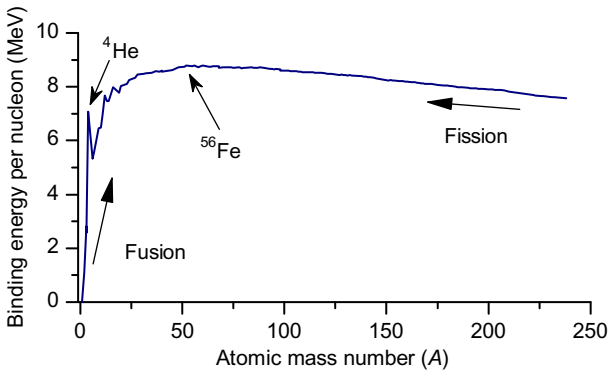

FIG. 2.9

Binding energy per nucleon.

EXAMPLE 2.8

Let us calculate the mass defect and binding energy for tritium, the heaviest hydrogen atom, ${}_1^3\mathrm{H}$. Fig. 2.10 shows the dissociation that would take place if a sufficient energy were provided. Now $Z_T = 1$, $N_T = 2$, $m_n = 1.008665$, $M_H = 1.007825$, and $M_T = 3.016049$. Then the mass defect is

$$\begin{aligned}\Delta m_T &= N_T m_n + Z_T M_H - M_T \\ &= 2(1.008665) + 1(1.007825) - 3.016049 = 0.009106\,\text{amu}\end{aligned}$$

Converting by use of the relation 1 amu = 931.5 MeV, the binding energy is $BE = 8.48$ MeV.

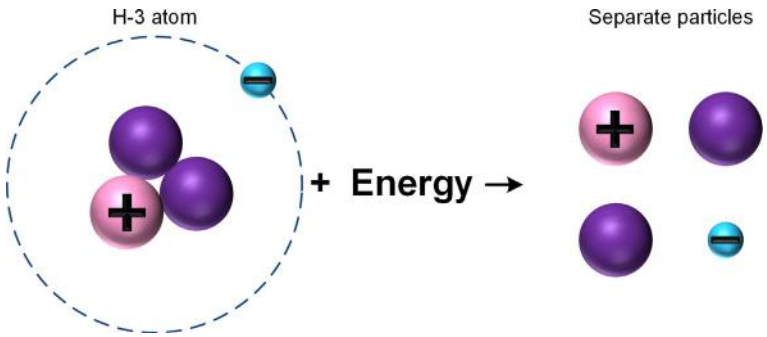

FIG. 2.10

Dissociation of tritium (^{3}H).

The preceding example shows the necessity of utilizing masses known to six or more significant digits in the computation of the mass defect. Calculations such as these are required for several purposes: to compare the stability of one nucleus with that of another, to find the energy release in a nuclear reaction, and to predict the possibility of fission of a nucleus.

We can speak of the binding energy associated with one particle such as a neutron. Suppose that M_1 is the mass of an atom and M_2 is its mass after absorbing a neutron. The binding energy of the additional neutron of mass m_n is then

$$S_n = [(M_1 + m_n) - M_2]\, c^2 \tag{2.14}$$

S_p, which is the binding energy associated with a proton, and S_n are the separation energies needed to remove the particular particle from the nucleus.

EXAMPLE 2.9

Determine the proton separation energy for boron-10. The energy to remove a proton from nuclide 2 to yield nuclide 1 must account for the additional electron present in the initial nuclide via

$$S_p = \left[\left(M_1 + m_e + m_p\right) - M_2\right] c^2 = [(M_1 + M_{H-1}) - M_2]\, c^2 \tag{2.15}$$

Referring to the periodic table of Fig. 2.1, the loss of a proton from boron decreases the atomic number Z by one to form beryllium while concurrently the atomic mass number A is reduced by unity (i.e., B-10 becomes Be-9). Inserting the appropriate atomic masses from Table A.5 gives

$$\begin{aligned} S_p^{B-10} &= [(M_{Be-9} + M_{H-1}) - M_{B-10}]c^2 \\ &= [(9.0121831 + 1.0078250) - 10.0129369]\text{u}(931.5\,\text{MeV/u}) \\ &= 6.59\,\text{MeV} \end{aligned}$$

Explanations of binding energy effects by means of physical logic and measured atomic masses have led to what are called semiempirical formulas for binding energy. The *BE* for any nuclide may be approximated using a liquid drop model that accounts for (1) attraction of nucleons for each other due to strong nuclear force, (2) electrostatic (Coulombic) repulsion, (3) surface tension effects, and (4) the imbalance of neutrons and protons in the nucleus. The Bethe-Weizsäcker formula is one such expression to calculate the binding energy:

$$BE[\text{MeV}] = a_v A - a_s A^{2/3} - a_c \frac{Z^2}{A^{1/3}} - a_a \frac{(A-2Z)^2}{A} + \frac{a_p}{A^{1/2}} \frac{\left[(-1)^Z + (-1)^{A-Z}\right]}{2} \tag{2.16}$$

From left to right, the terms correspond to contributions from volume, surface, Coulomb, asymmetry and pairing energy, and a reasonable set of fitting coefficients: $a_v = 15.56$, $a_s = 17.23$, $a_c = 0.697$, $a_a = 23.285$ and $a_p = 12$ (Williams, 1991).

EXAMPLE 2.10

Compute the binding energy per nucleon and the mass of ^{235}U using the Bethe-Weizsäcker formula. With $Z = 92$ and $A = 235$, the total binding energy is

$$\begin{aligned} BE = {} & (15.56)(235) - (17.23)(235)^{2/3} - 0.697\frac{(92)^2}{(235)^{1/3}} \\ & -23.285\frac{(235-2(92))^2}{235} + \frac{12}{(235)^{1/2}} \frac{\left[(-1)^{92} + (-1)^{235-92}\right]}{2} = 1786.8\,\text{MeV} \end{aligned}$$

The binding energy per nucleon is readily seen as $BE/A = (1786.8\,\text{MeV})/(235) = 7.60\,\text{MeV/nucleon}$, which compares favorably to the known value of 7.59 MeV/nucleon (see Fig. 2.9). Finally, combining Eqs. (2.12) and (2.13) provides a relation for the atomic mass

$$\begin{aligned} M &= (A-Z)m_n + ZM_H - BE/c^2 \\ &= (235-92)(1.008665\text{u}) + (92)(1.007825\text{u}) - (1786.8\,\text{MeV})/(931.49\,\text{MeV/u}) \\ &= 235.04\,\text{amu} \end{aligned}$$

This mass agrees with that in Table A.5.

2.8 SUMMARY

All material is composed of elements whose chemical interaction depends on the number of electrons (Z). Light is absorbed and emitted in the form of photons when atomic electrons jump between orbits. Isotopes of elements differ according to the number of nucleons (A). Nuclei are much smaller than atoms and contain most of the mass of the atom. The nucleons are bound together by a net force in which the nuclear attraction forces exceed the electrostatic repulsion forces. Energy must be supplied to dissociate a nucleus into its components.

2.9 EXERCISES

2.1 Find the number of (a) C-12 and (b) C-13 atoms in $1\,\text{cm}^3$ of graphite, density $1.65\,\text{g/cm}^3$.

2.2 Estimate the radius and volume of the gold atom, using the metal density of $19.3\,\text{g/cm}^3$. Assume that atoms are located at corners of cubes and that the atomic radius is that of a sphere with volume equal to that of a cube.

2.3 Calculate the most probable speed of a "neutron gas" at (a) 20°C (293 K) and (b) 500°C, noting that the mass of a neutron is $1.675 \times 10^{-27}\,\text{kg}$ (Table A.2).

2.4 Prove that the specific heat at constant volume of an atomic gas is given by $c_V = (3/2)(k/m)$, by use of the formula for average energy of a molecule, i.e., Eq. (1.4), and that heat added (Q) causes a temperature rise (ΔT) according to $Q = mc_V\Delta T$.

2.5 Use the formula derived in the previous exercise to determine the specific heat of helium, a common coolant for high-temperature gas reactors.

2.6 Calculate the energy in electronvolts of a (a) 280-nm photon of ultraviolet light, (b) 1.5-pm gamma ray, and (c) 0.10-nm X-ray.

2.7 What frequency of light is emitted when an electron jumps into the smallest orbit of hydrogen, coming from a very large radius (assume infinity)?

2.8 Calculate the energy in electronvolts of the electron orbit in hydrogen for which $n = 3$, and find the radius in centimeters. How much energy would be needed to cause an electron to go from the innermost orbit to this one? If the electron jumped back, what frequency of light would be observed?

2.9 Sketch the atomic and nuclear structure of carbon-14, noting Z and A values and the numbers of electrons, protons, and neutrons.

2.10 If A nucleons are visualized as spheres of radius r that can be deformed and packed tightly in a nucleus of radius R, show that $r = 1.25 \times 10^{-13}$ cm.

2.11 What is the radius of the nucleus of uranium-238 viewed as a sphere? What is the area of the nucleus, seen from a distance as a circle?

2.12 Find the fraction of the volume that is occupied by the nucleus in the gold-197 atom, by use of the relationship of radius R to mass number A. Recall from Exercise 2.2 that the radius of the atom is 1.59×10^{-8} cm.

2.13 Find the mass defect in amu and binding energy in MeV of ordinary (a) helium, ${}^{4}_{2}\mathrm{He}$, (b) carbon, ${}^{12}_{6}\mathrm{C}$, and (c) nitrogen, ${}^{14}_{7}\mathrm{N}$.

2.14 How much energy (in MeV) would be required to completely dissociate the (a) uranium-235, (b) gold-197, and (c) manganese-55 nucleus into its component protons and neutrons?

2.15 Find the mass density of the nucleus, the electrons, and the atom of U-235, assuming spherical shapes and the following data:

Atomic radius	1.7×10^{-10} m
Nuclear radius	8.6×10^{-15} m
Electron radius	2.8×10^{-15} m
Mass of 1 amu	1.66×10^{-27} kg
Mass of electron	9.11×10^{-31} kg

Discuss the results.

2.16 (a) Use the Maxwell-Boltzmann distribution of Eq. (2.4) to verify by differentiation that the peak of the curve occurs at v_p given by Eq. (2.5). (b) Confirm by integration that the average speed is given by Eq. (2.6). *Hint:* Let $mv^2/(2kT) = x$.

2.17 The temperature of the surface of the sun is approximately 5800 K. To what light frequency and wavelength does that correspond?

2.18 The division between ionizing and nonionizing electromagnetic radiation is sometimes quoted as 10 eV. Determine the corresponding frequency and wavelength.

2.19 Use the Bethe-Weizsäcker formula to determine the atomic mass of (a) ${}^{16}\mathrm{O}$, (b) ${}^{17}\mathrm{O}$, (c) ${}^{92}\mathrm{Rb}$, (d) ${}^{140}\mathrm{Cs}$, and (e) ${}^{238}\mathrm{U}$. Compare the resulting values to those in Table A.5.

2.20 Using Eqs. (2.9) and (2.10), make a log-log plot of $|E_n|$ versus R_n for $n = 1, 2, \ldots 6$. What is the shape of the resulting curve?

2.21 Using the liquid drop model, create an approximation of the binding energy per nucleon graph of Fig. 2.9. The atomic mass number of stable isotopes can be approximated as a power law function of the atomic number according to $A = 1.47Z^{1.123}$ (Paar et al., 2002) where the resulting value must be rounded to an integer for use in Eq. (2.16).

2.22 Use the isotopic data of Table A.5 to calculate the atomic weight of (a) lithium, (b) boron, (c) oxygen, (d) chlorine, and (e) uranium.

2.23 Use Eq. (2.10) to verify that the total energy of an electron in the first orbit is $-13.6\,\text{eV}$.

2.24 Determine the photon emission energy and wavelength due to an electron transition in the H atom (a) from $n = 2$ to $n = 1$, and (b) from $n = 4$ to $n = 2$.

2.25 Calculate the neutron separation energy for (a) lithium-7, (b) nitrogen-14, (c) uranium-235, and (d) plutonium-240.

2.26 Compute the proton separation energy for (a) carbon-12, (b) nitrogen-14, (c) oxygen-17, and (d) barium-141.

2.10 COMPUTER EXERCISES

2.A Use the program ALBERT (see Chapter 1) to complete the following table comparing basic quantities of the electron, proton, and neutron at 1 MeV

Particle	Total Energy (MeV)	Velocity (m/s)	Mass to Rest Mass Ratio	Momentum (kg m/s)
Electron				
Proton				
Neutron				

2.B Using Eq. (2.16), the program BINDING calculates the approximate binding energy BE and atomic mass M for any nuclide. Run the program on these isotopes:

$$^{2}_{1}\text{H},\ ^{12}_{6}\text{C},\ ^{23}_{11}\text{Na},\ ^{60}_{27}\text{Co},\ ^{144}_{56}\text{Ba},\ ^{235}_{92}\text{U}$$

How do the results compare with the values listed in Table A.5? To assess the relative importance of the first four terms of the Bethe-Weizsäcker formula, BINDING constructs an area graph of the contribution to the binding energy per nucleon (BE/A) for the volume, surface, Coulomb, and asymmetry energy terms such that the net BE/A is clearly distinguishable as a function of A.

REFERENCES

Bearden, J.A., 1967. X-ray wavelengths. Rev. Mod. Phys. 39 (1), 78–124.
Bohr, N., 1913. On the constitution of atoms and molecules. Philos. Mag. Ser. 6 26 (151), 1–25.

Geiger, H., Marsden, E., 1909. On a diffuse reflection of the α-particles. Proc. R. Soc. Lond. Ser. A 82 (557), 495–500.

Krane, K.S., 1988. Introductory Nuclear Physics. Wiley, New York.

Maiman, T.H., 1960. Stimulated optical radiation in ruby. Nature 187 (4736), 493–494.

Paar, V., Pavin, N., Rubčić, A., Rubčić, J., 2002. Power laws and fractal behavior in nuclear stability, atomic weights and molecular weights. Chaos, Solitons Fractals 14 (6), 901–916.

Rutherford, E., 1911. LXXIX. The scattering of α and β particles by matter and the structure of the atom. Philos. Mag. Ser. 6 21 (125), 669–688.

Williams, W.S.C., 1991. Nuclear and Particle Physics. Oxford University Press.

CHAPTER

RADIOACTIVITY

3

CHAPTER OUTLINE

Many naturally occurring and artificially produced isotopes have the property of radioactivity, which is the spontaneous transformation (decay) of the nucleus with the emission of a particle. The decay process takes place in minerals of the ground, in fibers of plants, in tissues of animals, and in the air and water, all of which contain traces of radioactive elements.

3.1 NUCLEAR STABILITY

Although the repulsive Coulombic forces of the protons attempt to separate the nucleons, the strong nuclear forces strive to keep the nucleus intact. Stable nuclei are found to have a balance between the number of repulsive protons and the additional neutrons providing cohesion. Fig. 3.1 plots the atomic number versus the number of neutrons (Z versus N) for the known nuclides, revealing a band of nuclear stability. Initially, $N \cong Z$ in the belt of stability, but for increasing Z values a greater number of neutrons than protons is progressively required. Most stable nuclei possess an even number of protons and/or neutrons. Moreover, *magic numbers* of 2, 8, 20, 28, 50, 82, and 126 define the total nucleons necessary to complete either the proton or the neutron shell (Goeppert-Mayer, 1949).

Nuclear Energy. https://doi.org/10.1016/B978-0-12-812881-7.00003-4

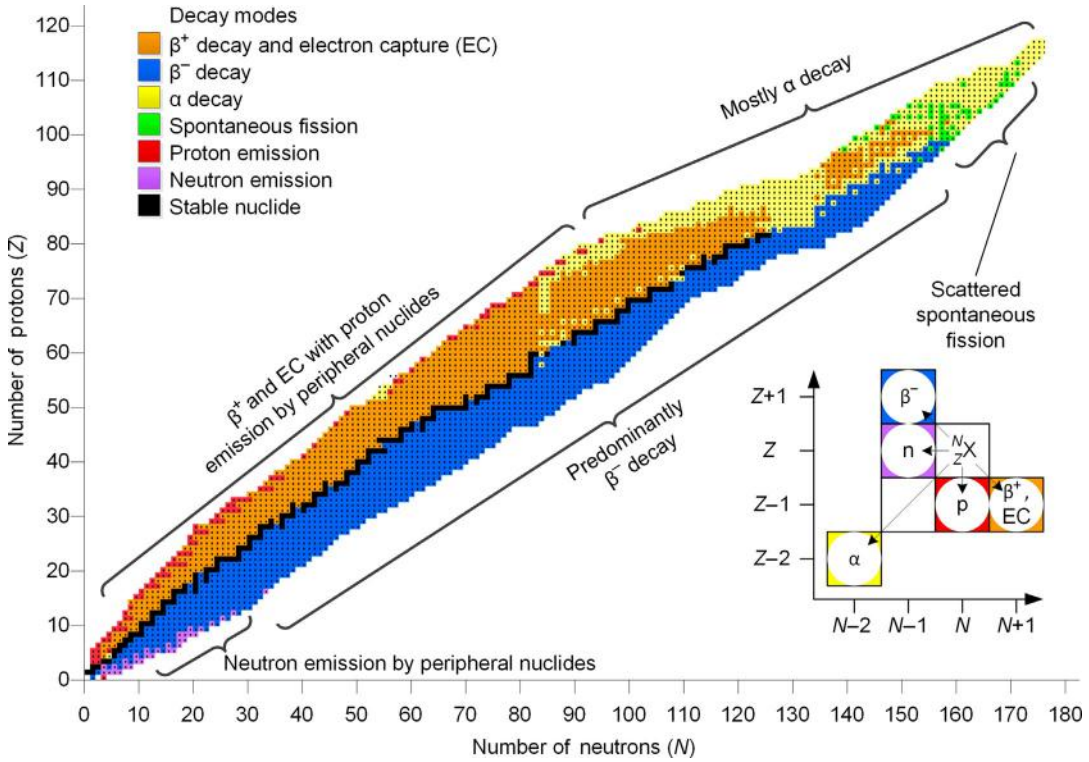

FIG. 3.1

Band of nuclear stability and decay modes. Created by Nucleus-Amdc (AMDC, 2012). Bottom right inset shows the direction that a radionuclide shifts for each decay mode.

EXAMPLE 3.1

Compare the N/Z ratio for a light and a heavy stable isotope. We arbitrarily select beryllium-9 ($^{9}_{4}$Be) and lead-208 ($^{208}_{82}$Pb). For the light Be-9, $N/Z = (9-4)/4 = 1.25$ while $N/Z = (208-82)/82 = 1.54$ for Pb-208, which is the heaviest stable nuclide.

Isotopes laying off the line of stability undergo radioactive decay in an effort to reduce their instability. Generally, those radioactive nuclides farthest from the belt of stability have the shortest decay times, commonly expressed as the half-life. Those nuclides positioned above the line are neutron-deficient while those below the line have a neutron excess. Radioactive decay seeks to rebalance the N/Z ratio through a variety of competing decay mechanisms, which are summarized in Table 3.1. Sometimes even after the decay emission, the nucleus remains in an excited state, which is relieved through gamma (γ) emission or internal conversion (IC).

The emanations from radioactive decay constitute the radiations. Fig. 3.1 reveals that alpha decay is more prevalent for the heavier nuclei, but another transformation mode exists for heavy radionuclides: spontaneous fission. The graph also discloses that neutron emission tends to occur in comparatively lighter nuclei only. Overall, beta and positron emission and electron capture (EC) are the dominant decay mechanisms.

Table 3.1 Radioactive Decay Processes

N/Z Ratio	Decay Modes	Decay Mechanisms
Neutron surplus	Beta	Neutron → proton + electron (β^-) emission
	Neutron	Neutron ejection from the nucleus
Neutron deficit	Alpha	Emission of a He-4 nucleus
	Positron	Proton → neutron + positron (β^+) emission
	Electron capture	Orbital electron + proton → neutron
	Proton	Proton ejection from the nucleus

3.2 RADIOACTIVE DECAY

Many heavy nuclides are unstable; in fact, all elements with $Z > 82$ (lead) are radioactive. An example is the decay of the most abundant isotope of uranium, in the reaction

$$^{238}_{92}\mathrm{U} \rightarrow {}^{234}_{90}\mathrm{Th} + {}^{4}_{2}\mathrm{He} \tag{3.1}$$

The particle released is the α (alpha) particle, which is merely the helium-4 nucleus. The newly formed isotope of thorium is also radioactive, according to

$$^{234}_{90}\mathrm{Th} \rightarrow {}^{234}_{91}\mathrm{Pa} + {}^{0}_{-1}\mathrm{e} + \bar{\nu} \tag{3.2}$$

The first product is the element protactinium (Pa). The second is an electron, which is called a β (beta) particle when it arises in a nuclear process. The nucleus does not contain electrons; they are produced in the reaction, as discussed next. The third is the antineutrino, symbolized by $\bar{\nu}$ (nu bar). It is a neutral particle that shares with the beta particle the reaction's energy release. On average, the (anti)neutrino carries two-thirds of the energy, the electron, one-third. The neutrino has zero or possibly a very small mass and readily penetrates enormous thicknesses of matter. We note that the A value decreases by 4 and the Z value by 2 on emission of an α particle, whereas the A remains unchanged but Z increases by 1 on emission of a β particle. In this case, these two events are the start of a long sequence or chain of disintegrations that produces isotopes of the elements radium, polonium, and bismuth, eventually yielding the stable lead isotope $^{206}_{82}\mathrm{Pb}$. Other chains found in nature start with $^{235}_{92}\mathrm{U}$ and $^{232}_{90}\mathrm{Th}$. Hundreds of artificial radioisotopes have been produced by bombardment of nuclei by charged particles or neutrons and by separation of the products of the fission process.

Table 3.2 gives several examples of radioactive materials with their emissions, product isotopes, and half-lives. The β particle energies are maximum values; on average, the emitted betas have only one-third as much energy, that is, $E_{\beta,\mathrm{avg}} \cong E_{\beta,\mathrm{max}}/3$. Included in the table are both natural and synthetic radioactive isotopes, also called *radioisotopes*. We note the special case of neutron decay according to

$$\underbrace{^{1}_{0}\mathrm{n}}_{\text{neutron}} \rightarrow \underbrace{^{1}_{1}\mathrm{p}}_{\text{proton}} + \underbrace{^{0}_{-1}\mathrm{e}}_{\text{electron}} \tag{3.3}$$

A free neutron has a half-life of 10.3 min. The conversion of a neutron into a proton can be regarded as the origin of beta emission in radioactive nuclei. Most of the radioisotopes in nature are heavy

Table 3.2 Selected Radioactive Isotopes

Isotope	Half-Life	Principal Radiations (Type, MeV, Frequency)
Neutron	614 s	β^-, 0.782 (100%)
Tritium (H-3)	12.32 y	β^-, 0.01859 (100%)
Carbon-14	5700 y	β^-, 0.156 (100%)
Nitrogen-13	9.965 m	β^+, 1.199 (99.8%); γ, 0.511 (199.6%) [annihilation]
Nitrogen-16	7.13 s	β^-, 4.289 (66.2%), 10.42 (28%); γ, 6.129 (67%), 7.115 (4.9%)
Flourine-18	109.77 m	β^+, 0.634 (96.7%); γ, 0.511 (193.5%) [annihilation]
Sodium-24	15.0 h	β^-, 1.393 (99.9%); γ, 1.369 (100%), 2.754 (99.9%)
Phosphorus-32	14.268 d	β^-, 1.711 (100%)
Sulfur-35	87.37 d	β^-, 0.167 (100%)
Chlorine-36	3.01×10^5 y	β^-, 0.710 (98.1%); EC (1.9%)
Argon-41	1.827 h	β^-, 1.198 (99.2%); γ, 1.294 (99.2%)
Potassium-40	1.248×10^9 y	β^-, 1.311 (89.1%); EC γ, 1.461 (10.7%)
Cobalt-60	5.271 y	β^-, 0.318 (99.9%); γ, 1.173 (99.85%), 1.332 (99.98%)
Copper-64	12.701 h	β^-, 0.579 (38.5%); β^+, 0.653 (17.6%)
Zinc-65	243.93 d	β^+, 0.330 (1.4%); γ, 0.511 (2.8%), 1.116 (50.0%)
Krypton-85	10.76 y	β^-, 0.687 (99.6%); γ, 0.514 (0.4%)
Strontium-90	28.79 y	β^-, 0.546 (100%)
Yttrium-90	64.0 h	β^-, 2.280 ($\sim$100%)
Molybdenum-99	65.98 h	β^-, 0.436 (16.4%), 1.214 (82.2%); γ, 0.740 (12.3%)
Technetium-99m	6.01 h	IT ($\sim$100%); γ, 0.141 (89%)
Iodine-129	1.57×10^7 y	β^-, 0.154 (100%); X, 0.0295 (20%), 0.0298 (37%)
Iodine-131	8.025 d	β^-, 0.248 (2.1%), 0.334 (7.2%), 0.606 (89.6%); γ, 0.284 (6.1%), 0.364 (81.5%), 0.637 (7.2%)
Xenon-135	9.14 h	β^-, 0.915 (96%); γ, 0.250 (90%)
Cesium-137	30.08 y	β^-, 0.514 (94.7%), 1.176 (5.3%); γ, 0.662 (85.1%)
Iridium-192	73.827 d	β^-, 0.259 (5.6%), 0.539 (41.4%), 0.675 (48.0%), γ, 0.296 (28.7%), 0.308 (30.0%), 0.317 (82.7%), 0.468 (47.8%); EC (4.9%)
Gold-198	2.694 d	β^-, 0.961 (99.0%); γ, 0.412 (95.6%)
Polonium-210	138.4 d	α, 5.304 (100%)
Radon-222	3.8235 d	α, 5.489 (99.9%); γ, 0.510 (0.08%)
Radium-226	1600 y	α, 4.601 (6.2%), 4.784 (93.8%); γ, 0.186 (3.6%)
Thorium-232	1.405×10^{10} y	α, 3.947 (21.7%), 4.012 (78.2%)
Uranium-234	2.455×10^5 y	α, 4.722 (28.4%), 4.775 (71.4%)
Uranium-235	7.038×10^8 y	α, 4.366 (17%), 4.398 (55%); X, 0.013 (37%); γ, 0.144 (11%), 0.186 (57%)
Uranium-238	4.468×10^9 y	α, 4.151 (21%), 4.198 (79%); X, 0.013 (7%)
Plutonium-238	87.7 y	α, 5.456 (29.0%), 5.499 (70.9%)

Table 3.2 Selected Radioactive Isotopes—cont'd

Isotope	Half-Life	Principal Radiations (Type, MeV, Frequency)
Plutonium-239	2.411×10^4 y	α, 5.106 (11.9%), 5.144 (17.1%), 5.157 (70.8%)
Americium-241	432.6 y	α, 5.443 (13.1%), 5.486 (84.8%); γ, 0.0595 (35.9%)
Californium-252	2.645 y	α, 6.076 (15.2%), 6.118 (81.6%); SF (3.1%)

Note: *for beta decay, the maximum energy is listed.* EC, *electron capture;* IT, *isomeric transition;* SF, *spontaneous fission. Data from NuDat 2.7 (National Nuclear Data Center (NNDC), 2017. NuDat: Nuclear Structure and Decay Data. Brookhaven National Laboratory.* www.nndc.bnl.gov/nudat2/.)

elements. One exception is potassium-40, half-life 1.25×10^9 y, with abundance 0.0117% in natural potassium. Others are carbon-14 and hydrogen-3 (tritium), which are produced continuously in small amounts by natural nuclear reactions. All three radioisotopes are found in plants and animals. Elaborating upon Table 3.2, Fig. 3.2 shows the decay characteristics of K-40.

In addition to the radioisotopes that decay by beta or alpha emission, there is a large group of artificial isotopes that decay by the emission of a positron (β+), which has the same mass as the electron and an equal but positive charge. An example is sodium-22, which decays with 2.6 y half-life into a neon isotope as

$$^{22}_{11}\mathrm{Na} \rightarrow {}^{22}_{10}\mathrm{Ne} + {}^{0}_{+1}\mathrm{e} + \nu \tag{3.4}$$

Whereas the electron (sometimes called negatron) is a normal part of any atom, the positron is not. It is an example of what is called an antiparticle because its properties are opposite to those of the normal particle. Just as particles form matter, antiparticles form antimatter.

The preceding Na-22 reaction can be regarded as involving the conversion of a proton into a neutron with the release of a positron and a neutrino (ν) by use of excess energy in the parent nucleus. This is an example of the conversion of energy into mass. Usually, the mass appears in the form of

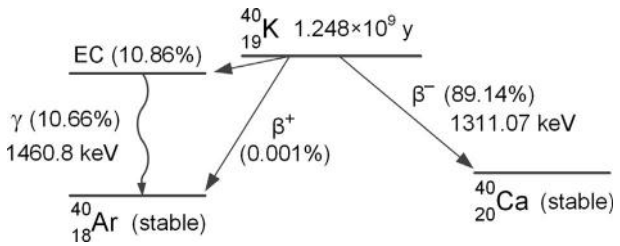

FIG. 3.2

Energy-level diagram for potassium-40.

pairs of particles of opposite charge. A positron-electron pair is one example. As discussed in Section 5.4.3, an electron and a positron will combine and both be annihilated to form two γ (gamma) rays.

A nucleus can shed excess internal energy by the emission of a gamma ray. When the emanation is delayed, leaving the nucleus in a metastable state (e.g., technetium-99m), the gamma decay process is known as isomeric transition. Alternatively, internal conversion imparts the excess energy directly to one of the atomic electrons, thereby ejecting it from the atom. In an inverse process, called electron capture, the nucleus spontaneously absorbs one of its own orbital electrons. Each of these two processes is followed by the production of characteristic X-rays as the inner shell vacancy is filled; the electronic transition energy can instead be transferred to an atomic electron, ejecting this so-called Auger electron.

3.3 THE DECAY LAW

The rate at which a radioactive substance transforms (and thus the rate of release of particles) depends on the isotopic species, but there is a definite decay law that governs the process. In a given time period, for example 1 s, each nucleus of a given isotopic species has the same chance of decay. If we were able to watch one nucleus, it might decay in the next instant, or a few days later, or even hundreds of years later. The *decay constant*, λ (lambda), is the "probability" that a particular nucleus will decay per unit time.

We should like to know how many nuclei of a radioactive species remain at any time. If λ is the chance one nucleus will decay in a second, then the chance in a time interval dt is λdt. For N nuclei, the change in number of nuclei is

$$dN = -\lambda N\, dt \tag{3.5}$$

Integrating and letting the number of nuclei at time zero be N_0 yields a general formula describing the number of radioisotopes at any time

$$N(t) = N_0 e^{-\lambda t} \tag{3.6}$$

Except for electron capture and internal conversion, the decay constant is unaffected by such factors as temperature, pressure, chemical form, and physical state (gas, liquid, or solid) (Emery, 1972).

Such statistical behavior is also described by a constant property of the atom called the *half-life*. This time interval, symbolized by t_H, is the period required for half the nuclei to decay, leaving half of them intact. If we start at time zero with N_0 nuclei, after a length of time t_H, there will be $N_0/2$; by the time $2t_H$ has elapsed, there will be $N_0/4$, and so on. A graph of the number of nuclei as a function of time is shown in Fig. 3.3. For any time t on the curve, the ratio of the number of nuclei present to the initial number is given by

$$N(t) = N_0 \left(\frac{1}{2}\right)^{t/t_H} \tag{3.7}$$

Half-lives range from very small fractions of a second to billions of years, with each radioactive isotope having a definite half-life.

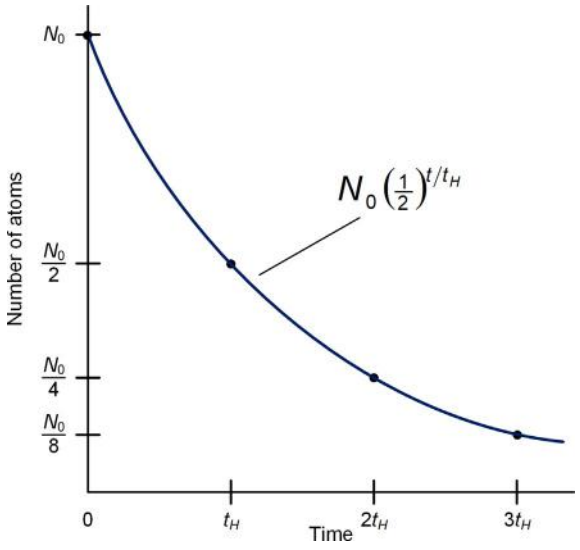

FIG. 3.3

Radioactive decay.

The relationship between the decay constant and half-life is readily obtained from

$$\frac{N(t_H)}{N_0} = \frac{1}{2} = \exp(-\lambda t_H) \tag{3.8}$$

We find that

$$\lambda = \ln(2)/t_H \tag{3.9}$$

EXAMPLE 3.2

To illustrate, let us calculate the ratio N/N_0 at the end of 2 y for cobalt-60, half-life 5.27 y. This artificially produced radioisotope has many medical and industrial applications. The decay reaction is

$$^{60}_{27}\mathrm{Co} \rightarrow {}^{60}_{28}\mathrm{Ni} + {}^{0}_{-1}\mathrm{e} + 2\gamma \tag{3.10}$$

in which the gamma ray energies are 1.17 and 1.33 MeV and the maximum beta energy is 0.315 MeV. The ratio may be computed using either Eq. (3.6) or (3.7); the latter is employed

$$\frac{N(t)}{N_0} = \left(\frac{1}{2}\right)^{t/t_H} = (0.5)^{(2\mathrm{y})/(5.27\mathrm{y})} = 0.769$$

The number of decays, or disintegrations, per second (dps) of a radioisotope is called the *activity*, A. Because the decay constant λ is the chance of decay each second of one nucleus, for N nuclei the activity is the product

$$A = \lambda N \tag{3.11}$$

The unit dps is called the becquerel (Bq), honoring the scientist Henri Becquerel, who discovered radioactivity. Another older and commonly used unit of activity is the curie (Ci), named after the French scientists Pierre and Marie Curie, who studied radium. The curie is 3.7×10^{10} Bq, which is an early measured value of the activity per gram of Ra-226.

Because the number of radioactive nuclei changes with time, the activity follows the same behavior

$$A(t) = \lambda N(t) = \lambda N_0 e^{-\lambda t} = A_0 e^{-\lambda t} \tag{3.12}$$

where A_0 is the initial activity.

EXAMPLE 3.3

Find the activity of a sample of cobalt-60 weighing 1 μg. First, the number of Co-60 atoms is found

$$N = \frac{mN_A}{M} = \frac{(10^{-6}\,\text{g})(6.022 \times 10^{23}\,\text{atom/mol})}{59.93\,\text{g/mol}} = 1.005 \times 10^{16}\,\text{atoms}$$

Next, the decay constant is calculated from the half-life

$$\lambda = \frac{\ln(2)}{t_H} = \frac{\ln(2)}{(5.27\,\text{y})}\left(\frac{1\,\text{y}}{365\,\text{d}}\right)\left(\frac{1\,\text{d}}{24\,\text{h}}\right)\left(\frac{1\,\text{h}}{3600\,\text{s}}\right) = 4.17 \times 10^{-9}/\text{s}$$

Finally, the cobalt sample activity is

$$\begin{aligned} A = \lambda N &= (4.17 \times 10^{-9}/\text{s})(1.005 \times 10^{16}\,\text{atoms}) = 4.19 \times 10^{7}\,\text{Bq} \\ &= (4.19 \times 10^{7}\,\text{Bq})(1\,\text{Ci}/3.7 \times 10^{10}\,\text{Bq}) = 0.0011\,\text{Ci} = 1.1\,\text{mCi} \end{aligned}$$

The half-life tells us how long it takes for half the nuclei to decay, whereas a related quantity, the mean life, τ (tau), is the average time elapsed for the decay of an individual nucleus. It turns out that (see Exercise 3.9)

$$\tau = \frac{1}{\lambda} = \frac{t_H}{\ln(2)} \tag{3.13}$$

Another measure that provides a comparison between the strength of various radioisotopes is the *specific activity*, which quantifies the activity per unit mass

$$SA = \lambda N_\text{A}/M \tag{3.14}$$

This expression demonstrates that the SA is constant.

EXAMPLE 3.4

Determine the mean life and specific activity for Co-60. These two quantities are quickly seen to be

$$\tau = t_H/\ln(2) = (5.27\,\text{y})/\ln(2) = 7.60\,\text{y}$$

$$SA = \frac{\lambda N_\text{A}}{M} = \frac{(4.17 \times 10^{-9}/\text{s})(6.022 \times 10^{23}\,\text{atom/mol})}{59.93\,\text{g/mol}} = 4.19 \times 10^{13}\,\text{Bq/g}$$

3.4 RADIOACTIVE CHAINS

Radionuclides arise in several processes. They may be produced by the bombardment of stable nuclei by charged particles, as in an accelerator, or by neutrons, as in a nuclear reactor. Or they may come from other radionuclides in which the parent nuclide decays and produces a daughter radioisotope. Still more generally, there may be a sequence of decays between a series of radionuclides, called a chain, leading eventually to a stable nucleus.

3.4.1 BUILDUP AND DECAY

Let us examine the method of calculating yields of some of these processes. The easiest case is a generation rate that is constant in time. For example, suppose that neutrons absorbed in cobalt-59 create cobalt-60 at a constant rate g. The net rate of change with time of the number of Co-60 atoms is

$$\text{Rate of change} = \text{Generation rate} - \text{Decay rate} \tag{3.15}$$

which may be written in the form of a differential equation,

$$dN/dt = g - \lambda N \tag{3.16}$$

If the initial number of radionuclides is zero, the solution is

$$N(t) = (g/\lambda)\left(1 - e^{-\lambda t}\right) \tag{3.17}$$

The function rises linearly at the start and then flattens out. At long times, the exponential term goes toward zero, leaving $N \cong g/\lambda$.

Fig. 3.4 shows what happens if the generation is stopped after six half-lives of the radionuclide. Prior to ceasing the production, the radionuclide is being created by the generation process and simultaneously depleted by the decay process. Once the generation mechanism is halted, only the decay process described by Eq. (3.6) remains.

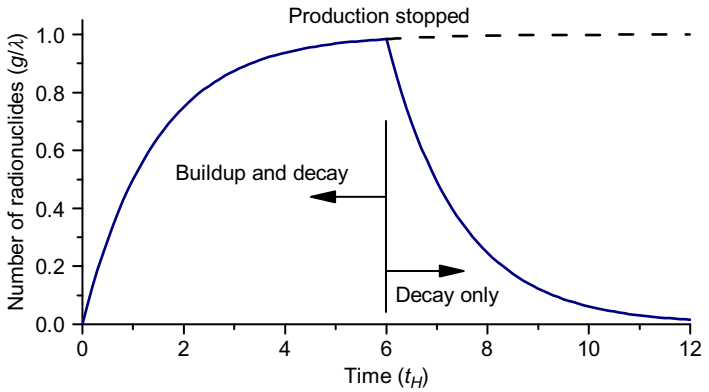

FIG. 3.4

Radionuclide buildup and decay.

3.4.2 COMPOUND DECAY

In compound decay, both the parent (P) and daughter (D) are radioactive. If the granddaughter (G) is stable, then the process may be depicted as

$$P \xrightarrow{\lambda_P} D \xrightarrow{\lambda_D} G(\text{stable}) \tag{3.18}$$

First, the dynamics of the decay of a parent radionuclide to form a daughter radionuclide are addressed. Let the initial number of atoms of a parent radioisotope be N_{P0}. At any time, the number of parent atoms as the result of decay is simply found from Eq. (3.6)

$$N_P(t) = N_{P0} \exp(-\lambda_P t) \tag{3.19}$$

As some radionuclides decay by multiple decay modes, let f be the fraction of parents that decay into a particular daughter. Then the generation rate for the daughter is

$$g(t) = f N_P(t) \lambda_P \tag{3.20}$$

Substituting this generation rate into Eq. (3.16) yields

$$dN_D/dt = f N_P(t) \lambda_P - \lambda_D N_D(t) \tag{3.21}$$

The solution of this differential equation for the daughter is

$$N_D(t) = \frac{f \lambda_P N_{P0}}{\lambda_D - \lambda_P} [\exp(-\lambda_P t) - \exp(-\lambda_D t)] \tag{3.22}$$

For $f = 1$, there are three distinct cases, depending on the relationship between the parent and daughter half-lives:

1. *Secular equilibrium* occurs when the parent is very long lived, compared to the daughter ($\lambda_P \ll \lambda_D$). In this case, the activity of the daughter rises up to equal the parent activity ($A_D \cong A_P$) within about seven half-lives of the daughter; see Fig. 3.5.

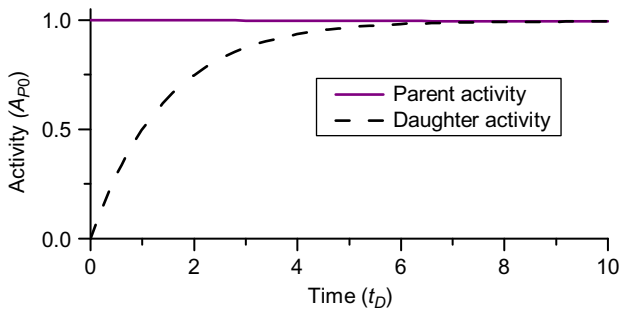

FIG. 3.5

Parent and daughter activities for compound decay with secular equilibrium.

2. *Transient equilibrium* exists when the parent is long-lived compared to the daughter ($\lambda_P < \lambda_D$). Consequently, after about seven half-lives of the daughter, the parent and daughter activities are related by

$$A_D = A_P \lambda_D / (\lambda_D - \lambda_P) \tag{3.23}$$

Exercise 3.13 reveals that the peak activity shown in Fig. 3.6 occurs at

$$t_{\max} = \frac{\ln(\lambda_D/\lambda_P)}{\lambda_D - \lambda_P} \tag{3.24}$$

3. In the general no equilibrium case ($\lambda_P > \lambda_D$), the total activity is eventually dominated by the daughter's activity; see Fig. 3.7.

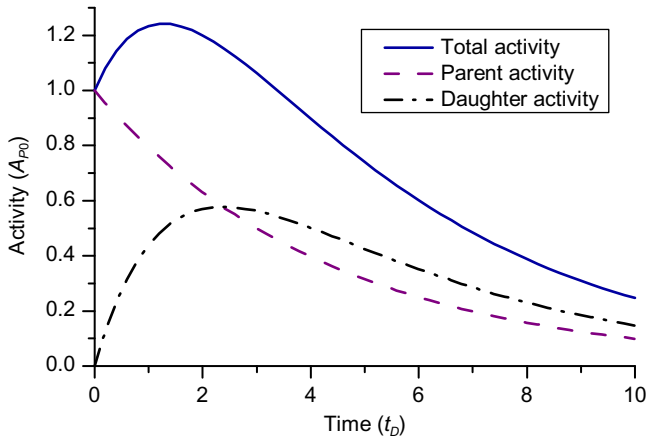

FIG. 3.6

Parent and daughter activities for compound decay with transient equilibrium.

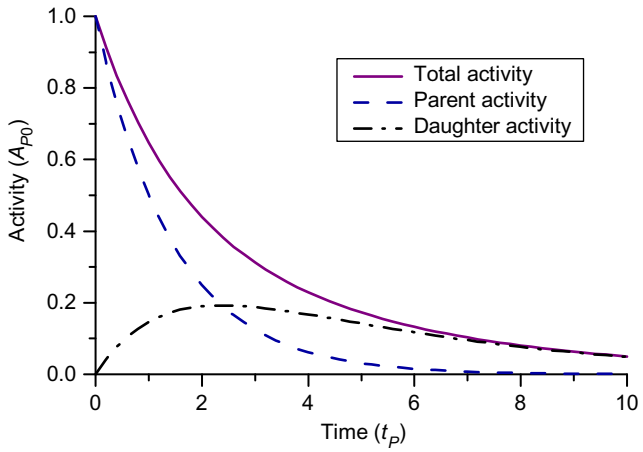

FIG. 3.7

Parent and daughter activities for general case of compound decay.

3.4.3 SERIAL DECAY CHAINS

Natural radioactive isotopes such as uranium-238 ($t_H = 4.47 \times 10^9$ y) and thorium-232 (1.4×10^{10} y) were produced billions of years ago but still persist because of their long half-lives. Their products form a long chain of radionuclides, with the emission of α and β particles. Those comprising the U-238 series are:

$$\begin{aligned} &{}^{238}_{92}\mathrm{U} \xrightarrow{\alpha} {}^{234}_{90}\mathrm{Th} \xrightarrow{\beta} {}^{234}_{91}\mathrm{Pa} \xrightarrow{\beta} {}^{234}_{92}\mathrm{U} \xrightarrow{\alpha} {}^{230}_{90}\mathrm{Th} \xrightarrow{\alpha} {}^{226}_{88}\mathrm{Ra} \\ &{}^{226}_{88}\mathrm{Ra} \xrightarrow{\alpha} {}^{222}_{86}\mathrm{Rn} \xrightarrow{\alpha} {}^{218}_{84}\mathrm{Po} \xrightarrow{\alpha} {}^{214}_{82}\mathrm{Pb} \xrightarrow{\beta} {}^{214}_{83}\mathrm{Bi} \xrightarrow{\beta} {}^{214}_{84}\mathrm{Po} \\ &{}^{214}_{84}\mathrm{Po} \xrightarrow{\alpha} {}^{210}_{82}\mathrm{Pb} \xrightarrow{\beta} {}^{210}_{83}\mathrm{Bi} \xrightarrow{\beta} {}^{210}_{84}\mathrm{Po} \xrightarrow{\alpha} {}^{206}_{82}\mathrm{Pb} \end{aligned} \tag{3.25}$$

Note that radium-226 (1600 y) is fairly far down the chain. The final product is stable lead-206. Because of the very long half-life of uranium-238, the generation rate of its daughters and their descendants is practically constant. Let us write $g \cong N_{238}\lambda_{238}$ and apply the expression for the number of atoms at long times to the Ra-226, $N_{226} \cong g/\lambda_{226}$. Rearranging, the activities are approximately equal,

$$A_{238} \cong A_{226} \tag{3.26}$$

and the condition is called *secular equilibrium*.

Table 3.3 summarizes the four long decay chains with the relatively shorter half-life of neptunium-237 implying its extinction from the natural environs of Earth. The U-235 and U-238 decay chains are illustrated in Fig. 3.8. The graphic conveys the differences in alpha and beta decay. In the list of Eq. (3.25) is the alpha particle emitter polonium-210, half-life 138 days. It was the poison that caused the death in 2006 of the former Russian KGB agent Litvinenko (Owen, 2016).

Bateman (1910) developed a general equation for serial decay chains such as

$$N_1 \xrightarrow{\lambda_1} N_2 \xrightarrow{\lambda_2} \ldots \xrightarrow{\lambda_{i-1}} N_i \xrightarrow{\lambda_i} \ldots \tag{3.27}$$

Assuming that there are no progeny atoms initially (i.e., $N_i(0) = 0$ for $i > 1$), the number of radionuclides of each member in the chain can be determined from

$$N_i(t) = \lambda_1\lambda_2\cdots\lambda_{i-1}N_1(0)\sum_{j=1}^{i}\frac{\exp\left(-\lambda_j t\right)}{\prod_{\substack{k=1\\k\neq j}}^{i}\left(\lambda_k - \lambda_j\right)} \tag{3.28}$$

Table 3.3 Natural Heavy Decay Chains

Series	Decay Chain	Parent	Parent Half-Life (y)	Stable End Product
$(4n+0)$	Thorium	${}^{232}_{90}\mathrm{Th}$	1.405×10^{10}	${}^{208}_{82}\mathrm{Pb}$
$(4n+1)$	Neptunium	${}^{237}_{93}\mathrm{Np}$	2.144×10^{6}	${}^{209}_{83}\mathrm{Bi}$
$(4n+2)$	Uranium	${}^{238}_{92}\mathrm{U}$	4.468×10^{9}	${}^{206}_{82}\mathrm{Pb}$
$(4n+3)$	Actinium	${}^{235}_{92}\mathrm{U}$	7.038×10^{8}	${}^{207}_{82}\mathrm{Pb}$

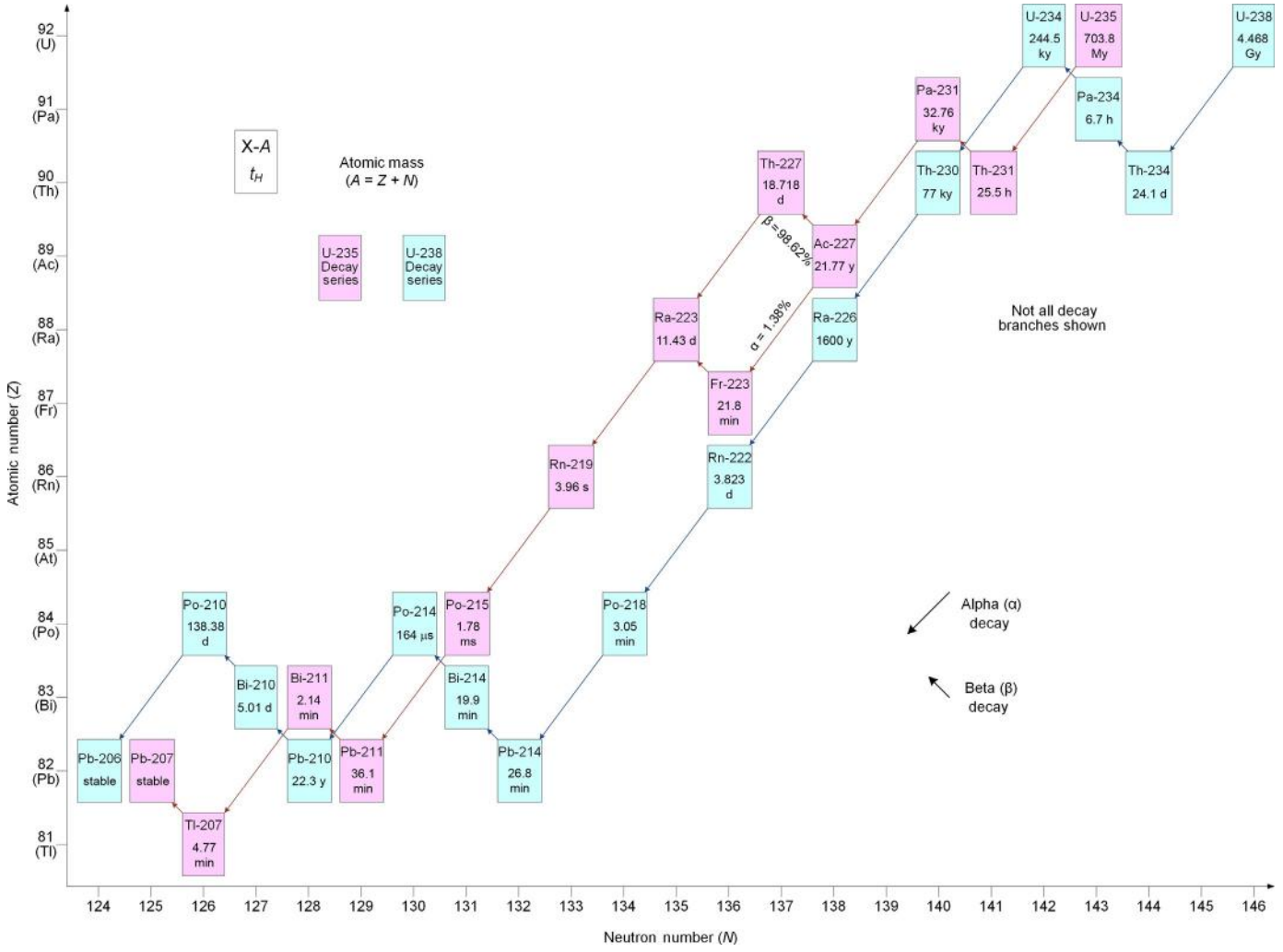

FIG. 3.8

Decay products and half-lives in the U-235 and U-238 serial decay chains.

EXAMPLE 3.5

Fig. 3.8 reveals that the half-lives of the first three progeny of U-238 are much smaller than that of U-238; hence, secular equilibrium exists between U-234 and U-238. This fact permits not only calculating the activity of U-234 but also the natural isotopic abundance ratio between ^{238}U and ^{234}U. Equating the activities of the two radioisotopes of interest

$$A_{\text{U-234}} = A_{\text{U-238}}$$

$$(\lambda N)_{\text{U-234}} = (\lambda N)_{\text{U-238}}$$

Rearranging this expression and substituting the half-lives from Fig. 3.8 gives

$$\frac{N_{\text{U-238}}}{N_{\text{U-234}}} = \frac{\lambda_{\text{U-234}}}{\lambda_{\text{U-238}}} = \frac{t_H^{238}}{t_H^{234}} = \frac{4.468 \times 10^9\,\text{y}}{244.5 \times 10^3\,\text{y}} = 18{,}270$$

The validity of this answer is confirmed by comparing the natural isotopic abundances γ given in Table A.5 in Appendix A, specifically

$$\frac{\gamma_{\text{U-238}}}{\gamma_{\text{U-234}}} = \frac{0.992742}{0.000054} = 18{,}000$$

3.4.4 COMPLEX DECAY

As multiple decay modes exist for some radionuclides, complex decay paths arise. The decay paths may result directly in distinct stable products, as seen in the case of K-40 (Fig. 3.2). In contrast, within the U-235 decay chain of Fig. 3.8, Ac-227 can either β decay to Th-227 or α decay to Fr-223, but both these daughters subsequently transform to the same radioisotope, Ra-223.

Suppose that parent P decays proportionally to B and C according to fractions f_B and f_C, respectively. Because λ_P represents the transformation probability for P, then the decay constant from P to B is $\lambda_1 = f_B\lambda_P$, and likewise to C is $\lambda_2 = f_C\lambda_P$. The parent decay constant is $\lambda_P = \lambda_1 + \lambda_2$.

EXAMPLE 3.6

The decay of Bi-212 within the thorium series involves a complex decay scheme whose daughters both decay to the same grandchild (stable Pb-208), as depicted in Fig. 3.9. Determine whether the mean time to decay from Bi-212 ($t_H = 60.55$ min) to Pb-208 differs based on the decay branch taken.

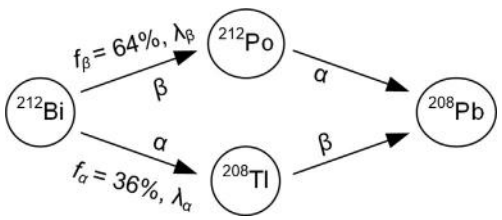

FIG. 3.9

Complex decay paths for Bi-212 to Pb-208 decay.

We begin by finding the decay constant of Bi-212

$$\lambda_{\text{Bi-212}} = \ln(2)/t_H = \ln(2)/(60.55\,\text{min}) = 0.01145/\text{min}$$

Next, determine the decay constants associated with the initial two (α and β) decay branches

$$\lambda_\beta = f_\beta \lambda_{\text{Bi-212}} = (0.6406)(0.01145/\text{min}) = 0.00733/\text{min}$$

$$\lambda_\alpha = f_\alpha \lambda_{\text{Bi-212}} = (0.3594)(0.01145/\text{min}) = 0.00412/\text{min}$$

The half-lives of Po-212 and Tl-208 are 0.30 μs and 3.05 min, respectively, such that the corresponding average lifetimes ($\tau = 1/\lambda$) of the radionuclides are

$$\text{Upper branch}: \quad \tau_{\text{Bi-212},\beta} = 1/\lambda_\beta = 1/(0.00733/\text{min}) = 136\,\text{min}$$
$$\tau_{\text{Po-212}} = t_H/\ln(2) = (0.30\mu s)/\ln(2) = 0.43\,\mu\text{s}$$

$$\text{Lower branch}: \quad \tau_{\text{Bi-212},\alpha} = 1/\lambda_\alpha = 1/(0.00412/\text{min}) = 243\,\text{min}$$
$$\tau_{\text{Tl-208}} = t_H/\ln(2) = (3.05\,\text{min})/\ln(2) = 4.40\,\text{min}$$

This implies that the average time in the upper (Bi-212 → Po-212 → Pb-208) branch is shorter than in the Bi-212 → Tl-208 → Pb-208 path. Note that both paths follow secular equilibrium behavior.

3.5 MEASUREMENT OF HALF-LIFE

Finding the half-life of an isotope provides part of its identification needed for beneficial use or for protection against radiation hazard. Let us look at a method for measuring the half-life of a radioactive substance. As in Fig. 3.10, a detector that counts the number of particles striking it is placed near the source of radiation. The counting rate C is computed from the number of counts observed in a known short time interval. It is proportional to the rates of emission of particles or rays from the sample and

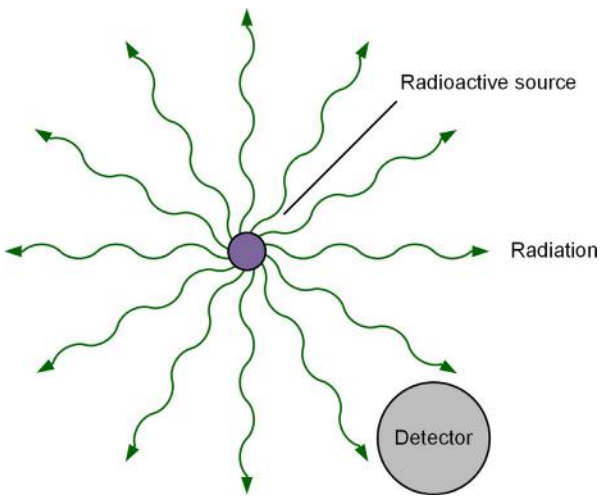

FIG. 3.10

Measurement of radiation from a radioactive source.

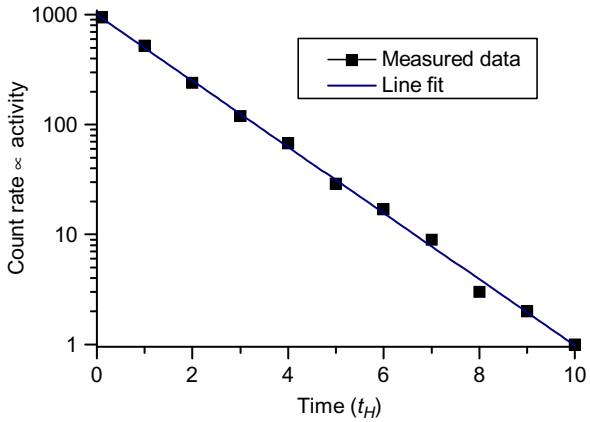

FIG. 3.11

Activity plot.

thus to the activity A of the source (i.e., $C \propto A$). The process is repeated after an elapsed time for decay. The resulting values of activity may be plotted on a semilogarithmic graph as in Fig. 3.11, and a straight line drawn through the observed points. A least-squares line fit permits determining λ, from which t_H can be calculated (see Exercise 3.10). The technique may be applied to mixtures of two radioisotopes. After a long time has elapsed, only the isotope of longer half-life will contribute counts. By extending its graph linearly back in time, one can find the counts to be subtracted from the total to yield the counts from the isotope of shorter half-life, a process known as exponential peeling.

Activity plots cannot be used for a substance with long half-life (e.g., strontium-90, $t_H = 28.79$ y). The change in activity is almost zero over the span of time one is willing to devote to a measurement. However, if one knows the number of atoms present in the sample and measures the activity, the decay constant can be calculated from $\lambda = A/N$, from which t_H can be found.

The measurement of the activity of a radioactive substance is complicated by the presence of background radiation, which is due to cosmic rays from outside the Earth or from the decay of minerals in materials of construction or in the ground. It is always necessary to measure the background counts and subtract them from those observed in the experiment (see Section 12.7).

3.6 SUMMARY

Many elements that are found in nature or are man-made are radioactive, emitting α particles, β particles, and γ-rays. The process is governed by an exponential relation such that half a sample decays in a time called the half-life, t_H. Values of t_H range from fractions of a second to billions of years among the hundreds of radioisotopes known. Measurement of the activity, as the transformation rate of a sample, yields half-life values of importance in radiation use and protection.

3.7 EXERCISES

3.1 Find the decay constant of cesium-137, half-life 30.1 y; then calculate the activity in becquerels and curies for a sample containing 3×10^{19} atoms.

3.2 Calculate the activity A for 1 g of radium-226 with the modern value of the half-life, and compare it with the definition of a curie.

3.3 The radioisotope sodium-24 ($^{24}_{11}$Na), half-life 15 h, is used to measure the flow rate of salt-water. By irradiation of stable $^{23}_{11}$Na with neutrons, suppose that we produce 5 μg of the radionuclide. How much Na-24 do we have at the end of 24 h?

3.4 For a 1-mg sample of Na-24, what is the initial activity and that after 24 h, in Bq and curies? (See Exercise 3.3.)

3.5 The isotope thorium-232 ($^{232}_{90}$Th) decays successively to form $^{228}_{88}$Ra, $^{228}_{89}$Ac, $^{228}_{90}$Th, and $^{224}_{88}$Ra, finally becoming radon-220 ($^{220}_{86}$Rn). What particles are emitted in each of these five steps? Draw a graph of this chain, using N and Z values on the horizontal and vertical axes, respectively.

3.6 A capsule of cesium-137, half-life 30.1 y, is used to check the accuracy of detectors of radioactivity in air and water. Create a semilogarithmic graph of the activity over a 10 y period, assuming the initial strength is 1 mCi. Explain the results.

3.7 There are approximately 140 g of potassium in a typical person's body (International Commission on Radiological Protection (ICRP), 1975). From this weight, the abundance of K-40, and Avogadro's number, find the number of atoms. Find the decay constant in per s. How many disintegrations per second are there in the body? How many becquerels and how many microcuries is this?

3.8 Using Eq. (3.9), derive Eq. (3.7) from Eq. (3.6).

3.9 Using integration, prove that the mean life is the reciprocal of the decay constant.

3.10 (a) Noting that the activity of a radioactive substance is $A = \lambda N_0 e^{-\lambda t}$, verify that the decay constant may be obtained from the counting rates C at two different time instants

$$\lambda = \frac{\ln(C_1/C_2)}{t_2 - t_1}$$

(b) Plot the following data on a semilogarithmic graph, and perform a linear regression fit using a $y = mx + b$ model where $y = \ln(C)$, $m = -\lambda$, $x = t$ and $b = \ln(C_0)$. Estimate the half-life of an unknown, and suggest what isotope it is (see Table 3.2 for a list of possible radioisotopes).

Time (s)	Counting Rate (counts/s)
0	200
1000	182
2000	162
3000	144
4000	131

3.11 By chemical means, we deposit 10^{-8} moles of a radioisotope on a surface and measure the activity to be 82,000 Bq. What is the half-life of the substance and what radionuclide is it (see Table 3.2)?

3.12 Determine the specific activity of (a) H-3, (b) P-32, (c) Pu-238, and (d) Cs-137.

3.13 Use Eq. (3.22) to form an expression for the activity of the daughter, and then differentiate to prove Eq. (3.24).

3.14 With the assistance of Fig. 3.8, categorize each of the first eight major decay steps in the (a) U-235 and (b) U-238 serial chain as secular, transient, or no equilibrium.

3.15 Assuming that the entire inventory of parent radionuclides and no daughter atoms were initially present, determine the time of peak activity for the (a) $^{234}\text{U} \rightarrow {}^{230}\text{Th}$ and (b) $^{227}\text{Th} \rightarrow {}^{223}\text{Ra}$ decays.

3.8 COMPUTER EXERCISES

3.A Program DECAY1.xls is convenient for calculating the amount of decay of a radioactive sample in a given time. DECAY1 has input of the original activity and the half-life; it calculates the final activity. Load the program, examine its form, and look at the results for the decay in 100 y of 2 Ci of Cs-137, half-life 30.1 y. (a) Find the activity after 10 half-lives. (b) Find the activity of 2 Ci of Co-60, half-life 5.27 y, after 100 y. (c) What is the activity of 2 Ci of C-14 after 100 y?

3.B Nucleus-Amdc (Atomic Mass Data Center (AMDC), 2012) was used to produce Fig. 3.1. Create similar color graphs for (a) binding energy per nucleon and (b) half-life using the same online or downloadable software. What is the trend of each of these two graphs?

3.C Computer program RADIOGEN uses Eqs. (3.19) and (3.22) to calculate the number of parent and daughter atoms as a function of time and their activities in compound decay. Test the program for the decay by beta emission of 10 Ci of reactor-produced plutonium-241, (14.4 y) into americium-241 (432 y), with $f = 1$.

REFERENCES

Atomic Mass Data Center (AMDC), 2012. Nucleus. Orsay, France, http://amdc.in2p3.fr/.

Bateman, H., 1910. The solution of a system of differentials occurring in the theory of radio-active transformations. Proc. Camb. Philos. Soc. 15, 423–427.

Emery, G.T., 1972. Perturbation of nuclear decay rates. Annu. Rev. Nucl. Part. Sci. 22, 165–202.

Goeppert-Mayer, M., 1949. On closed shells in nuclei. II. Phys. Rev. 75 (12), 1969–1970.

International Commission on Radiological Protection (ICRP), 1975. Report of the Task Group on Reference Man. Report No. 23. Pergamon Press, Oxford, p. 287.

National Nuclear Data Center (NNDC), 2017. NuDat: Nuclear Structure and Decay Data. Brookhaven National Laboratory, www.nndc.bnl.gov/nudat2/.

Owen, R., 2016. The Litvinenko Inquiry. Williams Lea Group, London.

FURTHER READING

Eisenbud, M., Gesell, T.F., 1997. Environmental Radioactivity: From Natural, Industrial, and Military Sources, fourth ed. Academic Press, San Diego, CA.

Evans, R.D., 1982. The Atomic Nucleus. Krieger, New York. Reprint of the McGraw-Hill 1955 Classic Advanced Textbook.

L'Annunziata, M.F., 2007. Radioactivity: Introduction and History. Elsevier, Amsterdam.

L'Annunziata, M.F. (Ed.), 2012. Handbook of Radioactivity Analysis, third ed. Academic Press, San Diego, CA.

CHAPTER

NUCLEAR PROCESSES

4

CHAPTER OUTLINE

Nuclear reactions—those in which atomic nuclei participate—may take place spontaneously, as in radioactivity, or may be induced by bombardment with a particle or ray. Nuclear reactions are much more energetic than chemical reactions, but they obey the same physical laws: conservation of momentum, energy, number of particles, and charge.

The number of possible nuclear reactions is extremely large because there are approximately 2000 known isotopes and many particles that can be either projectiles or products: photons, electrons, protons, neutrons, alpha particles, deuterons, and heavy charged particles. In this chapter, we will emphasize induced reactions, especially those involving neutrons.

4.1 TRANSMUTATION OF ELEMENTS

Nuclear reactions may be written using a general equation form

$$ {}^{A_1}_{Z_1}a + {}^{A_2}_{Z_2}X \rightarrow {}^{A_3}_{Z_3}Y + {}^{A_4}_{Z_4}b \tag{4.1} $$

Nuclear Energy. https://doi.org/10.1016/B978-0-12-812881-7.00004-6

All reactions obey four fundamental governing laws:

1. Conservation of nucleons: $A_1+A_2=A_3+A_4$
2. Conservation of charge: $Z_1+Z_2=Z_3+Z_4$
3. Conservation of momentum
4. Conservation of total energy

Sections 4.2 and 4.3 provide the relations for the latter two quantities.

Rutherford (1919) in England first achieved the conversion of one element into another, a process called *transmutation*. He bombarded nitrogen atoms with alpha particles from a radioactive source to produce an oxygen isotope and a proton, according to the equation

$$^{4}_{2}\mathrm{He}+{}^{14}_{7}\mathrm{N}\rightarrow {}^{17}_{8}\mathrm{O}+{}^{1}_{1}\mathrm{H} \tag{4.2}$$

We note that on both sides of the equation, the A values sum to 18 and the Z values total 9. Fig. 4.1 shows Rutherford's experiment. It is difficult for the positively charged α particle to enter the nitrogen nucleus because of the force of electrical repulsion between charged particles. Thus, the α particle must have several MeV of energy.

Nuclear transmutations can also be achieved by charged particles that are electrically accelerated to high speeds. The first such example discovered (Cockcroft and Walton, 1932) was the reaction

$$^{1}_{1}\mathrm{H}+{}^{7}_{3}\mathrm{Li}\rightarrow 2\,{}^{4}_{2}\mathrm{He} \tag{4.3}$$

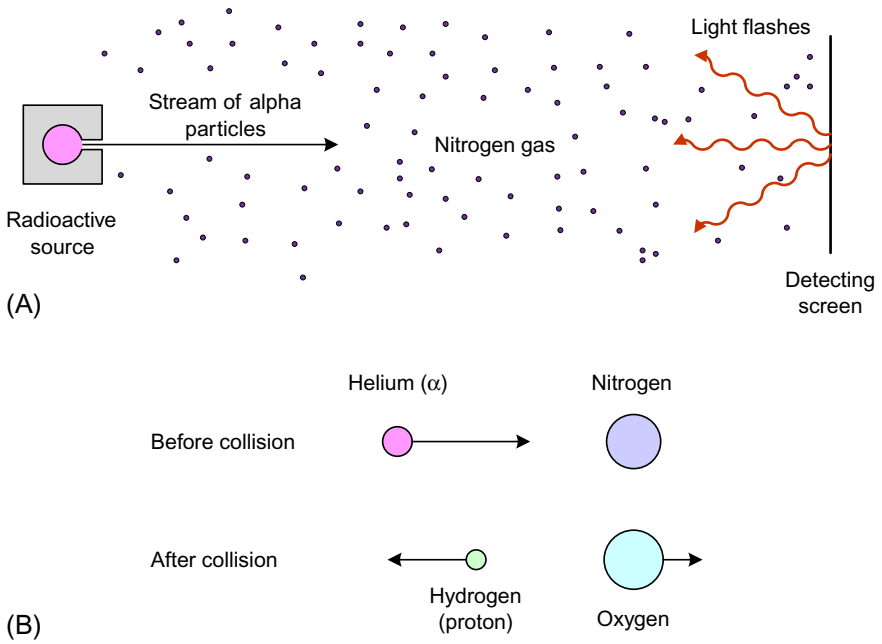

FIG. 4.1

Transmutation by nuclear reaction. (A) Rutherford's experiment and (B) nuclear reaction.

Another reaction,

$$^{1}_{1}\mathrm{H} + ^{12}_{6}\mathrm{C} \rightarrow ^{13}_{7}\mathrm{N} + \gamma \tag{4.4}$$

yields a gamma ray and an isotope of nitrogen. The latter decays with a half-life of 10 min, releasing a positron, the positive counterpart of the electron.

Because the neutron is a neutral particle, it does not experience electrostatic repulsion and can readily penetrate a target nucleus. Neutrons are thus especially useful as projectiles to induce reactions. Several examples are chosen here based on interest or usefulness. The conversion of mercury into gold, the alchemist's dream, is described by

$$^{1}_{0}\mathrm{n} + ^{198}_{80}\mathrm{Hg} \rightarrow ^{198}_{79}\mathrm{Au} + ^{1}_{1}\mathrm{H} \tag{4.5}$$

The production of cobalt-60 is governed by

$$^{1}_{0}\mathrm{n} + ^{59}_{27}\mathrm{Co} \rightarrow ^{60}_{27}\mathrm{Co} + \gamma \tag{4.6}$$

in which a capture gamma ray is produced, and Co-60 is termed a neutron *activation product*. Neutron capture in cadmium, sometimes used in nuclear reactor control rods, is given by

$$^{1}_{0}\mathrm{n} + ^{113}_{48}\mathrm{Cd} \rightarrow ^{114}_{48}\mathrm{Cd} + \gamma \tag{4.7}$$

A reaction that produces tritium, which may be a fuel for controlled fusion reactors of the future, is

$$^{1}_{0}\mathrm{n} + ^{6}_{3}\mathrm{Li} \rightarrow ^{3}_{1}\mathrm{H} + ^{4}_{2}\mathrm{He} \tag{4.8}$$

Later, in Section 6.1, we will discuss the absorption of neutrons in uranium isotopes to cause fission.

A shorthand notation is used to represent nuclear reactions. Let an incoming particle a strike a target nucleus X to produce a residual nucleus Y and an outgoing particle b, with equation

$$a + X \rightarrow Y + b \tag{4.9}$$

This binary reaction may be abbreviated $X(a, b)Y$, where a and b stand for the neutron (n), alpha particle (α), gamma ray (γ), proton (p), deuteron (d), and so on. For example, Rutherford's experiment can be written $^{14}\mathrm{N}(\alpha, \mathrm{p})^{17}\mathrm{O}$ and the reaction in control rods $^{113}\mathrm{Cd}(\mathrm{n}, \gamma)^{114}\mathrm{Cd}$. The Z value can be omitted because it is unique to the chemical element.

The interpretation of nuclear reactions often involves the concept of *compound nucleus*, C^*. This intermediate stage is formed by the combination of a projectile and target nucleus. The compound nucleus contains extra internal energy of motion of the nucleons, called *excitation energy*, as denoted by the asterisk. After a very short time, $\sim 10^{-14}$ s (Foster and Wright Jr., 1983), C^* breaks up into the outgoing particle or ray and the residual nucleus. The full nuclear reaction equation is therefore

$$a + X \rightarrow C^* \rightarrow Y + b \tag{4.10}$$

as depicted in Fig. 4.2. For reactions at low energy, <10 MeV, the same compound nucleus could be formed by several different pairs of interacting nuclei, and could decay into several different pairs of final products.

The reaction equations can be used to calculate balances in properties such as mass-energy, visualizing conditions before and after. In place of the symbols, the atomic masses are inserted. Strictly, the masses of the nuclei should be used, but in most reactions, the same number of electrons appears on

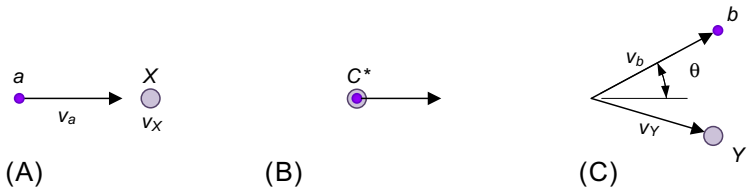

FIG. 4.2

General nuclear reaction. (A) Before collision, (B) compound nucleus, and (C) after collision.

both sides of the equation and cancels out. In the case of reactions that produce a positron, however, either nuclear masses or atomic masses with the subtraction of the mass-energy required to create an electron-positron pair should be used, 0.0011 amu or 1.02 MeV. The radioactive decay of fluorine-18 provides an example reaction of this type

$$^{18}_{9}\mathrm{F} \rightarrow {}^{18}_{8}\mathrm{O} + {}^{0}_{+1}\mathrm{e}^{+1} + \nu \tag{4.11}$$

In particular, a closer examination of positron decay reveals that the daughter carries an excess electron.

4.2 ENERGY CONSERVATION

The conservation of total energy is a firm requirement for any nuclear reaction, such that the sum of the reactant energies must equal the sum of the reaction product energies

$$\sum_{\text{reactants}} E_T = \sum_{\text{products}} E_T \tag{4.12}$$

For an $X(a, b)Y$ reaction, the conservation of energy is simply

$$E_T^X + E_T^a = E_T^b + E_T^Y \tag{4.13}$$

Recalling from Section 1.5 that the total energy is the sum of the rest mass energy E_0 and the kinetic energy E_K means that Eq. (4.13) can be rewritten as

$$E_0^X + E_K^X + E_0^a + E_K^a = E_0^b + E_K^b + E_0^Y + E_K^Y \tag{4.14}$$

or in terms of conservation of mass-energy

$$M_X c^2 + E_K^X + m_a c^2 + E_K^a = m_b c^2 + E_K^b + M_Y c^2 + E_K^Y \tag{4.15}$$

Oftentimes, the target nucleus X is stationary such that its kinetic energy is zero.

The reaction energy conservation also provides us the ability to calculate the energy either emitted by a nuclear reaction or required to cause the reaction. We shall refer to this energy as the reaction Q value. Rearranging Eq. (4.15) provides the definition of the Q value

$$Q = [(M_X + m_a) - (m_b + M_Y)]c^2 = \left(E_K^b + E_K^Y\right) - \left(E_K^X + E_K^a\right) \tag{4.16}$$

From the grouping of terms, we realize that Eq. (4.16) can be written in general as

$$Q = \sum_{\text{reactants}} Mc^2 - \sum_{\text{products}} Mc^2 = \sum_{\text{products}} E_K - \sum_{\text{reactants}} E_K \tag{4.17}$$

The utility of these two formulas is immediately evident as the reactant masses are known and thereby permit direct calculation of Q. Thereafter, the combined kinetic energies of the products are then obtainable.

A reaction that produces energy is *exothermic*, whereas a reaction requiring input energy to occur is said to be *endothermic*. The Q value allows us to determine the reaction type

$$Q\begin{cases} <0 & \text{Reaction is endothermic (or endoergic)} \\ >0 & \text{Reaction is exothermic (or exoergic)} \end{cases} \tag{4.18}$$

We seek exoergic reactions such as fission and fusion to provide power sources. Because radioactive decay is a spontaneous process that occurs without energy input, we surmise that all decay reactions are exothermic.

For endothermic reactions to occur, the needed energy must be brought to the reaction by the reactant kinetic energy. In fact, the incoming particle must meet or exceed the kinematic threshold energy of (Shultis and Faw, 2008)

$$E_{\text{th}} \cong -Q\,(1 + m_a/M_X) \tag{4.19}$$

Hence, the particle must bring more energy than $|Q|$. If the incident particle energy were simply equal to Q, then the reaction could occur, but conservation of momentum would be violated because the product kinetic energies (and velocities) would be zero. If the energy of the incident particle is too low, the projectile will merely be scattered by the target.

In addition, if the incoming particle is positively charged, then the nucleus repels the projectile. Therefore, the Coulombic threshold (see Exercise 4.22) must also be surpassed (Mayo, 1998)

$$E_C = \frac{(1.2\text{MeV})Z_a Z_X}{A_a^{1/3} + A_X^{1/3}} \tag{4.20}$$

Overall, for a reaction to occur $E_a > E_{\text{th}}$ and $E_a > E_C$. Table 4.1 delineates the governing threshold given the incident particle charge and the reaction type.

Table 4.1 Nuclear Reaction Threshold Energy

	Overall Reaction Threshold Energy	
Incident Particle Type	**$Q<0$ (Endoergic)**	**$Q>0$ (Exoergic)**
Neutral (n, γ)	Kinematic	None (n/a)
Charged (p, α)	Max(Kinematic, Coulombic)	Coulombic

EXAMPLE 4.1

Let us calculate the energy released when a slow neutron is captured in hydrogen, according to

$$ {}_0^1\mathrm{n} + {}_1^1\mathrm{H} \rightarrow {}_1^2\mathrm{H} + \gamma \tag{4.21} $$

This (n,γ) process occurs in reactors that use ordinary (light) water.

We use accurately known masses, as given in Table A.5, substituted into Eq. (4.16) along with a conversion factor 1 amu = 931.49 MeV, to find the Q value. Because the gamma ray has no rest mass,

$$ \begin{aligned} Q &= [(m_\mathrm{n} + M_{\mathrm{H}-1}) - M_{\mathrm{H}-2}]c^2 \\ &= (1.008665 + 1.007825 - 2.014102)\,\mathrm{amu}\,(931.49\,\mathrm{MeV/amu}) = 2.22\,\mathrm{MeV} \end{aligned} $$

Because both reactants have zero or near zero velocity, this exothermic energy is shared by the deuterium atom and the gamma ray in the form of kinetic energy.

EXAMPLE 4.2

A similar calculation can be made for the ^{7}Li(p,2α) reaction of Eq. (4.3). Suppose that the target nucleus is at rest and that the incoming proton has a kinetic energy of 2 MeV. This reaction is found to be exothermic via

$$ \begin{aligned} Q &= [(M_{\mathrm{H}-1} + M_{\mathrm{Li}-7}) - 2M_{\mathrm{He}-4}]c^2 \\ &= [1.007825 + 7.016003 - 2(4.002603)]\,\mathrm{u}\,(931.49\,\mathrm{MeV/u}) = 17.3\,\mathrm{MeV} \end{aligned} $$

Note that He-4 atomic mass ($M_{\mathrm{He}\text{-}4}$) is utilized, rather than alpha particle mass (m_α); otherwise the four electrons of the reactants would be lost. For the reaction to occur, the proton energy must exceed the Coulombic threshold of

$$ E_C = \frac{(1.2\,\mathrm{MeV})Z_{\mathrm{H}-1}Z_{\mathrm{Li}-7}}{A_{\mathrm{H}-1}^{1/3} + A_{\mathrm{Li}-7}^{1/3}} = \frac{(1.2\,\mathrm{MeV})(1)(3)}{(1)^{1/3} + (7)^{1/3}} = 1.2\,\mathrm{MeV} $$

And it does with 2 MeV. Using Eq. (4.17), the kinetic energy of the products is

$$ E_K^{\mathrm{prod}} = Q + E_K^{\mathrm{react}} = 17.3\,\mathrm{MeV} + 2\,\mathrm{MeV} = 19.3\,\mathrm{MeV} $$

The two α particles share this kinetic energy.

4.3 MOMENTUM CONSERVATION

The calculations just completed tell us the total kinetic energy of the product particles but do not reveal how much each has or what the speeds are. To find this information, we must apply the principle of conservation of momentum. Recall that the linear momentum p of a material particle of mass m and speed v is

$$ p = mv \tag{4.22} $$

This relation is correct in both the classical and relativistic senses. The total vector momentum of the interacting particles before and after the collision is

$$ \vec{\mathbf{p}}_a + \vec{\mathbf{p}}_X = \vec{\mathbf{p}}_Y + \vec{\mathbf{p}}_b \tag{4.23} $$

For Example 4.1 in which a very slow neutron strikes a hydrogen atom at rest, we can assume the initial momentum is zero. If momentum is to be zero finally, the ${}^{2}_{1}\mathrm{H}$ and γ-ray must fly apart with equal magnitudes of momentum $p_{\mathrm{D}} = p_{\gamma}$. The momentum of a γ-ray having the speed of light c may be written $p_{\gamma} = m_{\gamma}c$ if we regard the mass as an effective value, related to the photon energy E_{γ} by Einstein's formula $E = mc^2$. Thus

$$p_{\gamma} = m_{\gamma}c = \frac{E_{\gamma}}{c} \tag{4.24}$$

Most of the 2.22-MeV energy release of the neutron capture reaction goes to the γ-ray, as shown in Exercise 4.5. Assuming that to be correct, we can estimate the effective mass of this γ-ray. It is close to

$$m_{\gamma} = E_{\gamma}/c^2 = (2.22\,\mathrm{MeV})/(931.5\,\mathrm{MeV/u}) = 0.00238\,\mathrm{amu}$$

which is very small compared with 2.014 amu for the deuterium. Then from the momentum balance, we see that the speed of recoil of the deuterium is much smaller than the speed of light.

The calculation of the energies of the two α particles of Example 4.2 is a little complicated, even for the case in which they separate along the same line that the proton entered. The particle speeds of interest are low enough that relativistic mass variation with speed is small, and thus the classical formula for kinetic energy can be used, $E_K = \frac{1}{2}m_0v^2$. If we let m be the α particle mass and v_1 and v_2 be their speeds, with p_{H} the proton momentum, we must solve the two simultaneous equations (Exercise 4.6)

$$\begin{aligned} mv_1 - mv_2 &= p_{\mathrm{H}} \\ \frac{1}{2}mv_1^2 + \frac{1}{2}mv_2^2 &= E_K^{\mathrm{prod}} \end{aligned} \tag{4.25}$$

EXAMPLE 4.3

Derive a general expression for the kinetic energies of the recoiling daughter and emitted alpha particle upon radioactive decay. First, the Q value of the parent P decay to daughter D is

$$Q = [M_P - (M_D + M_{\mathrm{He-4}})]c^2 \tag{4.26}$$

in which the use of the He-4 atom mass ensures that two electron masses are not lost. With the parent initially stationary, the daughter and alpha particle momenta are equal but opposite in direction

$$M_D v_D = p = M_{\mathrm{He-4}} v_{\mathrm{He-4}} \tag{4.27}$$

And the Q value equals the kinetic energies of the products

$$Q = E_K^D + E_K^{\mathrm{He-4}} = \frac{1}{2}M_D v_D^2 + \frac{1}{2}M_{\mathrm{He-4}} v_{\mathrm{He-4}}^2 \tag{4.28}$$

Algebraically combining the preceding two expressions reveals that

$$\begin{aligned} E_K^D &= QM_{\mathrm{He-4}}/(M_D + M_{\mathrm{He-4}}) \\ E_K^{\mathrm{He-4}} &= QM_D/(M_D + M_{\mathrm{He-4}}) \end{aligned} \tag{4.29}$$

Fig. 3.1 indicates that most alpha emitters are heavy nuclei such that the α particle receives the majority of the decay energy.

4.4 REACTION RATES

When any two particles approach each other, their mutual influence depends on the nature of the force between them. Two electrically charged particles obey Coulomb's (1785) relation with the mutual force of attraction or repulsion being

$$F_C = \frac{q_1 q_2}{4\pi\varepsilon_0 r^2} \tag{4.30}$$

where the q's are the amounts of charge; ε_0 is the permittivity of free space; and r is the distance of separation of centers. There will be some influence no matter how far they are apart. However, two atoms, each of which is neutral electrically, will not interact until they get close to one another ($\cong 10^{-10}$ m). The special force between nuclei is limited still further ($\cong 10^{-15}$ m).

Although we cannot see nuclei, we imagine them to be spheres with a certain radius. To estimate that radius, we need to probe with another particle—a proton, an electron, or a photon. But the answer will depend on the projectile used and its speed, and thus it is necessary to specify the apparent radius and cross-sectional area for the particular reaction. This leads to the concept of cross-section as a measure of the chance of collision.

We can perform a set of imaginary experiments that will clarify the idea of cross-section. Picture, as in Fig. 4.3A, a tube of end area 1 cm^2 containing only one target particle. A single projectile is injected parallel to the tube axis, but its exact location is not specified. It is clear that the chance of collision,

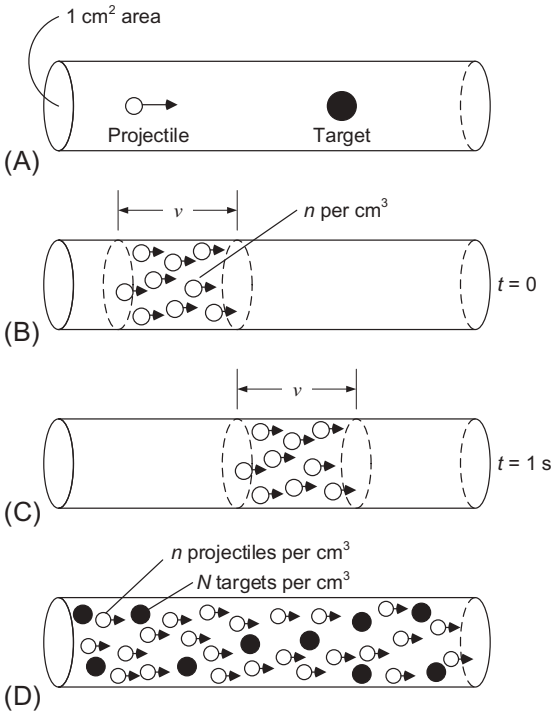

FIG. 4.3

Particle collisions.

denoted by σ (sigma) and called the *microscopic cross-section*, is the ratio of the target area to the area of the tube, which is $1\,\text{cm}^2$.

Now let us inject a continuous stream of particles of speed v into the empty tube (see Fig. 4.3B). In a time of 1 s, each of the particles has moved along a distance v cm (see Fig. 4.3C). All of them in a column of volume $(1\,\text{cm}^2)\ (v\ \text{cm}) = v\ \text{cm}^3$ will sweep past a point at which we watch each second. If there are n particles per cubic centimeter, then the number per unit time that crosses any unit area perpendicular to the stream direction is nv, called the *current density* j ($j = nv$).

Finally, in Fig. 4.3D, we fill each unit volume of the tube with N targets, each of area σ as seen by incoming projectiles (we presume that the targets do not "shadow" each other). If we focus attention on a unit volume, there is a total target area of $N\sigma$. This product is labeled Σ (capital sigma), the *macroscopic cross-section*, referring to the large-scale properties of the medium

$$\Sigma = N\sigma \tag{4.31}$$

Again, we inject the stream of projectiles. In a time of 1 s, the number of them that pass through the target volume is nv and because the chance of collision of each with one target atom is σ, the number of collisions is $nv\ N\sigma$. We can thus define the reaction rate per unit volume,

$$R = nvN\sigma \tag{4.32}$$

Then the reaction rate per cubic centimeter is simply $R = j\Sigma$. We can easily check that the units of j are per cm^2/s and those of Σ are per cm, so that the unit of R is per cm^3/s.

In a different experiment, we release particles in a medium and allow them to make many collisions with those in the material. In a short time, the directions of motion are random, as shown in Fig. 4.4. We will look only at particles of the same speed v, of which there are n per unit volume. The product nv in this situation is no longer called current density but is given a different name, the *flux*, symbolized by ϕ (phi). If we place a unit area anywhere in the region, there will be flows of particles across it each second from both directions, but it is clear that the current densities will now be less than nv. It turns out that they are each $nv/4$, and the total current density is $nv/2$ (Murray, 1957). The rate of reaction of

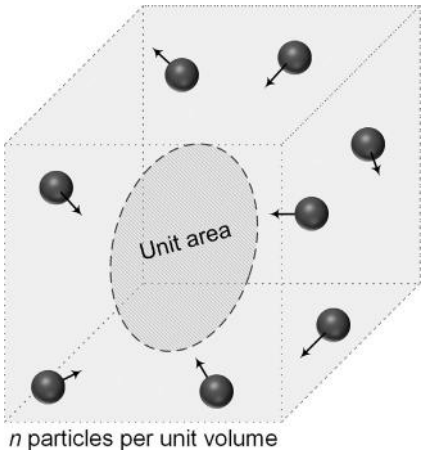

FIG. 4.4

Particles in random motion.

particles with those in the medium can be found by adding up the effects of individual projectiles. Each behaves the same way in interacting with the targets, regardless of direction of motion. The reaction rate is again $nvN\sigma$ or, for this random motion,

$$R = nvN\sigma = \phi\Sigma \tag{4.33}$$

Although j and ϕ possess the same scientific units, the current density as a vector quantity describes the net particle flow while the flux represents the gross number of particles passing through some arbitrary cross-sectional area per unit time. Integrating the flux over time forms the *fluence*, that is, $\Phi = \int \phi dt$.

The random motion of particles can be simulated mathematically by the use of random numbers, which form a collection of decimal fractions that are independent and are distributed uniformly over the range 0–1. They are useful for the study of neutron and gamma ray processes, both of which are governed by statistics. This Monte Carlo (named after the gambling casino in Monaco) approach is at the heart of various radiation transport computer codes, such as MCNP® (Monte Carlo *n*-particle transport code).

When a particle such as a neutron collides with a target nucleus, there is a certain chance of each of several reactions. The simplest is *elastic scattering*, in which the neutron is visualized as bouncing off the nucleus and moving in a new direction with a change in energy. Such a collision, governed by classical physics, is predominant in light elements. In the *inelastic scattering* collision—an important process for fast neutrons in heavy elements—the neutron becomes a part of the nucleus; the incident neutron energy provides excitation, and a neutron is released. The excited nucleus returns to its ground state through gamma-ray emission. The cross-section σ_s is the chance of a collision that results in neutron scattering. The neutron may instead be absorbed by the nucleus, with cross-section σ_a. Because σ_a and σ_s are chances of reaction, their sum is the chance for collision or total cross-section

$$\sigma_t = \sigma_a + \sigma_s \tag{4.34}$$

EXAMPLE 4.4

Let us illustrate these ideas by some calculations. In a typical nuclear reactor used for training and research in universities, a large number of neutrons will be present with energies near 0.0253 eV. This energy corresponds to a most probable speed of 2200 m/s for the neutrons viewed as a gas at room temperature, 293 K. Suppose that the flux of such neutrons is $\phi = 2 \times 10^{12}/(\text{cm}^2\,\text{s})$. The neutron density is then

$$n = \frac{\phi}{v} = \frac{2 \times 10^{12}/(\text{cm}^2\,\text{s})}{2.2 \times 10^5\,\text{cm/s}} = 9 \times 10^6/\text{cm}^3$$

Although this is a very large number by ordinary standards, it is exceedingly small compared with the number of water molecules per cubic centimeter (3.3×10^{22}) or even the number of air molecules per cubic centimeter (2.7×10^{19}). The "neutron gas" in a reactor is almost a perfect vacuum.

Now let the neutrons interact with uranium-235 fuel in the reactor. The U-235 cross-section for absorption σ_a is 681×10^{-24} cm^2. If the number density of fuel atoms is $N = 0.048 \times 10^{24}/\text{cm}^3$, as in uranium metal, then the macroscopic cross-section is

$$\Sigma_a = N\sigma_a = \left(0.048 \times 10^{24}/\text{cm}^3\right)\left(681 \times 10^{-24}\,\text{cm}^2\right) = 32.7/\text{cm}$$

The unit of area 10^{-24} cm^2 is conventionally called the barn. Early atomic scientists observed that "a cross-section of 10^{-24} cm^2 for nuclear processes was really as big as a barn" (Holloway and Baker, 1947). If we express the number of

targets per cubic centimeter in units of 10^{24} and the microscopic cross-section in barns, then $\Sigma_a = (0.048)\,(681) = 32.7/\text{cm}$ as previously shown. Using the given neutron flux, the reaction rate for absorption is

$$R_a = \Sigma_a \phi = (32.7/\text{cm})\left(2 \times 10^{12}/(\text{cm}^2\,\text{s})\right) = 6.54 \times 10^{13}/(\text{cm}^3\,\text{s})$$

This is also the rate at which U-235 nuclei are consumed.

The average energy of neutrons in a nuclear reactor used for electrical power generation is approximately 0.1 eV, almost four times the value used in our example. The effects of the high temperature of the medium (approximately 600°F) and of neutron absorption give rise to this higher energy.

Using the reaction rate permits writing a general expression for the generation rate g used in the buildup and decay equations of Section 3.4.1. Given a reaction cross-section σ for the target atoms N_T and constant particle flux ϕ, the production rate of radionuclides N_P is

$$g = R = \sigma N_T \phi \tag{4.35}$$

If $R \ll N_T$, then N_T may be assumed constant such that Eq. (3.17) becomes

$$N_P(t) = (\sigma N_T \phi/\lambda_P)\left(1 - e^{-\lambda_P t}\right) \tag{4.36}$$

4.5 PARTICLE ATTENUATION

Visualize an experiment in which a stream of particles of common speed and direction is allowed to strike the plane surface of a substance, as in Fig. 4.5. Collisions with the target atoms in the material will continually remove projectiles from the stream, which will thus diminish in strength with distance, a

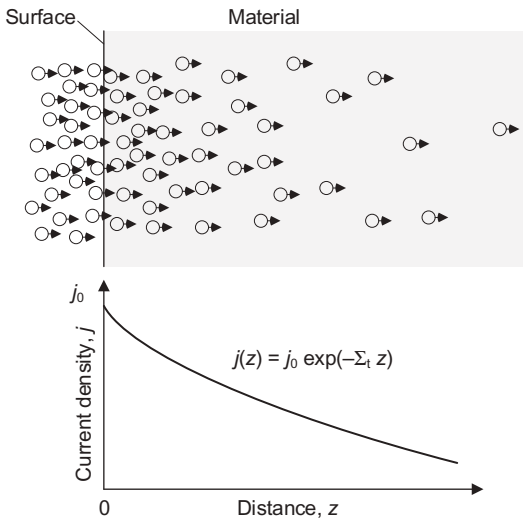

FIG. 4.5

Neutron penetration and attenuation.

process we label *attenuation*. If the current density incident on the substance at position $z=0$ is labeled j_0, the current of those not having made any collision on penetrating to a depth z is given by[1]

$$j = j_0 e^{-\Sigma_t z} \tag{4.37}$$

where Σ_t is the total macroscopic cross-section. The similarity in form to the exponential for radioactive decay is noted, and one can deduce by analogy that the *half-thickness*, the distance required to reduce j to half its initial value, is

$$z_H = \ln(2)/\Sigma_t \tag{4.38}$$

Another more frequently used quantity is the mean free path λ, the average distance a particle travels before making a collision. By analogy with the mean life for radioactivity, we can write[2]

$$\lambda_k = 1/\Sigma_k \tag{4.39}$$

where k signifies a particular reaction type. For instance, λ_a is the absorption mean free path (mfp). Thus, the macroscopic cross-sections Σ_s and Σ_a determine the scattering and absorption of neutrons, on average. For a given neutron, however, the number of scatterings before being absorbed can vary widely.

This relation is applicable as well to particles moving randomly in a medium. Consider a particle that has just made a collision and moves off in some direction. On the average, it will go a distance λ through the array of targets before colliding again.

EXAMPLE 4.5

Find the mean free path of 1 eV neutrons in water, assuming that scattering by hydrogen with cross-section 20 barns is the dominant process. The atomic number density of hydrogen in water was previously determined in Example 2.2 as $N_H = 6.68 \times 10^{22}/\text{cm}^3$. Because σ_s is 20×10^{-24} cm^2, therefore, the corresponding macroscopic scattering cross-section is

$$\Sigma_s^H = N_H \sigma_s = \left(6.68 \times 10^{22}/\text{cm}^3\right)\left(20 \times 10^{-24}\,\text{cm}^2\right) = 1.34/\text{cm}$$

Thus, the mean free path for scattering λ_s is approximately

$$\lambda_s^H = 1/\Sigma_s^H = 1/(1.34/\text{cm}) = 0.75\,\text{cm}$$

If scattering is the dominant interaction, this implies that $\lambda_t \cong \lambda_s$.

The cross-sections for atoms interacting with their own kind at the energies corresponding to room temperature conditions are of the order of 10^{-15} cm^2. If we equate this area to πr^2, the calculated radii are of the order of 10^{-8} cm. This is in rough agreement with the theoretical radius of electron motion in the hydrogen atom 0.53×10^{-8} cm (Mohr et al., 2015). On the other hand, the cross-sections for neutrons interacting with nuclei by scattering collisions, those in which the neutron is deflected in direction

[1]The derivation proceeds as follows. In a slab of material of unit area and infinitesimal thickness dz, the target area will be $N\sigma dz$. If the current at z is j, the number of collisions per second in the slab is $jN\sigma dz$, and thus the change in j on crossing the layer is $dj = -j\Sigma dz$, in which the reduction is indicated by the negative sign. By analogy with the solution of the radioactive decay law, we can write the formula cited.

[2]This relation can be derived directly by use of the definition of an average as the sum of the distances the particles travel divided by the total number of particles. When integrals are used, this is $\bar{z} = \int z dj / \int dj$.

and loses energy, are usually very much smaller than those for atoms. For the case of 1 eV neutrons in hydrogen with a scattering cross-section of 20 barns (i.e., 20×10^{-24} cm^2), one deduces a radius of approximately 2.5×10^{-12} cm. These results correspond to our earlier observation in Section 2.6 that the nucleus is thousands of times smaller than the atom.

4.6 NEUTRON CROSS-SECTIONS

The cross-section for neutron absorption in materials depends greatly on the isotope bombarded and on the neutron energy. For consistent comparison and use, the cross-section is often cited at 0.0253 eV, corresponding to the most probable neutron speed at 20°C. Table 4.2 lists capture cross-section σ_γ values for a number of isotopes at that energy. The dependence of the absorption cross-section (and its constituents such as capture and fission) on energy is of two types. The first is called $1/v$, in which σ_a varies inversely with neutron speed,

$$\sigma_a(v) = \sigma_{a0} v_0 / v \tag{4.40}$$

where σ_{a0} is the cross-section at v_0, typically taken as 2200 m/s. Qualitatively, a lower energy neutron spends more time in the vicinity of the nucleus, thereby increasing the likelihood of absorption. The second is termed *resonance*, in which there is a very strong absorption at certain neutron energies. Many materials exhibit both variations. Fig. 4.6 shows the dominant ^{10}B absorption cross-section, which displays the $1/v$ behavior from 10^{-5} to 10^5 eV, but no resonances. The use of the logarithmic plot enables one to display the large range of cross-section over the large range of energy of interest. Also shown in the graph is the ^{113}Cd capture cross-section, which exhibits a multitude of resonances from 2×10^{-5} to 6×10^{-3} MeV and a single resonance at 1.7×10^{-7} MeV forming the cadmium cutoff energy at about 0.5 eV. Measured cross-sections combined with nuclear model predictions are compiled into datasets such as the Evaluated Nuclear Data File version B-VII.1 (ENDF/B-VII.1) (Chadwick et al., 2011).

EXAMPLE 4.6

Find the absorption cross-section for B-10 at 1 keV. Table 4.2 gives $\sigma_a = \sigma_\gamma + \sigma_\alpha = 3837.5$ b at 0.0253 eV. Replacing velocity in Eq. (4.40) with kinetic energy yields an alternate general expression for $1/v$ cross-sections

$$\sigma_a(E) = \sigma_{a0} \frac{v_0}{v} = \sigma_{a0} \sqrt{\frac{E_0}{E}} \tag{4.41}$$

Substituting the given values results in

$$\sigma_a^{B-10}(1\text{keV}) = \sigma_{a0} \sqrt{\frac{E_0}{E}} = (3837.5\text{b}) \sqrt{\frac{0.0253\text{eV}}{1000\text{eV}}} = 19.3\text{b}$$

This value concurs with that in the graph of Fig. 4.6.

Neutron scattering cross-sections are comparatively similar for all elements and have less variation with neutron energy. Fig. 4.7 shows the trend of σ_s for hydrogen-1 as in water. Over a large range of neutron energy (~0.1 eV to 10 keV), the scattering cross-section is nearly constant, dropping off in the

Table 4.2 Selected Thermal Neutron Cross-sections at 0.0253 eV

Isotope	σ_s (barn)	σ_γ (barn)	Other σ (barn)
H-1	20.49	0.3326	
H-2	3.39	0.000519	
He-3	3.1	0.000031	$\sigma_p = 5333$
Li-6	0.75	0.0385	$\sigma_\alpha = 940$
Li-7	0.97	0.0454	
Be-9	6.151	0.0076	
B-10	2.23	0.5	$\sigma_\alpha = 3837$
B-11	4.84	0.0055	
C-12	4.746	0.00353	
C-13	4.19	0.00137	
N-14	10.05	0.075	$\sigma_p = 1.83$
N-15	4.59	2.4×10^{-5}	
O-16	3.761	0.00019	
O-17	3.61	0.000538	$\sigma_\alpha = 0.235$
O-18		0.00016	
Na-23	3.025	0.53	
Al-27	1.413	0.231	
Mn-55	2.2	13.3	
Co-59	6.0	20.4	
Nb-93	6.37	1.15	
Cd-113		2.06×10^4	
Xe-135		2.65×10^6	
Sm-149		4.014×10^4	
Au-197	7.84	98.65	
Th-232		7.37	$\sigma_f < 2.5 \times 10^{-6}$
U-233	12.8	45.5	$\sigma_f = 529.1$
U-235	14.3	98.3	$\sigma_f = 582.6$
U-238	9.38	2.68	$\sigma_f = 4 \times 10^{-6}$, $\sigma_\alpha = 1.3 \times 10^{-6}$
Pu-239	7.6	269.3	$\sigma_f = 748.1$
Pu-241	9.0	358.2	$\sigma_f = 1011.1$

Data from Mughabghab, S.F., Divadeenam, M., Holden, N.E., 1981. Neutron Cross-sections, vol. 1, Neutron Resonance Parameters and Thermal Cross-sections. Academic Press.

megaelectronvolt (MeV) region. This high-energy range is of special interest because neutrons produced by the fission process have such MeV energies.

The competition between scattering and absorption for neutrons in a medium is statistical in nature. The number of scattering collisions that occur before an absorption removes the neutron may be none, one, a few, or many. Even within absorption and scattering, there is further statistical competition between subdivisions of absorption and scattering. For instance, scattering can be either *elastic*, for which kinetic energy, in addition to total energy, is conserved; or *inelastic*, for which kinetic energy is imparted to the target nucleus, which is left in an excited state. Similarly, absorption may include

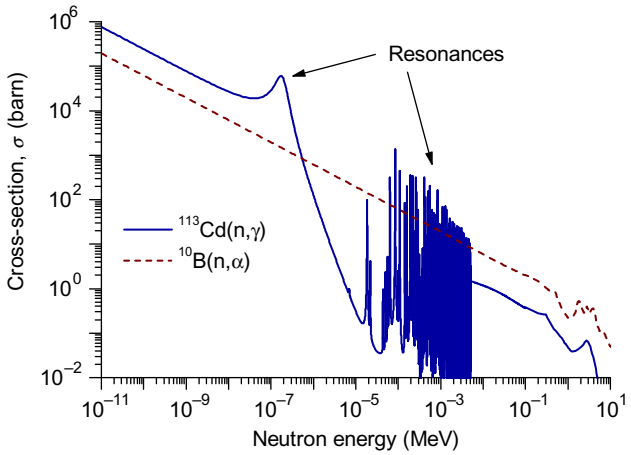

FIG. 4.6

Microscopic absorption cross-sections for boron-10 and cadmium-113.

Data from ENDF/B-VII.1 (Chadwick, M.B., Herman, M., Obložinský, P., Dunn, M.E., Danon, Y., Kahler, A.C., et al., 2011. ENDF/B-VII.1 Nuclear data for science and technology: cross-sections, covariances, fission product yields and decay data. Nucl. Data Sheets 112 (12), 2887–2996).

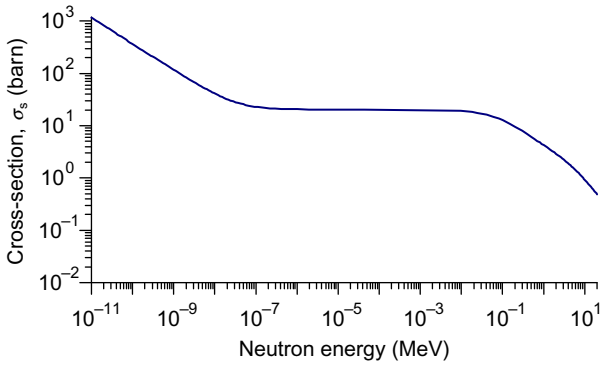

FIG. 4.7

Microscopic scattering cross-section for hydrogen-1.

Data from ENDF/B-VII.1 (Chadwick, M.B., Herman, M., Obložinský, P., Dunn, M.E., Danon, Y., Kahler, A.C., et al., 2011. ENDF/B-VII.1 Nuclear data for science and technology: cross-sections, covariances, fission product yields and decay data. Nucl. Data Sheets 112 (12), 2887–2996).

radiative capture, as from an (n, γ) reaction, fission, or other reactions in which a neutron enters the nucleus but another particle is expelled, as associated with reactions such as (n, p), (n, d), (n, t), and (n, α). The reaction hierarchy shown in Fig. 4.8 also directly applies to both microscopic and macroscopic cross-sections

$$\sigma_t = \sigma_s + \sigma_a = (\sigma_e + \sigma_i) + (\sigma_\gamma + \sigma_f + \ldots) \tag{4.42}$$

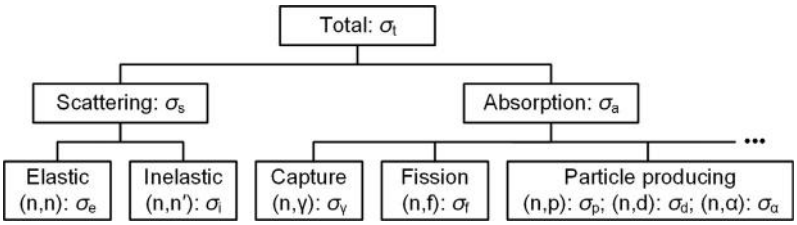

FIG. 4.8

Neutron reaction and cross-section hierarchy. Not shown are neutron and multiple particle producing reactions such as (n, 2n) and (n, np).

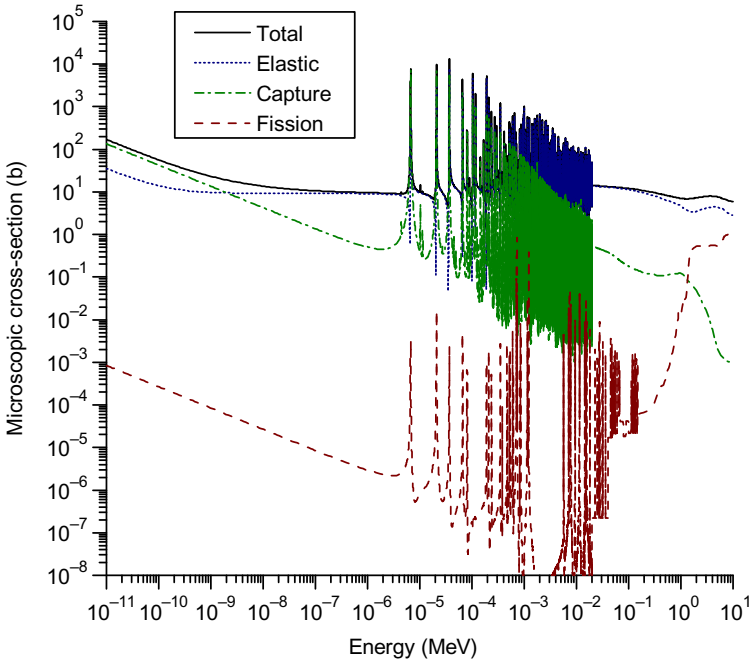

FIG. 4.9

Microscopic cross-sections for uranium-238.

Data from ENDF/B-VII.1 (Chadwick, M.B., Herman, M., Obložinský, P., Dunn, M.E., Danon, Y., Kahler, A.C., et al., 2011. ENDF/B-VII.1 Nuclear data for science and technology: cross-sections, covariances, fission product yields and decay data. Nucl. Data Sheets 112(12), 2887–2996).

where σ_γ and σ_f are for capture and fission, and σ_e and σ_i are for elastic (n, n) and inelastic (n, n′) scattering, respectively.

Fig. 4.9 shows four cross-sections for U-238: (1) total σ_t, (2) elastic scattering σ_e, (3) radiative capture σ_γ, and (4) fission σ_f. As seen, both the scattering and capture cross-sections exhibit resonances in the intermediate energy region from about 10^{-5} to 0.02 MeV. It is noteworthy that the fission cross-section does not become significant until 1 MeV.

EXAMPLE 4.7

Let us determine the total macroscopic cross-section for air that has a composition of simply nitrogen and oxygen, as listed in Table 4.3. To find Σ, the atomic number densities of N and O are needed. Eq. (2.2) can be modified for the situation in which the fraction weight ω_j of the j-th component in a mixture of density ρ_{mix} is known, in particular

$$N_j = \frac{\rho_j N_A}{M_j} = \frac{(\omega_j \rho_{\text{mix}}) N_A}{M_j} \tag{4.43}$$

Table 4.3 Basic Composition of Air

Constituent	Volume Fraction	Mass Fraction
Nitrogen, N_2	0.788	0.765
Oxygen, O_2	0.212	0.235

Therefore, the nitrogen and oxygen number densities in air with a density of 1.205×10^{-3} g/cm^3 are

$$N_N = \frac{\omega_N \rho_{\text{air}} N_A}{M_N} = \frac{\left(0.765 \frac{\text{g}-\text{N}}{\text{g}-\text{air}}\right)\left(1.205 \times 10^{-3} \frac{\text{g}-\text{air}}{\text{cm}^3}\right)\left(6.022 \times 10^{23} \frac{\text{atoms}}{\text{mol}}\right)}{14.0067 \frac{\text{g}}{\text{mol}}} = 3.96 \times 10^{19} \frac{\text{N}-\text{atoms}}{\text{cm}^3}$$

$$N_O = \frac{\omega_O \rho_{\text{air}} N_A}{M_O} = \frac{\left(0.235 \frac{\text{g}-\text{O}}{\text{g}-\text{air}}\right)\left(1.205 \times 10^{-3} \frac{\text{g}-\text{air}}{\text{cm}^3}\right)\left(6.022 \times 10^{23} \frac{\text{atoms}}{\text{mol}}\right)}{15.9994 \frac{\text{g}}{\text{mol}}} = 1.07 \times 10^{19} \frac{\text{O}-\text{atoms}}{\text{cm}^3}$$

The next challenge is to combine the cross-sections from the different isotopes of each element. The macroscopic cross-sections of the constituents comprise the overall material (element or mixture) cross-section of type k,

$$\Sigma_k^{\text{mat}} = \sum_j^{\text{constituents}} \Sigma_k^j = \sum_j^{\text{constituents}} N_j \sigma_k^j \tag{4.44}$$

We should recognize that the atomic density of the i-th isotope is the product of its abundance γ_i and the number density of the element N_{elem},

$$N_i = \gamma_i N_{\text{elem}} \tag{4.45}$$

Hence, the following general relation may be written for the type k macroscopic cross-section of an element composed of multiple isotopes

$$\Sigma_k^{\text{elem}} = \sum_i^{\text{isotopes}} N_i \sigma_k^i = \sum_i^{\text{isotopes}} \gamma_i N_{\text{elem}} \sigma_k^i = N_{\text{elem}} \sum_i^{\text{isotopes}} \gamma_i \sigma_k^i \tag{4.46}$$

which means that the overall microscopic cross-section for an element is

$$\sigma_k^{\text{elem}} = \sum_i^{\text{isotopes}} \gamma_i \sigma_k^i \tag{4.47}$$

Using these relations leads to the final numeric result of

$$\begin{aligned}\Sigma_t^{air} &= \Sigma_t^N + \Sigma_t^O = N_N\sigma_t^N + N_O\sigma_t^O \\ &= N_N\left(\gamma_{N-14}\sigma_t^{N-14} + \gamma_{N-15}\sigma_t^{N-15}\right) + N_O\left(\gamma_{O-16}\sigma_t^{O-16} + \gamma_{O-17}\sigma_t^{O-17} + \gamma_{O-18}\sigma_t^{O-18}\right) \\ &= \left(3.96\times10^{19}\right)[(0.9964)(11.96) + (0.0036)(4.59)]\left(10^{-24}\right) + \\ &\quad \left(1.07\times10^{19}\right)[(0.99757)(3.76) + (0.00038)(3.61) + (0.00205)(0)]\left(10^{-24}\right) \\ &= 0.000513/\text{cm}\end{aligned}$$

where the σ_t values are obtained from summing constituent cross-sections in Table 4.2, and the abundances are taken from Table A.5. Clearly, in this case, Σ_t could have been approximated well using only N-14 and O-16.

Although this section focuses on neutron cross-sections, the terminology is just as applicable to other particles causing nuclear reactions. For instance, the Van Allen radiation belts surrounding the Earth are laden with energetic protons. These protons may undergo reactions, such as (p, γ) and (p, α), with satellite materials.

4.7 NEUTRON MIGRATION

When fast neutrons, those of energy of the order of 2 MeV, are introduced into a medium, they make inelastic or elastic collisions with nuclei. On each elastic collision, neutrons are deflected in direction, they lose energy, and they tend to migrate away from their origin. Each neutron has a unique history, and it is impractical to keep track of all of them. Instead, we seek to deduce average behavior. First, we note that the elastic scattering of a neutron with an initially stationary nucleus of mass number A causes a reduction in neutron energy from E_0 to E and a change of direction through an angle θ (theta), as shown in Fig. 4.10. The length of arrows indicates the speeds of the particles. The example shown is but one of a great variety of possible results of scattering collisions. For each final energy, there is a unique angle of scattering, and vice versa, but the occurrence of a particular E and θ pair depends

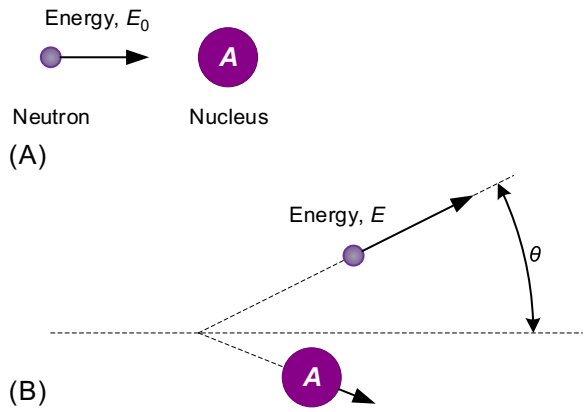

FIG. 4.10

Neutron scattering and energy loss. (A) Before collision and (B) after collision.

on chance. The neutron may ricochet directly backward, $\theta = 180°$, dropping down to a minimum energy αE_0, where

$$\alpha = \frac{(A-1)^2}{(A+1)^2} \tag{4.48}$$

or it may be undeflected, $\theta = 0°$ and retain its initial energy E_0, or it may be scattered through any other angle, with corresponding energy loss. The average E_{avg} and these extreme energies of the scattered neutron are summarized in

$$\begin{aligned} E_{\min} &= \alpha E_0 \\ E_{\text{avg}} &= E_0(1+\alpha)/2 \\ E_{\max} &= E_0 \end{aligned} \tag{4.49}$$

Hence, the energy loss of a neutron in an elastic collision with a nucleus can range from zero to $E_0(1-\alpha)$. For the special case of a hydrogen nucleus as scattering target, $A = 1$ and $\alpha = 0$, so that the neutron loses all its energy in a head-on collision. As we will see later, this makes water a useful material in a nuclear reactor.

The average elastic scattering collision is described by two quantities that depend only on the nucleus, not on the neutron energy. The first is $\overline{\mu}$, the average cosine of the scattering angles, given by

$$\overline{\mu} = \overline{\cos(\theta)} = \frac{2}{3A} \tag{4.50}$$

For hydrogen $\overline{\mu}$ is 2/3, meaning that the neutron tends to be scattered in the forward direction; for a very heavy nucleus such as uranium $\overline{\mu}$ is near zero, meaning that the scattering is almost equally likely in each direction. Forward scattering results in an enhanced migration of neutrons from their point of appearance in a medium. Their free paths are effectively longer, and it is conventional to use the *transport* mean free path

$$\lambda_{\text{tr}} = \frac{\lambda_s}{1-\overline{\mu}} \tag{4.51}$$

instead of λ_s to account for the effect. We note that λ_{tr} is always the larger. This formula for λ_{tr} is intended for materials such as moderators in which scattering dominates; otherwise, absorption must be incorporated via $\Sigma_{\text{tr}} = \Sigma_t - \overline{\mu}\Sigma_s$.

EXAMPLE 4.8

Consider slow neutrons in carbon, which is 99% ^{12}C for which $\sigma_s = 4.75$ barns and $N = 8.18 \times 10^{22}/\text{cm}^3$ (from Exercise 2.1 (a)), so that

$$\Sigma_s = N\sigma_s = \left(8.18 \times 10^{22}/\text{cm}^3\right)\left(4.75 \times 10^{-24}\,\text{cm}^2\right) = 0.389/\text{cm}$$

Using an A value of 12, the average cosine of the scattering angles is

$$\overline{\mu} = \frac{2}{3A} = \frac{2}{3(12)} = 0.0556$$

The transport mean free path of carbon is therefore

$$\lambda_{\text{tr}} = \frac{1}{\Sigma_s(1-\overline{\mu})} = \frac{1}{(0.389/\text{cm})(1-0.0556)} = 2.72\,\text{cm}$$

The second quantity that describes the average collision is ξ (xi), the average change in the natural logarithm of the energy, given by

$$\xi = 1 + \frac{\alpha \ln(\alpha)}{1-\alpha} \tag{4.52}$$

For hydrogen, ξ is exactly 1, the largest possible value, meaning that hydrogen is a good *moderator* for neutrons, its nuclei permitting the greatest neutron energy loss; for a heavy element, $\xi \cong 2/(A+2/3)$, which is much smaller than 1.

EXAMPLE 4.9

Determine the value of ξ for carbon, $A = 12$. First, Eq. (4.48) is used to find

$$\alpha = (A-1)^2/(A+1)^2 = (12-1)^2/(12+1)^2 = 0.716$$

Therefore, the average logarithmic energy decrement for carbon is

$$\xi = 1 + \alpha \ln(\alpha)/(1-\alpha) = 1 + (0.716)\ \ln(0.716)/(1-0.716) = 0.158$$

To find how many collisions C are required on the average to slow neutrons from an initial (higher) energy E_0 to a final (lower) energy E_F, we use

$$C = \frac{\ln(E_0/E_F)}{\xi} \tag{4.53}$$

The numerator of the previous relation is known as the lethargy (u).

EXAMPLE 4.10

Compare the number of collisions in going from the fission energy 2 MeV to the thermal energy 0.025 eV in both hydrogen and carbon. In both cases the lethargy is

$$u = \ln(E_0/E_F) = \ln\left(2 \times 10^6 \text{eV}/0.025 \text{eV}\right) = 18.2$$

Thus, neutrons require a significantly different number of collisions for slowing in the two media, as can be seen from the final results

$$\text{Hydrogen}: \ C = u/\xi = 18.2/1 = 18$$
$$\text{Carbon}: \ C = u/\xi = 18.2/0.158 = 115$$

Again, we see the virtue of hydrogen as a moderator. The fact that hydrogen has a scattering cross-section of 20 barns over a wide range, whereas carbon has a σ_s of only 4.8 barns, implies that collisions are more frequent and the slowing takes place in a smaller region. The only disadvantage is that hydrogen has a larger thermal neutron absorption cross-section σ_a, 0.333 barns versus 0.0035 barns for carbon.

The movement of individual neutrons through a moderator during slowing consists of free flights, interrupted frequently by collisions that cause energy loss. Picture, as in Fig. 4.11, a fast neutron starting at a point and migrating outward. At some distance r away, it arrives at the thermal energy. Other

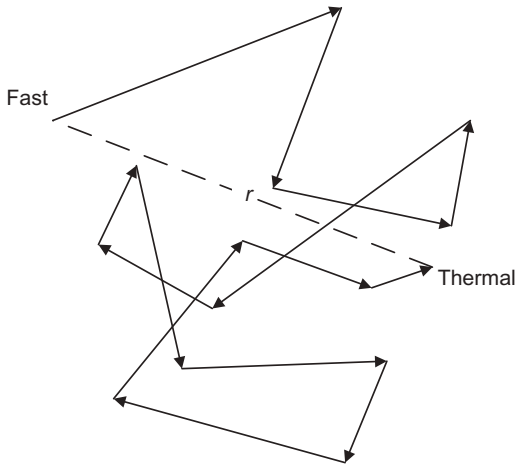

FIG. 4.11

Neutron migration during slowing.

Table 4.4 Common Moderator Properties

Moderator	τ, Age to Thermal (cm^2)	L, Diffusion Length (cm)
H_2O	31.4	2.85
D_2O (0.16% H_2O)	125	116
Be	97.2	20.8
BeO	105	28.6
C (graphite)	364	54

Data from Sodak, H., (Ed.) 1962. Reactor Handbook, second ed., Vol. III, Part A, Physics. Inter Science Publishers, New York, pp. 57–58.

neutrons become thermal at different distances, depending on their particular histories. If we were to measure all their r values and form the average of r^2, the result would be $\overline{r^2} = 6\tau$, where τ (tau) is called the Fermi "age" of the neutron. Approximate values of the age for various moderators, as obtained from experiment, are listed in Table 4.4. We thus note that water is a much better agent for neutron slowing than is graphite because of the larger scattering cross-section and energy loss.

As neutrons slow into the energy region that is comparable to thermal agitation of the moderator atoms, they may either lose or gain energy on collision. Members of a group of neutrons have various speeds at any instant and thus the group behaves as a gas with Maxwell-Boltzmann distribution, as was shown in Fig. 2.2 and discussed in Section 2.2. The neutron group has a temperature T that is close to that of the medium in which the neutrons are present. Thus, if the moderator is at room temperature 20°C, or 293 K, the most likely neutron speed from Eq. (2.5) is 2200 m/s. This corresponds to a kinetic energy of 0.0253 eV. The neutrons are said to be *thermal*, in contrast to fast or intermediate.

Another parameter that characterizes neutron migration while at thermal energy is the diffusion length, symbolized by L. By analogy to the slowing process, the average square distance between origin and absorption is given by $\overline{r^2} = 6L^2$. Table 4.4 lists approximate values of L for three moderators.

According to diffusion theory (see Section 19.1), the *diffusion length* is

$$L = \sqrt{D/\Sigma_a} \tag{4.54}$$

where the diffusion coefficient is

$$D = \lambda_{tr}/3 \tag{4.55}$$

This shows that the addition of an absorber to pure moderator reduces the distance neutrons travel, as expected.

The process of diffusion of gas molecules is familiar to us. If a bottle of perfume is opened, the scent is quickly detected because the molecules of the substance migrate away from the source. Because neutrons in large numbers behave as a gas, the descriptions of gas diffusion may be applied. The flow of neutrons through a medium at a location is proportional to the way the concentration of neutrons varies, in particular to the negative of the slope of the neutron number density. We can guess that the larger the neutron speed v and the larger the transport mean free path λ_{tr}, the more neutron flow will take place. Theory and measurement show that if n varies in the z-direction (refer to Fig. 4.5), the net flow of neutrons across a unit area each second, the net current density, is

$$j = \frac{-\lambda_{tr} v}{3} \frac{dn}{dz} \tag{4.56}$$

This is called Fick's (1855) law of diffusion, derived for the description of salt concentration in water. It applies to neutrons if absorption is small compared with scattering. In terms of the flux $\phi = nv$ and the diffusion coefficient $D = \lambda_{tr}/3$, this may be written compactly $j = -D\phi'$ where ϕ' is the derivative, or slope, of the neutron flux.

4.8 SUMMARY

Chemical and nuclear reactions have similarities in the form of equations and in the requirements on conservation of particles and charge. The bombardment of nuclei by charged particles or neutrons produces new nuclei and particles. Final energies are found from mass differences and final speeds from conservation of momentum. The cross-section for interaction of neutrons with nuclei is a measure of the chance of collision. Reaction rates depend mutually on neutron flows and the macroscopic cross-section. As a particle stream passes through a medium, the uncollided particle intensity is reduced exponentially. Neutron absorption cross-sections vary greatly with target isotope and with neutron energy, whereas scattering cross-sections are relatively constant. Neutrons are slowed readily by collisions with light nuclei and migrate from their point of origin. On reaching thermal energy, they continue to disperse, with the net flow dependent on the spatial variation of flux.

4.9 EXERCISES

4.1 The energy of formation of water from its constituent gases is said to be 54.5 kcal/mole. Verify that this corresponds to 2.4 eV per molecule of H_2O.

4.2 Complete the following nuclear reaction equations:

$$\text{(a)}\ {}^{1}_{0}\text{n} + {}^{14}_{7}\text{N} \rightarrow {}^{()}_{()}() + {}^{1}_{1}\text{H}$$
$$\text{(b)}\ {}^{2}_{1}\text{H} + {}^{9}_{4}\text{Be} \rightarrow {}^{()}_{()}() + {}^{1}_{0}\text{n}$$
$$\text{(c)}\ {}^{1}_{0}\text{n} + {}^{10}_{5}\text{B} \rightarrow {}^{()}_{()}() + {}^{4}_{2}\text{He}$$
$$\text{(d)}\ {}^{1}_{0}\text{n} + {}^{3}_{2}\text{He} \rightarrow {}^{()}_{()}() + {}^{1}_{1}\text{H}$$
$$\text{(e)}\ {}^{1}_{0}\text{n} + {}^{235}_{92}\text{U} \rightarrow {}^{()}_{()}() + {}^{94}_{38}\text{Sr} + 2{}^{1}_{0}\text{n}$$

4.3 Using the accurate atomic masses from Table A.5, find the minimum amount of energy an alpha particle must have to cause the transmutation of nitrogen-14 to oxygen-17.

4.4 Find the energy release in the reaction ^{6}Li(n,α)^{3}H.

4.5 A slow neutron is caught by the nucleus of a hydrogen atom and the final products are a deuterium atom and a gamma ray (see Example 4.1). The energy released is 2.22 MeV. If the γ-ray is assumed to have almost all this energy, what is its effective mass in kg? What is the speed of the ^{2}H particle in m/s, using equality of momenta on separation? What is the recoil energy of ^{2}H in MeV? How does this compare with the total energy released? Was the assumption about the γ-ray reasonable?

4.6 Calculate the speeds and energies of the individual α particles in the ^{7}Li(p,2α) reaction of Eq. (4.3), assuming that they separate along the line of the 2 MeV proton motion; see Example 4.2.

4.7 Determine the energy release in the reaction

$$^{13}_{7}\text{N} \rightarrow {}^{13}_{6}\text{C} + {}^{0}_{+1}\text{e}$$

Calculate (a) using nuclear masses, formed by subtracting the proper number of electron masses from the atomic masses, and (b) using atomic masses while accounting for the energy of pair production.

4.8 Calculate the macroscopic cross-section for scattering of 1 eV neutrons in water, using N for water as $3.34 \times 10^{22}/\text{cm}^3$ and scattering cross-sections of 20 barns for hydrogen and 3.8 barns for oxygen. Find the scattering mean free path λ_s.

4.9 Find the speed v and the number density of neutrons of energy 1.5 MeV in a flux $7 \times 10^{13}/(\text{cm}^2\ \text{s})$.

4.10 Compute the flux, macroscopic cross-section and reaction rate for the following data: $n = 2 \times 10^5/\text{cm}^3$, $v = 3 \times 10^8$ cm/s, $N = 0.04 \times 10^{24}/\text{cm}^3$, $\sigma = 0.5 \times 10^{-24}$ cm^2.

4.11 What are the values of the average logarithmic energy change ξ and the average cosine of the scattering angle $\overline{\mu}$ for neutrons in beryllium, $A = 9$? How many collisions are needed to slow neutrons from 2 MeV to 0.025 eV in Be? What is the value of the diffusion coefficient D for 0.025 eV neutrons if Σ_s is 0.90/cm?

4.12 (a) Verify that neutrons of speed 2200 m/s have an energy of 0.0253 eV. (b) If the neutron absorption cross-section of B-10 at 0.0253 eV is 3842 barns, what would it be at 0.1 eV? Does this result agree with that shown in Fig. 4.6?

4.13 Calculate the rate of consumption of U-235 and U-238 in a flux of $2.5 \times 10^{13}/(\text{cm}^2\ \text{s})$ if the uranium atom number density is $0.0223 \times 10^{24}/\text{cm}^3$, the atom number fractions of the two isotopes are 0.0072 and 0.9928, and cross-sections are 681 barns and 2.68 barns, respectively. Comment on the results.

4.14 What concentration of impurity atoms of B-10 per atom of C-12 would result in an increase of 50% in the macroscopic absorption cross-section of graphite? How many ^{10}B contaminate atoms would there then be per million ^{12}C atoms?

4.15 Calculate the absorption cross-section of the element zirconium using the isotopic data in the following table (Holden, 2016):

Mass Number	Abundance (atom %)	Cross-Section, σ_γ (barn)
90	51.45	0.014
91	11.22	1.2
92	17.15	0.2
94	17.38	0.049
96	2.80	0.020

4.16 The total cross-section for uranium dioxide of density $10\,\text{g/cm}^3$ is to be measured by a transmission method. To avoid multiple neutron scattering, which would introduce error into the results, the sample thickness is chosen to be much smaller than the mean free path of neutrons in the material. Using approximate cross-sections for UO_2 of $\sigma_s = 15$ barns and σ_a of 7.6 barns, find the total macroscopic cross-section Σ_t. Then find the thickness of target t such that $t/\lambda_t = 0.05$. How much attenuation in neutron beam would that thickness give?

4.17 The manganese content of a certain stainless steel is to be verified by an activation measurement. The activity induced in a sample of volume V by neutron capture during a time t is given by

$$A = \phi \Sigma_\gamma V [1 - \exp(-\lambda t)]$$

A foil of area $1\,\text{cm}^2$ and thickness 2 mm is irradiated in a thermal neutron flux of $3 \times 10^{12}/(\text{cm}^2\ \text{s})$ for 2 h. Counts taken immediately afterward yield an activity of 150 mCi for the induced Mn-56, half-life 2.58 h. Assuming that the atom number density of the alloy is $0.087 \times 10^{24}/\text{cm}^3$ and that the cross-section for capture in Mn-55 is 13.3 barns, find the percent of Mn in the sample.

4.18 For fast neutrons in uranium-235 metal, find the density ρ, the number of atoms per cubic centimeter N, the macroscopic cross-sections Σ_a and Σ_{tr}, the transport mean free path λ_{tr}, the diffusion coefficient D, and the diffusion length L. *Note:* the density of natural U (99.3% U-238) is approximately 19.05 g/cm^3; for U-235, $\sigma_\gamma = 0.25$ barns, $\sigma_f = 1.4$ barns, and $\sigma_{tr} = 6.8$ barns (Argonne National Laboratory (ANL), 1963).

4.19 When a projectile of mass m_1 and vector velocity $\mathbf{u}_1$ collides elastically with a target of mass m_2 and vector velocity $\mathbf{u}_2$, the final velocities are:

$$\begin{aligned} \mathbf{v}_1 &= [2m_2\mathbf{u}_2 + (m_1 - m_2)\mathbf{u}_1]/(m_1 + m_2) \\ \mathbf{v}_2 &= [2m_1\mathbf{u}_1 + (m_2 - m_1)\mathbf{u}_2]/(m_1 + m_2) \end{aligned} \tag{4.57}$$

Find the velocities if $\mathbf{u}_2 = 0$ and $m_2 \gg m_1$. Discuss the results.

4.20 A neutron of energy E_0 collides head-on with a heavy nucleus of mass number A. Using the velocity equations of Exercise 4.19, verify that the minimum neutron energy after collision is $E_1 = \alpha E_0$, where $\alpha = [(A-1)/(A+1)]^2$. Evaluate α and ξ for U-238.

4.21 Show for the case of $\mathbf{u}_2 = 0$ (Exercise 4.19) that kinetic energy is conserved.

4.22 (a) Derive the Coulombic threshold by integrating Eq. (4.30) from an infinite separation to where the particles contact, specifically

$$E_C = -\int_{\infty}^{d} F_C\, dr = \frac{q_1 q_2}{4\pi\varepsilon_0 d} \tag{4.58}$$

Where the closest distance d is found from the nuclei radii using Eq. (2.11), $d = 1.25 \times 10^{-13}\,\text{cm}(A_1^{1/3} + A_2^{1/3})$. (b) For particle charges of $q_1 = eZ_1$ and $q_2 = eZ_2$, substitute the appropriate constants to verify the 1.2 MeV value in the numerator of Eq. (4.20).

4.23 Calculate the Q value of the following reactions, and state whether the reaction is endothermic or exothermic.

(a) ${}^4_2\text{He} + {}^{14}_7\text{N} \rightarrow {}^{17}_8\text{O} + {}^1_1\text{H}$
(b) ${}^1_1\text{H} + {}^{12}_6\text{C} \rightarrow {}^{13}_7\text{N} + \gamma$
(c) ${}^1_0\text{n} + {}^6_3\text{Li} \rightarrow {}^3_1\text{H} + {}^4_2\text{He}$
(d) ${}^1_1\text{H} + {}^6_3\text{Li} \rightarrow {}^3_2\text{He} + {}^4_2\text{He}$
(e) ${}^1_0\text{n} + {}^{17}_8\text{O} \rightarrow {}^4_2\text{He} + {}^{14}_6\text{C}$
(f) ${}^4_2\text{He} + {}^7_3\text{Li} \rightarrow {}^1_0\text{n} + {}^{10}_5\text{B}$

4.24 In Example 4.7, the atom densities were determined using the mass fractions of nitrogen and oxygen in air. Repeat the calculations of N_N and N_O using the volume fractions of Table 4.3 instead. Note that for gases, volume fraction is the same as atom fraction.

4.25 Determine the average number of collisions to reduce the energy of a 1 MeV neutron to 0.030 eV in (a) beryllium and (b) deuterium.

4.26 Compute the alpha emission energy from the decay of (a) Po-210 and (b) Rn-222.

4.10 COMPUTER EXERCISE

4.A Extensive tabulations of cross-sections are available online (e.g., www.nndc.bnl.gov/exfor/endf00.jsp) within the evaluated nuclear data file (ENDF). Use this website to create a single graph similar to Fig. 4.9 of the total, fission, capture, and elastic scattering cross-sections for (a) Th-232, (b) U-233, (c) U-235, and (d) Pu-239.

REFERENCES

Argonne National Laboratory (ANL), 1963. Reactor Physics Constants. ANL-5800, second ed. p. 581.
Chadwick, M.B., Herman, M., Obložinský, P., Dunn, M.E., Danon, Y., Kahler, A.C., et al., 2011. ENDF/B-VII.1 Nuclear data for science and technology: cross-sections, covariances, fission product yields and decay data. Nucl. Data Sheets 112 (12), 2887–2996.
Cockcroft, J.D., Walton, E.T.S., 1932. Experiments with high velocity positive ions. II.–The disintegration of elements by high velocity protons. Proc. R. Soc. Lond. Ser. A 137 (831), 229–242.
Coulomb, M., 1785. Premier mémoire sur l'électricité et le magnétisme. Histoire de l'Académie Royale des Sciences. Paris, pp. 569–577.
Fick, A., 1855. V. On liquid diffusion. Phil. Mag. Ser. 4 10 (63), 30–39.
Foster, A.R., Wright Jr., R.L., 1983. Basic Nuclear Engineering, fourth ed. Allyn and Bacon, Inc., Boston.
Holden, N.E., 2016. Neutron scattering and absorption properties. In: Haynes, W.M. (Ed.), CRC Handbook of Chemistry and Physics. ninty-sixth ed. CRC Press/Taylor & Francis, Boca Raton, FL.
Holloway, M.G., Baker, C.P., 1947. Note on the origin of the term "barn". Los Alamos National Laboratory Report LAMS-523.
Mayo, R.M., 1998. Introduction to Nuclear Concepts for Engineers. American Nuclear Society, La Grange Park.
Mohr, P.J., Newell, D.B., Taylor, B.N., 2015. CODATA recommended values of the fundamental physical constants: 2014. arXiv:1507.07956v1 [physics.atom-ph].
Murray, R.L., 1957. Nuclear Reactor Physics. Prentice-Hall, Inc., Englewood Cliffs, p. 27
Rutherford, E., 1919. LIV. Collision of α particles with light atoms. IV. An anomalous effect in nitrogen. Phil Mag. Ser. 6 37 (222), 581–587.
Shultis, J.K., Faw, R.E., 2008. Fundamentals of Nuclear Science and Engineering, second ed. CRC Press, Boca Raton.

FURTHER READING

Atomic Mass Data Center, http://amdc.impcas.ac.cn/ https://www-nds.iaea.org/amdc/. Select AME.
Bertulani, C.A., Danielewicz, P., 2004. Introduction to Nuclear Reactions. Taylor & Francis, Bristol.
Bethe, H.A., Bacher, R.F., Livingston, M.S., 1986. Basic Bethe: Seminal Articles on Nuclear Physics, 1936–1937. American Institute of Physics and Springer-Verlag, New York.
Bodansky, D., 2003. Nuclear Energy: Principles, Practices, and Prospects, second ed. Springer/AIP Press, New York.
Duderstadt, J.J., Hamilton, L.J., 1976. Nuclear Reactor Analysis. Wiley, New York.
Lamarsh, J.R., 1972. Introduction to Nuclear Reactor Theory. Addison-Wesley Classic textbook reprinted by American Nuclear Society, La Grange Park, IL, 2002.
Lamarsh, J.R., Baratta, A.J., 2018. Introduction to Nuclear Engineering, fourth ed. Pearson, Hoboken.

McLane, V., Dunford, C.L., Rose, P.F., 1988. Neutron Cross-Sections, Vol. 2, Neutron Cross-section Curves. Academic Press, San Diego.

Mughabghab, S.F., 2006. Atlas of Neutron Resonances: Resonance Parameters and Thermal Cross-Sections, Z = 1-100, fifth ed. Elsevier Science, Amsterdam.

National Nuclear Data Center (NNDC), Atomic Mass Evaluation. Brookhaven National Laboratory. www.nndc.bnl.gov/masses.

Mughabghab, S.F., Divadeenam, M., Holden, N.E., 1981. Neutron Cross-sections. Neutron Resonance Parameters and Thermal Cross-sections, vol. 1. Academic Press, New York.

Sodak, H. (Ed.), 1962. Reactor Handbook. second ed. In: Part A, Physics, vol. III. Inter Science Publishers, New York, pp. 57–58.

CHAPTER

RADIATION AND MATERIALS

5

CHAPTER OUTLINE

In this chapter, the word *radiation* embraces all particles, whether they are of material or electromagnetic origin. We include those particles produced by both atomic and nuclear processes and those resulting from electrical acceleration, noting that there is no essential difference between X-rays from atomic collisions and gamma rays from nuclear decay; protons can come from a particle accelerator, from cosmic rays, or from a nuclear reaction in a reactor. The word *materials* refers to bulk matter, whether of mineral or biological origin, as well as to the particles of which the matter is composed, including molecules, atoms, electrons, and nuclei.

When we put radiation and materials together, a great variety of possible situations must be considered. Bombarding particles may have low or high energy; they may be charged, uncharged, or photons; and they may be heavy or light in the scale of masses. The targets may be similarly distinguished, but they may also exhibit degrees of binding that range from (a) none, as for free particles, to (b) weak, as for atoms in molecules and electrons in atoms, to (c) strong, as for nucleons in nuclei. In most interactions, the higher the projectile energy in comparison with the binding energy of the structure, the greater the effect.

Nuclear Energy. https://doi.org/10.1016/B978-0-12-812881-7.00005-8

Out of the broad subject, we will select for review some of the reactions that are important in the nuclear energy field. Looking ahead, we will need to understand the effects produced by the particles and rays from radioactivity and other nuclear reactions. Materials affected may be in or around a nuclear reactor, as part of its construction, or inserted to be irradiated. Materials may be of biological form, including the human body, or they may be inert substances used for protective shielding against radiation. We will not attempt to explain the processes rigorously but be content with qualitative descriptions based on analogy with collisions viewed on an elementary physics level.

5.1 IONIZING RADIATION

Ionizing radiation can be categorized into charged particles and neutral radiations. The charged radiations consist of a variety of particles, including electrons, protons, and *ions*, which are typically atoms missing one or more electrons. The neutral radiations are the photons, such as gamma rays and X-rays, and the neutrons. Table 5.1 compares some key characteristics of the ionizing radiations of interest. To describe the interaction of charged radiation with matter, the particles are classified according to their mass. Charged particles participate in a number of interactions, including excitation, ionization, scattering, nuclear reactions, and bremsstrahlung production. Unlike the neutral radiations, the charged particles are subjected to the Coulombic forces from electrons and nuclei within the material through which they pass. Analysis of nuclear interactions (by both heavy ions and neutrons) requires consideration of the kinematic and Coulombic thresholds. The range of neutral radiations into incident material is described by a decaying exponential function, whereas the complexity of the charged particle interactions requires the use of a (semi-)empirical formula to describe the penetration depth.

Radiation may interact with the atomic electrons or the nucleus or both. As a charged particle passes through a material, the particle slows as it loses kinetic energy. The energy loss by charged particles traveling through a material is broken into two components based on the mechanism of energy transfer: collisional and radiative/nuclear energy loss, as shown in Fig. 5.1. The latter component is generally referred to as the *radiative energy loss* for electrons and the *nuclear energy loss* for heavy charged particles because those are the dominant noncollisional interactions for those respective particles.

Although elastic collisions between charged particles are possible, the inelastic collisions from excitation and ionization are more prevalent. As depicted in Fig. 5.2, *excitation* raises an atomic electron to a higher energy shell, whereas *ionization* completely removes the electron from the atom. Ionization creates an *ion pair*, which is the (now) free electron and the positively charged atom from which the electron was removed. The kinetic energy of the ionized electron equals the energy given up by the

Table 5.1 Comparison of Ionizing Radiation

Characteristic	Photon (γ or X-ray)	Neutron	Proton	Alpha Particle	Electron or Beta Particle
Charge	0	0	+1	+2	−1
Mass relative to electron	0	1839	1836	7294	1
Percentage of speed of light for 1 MeV radiation	100%	4.6%	4.6%	2.3%	94.1%

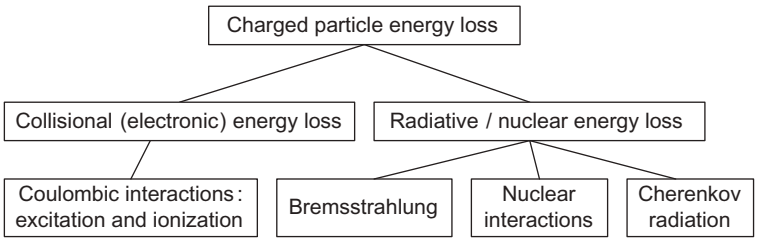

FIG. 5.1

Mechanisms for charged particle energy loss.

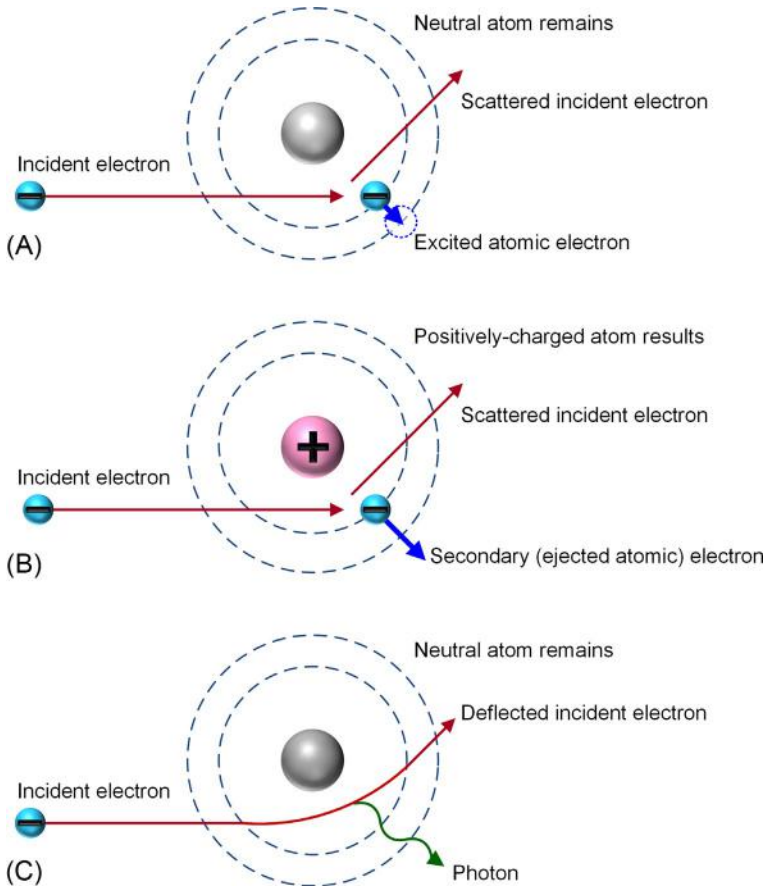

FIG. 5.2

Three electron interaction processes. Other charged particles routinely cause excitation and ionization too. (A) Excitation, (B) ionization, and (C) bremsstrahlung.

incident particle less the ionization potential of the atomic electron. The freed electron may possess sufficient kinetic energy to cause further (i.e., secondary) ionization events. Secondary ionization often frees more electrons than the primary ionization; however, the energies of the secondary electrons are lower than those of the primary ionization electrons.

The energy required to create an ion pair depends on the irradiated material. Experimental results have shown that the actual energy necessary to create an ion pair is about 2–3 times greater than the *ionization potential*, which is the energy required to remove the most loosely bound electron from an atom in the gaseous state. For instance, the ionization energies of oxygen and nitrogen are 13.6 and 14.5 eV, respectively (Martin et al., 2011), whereas the mean energy W to create an ion pair in air is 34 eV (International Atomic Energy Agency (IAEA), 1995). In contrast, the work function of metallic solids is approximately half the ionization energy of gaseous atoms (Gallo and Lama, 1974). In the case of semiconductors, the favored descriptor is the electron-hole pair (ehp) generation energy, which is about three times the material bandgap energy. For example, silicon has bandgap and ehp generation energies of 1.1 and 3.6 eV, respectively, at 300 K (Knoll, 2000).

EXAMPLE 5.1

The number of ion pairs (ip) created by a 4-MeV alpha particle as it is stopped in air is calculated readily from

$$N_{IP} = \frac{E}{W} = \frac{4 \times 10^6 \text{ eV}}{34 \text{ eV/ip}} = 120{,}000 \text{ ion pairs}$$

This ionization equates to a charge deposition of

$$q = N_{IP} e = \left(1.2 \times 10^5 \text{ ip}\right)\left(1.602 \times 10^{-19} \text{ C/ip}\right) = 1.9 \times 10^{-14} \text{ C}$$

We begin our study with the general issues related to charged particle interactions. Because all the other radiations either directly or indirectly affect the electron, we address electron interactions first.

5.2 LIGHT CHARGED PARTICLE INTERACTIONS

For our purposes, light charged particles are electrons (e^-), positrons (e^+), and beta (β) particles. When electrons pass through matter, several possible processes may occur, including ionization, excitation, and bremsstrahlung, as illustrated in Fig. 5.2. The former two processes occur in the familiar fluorescent light bulb, in an X-ray machine, or in matter exposed to beta particles. If an electron that enters a material has a very low energy, it will merely migrate without affecting the molecules significantly. If its energy is large, it may impart energy to atomic electrons as described by the Bohr theory (Section 2.3), causing excitation of electrons to higher energy states or producing ionization with subsequent emission of light. When electrons of inner orbits in heavy elements are displaced, the resultant high-energy radiations are classed as X-rays. These rays, which are so useful for internal examination of the human body, are produced by accelerating electrons in a vacuum chamber to energies in the kilovolt range and allowing them to strike a heavy element target, such as tungsten (see Section 13.8).

In addition to the X-rays as a result of transitions in the electron orbits, a similar radiation called *bremsstrahlung* (German for braking radiation) can be produced. It arises from the deflection and resulting rapid change in velocity—direction and speed—of electrons as they encounter nuclei. When the negatively charged electron passes near the nucleus, the high-speed electron undergoes radial acceleration toward the nucleus. Classical electromagnetic theory states that the electron loses energy, in the form of a photonic emission, in proportion to the square of the acceleration. The fraction of beta particle or monoenergetic electron *energy* converted to X-rays in a material of atomic number Z is (Cember and Johnson, 2009)

$$\begin{aligned} f_\beta &= 3.5 \times 10^{-4}\, Z E_\beta \\ f_e &= 10^{-3}\, Z E_e \end{aligned} \tag{5.1}$$

in which E_β and E_e are the maximum beta and electron energy, respectively, in MeV. Another radiative energy loss mechanism for fast electrons is Cherenkov radiation, which causes the famous bluish glow of nuclear reactors in water.

Beta particles as electrons from nuclear reactions have energies in the range of 0.01–1 MeV and thus are capable of producing large amounts of ionization as they penetrate a substance. Electrons are easily scattered due to their small mass and charge and therefore travel a nonlinear path. The beta particles lose energy with each event and eventually are stopped. The tracks and ranges of positrons are about the same as negatrons with the major difference between positrons and negatrons being that positrons undergo annihilation at the end of their track. For electrons of 1 MeV energy, the range, as the typical distance of penetration, is no more than a few millimeters in liquids and solids or a few meters in air. The maximum range R_{max} (material independent) of a beta particle or electron can be computed from an empirical formula given by Katz and Penfold (1952)

$$R_{max}\left[\mathrm{g/cm^2}\right] = \begin{cases} 0.412\, E^{1.265-0.0954\ \ln(E)} & 0.01 \le E \le 2.5\,\mathrm{MeV} \\ 0.530\, E - 0.106 & 2.5 \le E \le 20\,\mathrm{MeV} \end{cases} \tag{5.2}$$

where E is the maximum beta energy or the kinetic energy of monoenergetic electrons in MeV. This density thickness (g/cm^2) of the material gives a generic quantifier by which various absorbers can be compared. With the maximum range known, the actual penetration depth can be computed from R_{max}/ρ where ρ is the material density. A thin sheet of metal or glass easily stops beta particles from natural radionuclides; however, shielding with high-Z materials such as lead must be avoided due to bremsstrahlung production.

EXAMPLE 5.2

Determine the copper thickness necessary to stop the beta particles emitted from Co-60. Cobalt-60 emits beta particles with a maximum energy of 0.3179 MeV (see Table 3.2), hence the maximum range of those particles is

$$R_{max} = (0.412)(0.3179)^{1.265-0.0954\ \ln(0.3179)} = 0.08529\,\mathrm{g/cm^2}$$

Copper has a density of 8.933 g/cm^3 (Table A.4), so the actual shield thickness necessary is

$$\frac{R_{max}}{\rho} = \frac{0.08529\,\mathrm{g/cm^2}}{8.933\,\mathrm{g/cm^3}} = 0.00955\,\mathrm{cm}$$

The range of beta particles and electrons in several common materials is plotted in Fig. 5.3.

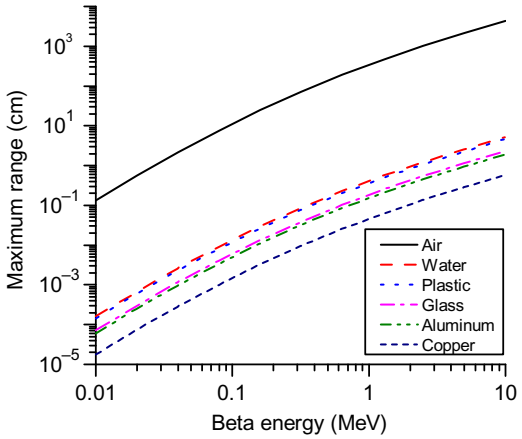

FIG. 5.3

Beta particle range in common materials.

5.3 HEAVY CHARGED PARTICLE STOPPING BY MATTER

Charged particles such as protons, alpha particles, and fission fragment ions are classified as heavy, being much more massive than the electron. For a given energy, their speed is lower than that of an electron, but their momentum is greater, and they are less readily deflected on collision. The mechanism by which they slow down in matter is mainly electrostatic interaction with the atomic electrons and with nuclei. In each case, the Coulomb force, varying as $1/r^2$ with distance of separation r, determines the result of a collision. Fig. 5.4 illustrates the effect of the passage of an ion by an atom. An electron is displaced and gains energy in a large amount compared with its binding in the atom, leaving behind a new ion. Application of the collision formulas of Eq. (4.57) leads to the energy change when a heavy particle of mass m_H and energy E_0 collides head-on with an electron of mass m_e, as approximately $4(m_e/m_H)\ E_0$ (see Exercise 5.15). For example, for an alpha particle of 5 MeV, the loss by the projectile and the gain by the target are $4(0.000549/4.00)\ 5\,\text{MeV} = 0.00274\,\text{MeV}$ or 2.74 keV. The electron is energetic enough to produce secondary ionization, whereas hundreds of collisions are needed to reduce the alpha particle's energy by as little as 1 MeV. As the result of primary and secondary processes, a great deal of ionization is produced by heavy ions as they move through matter.

In contrast, when a heavy charged particle comes close to a nucleus, the electrostatic force causes it to move in a hyperbolic path, as in Fig. 5.5. The projectile is scattered through an angle that depends on the detailed nature of the collision (i.e., the initial energy and direction of motion of the incoming ion relative to the target nucleus) and the magnitudes of electric charges of the interacting particles. The charged particle loses a significant amount of energy in the process, in contrast with the slight energy loss on collision with an electron. Unless the energy of the bombarding particle is very high and it comes within the short range of the nuclear force, there is a small chance that it can enter the nucleus and cause a nuclear reaction.

Heavy charged particles are much more massive than electrons; therefore, such heavy ions are only slightly deflected by the atomic electrons. Consequently, heavy charged particles travel in nearly

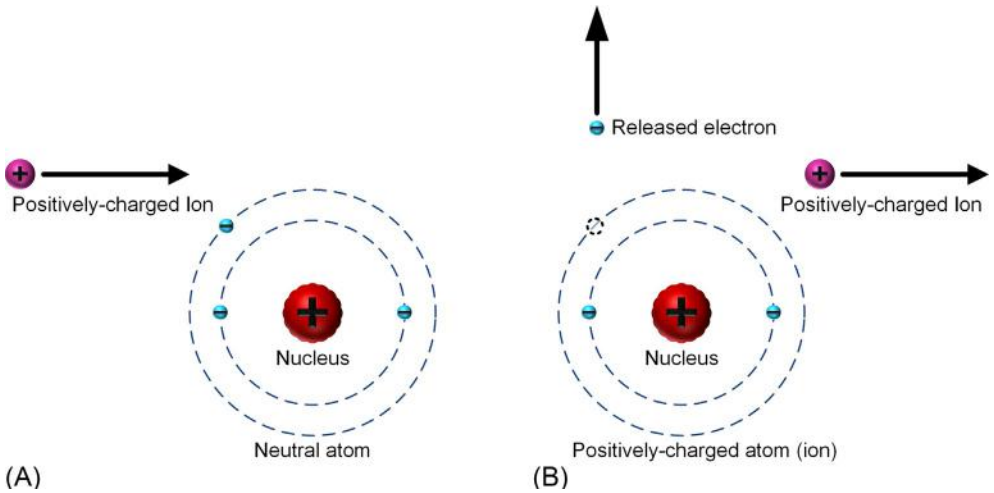

FIG. 5.4

Interaction of heavy ion with outer shell atomic electron: (A) before and (B) after.

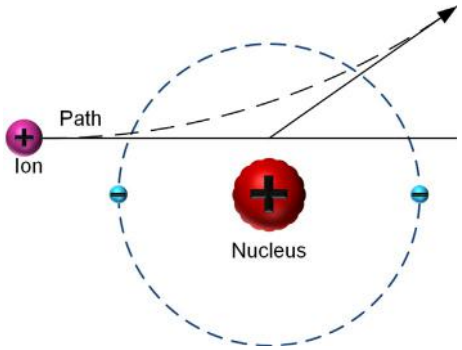

FIG. 5.5

Interaction of heavy ion with nucleus.

straight lines through matter. Because of the small, gradual amount of energy transferred from the ion to the absorber material, the particle passage may be treated as a continuous slowing down process. Near the end of its track, an ion experiences charge exchange between the absorbing material, and picks up electrons until it becomes a neutral atom. The heavy charged particles are the least penetrating radiations for a given energy.

A measure of the rate of ion energy loss with distance x traveled is the *stopping power* S. In the absence of radiative energy loss, S is the local energy deposition into the material known as the linear energy transfer

$$\text{LET} = -dE/dx \tag{5.3}$$

Two separate stopping power components, atomic and nuclear/radiative, add to give the total, as tabulated in the NIST website for electrons, protons, and alpha particles in various materials

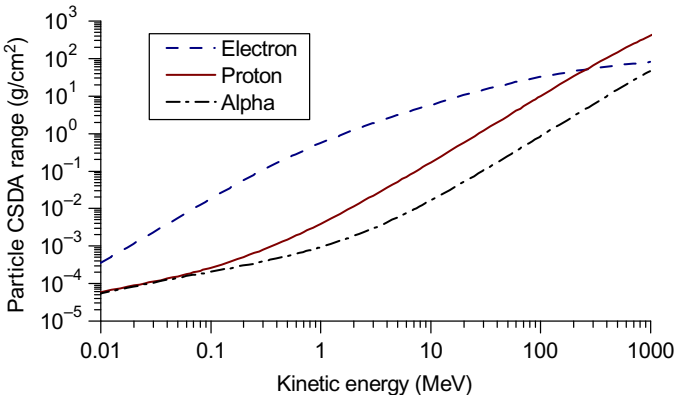

FIG. 5.6

Continuous slowing down approximation (CSDA) range of protons and alpha and beta particles in aluminum.

Data obtained from PSTAR, ASTAR, and ESTAR (Berger, M.J., Coursey, J.S., Zucker, M.A., Chang, J., 2005. Stopping-Power and Range Tables for Electrons, Protons, and Helium Ions (Version 1.2.3), NISTIR 4999. National Institute of Standards and Technology, Gaithersburg, MD).

(Berger et al., 2005). Theoretical formulas giving the dependence on electric charges, masses, and energy are given by Mayo (1998). A related quantity is the *range*, which is the maximum distance of travel of a projectile as it makes multiple collisions in matter. Integration of the reciprocal of the stopping power yields values of the range. A comparison of the continuous slowing down ranges for alphas, betas, and protons in aluminum is given in Fig. 5.6.

The range of an alpha particle in air (at 15°C and 1 atm) is closely approximated by (Sodak, 1962):

$$R_{\text{air}}[\text{cm}] = \begin{cases} 0.56\,E_\alpha & \text{for } E_\alpha < 4\,\text{MeV} \\ 1.24\,E_\alpha - 2.62 & \text{for } 4 \le E_\alpha < 8\,\text{MeV} \end{cases} \tag{5.4}$$

where E_α is the alpha energy in MeV. If the range (R_1) of a heavy particle in one material is known, then the range (R_2) in a second material can be estimated using the Bragg-Kleeman (1905) rule

$$\frac{R_1}{R_2} = \frac{\rho_2}{\rho_1}\sqrt{\frac{M_1}{M_2}} \tag{5.5}$$

where ρ_i and M_i are the density and atomic mass, respectively, of the i-th absorbing material.

EXAMPLE 5.3

Find a relation to convert the heavy ion range in air to a range in an arbitrary material. Air density is taken as 1.205×10^{-3} g/cm^3, but the effective atomic weight of a compound or mixture such as air must be determined from (Bragg and Kleeman, 1905)

$$\sqrt{M_{eff}} = \sum_i \gamma_i \sqrt{M_i} \quad \text{or} \quad \frac{1}{\sqrt{M_{eff}}} = \sum_i \frac{\omega_i}{\sqrt{M_i}} \tag{5.6}$$

where ω_i and γ_i are the weight and atomic fractions, respectively, of the i-th constituent. Using the mass fractions listed in Table 4.3 for nitrogen and oxygen yields

$$\frac{1}{\sqrt{M_{\text{air}}}}=\frac{\omega_{\text{N}}}{\sqrt{M_{\text{N}}}}+\frac{\omega_{\text{O}}}{\sqrt{M_{\text{O}}}}=\frac{0.768}{\sqrt{14.007}}+\frac{0.233}{\sqrt{15.999}}=0.2635$$
$$M_{\text{air}}=14.4\,\text{g/mol}$$

Substituting these values into Eq. (5.5) gives a range in other materials of

$$R=R_{\text{air}}\frac{\rho_{\text{air}}}{\rho}\sqrt{\frac{M}{M_{\text{air}}}}=R_{\text{air}}\frac{1.205\times10^{-3}}{\rho}\sqrt{\frac{M}{14.4}}=3.2\times10^{-4}\frac{\sqrt{M}}{\rho}R_{\text{air}} \tag{5.7}$$

Although air consists of diatomic N_2 and O_2, the effective atomic, rather than molecular, mass must be utilized in these formulas.

EXAMPLE 5.4

Determine the range of a 2 MeV alpha particle in air and the thickness of aluminum needed to stop the alpha particle. Using the first expression of Eq. (5.4), the alpha particle range in air is computed

$$R_{\text{air}}=(0.56\text{cm/MeV})(2\text{MeV})=1.12\text{cm}$$

The aluminum thickness required to shield the 2 MeV alpha is determined from the Bragg-Kleeman rule using the fact that aluminum has an atomic mass of 26.98 and a density of 2.70 g/cm^3

$$R_{\text{Al}}=3.2\times10^{-4}\frac{\sqrt{26.98}}{2.70}(1.12\text{cm})=0.00069\text{cm}=6.9\,\mu\text{m (microns)}$$

An alpha particle has a very small range in solid materials: a sheet of paper is sufficient to stop it and the outer layer of human skin provides protection for sensitive tissue.

Many other simple and detailed range formulas exist for charged particles within a plethora of media. For instance, the approximate range in air of a proton having energy E_{p} of a few MeV to 200 MeV is (Wilson, 1947)

$$R_{\text{air}}\,[\text{m}]=\left(E_{\text{p}}/9.3\right)^{1.8} \tag{5.8}$$

5.4 GAMMA RAY INTERACTIONS WITH MATTER

We now turn to a group of three related processes involving gamma ray photons produced by nuclear reactions. These have energies as high as a few MeV. The interactions include simple scattering of the photon, ionization by it, and a special nuclear reaction known as pair production. Gamma rays are sometimes represented as having higher energies than X-rays, and while this may be true generally, it is not universally valid. Photons such as X-rays and bremsstrahlung with energies in the keV to MeV range undergo these same three processes. Soft x-rays have energies $\lesssim 10$ keV while hard X-rays have higher energies. Other photon interactions include (a) coherent (Rayleigh) scattering, which is elastic scattering with the entire atom, and (b) photonuclear reactions such as fissioning of an atom via a gamma ray at very high energy (see Section 6.2).

5.4.1 PHOTON-ELECTRON SCATTERING

One of the easiest processes to visualize is the interaction of a photon of energy $E = h\nu$ and an electron of rest mass m_e. Although the electrons in a target atom can be regarded as moving and bound to their nucleus, the energies involved are very small (eV) compared with those of typical gamma rays (keV or MeV). Thus, the electrons may be viewed as free stationary particles. The collision may be treated by the physical principles of energy and momentum conservation. As shown in Fig. 5.7, the photon is deflected in its direction and loses energy, becoming a photon of new energy $E' = h\nu'$, which depends on the photon scattering angle θ according to

$$\frac{1}{E'} - \frac{1}{E} = \frac{1}{m_e c^2}[1 - \cos(\theta)] \tag{5.9}$$

Conservation of energy asserts that the kinetic energy of the recoil electron is equal to the energy lost by the photon

$$E_K^e = E - E' \tag{5.10}$$

The electron gains energy and moves away with high-speed v and total mass-energy mc^2, leaving the atom ionized.

EXAMPLE 5.5

Find the recoil energy of an electron that deflects a 1-MeV photon 45°. Combining Eqs. (5.9) and (5.10) leads to

$$\begin{aligned} E_K^e = E - E' &= \frac{(E^2/m_e c^2)[1 - \cos(\theta)]}{1 + (E/m_e c^2)[1 - \cos(\theta)]} \\ &= \frac{\left[(1\,\text{MeV})^2/0.511\,\text{MeV}\right]\left[1 - \cos\left(45^\circ\right)\right]}{1 + (1\,\text{MeV}/0.511\,\text{MeV})\left[1 - \cos\left(45^\circ\right)\right]} = 0.36\,\text{MeV} \end{aligned} \tag{5.11}$$

This is a relativistic electron moving at 81% of the speed of light.

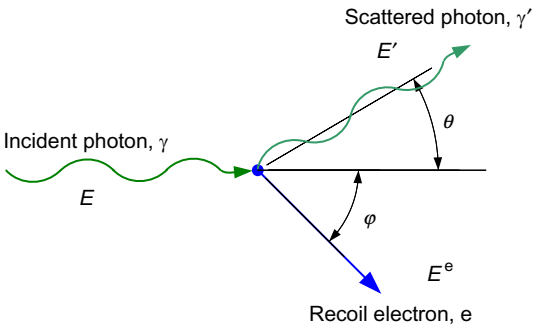

FIG. 5.7

Photon electron scattering (Compton effect).

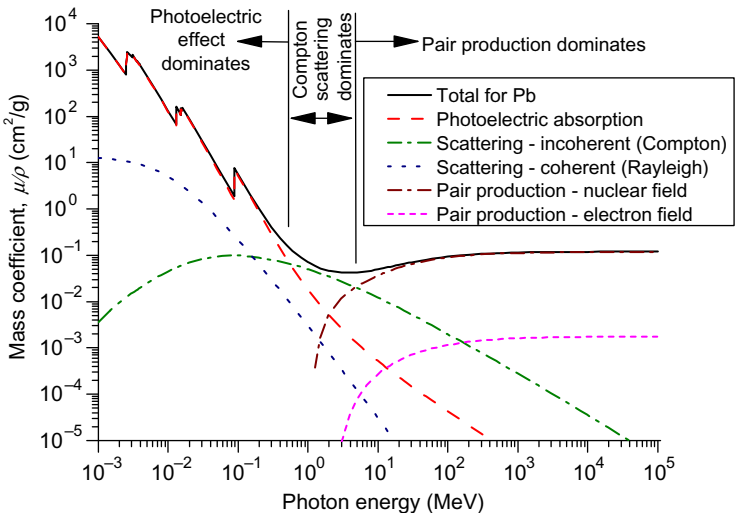

FIG. 5.8

Gamma ray cross-sections in lead, Pb.

Plotted using data from NIST XCOM (Berger et al., 2010) photon cross-sections database.

In this Compton effect (Compton, 1923), named after its discoverer, the greatest photon energy loss occurs when it is scattered backward (180°) from its original direction. Then, if E is much larger than the rest energy of the electron $E_0 = m_e\, c^2 = 0.511\,\text{MeV}$, it is found that the final photon energy E' is equal to $E_0/2$. On the other hand, if E is much smaller than E_0, the fractional energy loss of the photon is $2E/E_0$ (see also Exercise 5.3). The derivation of the photon energy loss in general is complicated by the fact that the special theory of relativity must be applied. In particular, the angular distribution of scattered photons is described by the Klein and Nishina (1929) formula.

The probability of Compton scattering is expressed by a cross-section, which is smaller for larger gamma energies, as shown in Fig. 5.8 for the element lead, a common material for shielding against X-rays or gamma rays. We can deduce that the chance of collision increases with each successive loss of energy by the photon, and eventually the photon disappears.

5.4.2 PHOTOELECTRIC EFFECT

This process is in competition with scattering and dominates at lower photon energy. An incident photon of high enough energy dislodges an electron from the atom, leaving a positively charged ion. In so doing, the photon is absorbed and thus lost (see Fig. 5.9). The ejected electron, known as a *photoelectron*, leaves the atom with a kinetic energy of

$$E_K^e = E_\gamma - I_e \tag{5.12}$$

where E_γ is the energy of the incident photon, and I_e is the ionization potential (or binding energy) of the particular electron to the atom.

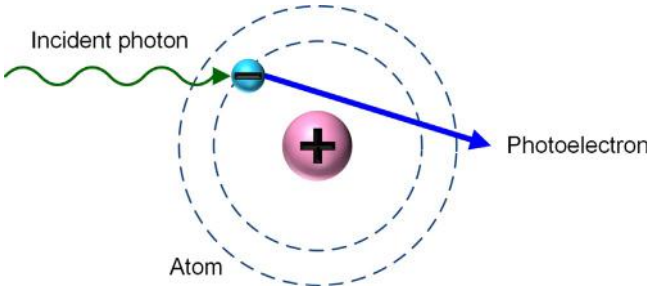

FIG. 5.9

Photoelectric effect, which typically involves an inner shell electron.

The cross-section for the photoelectric effect decreases with increasing photon energy, as graphed in Fig. 5.8 for the element lead. We note discontinuities in μ/ρ near 2.5, 13, and 88 keV corresponding to M, L, and K shell edges, respectively, of Pb (the K, L, M, …, Q shells match to quantum numbers $n = 1$, 2, 3, …, 7 of Section 2.3). Such absorption edges denote energies below which insufficient photon energy exists to eject an atomic electron from that shell.

The preceding two processes are usually treated separately even though both result in ionization. In the Compton effect, a photon of lower energy survives, but in the photoelectric effect, the photon is eliminated. In each case, the electron released may have enough energy to excite or ionize other atoms by the mechanism described in Section 5.2. In addition, the ejection of the electron is followed by characteristic (fluorescent) X-ray or Auger electron emission.

5.4.3 ELECTRON-POSITRON PAIR PRODUCTION

The third process to be considered is one in which the photon is converted into matter. This is entirely in accord with Einstein's theory of the equivalence of mass and energy. In the presence of a strong electromagnetic field such as the Coulombic field generated by the nucleus, as shown in Fig. 5.10, a gamma ray photon disappears and two particles appear: an electron (i.e., negatron e^-) and a positron (e^+).

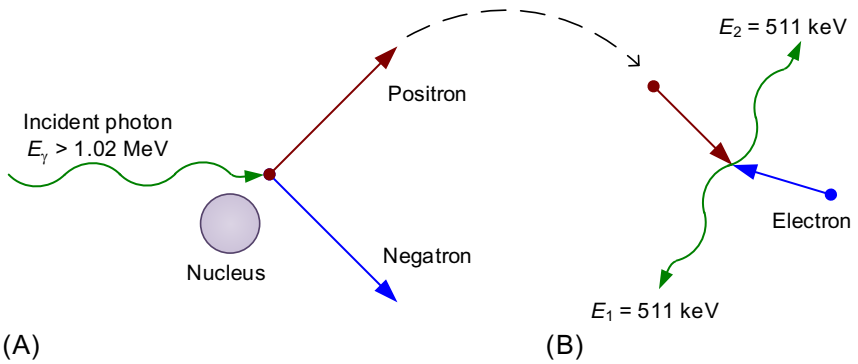

FIG. 5.10

Pair production near the nucleus (A), and later annihilation process (B).

Because these are of equal charge but of opposite sign, there is no net charge after the reaction, just as at the onset, the gamma ray having zero charge. The law of conservation of charge is thus met. The total new mass produced is twice the mass-energy of an electron, $2(0.51) = 1.02\,\text{MeV}$, which means that the reaction can occur only if the gamma ray has at least this amount of energy. Photon energy in excess of 1.02 MeV is equally distributed ($E_K^{e+} = E_K^{e-}$) to the electron-positron pair in the form of kinetic energy

$$E_K^{\text{pair}} = E_K^{e+} + E_K^{e-} = E_\gamma - 2E_0^e \tag{5.13}$$

Considering conservation of momentum, the positron and negatron are propelled in a forward direction relative to the photon direction.

The cross-section for the process of pair production rises from zero, as shown in Fig. 5.8 for lead. The graphical data demonstrate that pair production more often takes place in the vicinity of the nuclear rather than the atomic electron Coulomb field.

The reverse process also takes place. After losing its kinetic energy, the positron has a very short lifetime as it combines with a free electron. As shown in Fig. 5.10, when an electron and a positron combine, they are annihilated as material particles, and two new gamma rays—termed *annihilation radiation*—of energy totaling 1.02 MeV are released. That there must be two photons emitted in opposite directions is a consequence of the principle of momentum conservation.

The reverse process, in which two high-energy photons collide to form an electron-positron pair, is believed to have been common in early times after the Big Bang.

5.4.4 PHOTON ATTENUATION

In contrast with α and β particles, which have a definite range, a certain fraction of incident gamma rays can pass through any thickness of material. The exponential expression $e^{-\Sigma z}$ as used to describe neutron behavior (see Section 4.5) can be carried over to the attenuation of gamma rays in matter. In the case of photons, the scientific community prefers to express interaction probabilities as linear attenuation coefficients μ, which are analogous to neutron macroscopic cross-sections Σ. However, the photon coefficients are tabulated in terms of μ/ρ, being known as the *mass attenuation coefficient* because ρ is the material density. Consider a monoenergetic, unidirectional beam of photons: the Beer-Lambert law describes the uncollided photon intensity as a function of depth x into the material

$$I(x) = I_0 e^{-\mu x} \tag{5.14}$$

To quantify the photon range, one can use the mean free path $\lambda = 1/\mu$ or, better, the half-thickness $x_H = \ln(2)/\mu$ (also called the half-value layer), the distance in which the intensity of a gamma ray beam is reduced by a factor of two.

Similar to neutron cross-sections, the attenuation coefficients are material-specific quantities that vary as a function of energy. Attenuation coefficients for the interaction of photons with most elements are found in the NIST website (Hubbell and Seltzer, 2004). For a chemical compound based on constituent weight fractions ω_i, the mass attenuation coefficient of the mixture is

$$(\mu/\rho)_{\text{mix}} = \sum \omega_i (\mu/\rho)_i \tag{5.15}$$

Fig. 5.8 shows that the total gamma ray cross-section curve for lead (Pb), as the sum of the components for the Compton effect, photoelectric effect, and pair production, exhibits a minimum at approximately 3 MeV energy. This implies that gamma rays in this vicinity are more penetrating than those of higher or lower energy.

EXAMPLE 5.6

Determine the Pb thickness needed to reduce the original gamma flux from Co-60 by a factor of 10. According to Table 3.2, Co-60 emits photons at 1.173 and 1.332 MeV. Using an average gamma energy of 1.25 MeV, an attenuation coefficient of $0.05876\,\text{cm}^2/\text{g}$ is taken from Table A.6. Lead has a density of $11.35\,\text{g/cm}^3$, such that the thickness d may be found from

$$I(d)/I_0 = \exp[-(\mu/\rho)\rho d]$$

$$d = \frac{-\ln[I(d)/I_0]}{(\mu/\rho)\rho} = \frac{-\ln(0.1)}{(0.05876\,\text{cm}^2/\text{g})(11.35\,\text{g/cm}^3)} = 3.45\,\text{cm}$$

Later in Section 11.3, we will realize that this example has been worded carefully because scattering does not destroy a photon, but merely reduces its energy.

Because photon attenuation does not mean that all the photon energy is absorbed (e.g., consider Compton scattering in which only a fraction of the photon energy is transferred to an electron), it is necessary to introduce another quantity—the energy-absorption coefficient μ_{en}. To contrast the attenuation and absorption coefficients, we should employ μ in the calculation of probabilities of removing radiation from a beam, and use μ_{en} in the calculation of radiation dose (i.e., energy deposition), as will be done in Chapter 11. Comparing photon attenuation versus absorption coefficients reveals that $\mu \geq \mu_{\text{en}}$.

5.5 NEUTRON REACTIONS

For completeness, we briefly review the interaction of neutrons with matter. While the massless photon predominantly interacts with the atomic electrons, a neutron interacts with the nucleus. Neutrons may be scattered by nuclei elastically or inelastically, may be captured with resulting gamma ray emission, or may cause fission. If their energy is high enough, neutrons may induce (n, p), (n, d), and (n, α) reactions as well. Because the direct ionization from photons and neutrons is insignificant compared to the ionization from their secondary radiation, they are referred to as *indirectly ionizing radiation*. It is noteworthy that the neutral radiations are most often detected and measured through their interactions that produce charged particles.

We are now in a position to understand the connection between neutron reactions and atomic processes. When a high-speed neutron strikes the hydrogen atom in a water molecule, a proton is ejected, resulting in chemical dissociation of the H_2O. A similar effect takes place in molecules of cells in any biological tissue. The proton compared with the electron is a heavy charged particle. It passes through matter, slowing and creating ionization along its path. Thus, two types of neutron radiation damage take place: primary (chemical dissociation) and secondary (ionization).

After many collisions, the neutron arrives at a low enough energy that it can be readily absorbed. If it is captured by the proton in a molecule of water or some other hydrocarbon, a gamma ray is released, as discussed in Chapter 4. The resulting deuteron recoils with energy that is much smaller than that of the gamma ray (see Exercise 4.5) but still is far greater than the energy of binding of atoms in the water molecule. Again, dissociation of the compound takes place, which can be regarded as a form of radiation damage. Alternatively, the neutron could have been absorbed by a different nuclide resulting in radioactive decay to a different element, constituting an impurity, as discussed in the next section.

5.6 RADIATION EFFECTS AND DAMAGE

With knowledge of the basic interactions that radiation undergoes at the atomic level, the engineer/scientist can propagate these mechanisms to the resultant macroscopic (radiation) effects on the materials present. The radiation effects can be either beneficial or detrimental. For instance, ionization may manifest itself in terms of reduced performance and inoperability in electronic devices and circuits; consider the discoloration of fiber optics due to photon irradiation, resulting in the loss of light transmissibility. Conversely, knowledge of radiation has led to the development of novel processing approaches, for instance neutron transmutation doping of semiconductors (see Section 14.8).

Ionizing radiation tends to be increasingly damaging in the following order of molecular formation (largely due to the ability of ionization to disrupt the bonds):

(a) Metallic bond (least damaged).
(b) Ionic bond.
(c) Covalent bond (most damaged).

Because biological tissue is characterized by substantial covalent bonding, it is generally more susceptible to radiation damage than metallic-bonded structural components.

EXAMPLE 5.7

Let us use salt (NaCl) as an example. Sodium transfers its loosely bound valence electron to chlorine, such that Na^+Cl^- is formed. Ionization of the sodium cation would result in a doubly charged Na ion, and the Na^{2+} would continue to be attracted to the Cl^- anion. Conversely, ionization of the Cl^- anion would result in the chlorine atom returning to a neutral state, and the Na^+ cation is no longer attracted to the chlorine atom, and hence, the ionic bond is broken.

Another radiation effect, termed displacement damage, is the result of nuclear interactions, typically scattering, that cause lattice defects within the absorbing material. The atomic scattering can be studied via kinematic and/or Monte Carlo analyses. Neutrons are particularly adept at causing atomic displacements.

Besides ionization and energy deposition, introduction of radiation into a material can result in detrimental or purposeful creation of impurities. For instance, as an ion slows, it captures electron(s) to form a neutral atom (e.g., a proton becomes hydrogen, and an alpha particle forms helium). As another example, an absorbed neutron may create a radionuclide that subsequently decays into a different element. Even ionization itself can cause impurity production, as illustrated in the following example.

EXAMPLE 5.8

Beta and gamma radiation can ionize an electron from a water molecule, thereby causing *radiolysis*—radiation-induced molecular decomposition. The ionization of the electron results in

$$H_2O \xrightarrow{\text{ionizing radiation}} H_2O^+ + e^- \tag{5.16}$$

Then the free electron and ionized water molecule may react with other water molecules, according to (Stephenson, 1958)

$$\begin{aligned} H_2O^+ + H_2O &\rightarrow H_3O^+ + OH \\ e^- + H_2O &\rightarrow OH^- + H \end{aligned} \tag{5.17}$$

where OH^- is hydroxide and H_3O^+ is hydronium. Further reactions may produce hydrogen (H_2) and hydrogen peroxide (H_2O_2), which is a strong oxidizing agent. As an adult human comprises 60% water (International Commission on Radiological Protection (ICRP), 1975), we surmise that ionizing radiation negatively impacts cellular functionality.

At the macroscopic level, radiation can cause changes to a variety of material properties, including chemical, electrical, magnetic, mechanical, optical, and so on. The effects of radiation on the mechanical (and metallurgical) properties include changes to strength and ductility. Neutron irradiation increases the yield strength and decreases the ductility of most metals (Was, 2007) while polymers experience a loss of tensile strength (Van Vlack, 1985).

5.7 SUMMARY

Radiation of special interest includes electrons, heavy charged particles, photons, and neutrons. Each of the particles tends to lose energy by interaction with the electrons and nuclei of matter, and each creates ionization in different degrees. The ranges of beta particles and alpha particles are short, but gamma rays and neutrons penetrate in accord with an exponential law. Gamma rays can also produce electron-positron pairs. Neutrons of both high and low energy can create radiation damage in molecular materials.

5.8 EXERCISES

5.1 The charged particles in a highly ionized electrical discharge in hydrogen gas—protons and electrons, mass ratio $m_p/m_e = 1836$—have the same energies. What is the ratio of the speeds v_p/v_e? Of the momenta p_p/p_e?

5.2 A gamma ray from neutron capture has an energy of 6 MeV. What is its frequency? What is its wavelength?

5.3 For 180° scattering of gamma or X-rays by electrons of rest mass E_0, (a) verify that the final energy of the photon is

$$E' = \left(\frac{1}{E} + \frac{2}{E_0}\right)^{-1}$$

(b) What is the final photon energy for the 6 MeV gamma ray of Exercise 5.2? (c) Verify that if $E \gg E_0$, then $E' \cong E_0/2$ and if $E \ll E_0$, $(E - E')/E \cong 2E/E_0$. (d) Which approximation should be used for a 6-MeV gamma ray? Verify numerically. (e) Show that the final (maximum) electron energy is

$$E^e_{K,\max} = \frac{E}{1 + E_0/(2E)}$$

5.4 An electron-positron pair is produced by a gamma ray of 2.26 MeV. What is the kinetic energy imparted to each of the charged particles?

5.5 Estimate the thickness of paper required to stop 2 MeV alpha particles, assuming the paper to be of density 1.29 g/cm^3, about the same effective atomic mass as air (i.e., $M_{paper} \approx M_{air}$), density 1.29×10^{-3} g/cm^3.

5.6 The element lead, $M = 207.2$, has a density of $11.35\,\text{g/cm}^3$. (a) Find the number of atoms per cubic centimeter. If the total gamma ray cross-section at 3 MeV is 14.6 barns, what are (b) the linear attenuation coefficient and (c) the half-thickness?

5.7 The range of beta particles of maximum energy between 0.8 and 3.0 MeV is given roughly by the Feather (1938) relation

$$R[\text{cm}] = \frac{0.543E[\text{MeV}] - 0.160}{\rho[\text{g/cm}^3]}$$

(a) Using this formula, find what thickness of aluminum sheet (density $2.7\,\text{g/cm}^3$) is enough to stop the betas from phosphorus-32 (see Table 3.2). (b) Repeat the calculation using the Katz-Penfold relation of Eq. (5.2).

5.8 A radiation worker's hands are exposed for 5 s to a $3 \times 10^8/(\text{cm}^2\ \text{s})$ beam of 1 MeV beta particles. Find the range in tissue of density $1.0\,\text{g/cm}^3$ and calculate the amounts of charge and energy deposition in C/cm^3 and J/g. Note that the charge on the electron is 1.60×10^{-19} C. For tissue, use the equation in Exercise 5.7.

5.9 Calculate the energy gain by an electron struck head-on by an alpha particle of energy 4 MeV; see Exercise 4.19. How many such collisions would it take to reduce the alpha particle energy to 1 MeV?

5.10 At a certain time after the Big Bang, high-speed photons collided to form electrons and positrons. Assuming energies of 0.51 MeV each, what temperature is implied?

5.11 Find the percentage reduction through 1.5 cm of lead from a gamma-ray flux produced by (a) ^{137}Cs, (b) ^{40}K, and (c) ^{99}Mo.

5.12 Find the resultant maximum and minimum photon energies of incident 50-keV X-rays passing through a thin aluminum foil and making no more than one collision.

5.13 Compare the percent energy change of 10 keV and 10 MeV photons scattered at 90°. What conclusion do these results suggest?

5.14 (a) Find the fractional energy loss for a 20-keV X-ray scattered from an electron at angle 180° and compare with $2E/E_0$. (b) Find the final energy for a 10-MeV gamma ray scattered from an electron at 180° and compare with $E_0/2$.

5.15 Revisit Exercise 4.19 for the case of $\mathbf{u_2} = 0$ with $m_2 \ll m_1$. Verify that the final energy of m_2 is $E_2 = 4\,E_1 m_2/m_1$ where E_1 is the initial energy of m_1.

5.16 Determine the kinetic energy (in MeV) at which the following particles can be considered relativistic: (a) electron, (b) proton, (c) neutron, (d) deuteron, (e) triton, and (f) alpha.

5.17 Confirm the consistency between the two expressions of Eq. (5.1) when considering that $E_{\beta,\text{avg}} \cong E_{\beta,\text{max}}/3$.

5.18 Compute the mass attenuation coefficient for U_3O_8 at 1.25 MeV given that μ/ρ for uranium and oxygen are 0.06370 and $0.05697\,\text{cm}^2/\text{g}$, respectively.

5.19 Compute the half-thickness of gamma rays from Cs-137 for shielding composed of (a) lead, (b) iron, (c) concrete, and (d) water.

5.20 Find the range in (a) air and (b) tissue of an alpha particle emitted by Po-210. Tissue has a similar effective atomic mass as air (i.e., $M_{\text{tissue}} \approx M_{\text{air}}$), but a density more like water.

5.21 Use Eq. (4.17) and the data of Table A.5 to compute the −13.6 eV electron ionization energy of hydrogen.

5.9 COMPUTER EXERCISES

5.A The ESTAR, PSTAR, and ASTAR programs (Berger et al., 2005) from NIST[1] compute stopping power and range tables for electrons, protons, and alpha particles, respectively. Similar to Fig. 5.6, make a graph comparing the continuous slowing down range of these particles in (a) graphite, (b) silicon, (c) dry air, (d) Pyrex glass, (e) polyethylene, and (f) tissue.

5.B Use the compilations of X-ray mass attenuation and energy-absorption coefficients available from NIST[2] to create a graph of both μ/ρ and μ_{en}/ρ for each of the following: (a) Pb, (b) lead glass, (c) cadmium telluride, (d) water, and (e) SiO_2 (see Fig. 11.2 for an example using tissue).

5.C The XCOM program (Berger et al., 2010) from NIST[3] calculates photon cross-sections for scattering, photoelectric absorption, and pair production. Akin to Fig. 5.8, create a plot of photon mass coefficients for (a) iron, (b) water, (c) dry air, (d) ordinary concrete, and (e) soft tissue. Elemental compositions of the latter three mixtures can be found at http://physics.nist.gov/PhysRefData/XrayMassCoef/tab2.html.

REFERENCES

Berger, M.J., Coursey, J.S., Zucker, M.A., Chang, J., 2005. Stopping-Power and Range Tables for Electrons, Protons, and Helium Ions (Version 1.2.3). NISTIR 4999, National Institute of Standards and Technology, Gaithersburg, MD.

Berger, M.J., Hubbell, J.H., Seltzer, S.M., Chang, J., Coursey, J.S., Sukumar, R., Zucker, D.S., Olsen, K., 2010. XCOM: Photon Cross Sections Database (Version 1.5). NBSIR 87-3597, National Institute of Standards and Technology, Gaithersburg, MD.

Bragg, W.H., Kleeman, R., 1905. On the α particles of radium, and their loss of range in passing through various atoms and molecules. Philos. Mag. Ser. 6 10 (57), 318–340.

Cember, H., Johnson, T.E., 2009. Introduction to Health Physics, fourth ed. McGraw-Hill, New York.

Compton, A.H., 1923. A quantum theory of the scattering of X-rays by light elements. Phys. Rev. 21 (5), 483–502.

Feather, N., 1938. Further possibilities for the absorption method of investigating the primary β-particles from radioactive substances. Math. Proc. Camb. Philos. Soc. 34 (4), 599–611.

Gallo, C.F., Lama, W.L., 1974. Electrostatic model for the correlation between the work function and the ionization energy of the metallic elements. IEEE Trans. Ind. Appl. 10 (4), 496–500.

Hubbell, J.H., Seltzer, S.M., 2004. Tables of X-Ray Mass Attenuation Coefficients and Mass Energy-Absorption Coefficients (Version 1.4). NISTIR 5632, National Institute of Standards and Technology, Gaithersburg, MD. http://physics.nist.gove/xaamdi.

International Atomic Energy Agency (IAEA), 1995. Atomic and Molecular Data for Radiotherapy and Radiation Research. IAEA-TECDOC-799, IAEA, Vienna. pp. 396, 576.

International Commission on Radiological Protection (ICRP), 1975. Report of the Task Group on Reference Man. Report No. 23. Pergamon Press, Oxford, p. 24.

Katz, L., Penfold, A.S., 1952. Range-energy relations for electrons and the determination of beta-ray end-point energies by absorption. Rev. Mod. Phys. 24 (1), 28–44.

[1] http://physics.nist.gov/Star
[2] http://physics.nist.gov/xaamdi
[3] http://physics.nist.gov/xcom

Klein, O., Nishina, Y., 1929. Über die Streuung von Strahlung durch freie Elektronen nach der neuen relativistischen Quantendynamik von Dirac (On the scattering of radiation by free electrons according to Dirac's new relativistic quantum dynamics). Z. Phys. 52 (11), 853–868.
Knoll, G.F., 2000. Radiation Detection and Measurement, third ed. Wiley, New York.
Martin, W.C., Musgrove, A., Kotochigova, S., Sansonetti, J.E., 2011. Ground Levels and Ionization Energies for the Neutral Atoms (version 1.4.1). physics.nist.gov/IonEnergy, National Institute of Standards and Technology, Gaithersburg, MD.
Mayo, R.M., 1998. Introduction to Nuclear Concepts for Engineers. American Nuclear Society, La Grange Park.
Sodak, H. (Ed.), 1962. Reactor Handbook, Vol. III, Part A Physics, second ed. Inter Science Publishers, New York, p. 30.
Stephenson, R., 1958. Introduction to Nuclear Engineering, second ed. McGraw-Hill, New York, pp. 244–245.
Van Vlack, L.H., 1985. Elements of Materials Science and Engineering, fifth ed. Addison-Wesley Publishing Co., Reading.
Was, G.S., 2007. Fundamentals of Radiation Materials Science. Springer, Berlin.
Wilson, R.R., 1947. Range, straggling, and multiple scattering of fast protons. Phys. Rev. 71 (6), 385–386.

FURTHER READING

Bethe, H.A., Bacher, R.F., Livingston, M.S., 1986. Basic Bethe, Seminal Articles on Nuclear Physics, 1936–1937. American Institute of Physics and Springer-Verlag, New York.
Choppin, G., Liljenzin, J.-O., Rydberg, J., 2002. Radiochemistry and Nuclear Chemistry, third ed. Butterworth-Heinemann, Woburn.
Faw, R.E., Shultis, J.K., 1999. Radiological Assessment: Sources and Doses. American Nuclear Society, La Grange Park, IL.
Segrè, E., 1977. Nuclei and Particles, second ed. Benjamin-Cummings, Reading, MA.
Shultis, J.K., Faw, E.R., 1996. Radiation Shielding. Prentice-Hall, Upper Saddle River, NJ.
Turner, J.E., 2005. Interaction of ionizing radiation with matter. Health Phys. 88 (6), 520–544.
Turner, J.E., 2007. Atoms, Radiation, and Radiation Protection, third ed. Wiley, New York.

CHAPTER

FISSION

6

CHAPTER OUTLINE

Out of the many nuclear reactions known, the reaction that results in fission has, at present, the greatest practical significance. In this chapter, we will describe the mechanism of the process, identify the byproducts, introduce the concept of the chain reaction, and look at the energy yield from the consumption of nuclear fuels.

6.1 THE FISSION PROCESS

The absorption of a neutron by most isotopes involves radiative capture, with the nuclear excitation energy appearing as a gamma ray. In certain heavy elements, notably uranium and plutonium, an alternate consequence is observed: the splitting of the nucleus into two massive fragments, a process called *fission*—a term from cellular division adopted by Meitner and Frisch (1939). Fig. 6.1 shows the sequence of events by use of the reaction with U-235. In Stage A, the neutron approaches the U-235 nucleus. In Stage B, the U-236 compound nucleus has been formed in an excited state. The excess energy in some cases may be released as a gamma ray, but more frequently, the energy causes distortions of the nucleus into a dumbbell shape, as in Stage C. The parts of the nucleus oscillate in a manner analogous to the motion of a drop of liquid (Bohr and Wheeler, 1939). Because of the dominance of electrostatic repulsion over nuclear attraction, the two parts can separate, as in Stage D. They are then called fission fragments, bearing most of the energy released. They fly apart at high speeds, carrying some 166 MeV of kinetic energy out of the total of approximately

Nuclear Energy. https://doi.org/10.1016/B978-0-12-812881-7.00006-X

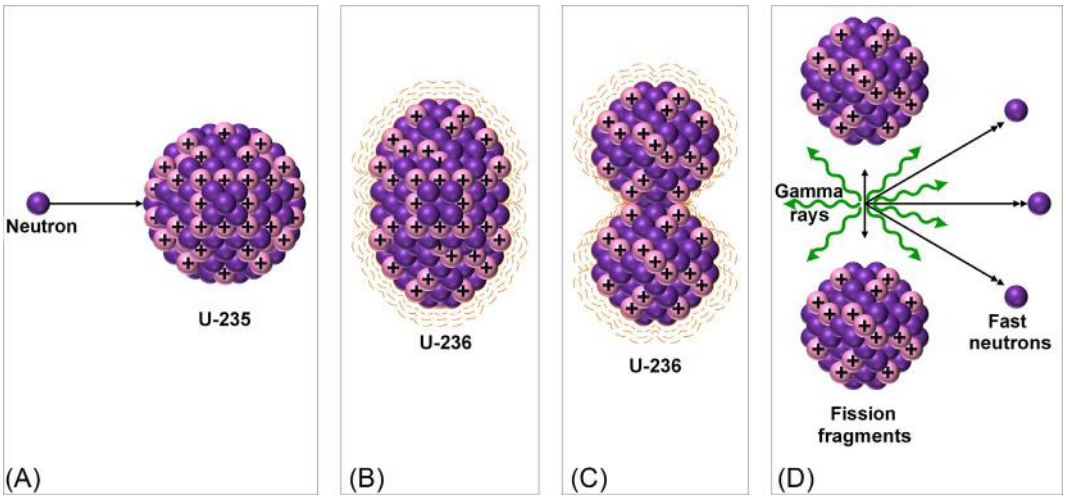

FIG. 6.1

The fission process. (A) A neutron approaches a U-235 nucleus; (B) the U-236 compound nucleus is formed in an excited state and elongated; (C) the nucleus further distorts into the shape of a dumbbell; and (D) the nucleus separates into fission fragments, fast neutrons, and gamma rays.

200 MeV released in the whole process. As the fragments separate, they lose atomic electrons, and the resulting high-speed ions lose energy by interaction with the atoms and molecules of the surrounding medium. The resultant thermal energy is recoverable if the fission takes place in a nuclear reactor. Also shown in the Stage D diagram are the prompt gamma rays and fast neutrons that are released at the time of splitting. This entire fission process occurs over a period of about 10^{-15} s (Gozani, 1981).

6.2 ENERGY CONSIDERATIONS

The absorption of a neutron by a nucleus such as U-235 gives rise to extra internal energy of the product because the sum of the masses of the two interacting particles is greater than that of a normal U-236 nucleus. We write the first step in the reaction

$$^{235}_{92}\mathrm{U} + ^{1}_{0}\mathrm{n} \rightarrow \left(^{236}_{92}\mathrm{U}\right)^{*} \tag{6.1}$$

where the asterisk (*) signifies the excited state. The mass of (U-236)* in atomic mass units is

$$M_{\text{U-236}^*} = M_{\text{U-235}} + m_{\text{n}} = 235.043930 + 1.008665 = 236.052595$$

However, U-236 in its ground state has a mass of only 236.045568 (see Table A.5), lower by 0.007027 amu or 6.55 MeV. This amount of excess energy is sufficient to cause fission. Fig. 6.2 shows these energy relationships.

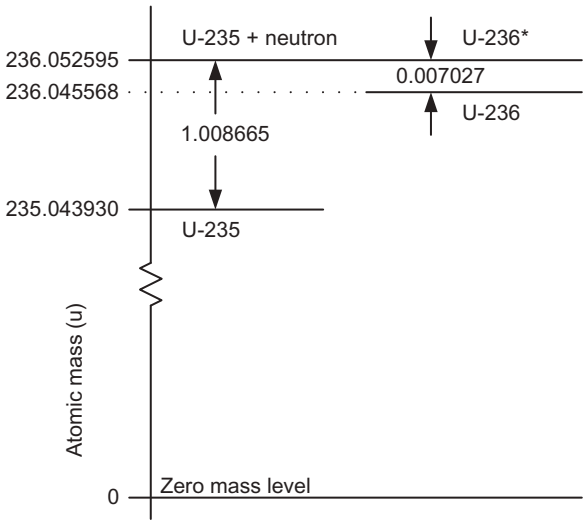

FIG. 6.2

Excitation energy caused by neutron absorption.

It may be surprising that the introduction of only 6.55 MeV of excitation energy can produce a reaction yielding as much as 200 MeV. The explanation is that the excitation triggers the separation of the two fragments and the powerful electrostatic force provides them a large amount of kinetic energy. By conservation of mass-energy, the mass of the nuclear products is smaller than the mass of the compound nucleus from which they emerge.

The preceding calculation did not include any kinetic energy brought to the reaction by the neutron, on the grounds that fission can be induced by absorption in U-235 of very slow neutrons. Only one natural isotope, ^{235}U, undergoes fission in this way, whereas ^{239}Pu and ^{233}U are the main artificial isotopes that do so. Most other heavy isotopes require significantly larger excitation energy to bring the compound nucleus to the required energy level for fission to occur, and the extra energy must be provided by the motion of the incoming neutron. For example, neutrons of at least 0.9 MeV are required to cause significant fission from U-238, and other isotopes require even higher energy. The resultant terminology is as follows: *fissionable* isotopes are those nuclides that can undergo fission while *fissile* materials are fissioned readily with slow (thermal) neutrons. Common fissionable isotopes are ^{232}Th and ^{238}U, and the subset of fissile materials including ^{233}U, ^{235}U, and ^{239}Pu. Fig. 6.3 compares the fission cross-sections for fissile ^{235}U and ^{239}Pu to that of ^{238}U, which has a σ_f that is more than seven orders of magnitude smaller at thermal energies. It is advantageous to use fast neutrons—of the order of 1 MeV energy—to cause fission. As will be discussed in Chapter 25, the fast reactor permits the breeding of nuclear fuel.

In a few elements, such as californium, *spontaneous fission* takes place. The isotope ^{252}Cf, produced artificially by a sequence of neutron absorptions, has a half-life of 2.645 y and undergoes complex decay by alpha emission (96.9%) and spontaneous fission (3.1%). A small but important amount of spontaneous fission occurs in Pu-240 in competition with alpha decay.

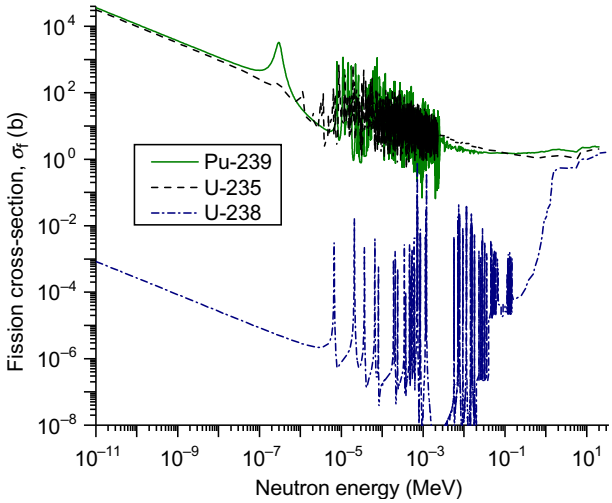

FIG. 6.3

Microscopic fission cross-sections for two fissile materials (U-235 and Pu-239) and a fissionable nuclide (U-238).
Data from ENDF/B-VII.1 (Chadwick, M.B., Herman, M., Obložinský, P., Dunn, M.E., Danon, Y., Kahler, A.C., et al., 2011. ENDF/B-VII.1 Nuclear data for science and technology: cross-sections, covariances, fission product yields and decay data. Nucl. Data Sheets 112 (12), 2887–2996).

EXAMPLE 6.1

Find the neutron emission rate per gram of Cf-252. The specific activity of ^{252}Cf is

$$SA = \frac{\lambda N_A}{M} = \frac{\ln(2)\left(6.022 \times 10^{23}\,\text{atom/mol}\right)}{\left(3.1558 \times 10^{7}\,\text{s/y}\right)(2.645\,\text{y})(252\,\text{g/mol})} = 1.98 \times 10^{13}\,\text{Bq/g}$$

Because only 3.1% of the decays are spontaneous fission (SF) events in which ^{252}Cf emits 3.757 neutrons (see Table 6.1), the SF neutron yield is

$$Y = \left(1.98 \times 10^{13}\,\text{decay/(gs)}\right)(0.031\,\text{SF/decay})(3.757\,\text{n/SF}) = 2.31 \times 10^{12}\,\text{n/(gs)}$$

Table 6.1 Spontaneous Fission Data

Isotope	Total Half-Life (y)	Spontaneous Fission Half-Life (y)	Spontaneous Neutron Yield per Fission, ν (n/fission)
U-232	71.7	8×10^{13}	1.71
U-238	4.47×10^{9}	8.20×10^{15}	2.01
Pu-238	87.74	4.77×10^{10}	2.21
Pu-239	2.41×10^{4}	5.48×10^{15}	2.16
Pu-240	6.56×10^{3}	1.16×10^{11}	2.16
Am-241	433.6	1.05×10^{14}	3.22
Cf-252	2.646	85.5	3.757

Data from Reilly, D., Ensslin, N., Smith, Jr. H., 1991. Passive Nondestructive Assay of Nuclear Materials, NUREG/CR-5550, 339. Referred to as PANDA.

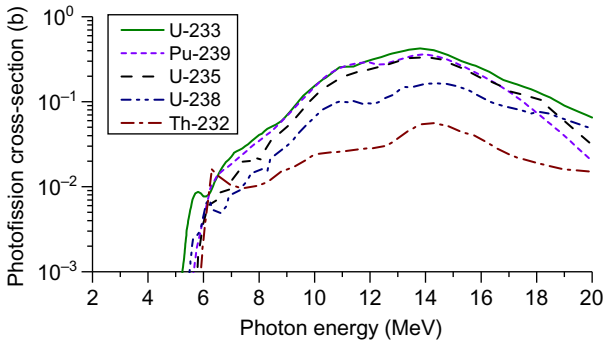

FIG. 6.4

Microscopic photofission cross-sections for a few fissionable nuclides.

Data from ENDF/B-VII.1 (Chadwick, M.B., Herman, M., Obložinský, P., Dunn, M.E., Danon, Y., Kahler, A.C., et al., 2011. ENDF/B-VII.1 Nuclear data for science and technology: cross-sections, covariances, fission product yields and decay data. Nucl. Data Sheets 112 (12), 2887–2996).

Fission can also be initiated by high-energy gamma rays. Fig. 6.4 shows that the photofission (γ, f) cross-sections are less than one barn. Photofission requires a threshold energy of around 5 MeV (Hyde, 1964).

6.3 BYPRODUCTS OF FISSION

Accompanying the fission process is the release of several neutrons, which are all important for the practical application to a self-sustaining chain reaction. The numbers of neutrons per fission that appear, ν (nu), range from 1 to 7, with an average in the range of 2–3, depending on the isotope and the bombarding neutron energy; see Table 6.2. For example, in U-235 with slow neutrons, the average number ν is 2.44. Most of these are released instantly, the so-called prompt neutrons, whereas a small percentage, 0.65% for U-235, appear later as the result of radioactive decay of certain fission fragments. These delayed neutrons provide considerable inherent safety and controllability in the operation

Table 6.2 Neutron Yield From Fission

Nuclide	Fission Type	Prompt Neutron Yield (ν_p)	Delayed Neutron Yield (ν_d)	Total Neutron Yield (ν)
Th-232	Fast	2.406	0.0499	2.456
U-233	Thermal	2.490	0.0067	2.4968
U-235	Thermal	2.419	0.0162	2.4355
U-238	Fast	2.773	0.0465	2.819
Pu-239	Thermal	2.877	0.0065	2.8836
Am-241	Thermal	3.235	0.0043	3.239

Data from International Atomic Energy Agency (IAEA), 2008. Handbook of Nuclear Data for Safeguards: Database Extensions. IAEA, INDC(NDS)-0534.

of nuclear reactors, as we will see in Section 20.2. The number of neutrons produced increases linearly with the bombarding neutron energy (Gozani, 1981). The mechanism initiating fission also affects the number of neutrons produced; for example, the ν for Pu-239 thermal fission in Table 6.2 is 34% larger than that for spontaneous fission in Table 6.1.

The nuclear reaction equation for fission resulting from neutron absorption in U-235 may be written in general form, letting the chemical symbols for the two fragments be labeled F_1 and F_2 to indicate many possible ways of splitting. Thus

$$^{235}_{92}\mathrm{U} + {}^{1}_{0}\mathrm{n} \rightarrow {}^{A_1}_{Z_1}F_1 + {}^{A_2}_{Z_2}F_2 + \nu\ {}^{1}_{0}\mathrm{n} + \text{energy} \tag{6.2}$$

The appropriate mass numbers and atomic numbers are attached. One example, in which the fission fragments are isotopes of krypton and barium, is

$$^{235}_{92}\mathrm{U} + {}^{1}_{0}\mathrm{n} \rightarrow {}^{90}_{36}\mathrm{Kr} + {}^{144}_{56}\mathrm{Ba} + 2{}^{1}_{0}\mathrm{n} + Q \tag{6.3}$$

EXAMPLE 6.2

Determine the immediate energy release from the fission reaction of Eq. (6.3). Using Eq. (4.17) and the atomic masses from Table A.5 (Appendix A) gives

$$\begin{aligned} Q &= [(M_{\text{U-235}} + m_{\text{n}}) - (M_{\text{Kr-90}} + M_{\text{Ba-144}} + 2m_{\text{n}})]c^2 \\ &= [(235.043930131) - (89.919527931 + 143.922954866 + 1.008664916)]\,\text{u}\,(931.5\,\text{MeV/u}) \\ &= 179.6\,\text{MeV} \end{aligned}$$

Mass numbers ranging from 70 to 164 are observed with the most probable at approximately 95 and 134 for thermal fission, as plotted in Fig. 6.5. The ordinate on this graph is the percentage yield of each mass number (e.g., approximately 6% for mass numbers 92 and 143). If the number of fissions is given,

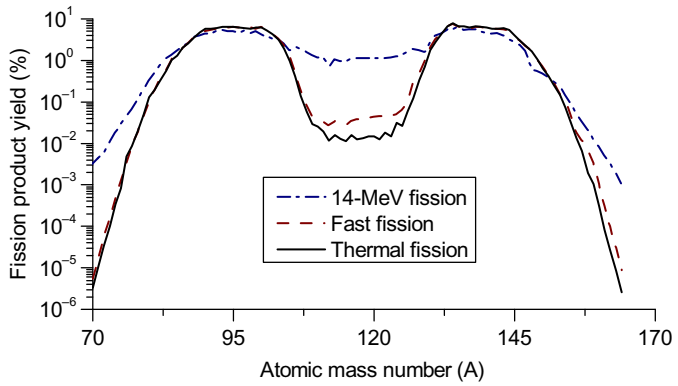

FIG. 6.5

Yield of U-235 fission products according to mass number.

Data from International Atomic Energy Agency (IAEA), 2008. Handbook of Nuclear Data for Safeguards: Database Extensions. IAEA, INDC(NDS)-0534.

the number of atoms of those types is 0.06 as large. The graph reveals that the energy of the neutron initiating the reaction affects the fission product yield. Not shown on the plot is the fact that some low A nuclides are produced by *ternary fission*, which yields three fission fragments. For instance, 0.17% of the fission products from U-235 thermal fission have an A of 4 (International Atomic Energy Agency (IAEA), 2008).

As a collection of isotopes, these byproducts are called fission products. The isotopes have an excess of neutrons or a deficiency of protons compared with naturally occurring elements. For example, consider the fission product $^{144}_{56}$Ba; the most abundant isotope of barium is $^{138}_{56}$Ba, and a prominent element of mass 144 is $^{144}_{60}$Nd. Thus, there are six extra neutrons or four too few protons in the barium isotope from fission, and $^{144}_{56}$Ba is highly unstable. Radioactive decay, usually involving several emissions of beta particles and delayed gamma rays in a chain of events, brings the fragments down to stable forms. For instance, Kr-90 undergoes successive β^- decays accompanied by emissions of gamma rays with various energies

$$^{90}_{36}\mathrm{Kr} \xrightarrow{32.3\ \mathrm{s}} {}^{90}_{37}\mathrm{Rb} \xrightarrow{2.6\ \mathrm{min}} {}^{90}_{38}\mathrm{Sr} \xrightarrow{29.1\ \mathrm{y}} {}^{90}_{39}\mathrm{Y} \xrightarrow{2.67\ \mathrm{d}} {}^{90}_{40}\mathrm{Zr} \tag{6.4}$$

The hazard associated with the radioactive emanations from fission products is evident when we consider the large yields and the short half-lives.

EXAMPLE 6.3

Determine the delayed energy release from the Kr-90 decay chain of Eq. (6.4). For each decay step, the parent P emits a β particle while leaving the daughter D missing an electron; hence, the Q value of each transformation is

$$Q_\beta = \left[M_P - (M_D - m_e) - m_{\beta-}\right] c^2 = \left[M_P - M_D\right] c^2 \tag{6.5}$$

The overall energy release due to the four beta decays is

$$\begin{aligned} Q &= (M_{\text{Kr-90}} - M_{\text{Zr-90}})c^2 \\ &= (89.919527931\,\text{u} - 89.904697659\,\text{u})(931.5\,\text{MeV/u}) \\ &= 13.8\,\text{MeV} \end{aligned}$$

Based on the half-lives shown in Eq. (6.4) and a fuel residence time of several years, we surmise that much of the energy release from the first two decay steps occurs while the fuel is within the reactor, but recognize that some energy is carried away by neutrinos.

The total energy from fission, after all the particles from decay have been released, is approximately 200 MeV. This is distributed among the various processes, as shown in Table 6.3. Approximately seven prompt gamma rays with an energy of ~1 MeV each (Verbinski et al., 1973) are emitted as a part of fission; the rest are fission product decay gammas. Neutrinos accompany the beta particle emission, but because they are such highly penetrating particles, their energy cannot be counted as part of the useful thermal energy yield of the fission process. Thus, only approximately 190 MeV of the fission energy is effectively available for recovery. However, several MeV of energy from gamma rays released from nuclei that capture neutrons can also be extracted as useful heat.

The average total neutron energy is noted to be 5 MeV. If there are approximately 2.5 neutrons per fission, the average neutron energy is 2 MeV. When one observes many fission events, the neutrons are found to range in energy from nearly zero to more than 10 MeV, as seen in Fig. 6.6, with a most likely

Table 6.3 Average Energy (MeV) Released from Fission

Fission Energy Component	U-233	U-235	Pu-239
Fission fragment kinetic energy	168.2	169.1	175.8
Prompt neutron kinetic energy	4.9	4.8	5.9
Prompt gamma rays	7.7	7.0	7.8
Decay gamma rays	5.0	6.3	5.2
Decay beta particles	5.2	6.5	5.3
Decay neutrinos	6.9	8.8	7.1
Total	197.9	202.5	207.1

Data from Sher, R., 1981. Fission energy release for 16 fissioning nuclides, In: Proceedings of the Conference on Nuclear Data Evaluation Methods and Procedures, Brookhaven National Laboratory, 22–25 September 1980, BNL-NCS-51363, vol. II, pp. 835–860.

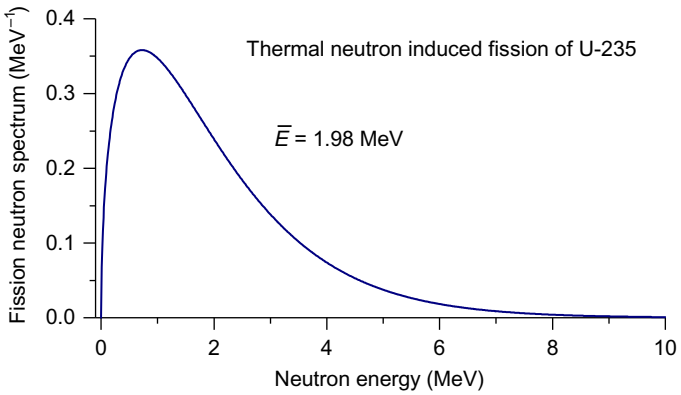

FIG. 6.6

Watt fission neutron spectrum.

value of 0.7 MeV. The U-235 fission neutron energy distribution may be described according to a semi-empirical formula known as the Watt fission spectrum (Cranberg et al., 1956)

$$\chi = 0.453 \exp(-E/0.965) \sinh\left(\sqrt{2.29E}\right) \tag{6.6}$$

We note that the neutrons produced by fission are fast, whereas the cross-section for the fission reaction is high for slow neutrons (see Fig. 6.3). This fact serves as the basis for the use of a reactor moderator containing a light element that permits neutrons to slow down, by a succession of collisions, to energies favorable for fission.

Although fission is the dominant process, a certain fraction of the absorptions of neutrons in uranium merely results in radiative capture, according to

$$^{235}_{92}\mathrm{U} + ^{1}_{0}\mathrm{n} \rightarrow ^{236}_{92}\mathrm{U} + \gamma \tag{6.7}$$

Table 6.4 Thermal Microscopic Cross-Sections

Nuclide	Capture (σ_γ)	Fission (σ_f)
Th-232	7.35	–
U-233	45.5	529.1
U-234	99.8	–
U-235	98.8	582.6
U-236	5.09	–
U-238	2.683	–
Pu-238	540	17.9
Pu-239	269.3	748.1
Pu-240	289.5	–
Pu-241	362.1	1011.1
Pu-242	18.5	–
Am-241	587	3.20

Data from International Atomic Energy Agency (IAEA), 2008. Handbook of Nuclear Data for Safeguards: Database Extensions. IAEA, INDC(NDS)-0534.

The U-236 is relatively stable, having a half-life of 2.34×10^7 y. Using the U-235 cross-sections in Table 6.4, we find that approximately 14% (σ_γ/σ_a) of the absorptions are due to an (n, γ) reaction, with fission occurring in the remaining 86%. The capture-to-fission ratio, $\alpha = \sigma_\gamma/\sigma_f$, quantifies the competition between these two reactions. This means that η (eta), the number of neutrons produced per *absorption* in U-235, is smaller than ν, the number per *fission*. In particular, η is known as the *reproduction factor* and for a single fuel nuclide is defined by

$$\eta = \nu\sigma_f/\sigma_a \tag{6.8}$$

The effectiveness of any nuclear fuel is sensitively dependent on the value of η. We find that η is larger for fission induced by fast neutrons than that by slow neutrons (see Section 25.1).

EXAMPLE 6.4

The reproduction factor for U-235 thermal fission may be determined from the data in Tables 6.2 and 6.4,

$$\eta = \frac{\nu\sigma_f}{\sigma_a} = \frac{\nu\sigma_f}{\sigma_\gamma + \sigma_f} = \frac{(2.4355)(582.6)}{98.8 + 582.6} = 2.082$$

The possibility of a *chain reaction* was recognized as soon as it was known that neutrons were released in the fission process (Anderson et al., 1939). If a neutron is absorbed by the nucleus of one atom of uranium and one neutron is produced, the latter can be absorbed in a second uranium atom, and so on. To sustain a chain reaction, as in a nuclear reactor or in a nuclear weapon, the value of η must be somewhat greater than one because of processes that compete with absorption in uranium, such as capture in other materials and escape from the system. The size of η has two important consequences. First, there is a possibility of a growth of the freed neutron population with time. After all extraneous absorption

and losses have been accounted for, if one absorption in uranium ultimately gives rise to, for instance on average, 1.1 neutrons, these can be absorbed to give (1.1) (1.1) = 1.21, which produce 1.331, and so on. The number available increases rapidly with time. Second, there is a possibility of the use of the extra neutron, over and above the one required to maintain the chain reaction, to produce new fissile materials. *Conversion* involves the production of some new nuclear fuel to replace that used up, whereas *breeding* is achieved if more fuel is produced than is used.

Out of the hundreds of isotopes found in nature, only one is fissile, $^{235}_{92}\mathrm{U}$. Unfortunately, it is the less abundant of the isotopes of uranium, with weight percentage in natural uranium of only 0.711 in comparison with 99.3% of the heavier isotope $^{238}_{92}\mathrm{U}$. The two other most important fissile materials, plutonium-239 and uranium-233, are artificial in the sense that they are created by use of neutron irradiation of two *fertile* materials, uranium-238 and thorium-232, respectively. The reactions by which $^{239}_{94}\mathrm{Pu}$ is produced are

$$\begin{aligned} &^{238}_{92}\mathrm{U} + {}^{1}_{0}\mathrm{n} \rightarrow {}^{239}_{92}\mathrm{U} \\ &^{239}_{92}\mathrm{U} \xrightarrow{23.5\,\mathrm{min}} {}^{239}_{93}\mathrm{Np} + {}^{0}_{-1}\mathrm{e} \\ &^{239}_{93}\mathrm{Np} \xrightarrow{2.355\,\mathrm{d}} {}^{239}_{94}\mathrm{Pu} + {}^{0}_{-1}\mathrm{e} \end{aligned} \tag{6.9}$$

whereas those yielding $^{233}_{92}\mathrm{U}$ are

$$\begin{aligned} &^{232}_{90}\mathrm{Th} + {}^{1}_{0}\mathrm{n} \rightarrow {}^{233}_{90}\mathrm{Th} \\ &^{233}_{90}\mathrm{Th} \xrightarrow{22.3\,\mathrm{min}} {}^{233}_{91}\mathrm{Pa} + {}^{0}_{-1}\mathrm{e} \\ &^{233}_{91}\mathrm{Pa} \xrightarrow{27.0\,\mathrm{d}} {}^{233}_{92}\mathrm{U} + {}^{0}_{-1}\mathrm{e} \end{aligned} \tag{6.10}$$

The half-lives for decay of the intermediate isotopes are short compared with times involved in the production of these fissile materials. For many purposes, these decay steps can be ignored. It is important to note that although U-238 is not fissile, it can be put to good use as a fertile material for the production of Pu-239, as long as enough free neutrons are available.

6.4 ENERGY FROM NUCLEAR FUELS

The practical significance of the fission process is revealed by calculating the amount of fuel that is consumed to obtain a given amount of energy. Each fission yields about $w = 190\,\mathrm{MeV}$ of useful energy, that is, *recoverable energy*. Thus, the number of fissions required to obtain 1 W s of energy is

$$\frac{1}{w} = \left(\frac{1\,\mathrm{fission}}{190\,\mathrm{MeV}}\right)\left(\frac{1\,\mathrm{MeV}}{1.602\times10^{-13}\,\mathrm{J}}\right) = 3.29\times10^{10}\,\frac{\mathrm{fissions}}{\mathrm{W\,s}} \tag{6.11}$$

Hence, the fission rate required to produce a given thermal power output P_{th} is

$$R_{\mathrm{f}} = P_{\mathrm{th}}/w \tag{6.12}$$

Each fission requires one fuel atom to be *burned*. In one day's operation of a reactor per megawatt of thermal power (MWt), the number of nuclei burned by fission is

$$\left(\frac{10^6\,\mathrm{W}}{\mathrm{MW}}\right)\left(\frac{3.29\times10^{10}\,\mathrm{fissions}}{\mathrm{Ws}}\right)\left(\frac{86{,}400\,\mathrm{s}}{\mathrm{d}}\right)=2.84\times10^{21}\,\frac{\mathrm{atoms}}{\mathrm{MWtd}} \tag{6.13}$$

Using the atomic mass M, the burnup rate quantifies the pace at which fuel mass diminishes due to the fission process

$$\dot{m}_\mathrm{B}=R_\mathrm{f}\frac{M}{N_\mathrm{A}}=\frac{P_\mathrm{th}M}{wN_\mathrm{A}} \tag{6.14}$$

However, the number of atoms *consumed* in a reactor is larger by the factor $\sigma_\mathrm{a}/\sigma_\mathrm{f}$ because of the radiative capture reactions. Therefore, the total consumption rate of fuel mass is

$$\dot{m}_\mathrm{C}=\dot{m}_\mathrm{B}\frac{\sigma_\mathrm{a}}{\sigma_\mathrm{f}} \tag{6.15}$$

Differentiation between burned and consumed fuel is significant in the context of waste production—a topic for Chapter 23.

EXAMPLE 6.5

The U-235 consumed to generate 1 MW of thermal power for a day is

$$\left(2.84\times10^{21}\,\frac{\mathrm{atoms\,fissioned}}{\mathrm{MWtd}}\right)\frac{\sigma_\mathrm{a}}{\sigma_\mathrm{f}}=\left(2.84\times10^{21}\right)\left(\frac{582.6+98.3}{582.6}\right)=3.32\times10^{21}\,\frac{\mathrm{atoms\,consumed}}{\mathrm{MWtd}}$$

From this, it becomes clear that various fuels will be consumed in differing amounts dependent on their cross-sections. Furthermore, because 235 g corresponds to Avogadro's number of atoms, the U-235 mass consumed is

$$\frac{\dot{m}_\mathrm{C}}{P_\mathrm{th}}=\frac{\left(3.32\times10^{21}\,\mathrm{atoms/(MWtd)}\right)(235\,\mathrm{g/mol})}{6.022\times10^{23}\,\mathrm{atoms/mol}}=1.30\,\mathrm{g/(MWtd)} \tag{6.16}$$

Of this, the U-235 mass that is actually fissioned, or burned, is

$$\frac{\dot{m}_\mathrm{B}}{P_\mathrm{th}}=\frac{\left(2.84\times10^{21}\,\mathrm{atoms/(MWtd)}\right)(235\,\mathrm{g/mol})}{6.022\times10^{23}\,\mathrm{atoms/mol}}=1.11\,\mathrm{g/(MWtd)} \tag{6.17}$$

In other words, 1.3 g of U-235 fuel is used per megawatt-day (MWtd) of useful thermal energy released. In a typical reactor, which produces 3000 MWt, the U-235 fuel consumption is

$$\dot{m}_\mathrm{C}=(1.3\,\mathrm{g/(MWtd)})\,P_\mathrm{th}=(1.3\,\mathrm{g/(MWtd)})(3000\,\mathrm{MWt})=3.9\,\mathrm{kg/d}$$

To produce the same energy using fossil fuels such as coal, oil, or gas, millions of times as much mass would be required (see Exercise 6.8).

EXAMPLE 6.6

Make a first-order estimate of the mass of fission products (FP) and actinides (Z from 89 to 103) created from the consumption of 1 g of U-235. Referring to Eq. (6.2), the fission fragment mass produced per thermal fission reaction is

$$\begin{aligned}M_\mathrm{FP}&=M_\mathrm{U\text{-}235}+m_\mathrm{n}-\nu m_\mathrm{n}-Q/c^2\\&=235.0439\,\mathrm{u}+1.0087\,\mathrm{u}(1-2.4355)-(202.5\,\mathrm{MeV})/(931.5\,\mathrm{MeV/u})=233.38\,\mathrm{u}\end{aligned}$$

Because only 86% ($\sigma_\mathrm{f}/\sigma_\mathrm{a}$) of each gram of U-235 reactant undergoes fission, the fission product mass per gram of U-235 consumed is

$$m_{\text{FP}} = \frac{\sigma_f M_{\text{FP}}}{\sigma_a M_{\text{U-235}}} = \left(\frac{582.6}{98.8 + 582.6}\right)\left(\frac{233.38\ \text{gFP}}{235.04\ \text{g}^{235}\text{U}}\right) = 0.849\,\frac{\text{gFP}}{\text{g}^{235}\text{U}}$$

We shall assume that the U-236 produced in Eq. (6.7) does not undergo further neutron absorption such that it is the sole actinide created. Hence, the actinide production per gram of U-235 consumed is

$$m_{\text{Act}} = \frac{\sigma_\gamma M_{\text{U-236}}}{\sigma_a M_{\text{U-235}}} = \left(\frac{98.8}{98.8 + 582.6}\right)\left(\frac{236.05\,\text{g}^{236}\text{U}}{235.04\,\text{g}^{235}\text{U}}\right) = 0.146\,\frac{\text{gAct}}{\text{g}^{235}\text{U}}$$

With U-238 also present in reactors, we recognize additional paths for generating transuranics ($Z > 92$) and fission products; see Eq. (6.9).

6.5 SUMMARY

Neutron absorption by the nuclei of heavy elements gives rise to fission, in which heavy fragments, fast neutrons, and other radiations are released. Fissile materials are natural U-235 and the man-made isotopes Pu-239 and U-233. Many different radioactive isotopes are released in the fission process, and more neutrons are produced than are used, which makes possible a chain reaction and, under certain conditions, conversion and breeding of new fuels. Useful energy amounts to 190 MeV per fission, requiring only 1.3 g of U-235 to be consumed to obtain 1 MW d of thermal energy.

6.6 EXERCISES

6.1 Calculate the mass of the excited nucleus of plutonium-240 as the sum of the neutron mass and the Pu-239 mass. How much larger is that sum than the mass of stable Pu-240? What energy in MeV is that?

6.2 If three neutrons are produced when a neutron bombards a U-235 atom, determine the second fission product isotope when the first fission fragment is (a) xenon-133, (b) barium-144, (c) cesium-143, (d) tellurium-137, and (e) lanthanum-146.

6.3 The total kinetic energy of two fission fragments is 166 MeV. (a) Assuming that the momenta of the fission neutrons are negligible, what are the energies of each fragment if the mass ratio is 3/2? (b) What are the two mass numbers if three neutrons were released in U-235 fission? (c) What are the velocities of the fragments? (d) What is the ratio of the momentum of a fission fragment to that of a fission neutron?

6.4 Calculate the energy yield from the following fission reactions

(a) $^{235}_{92}\text{U} + {}^{1}_{0}\text{n} \rightarrow {}^{92}_{37}\text{Rb} + {}^{140}_{55}\text{Cs} + 4{}^{1}_{0}\text{n} + Q$

(b) $^{235}_{92}\text{U} + {}^{1}_{0}\text{n} \rightarrow {}^{94}_{38}\text{Sr} + {}^{140}_{54}\text{Xe} + 2{}^{1}_{0}\text{n} + Q$

(c) $^{235}_{92}\text{U} + {}^{1}_{0}\text{n} \rightarrow {}^{92}_{36}\text{Kr} + {}^{141}_{56}\text{Ba} + 3{}^{1}_{0}\text{n} + Q$

(d) $^{233}_{92}\text{U} + {}^{1}_{0}\text{n} \rightarrow {}^{94}_{38}\text{Sr} + {}^{137}_{54}\text{Xe} + 3{}^{1}_{0}\text{n} + Q$

(e) $^{239}_{94}\text{Pu} + {}^{1}_{0}\text{n} \rightarrow {}^{103}_{40}\text{Zr} + {}^{134}_{54}\text{Xe} + 3{}^{1}_{0}\text{n} + Q$

6.5 Compute the reproduction factor for (a) U-233, (b) Pu-239, and (c) Am-241.

6.6 A mass of 8000 kg of slightly enriched uranium (2% U-235, 98% U-238) is exposed for 30 days in a reactor operating at heat power 2000 MW. Neglecting consumption of U-238, what is the final fuel enrichment?

6.7 The per capita consumption of electrical energy in the United States is approximately 35 kWh/d. If this energy were provided by fission with 2/3 of the heat wasted, how much U-235 would each person use per day?

6.8 Calculate the number of kilograms of coal, oil, and natural gas that must be burned each day to operate a 3000-MW thermal power plant, which otherwise consumes 3.9 kg/d of U-235. The heats of combustion of the three fuels (in kJ/g) are, respectively, 32, 44, and 50.

6.9 Given the spontaneous fission half-lives and neutron yields per fission in Table 6.1, determine the spontaneous fission yield (n/(g s)) for (a) U-232, (b) U-238, (c) Pu-238, (d) Pu-239, and (e) Am-241.

6.10 Determine the consumption rate (g/(MW d)) for fuels of (a) U-233 and (b) Pu-239.

6.11 Show that atom fraction γ_k and mass fraction ω_k of isotope k are related by

$$\gamma_k / M = \omega_k / M_k \tag{6.18}$$

where M and M_k are the atomic masses of the element and isotope, respectively.

6.12 Determine the final stable nuclide formed from the decay of the fission product (a) Ba-144, (b) Xe-141, (c) Zr-103, (d) Kr-93, and (e) Br-89. *Hint*: except for Th-232, all elements having a single naturally occurring isotope are stable.

6.13 Use the Cf-252 half-lives of Table 6.1 to verify the spontaneous fission branching ratio of 3.1%.

6.14 (a) Calculate separately the total energy release from the first two and last two transitions in the decay chain of Eq. (6.4). (b) What fraction of the total decay energy does each of these pairs of transitions constitute?

6.7 COMPUTER EXERCISES

6.A Monte Carlo analyses are employed to model radiation transport and nuclear processes such as fission. The MONTEPI code performs a Monte Carlo simulation that estimates the constant pi (π). The comments in the program describe the theoretical basis for the computation. (a) Run the program and note the pi estimate and its error for increasing numbers of trials. (b) Determine the effect of changing the random number function from *rand* for producing a uniform distribution to *randn*, which provides a normal distribution.

6.B Use a symbolic or numerical equation solver to compute the integral of Eq. (6.6) from zero to infinite energy.

REFERENCES

Anderson, H.L., Fermi, E., Szilard, L., 1939. Neutron production and absorption in uranium. Phys. Rev. 56 (3), 284–286.

Bohr, N., Wheeler, J.A., 1939. The mechanism of nuclear fission. Phys. Rev. 56 (5), 426–450.

Cranberg, L., Frye, G., Nereson, N., Rosen, L., 1956. Fission neutron spectrum of U^{235}. Phys. Rev. 103 (3), 662–670.

Gozani, T., 1981. Active Nondestructive Assay of Nuclear Materials, NUREG/CR-0602; 1981. p. 174. Referred to as ANDA.

Hyde, E.K., 1964. The Nuclear Properties of the Heavy Elements, vol. 3. Fission Phenomena. Prentice-Hall, Englewood Cliffs, p. 503.

International Atomic Energy Agency (IAEA), 2008. Handbook of Nuclear Data for Safeguards: Database Extensions. 2008. IAEA, INDC(NDS)-0534.

Meitner, L., Frisch, O.R., 1939. Disintegration of uranium by neutrons: a new type of nuclear reaction. Nature 143 (3615), 239–240.

Verbinski, V.V., Weber, H., Sund, R.E., 1973. Prompt gamma rays from ^{235}U(n,f), ^{239}Pu(n,f), and spontaneous fission of ^{252}Cf. Phys. Rev. C 7 (3), 1173–1185.

FURTHER READING

Alter, H., 1986. Glossary of Terms in Nuclear Science and Technology. American Nuclear Society, La Grange Park, IL.

American Institute of Physics (AIP), 2003. Discovery of fission. http://aip.org/history/mod/fission/fission1/03.html. Includes quotations from the scientists.

Bodansky, D., 2003. Nuclear Energy: Principles, Practices, and Prospects, second ed. Springer/AIP Press, New York.

Bohr, N., 1939. Disintegration of heavy nuclei. Nature 143 (3617), 330.

Chadwick, M.B., Herman, M., Obložinský, P., Dunn, M.E., Danon, Y., Kahler, A.C., et al., 2011. ENDF/B-VII.1 Nuclear data for science and technology: cross-sections, covariances, fission product yields and decay data. Nucl. Data Sheets 112 (12), 2887–2996.

Lamarsh, J.R., Baratta, A.J., 2018. Introduction to Nuclear Engineering, fourth ed. Pearson, Hoboken.

Reilly, D., Ensslin, N., Smith Jr., H., 1991. Passive Nondestructive Assay of Nuclear Materials. 1991. NUREG/CR-5550, 339. Referred to as PANDA.

Segrè, E., 1989. The discovery of nuclear fission. Phys. Today 42 (7), 38–43.

Sher, R., 1981. Fission energy release for 16 fissioning nuclides. In: Proceedings of the Conference on Nuclear Data Evaluation Methods and Procedures, Brookhaven National Laboratory, 22–25 September 1980, BNL-NCS-51363, vol. II, pp. 835–860.

Sime, R.L., 1998. Lise Meitner and the discovery of nuclear fission. Sci. Am. 278 (1), 80–85. Contributions of the scientist who should have received the Nobel Prize.

CHAPTER

FUSION

7

CHAPTER OUTLINE

When two light nuclear particles combine or fuse together, energy is released because the product nuclei have less mass than the original particles. Such fusion reactions can be caused by bombarding targets with charged particles, by use of an accelerator, or by raising the temperature of a gas to a high enough level for nuclear reactions to take place. In this chapter, we will describe the interactions in the microscopic sense and discuss the phenomena that affect our ability to achieve a practical large-scale source of energy from fusion.

7.1 FUSION REACTIONS

The possibility of release of large amounts of nuclear energy can be seen by comparing the masses of nuclei of low atomic number. Suppose that one could combine two hydrogen nuclei and two neutrons to form the helium nucleus. In the reaction

$$2{}_1^1\mathrm{H} + 2{}_0^1\mathrm{n} \rightarrow {}_2^4\mathrm{He} \tag{7.1}$$

the mass-energy difference (by use of atom masses) is

$$\begin{aligned}\Delta m &= \sum M_{\text{react}} - M_{\text{prod}} = 2M_{\text{H-1}} + 2m_{\text{n}} - M_{\text{He-4}} \\ &= 2(1.007825) + 2(1.008665) - 4.002603 = 0.030377\,\text{amu}\end{aligned} \tag{7.2}$$

Nuclear Energy. https://doi.org/10.1016/B978-0-12-812881-7.00007-1

which corresponds to 28.3 MeV energy. A comparable amount of energy would be obtained by combining four hydrogen nuclei to form helium plus two positrons

$$4\,{}^{1}_{1}\mathrm{H} \rightarrow {}^{4}_{2}\mathrm{He} + 2\,{}^{0}_{+1}\mathrm{e}^{+1} \tag{7.3}$$

This reaction in effect takes place in the sun and in other stars through the so-called *carbon cycle*, a complicated chain of events involving hydrogen and isotopes of the elements carbon, oxygen, and nitrogen. The cycle is extremely slow, however, and is not suitable for terrestrial application.

In the hydrogen bomb, on the other hand, the high temperatures created by a fission reaction cause the fusion reaction to proceed in a rapid and uncontrolled manner. Between these extremes is the possibility of achieving a controlled fusion reaction that uses inexpensive and abundant fuels. As yet, a practical fusion power device has not been demonstrated, and considerable research and development will be required to reach that goal. Let us now examine the nuclear reactions that might be used. There seems to be no mechanism by which four separate nuclei can be made to fuse directly, and thus combinations of two particles must be sought.

The most promising reactions make use of the isotope deuterium, ${}^{2}_{1}\mathrm{H}$, abbreviated D. According to Table A.5 in Appendix A, D is present in hydrogen, as in water, with an abundance of only 0.0156% (i.e., there is one atom of ${}^{2}_{1}\mathrm{H}$ for every 6413 atoms of ${}^{1}_{1}\mathrm{H}$), but because our planet has enormous amounts of water, the fuel available is almost inexhaustible. Four reactions are important:

$$\begin{aligned}
&\text{D-D:} && {}^{2}_{1}\mathrm{H} + {}^{2}_{1}\mathrm{H} \rightarrow \begin{cases} {}^{3}_{1}\mathrm{H} + {}^{1}_{1}\mathrm{H} + 4.03\,\mathrm{MeV} \\ {}^{3}_{2}\mathrm{He} + {}^{1}_{0}\mathrm{n} + 3.27\,\mathrm{MeV} \end{cases} \\
&\text{D-T:} && {}^{2}_{1}\mathrm{H} + {}^{3}_{1}\mathrm{H} \rightarrow {}^{4}_{2}\mathrm{He} + {}^{1}_{0}\mathrm{n} + 17.59\,\mathrm{MeV} \\
&\text{D-}{}^{3}\text{He:} && {}^{2}_{1}\mathrm{H} + {}^{3}_{2}\mathrm{He} \rightarrow {}^{4}_{2}\mathrm{He} + {}^{1}_{1}\mathrm{H} + 18.35\,\mathrm{MeV}
\end{aligned} \tag{7.4}$$

The fusion of two deuterons—deuterium nuclei—in what is designated the D-D reaction, as shown in Fig. 7.1, results in two processes of nearly equal likelihood. The other reactions yield more energy but involve the artificial isotopes tritium, ${}^{3}_{1}\mathrm{H}$, abbreviated T, with the ion called the triton, and the rare isotope ${}^{3}_{2}\mathrm{He}$, helium-3. We note that the products of the first and second equations appear as reactants in the third and fourth equations. This suggests that a composite process might be feasible. Suppose that each of the reactions could be made to proceed at the same rate, along with twice the reaction of neutron capture in hydrogen

$${}^{1}_{1}\mathrm{H} + {}^{1}_{0}\mathrm{n} \rightarrow {}^{2}_{1}\mathrm{H} + 2.22\,\mathrm{MeV} \tag{7.5}$$

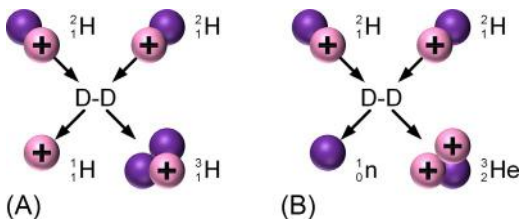

FIG. 7.1

Deuterium-deuterium (D-D) fusion reactions. (A) D-D (p) and (B) D-D (n).

Adding twice this equation to the preceding four, we find that the net effect is to convert deuterium into helium according to

$$4\,{}_1^2\mathrm{H} \rightarrow 2\,{}_2^4\mathrm{He} + 47.7\,\mathrm{MeV} \tag{7.6}$$

The energy yield per atomic mass unit of deuterium fuel would thus be approximately 6 MeV, which is much more favorable than the yield per atomic mass unit of U-235 burned, which is only 190/235 = 0.81 MeV/u.

EXAMPLE 7.1

Verify the D-T energy release value of 17.59 MeV. Using the masses in Table A.5 and Eq. (4.17) gives

$$\begin{aligned} Q_{\mathrm{DT}} &= [(M_{\mathrm{D}} + M_{\mathrm{T}}) - (m_{\mathrm{n}} + M_{\mathrm{He-4}})]c^2 \\ &= [(2.01410178 + 3.01604928) - (1.00866492 + 4.00260325)](931.5) = 17.59\,\mathrm{MeV} \end{aligned}$$

7.2 ELECTROSTATIC AND NUCLEAR FORCES

The reactions previously described do not take place merely by mixing the ingredients because of the very strong force of electrostatic repulsion between the charged nuclei. Only by giving one or both of the particles a high speed can they be brought close enough to each other for the strong nuclear force to dominate the electrical force. This behavior is in sharp contrast to the ease with which neutrons interact with nuclei.

There are two consequences of the fact that the Coulomb force between two charges of atomic numbers Z_1 and Z_2 varies with separation r according to

$$F_C = \frac{Z_1 e Z_2 e}{4\pi\varepsilon_0 r^2} \tag{7.7}$$

where e is the elementary charge (1.602×10^{-19} C). First, we see that fusion is unlikely in elements other than those low on the periodic table (small Z). Second, the force and corresponding potential energy of repulsion is very large at the 10^{-15} m range of nuclear forces, and thus the chance of reaction is negligible unless particle energies are of the order of keV. Fig. 7.2 shows the cross-section for four fusion reactions. The strong dependence on energy is noted, with σ_{DT} rising by a factor of 1000 in the range 10–75 keV.

EXAMPLE 7.2

The energy required to overcome the Coulombic barrier for the D-T reaction may be computed with Eq. (4.20)

$$E_{\mathrm{C}} = \frac{(1.2\,\mathrm{MeV})Z_{\mathrm{D}}Z_{\mathrm{T}}}{A_{\mathrm{D}}^{1/3} + A_{\mathrm{T}}^{1/3}} = \frac{(1.2\,\mathrm{MeV})(1)(1)}{(2)^{1/3} + (3)^{1/3}} = 0.44\,\mathrm{MeV}$$

This is an overestimation of the energy needed for fusion because quantum mechanics permits tunneling through the potential barrier (Atzeni and Meyer-ter-vehn, 2004).

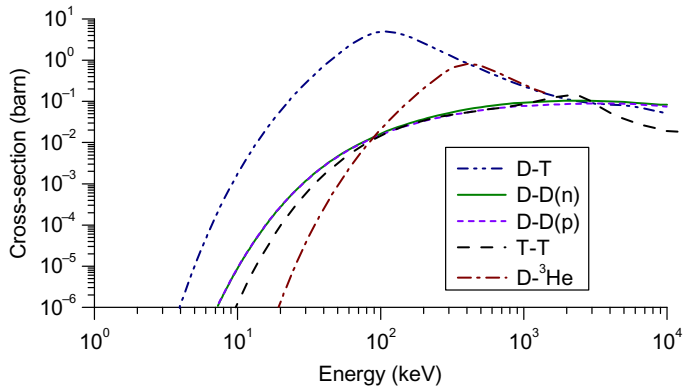

FIG. 7.2

Cross-sections for fusion reactions.

Data from ENDF/B-VII.1 (Chadwick, M.B., Herman, M., Obložinský, P., Dunn, M.E., Danon, Y., Kahler, A.C., et al., 2011. ENDF/B-VII.1 Nuclear data for science and technology: cross-sections, covariances, fission product yields and decay data. Nucl. Data Sheets 112 (12), 2887–2996).

Energies in the kiloelectronvolt and megaelectronvolt range can be achieved by a variety of charged particle accelerators. Bombardment of a solid or gaseous deuterium target by high-speed deuterons produces fusion reactions, but most of the particle energy goes into electrostatic interactions that merely heat up the bulk of the target. For a practical system, the recoverable fusion energy must significantly exceed the energy required to operate the accelerator. Special equipment and processes are required to achieve that objective.

EXAMPLE 7.3

Some commercially available neutron generators utilize the D-D or D-T reaction to produce the neutrons. Assuming an initial net momentum of zero, we may draw upon the results of Example 4.3 to compute the energies of the two reaction products. The D-T reaction energy Q_{DT} distributes according to the product masses

$$E_K^{\mathrm{n}} = Q_{\mathrm{DT}} M_{\mathrm{He\text{-}4}} / (m_{\mathrm{n}} + M_{\mathrm{He\text{-}4}})$$
$$E_K^{\mathrm{He\text{-}4}} = Q_{\mathrm{DT}} m_{\mathrm{n}} / (m_{\mathrm{n}} + M_{\mathrm{He\text{-}4}})$$

Hence, the expected neutron kinetic energy is

$$E_K^{\mathrm{n}} = \frac{Q_{\mathrm{DT}} M_{\mathrm{He\text{-}4}}}{m_{\mathrm{n}} + M_{\mathrm{He\text{-}4}}} = \frac{(17.59\,\mathrm{MeV})(4.0026)}{1.0087 + 4.0026} = 14.05\,\mathrm{MeV}$$

7.3 THERMONUCLEAR REACTIONS IN A PLASMA

A medium in which high particle energies are obtained is the *plasma*. It consists of a highly ionized gas as in an electrical discharge created by the acceleration of electrons. Equal numbers of electrons and positively charged ions are present, making the medium electrically neutral. The plasma is often called

the fourth state of matter. Through the injection of enough energy into the plasma, its temperature can be increased, and particles such as deuterons reach the speed for fusion to be favorable. The term *thermonuclear* is applied to reactions induced by high thermal energy, and the particles obey a Maxwellian speed distribution similar to that of a gas, as discussed in Section 2.2.

The temperatures to which the plasma must be raised are extremely high, as we can see by expressing an average particle energy in terms of temperature, by use of the kinetic relation

$$\overline{E} = \frac{3}{2}kT \tag{7.8}$$

EXAMPLE 7.4

For example, even if $\overline{E}$ is as low as 10 keV, the temperature is

$$T = \frac{2\overline{E}}{3k} = \frac{2\left(10^4\,\text{eV}\right)}{3\left(8.62\times10^{-5}\,\text{J/K}\right)} = 7.7\times10^7\,\text{K}$$

Such a temperature greatly exceeds the temperature of the surface of the sun and is far beyond any temperature at which ordinary materials melt and vaporize. The plasma must be created and heated to the necessary temperature under some constraint provided by a physical force. In stars, gravity provides that force, but that is not feasible on Earth. Compression by reaction to ablation is designated as inertial confinement; restraint by electric and magnetic fields is called magnetic confinement. These methods will be discussed in Chapter 26. Such forces on the plasma are required to assure that thermal energy is not prematurely lost. Moreover, the plasma must remain intact long enough for many nuclear reactions to occur, which is difficult because of inherent instabilities of such highly charged media. Recalling from Section 2.2 the relationship $pV = nkT$, we note that even though the temperature T is very high, the particle density n/V is low, allowing the pressure p to be manageable.

The achievement of a practical fusion energy source is further limited by the phenomenon of radiation losses. In Section 5.2 we discussed the *bremsstrahlung* radiation produced when electrons experience acceleration. Conditions are ideal for the generation of such electromagnetic radiation because the high-speed electrons in the plasma at elevated temperature experience continuous accelerations and decelerations as they interact with other charges. The photon radiation can readily escape from the region because the number of target particles is very small. In typical plasma, the number density of electrons and deuterons is $10^{15}/\text{cm}^3$, which corresponds to a rarefied gas. The bremsstrahlung generated radiation losses in W/cm^3 are (Glasstone and Lovberg, 1975)

$$P_{\text{br}} = 5.35\times10^{-31} n_{\text{e}} \sqrt{kT_{\text{e}}} \sum_{j}^{\text{ions}} n_j Z_j^2 \tag{7.9}$$

where Z_i is the ion atomic number; n_j and n_{e} are the ion and electron densities per cm^3 ($n_{\text{e}} = n_i = \sum n_j$); and kT_{e} is the electron gas temperature in keV. Other energy loss mechanisms include particle diffusion, and, in the case of magnetic confinement, synchrotron/cyclotron radiation.

As both reactants have random motion, the reaction rate is conventionally expressed in terms of the *reactivity*, defined as the product of the reaction cross-section and relative ion speed. This reaction probability may be averaged over the Maxwell-Boltzmann velocity distribution to obtain $\overline{\sigma v}$. Some

simple formulas are available for quantifying the reactivity at low ion energies kT_i. For the D-T reaction, Hivey (1983) provides

$$(\overline{\sigma v})_{\mathrm{DT}} = 9.131 \times 10^{-16} \exp\left[-0.5716 \left| \ln\left(\frac{kT_i}{64.22}\right)\right|^{2.137}\right] \frac{\mathrm{cm}^3}{\mathrm{s}} \tag{7.10}$$

in which kT_i is in units of keV and valid for 1–100 keV. For the two D-D reactions, Hivey (1977) gives for 1–80 keV

$$\begin{aligned}(\overline{\sigma v})_{\mathrm{DDp}} &= 2.002 \times 10^{-14} \frac{1 + 0.005776(kT_i)^{0.9496}}{(kT_i)^{2/3}} \exp\left[\frac{-19.307}{(kT_i)^{1/3}}\right] \frac{\mathrm{cm}^3}{\mathrm{s}} \\ (\overline{\sigma v})_{\mathrm{DDn}} &= 2.722 \times 10^{-14} \frac{1 + 0.005389(kT_i)^{0.9172}}{(kT_i)^{2/3}} \exp\left[\frac{-19.796}{(kT_i)^{1/3}}\right] \frac{\mathrm{cm}^3}{\mathrm{s}}\end{aligned} \tag{7.11}$$

In the case of a plasma relying upon the D-D reaction, the deuterium density equals the ion density ($n_{\mathrm{D}} = n_i$); however, for the D-T-based plasma, equal numbers of deuterons and tritons are assumed such that $n_{\mathrm{D}} = n_i/2 = n_{\mathrm{T}}$. Because $n_i = n_{\mathrm{D}} + n_{\mathrm{T}}$, the D-T reaction rate is

$$R_{\mathrm{DT}} = n_{\mathrm{D}} n_{\mathrm{T}} (\overline{\sigma v})_{\mathrm{DT}} = \frac{n_i^2}{4} (\overline{\sigma v})_{\mathrm{DT}} \tag{7.12}$$

In contrast, for the D-D reaction, $n_i = n_{\mathrm{D}}$, but the reaction rate formula must include a factor of one-half to avoid double counting particle reactions

$$R_{\mathrm{DD}} = \frac{1}{2} n_{\mathrm{D}} n_{\mathrm{D}} (\overline{\sigma v})_{\mathrm{DD}} = \frac{n_i^2}{2} (\overline{\sigma v})_{\mathrm{DD}} \tag{7.13}$$

where $(\overline{\sigma v})_{\mathrm{DD}}$ accounts for both the proton and neutron branches of the D-D reaction, that is, $(\overline{\sigma v})_{\mathrm{DD}} = (\overline{\sigma v})_{\mathrm{DDp}} + (\overline{\sigma v})_{\mathrm{DDn}}$.

Like fission, the product of the energy release per reaction and the reaction rate provides the energy liberated from fusion; however, the uncharged neutron leaves the plasma such that the retained energy is smaller than the reaction Q value. Consequently, the corresponding fusion power generation is expressed in terms of the energy release E_{ch} in the form of charged particles

$$P_{\mathrm{fus}} = E_{\mathrm{ch}} R \tag{7.14}$$

Using the results of Example 7.2, the D-T plasma keeps only 20.1% [(17.59 – 14.05)/17.59] of its fusion energy while 66.4% of the overall D-D reaction energy is retained. The neutron energy may be recovered within peripheral materials. Thus, the reaction energy deposited within the plasma is

$$P_{\mathrm{DT}} = (3.54\,\mathrm{MeV}) n_{\mathrm{D}} n_{\mathrm{T}} (\overline{\sigma v})_{\mathrm{DT}} \tag{7.15}$$

$$P_{\mathrm{DD}} = (4.03\,\mathrm{MeV})\left(n_{\mathrm{D}}^2/2\right)(\overline{\sigma v})_{\mathrm{DDp}} + (0.82\,\mathrm{MeV})\left(n_{\mathrm{D}}^2/2\right)(\overline{\sigma v})_{\mathrm{DDn}} \tag{7.16}$$

Some formulations (Huba, 2016) for P_{DD} also incorporate the subsequent prompt D-T reaction (see Exercise 7.12).

The amount of radiation production (and loss) increases with temperature at a slower rate than does the energy released by fusion, as shown in Fig. 7.3. At what is called the *ideal ignition temperature*, the lines cross. Only for temperatures greater than that value, 560 million K in the case of the D-D reaction, will there be a net energy yield, assuming that the radiation is lost. As reaction products and impurities

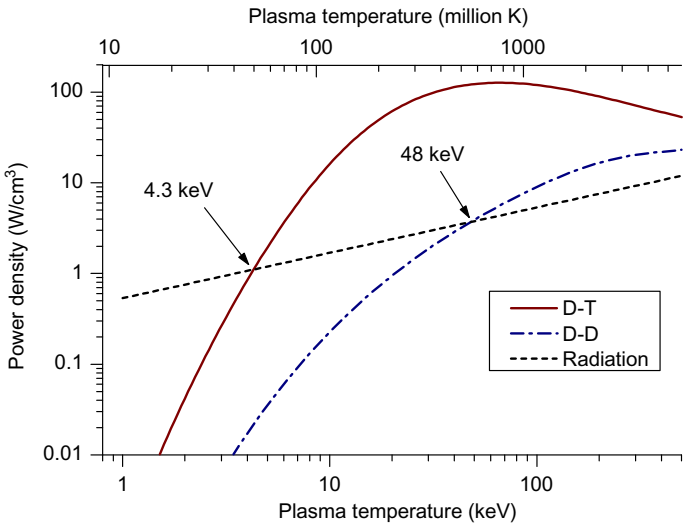

FIG. 7.3

Fusion and radiation energies for ion and electron densities of $10^{15}/\text{cm}^{-3}$.

with $Z>1$ build up, the bremsstrahlung losses increase, thus raising the ignition temperature. In Chapter 26, we will describe some of the devices that have been used to explore the possibility of achieving a fusion reactor.

EXAMPLE 7.5

Estimate the ideal ignition temperature for the D-T reaction with a plasma density of $10^{15}/\text{cm}^3$. For this reaction $Z_D=1=Z_T$, such that the expression (Eq. 7.9) for radiation losses may be reduced to

$$P_{br}^{DT}=\left(5.35\times10^{-31}\,\text{W cm}^3\right)n_e\left(n_D+n_T\right)\sqrt{kT_e} \tag{7.17}$$

Substituting Eq. (7.10) into (7.15) gives the D-T reaction produced power

$$P_{DT}=\left(5.18\times10^{-28}\,\text{W cm}^3\right)n_D n_T \exp\left[-0.5716\left|\ln\left(\frac{kT_i}{64.22}\right)\right|^{2.137}\right] \tag{7.18}$$

Finally, equating the bremsstrahlung loss to the fusion generated power ($P_{br}=P_{DT}$) and recalling that $n_D=n_i/2=n_T$ and $n_e=n_i$ yields

$$\left(5.35\times10^{-31}\right)n_i^2\sqrt{kT_e}=\left(5.18\times10^{-28}\right)\frac{n_i^2}{4}\exp\left[-0.5716\left|\ln\left(\frac{kT_i}{64.22}\right)\right|^{2.137}\right]$$

This demonstrates that the ideal ignition temperature is independent of the particle density. Now, assuming that the electron and ion temperatures are the same, the above expression reduces to

$$4.13\times10^{-3}=\left(kT_i\right)^{-1/2}\exp\left[-0.5716\left|\ln\left(\frac{kT_i}{64.22}\right)\right|^{2.137}\right]$$

Numerically solving this equation gives an ideal ignition temperature of 4.3 keV (50 million K) in agreement with the value in Fig. 7.3, which utilizes reactivity relations from Bosch and Hale (1992).

As n is already on a per unit volume basis, the corresponding plasma pressure is

$$\begin{aligned} p &= nkT = (n_e + n_D + n_T)kT = 2n_i kT \\ &= \left(2\times10^{15}\,\mathrm{cm^{-3}}\right)\left(10^6\,\mathrm{cm^3/m^3}\right)(4.3\,\mathrm{keV})\left(1.602\times10^{-16}\,\mathrm{J/keV}\right)\left(\mathrm{Pa\,m^3/J}\right) \\ &= \left(1.38\times10^6\,\mathrm{Pa}\right)\left(1\,\mathrm{atm}/1.013\times10^5\,\mathrm{Pa}\right) = 14\,\mathrm{atm} \end{aligned}$$

7.4 SUMMARY

Nuclear energy is released when nuclei of two light elements combine. The most favorable fusion reactions involve deuterium, which is a natural component of water and thus is a very abundant fuel. The reaction takes place only when the nuclei have a high enough speed to overcome the electrostatic repulsion of their charges. At temperatures of the order of 50 million K within a highly ionized electrical medium (i.e., a plasma), the D-T fusion energy can exceed the energy loss due to radiation.

7.5 EXERCISES

7.1 Calculate the energy release in amu and MeV from the combination of four protons to form a helium nucleus and two positrons (each of mass 0.000549 amu).

7.2 Verify the energy yield for the (a) D-^{3}He and (b) both D-D reactions.

7.3 To obtain 3000 MW of thermal power from a fusion reactor, in which the effective reaction is $2{}_1^2\mathrm{H} \rightarrow {}_2^4\mathrm{He} + 23.85$ MeV, how many grams per day of deuterium would be needed? If all the deuterium could be extracted from water, how many kilograms of water would have to be processed per day?

7.4 The reaction rate relation $nvN\sigma$ can be used to estimate the power density of a fusion plasma. (a) Find the speed v_D of 100 keV deuterons. (b) Assuming that deuterons serve as both target and projectile, such that the effective v is $v_D/2$, find what particle number density would be needed to achieve a power density of 1 kW/cm^3.

7.5 Estimate the temperature of the electrical discharge in a 120-V fluorescent light bulb.

7.6 Calculate the potential energy in MeV of a deuteron in the presence of another when their centers are separated by three nuclear radii (*Note:* $E_P = E_C = -\int_\infty^d F_C dr$).

7.7 Determine the energy needed to overcome electrostatic repulsion in the (a) D-D, (b) D-^{3}He, and (c) T-T reactions.

7.8 Find the temperature needed to overcome the Coulombic repulsion for the D-T reaction.

7.9 For the following fusion reactions, determine the energy release and the Coulombic threshold energy.

$$\begin{aligned}&\text{(a) T-T:} && {}^3_1\text{H} + {}^3_1\text{H} \rightarrow {}^4_2\text{He} + 2\,{}^1_0\text{n}\\ &\text{(b) T-}{}^3\text{He:} && {}^3_1\text{H} + {}^3_2\text{He} \rightarrow {}^4_2\text{He} + {}^2_1\text{H}\\ &\text{(c) }{}^3\text{He-}{}^3\text{He:} && {}^3_2\text{He} + {}^3_2\text{He} \rightarrow {}^4_2\text{He} + 2\,{}^1_1\text{H}\end{aligned}$$

7.10 Determine the expected neutron kinetic energy from the D-D reaction.

7.11 Use the following formulation (Gross, 1985) to verify the leading coefficient of 5.35×10^{-31} in Eq. (7.9)

$$P_{\text{br}} = g_{\text{ff}} \frac{32\pi e^6}{3(4\pi\varepsilon_0)^3 c^3 m_{\text{e}} h} \sqrt{\frac{2\pi k T_{\text{e}}}{3m_{\text{e}}}} n_{\text{e}} \sum_j^{\text{ions}} n_j Z_j^2 \tag{7.19}$$

where the Gaunt factor $g_{\text{ff}} = 2\sqrt{3}/\pi \cong 1.10$ corrects for quantum effects.

7.12 Estimate the ideal ignition temperature for the D-D reaction (a) excluding and (b) including the subsequent prompt D-T reaction energy. In the latter case, the power density is

$$P_{\text{DD}} = (4.03 + 3.54\,\text{MeV})\left(n_{\text{D}}^2/2\right)\langle\overline{\sigma v}\rangle_{\text{DDp}} + (0.82\,\text{MeV})\left(n_{\text{D}}^2/2\right)\langle\overline{\sigma v}\rangle_{\text{DDn}} \tag{7.20}$$

7.6 COMPUTER EXERCISE

7.A Use the relations within Section 7.3 to recreate a graph like that of Fig. 7.3.

REFERENCES

Atzeni, S., Meyer-ter-vehn, J., 2004. The Physics of Inertial Fusion. Clarendon Press, Oxford.

Bosch, H.-S., Hale, G.M., 1992. Improved formulas for fusion cross-sections and thermal reactivities. Nucl. Fusion 32 (4), 611–631.

Glasstone, S., Lovberg, R.H., 1975. Controlled Thermonuclear Reactions: An Introduction to Theory and Experiment. Krieger, New York (Reprint of 1960 edition.).

Gross, R.A., 1985. Fusion Energy. Wiley, New York.

Hivey, L.M., 1977. Convenient computational forms for Maxwellian reactivities. Nucl. Fusion 17 (4), 873–876.

Hivey, L.M., 1983. A simple computational form for Maxwellian reactivities. Fusion Sci. Technol. 3 (2), 199–200.

Huba, J.D., 2016. NRL Plasma Formulary. Naval Research Laboratory, Washington, DC.

FURTHER READING

Chadwick, M.B., Herman, M., Obložinský, P., Dunn, M.E., Danon, Y., Kahler, A.C., et al., 2011. ENDF/B-VII.1 Nuclear data for science and technology: cross-sections, covariances, fission product yields and decay data. Nucl. Data Sheets 112 (12), 2887–2996.

Duderstadt, J.J., Moses, G.A., 1982. Inertial Confinement Fusion. Wiley, New York An excellent complement to the book by Gross.

European Fusion Development Agreement (EFDA), About the Joint European Torus (JET). www.efda.org.

Freidberg, J.P., 2007. Plasma Physics and Fusion Energy. Cambridge University Press, Cambridge.

Harms, A.A., Schoepf, K.F., Miley, G.H., Kingdon, D.R., 2000. Principles of Fusion Energy: An Introduction to Fusion Energy for Students of Science and Engineering. World Scientific Publishing Co., Singapore

Heppenheimer, T.A., 1984. The Man-Made Sun, The Quest for Fusion Power. Little, Brown & Co, Boston, MA.

Miley, G.H., 1976. Fusion Energy Conversion. American Nuclear Society, La Grange Park.

Miyamoto, K., 2005. Plasma Physics and Controlled Nuclear Fusion. Springer-Verlag, Dordrecht.

Pfalzner, S., 2006. An Introduction to Inertial Confinement Fusion. CRC Press, New York.

Robin, H., 1990. Fusion: The Search for Endless Energy. Cambridge University Press A well-written and interesting account.

Smid, T., n.d. Theoretical Principles of Plasma Physics and Atomic Physics. www.plasmaphysics.org.uk. Highly technical but comprehensive.

PART

RADIATION AND ITS USES

II

Part II of this book addresses radiation, including its generation and utilization. With fundamental nuclear concepts established, we pause to review the history of nuclear energy, which begins with discoveries associated with atomic structure and radiation. The particle accelerator was one of the first radiation-producing devices to be developed, but it remains an essential means of conducting research and producing medical isotopes.

After establishing knowledge of the effects of ionizing radiation on biological entities, we examine the techniques for protecting people from radiation. Radiation doses can be received from external or internal sources originating from either natural or artificial processes. To sense and measure radiation requires specialized instrumentation and detectors that exploit the atomic and nuclear reactions explained in Part I.

Next, various applications are described in which radioisotopes are employed for beneficial purposes, including radiography, radiopharmaceuticals, and radiometric dating. Part II closes with general uses of radiation that further the goals of humanity, such as insect control and food preservation.

CHAPTER

THE HISTORY OF NUCLEAR ENERGY

8

CHAPTER OUTLINE

The development of nuclear energy exemplifies the consequences of scientific study, technological effort, and commercial application. We will review the history for its relation to our cultural background, which should include human endeavors in the broadest sense. The authors subscribe to the traditional conviction that history is relevant. Present understanding is grounded in recorded experience, and although we cannot undo errors, we can avoid them in the future. We can hopefully establish concepts and principles about human attitudes and capabilities that are independent of time to help guide future action. Finally, we can draw confidence and inspiration from the knowledge of what human beings have been able to accomplish.

8.1 THE RISE OF NUCLEAR PHYSICS

The science on which practical nuclear energy is based can be categorized as classical, evolving from studies in chemistry and physics for the last several centuries, and modern, which relates to investigations over the past century into the structure of the atom and nucleus. The modern era begins with Crookes' (1879) achievement of ionization of a gas by an electric discharge. Thomson (1897) identified the electron as the charged particle responsible for electricity. Roentgen (1895) discovered penetrating X-rays from a discharge tube, and Becquerel (1896) found similar rays—now known as gamma rays—from an entirely different source, the same element that exhibited the phenomenon of radioactivity: uranium. The Curies (1898) isolated the radioactive element radium. As a part of his revolutionary

Nuclear Energy. https://doi.org/10.1016/B978-0-12-812881-7.00008-3

theory of motion, Einstein (1905) concluded that the mass of any object increased with its speed and stated his now-famous formula $E = mc^2$, which expresses the equivalence of mass and energy. At that time, no experimental verification was available, and Einstein could not have foreseen the implications of his equation.

In the first third of the 20th century, a host of experiments with the various particles coming from radioactive materials led to a rather clear understanding of the structure of the atom and its nucleus. The works of Rutherford (1911) and Bohr (1913) led to the understanding that the electrically neutral atom is constructed from negative charge in the form of electrons surrounding a central positive nucleus, which contains most of the matter of the atom. Through further work by Rutherford (1919) in England, it was revealed that even though the nucleus is composed of particles bound together by forces of great strength, nuclear transmutations could be induced (e.g., the bombardment of nitrogen by helium yields oxygen and hydrogen, see Eq. 4.2).

Bothe and Becker (1930) bombarded beryllium with alpha particles from polonium and found what they thought were gamma rays but which Chadwick (1932) showed to be neutrons (see Exercise 8.3). A similar reaction is now used in nuclear reactors to provide a source of neutrons. Joliot and Curie (1934) first reported artificial radioactivity. Particles injected into nuclei of boron, magnesium, and aluminum gave new radioactive isotopes of several elements. The development of machines to accelerate charged particles to high speeds opened up new opportunities to study nuclear reactions. The cyclotron, developed by Lawrence and Livingston (1932), was the first of a series of devices of ever-increasing capability.

8.2 THE DISCOVERY OF FISSION

During the 1930s, Enrico Fermi and his coworkers in Italy performed a number of experiments with the newly discovered neutron. He reasoned correctly that the lack of charge on the neutron would make it particularly effective in penetrating a nucleus. Among his discoveries was the great affinity of slow neutrons for many elements and the variety of radioisotopes that could be produced by neutron capture. Breit and Wigner (1936) provided the theoretical explanation of slow neutron processes. Fermi made measurements of the distribution of both fast and thermal neutrons and explained the behavior in terms of elastic scattering, chemical binding effects, and thermal motion in the target molecules. During this period, many cross sections for neutron reactions were measured, including that of uranium, but the fission process was not identified.

It was not until January 1939 that Hahn and Strassmann (1939) of Germany reported that they had found the element barium as a product of neutron bombardment of uranium. Meitner and Frisch (1939) made the guess that *fission*, a term borrowed from the biological sciences, was responsible for the appearance of an element that is only half as heavy as uranium and that the fragments would be very energetic. Fermi then suggested that neutrons might be emitted during the process, and the idea was born that a chain reaction that releases great amounts of energy might be possible. The press picked up the idea, and many sensational articles were written. The information on fission, brought to the United States by Bohr on a visit from Denmark, prompted a flurry of activity at several universities, and by 1940, nearly a hundred papers had appeared in the technical literature. All the qualitative characteristics of the chain reaction were soon learned—the moderation of neutrons by light elements, thermal and resonance capture, the existence of fission in U-235 by thermal neutrons, the large energy of fission fragments, the release of neutrons, and the possibility of producing transuranic elements, those beyond uranium in the periodic table.

8.3 THE DEVELOPMENT OF NUCLEAR WEAPONS

The discovery of fission, with the possibility of a chain reaction of explosive violence, was of special importance at this particular time in history because World War II had begun in 1939. Because of the military potential of the fission process, in 1940 scientists established a voluntary censorship of publication on the subject. The studies that showed U-235 to be fissile suggested that the new element plutonium, discovered in 1941 by Seaborg et al. (1946), might also be fissile and thus also serve as a weapon material. As early as July 1939, four leading scientists—Szilard, Wigner, Sachs, and Einstein—had initiated contact with US President Franklin D. Roosevelt (see Exercise 8.2), explaining the possibility of an atomic bomb based on uranium. Consequently, a small grant of $6000 was made by the military to procure materials for experimental testing of the chain reaction. Before the end of World War II, a total of $2 billion had been spent (Hewlett and Anderson Jr., 1962), an almost inconceivable sum in those times. After a series of studies, reports, and policy decisions, a major effort was mounted through the US Army Corps of Engineers under General Leslie Groves. The code name Manhattan District (or Manhattan Project) was devised, with military security mandated on all information.

Although a great deal was known about the individual nuclear reactions, there was great uncertainty as to the practical behavior. Could a chain reaction be achieved at all? If so, could Pu-239 in adequate quantities be produced? Could a nuclear explosion be made to occur? Could U-235 be separated on a large scale? These questions were addressed at several institutions, and design of production plants began almost concurrently, with great impetus provided by the involvement of the United States in World War II after the attack on Pearl Harbor by Japan in December 1941. The distinct possibility that Germany was actively engaged in the development of an atomic weapon served as a strong stimulus to the work of scientists in the United States, most of whom were in universities. They and their students dropped their normal work to enlist in some phase of the project.

As was revealed by the Alsos Mission (Goudsmit, 1947; Pash, 1980), a military investigation project, Germany had actually made little progress toward an atomic bomb. Controversy surrounds the possible reasons for its failure. One theory is that the critical mass of enriched uranium was overestimated—as tonnes rather than kilograms—with the conclusion that such amounts were not achievable (Rose, 1998). Another theory is that scientist Werner Heisenberg, the leader of the German effort, had deliberately stalled the project to prevent Hitler from having a nuclear weapon to use against the Allies.

The Manhattan Project consisted of several parallel endeavors. The major effort was in the United States, with cooperation from the United Kingdom, Canada, and France.

An experiment at the University of Chicago was crucial to the success of the Manhattan Project and also set the stage for future nuclear developments. The team under Enrico Fermi assembled blocks of graphite and embedded spheres of uranium oxide and uranium metal into what was called a *pile*. The main control rod was a wooden stick wrapped with cadmium foil. One safety rod would automatically drop upon high neutron level; one was attached to a weight with a rope, ready to be cut with an axe if necessary. Containers of neutron-absorbing cadmium-salt solution were ready to be dumped on the assembly in case of emergency. On December 2, 1942, the system was ready. The team gathered for the key experiment, as shown in an artist's recreation of the scene in Fig. 8.1. Fermi calmly made calculations with his slide rule and called for the main control rod to be withdrawn in steps.

FIG. 8.1

The first man-made chain reaction, December 2, 1942.

Reproduced from The Birth of the Atomic Age *by Gary Sheahan, courtesy Chicago Historical Society.*

The counters clicked faster and faster until it was necessary to switch to a recorder, whose pen kept climbing. Finally, Fermi closed his slide rule and said, "The reaction is self-sustaining. The curve is exponential." (Allardice and Trapnell, 2002).

This first man-made chain reaction gave confidence to the possibility of producing weapons material and was the basis for the construction of the natural-uranium-fueled graphite-moderated pile at Oak Ridge, Tennessee; see Fig. 8.2. By 1944, several large-scale water-cooled nuclear reactors at Hanford, Washington, were producing plutonium in kilogram quantities.

At the University of California at Berkeley, under the leadership of Ernest O. Lawrence, the electromagnetic separation calutron process for isolating U-235 was perfected, and government production plants at Oak Ridge, Tennessee, were built in 1943. At Columbia University, the gaseous diffusion process for isotope separation was studied, forming the basis for that production system, the first units of which were built at Oak Ridge. At Los Alamos, New Mexico, a research laboratory was established under the direction of J. Robert Oppenheimer. Theory and experiment led to the development of the nuclear weapons, first tested at Alamogordo, New Mexico, on July 16, 1945, and used in the next month at Hiroshima and Nagasaki in Japan.

The brevity of this account fails to describe adequately the dedication of scientists, engineers, and other workers to the accomplishment of wartime objectives or the magnitude of the design and construction effort by American industry. Two questions are inevitably raised. Should the atomic bombs have been developed? Should they have been used? Some of the scientists who worked on the Manhattan Project have expressed their feelings of guilt for having participated. Some insist that a lesser demonstration of the destructive power of the weapon should have been arranged, which would have been sufficient to end the conflict (Rabinowitch, 1946). Many others believed that the security of

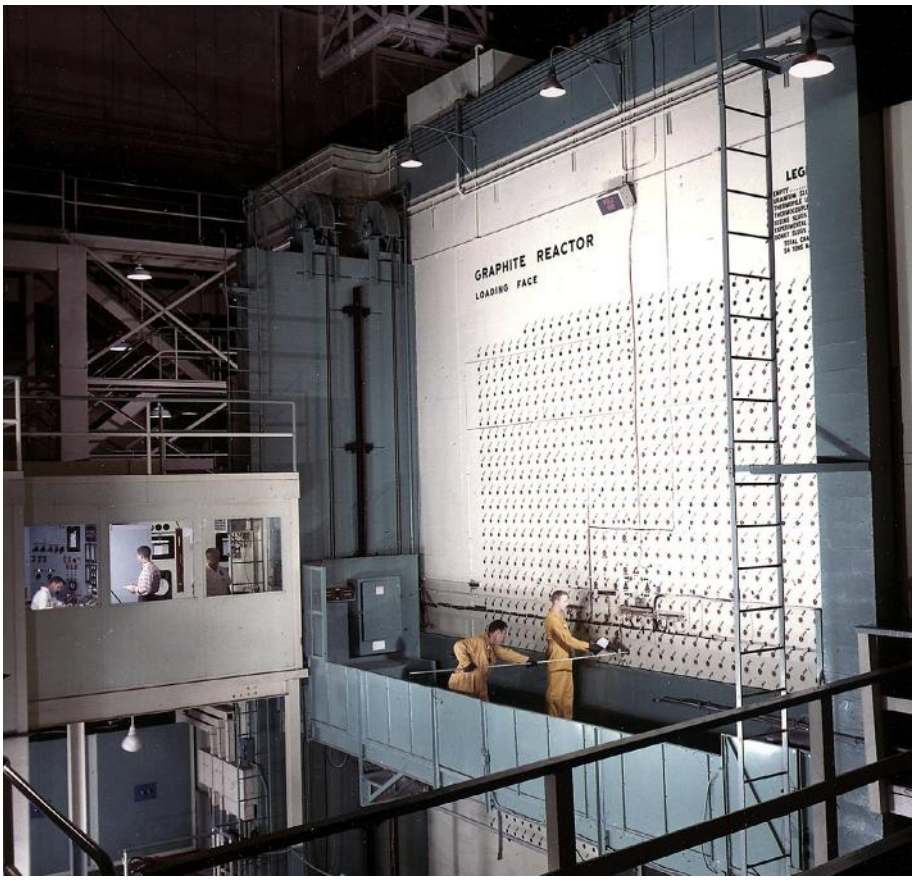

FIG. 8.2

Uranium slugs are loaded into fuel channels of the air-cooled X-10 pile at Oak Ridge.

Courtesy US Department of Energy (DOE).

the United States was threatened and that the use of the weapon shortened World War II greatly and thus saved a large number of lives on both sides. Many surviving military personnel scheduled to invade Japan have expressed gratitude for the action taken.

In the ensuing years, the buildup of nuclear weapons continued despite efforts to achieve disarmament. The dismantling of excess weapons will require many years. It is of some comfort, albeit small, that the existence of nuclear weapons has served for several decades as a deterrent to a direct conflict between major powers.

The discovery of nuclear energy has the potential for the betterment of humanity through fission and fusion energy resources and through radioisotopes and their radiation for research and medical purposes. The benefits can outweigh the detriments if humans are wise enough not to use nuclear weapons again.

8.4 THE ATOMIC ENERGY ACTS

After World War II, Congress addressed the problem of exploiting the new source of energy for peaceful purposes. The first law in the United States dealing with control of nuclear energy was the Atomic Energy Act of 1946, which was expanded in 1954. Issues of the times were involvement of the military, security of information, and freedom of scientists to do research.

In the declaration of policy, the Act says, "… the development and utilization of atomic energy shall, so far as practicable, be directed toward improving the public welfare, increasing the standard of living, strengthening free competition in private enterprise, and promoting world peace." The stated purposes of the Act were to carry out that policy through both private and federal research and development (R&D), to control information and fissionable material, and to provide regular reports to Congress. Special mention was given to the distribution of *byproduct material*, which includes the radioactive substances used for medical therapy and research. The Act created the US Atomic Energy Commission (AEC), consisting of five commissioners and a general manager. The AEC was given broad powers to preserve national security while advancing the nuclear field. A Joint Committee on Atomic Energy (JCAE) provided oversight for the new AEC. It included nine members each from the Senate and the House of Representatives. The civilian General Advisory Committee and the Military Liaison Committee provided advice to the AEC.

The Atomic Energy Act of 1954 revised and liberalized the previous legislation and expanded the AEC's role in disseminating unclassified information while retaining control of restricted weapons data. The groundwork was laid for a national program of reactor R&D with cooperation between the AEC and industry, including some degree of private ownership. The act authorized sharing of atomic technology with other countries, spelled out licensing procedures for the use of nuclear materials, and clarified the status of patents and inventions.

The powerful AEC carried out its missions of supplying material for defense, promoting beneficial applications, and regulating uses in the interests of public health and safety. It managed some 50 sites around the United States. Seven of the sites were labeled national laboratories, each with many R&D projects underway. The AEC owned the facilities, but contractors operated them. For example, Union Carbide Corporation had charge of Oak Ridge National Laboratory. During the Cold War of the late 1940s and early 1950s, new plutonium and enriched uranium plants were built, weapons tests were conducted in the South Pacific, and a major uranium exploration effort was begun. Under AEC sponsorship, a successful power reactor R&D program was carried out. Both the United States and the former Soviet Union developed the hydrogen bomb, and the nuclear arms race escalated.

Critics pointed out that the promotional and regulatory functions of the AEC were in conflict, despite an attempt to separate them administratively. Eventually, in 1974, the activities of the AEC were divided between two new agencies, the Energy Research and Development Administration (ERDA) and the Nuclear Regulatory Commission (NRC). In 1977, the cabinet-level Department of Energy (DOE) was formed from several other groups, including ERDA.

The DOE supports basic research in science and engineering and engages in energy technology development. It also manages defense programs such as nuclear weapons design, development, and testing. The DOE operates several multiprogram laboratories[1] and many smaller facilities around the United States.

[1]Argonne National Laboratory, Brookhaven National Laboratory, Idaho National Laboratory, Lawrence Berkeley Laboratory, Lawrence Livermore National Laboratory, Los Alamos National Laboratory, Oak Ridge National Laboratory, Pacific Northwest Laboratory, and Sandia National Laboratories.

8.5 INTERNATIONAL ATOMIC ENERGY AGENCY

In 1953, US President Dwight Eisenhower gave a speech titled "Atoms for Peace" that had an important influence on all aspects of nuclear energy. After describing the danger of nuclear war, he proposed the formation of an Atomic Energy Agency that would be responsible for receiving contributed fissionable materials, storing them, and making them available for peaceful purposes. Thus, he hoped to prevent the proliferation of nuclear weapons. For copies of the speech, see Eisenhower (1953).

In response to the speech, the United Nations established the International Atomic Energy Agency (IAEA) through a statute ratified by the necessary number of countries in 1957. More than 160 nations support and participate in the programs administered by headquarters in Vienna. The objective of the IAEA is "to accelerate and enlarge the contribution of atomic energy to peace, health, and prosperity throughout the world."

International conferences sponsored by the IAEA were held in 1955, 1958, 1964, and 1971 in Geneva, with all countries of the world invited to participate. The first of these revealed the progress made by the USSR in nuclear R&D.

The main functions of the IAEA are:

(a) To help its members develop nuclear applications to agriculture, medicine, science, and industry. Mechanisms are conferences, expert advisor visits, publications, fellowships, and the supply of nuclear materials and equipment. Special emphasis is placed on isotopes and radiation. Local research on the country's problems is encouraged. Nuclear programs sponsored by IAEA often help strengthen basic science in developing countries, even if they are not yet ready for nuclear power.

(b) To administer a system of international safeguards to prevent diversion of nuclear materials to military purposes. This involves the review by the IAEA of reports by individual countries on their fissionable material inventories and on-the-spot inspections of facilities, including reactors, fuel fabrication plants, and reprocessing facilities. Such monitoring is done for countries that signed the Nonproliferation Treaty (NPT) of 1968 and do not have nuclear weapons. The form of the monitoring is set by agreement. If a serious violation is found, the offending nation could lose its benefits from the IAEA.

The IAEA is one of the largest science publishers in the world because it sponsors a number of symposia on nuclear subjects each year and publishes the proceedings of each. The IAEA also promotes international rules, for example, in the area of transportation safety.

Recent initiatives of the IAEA include the establishment of agreements with countries on the application of safeguards. A large number of seminars addressing safeguards are given each year. Annual reports on nuclear-related information are available online. Unfortunately, the IAEA has had difficulties in making inspections in certain countries (e.g., Iran and North Korea).

8.6 REACTOR RESEARCH AND DEVELOPMENT

The AEC was charged with the management of the US nuclear programs, including military protection and development of peaceful uses of the atom. Several national laboratories were established to continue nuclear research, including sites such as Oak Ridge, Argonne (near Chicago), Los Alamos, and Brookhaven (on Long Island). A major objective was to achieve practical commercial nuclear power

through research and development. Oak Ridge first studied a gas-cooled reactor and later planned a high-flux reactor fueled with highly enriched uranium alloyed with and clad with aluminum that used water as moderator and coolant. A reactor was eventually built at the National Reactor Testing Station (NRTS) in Idaho as the Materials Testing Reactor (MTR). Table 8.1 compares some of the early reactors in the United States; Stacy (2000) lists 52 reactors at the NRTS alone. The submarine reactor (described in Section 22.1) was adapted by Westinghouse Electric Corporation for use as the first commercial power plant at Shippingport, Pennsylvania. It began operation in 1957 at an electric power output of 60 MW. Uranium dioxide (UO_2) pellets as fuel were first introduced in this pressurized water reactor (PWR) design (see Fig. 8.3).

In the 1950s, several reactor concepts were tested and dismissed for various reasons (Dawson, 1976; Simpson, 1995; Holbert, 2017). One used an organic liquid diphenyl ($C_{12}H_{10}$) as a coolant based on a high boiling point. Unfortunately, radiation caused deterioration of the compound. Another was the homogeneous aqueous reactor, with a uranium salt in water solution that was circulated through the core and heat exchanger. Deposits of uranium led to excess heating and corrosion of wall materials. The sodium-graphite reactor had liquid metal coolant and carbon moderator. Only one commercial reactor of this type was built. The high-temperature gas-cooled reactor, developed by General Atomics, has not been widely adopted but is a potential alternative to light water reactors by virtue of its graphite moderator, helium coolant, and uranium-thorium fuel cycle.

Table 8.1 Early Reactors in the United States

Reactor	Location	Operation	Full Power	Fuel	Moderator/Coolant
CP-1	Chicago, IL	1942	200 W	Natural U	Graphite/Air
X-10	Oak Ridge, TN	1943	4 MW	Natural U	Graphite/Air
CP-3	Argonne, IL	1944	300 kW	Natural U	D_2O
LOPO	Los Alamos, NM	1944	1 W	Uranyl sulfate	H_2O
B reactor	Hanford, WA	1944	~100–1000 MW	Natural U	Graphite/H_2O
Clementine	Los Alamos, NM	1946	25 kW	Plutonium	None (fast)/Hg
BSR	Oak Ridge, TN	1950	100 kW	Enriched U	H_2O
EBR-I	NRTS, ID	1951	100 kW	Highly enriched U	None (fast)/NaK
MTR	NRTS, ID	1952	40 MW	Enriched U	H_2O
HRE	Oak Ridge, TN	1952	150 kWe	Uranyl sulfate	H_2O
STR-II	USS Nautilus	1955	~100 MW	Highly enriched U	H_2O
EBWR	Argonne, IL	1956	5000 kWe	Low enriched U	H_2O
PWR	Shippingport, PA	1957	60 MWe	Highly enriched U	H_2O
BWR	Dresden, IL	1959	200 MWe	Low enriched U	H_2O

Data from Landis, J.W., 1957. Nuclear Engineering. McGraw-Hill, pp. 764–768; Stephenson, R., 1958. Introduction to Nuclear Engineering, second ed., McGraw-Hill, pp. 86, 98, 102, 107, 115, 118; Jacobs, A.M., Kline, D.E., Remick, F.J., 1960. Basic Principles of Nuclear Science and Reactors. D. Van Nostrand, Princeton; Murray, R.L., 1961. Introduction to Nuclear Engineering, second ed. Prentice-Hall, pp. 128–129; Foster, A.R., Wright, R.L., 1983. Basic Nuclear Engineering, fourth ed. Allyn and Bacon, Inc.
BSR, *Bulk Shielding Reactor-swimming pool;* CP, *Chicago Pile;* EBR, *Experimental Breeder Reactor;* EBWR, *Experimental Boiling Water Reactor;* HRE, *Homogeneous Reactor Experiment;* LOPO, *LOw POwer water boiler;* MTR, *Materials Test Reactor;* STR, *Submarine Thermal Reactor.*

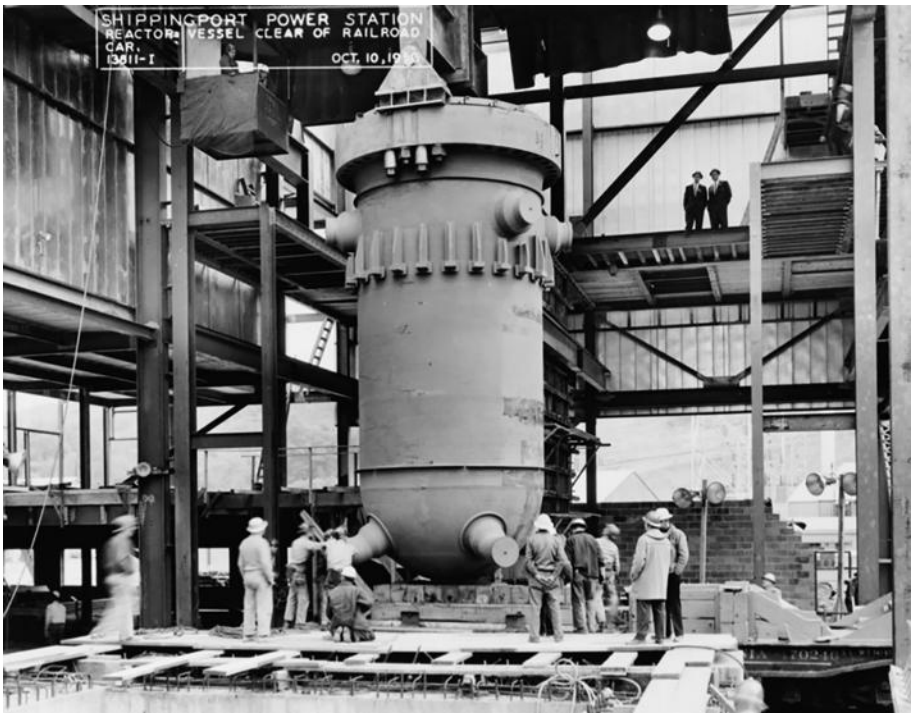

FIG. 8.3

Shippingport reactor vessel, October 10, 1956.

Courtesy Library of Congress, Prints and Photographs Division, HAER, Reproduction number HAER PA,4-SHIP,1-87.

Two other reactor R&D programs were underway at Argonne over the same period. The first program was aimed at achieving power plus breeding of plutonium by use of the fast reactor concept with liquid sodium coolant. The first electric power from a nuclear source was produced in late 1951 in the Experimental Breeder Reactor, and the possibility of breeding was demonstrated. The second program consisted of an investigation of the possibility of allowing water in a reactor to boil and generate steam directly. The principal concern was with the fluctuations and instability associated with the boiling. Tests called BORAX were performed that showed that a boiling reactor could operate safely, and work progressed that led to electrical generation in 1955. The General Electric Company then proceeded to develop the boiling water reactor (BWR) concept further, with the first commercial reactor of this type put into operation at the 200 MWe plant at Dresden, Illinois, in 1960.

Based on the initial success of the PWR and BWR, and with the application of commercial design and construction expertise, Westinghouse and General Electric were able, in the early 1960s, to advertise large-scale nuclear plants with a power of approximately 500 MWe that would be competitive with fossil fuel plants in the cost of electricity. Immediately thereafter, there was a rapid move on the part of the electric utilities to order nuclear plants, and the growth in the late 1960s was phenomenal. Orders for nuclear steam supply systems for 1965–70 amounted to approximately 88,000 MWe, which was

more than a third of all orders, including fossil-fueled plants. The corresponding nuclear electric capacity was approximately a quarter of the total US capacity at the end of the period of rapid growth.

After 1970, the rate of installation of nuclear plants in the United States declined, for a variety of reasons: (a) the very long time required—greater than 10 years—to design, license, and construct nuclear facilities; (b) the energy conservation measures adopted as a result of the Arab oil embargo of 1973–74, which produced a lower growth rate of demand for electricity; and (c) public opposition in some areas. The last order for nuclear plants in the 20th century was in 1978. A number of orders were canceled, and construction was stopped before completion on others.

This large new power source was put in place in a relatively brief period of 40 years after the end of World War II. The endeavor revealed a new concept: that large-scale national technological projects could be undertaken and successfully completed by the application of large amounts of money and the organization of the efforts of many sectors of society. The nuclear project in many ways served as a model for the US space program of the 1960s. The important lesson that the history of nuclear energy development may have for us is that urgent national and world problems can be solved by wisdom, dedication, and cooperation.

For economic and political reasons, considerable uncertainty developed about the future of nuclear power in the United States and many other countries. In the next section, we will discuss the nuclear controversy and later (in Chapter 24) describe the stagnation of nuclear power before the turn of the millennium and the future of nuclear energy in the coming decades.

8.7 THE NUCLEAR CONTROVERSY

The popularity of nuclear power decreased during the 1970s and 1980s, with adverse public opinion threatening to prevent the construction of new reactors. We can attempt to analyze this situation, explaining causes and assessing effects.

In the 1950s, the AEC and the press heralded nuclear power as inexpensive, inexhaustible, and safe. Congress was highly supportive of reactor development, and the public seemed to feel that great progress toward a better life was being made. In the 1960s, however, a series of events and trends raised public concerns and began to reverse the favorable opinion.

First was the youth movement against authority and constraints. In that generation's search for a simpler and more primitive or natural lifestyle, the use of wood and solar energy was preferred to energy based on the high technology of the "establishment." Another target for opposition was the military-industrial complex, blamed for the generally unpopular Vietnam War. A 1980s version of the antiestablishment philosophy advocated decentralization of government and industry, favoring small locally controlled power units based on renewable resources.

Second was the 1960s environmental movement, which revealed the extent to which industrial pollution in general was affecting wildlife and human beings, with its related issue of the possible contamination of air, water, and land by accidental releases of radioactivity from nuclear reactors. Continued revelations about the extent of improper management of hazardous chemical waste had a side effect of creating adverse opinion about radioactive waste.

Third was a growing loss of respect for government, with public disillusionment becoming acute as an aftermath of the Watergate affair. Concerned observers cited actions taken by the AEC or the DOE without informing or consulting those affected. Changes in policy about radioactive waste management

from one administration to another resulted in inaction, interpreted as evidence of ignorance or ineptitude. A common opinion was that no one knew what to do with nuclear waste.

A fourth development was the confusion created by the sharp differences in opinion among scientists about the wisdom of developing nuclear power. Nobel Prize winners were arrayed on both sides of the argument; the public understandably could hardly fail to be confused and worried about where the truth lay.

The fifth was the fear of the unknown hazard represented by reactors, radioactivity, and radiation. It may be agreed that an individual has a much greater chance of dying in an automobile accident than from exposure to fallout from a reactor accident. However, because the hazard of the roads is familiar and believed to be within the individual's control, it does not evoke nearly as great a concern as does a nuclear event.

The sixth was the association between nuclear power and nuclear weapons. This is in part inevitable because both involve plutonium, use the physical process of fission with neutrons, and have radioactive byproducts. On the other hand, opponents of nuclear power, who stress the similarities rather than the differences, have cultivated the connection.

As with any subject, there is a spectrum of opinions. At one end are the dedicated advocates who believe nuclear power to be safe, badly needed, and capable of success only if opposition can be reduced. A large percentage of physical scientists and engineers fall into this category, believing that technical solutions for most problems are possible.

Next are those who are technically knowledgeable but are concerned about the ability of man to avoid reactor accidents or to design and build safe waste facilities. Depending on the strength of their concerns, they may believe that consequences outweigh benefits.

Next are average citizens who are suspicious of government and who believe in Murphy's Law, being aware of failures such as Three Mile Island, the space shuttle Challenger, Chernobyl, Deepwater Horizon, and Fukushima. They have been influenced as well by strong antinuclear claims and tend to be opposed to further nuclear power development, although they recognize the need for continuous electric power generation.

At the other end of the spectrum are ardent opponents of nuclear power who actively speak, write polemics, intervene in licensing hearings, lead demonstrations, or take physical action to try to prevent power plants from reaching fruition.

Attitudes vary among representatives of the news and entertainment media—newspapers, magazines, radio, television, and movies—but there is an apparent tendency toward skepticism. Nuclear advocates are convinced that any incident involving reactors or radiation is given undue emphasis by the media. They believe that if people were adequately informed, they would find nuclear power acceptable. This view is only partially accurate for two reasons: (1) some technically knowledgeable people are strongly antinuclear, and (2) irrational fears cannot be removed by additional facts. Many people have sought to analyze the phenomenon of nuclear fear, but the study by Weart (1988) is one of the best.

Nevertheless, in recent years public acceptance of nuclear power has held steady in the United States for several reasons: (a) the industry has maintained an excellent nuclear safety record, through actions by utilities, the Nuclear Regulatory Commission, and the Institute of Nuclear Power Operations; (b) increased awareness of energy needs, related to the continued demand for expensive and uncertain foreign oil; and (c) realization that the generation of electricity by fission does not release greenhouse gases that contribute to global warming.

8.8 SUMMARY

A series of investigations in atomic and nuclear physics from 1879 to 1939 led to the discovery of fission. New knowledge was developed about particles and rays, radioactivity, and the structures of the atom and the nucleus. The existence of fission suggested that a chain reaction involving neutrons was possible and that the process had military significance. A major national program was initiated in the United States during World War II. The ensuing development of uranium isotope separation methods, nuclear reactors for plutonium production, and weapons technology culminated in the use of atomic bombs to end the war.

In the postwar period, emphasis was placed on maintenance of nuclear protection and on peaceful applications of nuclear processes under the AEC. Four reactor concepts—pressurized water, boiling water, fast breeder, and gas-cooled—evolved through work by national laboratories and industry. The first two concepts were brought to commercial status in the 1960s. The AEC had functions of promotion and regulation for 28 years while the DOE and NRC, respectively, shoulder those roles now. Internationally, the IAEA helps developing countries and monitors nuclear inventories.

8.9 EXERCISES

8.1 Enter into an Internet search engine the phrase "nuclear age timeline" and consult several sources to develop a list of the most important single events in each decade.

8.2 Perform an Internet search using the phrase "Einstein letter Roosevelt" and read the letter of August 2, 1939.

8.3 Using the nuclear data of Appendix A, determine the Q value and Coulombic threshold energy of the neutron-emitting reaction:

$$^{4}_{2}\alpha + {}^{9}_{4}\mathrm{Be} \rightarrow {}^{12}_{6}\mathrm{C} + {}^{1}_{0}\mathrm{n} \tag{8.1}$$

Does the alpha emitted from the decay of Po-210 have sufficient energy to initiate this reaction?

8.4 Highly enriched uranium (HEU) produced at Oak Ridge was called oralloy. For an isotopic content of 1% U-234, 93% U-235, and 6% U-238, and density of 18.7 g/cm^3, compute the thermal macroscopic cross-section for (a) capture and (b) fission.

8.5 The CP-1 utilized four grades of graphite, each with a different thermal absorption cross section: (a) AGOT 4.97 mb, (b) Speer 5.51 mb, (c) US 6.38 mb, and (d) AGX 6.68 mb (Nightingale, 1962). Assuming that boron contaminants cause the cross-section deviation from pure carbon, determine the atomic fraction of boron in each graphite type.

8.6 Make a list of fictional superheroes who owe their powers to radiation.

REFERENCES

Allardice, C., Trapnell, E.R., 2002. The first pile. Nucl. News 45 (12), 34.

Becquerel, H., 1896. On the invisible rays emitted by phosphorescent bodies. Comptes Rendus 122, 501.

Bohr, N., 1913. On the constitution of atoms and molecules. Philos. Mag. Ser. 6 26 (151), 1–25.

Bothe, W., Becker, H., 1930. Künstliche erregung von kern-γ-strahlen (Artificial excitation of nuclear γ-rays). Z Phys. 66 (5-6), 289–306.

Breit, G., Wigner, E., 1936. Capture of slow neutrons. Phys. Rev. 49 (7), 519–531.

Chadwick, J., 1932. The existence of a neutron. Proc. R. Soc. Lond. Ser. A 136 (830), 692–708.

Crookes, W., 1879. On the illumination of lines of molecular pressure, and the trajectory of molecules. Philos. Trans. R Soc. Lond. 170, 135–164.

Curie, P., Curie, M.S., 1898. On a new radioactive substance contained in pitchblende. Comptes Rendus 127, 175–178.

Dawson, F.G., 1976. Nuclear Power: Development and Management of a Technology. University of Washington Press, Seattle, WA.

Einstein, A., 1905. Zur elektrodynamik bewegter körper (On the electrodynamics of moving bodies). Ann. Phys. 17, 891.

Eisenhower, D.D., 1953. Atoms for Peace Address to the 470th Plenary Meeting of the United Nations General Assembly. New York. Full text and video excerpt. Available from: https://www.iaea.org/newscenter/multimedia/videos/atoms-peace-speech.

Goudsmit, S.A., 1947. Alsos; 1947. (Reprinted in 1983 by Tomash Publishers and American Institute of Physics (AIP), with a new introduction by R.V. Jones and supplemental photographs).

Hahn, O., Strassmann, 1939. Über den nachweis und das verhalten der bei der bestrahlung des urans mittels neutronen entstehenden erdalkalimetalle (On the detection and characteristics of the alkaline earth metals formed by irradiation of uranium with neutrons). Naturwissenschaften 27 (1), 11–15.

Hewlett, R.G., Anderson Jr., O.E., 1962. A History of the United States Atomic Energy Commission: The New World, 1939/1946. vol. I. The Pennsylvania State University Press, University Park.

Holbert, K.E., 2017. Nuclear reactors. In: Seidel, A. (Ed.), Kirk-Othmer Encyclopedia of Chemical Technology. Wiley, New York.

Joliot, F., Curie, I., 1934. Artificial production of a new kind of radio-element. Nature 133, 201–202.

Lawrence, E.O., Livingston, M.S., 1932. The production of high speed light ions without the use of high voltages. Phys. Rev. 40 (1), 19–37.

Meitner, L., Frisch, O.R., 1939. Disintegration of uranium by neutrons: a new type of nuclear reaction. Nature 143 (3615), 239–240.

Nightingale, R.E., 1962. Nuclear Graphite. Academic Press, New York, p. 4.

Pash, B.T., 1980. The Alsos Mission. Ace Books, New York.

Rabinowitch, E., 1946. Before Hiroshima. Bull. Atom. Sci. 1 (10), 1–4. 16.

Roentgen, W.C., 1895. On a new kind of rays. Nature 53 (1369), 274–276.

Rose, P.L., 1998. Heisenberg and the Nazi Atomic Bomb Project: A Study in German Culture. University of California Press, Berkeley.

Rutherford, E., 1911. LXXIX. The scattering of α and β particles by matter and the structure of the atom. Philos. Mag. Ser. 6 21 (125), 669–688.

Rutherford, E., 1919. LIV. Collision of α particles with light atoms. IV. An anomalous effect in nitrogen. Philos. Mag. Ser. 6 37 (122), 581–587.

Seaborg, G.T., McMillan, E.M., Kennedy, J.W., Wahl, A.C., 1946. Radioactive element 94 from deuterons on uranium. Phys. Rev. 69, 366–367.

Simpson, J.W., 1995. Nuclear Power from Underseas to Outer Space. American Nuclear Society, La Grange Park, IL.
Stacy, S.M., 2000. Proving the Principle. Idaho National Engineering and Environmental Laboratory, Idaho Falls.
Thomson, J.J., 1897. XL. Cathode rays. Philos. Mag. Ser. 5 44 (269), 293–316.
Weart, S.R., 1988. Nuclear Fear: A History of Images. Harvard University Press, Cambridge.

FURTHER READING

American Nuclear Society (ANS), 1992. Controlled Nuclear Chain Reaction: The First 50 Years. ANS, La Grange Park, IL.
Atomic Heritage Foundation, http://www.atomicheritage.org/. Information on the nuclear effort of WWII.
Bird, K., Sherwin, M.J., 2005. American Prometheus: The Triumph and Tragedy of J. Robert Oppenheimer. Knopf, New York.
Charles, F., 1993. Operation Epsilon: The Farm Hall Transcripts. University of California Press, Berkeley Recorded conversations among German scientists captured at the end of World War II.
Cohen, B.L., 1983. Before It's Too Late: A Scientist's Case for Nuclear Energy. Plenum Press, New York.
Davis, N.P., 1968. Lawrence and Oppenheimer. Simon & Schuster, New York.
Foster, A.R., Wright, R.L., 1983. Basic Nuclear Engineering, fourth ed. Allyn and Bacon, Inc., Boston.
Goldschmidt, B., 1982. The Atomic Complex. American Nuclear Society, La Grange Park.
Gosling, F.G., 2010. The Manhattan Project: Making the Atomic Bomb. DOE/MA-0002, http://energy.gov/management/downloads/gosling-manhattan-project-making-atomic-bomb.
Groueff, S., 1967. Manhattan Project: The Untold Story of the Making of the Atomic Bomb. Little, Brown & Co, Boston, The author benefited from material published right after WWII and interviews with participants; both General Leslie Groves and AEC Commissioner Glenn Seaborg praised the book.
Groves Lt. General, L.R., 1962. Now It Can Be Told. Harper & Row, New York, The account of the Manhattan Project by the person in charge.
Hewlett, R.G., Duncan, F., 1972. A History of the United States Atomic Energy Commission: Atomic Shield, 1947/1952. vol. II. U.S. Atomic Energy Commission (AEC), Washington, DC.
Hilgartner, S., Bell, R.C., O'Connor, R., 1982. Nukespeak: Nuclear Language, Visions, and Mindset. Sierra Club Books, San Francisco.
Jacobs, A.M., Kline, D.E., Remick, F.J., 1960. Basic Principles of Nuclear Science and Reactors. D. Van Nostrand, Princeton, NJ.
Jungk, R., 1958. Brighter Than a Thousand Suns. Harcourt Brace & Co., San Diego.
Kelly, C.C. (Ed.), 2007. The Manhattan Project: The Birth of the Atomic Bomb in the Words of Its Creators, Eyewitnesses, and Historians. Black Dog & Leventhal Publishers, Inc., New York.
Landis, J.W., 1957. Nuclear-reactor types. In: Bonilla, C.F. (Ed.), Nuclear Engineering. McGraw-Hill, New York, pp. 764–768.
Loeber, C.R., 2005. Building the Bombs: A History of the Nuclear Weapons Complex, second ed. Sandia National Laboratories, Albuquerque, SAND2005-5648P.
Michal, R., 2004. Atoms for Peace—Updating the Vision. Nucl. News 47 (1), 55–57.
Murray, R.L., 1961. Introduction to Nuclear Engineering, second ed. Prentice-Hall, Englewood Cliffs, pp. 128–129.
National Health Museum, Access Excellence, Radioactivity: Historical Figures. www.accessexcellence.org/AE/AEC/CC/historical_background.html. Biographies of Roentgen, Becquerel, the Curies, and Rutherford.
Nuclear News, 2013. Reference special section. Nucl. News 56 (3), 45–77.
Rhodes, R., 1986. The Making of the Atomic Bomb. Simon & Schuster, New York.
Rhodes, R., 1995. Dark Sun: The Making of the Hydrogen Bomb. Simon & Schuster, New York.

Smyth, H.D., 1945. Atomic Energy for Military Purposes. Princeton University Press (Republished in *Reviews of Modern Physics* 17 (4): 351–471, 1945 and reprinted with additional commentary by Stanford University Press, 1989). The first unclassified account of the nuclear effort of World War II; also known as the "Smyth Report".

Stephenson, R., 1958. Introduction to Nuclear Engineering, second ed. McGraw-Hill, New York, pp. 86, 98, 102, 107, 115, 118.

U.S. Department of Energy, Energy Information Administration, 2018. Electric Power Annual 2016. www.eia.gov/electricity/annual/.

U.S. Department of Energy, Manhattan Project Resources. https://www.osti.gov/opennet/manhattan_resources.jsp. Comprehensive account of WWII project.

U.S. Department of Energy, Office of Scientific and Technical Information (OSTI), History of the Department of Energy's National Laboratories. www.osti.gov/accomplishments/nuggets/historynatlabs.html.

U.S. Department of Energy. History Publications. Available from: https://energy.gov/management/history/historical-resources/history-publications.

U.S. Department of Energy, The History of Nuclear Energy, DOE/NE-0088. https://energy.gov/ne/downloads/history-nuclear-energy.

Walker, M., 1989. German National Socialism and the Quest for Nuclear Power, 1939–1949. Cambridge University Press, Cambridge.

Walker, M., 1990. Heisenberg, Goudsmit, and the German atomic bomb. Phys. Today 43 (1), 52–60. This article prompted a series of letters to the editor in the issues of May 1991 and February 1992.

CHAPTER

PARTICLE ACCELERATORS

9

CHAPTER OUTLINE

A device that provides forces on charged particles by some combination of electric and magnetic fields and brings the ions to high speed and kinetic energy is called an *accelerator*. Many types have been developed for the study of nuclear reactions and basic nuclear structure, with an ever-increasing demand for higher particle energy. In this chapter, we will review the nature of the forces on charges and describe the arrangement and principle of operation of several important kinds of particle accelerators. In later chapters, we describe some of the many applications.

9.1 ELECTRIC AND MAGNETIC FORCES

Let us recall how charged particles are influenced by electric and magnetic fields. First, visualize a pair of parallel metal plates separated by a distance d, as in the simple capacitor shown in Fig. 9.1. A direct-current voltage supply, such as a battery, provides a potential difference V to the region of low gas pressure, thereby producing an electric field of

$$\mathcal{E} = V/d \tag{9.1}$$

between the parallel plates. If a particle of mass m and charge q is released at the plate of like charge, it will experience an electric force

$$F_E = \mathcal{E}q \tag{9.2}$$

Nuclear Energy. https://doi.org/10.1016/B978-0-12-812881-7.00009-5

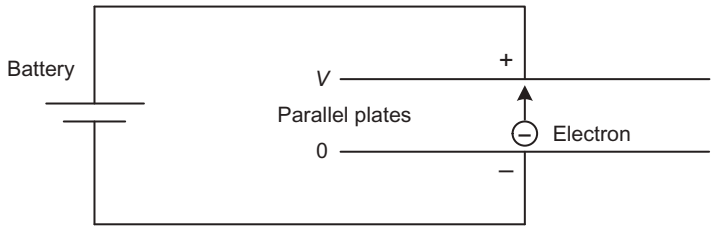

FIG. 9.1

Capacitor as accelerator.

and its acceleration will be

$$a = F_E/m = \mathcal{E}q/m \tag{9.3}$$

The particle will gain speed, and on reaching the opposite plate, it will have reached a kinetic energy

$$\frac{1}{2}mv^2 = Vq \tag{9.4}$$

Thus, its speed is

$$v = \sqrt{2Vq/m} \tag{9.5}$$

EXAMPLE 9.1

If the voltage between two parallel plates is 100 V, an electron ($e = 1.602 \times 10^{-19}$ C) placed initially at the negative plate achieves a terminal speed of

$$v = \sqrt{\frac{2Ve}{m_e}} = \sqrt{\frac{(2)(100\,\mathrm{V})(1.602 \times 10^{-19}\,\mathrm{C})[(\mathrm{J/C})/\mathrm{V}]}{(9.109 \times 10^{-31}\,\mathrm{kg})[\mathrm{J}/(\mathrm{kg\,m^2/s^2})]}} = 5.93 \times 10^6\,\mathrm{m/s}$$

This is a nonrelativistic velocity, justifying the use of $\frac{1}{2}mv^2$.

Next, let us introduce a charged particle of mass m, charge q, and speed v into a region with uniform magnetic field B, as in Fig. 9.2. The particle experiences a magnetic force of

$$F_M = qvB\,\sin(\varphi) \tag{9.6}$$

in which φ is the angle between the magnetic field and the particle direction. If the charge enters along or opposite the direction of the field lines ($\sin(\varphi) = 0$), it will not be affected. However, if the charged particle enters perpendicularly to the field ($\sin(\varphi) = 1$), it will undergo centripetal acceleration a_c from the force such that

$$F_M = ma_c = m(v^2/R) \tag{9.7}$$

Hence, the charge moves at constant speed on a circle with a *radius of gyration* of

$$R = mv^2/F_M = mv/(qB) \tag{9.8}$$

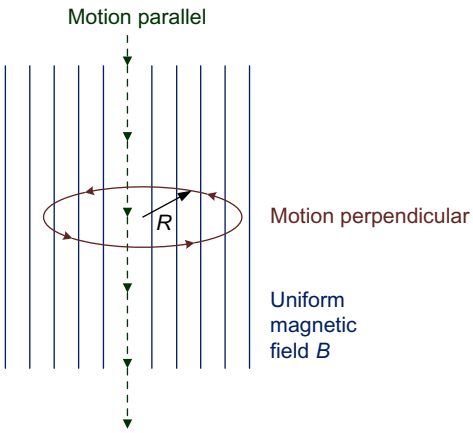

FIG. 9.2

Electric charge motion in uniform magnetic field B.

such that the stronger the field or the lower the speed, the smaller will be the radius of motion. Note that the angular frequency ω (omega) is equal to

$$\omega = v/R = qB/m \tag{9.9}$$

If the charge enters at some other angle, it will move in a helical path.

Instead, let us release a charge in a region where the magnetic field B is changing with time. If an electron were inside the metal of a circular loop of wire of area A as in Fig. 9.3, it would experience an electric force induced by the change in magnetic flux $\Phi = BA$. The same effect would take place without the presence of the wire, of course. Finally, if the magnetic field varies with position, additional forces act on the charged particles.

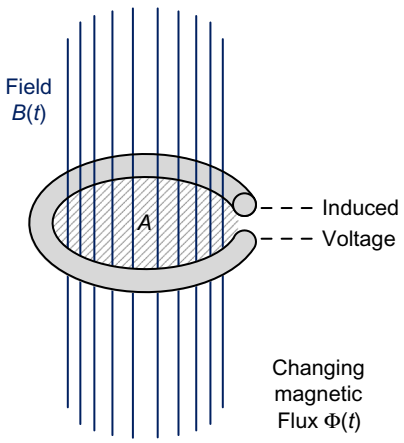

FIG. 9.3

Magnetic induction.

9.2 HIGH-VOLTAGE MACHINES

One way to accelerate ions to high speed is to provide a large potential difference between a source of charges and a target. In effect, the phenomenon of lightning, in which a discharge from charged clouds to the ground takes place, is produced in the laboratory. Two devices of this type are commonly used. The first is the voltage multiplier or Cockcroft and Walton (1932) machine, Fig. 9.4, which has a circuit that charges capacitors in parallel and discharges them in series. The second is the electrostatic generator or Van de Graaff et al. (1933) accelerator, the principle of which is shown in Fig. 9.5. An insulated metal shell is raised to high potential by bringing it charge on a moving belt, permitting the acceleration of positive charges such as protons or deuterons. Particle energies of the order of 5 MeV are possible, with a very small spread in energy.

9.3 LINEAR ACCELERATOR

Rather than giving a charge one large acceleration with a high voltage, it can be brought to high speed by a succession of accelerations through relatively small potential differences (Wideröe, 1928), as in the linear accelerator (LINAC) in Fig. 9.6. It consists of a series of accelerating electrodes in the form of tubes with alternating electric potentials applied as shown. An electron or ion gains energy in the gaps between tubes and drifts without change of energy while inside the tube, where the field is nearly zero. By the time the charge reaches the next gap, the voltage is again correct for acceleration.

From the ion source to the entrance of the first tube, the particle kinetic energy increases to qV_p where V_p is the peak voltage, and its speed is $v_1 = \sqrt{2V_p q/m}$. Within the gap between the first and

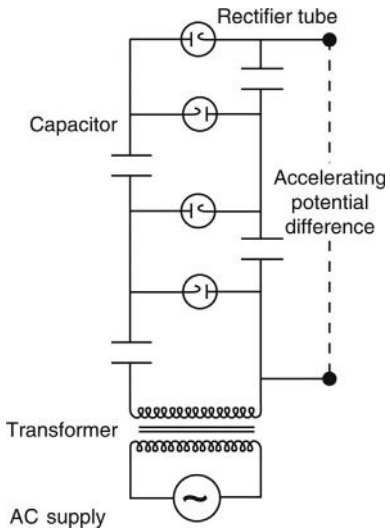

FIG. 9.4

Cockcroft-Walton circuit.

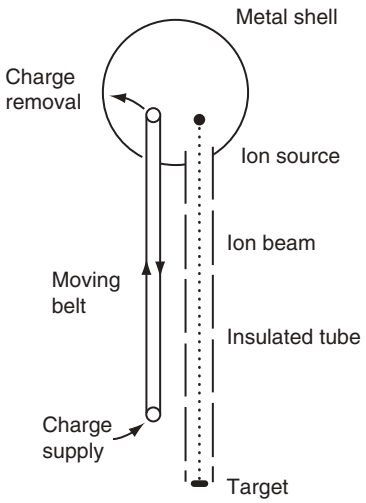

FIG. 9.5

Van de Graaff accelerator.

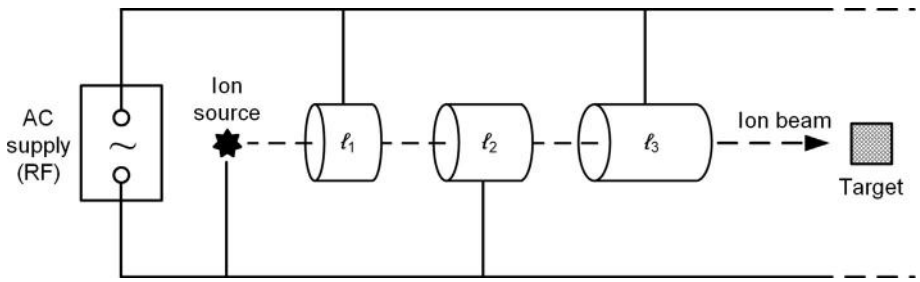

FIG. 9.6

Simple linear accelerator.

second tubes, the particle energy rises by an additional qV_p such that its velocity entering the second tube is $v_2 = \sqrt{4V_p q/m} = v_1\sqrt{2}$. Extrapolating this behavior reveals a speed of

$$v_n = v_1\sqrt{n} \tag{9.10}$$

at the n-th tube. The time to traverse a distance ℓ is ℓ/v, which is equal to the half-period $T/2$ of the voltage cycle of frequency $f = 1/T$. As the transit time within each drift tube is identical,

$$t = \ell_n/v_n = T/2 \tag{9.11}$$

Because the ion is gaining speed along the path down the row of tubes, their lengths ℓ must be successively longer for the time of flight in each to be constant. If the gap spacings are comparatively short, the accelerator length is

$$\sum_{k=1}^{n} \ell_k = \ell_1 \sum_{k=1}^{n} \sqrt{k} \cong \frac{2}{3} n^{3/2} \ell_1 \tag{9.12}$$

The LINAC at the Stanford Linear Accelerator Center (SLAC) is the world's longest at 2 miles (3.2 km). It produces electron and positron beams with energies up to 50 GeV (Rees, 1989). Such an extensive linear dimension encourages a more compact accelerator such as the cyclotron.

EXAMPLE 9.2

A helion ($^3He^{2+}$) has a charge of $2e$ and mass of 5.006×10^{-27} kg. For a 20 MHz, 15 kV peak voltage supply, the speed of a helion after crossing the initial gap is

$$v_1 = \sqrt{\frac{2V_p q_h}{m_h}} = \sqrt{\frac{2(15,000\,\text{V})(2)(1.602 \times 10^{-19}\,\text{C})}{5.006 \times 10^{-27}\,\text{kg}}} = 1.39 \times 10^6\,\text{m/s}$$

The corresponding length of the first tube should be

$$\ell_1 = \frac{v_1 T}{2} = \frac{v_1}{2f} = \frac{1.39 \times 10^6\,\text{m/s}}{2(20 \times 10^6\,\text{Hz})} = 0.035\,\text{m}$$

9.4 CYCLOTRON AND BETATRON

Successive electrical acceleration by electrodes and circular motion within a magnetic field are combined in the cyclotron, invented at the University of California (Lawrence and Livingston, 1932). As shown in Fig. 9.7, ions such as protons, deuterons, or alpha particles are provided by a source at the center of a vacuum chamber located between the poles of a large electromagnet. Two hollow metal boxes called "dees" (in the shape of the letter D) are supplied with alternating voltages in correct frequency and opposite polarity. In the gap between dees, an ion gains energy as in the linear accelerator, then moves on a circle while inside the electric-field-free region, guided by the magnetic field. Each crossing of the gap with potential difference V gives impetus to the ion with an energy gain Vq, and the radius of motion increases according to $R = v/\omega$, where $\omega = qB/m$ is the angular speed. The unique feature of the cyclotron is that the time required for one complete revolution, $T = 2\pi/\omega$, is independent of the radius of motion of the ion. Thus, it is possible to use a synchronized alternating potential of constant frequency f, angular frequency $\omega = 2\pi f$, to provide acceleration at the right instant.

The path of ions is approximately a spiral. When the outermost radius is reached and the ions have full energy, a beam is extracted from the dees by special electric and magnetic fields and allowed to strike a target, in which nuclear reactions take place.

The first artificial plutonium was created at Berkeley with a 60-in. cyclotron that produced 16-MeV deuterons that bombarded uranium, thereby forming neptunium that decayed to plutonium (Seaborg, 1981). The cyclotron is primitive compared with new machines but is still widely used in hospitals to produce radioisotopes such as Mo-99. Canada's TRIUMF boasts the world's largest cyclotron, which provides 520 MeV protons.

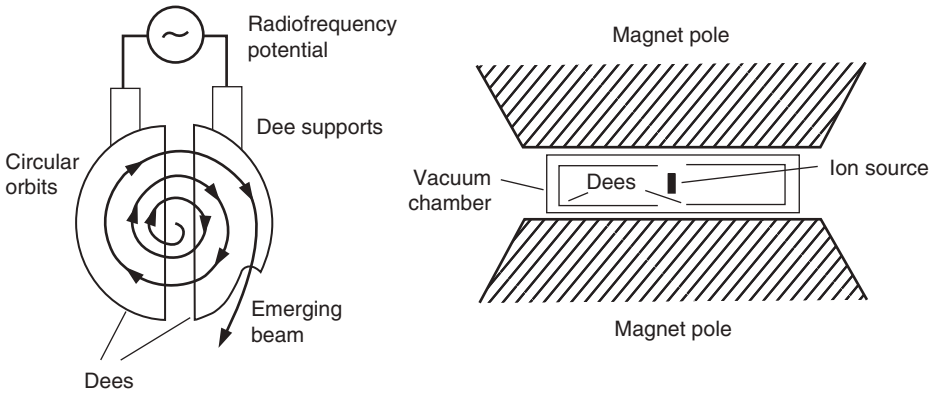

FIG. 9.7

Cyclotron.

EXAMPLE 9.3

In a cyclotron magnetic field B of 0.5 Wb/m^2 (tesla), the angular speed for deuterons of mass 3.34×10^{-27} kg and charge $q_d = e$ is

$$\omega = \frac{q_d B}{m_d} = \frac{(1.602 \times 10^{-19}\,\text{C})(0.5\,\text{T})}{3.34 \times 10^{-27}\,\text{kg}} = 2.4 \times 10^7\,\text{rad/s}$$

Equating this to the angular frequency for the power supply, $\omega = 2\pi f$, we find

$$f = \omega/(2\pi) = (2.4 \times 10^7\,\text{rad/s})/(2\pi) = 3.8 \times 10^6\,\text{Hz}$$

This is in the radiofrequency (RF) range according to Fig. 1.1.

In the betatron, the induction accelerator first built by Kerst (1941), electrons are brought to high speeds. A changing magnetic flux provides an electric field and a force on the charges while they are guided in a path of constant radius. Fig. 9.8 shows the vacuum chamber in the form of a doughnut placed between specially shaped magnetic poles. The force on electrons of charge e is in the direction tangential to the orbit of radius R. The rate at which the average magnetic field within the loop changes is $\Delta B/\Delta t$, provided by varying the current in the coils of the electromagnet. Note that the area within the circular path is $A = \pi R^2$ and the magnetic flux is $\Phi = BA$. According to Faraday's law of induction, if the flux changes by $\Delta\Phi$ in a time Δt, a potential difference around a circuit of $V = \Delta\Phi/\Delta t$ is produced. The corresponding electric field is $\mathcal{E} = V/(2\pi R)$, and the force is $e\mathcal{E}$. Combining these relations, the magnitude of the force is

$$F = \frac{eR}{2}\frac{\Delta B}{\Delta t} \tag{9.13}$$

The charge continues to gain energy while remaining at the same radius if the magnetic field at that location is half the average field within the loop. The acceleration to energies in the megaelectronvolt

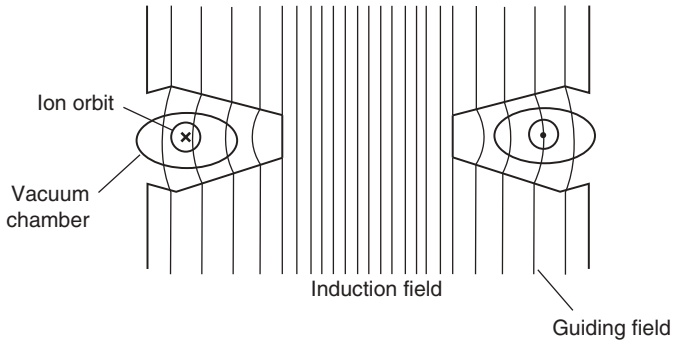

FIG. 9.8

Betatron. The × and • indicate magnetic field direction into and out of the page, respectively.

range takes place in the fraction of a second that it takes for the alternating magnetic current to progress through a quarter-cycle.

The speeds reached in a betatron are high enough to require the use of relativistic formulas (Section 1.5).

EXAMPLE 9.4

Let us find the mass m and speed v for an electron of kinetic energy $E_K = 1\,\text{MeV}$. Recall that the rest energy $E_0 = m_0c^2$ for an electron is 0.511 MeV. Rearranging Eq. (1.11) for kinetic energy, the ratio of m to the rest mass m_0 is

$$\frac{m}{m_0} = 1 + \frac{E_K}{m_0c^2} = 1 + \frac{1\,\text{MeV}}{0.511\,\text{MeV}} = 2.96$$

Solving Einstein's equation for the speed, $m/m_0 = 1/\sqrt{1-(v/c)^2}$, we find that

$$v = c\sqrt{1-(m_0/m)^2} = c\sqrt{1-(1/2.96)^2} = 0.94c$$

Thus the 1-MeV electron's speed is close to that of light, $c = 3.0 \times 10^8$ m/s (i.e., $v = 2.8 \times 10^8$ m/s). If instead we impart a kinetic energy of 100 MeV to an electron, its mass increases by a factor of 197 and its speed becomes $0.999987c$ (see Exercise 9.8(c)).

Calculations of this type are readily made by use of the computer program ALBERT, introduced in Chapter 1 Exercises (Section 1.8). Some other applications to ion motion in modern accelerators are found in Computer Exercises 9.A and 9.B.

9.5 SYNCHROTRON AND COLLIDER

Over the past half-century, the science and engineering of accelerators has evolved dramatically, with ever-increasing beam currents and energy of the charged particles. A major step was the invention independently of the synchrotron by Veksler (1944) and McMillan (1945). It consists of the periodic acceleration of the particles by radiofrequency electric fields but with a time-varying magnetic field

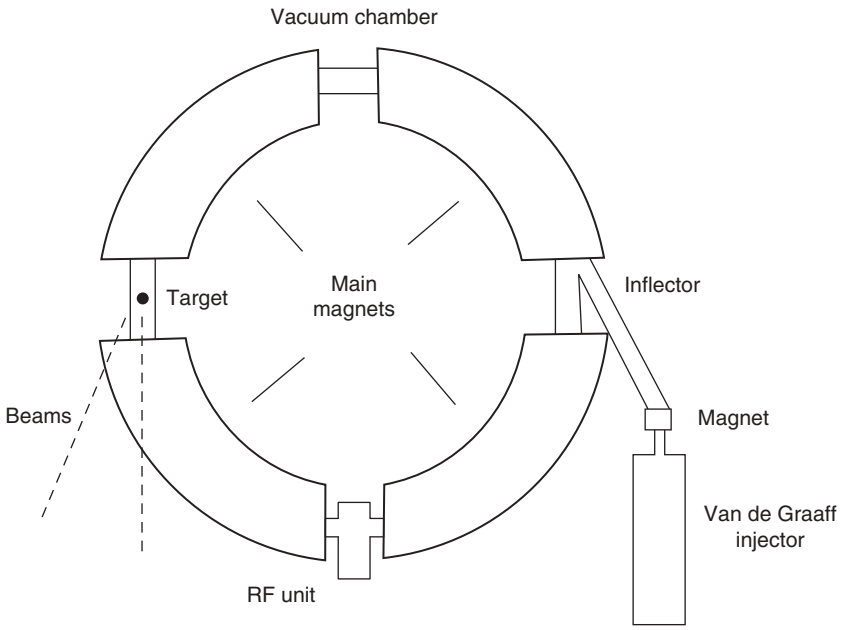

FIG. 9.9

Cosmotron proton synchrotron at Brookhaven National Laboratory.

that keeps the charges on a circular path. Ions that are out of step are brought back into step (i.e., they are synchronized). Fig. 9.9 shows schematically the Cosmotron, operated from 1953 to 1966 at Brookhaven National Laboratory. An ion source provided protons that were injected at 4 MeV into a vacuum chamber by a Van de Graaff accelerator. The inflector sent the charges into the magnet. There, the magnetic field rose to 1.4 tesla in 1 s to provide the constant radius condition $R = mv/(qB)$ as the protons gained energy. The field was shaped to assure proper focusing. The radiofrequency unit accelerated the particles with initial voltage 2000 V at frequency 2000 Hz. Ions at final energy 3 GeV struck an internal target to yield neutrons or mesons, which are subatomic particles.

In a more modern version of the synchrotron, the magnetic field that bends the particles in a circular orbit is provided by a series of separate magnets, like beads on a necklace. In between the magnets are quadrupole (two north and two south) magnets that provide beam focusing, helping compensate for space charge spreading.

Most of the early accelerators involved charge bombardment of a fixed target. Recently, much larger energies are achieved by causing two oppositely circulating beams to collide in what is called a storage ring. The pairs of particles used in a collider include (a) electrons and positrons, (b) protons and antiprotons, (c) protons and protons, and (d) electrons and protons. The accelerating cavity of the electron-positron collider at the Thomas Jefferson Accelerator Laboratory is constructed of superconducting niobium to minimize energy losses. It provides a total energy of 12 GeV. The Large Electron Positron (LEP) collider at the European Laboratory for Particle Physics (CERN) gave particles of 209 GeV before being shut down in 2000.

To reach high particle energies, a combination of accelerators of different types is used, as in the Tevatron (Lederman, 1991) at the Fermi National Accelerator Laboratory (Fermilab) near Chicago. The Tevatron, which was shut down in 2011, involved a circular underground tunnel of diameter 3 m and length 6.3 km, containing the beam tube and a series of hundreds of magnets that provided ion bending. Negative hydrogen ions were first accelerated to 0.75 MeV by a Cockcroft-Walton machine (Section 9.2), then raised to 200 MeV by a linear accelerator (Section 9.3). Electrons were stripped from the ions by a carbon foil, leaving protons. These were brought to 8 GeV by a small booster synchrotron. The ions were then injected into the Main Ring synchrotron and brought to 150 GeV. They were focused into short pulses and extracted to strike a copper target, creating large numbers of antiprotons. These were drawn off into a storage ring where they circulated and the beam was compressed, then transferred to an accumulator ring, and then put in the Tevatron ring. In the meantime, a batch of protons from the Main Ring had also been put in the Tevatron ring. Along the path of that ring were 1000 superconducting magnets that used liquid nitrogen and helium for cooling. Finally, the two countercurrent beams, of diameter approximately 0.1 mm, were accelerated to their peak energy of nearly 1 TeV. Detection of the byproducts of collisions was by the Collider Detector Fermilab (CDF), a complex particle-tracking device.

Another example of combining accelerators is the Bevalac, which linked the Bevatron (Billions of eV Synchrotron) and SuperHILAC (Super Heavy Ion Linear Accelerator) at Lawrence Berkeley Laboratory (LBL). As a side note, one might say that alchemy, the conversion of a base metal into gold, was achieved in one set of experiments. Specifically, Aleklett et al. (1981) used the Bevalac to irradiate Bi-209 with relativistic (GeV) C-12 and Ne-20 heavy ions to produce gold isotopes.

9.6 ACCELERATOR APPLICATIONS

Among the purposes of accelerators is the search for new particles in nature, which can be created only by transforming the energy of accelerated charges, in accord with Einstein's theory. Colliding high-energy beams of particles and antiparticles can create far more massive nuclear species than can simple ion bombardment of stationary targets. The reason is that a high-energy charge expends most of its energy in accelerating new particles to meet momentum conservation requirements. In contrast, when a particle collides with an antiparticle, the momentum is zero, allowing all the energy to go into new mass.

One major accomplishment of high-energy machines was the discovery of the "top" quark (Liss and Tipton, 1997). Its existence is crucial to the correctness of the theory called the Standard Model. According to that picture, matter is composed of leptons (electron, muon, tau, and neutrinos) and quarks (types: up, down, charm, strange, top, and bottom), along with their antiparticle forms. The up quark has a charge 2/3 while the down quark has a charge of $-1/3$. Quarks are believed to have been free just after the Big Bang, forming what is viewed as a perfect liquid. They clustered together with the help of gluons to form protons and neutrons. The proton is made of two ups and one down (uud), whereas the neutron is two downs and one up (udd). In the collision of protons and antiprotons, it is actually the component quarks that collide. It is believed that the top quark existed in nature only in the first 10^{-16} s from the Big Bang that started the universe. Quarks can be freed with difficulty in the laboratory by collisions of very high-energy gold atoms. The Relativistic Heavy Ion Collider (RHIC) at Brookhaven National Laboratory has detected the products of quark combination.

Forces in nature are thought to be provided by the exchange of bosons, an example of which is the photon, for electromagnetic force. There are three other forces: weak (involved in radioactivity), strong (for binding in nuclei), and gravity. The electromagnetic and weak forces are viewed as different aspects of a more general *electroweak* force.

EXAMPLE 9.5

Knowledge of these fundamental particles aids in understanding nuclear reactions. Consider the beta decay of a free neutron (udd) as shown in Fig. 9.10. A virtual W^- boson mediates the transformation of a down quark within the neutron to an up quark, leading to the appearance of a proton (uud). Meanwhile the W^- forms an electron and antineutrino. Charge conservation (neutrality) is maintained because

$$\text{udd} \rightarrow \text{uud} + e^- + \bar{\nu}$$

$$\left(\frac{2}{3} - \frac{1}{3} - \frac{1}{3}\right) = \left(\frac{2}{3} + \frac{2}{3} - \frac{1}{3}\right) - 1 + 0$$

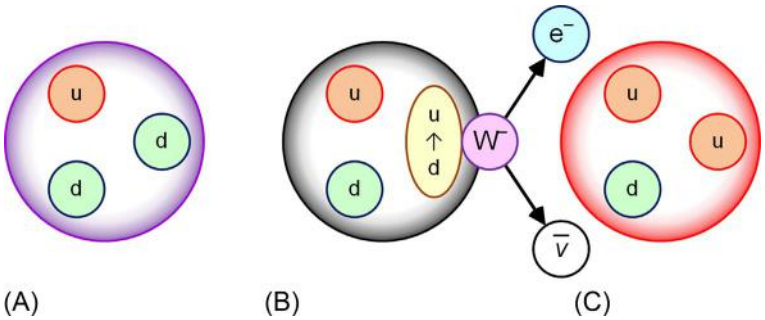

FIG. 9.10

Beta decay of an unbound neutron. (A) Free neutron, (B) beta decay, and (C) proton formed.

Studies of collisions of high-energy particles are intended to obtain information on the origin of mass, along with an answer as to why there is so much invisible mass (dark matter) in the universe and the cause of accelerated expansion of the universe (dark energy). Questions to be addressed are the mass of neutrinos, the scarcity of antimatter, and extra dimensions of space.

In the early 1990s, the United States had started to build in Texas a large superconducting supercollider (SSC) to give a beam of 20 TeV, but Congress canceled the project, citing excessive cost. With the demise of the SSC, a considerable part of high-energy particle research by US physicists was shifted to CERN, the European Laboratory for Particle Physics. The US Department of Energy allocated funds to help construct the Large Hadron Collider (LHC) and the ATLAS detector, which analyzes the products of proton-proton collisions. The LHC utilizes a 27 km circumference tunnel at the French-Swiss border. By use of superconducting magnets and advanced accelerator technology, it is designed to collide protons each of 7 TeV. Alternatively, it will handle beams of heavy ions such as lead with total energy 1250 TeV. In July 2012, it was announced that the previously hypothetical heavy particle called the Higgs boson, which is thought to relate the vacuum of space to the existence of particles, had been detected at the facility (ATLAS Collaboration, 2012).

Two extensions of particle accelerators have opened up new opportunities for research and industrial applications. The first is synchrotron radiation (SR), based on the fact that if an electric charge is given acceleration, it radiates light. At each of the bending magnets of a synchrotron or storage ring, experimental beams of X-rays are available. The beams are very narrow, with an angle given by E_0/E_K, the ratio of rest energy and kinetic energy. An example of an SR facility is the National Synchrotron Light Source at Brookhaven National Laboratory. The second is a free electron laser (FEL), in which electrons are brought to high speed in a LINAC and injected into a tube with magnets along its length. These provide an alternating field that accelerates the electrons to radiate photons. The light is reflected back and forth by mirrors at the ends of the tube and interacts with the circulating electrons rather than with atoms, as in a conventional laser. FELs can produce frequencies ranging from infrared to gamma rays.

D-D and D-T neutron generators accelerate deuterons to impact a deuterium and tritium target, respectively, to produce 2.45 and 14.1 MeV neutrons.

9.7 SPALLATION

High-energy charged particles from an accelerator can disrupt the nuclei of target materials. Experiments at California radiation laboratories showed that large neutron yields were achieved in targets bombarded by charged particles such as deuterons or protons of several hundred MeV energy. Dramatic nuclear reactions occur. One is the *stripping* reaction, Fig. 9.11A, in which a deuteron is broken into a proton and a neutron by the impact on a target nucleus. Another is the process of *spallation*, in which a nucleus is broken into pieces by an energetic projectile. Fig. 9.11B shows how spallation produces a cascade of nucleons. A third is *evaporation* in which neutrons fly out of a nucleus with some 100 MeV of internal excitation energy (see Fig. 9.11C). The average energy of evaporation of neutrons is approximately 3 MeV. The excited nucleus may undergo fission, which releases neutrons, and further evaporation from the fission fragments can occur.

It has been predicted that as many as 50 neutrons can be produced by a single high-energy (500 MeV) deuteron. The large supply of neutrons can be used for a number of purposes: (a) physics and chemistry research; (b) production of new nuclear fuel, beneficial radioisotopes, or weapons tritium; and (c) to burn unwanted plutonium or certain radioactive waste isotopes. In the last case, the radionuclides would be transmuted using an accelerator-driven reactor for which the target-produced particles stream into the fissionable material, thereby initiating and maintaining fission in an otherwise subcritical assembly (Nifenecker et al., 2001). Some of these applications will be discussed in later sections.

At Oak Ridge National Laboratory, the Spallation Neutron Source (SNS) was put into operation in 2006. Design and construction of the Department of Energy facility was a cooperative effort of six laboratories (Argonne, Brookhaven, Lawrence Berkeley, Los Alamos, Oak Ridge, and Jefferson). A large linear accelerator produces high-speed protons to bombard a liquid mercury target. The particle energy is 1 GeV; the beam power is 1.4 MW (Mason et al., 2006). Neutrons are moderated by water and liquid hydrogen, and a time-of-flight device selects neutrons of desired energy. The SNS will serve many hundreds of researchers in neutron science from the United States and abroad, facilitating a great variety of programs, as discussed in Section 14.9.

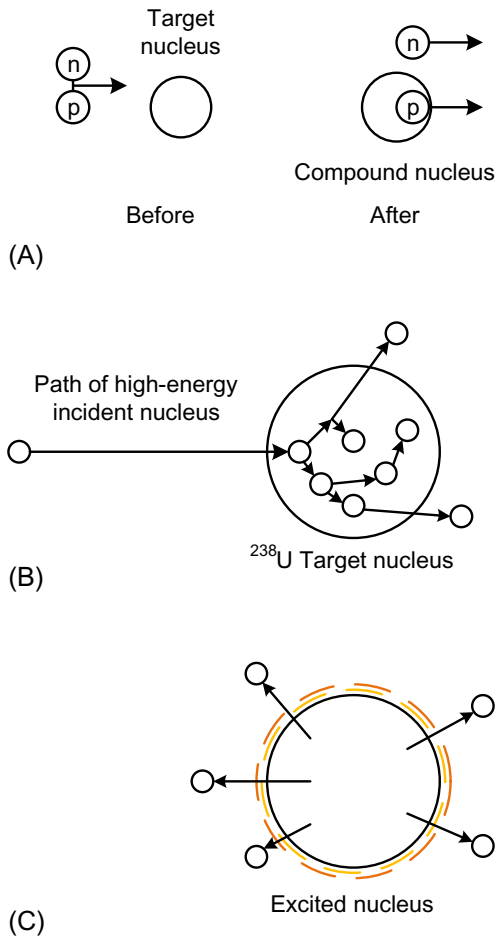

FIG. 9.11

Nuclear reactions produced by very high energy charged particles. (A) Stripping, (B) spallation, and (C) evaporation.

EXAMPLE 9.6

The SNS beam power can be used to determine the charge flow, or beam current,

$$\frac{dq}{dt} = I = \frac{P}{V} = \frac{P}{E_K/e} = \frac{\left[\left(1.4\times10^{6}\,\mathrm{W}\right)/\left(1.602\times10^{-19}\,\mathrm{J/eV}\right)\right]\left(\mathrm{As/C}\right)}{\left[\left(1\times10^{9}\,\mathrm{eV/p}\right)/\left(1.602\times10^{-19}\,\mathrm{C/p}\right)\right]\left(\mathrm{Ws/J}\right)} = 0.0014\,\mathrm{A}$$

The corresponding number of protons accelerated per unit time is simply

$$I/e = \left(0.0014\,\mathrm{C/s}\right)/\left(1.602\times10^{-19}\,\mathrm{C/p}\right) = 8.7\times10^{15}\,\mathrm{p/s}$$

9.8 SUMMARY

Charged particles such as electrons and ions of light elements are brought to high speed and energy by particle accelerators, which use electric and magnetic fields in various ways. In the high-voltage machines, a beam of ions is accelerated directly through a large potential difference, produced by special voltage multiplier circuits or by carrying charge to a positive electrode. In the linear accelerator, ions are given successive accelerations in gaps between tubes lined up in a row. In the cyclotron, the ions are similarly accelerated but travel in circular orbits because of the applied magnetic field. In the betatron, a changing magnetic field produces an electric field that accelerates electrons to relativistic speeds. In the synchrotron, both radiofrequency and time-varying magnetic fields are used. High-energy nuclear physics research is carried out through the use of such accelerators. Through several spallation processes, high-energy charged particles can produce large numbers of neutrons that have a variety of applications.

9.9 EXERCISES

9.1 Calculate the potential difference (voltage) required to accelerate an electron to speed (a) 2×10^5 m/s, (b) 4×10^6 m/s, and (c) 1×10^7 m/s.

9.2 Find the voltage needed to accelerate (a) a proton, (b) an electron, (c) a deuteron, (d) a triton, and (e) an alpha particle to relativistic speed (i.e., $0.1c$).

9.3 What is the proper frequency for a voltage supply to a linear accelerator if the speed of protons in a tube of 0.6 m length is (a) 3×10^6 m/s and (b) 8×10^5 m/s?

9.4 Find the time for one revolution of a (a) deuteron, (b) proton, and (c) helion in a uniform magnetic field of 1 Wb/m^2.

9.5 Develop a working formula for the final energy of cyclotron ions of mass m, charge q, exit radius R, in a magnetic field B (use nonrelativistic energy relations).

9.6 What magnetic field strength (Wb/m^2) is required to accelerate (a) deuterons, (b) protons, and (c) helions in a cyclotron of radius 2.5 m to energy 5 MeV?

9.7 Performance data on the Main Ring proton synchrotron of Fermilab at Batavia, Illinois, were as follows (Wilson, 1974):
Diameter of ring: 2 km
Protons per pulse: 6×10^{12}
Number of magnets: 954
Initial proton energy: 8 GeV
Final proton energy: 400 GeV
Number of revolutions: 200,000
(a) Find the proton energy gain per revolution. (b) Find the speed of the protons at final energy by use of relativistic formulas of Sections 1.5 and 9.4. (c) Calculate the magnetic field at the final speed of the protons.

9.8 What is the factor by which the mass is increased, and what fraction of the speed of light do protons of (a) 200 GeV, (b) 150 GeV, and (c) electrons of 150 MeV have?

9.9 Calculate the steady deuteron beam current and the electric power required in a 500-GeV accelerator that produces 4 kg per day of plutonium-239 from neutron bombardment of U-238. Assume a conservative 25 neutrons per deuteron.

9.10 By use of the relativistic formulas from Section 1.5, show that for very large particle energies the fractional difference in speed from that of light, $f_c = (c - v)/c$, is accurately approximated by $f_c = (1/2)(m_0/m)^2$. Find f_c for 50 GeV electrons of rest energy 0.511 MeV.

9.11 The velocities of protons and antiprotons in the 2-km-diameter Tevatron ring are practically the same as the velocity of light. Find the time for particles of final energy 1 TeV to traverse the circumference. How much error is inherent in this approximation?

9.12 The synchrotron radiation loss in joules of a charge e with rest mass m_0 moving in a circle of radius R is given by Cohen (1995) as

$$\Delta E = e^2\gamma\left(\gamma^2 - 1\right)^{3/2}/(3\varepsilon_0 R)$$

where $\gamma = E/(m_0c^2)$, with $E = mc^2$ and $\varepsilon_0 \cong 8.8542 \times 10^{-12}$ F/m. (a) Find an approximate formula for ΔE in keV for an electron as a function of energy in GeV and R in meters, when the speed is very close to the speed of light. (b) How much lower than the radiation from an electron is that from a proton of the same radius and energy? (c) Find a formula for the power radiated from an electron moving in a circle with speed much less than the speed of light, in terms of its acceleration.

9.13 Show that the speed of a charged particle between two parallel plates is

$$v = \sqrt{2q\mathcal{E}x/m} \tag{9.14}$$

Where x is the distance from the plate at which the particle starts from rest.

9.14 Graph the Coulombic threshold energy for protons incident to nuclei having atomic numbers from 1 to 82. Use the atomic mass relationship from Exercise 2.21.

9.15 Using changes in constituent quarks, show that charge conservation is maintained in the case of positron radioactive decay.

9.16 Plot v/c (for 0–1) as a function of energy for (a) an electron and (b) a proton.

9.17 A linear proton accelerator utilizes a 50 MHz, 20 kV peak voltage supply. (a) Determine the particle speed after transiting the first gap. (b) Calculate the needed length of the first tube. (c) How many tubes are required to achieve an energy of 10 MeV? (d) What is the minimum length of this LINAC?

9.10 COMPUTER EXERCISES

9.A Verify with the computer program ALBERT that 1 TeV protons have a speed that seems to be almost the velocity of light. Calculate the fractional difference between v and c with the formula derived in Exercise 9.10.

9.B The electron-positron collider at Hamburg, Germany, produces 23 TeV particles. (a) What is the ratio of the electron's total energy to its rest energy? Check the result with the computer program ALBERT. (b) If 23 TeV electrons could be induced to travel around the Earth (radius 6378 km), how far behind a light beam would they arrive? See Exercise 9.10 for a useful formula.

REFERENCES

Aleklett, K., Morrissey, D.J., Loveland, W., McGaughey, P.L., Seaborg, G.T., 1981. Energy dependence of ^{209}Bi fragmentation in relativistic nuclear collisions. Phys. Rev. 23 (3), 1044–1046.

ATLAS Collaboration, 2012. Observation of a new particle in the search for the Standard Model Higgs boson with the ATLAS detector at the LHC. Phys. Lett. B 716 (1), 1–29.

Cockcroft, J.D., Walton, E.T.S., 1932. Experiments with high velocity positive ions. II.—The disintegration of elements by high velocity protons. Proc. R. Soc. Lond. Ser. A 137 (831), 229–242.

Cohen, E.R., 1995. The Physics Quick Reference Guide. AIP Press, New York.

Kerst, D.W., 1941. The acceleration of electrons by magnetic induction. Phys. Rev. 60 (1), 47–53.

Lawrence, E.O., Livingston, M.S., 1932. The production of high speed light ions without the use of high voltages. Phys. Rev. 40 (1), 19–37.

Lederman, L.M., 1991. The Tevatron. Sci. Am. 264 (3), 48–55.

Liss, T.M., Tipton, P.L., 1997. The discovery of the top quark. Sci. Am. 277 (3), 54–59.

Mason, T.E., Abernathy, D., Anderson, I., Ankner, J., Egami, T., Ehlers, G., et al., 2006. The Spallation Neutron Source in Oak Ridge: a powerful tool for materials research. Physica B 385–386 (2), 955–960.

McMillan, E.M., 1945. The synchrotron—a proposed high energy accelerator. Phys. Rev. 68, 143–144.

Nifenecker, H., David, S., Loiseaux, J.M., Meplan, O., 2001. Basics of accelerator driven subcritical reactors. Nucl. Inst. Methods Phys. Res. A 463 (3), 428–467.

Rees, J.R., 1989. The Stanford linear collider. Sci. Am. 261 (4), 58–65.

Seaborg, G.T., 1981. The Plutonium Story. 1981. Lawrence Berkeley Laboratory. LBL-13492.

Van de Graaff, R.J., Compton, K.T., Van Atta, L.C., 1933. The electrostatic production of high voltage for nuclear investigations. Phys. Rev. 43 (3), 149–157.

Veksler, V.I., 1944. A new method of accelerating relativistic particles. Compt. Rend. Acad. Sci. URSS 43 (8), 329–331.

Wideröe, R., 1928. Über ein neues Prinzip zur Herstellung hoher Spannungen. Archiv für Elektrotechnik 21, 387–406. translated by Fischer, G.E., Brasse, F.W., Kumpfert, H., Hartmann, H. as "A new principle for the generation of high voltages" in *The Development of High-Energy Accelerators*, Livingston, M.S., ed., Dover, NY, 1966, pp. 92–114.

Wilson, R.R., 1974. The Batavia accelerator. Sci. Am. 230 (2), 72–83.

FURTHER READING

American Institute of Physics (AIP), n.d. Early Particle Accelerators, Lawrence and the Cyclotron. https://history.aip.org/exhibits/lawrence/epa.htm. New systems, from the 1930s.

Brookhaven National Laboratory, National Synchrotron Light Sources. http://www.bnl.gov/ps/. (select "News & Events/Multimedia" to take an online tour).

European Organization for Nuclear Research (CERN), http://home.cern/. Large Hadron Collider.

Fermi National Accelerator Laboratory (Fermilab), Fermilab History and Archives Project. http://history.fnal.gov. Features Robert R. Wilson, first director.

Frommberger, F., 2017. Particle Accelerators Around the World. http://www-elsa.physik.uni-bonn.de/accelerator_list.html. Links to facilities sorted by location and by accelerator type.

Humphries Jr., S., 1986. Principles of Charged Particle Acceleration. Wiley, New York.

Lightsources.org, News, information, and educational materials about the world's synchrotron and free electron laser light source facilities. http://www.lightsources.org/.

Oak Ridge National Laboratory, Spallation Neutron Source. https://neutrons.ornl.gov/. Extensive information about features of the system and prospective applications.

Scharf, W.H., 1997. Biomedical Particle Accelerators. AIP Press, New York.

Sessler, A., Wilson, E., 2007. Engines of Discovery: A Century of Particle Accelerators. World Scientific Publishing Co., Singapore Accelerators for research, medicine, and industry.

Shafroth, S.M., Austin, J.C. (Eds.), 1997. Accelerator-Based Atomic Physics Techniques and Applications. AIP Press, Woodbury, NY.

WWW Virtual Library, Free Electron Laser Research and Applications. http://sbfel3.ucsb.edu/www/vl_fel.html. Select Jefferson Lab or University of California at Santa Barbara.

CHAPTER

BIOLOGICAL EFFECTS OF RADIATION

10

CHAPTER OUTLINE

All living species are exposed to a certain amount of natural radiation in the form of particles and rays. In addition to the sunlight, without which life would be impossible to sustain, all beings experience cosmic radiation from space outside Earth and natural background radiation from materials on Earth. Rather large variations occur in the radiation from one place to another, depending on the mineral content of the ground and on the elevation above sea level. Humans and other species have survived and evolved within such an environment despite the fact that radiation has a damaging effect on biological tissue. The situation has changed somewhat by the discovery of the means to generate high-energy radiation with various devices such as X-ray machines, particle accelerators, and nuclear reactors. In the assessment of the potential hazard of the new artificially generated radiation, comparison is often made with levels in naturally occurring background radiation.

We will now describe the biological effect of radiation on cells, tissues, organs, and the whole person; identify the units of measurement of radiation and its effect; and review the philosophy and practice of setting limits on exposure. Special attention will be given to regulations related to the nuclear power industry.

A brief summary of modern biological information will be useful in understanding radiation effects. As we know, living beings comprise a great variety of species of plants and animals; they are all composed of cells, which carry on the processes necessary for survival. The simplest organisms such as algae and protozoa consist of only one cell, whereas complex beings such as humans are composed of specialized organs and tissues that contain large numbers of cells, examples of which are nerve, muscle, epithelial, blood, skeletal, and connective. The principal components of a cell are the *nucleus*

Nuclear Energy. https://doi.org/10.1016/B978-0-12-812881-7.00010-1

as the control center, the *cytoplasm* containing vital substances, and the surrounding *membrane* as a porous cell wall. Within the nucleus are the *chromosomes*, which are long threads containing hereditary material. The growth process involves a form of cell multiplication called *mitosis* in which the chromosomes separate to form two new cells identical to the original one. The reproduction process involves a cell division process called *meiosis* in which germ cells are produced with only half the necessary complement of chromosomes, such that the union of sperm and egg creates a complete new entity. The laws of heredity are based on this process. The genes are the distinct regions on the chromosomes that are responsible for the inheritance of certain body characteristics. They are constructed of a universal molecule called DNA (deoxyribonucleic acid), a very long spiral staircase structure with the stair steps consisting of paired molecules, called nucleotides, of four nitrogen base types: adenine (A), thymine (T), guanine (G), and cytosine (C). Duplication of cells in complete detail involves the splitting of the DNA molecule along its length, followed by the accumulation of the necessary materials from the cell to form two new ones. In the case of humans, 23 pairs of chromosomes are present, containing approximately 4 billion of the DNA molecule steps in an order that describes each unique person.

10.1 PHYSIOLOGICAL EFFECTS

The various ways that moving particles and rays interact with matter discussed in earlier chapters can be reexamined in terms of biological effect. Our emphasis previously was on what happened to the radiation. Now, we are interested in the effects on the medium, which are viewed as damage in the sense that disruption of the original structure takes place, usually by *ionization*. We saw that energetic electrons and photons are capable of removing electrons from an atom to create ions; that heavy charged particles slow down in matter by successive ionizing events; that fast neutrons in slowing impart energy to target nuclei, which in turn serve as ionizing agents; and that capture of a slow neutron results in a gamma ray and a new nucleus. In Section 5.3, we defined linear energy transfer (LET). A distinction is made between radiation exhibiting low LET (electrons and gamma rays) and high LET (alpha particles and neutrons).

As a good rule, 34 eV of energy is required on average to create an ion pair in soft tissue and air. For gases, this figure (W) is reasonably independent of the type of ionizing radiation and its energy. Part of the deposited energy goes into molecular excitation and the formation of new chemicals. Water in cells can be converted into free radicals such as H, OH, H_2O_2, and HO_2. Because the human body is largely water, much of the indirect effect of radiation can be attributed to the chemical reactions of such products. In addition, direct damage can occur in which the radiation strikes certain molecules of the cells, especially the DNA that controls all growth and reproduction. Turner (2007) displays computer-generated diagrams of ionization effects.

EXAMPLE 10.1

Determine the charge deposition in tissue from a single 4-MeV alpha particle. As each ion pair requires 34 eV, the α creates a large number of ion pairs before stopping, specifically

$$N_{IP} = E_K/W = \left(4 \times 10^6 \text{ eV}\right)/(34 \text{ eV/ip}) = 1.2 \times 10^5 \text{ ion pairs}$$

Each ion pair represents the release of one fundamental charge unit such that the charge accumulation is

$$Q = eN_{IP} = \left(1.6 \times 10^{-19} \text{ C/ip}\right)\left(1.2 \times 10^5 \text{ ip}\right) = 1.9 \times 10^{-14} \text{ C}$$

The most important point from the biological standpoint is that the bombarding particles have energy, which can be transferred to atoms and molecules of living cells with a disruptive effect on their normal function. Because an organism is composed of very many cells, tissues, and organs, a disturbance of one atom is likely to be imperceptible, but exposure to many particles or rays can alter the function of a group of cells and thus affect the whole system. It is usually assumed that damage is cumulative, even though some accommodation and repair take place.

The physiological effects of radiation may be classified as *somatic*, which refers to the body and its state of health; *genetic*, involving the genes that transmit hereditary characteristics; and *teratogenic*, related to embryo or fetus development. The somatic effects range from temporary skin reddening when the body surface is irradiated, to a life shortening of an exposed individual because of general impairment of the body functions, to the initiation of cancer in the form of tumors in certain organs or as the blood disease, leukemia. The term *radiation sickness* is loosely applied to the immediate effects of exposure to very large amounts of radiation (greater than 70 rad to the entire body). Symptoms of radiation sickness, also called acute radiation syndrome, include nausea, hair loss, bleeding, and fatigue. The genetic effect consists of mutations in which progeny are significantly different in some respect from their parents, usually in ways that tend to reduce the chance of survival. The effect may extend over many generations. Teratogenic effects include microcephaly (small head size) and mental retardation.

Although the amount of ionization produced by radiation of a certain energy is rather constant, the biological effect varies greatly with the type of tissue involved. For radiation of low penetrating power such as alpha particles, the outside skin can receive some exposure without serious hazard, but for radiation that penetrates tissue readily such as X-rays, gamma rays, and neutrons, the critical parts of the body are bone marrow as blood-forming tissue, the reproductive organs, and the lenses of the eyes. The thyroid gland is important because of its affinity for the fission product iodine, whereas the gastrointestinal tract and lungs are sensitive to radiation from radioactive substances that enter the body through eating or breathing.

If a radioactive substance enters the body, radiation exposure to organs and tissues will occur. However, the foreign substance will not deliver all of its energy to the body because of partial elimination. In particular, the body excretes substances taken in by inhalation and ingestion. If there are N atoms present, the physical (radioactive) decay rate is λN and the biological elimination rate is $\lambda_B N$. The total elimination rate of the radionuclide within the body is the sum

$$dN/dt = -\lambda_E N = -\lambda N - \lambda_B N \tag{10.1}$$

where the effective decay constant is readily identified as

$$\lambda_E = \lambda + \lambda_B \tag{10.2}$$

Thus, the fraction of the radioisotope that is removed by the body before decay is λ_B/λ_E, and the fraction decaying within the body is λ/λ_E. The corresponding relation between half-lives is

$$1/t_E = 1/t_H + 1/t_B \tag{10.3}$$

where each half-life is related to its decay constant via $t_k = \ln(2)/\lambda_k$.

EXAMPLE 10.2

Iodine-131 has an 8-day physical half-life and an 80-day biological half-life for an adult thyroid gland (International Commission on Radiological Protection (ICRP), 1993). Thus its effective half-life is

$$t_E = (1/t_H + 1/t_B)^{-1} = [1/(8\text{d}) + 1/(80\text{d})]^{-1} = 7.3\text{d}$$

10.2 RADIATION DOSE UNITS

A number of specialized terms need to be defined for discussion of the biological effects of radiation. First is the *absorbed dose* (D), which is the amount of energy imparted (ΔE) to the exposed material mass (m)

$$D = \Delta E/m \tag{10.4}$$

The deposited energy appears as excitation or ionization of the molecules or atoms of the medium. The SI unit of dose is the *gray* (Gy), which is 1 J/kg. An older unit of energy absorption is the *rad* (**r**adiation **a**bsorbed **d**ose), which equals 0.01 J/kg (i.e., 1 Gy = 100 rad).

EXAMPLE 10.3

Suppose that an adult's gastrointestinal (GI) tract weighing 2 kg receives energy of amount 6×10^{-5} J as the result of ingesting some radioactive material. The dose would be

$$D = \frac{\Delta E}{m} = \frac{6 \times 10^{-5}\,\text{J}}{2\text{kg}} = 3 \times 10^{-5}\,\text{J/kg} = 3 \times 10^{-5}\,\text{Gy}$$

The preceding dose to the GI tract would be 0.003 rad or 3 millirad.

The biological effect of energy deposition may be large or small depending on the type of radiation. For instance, a radiation dose caused by fast neutrons or alpha particles is much more damaging than a radiation dose by X-rays or gamma rays. In general, heavy particles create a more serious effect than do photons because of the greater energy loss with distance (i.e., high LET) and resulting higher concentration of ionization. The *dose equivalent* (H) as the biologically important quantity takes account of those differences by scaling the energy absorption up by a *quality factor* (QF), with values as in Table 10.1. The US Nuclear Regulatory Commission (NRC) ascribes to this biological dose equivalent of

$$H = D\,QF \tag{10.5}$$

If D is expressed in Gy, then H is in *sieverts* (Sv); if D is in rad, then H is in *rem* (**r**adiation, or roentgen, **e**quivalent **m**an). In scientific research and the analysis of the biological effects of radiation, the SI units gray and sievert are used; in nuclear plant operation, rad and rem are more commonly used. Hence, the quality factor has implicit units of either Sv/Gy or rem/rad. Summarizing, conversion factors commonly needed:

$$1\,\text{gray(Gy)} = 100\ \text{rad} \quad 1\,\text{sievert(Sv)} = 100\ \text{rem}$$

Table 10.1 Radiation Quality Factors

Type of Radiation	QF
X-rays, gamma rays, beta particles	1
Lower energy neutrons ($\leq$1 keV)	2
Neutrons of 1 MeV energy	11
Neutrons of unknown energy	10
High-energy protons	10
Heavy ions, including alpha particles	20

Data from U.S. Nuclear Regulatory Commission (NRC), Standards for Protection Against Radiation, Part 20 of the Code of Federal Regulations—Energy, 10CFR20. www.nrc.gov/reading-rm/doc-collections/cfr/part020.

The great variety of radioactivity and radiation units can be confusing. Although it would be desirable to switch completely to the newer units, it is unrealistic to expect it to happen soon. The United States at least will continue to be burdened with a dual system of units. We will frequently include the SI units in parentheses. Adding perhaps additional confusion is the more recent use of the ICRP-defined equivalent dose H_T, which is the product of the absorbed dose and a radiation-weighting factor W_R.

EXAMPLE 10.4

Suppose that the GI tract dose of Example 10.3 were due to plutonium, an alpha particle emitter. According to Table 10.1, the quality factor for an alpha particle is 20. The dose equivalent would then be

$$H = DQF = (3 \times 10^{-5}\,\text{Gy})(20\,\text{Sv/Gy}) = 6 \times 10^{-4}\,\text{Sv} = 0.6\ \text{mSv}$$

Alternately, the H would be (20 rem/rad)(0.003 rad) = 0.06 rem or 60 millirem.

The long-term effect of radiation on an organism also depends on the rate at which energy is deposited. Thus the *dose rate*, expressed in convenient units such as rad per hour $(\dot{D})$ or millirem per year $(\dot{H})$, is used. Note that if dose is an energy, the dose rate is a power.

We will describe the methods of calculating dosage in Chapter 11. For perspective, however, we can cite some typical values. A single sudden exposure that gives the whole body of a person 20 rem (0.2 Sv) will exhibit no perceptible clinical effect, but a dose of 400 rem (4 Sv) will probably be fatal without medical treatment. The NRC defines the *lethal dose* as that expected to cause death to 50% of an exposed population within 30 days, abbreviated LD 50/30. The typical annual natural (background) radiation exposure, including radon, of the average US resident is around 300 millirem. Table 10.2 details the sources of the total effective dose to an individual, and compares estimates from the early 1980s and 2006. The most recent evaluation reveals a stark increase in the dose from medical diagnostic and treatment procedures, primarily from the use of computed tomography (CT) for medical X-ray imaging. The consumer category includes doses from a variety of sources such as smoking, building materials, commercial air travel, fossil fuel combustion, mining, and agriculture. As the given occupational dose is averaged across the entire national population, it is perhaps more instructive to examine

Table 10.2 Effective Annual Dose to Members of US Population

Exposure Category	Early 1980s Dose (mrem)	2006 Dose (mrem)
Ubiquitous background	300	311
Radon and thoron	200	228
Other	100	83
Medical	53	300
Computed tomography (CT)		147
Conventional radiography and fluoroscopy		33
All diagnostic	39	
Nuclear medicine	14	77
Interventional fluoroscopy		43
Consumer	5–13	13
Industrial, security, medical, educational, and research	0.1	0.3
Occupational	0.9	0.5
Total	**360**	**620**

Data from National Council on Radiation Protection, Measurements (NCRP), 2009. Ionizing Radiation Exposure of the Population of the United States, NCRP Report No. 160.

average doses to only those individuals in the exposed workforce. Table 10.3 shows that workers in the aviation field receive on average 50% more dose than those employed in the nuclear power industry.

Geographically, the annual dose varies widely. The radiation level in many parts of the world is larger than the average annual US statistic of 620 mrem (6.2 mSv) and greatly exceeds the NRC limits of 0.1 rem/y (1 mSv/y) for members of the public and 5 rem/y (50 mSv/y) for nuclear workers. According to Eisenbud and Gesell (1997), in countries such as India, the presence of thorium gives exposures of approximately 600 mrem/y (6 mSv/y). Many waters at health spas give rates that are orders of magnitude higher, mostly due to the presence of radium and radon. Other examples are Brazil with an annual dose of 17,500 mrem (175 mSv) and the city of Ramsar, Iran, where hot springs bring up

Table 10.3 Annual Occupational Dose

Occupational Field	Number of People Exposed	Dose (mrem)
Medical	735,000	80
Aviation	173,000	310
Commercial nuclear power	59,000	190
Industry and commerce	134,000	80
Education and research	84,000	70
Government, DOE, military	31,000	60
Average occupational	1,216,000	110

Data from National Council on Radiation Protection, Measurements (NCRP), 2009. Ionizing Radiation Exposure of the Population of the United States, NCRP Report No. 160.

radium-226, with an annual figure of 26,000 mrem (260 mSv). The frequency of cancer and the life span of people in that area are not noticeably different from other populations.

The amounts of energy that result in biological damage are remarkably small. A gamma dose of 400 rem (4 Sv), which is very large in terms of biological hazard, corresponds to 4 J/kg, which would be insufficient to raise the temperature of a kilogram of water as much as 0.001°C (Exercise 10.11). This fact shows that radiation affects the function of the cells by action on certain molecules, not by a general heating process. Cember and Johnson (2009) estimate that for the LD 50/30, only about 1 in 10 million atoms is directly affected (ionized).

10.3 BASIS FOR LIMITS OF EXPOSURE

A typical bottle of aspirin will specify that no more than two tablets every 4 h should be administered, implying that a larger or more frequent dose would be harmful. Such a limit is based on experience accumulated over the years with many patients. Although radiation has a medical benefit only in certain treatments, the idea of the need for a limit is similar.

As we seek to clean up the environment by controlling emissions of waste products from industrial plants, cities, and farms, it is necessary to specify water or air concentrations of materials such as sulfur or carbon monoxide that are below the level of danger to living beings. Ideally, there would be zero contamination, but it is generally assumed that some releases are inevitable in an industrialized world. Again, limits based on the knowledge of effects on living beings must be set.

For the establishment of limits on radiation exposure, agencies have been in existence for many years. Examples are the International Commission on Radiological Protection (ICRP) and the US National Council on Radiation Protection and Measurements (NCRP). Their general procedure is to study data on the effects of radiation and to arrive at practical limits that take into consideration both risk and benefit of the use of nuclear equipment and processes.

Extensive studies of the survival of colonies of cells exposed to radiation have led to the conclusion that double-strand breaks in DNA are responsible for cell damage. Hall (1984) shows diagrams of various types of breaks. Much of the research was prompted by the need to know the best way to administer radiation for the treatment of cancer. A formula for the number of breaks N as a function of dose D is

$$N = aD + bD^2 \tag{10.6}$$

where the first term refers to the effect of a single particle and the second to that of two successive particles. This is the so-called linear-quadratic model. The fraction S of the cells surviving a dose D is deduced to be

$$S = \exp(-pN) \tag{10.7}$$

where p is the probability that a break causes cell death. The formula is somewhat analogous to that for radioactive decay or the burn up of an isotope. Cell survival data are fitted to graphs where near zero dose, the curve is linear.

There have been many studies of the effect of radiation on animals other than human beings, starting with early observations of genetic effects on fruit flies. Small mammals such as mice provide a great deal of data rapidly. Because controlled experiments on humans are unacceptable, most of the available information on somatic effects comes from improper practices or accidents. Data are available, for

example, on the incidence of sickness and death from exposure of workers who painted radium on luminous-dial watches or of doctors who used X-rays without proper precautions. The number of serious radiation exposures in the nuclear industry is too small to be of use on a statistical basis. The principal source of information is the comprehensive study of the victims of the atomic bomb explosions in Japan in 1945. Continued studies of effects are being made and then evaluated by such organizations as the National Research Council (2006), the United Nations Scientific Committee on the Effects of Atomic Radiation (UNSCEAR) (2010), and the Radiation Effects Research Foundation (RERF) (2005).

The incidence of cancer fatalities as a function of dose is plotted on a graph similar to Fig. 10.1, where the available data are seen to lie only in the high dosage range. In the range below 10 rad (0.1 Gy), there is no statistical indication of any increase in incidence of solid cancer or leukemia fatalities over the number in unexposed populations. The nature of the graph of cancer risk versus dose in the low-dose range is unknown. One can draw various curves starting with one based on the linear-quadratic model. Another would involve a threshold below which there is no effect. To be conservative (i.e., to overestimate effects in the interest of providing protection) organizations such as NCRP and NRC support a linear extrapolation to zero as shown in Fig. 10.1. This assumption is given the acronym LNT (linear no-threshold). Other organizations such as the American Nuclear Society (American Nuclear Society (ANS), 2001) believe that there is insufficient evidence for the LNT curve. Critics believe that the insistence on conservatism and the adoption by the NRC of the LNT recommendation causes an

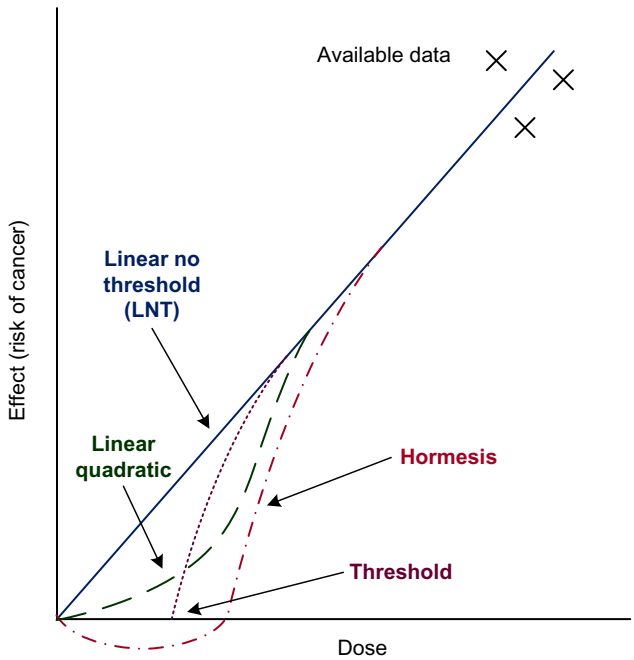

FIG. 10.1

Radiation hazard analysis.

unwarranted expense for radiation protection. Jaworowski (1999) calls the ethics of the use of the LNT into question.

There is considerable support for the existence of a process called *hormesis,* in which a small amount of a substance such as aspirin is beneficial, whereas a large amount can cause bleeding and even death. When applied to radiation, the curve of effect versus dose labeled "hormesis" in Fig. 10.1 would dip below the horizontal axis near zero. The implication is that a small amount of radiation can be beneficial to health. A definitive physiological explanation for the phenomenon is not available, but it is believed that small doses stimulate the immune system of organisms—a cellular effect. There also may be molecular responses involving DNA repair or free radical detoxification. A book by Luckey (1991) is devoted to the subject of hormesis.

The National Academies sponsored a study designed to settle the matter. In report BEIR VII (National Research Council, 2006), the linear no-threshold theory is preserved. The report states that it is unlikely that there is a threshold in the dose-effect relation. The authors of BEIR VII dismiss reports supporting hormesis by saying they are "… based on ecological studies…." However, research on the subject is recommended. No explanation is given in the report for the low cancer incidence in regions of the United States with much higher radiation dosage than the average.

There are significant economic implications of the distinction among models of radiation effect. The LNT version leads to regulations on the required degree of cleanup of radioactivity-contaminated sites and the limits on doses to workers in nuclear facilities.

The consequences of an *acute exposure*, which is a short-term exposure with a large total dose, differ from *chronic exposure*, which is long-term exposure at a low dose rate. There is evidence that the biological effect of a given dose administered almost instantly is greater than if it were given over a long period. In other words, the hazard is less for low dose rates, presumably because the organism has the ability to recover or adjust to the radiation effects. If, for example (see Exercise 10.2), the effect actually varied as the square of the dose, the linear curve would overestimate the effect by a factor of 100 in the vicinity of 1 rem (10 mSv). Although the hazard for low dose rates is small, and there is no clinical evidence of permanent injury, it is *not* assumed that there is a threshold dose (i.e., one below which no biological damage occurs). Instead, it is assumed that there is always some risk. The linear hypothesis is retained despite the likelihood that it is overly conservative. The basic question then faced by standards-setting bodies is "what is the maximum acceptable upper limit for exposure?" One answer is zero, on the grounds that any radiation is deleterious. The view is taken that it is unwarranted to demand zero, as both maximum and minimum, because of the benefit from the use of radiation or from devices that have potential radiation as a byproduct.

The limits adopted by the NRC and promulgated in 10CFR20[1] are 5 rem/y (0.05 Sv/y) for the total body dose of adult occupational exposure. Alternate limits for worker dose are 50 rem/y (0.5 Sv/y) to any individual organ or tissue other than the eye, 15 rem/y (0.15 Sv/y) for the eye, and 50 rem/y (0.5 Sv/y) to the skin or any extremity. In contrast, the limits for individual members of the public are set at 0.1 rem/y (1 mSv/y) (i.e., 2% of the worker dose) and 2 mrem/h (20 μSv/h). Because of concerns for an unborn child, the limit for a pregnant worker is 0.5 rem (5 mSv) over the term of the pregnancy. These figures take into account all radiation sources and all affected organs. It must be noted that the NRC does not limit patient exposures for medical purposes—the benefits should outweigh the risks.

[1] 10CFR20 is Title 10 of the US Code of Federal Regulations part 20.

For the special case of the site boundary of a low-level radioactive waste disposal facility, the NRC specifies a lower figure for the general public, 25 mrem/y (0.25 mSv/y) pursuant to 10CFR61.41, and for a nuclear power plant, a still lower 3 mrem/y (0.03 mSv/y) per 10CFR50 Appendix I.

The occupational dose limits are considerably higher than the average US resident's background dose of 0.31 rem/y (3.1 mSv/y), whereas those for the public are only a fraction of that dose. The National Academy of Sciences Committee on the Biological Effects of Ionizing Radiation (BEIR) analyzes new data and prepares occasional reports, such as BEIR V and VII (National Research Council, 2006). In the judgment of that group, the lifetime increase in risk of a radiation-induced cancer fatality for workers when the official dose limits are used is 8×10^{-4} per rem, and the NRC and other organizations assume half that figure, 4×10^{-4} per rem. However, because the practice of maintaining doses as low as reasonably achievable (ALARA) in nuclear facilities keeps doses well below the limit, the increase in chance of cancer is only a few percent. Measured dose figures have decreased considerably over the years, as reported by the NRC. Fig. 10.2 shows the trend.

For the general public, the radiation exposure from nuclear power plants is negligible compared with other hazards of existence. Specifically, NCRP report 160 (National Council on Radiation Protection, Measurements (NCRP), 2009) estimates that 15% of the annual 0.003 mSv from all industrial, security, medical, educational, and research activities is attributable to nuclear power generation, that is, 0.00045 mSv (0.045 mrem).

It has been said that knowledge about the origins and effects of radiation is greater than that for any chemical contaminant. The research over decades has led to changes in acceptable limits. In the very early days, soon after radioactivity and X-rays were discovered, no precautions were taken, and indeed radiation was thought to be healthful, hence the popularity of radioactive caves and springs that one might frequent for health purposes. Later, reddening of the skin was a crude indicator of exposure. Limits have decreased a great deal in recent decades, making the older literature outdated. A further

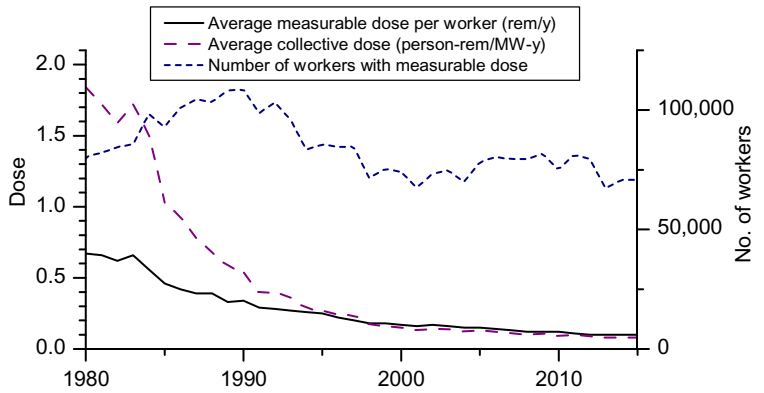

FIG. 10.2

Dose to workers at commercial light water reactors in the United States.

Data from NUREG-0713 (U.S. Nuclear Regulatory Commission (NRC), 2000. Occupational Radiation Exposure at Commercial Nuclear Power Reactors and Other Facilities, NUREG-0713, vol. 22; vol. 32, 2010; vol. 37, 2017.).

complication is the development cycle: research and analysis of effects; discussion, agreement, and publication of conclusions as by ICRP and NCRP; and proposal, review, and adoption of rules by an agency such as the NRC. This cycle requires considerable time. For example, recommendations made in 1977 were not put into effect until 1994, leaving some later suggested modifications in limbo. The time lag can sometimes be different for various applications, leading to apparent inconsistencies.

10.4 SOURCES OF RADIATION DOSAGE

The term *radiation* has come to imply something mysterious and harmful. We will try to provide here a more realistic perspective. The key points are that (a) people are more familiar with radiation than they believe; (b) there are sources of natural radiation that parallel the man-made sources; and (c) radiation can be both beneficial and harmful.

First, solar radiation is the source of heat and light that supports plant and animal life on Earth. We use its visible rays for sight; the ultraviolet rays provide vitamin D, cause tanning, and produce sunburn; the infrared rays give us warmth; and finally, solar radiation is the ultimate source of all weather. Manufactured devices produce electromagnetic radiation that is identical physically to solar radiation and has the same biological effect. Familiar equipment includes microwave ovens, radio and television transmitters, infrared heat lamps, ordinary light bulbs and fluorescent lamps, ultraviolet tanning sources, and X-ray machines. The gamma rays from nuclear processes have higher frequencies and thus greater penetrating power than X-rays but are no different in kind from other electromagnetic waves.

Consider ultraviolet light in the context of radiation effects on human skin. Fig. 1.1 revealed that the border between ionizing and nonionizing electromagnetic radiation lies within the UV wavelengths. Fig. 10.3 shows three representative divisions of UV light (International Agency for Research on Cancer (IARC), 2009). Fortunately, the stratospheric ozone layer blocks the higher energy UVC rays and absorbs much of the UVB as well. Recognizing that skin is composed of multiple elements having various ionization energies leads to the realization that an exact boundary between the ionizing and nonionizing regions does not exist. Although the UVA penetrates deeper than the UVB (Moan, 2001), the higher energy UVB is more carcinogenic.

In recent years, concern has been expressed about a potential cancer hazard because of electromagnetic fields (EMF) from alternating current (e.g., 60 Hz) sources such as power lines or even household circuits or appliances. Biological effects of EMF on lower organisms have been demonstrated, but research on physiological effects on humans is inconclusive and is continuing. More recently, concerns have arisen about the possibility of brain tumors caused by cell phone use.

The ubiquitous background radiation originates from a variety of sources including radon; terrestrial radionuclides such as uranium, thorium, and their progeny; cosmic rays; and even radionuclides within our own bodies. Human beings are continually exposed to gamma rays, beta particles, and alpha particles from radon and its daughters. Radon gas is present in homes and other buildings as a decay product of natural uranium, a mineral occurring in many types of soil. Neutrons as a part of cosmic radiation bombard all living things. Radionuclides internal to the human body include C-14 and K-40.

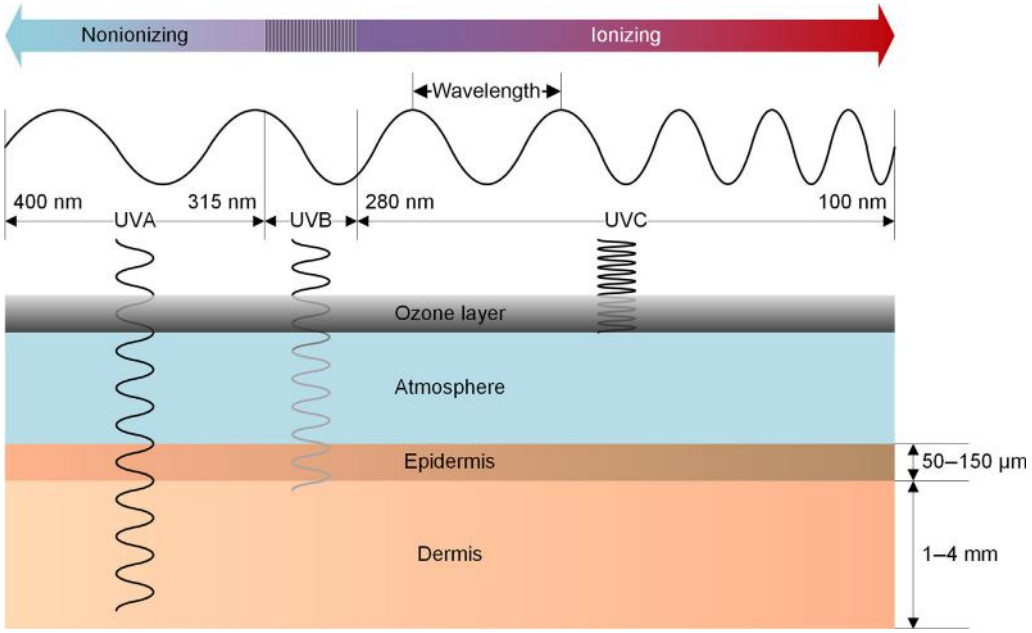

FIG. 10.3

Ultraviolet (UV) radiation passage through atmosphere and penetration into skin.

EXAMPLE 10.5

According to ICRP 30, a 70-kg person contains about 22 ng of C-14. The corresponding activity is

$$A = \lambda n = \frac{\ln(2)}{t_H}\frac{mN_A}{M} = \frac{\ln(2)\left(22\times10^{-9}\,\text{g}\right)\left(6.022\times10^{23}\,\text{atom/mol}\right)}{(5700\,\text{y})\left(3.156\times10^{7}\,\text{s/y}\right)(14\,\text{g/mol})} = 3600\,\text{Bq}$$

The average energy of a beta particle emitted by C-14 is $E_{\beta,avg} \cong E_{\beta,max}/3 = (0.156\,\text{MeV})/3 = 0.052\,\text{MeV}$. If none of the beta radiation escapes the body, then the absorbed dose rate due to C-14 is

$$\dot{D} = \frac{\Delta\dot{E}}{m} = \frac{A E_{\beta,avg}}{m} = \frac{(3600\,\text{Bq})(0.052\,\text{MeV/decay})\left(3.156\times10^{7}\,\text{s/y}\right)}{(70\,\text{kg})\left(1\,\text{MeV}/1.6022\times10^{-13}\,\text{J}\right)\left(10^{-6}\,\text{J/kg}/\mu Gy\right)} = 14\,\mu Gy/\text{y}$$

This corresponds to a dose equivalent rate of 14 μSv/y or 1.4 mrem/y.

It is often said that all nuclear radiation is harmful to biological organisms. There is evidence, however, that the statement is not quite true. First, there seems to be no increase in cancer incidence in the geographic areas where natural radiation background is high. Second, in the application of radiation for the treatment of disease such as cancer, advantage is taken of differences in response of normal and abnormal tissue. The net effect in many cases is of benefit to the patient. Third, it is possible that the phenomenon of hormesis occurs with small doses of radiation, as discussed in Section 10.3.

In the next chapter, we will discuss radiation protective measures and the application of regulatory limits on exposure.

10.5 RADIATION AND TERRORISM

One of the weapons that terrorists could use is the *dirty bomb* or technically a radiological dispersal device (RDD). It could consist of a gamma-emitting radioactive substance such as cobalt-60 ($t_H = 5.27$ y) or cesium-137 (30.1 y), combined with an explosive such as dynamite. An explosion would kill or maim those nearby but the dispersed radioactivity would harm relatively few people.

The resulting physical damage would be very small compared with that of a nuclear bomb, which is the subject of Chapter 27. The main effects of an RDD would be to create fear and panic, to cause serious property damage, and to require extensive decontamination over an area such as a city block. It can be called a "weapon of mass disruption." The effect would be psychological because of public fear of radiation. Also, as noted by Hart (2002) "… effectiveness [of an RDD] can be unintentionally enhanced by professionals and public officials." The news media could also contribute to terror. With the public in panic, the intent of terrorists would be achieved.

To reduce the chance of terrorist action, tight control must be maintained over radiation sources used in research, processing, and medical treatment. The U.S. Nuclear Regulatory Commission (NRC) (2012) addresses the main features of dirty bombs. The National Academy of Sciences (National Academy of Sciences (NAS), 2004) has authored a four-page fact sheet addressing the dangers of and response to a radiological attack.

EXAMPLE 10.6

A London-based terrorist contemplated using americium-241 harvested from smoke detectors to construct an RDD (Carlisle, 2007). The NRC defines risk-significant quantities of radioactive materials as those considered Category 1 and 2 by the International Atomic Energy Agency (IAEA) (2004). A smoke alarm contains about 1 μCi (37 kBq) of Am-241 while the Category 1 and 2 activities are 2000 and 20 Ci (74 and 0.74 TBq), respectively, for Am-241. Therefore, one would need to purchase 20 million (=20 Ci/10^{-6} Ci) of these to reach a risk-significant ^{241}Am activity.

10.6 SUMMARY

When radiation interacts with biological tissue, energy is deposited and ionization takes place that potentially causes damage to cells. The effect on organisms may be somatic (related to body health) and genetic (related to inherited characteristics). Radiation dose equivalent as a biologically effective energy deposition per unit mass is usually expressed in rem, with natural background giving approximately 0.31 rem/y (3.1 mSv/y) in the United States. Exposure limits are set by use of data on radiation effects at high dosages with a conservative linear no-threshold hypothesis applied to predict effects at low dose rates. Such assumptions have been questioned. The terrorist use of a radiological dispersal device (dirty bomb) is of concern.

10.7 EXERCISES

10.1 A beam of 2-MeV alpha particles with current density 10^6/(cm^2 s) is stopped in a distance of 1 cm in air, number density 2.7×10^{19} cm^{-3}. How many ion pairs per cm^3 are formed each second? What fraction of the targets experience ionization per second?

10.2 If the chance of fatality from a radiation dose is taken as 0.5 for 400 rem, by what factor would the chance at 2 rem be overestimated if the effect varied as the square of the dose rather than linearly?

10.3 A worker in a nuclear laboratory receives a whole-body exposure for 5 min by a thermal neutron beam at a rate of 20 millirad per hour. What dose (in mrad) and dose equivalent (in mrem) does he receive? What fraction of the yearly dose limit of 5000 mrem/y for an individual is this?

10.4 A person receives the following exposures in millirem in a year: one medical X-ray, 100; drinking water, 50; cosmic rays, 30; radon in house, 150; K-40 and other isotopes, 25; airplane flights, 10. Find the percentage increase in exposure that would be experienced if he also lived at a reactor site boundary, assuming that the maximum NRC radiation level existed there.

10.5 A plant worker accidentally breathes some stored gaseous tritium, a beta emitter with maximum particle energy 0.0186 MeV. The energy absorbed by the lungs, of total weight 1 kg, is 4×10^{-3} J. How many millirem dose equivalent was received? How many millisieverts?

10.6 If a radioisotope has a physical half-life t_H and a biological half-life t_B, what fraction of the substance decays within the body? Calculate that fraction for I-131 with radioactive half-life 8 days and biological half-life 4 days.

10.7 A mixture of radiation and radioactivity units is used in an article on high natural doses (Ahmed, 1991), as follows: (a) average radiation exposure in the world, 2.4 mSv/y; (b) average radiation exposure in southwest India, 10 mGy/y; (c) high outdoor dose in Iran, 9 mrem/h; (d) radon concentration at high altitudes in Iran, 37 kBq/m^3; (e) radon concentration in Czech houses, 10 kBq/m^3; and (f) high outdoor dose in Poland, 190 nGy/h. Convert each of these numbers into traditional units mrad/y, mrem/y, or pCi/L.

10.8 An employee is seeking hazard pay as compensation for chronic occupational radiation exposure. Data compiled by Cohen (1991) indicate that a person's lifespan is reduced by 51 days if exposed to 1 rem/y from age 18 to 65. If the person's time is valued at \$100/h, estimate the reparation per mrem.

10.9 Use integration to show that the number of initial radionuclides, N_0, that are eliminated from the body before undergoing radioactive decay is $\lambda_B N_0/\lambda_E$.

10.10 (a) Dose rate estimates for a mission to Mars consist of 1.9 mSv/d during each 180-d outbound and return flight, and 0.7 mSv/d while on Mars for nearly 2 y. What fraction or multiple of the annual NRC dose limits do the astronauts receive during total flight time and while exploring the planet each year? (b) How many days before the occupational dose limit is reached on the International Space Station where the dose rate is approximately 0.25 mSv/d?

10.11 Calculate the temperature rise due to a dose of 4 Gy (400 rad) in water.

10.12 Some computer programs compute the dose in units of MeV/g. Provide a conversion factor (multiplier) to change such results into (a) rad and (b) Gy.

10.13 If a cell is 10 μm thick, how many cells do (a) a 3-MeV and (b) a 6-MeV alpha particle pass through fully before being stopped?

10.14 Calculate the bounding frequencies and energies (in eV) for (a) UVA, (b) UVB, and (c) UVC.

10.8 COMPUTER EXERCISE

10.A Perform a literature search to ascertain natural radionuclide concentrations in food routinely consumed by the public. For example, determine K-40 concentrations in bananas.

REFERENCES

Ahmed, J.U., 1991. High levels of natural radiation: report of an international conference in Ramsar. IAEA Bull 33 (2), 36–38.

American Nuclear Society (ANS), 2001. Health Effects of Low-Level Radiation. ANS Position Statement No. 41, http://www.ans.org/pi/ps.

Carlisle, D., 2007. Dhiren Barot: was he an Al Qaeda mastermind or merely a hapless plotter? Stud. Confl. Terror. 30 (12), 1057–1071.

Cember, H., Johnson, T.E., 2009. Introduction to Health Physics, fourth ed. McGraw-Hill, New York.

Cohen, B.L., 1991. Catalog of risks extended and updated. Health Phys. 61 (3), 317–335.

Eisenbud, M., Gesell, T.F., 1997. Environmental Radioactivity: From Natural, Industrial, and Military Sources, fourth ed. Academic Press, San Diego, CA.

Hall, E.J., 1984. Radiation and Life, second ed. Pergamon Press, Oxford.

Hart, M.M., 2002. Disabling Radiological Dispersal Terror; 2002. Lawrence Livermore National Laboratory, UCRL-JC-150849.

International Agency for Research on Cancer (IARC), 2009. A Review of Human Carcinogens. IARC Monograph, vol. 100. IARC, Lyon.

International Atomic Energy Agency (IAEA), 2004. Code of Conduct on the Safety and Security of Radioactive Sources. IAEA, Vienna.

International Commission on Radiological Protection (ICRP), 1993. Ann. ICRP 23 (3–4), 141–167.

Jaworowski, Z., 1999. Radiation risk and ethics. Phys. Today 52 (9), 58. The article prompted a number of Letters in the April 2000 issue, p. 11.

Luckey, T.D., 1991. Radiation Hormesis. CRC Press, Boca Raton.

Moan, J., 2001. Visible light and UV radiation. In: Brune, D., Hellborg, R., Persson, B.R.R., Paakkonen, R. (Eds.), Radiation at Home, Outdoors and in the Workplace. Scandinavian Science Publisher, Oslo, pp. 69–85.

National Academy of Sciences (NAS), 2004. Radiological attack: dirty bombs and other devices. U.S. Department of Homeland Security, https://www.dhs.gov/xlibrary/assets/prep_radiological_fact_sheet.pdf.

National Council on Radiation Protection, Measurements (NCRP), 2009. Ionizing radiation exposure of the population of the United States. NCRP Report No. 160.

National Research Council, 2006. Health Risks from Exposure to Low Levels of Ionizing Radiation (BEIR VII—Phase 2). National Academies Press, Washington, DC an update to BEIR V from 1990.

Radiation Effects Research Foundation (RERF), 2005. Reassessment of the Atomic Bomb Radiation Dosimetry for Hiroshima and Nagasaki: Dosimetry System 2002. Hiroshima, Japan.

Turner, J.E., 2007. Atoms, Radiation, and Radiation Protection, third ed. Wiley, New York.
U.S. Nuclear Regulatory Commission (NRC), 2012. Fact Sheet on Dirty Bombs. http://www.nrc.gov/reading-rm/doc-collections/fact-sheets.
United Nations Scientific Committee on the Effects of Atomic Radiation (UNSCEAR), 2010. Sources and Effects of Ionizing Radiation. United Nations, New York.

FURTHER READING

Alberts, B., Bray, D., Johnson, A., Lewis, J., Raff, M., Roberts, K., Walter, P., 1997. Essential Cell Biology: An Introduction to the Molecular Biology of the Cell. Garland Publishing, New York, Highly recommended; stunning diagrams and readable text.
Hall, E.J., Giaccia, A.J., 2012. Radiobiology for the Radiologist, seventh ed. J.B. Lippincott Co., Philadelphia, Authoritative work that explains DNA damage, cell survival curves, and radiotherapy techniques.
Health Physics Society, Radiation Dose and Biological Effects. http://www.hps.org. Select "Radiation Terms" and "Position Statements".
Mettler, F.A., Upton, A.C., Moseley, R.D., 1995. Medical Effects of Ionizing Radiation. Elsevier, Netherlands.
National Health Museum, Access Excellence. DNA Structure. http://www.accessexcellence.org/AE/AEC/CC. Explains the role of radioactive labeling and displays the structure of DNA.
Pochin, E., 1985. Nuclear Radiation: Risks and Benefits. Clarendon Press, Oxford University Press, Oxford, UK/New York. Sources of radiation and biological effects, including cancer and damage to cells and genes.
Shapiro, J., 2002. Radiation Protection: A Guide for Scientists, Regulators and Physicians, fourth ed. Harvard University Press, Cambridge. A very readable textbook.
U.S. Nuclear Regulatory Commission (NRC), 2000. Occupational Radiation Exposure at Commercial Nuclear Power Reactors and Other Facilities, NUREG-0713. vol. 22. 32, 2010; 37, 2017.
U.S. Nuclear Regulatory Commission (NRC), Standards for Protection Against Radiation, Part 20 of the Code of Federal Regulations—Energy, 10CFR20. http://www.nrc.gov/reading-rm/doc-collections/cfr/part020.
U.S. Environmental Protection Agency (EPA), Health Effects of Radiation. http://www.epa.gov/rpdweb00/understand/health_effects.html. Questions and answers from the EPA.
U.S. Nuclear Regulatory Commission (NRC), Fact Sheet on Biological Effects of Radiation. http://www.nrc.gov/reading-rm/doc-collections/fact-sheets/. Extensive discussion.
U.S. Nuclear Regulatory Commission (NRC), Standards for Protection Against Radiation, Part 20 of the Code of Federal Regulations—energy, 10CFR20. http://www.nrc.gov/reading-rm/doc-collections/cfr/part020.
Wilson, R., 1999. Resource letter EIRLD-1: effects of ionizing radiation at low doses. Am J Phys 67, 372–377 Puts radiation risks into perspective.
Wilson, R., Crouch, E.A.C., 2001. Risk-Benefit Analysis. Harvard University Press, Cambridge, MA.

CHAPTER

RADIATION PROTECTION 11

CHAPTER OUTLINE

Protection of biological entities from the hazard of radiation exposure is a fundamental requirement in the application of nuclear energy. Safety is provided by the use of one or more general methods that involve control of the source of radiation or its ability to affect living organisms. We will identify these methods and describe the role of calculations in the field of radiation protection.

11.1 PROTECTIVE MEASURES

Radiation and radioactive materials are the link between a device or process as a source and the living being to be protected from hazard. To diminish the risk, we can try to eliminate the source, remove the individual, or insert some barrier between the two. Heightened safety can be accomplished by several means.

The first is to avoid the generation of radiation or isotopes that emit radiation. For example, the production of undesirable emitters from reactor operation can be minimized by the control of impurities in materials of construction and in the cooling agent. The second is to ensure that any radioactive substances are kept within containers or multiple barriers to prevent dispersal. Isotope sources and waste products are frequently sealed within one or more independent layers of metal or other impermeable substance, and nuclear reactors and chemical processing equipment are housed within leak-tight

Nuclear Energy. https://doi.org/10.1016/B978-0-12-812881-7.00011-3

buildings. The third is to provide layers of shielding material between the source of radiation and the individual and to select favorable characteristics of geological media in which radioactive wastes are buried. The fourth is to restrict access to the region where the radiation level is hazardous and take advantage of the reduction of intensity with distance. The fifth is to dilute a radioactive substance with very large volumes of air or water on release to lower the concentration of harmful material. The sixth is to limit the time that a person remains within a radiation zone to reduce the dose received. We thus see that radioactive materials may be managed in several different ways: *retention*, *isolation*, and *dispersal*; whereas exposure to radiation can be reduced by methods involving *distance*, *shielding*, and *time*. Signage and labeling using the trefoil symbol drawn in Fig. 11.1A aims to bring awareness by warning of a radiation hazard in an area or package. In February 2007, the International Atomic Energy Agency (IAEA) and the International Organization for Standardization (ISO) launched a supplementary symbol shown in Fig. 11.1B for high-level sealed sources (IAEA Category 1, 2, and 3).

The analysis of radiation hazard and protection along with the establishment of safe practices are part of the function of the science of radiological protection, known as *health physics*. Every user of radiation must follow accepted procedures, and health physicists provide specialized technical advice and monitor the user's methods. In the planning of research involving radiation or in the design and operation of a process, calculations must be made that relate the radiation source to the biological entity by use of exposure limits provided by regulatory bodies. Included in the evaluation are necessary protective measures for known sources, or limits that must be imposed on the radiation source, the rate of release of radioactive substances, or the concentration of radioisotopes in air, water, and other materials.

The detailed calculations of radiological protection are very involved for several reasons. A great variety of situations should be considered, including reactor operations and uses of isotopes. Many scientific and engineering disciplines are needed: physics, chemistry, biology, geology, meteorology, and several engineering fields. Increased use of computers favors the development of more sophisticated calculation methods while providing increased convenience. The collection of new experimental data on the interaction of radiation and matter and the relationship of dose and effect results in evolving recommendations and regulations. Finally, the enhanced awareness of radiation and concern for safety

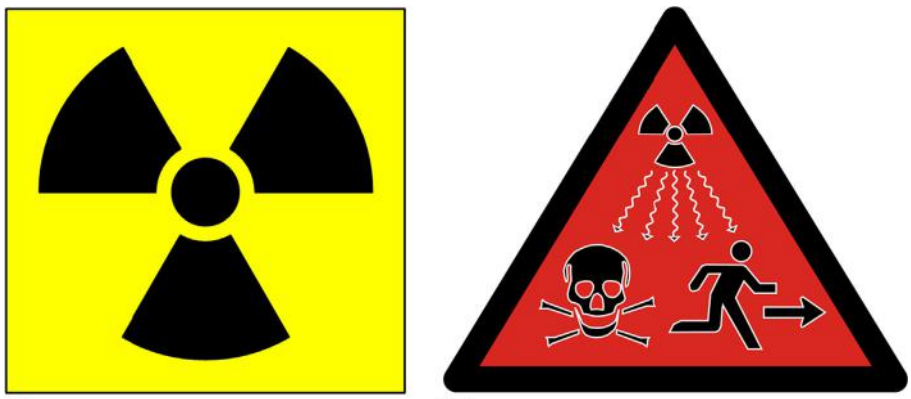

FIG. 11.1

(A) International radiation hazard (trefoil) symbol. (B) IAEA-ISO21482 supplementary ionizing radiation symbol.

on the part of the public have prompted increased conservatism, which entails refinement in methods and a requirement for fuller justification of methods and results.

In the operation of nuclear power plants and uses of radioisotopes, adherence to government regulations is mandatory to maintain a license. The principal document of the US Nuclear Regulatory Commission (NRC) is the *Code of Federal Regulations: 10 Energy*. Part 20, "Standards for Protection Against Radiation," has an abbreviated designation 10CFR20 (U.S. Nuclear Regulatory Commission (NRC), n.d.).

The establishment of regulations is a slow process, starting with the study of research information by advisory bodies such as the International Commission on Radiological Protection (ICRP) and the National Council on Radiation Protection and Measurements (NCRP); recommendations for dose limits and protection policies; review by the regulatory body with input from the public, institutions, and industry; and final issuance of mandatory requirements, along with guidance documents. Therefore, the limits and methods for different situations may be inconsistent but fundamentally safe. A case in point is the older use of a critical organ and maximum permissible concentrations of radionuclides, and the newer use of committed effective dose equivalent, referring to the summation of all effects on the body. The old and the new are contrasted in the NRC's discussion of regulation 10CFR20 in the *Federal Register* (U.S. Nuclear Regulatory Commission (NRC), 1986). Some of the earlier regulations are still applicable. We will present examples of both methods for two reasons: (1) to help the reader make use of all pertinent literature of radiological protection and (2) to illustrate the trend toward greater precision and realism in radiation protection.

We now discuss the relationship of dose to flux, the effect of distance and shielding materials, internal exposure, environmental assessment, and dose limits for workers and the public.

11.2 CALCULATION OF DOSE

Some simple idealized situations will help the reader understand concepts without becoming involved in intricate calculations. The estimation of radiation dose or dose rate is central to radiation protection. The dose is an energy absorbed per unit mass as discussed in Section 10.2. It depends on the type, energy, and intensity of the radiation as well as on the physical features of the target.

Let us imagine a situation in which the radiation field consists of a stream of gamma rays of a single energy, E_γ. The beam of photons might be coming from a piece of radioactive equipment in a nuclear plant. The stream passes through a substance such as tissue with negligible attenuation. This situation of radiation arising from a source outside the material of interest is said to lead to an *external dose*. We use the principles of Chapter 4 to calculate the energy deposition. Flux and current are the same for this beam (i.e., j and ϕ are both equal to nv). Section 5.4.4 introduced both the linear attenuation coefficient μ and the *energy-absorption coefficient* μ_{en} for photons, which are utilized for shielding and radiation dose calculations, respectively. Fig. 11.2, which compares the mass attenuation and energy-absorption coefficients of tissue, shows that $\mu \geq \mu_{\text{en}}$. With a flux ϕ and cross-section μ_{en}, the reaction rate is $\phi\mu_{\text{en}}$. If the gamma ray energy is E_γ, then the energy deposition rate per unit volume is $\phi E_\gamma\, \mu_{\text{en}}$. If the target density is ρ, the dose rate is

$$\dot{D} = \phi E_\gamma (\mu_{\text{en}}/\rho) \tag{11.1}$$

This relationship can be used to calculate a photon dose for given conditions or to find limits on flux or exposure time.

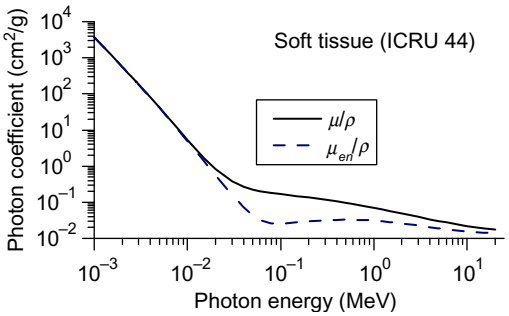

FIG. 11.2

Photon mass attenuation (μ/ρ) and energy-absorption (μ_{en}/ρ) coefficients for tissue.

Data from Hubbell, J.H., Seltzer, S.M., 2004. Tables of X-Ray Mass Attenuation Coefficients and Mass Energy-Absorption Coefficients. National Institute of Standards and Technology, Gaithersburg, MD. http://physics.nist.gove/xaamdi.

EXAMPLE 11.1

Let us find the gamma-ray flux that yields an external dose of 0.1 rem in 1 y with continuous exposure. This is the dose limit to members of the public according to 10CFR20 (Section 10.2). Suppose that the gamma rays have an energy of 1 MeV and that the energy-absorption coefficient for soft tissue of density 1.0 g/cm^3 is 0.03074/cm (which is similar to water). With a quality factor of 1 for this photon radiation, the numerical values of the absorbed dose D and the dose equivalent H are the same, so

$$D = H/QF = (0.1\,\text{rad})\left(1\times10^{-5}\,\text{J}/(\text{g rad})\right) = 1\times10^{-6}\,\text{J/g}$$

Also $E_\gamma = 1\,\text{MeV} = 1.60\times10^{-13}\,\text{J}$. Noting that for constant dose rate over time t, $D = \dot{D}t$, we solve for the flux,

$$\phi = \frac{D\rho}{\mu_{en}E_\gamma t} = \frac{\left(1.0\times10^{-6}\,\text{J/g}\right)\left(1\,\text{g/cm}^3\right)}{(0.03074/\text{cm})\left(1.602\times10^{-13}\,\text{J}\right)\left(3.1558\times10^{7}\,\text{s}\right)} = 6.43/\left(\text{cm}^2\,\text{s}\right)$$

This value of the gamma ray flux may be scaled up or down if another dose limit is specified. In the absence of soft tissue mass coefficients, those of water provide a reasonable approximation. The fluxes of various particles corresponding to 0.1 rem/y (1 mSv/y) are listed in Table 11.1.

Table 11.1 Representative Radiation Fluxes (0.1 rem/y)

Radiation Type	Flux (per cm^2 per s)
X- or gamma rays (1 MeV)	6.4
Beta particles	0.10
Thermal neutrons (0.025 eV)	3.1
Fast neutrons (1 MeV)	0.086
Alpha particles	10^{-5}

Another situation is the exposure of a person to air containing a radioactive contaminant. Let us derive and apply a formula for the case of continuous exposure during working hours. We wish to relate

dose H to the activity A per unit volume, with an exposure time of t seconds. A rough estimate comes from a simple assumption: that the person is immersed in a large radioactive cloud, and that the energy absorption in air, ΔE_a, is the same as in the human body and the same as that released by decay of the radionuclide, ΔE_r. Writing expressions for each of these gives

$$\Delta E_a = Hm/QF \tag{11.2}$$

$$\Delta E_r = AtE_d \tag{11.3}$$

where E_d is the average energy per decay. Equating these expressions and solving for the dose yields

$$H = AtE_dQF/m = (A/V)tE_dQF/\rho \tag{11.4}$$

If the person is at ground level, this dose should be divided by two because the cloud occupies only half of space, that is, there is no radionuclide-laden air below ground to act as a radiation source.

EXAMPLE 11.2

Let us find the activity of the noble gas krypton-85, half-life 10.76 y and an emitter of beta particles of average energy 0.251 MeV, that leads to a worker reaching the annual dose limit of $H = 5$ rem (50 mSv). Assume continuous exposure for 40 h/wk and 50 wk/y with 3600 s/h, so that $t = 7.2 \times 10^6$ s. Insert $E_d = 0.251$ MeV into Eq. (11.4), and solve for the activity

$$\frac{A}{V} = \frac{2H\rho}{tE_dQF} = \frac{(2)(5\,\text{rem})\left(1.293 \times 10^{-3}\,\text{g/cm}^3\right)\left(10^{-5}\,\text{J/(grad)}\right)\left(1\,\mu\text{Ci}/3.7 \times 10^4\,\text{decay/s}\right)}{\left(7.2 \times 10^6\,\text{s}\right)(0.251\,\text{MeV/decay})(1\,\text{rem/rad})\left(1.6 \times 10^{-13}\,\text{J/MeV}\right)}$$
$$= 1.2 \times 10^{-5}\,\mu\text{Ci/cm}^3$$

This agrees fairly well with the figure of 1×10^{-5} listed in the 1993 edition of the old NRC 10CFR20. We will see in Section 11.8 that the latest method yields a larger dose limit.

Unlike photons and neutrons, some radiations such as alphas and betas are stopped more readily. For a monodirectional particle stream incident to a material and not completely penetrating through the material, the primary radiation delivers its dose within the particle range R such that the absorbed dose rate can be expressed as

$$\dot{D} = \phi E/(\rho R) \tag{11.5}$$

in which E is the particle energy.

EXAMPLE 11.3

Let's determine the electron energy corresponding to the 0.1-rem/y (1-mSv/y) flux of 0.10/(cm^2 s) given in Table 11.1. Assuming that the electron energy E_e exceeds 2.5 MeV, the second relation of Eq. (5.2) may be used to describe the maximum range R_{max} in g/cm^2. Recognizing that $QF = 1$ for electrons, the dose is obtained from

$$\dot{H} = \dot{D}QF = \frac{\phi E_e}{\rho R} = \frac{\phi E_e}{R_{max}} = \frac{\phi E_e}{0.530E_e - 0.106}$$

Solving algebraically for the electron energy and paying particular attention to the implied units within the empirical relation for R_{max} gives

$$E_e = \frac{\dot{D}0.106}{\dot{D}0.530 - \phi}$$
$$= \frac{(0.106\,\mathrm{g/cm^2})(0.1\mathrm{rad/y})(\mathrm{MeV/g}/1.6\times10^{-8}\,\mathrm{rad})}{(0.530\,\mathrm{g/cm^2/MeV})(0.1\mathrm{rad/y})(\mathrm{MeV/g}/1.6\times10^{-8}\,\mathrm{rad}) - (0.10/(\mathrm{cm^2\,s}))(3.1558\times10^{7}\,\mathrm{s/y})}$$
$$= 4.2\,\mathrm{MeV}$$

in which the conversion from MeV/g to rad originates from Exercise 10.12(a).

11.3 EFFECTS OF DISTANCE AND SHIELDING

For protection, advantage can be taken of the fact that radiation intensities decrease with distance from the source, varying as the *inverse square of the distance*. Let us illustrate by an idealized case of a small source, regarded as a mathematical point, emitting S particles per second—the source strength. As in Fig. 11.3, let the rate of flow through each unit of area of a sphere of radius r about the point be labeled ϕ [/(cm^2 s)]. The flow through the whole sphere surface of area $4\pi r^2$ is then $\phi\, 4\pi r^2$, and if there is no intervening material, it can be equated to the source strength S. Then the flux from a point source in a vacuum is

$$\phi = \frac{S}{4\pi r^2} \tag{11.6}$$

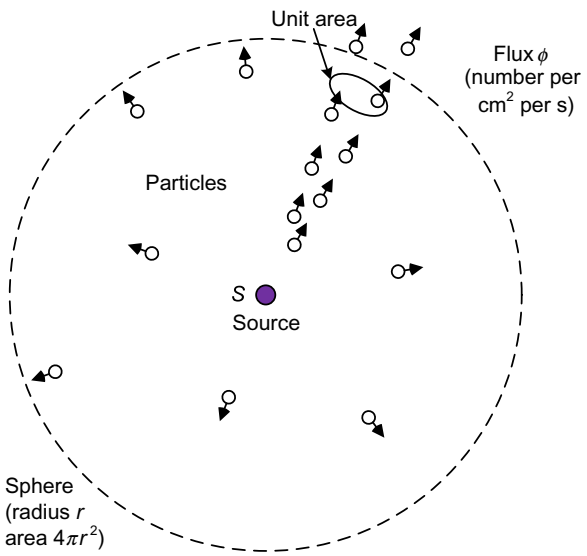

FIG. 11.3

Inverse square spreading of radiation.

This relation expresses the inverse square spreading effect. If we have a surface covered with radioactive material or an object that emits radiation throughout its volume, the flux at a point of measurement can be found by the addition of elementary contributions.

EXAMPLE 11.4

Let us consider the neutron radiation at a large distance from an unreflected and unshielded reactor operating at a power level of 1 MW. Because 1 W gives 3.3×10^{10} fissions per second (Section 6.4) and the number of neutrons per fission is 2.42 (Section 6.3), the reactor produces 8.0×10^{16} neutrons per second. Suppose that 20% of these escape the core as fast neutrons, so that S is 1.6×10^{16} n/s. Apply the inverse square relation, neglecting attenuation in air, an assumption that would only be correct if the reactor were in a deployed spacecraft. Let us find the closest distance of approach to the reactor surface to keep the dose below 100 mrem/y as in Table 11.1. The limiting fast flux is 0.086 n/(cm^2 s). Solving the inverse-square formula, we obtain

$$R = \sqrt{\frac{S}{4\pi\phi}} = \sqrt{\frac{1.6 \times 10^{16}\,\text{n/s}}{4\pi(0.086\,\text{n/(cm}^2\,\text{s))}}} = 1.22 \times 10^8\,\text{cm}$$

This is a surprisingly large distance, approximately 760 miles. If the same reactor were on the Earth, neutron attenuation in air would reduce this figure greatly, but the necessity for shielding by solid or liquid materials is clearly revealed by this calculation.

EXAMPLE 11.5

As another example, let us find how much radiation is received at a distance of 1 mile from a nuclear power plant, if the dose rate at the plant boundary, 0.25-mile radius, is 5 mrem/y. Neglecting attenuation in air, the inverse-square reduction factor is 1/16 according to

$$\frac{\phi_2}{\phi_1} = \frac{S/(4\pi r_2^2)}{S/(4\pi r_1^2)} = \frac{r_1^2}{r_2^2} = \frac{(0.25mi)^2}{(1mi)^2} = \frac{1}{16}$$

Because the dose is directly proportional to the flux, the dose rate a mile from the plant is

$$\dot{D}_2 = \dot{D}_1(r_1/r_2)^2 = (5\,\text{mrem/y})/16 = 0.31\,\text{mrem/y}$$

Air attenuation would reduce the dose to a negligible value.

The evaluation of necessary protective shielding from radiation makes use of the basic concepts and facts of radiation interaction with matter described in Chapters 4 and 5. Let us consider the particles with which we must deal. Because charged particles (electrons, alpha particles, protons, etc.) have a very short range in matter, attention needs to be given primarily to the penetrating radiation: gamma rays (or X-rays) and neutrons. The attenuation factor with distance of penetration for photons and neutrons may be expressed in exponential form $\exp(-\Sigma r)$, where r is the distance from source to observer and Σ is an appropriate macroscopic cross-section for neutrons. As noted in Section 5.4.4, for photons the linear attenuation coefficient μ is utilized. Both Σ and μ depend on the number of target atoms, and through the microscopic cross-section they also depend on the type of radiation, its energy, and the chemical and nuclear properties of the target.

For fast neutron shielding, a light element is preferred because of the large neutron energy loss per collision. Thus, hydrogenous materials such as water, concrete, or polyethylene are effective shields. The objective is to slow neutrons within a small distance from their origin and to allow them to be

absorbed at thermal energy. Many materials readily capture thermal neutrons, but boron is preferred because accompanying gamma rays are very weak.

EXAMPLE 11.6

Let us compute the effect of a water shield on the fast neutrons from the reactor of Example 11.4. The macroscopic cross-section appearing in the exponential formula $\exp(-\Sigma_r r)$ is now called a *removal cross-section* because many fast neutrons are removed from the high-energy region by one collision with hydrogen and eventually are absorbed as thermal neutrons. For fission neutrons in water, Σ_r is approximately 0.10/cm. The reduction of flux as a function of distance is the product of the inverse-square reduction with distance and the exponential reduction

$$\phi = \frac{S\exp(-\Sigma_r r)}{4\pi r^2} \tag{11.7}$$

A shield of thickness 2.5 m would reduce the flux to

$$\phi = \frac{S\exp(-\Sigma_r r)}{4\pi r^2} = \frac{(1.6\times 10^{16}\,\text{n/s})\exp(-(0.10/\text{cm})(250\,\text{cm}))}{4\pi(250\,\text{cm})^2} = 0.28\,\text{n}/(\text{cm}^2\,\text{s})$$

This flux is somewhat higher than the safe level of 0.086 n/(cm^2 s) as shown in Table 11.1. The addition of a few centimeters of water shield would provide adequate protection for steady reactor operation, at least. Computer Exercise 11.B utilizes a program NEUTSHLD that finds fast flux from a fission source as a point or a plane.

For gamma ray shielding, in which the main interaction takes place with atomic electrons, a substance of high atomic number is desired. Compton scattering varies as Z, pair production as Z^2, and the photoelectric effect as Z^4 (Evans, 1982). Elements such as iron and lead are particularly useful for gamma shielding. The amount of attenuation depends on the material of the shield, its thickness, and the photon energy. The literature gives values of the mass attenuation coefficient μ/ρ, which is the ratio of the linear attenuation coefficient μ (macroscopic cross-section Σ) and the material density ρ; thus, it has units cm^2/g. Typical values for a few elements at different energies are shown in Table 11.2; a more extensive listing is provided in Table A.6.

EXAMPLE 11.7

For 1 MeV gamma rays in iron, density 7.874 g/cm^3, the linear attenuation coefficient is

$$\mu = (\mu/\rho)\,\rho = (0.05995\,\text{cm}^2/\text{g})(7.874\,\text{g/cm}^3) = 0.472/\text{cm}$$

In contrast, for water H_2O, Eq. (5.15) must be employed with mass fractions obtained from the atomic weights; for example, the molecular weight of water is $2(1.008)+15.999 = 18.015$ g/mol. The average value of the mass attenuation coefficient with numbers from Table 11.2 and component weight fractions of M_i/M_{water} is

$$\begin{aligned}(\mu/\rho)_{\text{water}} &= \omega_H(\mu/\rho)_H + \omega_O(\mu/\rho)_O \\ &= [2(1.008)(0.1263\,\text{cm}^2/\text{g}) + (15.999)(0.0672\,\text{cm}^2/\text{g})]/18.015 \\ &= 0.0738\,\text{cm}^2/\text{g}\end{aligned}$$

This is also the value of μ because $\rho = 1$ g/cm^3. Thus to achieve the same reduction in gamma flux in iron as in water, the thickness only need be (0.0738)/(0.472) = 16% as much.

Table 11.2 Photon Mass Attenuation Coefficients, μ/ρ (cm^2/g)

Energy (MeV)	H	O	Al	Fe	Pb	U
0.01	0.3854	5.952	26.23	170.6	130.6	179.1
0.1	0.2944	0.1551	0.1704	0.3717	5.549	1.954
1	0.1263	0.0672	0.06146	0.05995	0.07102	0.07896
2	0.08769	0.04459	0.04324	0.04265	0.04606	0.04878
10	0.03254	0.02089	0.02318	0.02994	0.04972	0.05195

Data from NISTIR 5632 (Hubbell, J.H., Seltzer, S.M., 2004. Tables of X-Ray Mass Attenuation Coefficients and Mass Energy-Absorption Coefficients. National Institute of Standards and Technology, Gaithersburg, MD. http://physics.nist.gove/xaamdi).

The importance of photon radiation leads to defining a specific gamma-ray dose constant Γ. If one assumes a point source of activity A for a particular radionuclide, then its gamma-ray constant may be obtained by combining Eqs. (11.1) and (11.6), that is,

$$\dot{H} = \dot{D}\,QF = \phi E_\gamma (\mu_{en}/\rho)_{\text{air}} = \frac{AE_\gamma (\mu_{en}/\rho)_{\text{air}}}{4\pi r^2} = \frac{\Gamma A}{r^2} \tag{11.8}$$

in which $QF = 1$ for photons. The calculation and utility of Γ are illustrated by example.

EXAMPLE 11.8

Cobalt-60 emits two gamma rays of average energy 1.25 MeV for each decay. From Table A.6, the mass energy-absorption coefficient for water is $0.02965\,cm^2/g$. Rearranging the preceding equation gives

$$\Gamma = \frac{E_\gamma (\mu_{\text{en}}/\rho)_{\text{air}}}{4\pi} = \frac{(2.50\,\text{MeV/decay})(0.02965\,\text{cm}^2/\text{g})(1\,\text{Sv}/(\text{J/kg}))}{(4\pi)(1\,\text{MeV}/1.6022\times10^{-13}\,\text{J})(1\,\text{kg}/1000\,\text{g})(100\,\text{cm/m})^2}$$

$$= \left(\frac{9.45\times10^{-17}\,\text{Sv m}^2}{\text{decay}}\right)\frac{(10^3\,\text{mSv/Sv})(3600\,\text{s/h})}{(1\,\text{GBq}/10^9\,\text{decay/s})} = 0.34\,\frac{\text{mSv m}^2}{\text{GBq h}}$$

This Γ value compares favorably to that of Unger and Trubey (1982).

We can use Γ to calculate the dose rate at arbitrary distances from a point source. The dose equivalent rate 50 cm away from a 20-MBq Co-60 disc source is

$$\dot{H} = \frac{\Gamma A}{r^2} = \left(0.34\,\frac{\text{mSv m}^2}{\text{GBq h}}\right)\frac{(0.02\,\text{GBq})}{(0.05\,\text{m})^2} = 2.7\,\text{mSv/h}$$

For gamma shielding calculations, we may find the flux of photons that have made no collision in arriving from a point source. This *uncollided flux* is a product of a source strength S, an exponential attenuation factor $\exp(-\mu r)$, and an inverse square spreading factor $1/(4\pi r^2)$, that is,

$$\phi_u = \frac{S\exp(-\mu r)}{4\pi r^2} \tag{11.9}$$

This is not the complete flux that strikes a receptor at a given distance because those photons scattered by the Compton effect can return to the stream and contribute, as shown in Fig. 11.4. To account for this

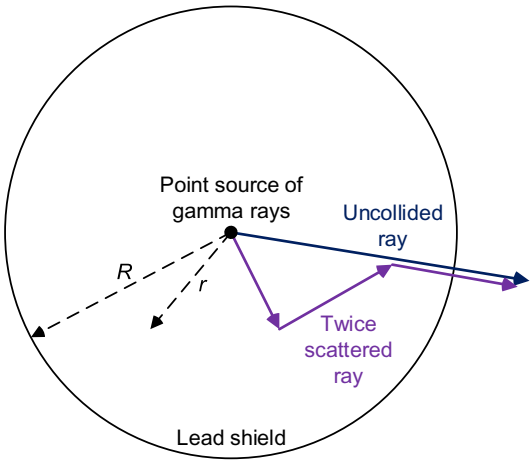

FIG. 11.4

Photon buildup effect.

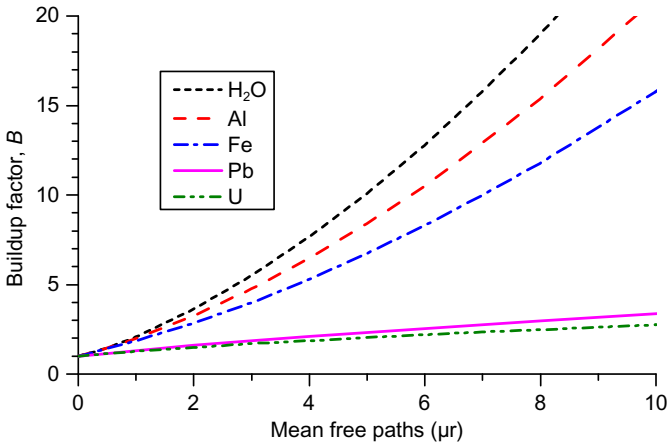

FIG. 11.5

Buildup factors, 1 MeV gammas. *B* for concrete and aluminum are about the same, and likewise *B* for air is similar to that of water.

Data from ORNL/RSIC-49 (Trubey, D.K., 1988. New Gamma-Ray Buildup Factor Data for Point Kernel Calculations: ANS-6.4.3 Standard Reference Data, Oak Ridge National Laboratory, ORNL/RSIC-49.)

buildup of radiation, a multiplying *buildup factor B* depending on μr is introduced. Fig. 11.5 shows *B* for 1 MeV gammas in the most common shielding materials: lead, iron, and water. The total flux is then

$$\phi = B\phi_u \tag{11.10}$$

This shows that the buildup factor is the ratio of the actual flux to the uncollided flux.

EXAMPLE 11.9

Find the uncollided 1-MeV flux from a 1 millicurie source ($S = 3.7 \times 10^7$/s) through 10 cm of lead. We readily calculate the linear attenuation coefficient for Pb, $\mu/\rho = 0.07102\,\text{cm}^2/\text{g}$, density $11.35\,\text{g/cm}^3$, to be 0.806/cm. Inserting the numbers into Eq. (11.9) gives

$$\phi_u = \frac{S\exp(-\mu r)}{4\pi r^2} = \frac{(3.7\times10^7/\text{s})\exp(-(0.806/\text{cm})(10\text{cm}))}{4\pi(10\text{cm})^2} = 9.30/(\text{cm}^2\,\text{s})$$

It remains to find B from the graph of Fig. 11.5 or external tables (Trubey, 1988), as 3.04, so that the total flux is

$$\phi = B\phi_u = (3.04)(9.30/(\text{cm}^2\,\text{s}) = 28.3/(\text{cm}^2\,\text{s})$$

This calculation was rather straightforward, but it is more difficult if one wants to find the distance, that is, the shielding thickness, to reduce the flux to a particular value. Note that r appears in three places in the total flux formula, so trial-and-error or iterative methods are needed. This tedious process is assisted by use of the computer program EXPOSO; see Computer Exercise 11.A. To bring the exposure down to 5 mrem/y, the value of r is approximately 15 cm.

Although calculations are performed in the design of equipment or experiments involving radiation, characterization of the radiation environment is ultimately assured by its measurement. Portable detectors used as survey meters are available commercially. They use the various detector principles described in Chapter 12, with the Geiger-Müller counter having the greatest general usefulness. Special detectors are installed to monitor general radiation levels or the amount of radioactivity in effluents. The possibility of accidental exposure to radiation always exists in a laboratory or plant despite all precautions. To have information immediately, personnel wear direct reading dosimeters that detect and measure dose. Contemporary devices include the thermoluminescent dosimeter (TLD), discussed in Section 12.5, which when heated releases photons in proportion to the dose received during the monitoring period.

Operation, maintenance, and repair of nuclear equipment involve some possible exposure to radiation. Even though it is assumed that any radiation is undesirable, it is necessary on practical grounds to allow a certain amount of exposure. It would be prohibitively expensive to reduce the level to zero. A basis for what action to take is the philosophy expressed in the phrase, "as low as is reasonably achievable," with the acronym ALARA (10CFR20). Planning, design, and operation are done with the ALARA principle in mind. For example, a repair job on contaminated equipment is planned after making careful surveys of radiation levels. The repair is to be carried out by a small crew of well-trained people who will perform the work quickly and with minimum contact with the radiation sources. Temporary shielding, special clothing, and respirators are used as needed to minimize doses. The following factors are considered:

(a) Maximum exposure both to individuals and to the group of workers as a whole,
(b) Other nonradiological risks,
(c) State of technology, and
(d) Economic importance of the operation being performed.

If the expected total dosage to the group is more than a fraction of the allowed quarterly dose, a formal ALARA evaluation is made, accounting for both the dollar costs and the dose costs.[1]

[1]For a complete discussion by the NRC of the regulatory implications of ALARA, see NRC Regulatory Guides 8.1-8.20, www.nrc.gov/reading-rm/doc-collections/reg-guides.

11.4 INTERNAL EXPOSURE

We now turn to the exposure of internal parts of an organism as a result of having taken in radioactive substances. Special attention will be given to the human body, but similar methods will apply to other animals and even to plants. Radioactive materials can enter the body by breathing, drinking, or eating, and to a certain extent can be absorbed through pores or wounds. The resulting internal dosage depends on many factors:

1. Amount that enters, which in turn depends on the rate of intake and elapsed time.
2. Chemical nature of the substance, which affects affinity with molecules of particular types of body tissue and which determines the rate of elimination (the term *biological half-life* is used in this connection, being the time for half an initial amount to be removed).
3. Particle size, which relates to progress of the material through the body.
4. Radioactive half-life, the energy, and kind of radiation, which determine the activity and energy deposition rate, and the length of time the radiation exposure persists.
5. Radiosensitivity of the tissue, with the gastrointestinal tract, reproductive organs, and bone marrow as the most important.

In the older regulatory framework, limiting concentrations of radionuclides in air or water are calculated with the concept of *critical organ*, the one receiving the greatest effective dose from a certain ingested or inhaled radionuclide. The organ selected thus dominates the hazard to the body, and effects on other organs are neglected.

EXAMPLE 11.10

We apply the method to calculate the maximum permissible concentration (MPC) in units $\mu Ci/cm^3$ of iodine-131 in water consumed by plant workers. I-131 has a half-life of 8.0 d and releases 0.23 MeV of beta-gamma energy per decay. The thyroid gland, of mass 20 g, will be taken as the critical organ because of the affinity of the thyroid for iodine. According to International Commission on Radiological Protection (ICRP) (1960), the allowed annual dose is 30 rad. The method of Section 11.2 is applied again with a slight modification to Eq. 11.4

$$D = AtE_d/m \tag{11.11}$$

We first find the activity A that will yield that dose

$$A = \frac{Dm}{tE_d} = \frac{(30\text{rad})(20\text{g})\left(10^{-5}\text{J}/(\text{grad})\right)\left(1\mu Ci/3.7\times10^{4}\text{decay/s}\right)}{\left(3.16\times10^{7}\text{s}\right)(0.23\text{MeV/decay})\left(1.60\times10^{-13}\text{J/MeV}\right)} = 0.139\mu\text{Ci}$$

Now we find the rates of supply and elimination of I-131 to the organ, assumed to be in balance in steady state. Using the formulas of Section 10.1, with a biological half-life of 138 days (unbound iodine), the effective half-life t_E is 7.56 d and the decay constant λ_E is 0.0917/d. Thus, the elimination rate is proportional to $\lambda_E A = (0.0917)(0.139)$. The consumption rate of water for the standard man is $2200\,cm^3$/d, but it is assumed that workers drink 1.5 times the average during their 8-h day, and they work only 50 wk at 40 h/wk. The rate of intake of contaminated water per calendar day is thus

$$(1.5)\left(2200\text{cm}^3/\text{d}\right)\frac{(40\text{h/wk})(50\text{wk/y})}{(24\text{h/d})(365\text{d/y})} = 753\text{cm}^3/\text{d}$$

If 30% of the iodine goes to the thyroid, the supply rate of I-131 is (0.3)(753)(MPC). Equate rates and solve for

$$\text{MPC} = \frac{(0.0917/\text{d})(0.139\mu\text{Ci})}{(0.3)(753\text{cm}^3/\text{d})} = 5.6\times10^{-5}\,\mu\text{Ci/cm}^3$$

This rounds off to $6\times10^{-5}\,\mu Ci/cm^3$, the value appearing in the older (1993) version of 10CFR20.

The existence of a biological half-life leads to a radiation protection strategy in the case of iodine. Potassium iodide (KI) composed of stable (nonradioactive) iodine may be prescribed and taken when radioactive iodine is present in air, food, or water. The KI tablets do not stop the radiation; rather the thyroid is saturated with iodine such that uptake of radioiodine into this gland is inhibited, but this treatment is temporary. In contrast, Prussian blue was given to victims of the Goiania, Brazil, incident to remove radiocesium (Thompson and Church, 2001).

When there is more than one radioisotope present, the allowed concentrations must be limited. The criterion used is

$$\sum_i \frac{C_i}{(\mathrm{MPC})_i} \leq 1 \tag{11.12}$$

where i is an index of the isotope. This equation says the sum of quotients of actual concentrations and maximum permissible concentrations must be no greater than 1.

11.5 RADIONUCLIDES IN THE ENVIRONMENT

The National Environmental Policy Act (NEPA) of 1969 included a Council on Environmental Quality in the executive branch and required environmental impact statements on all federal projects. The Environmental Protection Agency (EPA) was then proposed and accepted. A prominent part of the EPA is the administration of the Superfund to clean up old waste sites. The EPA has responsibility for standards on hazardous, solid, and radioactive wastes. The role of the EPA that is most relevant to nuclear energy is radiation protection.[2] Specifically, the EPA also sets standards for radiation protection that are used by the NRC in its licensing and regulation.

The EPA provides key nuclear regulations, appearing in the Code of Federal Regulations.[3] In Title 40 Part 61.102, the release of radionuclides is limited to a value calculated to be less than 10 mrem/y with the computer code to evaluate compliance being specified. In 40CFR191.15, dealing with disposal of high-level wastes and spent fuel, it is required that during the first 10,000 years no member of the public will receive an annual dose larger than 15 mrem (150 μSv). In addition, release limits are given for several radionuclides, expressed as curies per thousand metric tons of heavy metal (U, Pu, etc.). The lowest figure, 10 Ci, is for Th-230 or Th-232; most isotopes are at 100 Ci; the highest figure, 10,000 Ci, is for Tc-99.

The various naturally occurring radionuclides in the environment can be categorized in terms of their origins. The *primordial* radioisotopes have existed since before the formation of the Earth; examples include the heavy decay chains of Th-232, U-235, and U-238 as well as K-40 and Rb-87. The *cosmogenic* radionuclides are products of high-energy cosmic ray interactions with terrestrial nuclides; examples are H-3 and C-14, which are formed via (n, t) and (n, p) reactions with N-14, respectively. Environmental radioactivity also includes radioisotopes of *anthropogenic* (human-caused) origins such as nuclear weapons testing, industrial releases, and accidents. All the emanations from these radioactive species contribute to the natural and artificial background radiation levels in the biosphere.

[2] *www.epa.gov/radiation*.

[3] Complete copies of the regulations are available online: *www2.epa.gov/laws-regulations*.

Table 11.3 Radionuclide Contaminant Limits in Drinking Water

Contaminant	Maximum Contaminant Level
Alpha emitters excluding Ra-226, Rn, and U	15 pCi/L
Combined Ra-226 and Ra-228	5 pCi/L
Beta and photon emitters	4 mrem/y
Uranium	30 μg/L

From U.S. EPA, 10CFR141.66.

These radionuclides can manifest themselves as contaminants within food and water. Consequently, the EPA has established drinking water standards to reduce the incidence of cancer. The limits listed in Table 11.3 are in terms of the activity or dose, except for the uranium limit that is expressed on a mass basis because its maximum contamination level (MCL) is based on chemical toxicity to the kidneys.

11.6 THE RADON PROBLEM

The hazard of breathing air in a poorly ventilated uranium mine has long been recognized. The death rate of miners has historically been higher than that for the general population. The suspected source is the radiation from radioactive isotopes in the decay chain of uranium-238, which by emission of a series of alpha and beta particles eventually becomes lead-206. The data are clouded by the fact that uranium miners tend to be heavy smokers.

Appreciably down the chain is radium-226, half-life 1600 years. As shown in Fig. 3.8, Ra-226 decays into radon-222, half-life 3.82 days. Although Rn-222 is an alpha emitter, its shorter-lived daughters provide most of the dosage

$$\begin{aligned} {}^{222}_{86}\mathrm{Rn} &\xrightarrow{3.82\,\mathrm{d}} {}^{218}_{84}\mathrm{Po} \xrightarrow{3.05\,\mathrm{m}} {}^{214}_{82}\mathrm{Pb} \xrightarrow{26.8\,\mathrm{m}} {}^{214}_{83}\mathrm{Bi} \\ {}^{214}_{83}\mathrm{Bi} &\xrightarrow{19.9\,\mathrm{m}} {}^{214}_{84}\mathrm{Po} \xrightarrow{164\,\mu\mathrm{s}} {}^{210}_{82}\mathrm{Pb} \xrightarrow{22.3\,\mathrm{y}} \end{aligned} \tag{11.13}$$

Radon as a noble gas along with its suspended particulate decay products is breathed in with air. Some radioactive particles deposit on the lung surfaces. Decay of radon and its progeny releases ionizing radiation.

The problem of radon near piles of residue from uranium mining—the *mill tailings*—has been known. Rules have been adopted requiring earth covers to inhibit radon release and prohibiting the use of the tailings for fill or construction. More recently it has been discovered that a large number of US homes have higher than normal concentrations of radon. Such excessive levels are due to the particular type of rock over which houses are built. Many homes have a concentration of 20 pCi/L, in contrast with the average of approximately 1.5 pCi/L and in excess of the EPA limit of 4 pCi/L. The U.S. Environmental Protection Agency (EPA) (1986) has given the subject a great deal of attention.

Application of dose-effect relationships yields estimates of a large number of cancer deaths from the radon effect, as high as 20,000 per year in the United States. Such numbers depend on the validity of

the linear relationship of dose and effect discussed in Section 10.3. If there were a threshold or if there were a hormesis effect, the hazard would be very much smaller and mitigation costs greatly reduced. See Lewis (2006) for a history of radon in mines, spas, and homes.

It was originally believed that the radon concentrations in houses were high because of energy conservation measures that reduced ventilation. Investigations revealed that the radon comes out of the ground and is brought into the home by drafts, similar to chimney action. Temperature differences between the air in the house and in the ground beneath cause pressure differences that induce the flow. One might think that covering the earth under a house with plastic would solve the problem, but even slight leaks let the radon through. In areas known to have significant radon levels, it is considered wise for homeowners to obtain radon test kits, which are rather inexpensive. If levels well above 4 pCi/L are found, action is recommended. The best solution is to ventilate a crawl space or to provide a basement with a small blower that raises the pressure and prevents radon from entering. Computer Exercise 11.D investigates the buildup of radon in an enclosed space without ventilation.

The dimensions of the problem are yet not fully appreciated nationally; continued study is required to determine the proper course of action.

11.7 ENVIRONMENTAL RADIOLOGICAL ASSESSMENT

The NRC requires that the ALARA principle, discussed in Section 11.3, be applied to the releases of radioactive materials from a nuclear power plant. A deliberate effort is to be made to stay below the specified limits. These refer to any person in the unrestricted area outside the plant (see Section 21.11). According to 10CFR50, Appendix I, the annual dose resulting from a liquid effluent must be less than 3 mrem to the individual's total body or 10 mrem to any organ. The dose from air release must be less than 10 mrem from gamma rays and 20 mrem from beta particles. To comply with ALARA, it is necessary for the plant to correlate a release of contaminated water or air to the maximum effect on the most sensitive person. An acceptable method to calculate releases and doses is found in the NRC's Regulatory Guide 1.109 (U.S. Nuclear Regulatory Commission (NRC), 1977). This Regulatory Guide discusses the factors to be considered, gives useful formulas, and provides basic data. Older health physics methods are used, but because the dose limit sought is very small, the results are conservative. Among the important factors are:

(a) The amounts of each radioisotope in the effluent, with special attention to cesium-137, carbon-14, tritium, iodine, and noble gases.

(b) The mode of transfer of material. The medium by which radioactivity is received may be drinking water, aquatic food, shoreline deposits, or irrigated food (pathways include meat and milk). If the medium is air, human beings may be immersed in a contaminated cloud or breathe the air, or material may be deposited on vegetables.

(c) The distance between the source of radioactivity and person affected and how much dilution by spreading occurs.

(d) The time of transport, to account for decay during flow through air or by streams, or in the case of foodstuffs, during harvesting, processing, and shipment.

(e) The age group at risk: infant (0–1 year), child (1–11), teenager (11–17), and adult (17 and older). Sensitivities to radiation vary considerably with age.

(f) The dose conversion factor, which relates the dose to the activity. These numbers are tabulated according to isotope, age group, inhalation or ingestion, and organ (bone, liver, total body, thyroid, kidney, lung, and gastrointestinal (GI) tract).

EXAMPLE 11.11

Let us make an approximate calculation of the dose resulting from a continuous release of radioactive water from a nuclear power station into a nearby river. Assume that each day 1000 gallons of water contaminated with a single radioisotope cesium-137, half-life 30 y, is released. Also assume an activity in the water of 10^5 pCi/L. The activity in the discharge is diluted by a stream flow of 2×10^4 gal/min, down to

$$\frac{A}{V} = (10^5 \text{ pCi/L}) \frac{(1000 \text{ gal/d})(1 \text{ d}/1440 \text{ min})}{(2 \times 10^4 \text{ gal/min})} = 3.47 \text{ pCi/L}$$

The potential radiation hazard to the population downstream is by two types of ingestion: drinking the water or eating fish that live in the water. The age groups at risk are infants, children, teenagers, and adults. Consumption data are as shown in Table 11.4. The row in the table that refers to fish must be multiplied by a bioaccumulation factor of 2000 (its units are pCi/kg per pCi/L). *Bioaccumulation* occurs in an organism when the buildup of a substance, generally a toxin, exceeds the body's ability to remove it.

Table 11.4 Consumption by Age Group

	Infant	Child	Teen	Adult
Water (L/y)	330	510	510	730
Fish (kg/y)	0	6.9	16	21

From Table E-5, Reg. Guide 1.109 (U.S. Nuclear Regulatory Commission (NRC), 1977. Regulatory Guide 1.109 Calculation of Annual Doses to Man From Routine Releases of Reactor Effluents for the Purpose of Evaluating Compliance With 10CFR Part 50 Appendix I, October).

Consider the dose to an adult. To the consumption rate of water must be added the effect of eating fish, giving a total of

$$730 \text{ L/y} + (21 \text{ kg/y})(2000 \text{ L/kg}) = 42,700 \text{ L/y}$$

Now apply a dose conversion in mrem per pCi for Cs-137 as in Table 11.5. Because each number in the table should be multiplied by 10^{-5}, the adult total body dose conversion factor is 7.14×10^{-5} mrem/pCi. Thus, the yearly dose is

$$D = (3.47 \text{ pCi/L})(42,700 \text{ L/y})(7.14 \times 10^{-5} \text{ mrem/pCi}) = 10.6 \text{ mrem}$$

Because this is well above the limit of 3 mrem, a reduction in release rate is required.

Table 11.5 Ingestion Dose Conversion Factors (in units of 10^{-5} mrem/pCi) for Cs-137

Group	Bone	Liver	Total body	Kidney	Lungs	GI tract
Infant	52.2	61.1	4.33	16.4	6.64	0.191
Child	32.7	31.3	4.62	10.2	3.67	0.196
Teen	11.2	14.9	5.19	5.07	1.97	0.212
Adult	7.97	10.9	7.14	3.70	1.23	0.211

From Tables E-11 to E-14, Reg. Guide 1.109 (U.S. Nuclear Regulatory Commission (NRC), 1977. Regulatory Guide 1.109 Calculation of Annual Doses to Man From Routine Releases of Reactor Effluents for the Purpose of Evaluating Compliance With 10CFR Part 50 Appendix I, October).

The general environmental effect of supporting parts of the nuclear fuel cycle must be described in an application for a construction permit for a power reactor. Data acceptable to the NRC for that purpose appear in the 10CFR51.51, as "Table of Uranium Fuel Cycle Environmental Data."

11.8 CONTEMPORARY RADIATION STANDARDS

A major revision of regulations on radiation exposure was proposed by the NRC in 1986, published as a Final Rule in 1991, and required for use from January 1994. The newer version of the rule 10CFR20 (U. S. Nuclear Regulatory Commission (NRC), 1991) intended to provide greater protection for both workers and the public, was based on ICRP recommendations.

The improved regulations are more realistic in terms of hazards and bring to bear accumulated knowledge about radiation risk. The complicated task of deducing doses is accomplished by computer methods. Whereas the traditional limits on dose are based on the critical organ, the new 10CFR20 considers the dosage to the whole body from whatever sources of radiation are affecting organs and tissues. Radiations from external and internal sources are summed to obtain the total dose. In addition, the long-term effects of radionuclides fixed in the body are added to any short-term irradiation effects. The bases for the limits selected are the risk of cancer in the case of most organs and tissues, and the risk of hereditary diseases in offspring in the case of the gonads.

A new concept called *committed effective dose equivalent* is introduced. Recall from Section 10.2 that dose equivalent is the product of absorbed dose and the quality factor. The word "committed" implies taking into account future exposure after ingestion of radioactive material. The time span is taken to be a typical working life of 50 y (e.g., between ages 20 and 70). Suppose that a certain radionuclide is deposited in an organ of the human body. Over time thereafter, the nuclide decays and is eliminated but provides a dose to that organ. The total dose, labeled H_{50}, is called a committed dose equivalent. It is assumed that the dose is experienced within the year the nuclide is deposited, which will be more nearly true the shorter the effective life in the body.

To calculate H_{50}, suppose that N_0 atoms/cm^3 are deposited in an organ or tissue with density ρ. The number left there after a time t is

$$N = N_0 \left(\frac{1}{2}\right)^{t/t_E} \tag{11.14}$$

where t_E is the effective half-life, as discussed in Section 10.1. The number that has been eliminated is $N_E = N_0 - N$, and the fraction of these that decay is t_E/t_H, as shown in Exercise 11.6. Thus the number that decay is

$$N_D = N_E(t_E/t_H) \tag{11.15}$$

As each nucleus decays, it delivers energy E_d, and thus the committed dose equivalent is

$$H_{50} = N_D E_d/\rho \tag{11.16}$$

EXAMPLE 11.12

Let us apply these relations to some radionuclides. The 12.3-y (=4500 d) half-life of tritium is a fairly large fraction of 50 y, but the biological half-life is only $t_B = 10$ d, so t_E is also approximately 10 d. Hence, after 50 y very little of the original tritium remains in the body. The fraction that decays within the organ is

$$N_D/N_E = t_E/t_H = (10\text{d})/(4500\text{d}) = 0.0022$$

and the fraction leaving the tissue is almost exactly 1:

$$(N_E - N_D)/N_E = 1 - N_D/N_E = 1 - 0.0022 = 0.9978$$

In contrast, for plutonium-239, $t_H = 2.4 \times 10^4$ y, $t_B = 100$ y for bone, and $t_E = 99.6$ y. The fraction left after 50 y is

$$N/N_0 = \left(\frac{1}{2}\right)^{t/t_E} = \left(\frac{1}{2}\right)^{(50\text{y})/(100\text{y})} = 0.707$$

whereas the fraction eliminated is $N_E/N_0 = 1 - 0.707 = 0.293$. Of these, decay accounts for only

$$N_D/N_E = t_E/t_H = (99.6\text{y})/(24{,}000\text{y}) = 0.0042$$

Finally, the word "effective" accounts for the relative risk associated with different organs and tissues by forming a weighted sum by use of weighting factors w_T as listed in Table 11.6. If $(H_{50})_T$ represents the committed dose to organ or tissue T, the effective dose is a sum over T,

$$(H_{50})_E = \sum\nolimits_T \omega_T (H_{50})_T \tag{11.17}$$

If only one organ were important, as in the case of iodine-131 in the thyroid, the effective dose to the whole body would only be 3% of what it would be if the same dose were delivered throughout the body.

From the factors in Table 11.6 and from the knowledge of chemical properties, half-life, radiations, and organ and tissue data, the NRC has deduced the limits on concentrations of specific radionuclides. Dose restrictions are for an annual limit of intake (ALI) by inhalation or ingestion of a radionuclide that delivers 5 rem/y (or a 50-year dose of 50 rem) for a plant worker. The derived air concentration (DAC) would give one ALI in a working year (2000 h) through breathing contaminated air. Extensive tables of ALI and DAC for hundreds of radioisotopes are provided in the new 10CFR20. They allow the calculation of exposure to mixtures of isotopes. A few examples are exhibited in Table 11.7.

Table 11.6 Organ and Tissue Radiation Weighting Factors (10CFR20)

Organ or Tissue	Weighting Factor
Gonads	0.25
Breast	0.15
Red bone marrow	0.12
Lung	0.12
Thyroid	0.03
Bone surfaces	0.03
Remainder[a]	0.30
Whole body	1.00

[a] *0.06 each for five organs.*

Table 11.7 ALIs and DACs of Select Radionuclides for Occupational Exposure

		Oral Ingestion	Inhalation	
Radionuclide	**Class**	**ALI (μCi)**	**ALI (μCi)**	**DAC (μCi/mL)**
Kr-85	Submersion	–	–	1×10^{-4}
I-131	D	30	50	2×10^{-8}
Xe-133	Submersion	–	–	1×10^{-4}
Cs-137	D	100	200	6×10^{-8}

From 10CFR20, Appendix B.

The two quantities are related by

$$\text{DAC}\,[\mu\text{Ci/mL}] = \text{ALI}\,[\mu\text{Ci/y}]/\left(2.4 \times 10^9\,\text{mL/y}\right) \tag{11.18}$$

where the numerical factor is a product of four things: 50 wk/y, 40 h/wk, 60 min/h, and 2×10^4 mL of air breathed per minute.

A distinction is made between two types of doses. The first is *stochastic*, which is the same as probabilistic, defined as dosages related to the chance of cancer or hereditary effect, with the number of health effects proportional to the dose. The worker dose limit for stochastic effects is 5 rem/y. The second is nonstochastic or *deterministic*, which are doses to tissues for which there is a threshold dose for an effect, so that a definite limit can be set on an annual dose (e.g., 50 rem). The skin and the eye lens are examples. Fig. 11.6 distinguishes the terminology describing radiation effects on people.

We can revisit the situation of a cloud of radioactive Kr-85 as in Example 11.2. Detailed calculations on all organs lead to the conclusion that only the skin will be significantly affected and thus the nonstochastic limit applies. The ALI and DAC values are correspondingly higher, the latter being $1 \times 10^{-4}\,\mu\text{Ci/cm}^3$, 10 times the value in the old 10CFR20. For other radionuclides and modes of exposure, the new calculated concentrations can be smaller, the same, or larger than the old.

EXAMPLE 11.13

An example adapted from NRC material will be helpful in understanding the new rule. Suppose that a worker in a nuclear plant receives 1 rem of external radiation and also is exposed over 10 working days to concentrations in air of iodine-131 of $9 \times 10^{-9}\,\mu\text{Ci/mL}$ and of cesium-137 of $6 \times 10^{-8}\,\mu\text{Ci/mL}$ (these correspond to the older MPCs). What is the fraction (or multiple) of the annual effective dose equivalent limit? We sum the fractions that each exposure is of the annual limit of 5 rem. The external exposure contributes (1 rem)/(5 rem) = 0.2. The ALI figures, which consider the ICRP weighting factors for the various organs for the two isotopes, are 50 μCi for I-131 and 200 μCi for Cs-137 (see Table 11.7). We need to find the actual activities taken into the body. With the standard breathing rate of $1.2\,\text{m}^3$/h, in 80 h the air intake is $96\,\text{m}^3$. The activities received are thus

$$\text{I}-131: \left(9 \times 10^{-9}\,\mu\text{Ci/mL}\right)\left(96\text{m}^3\right)\left(10^6\,\text{mL/m}^3\right) = 0.86\,\mu\text{Ci}$$

$$\text{Cs}-137: \left(6 \times 10^{-8}\,\mu\text{Ci/mL}\right)\left(96\text{m}^3\right)\left(10^6\,\text{mL/m}^3\right) = 5.8\,\mu\text{Ci}$$

The corresponding I and Cs fractions are 0.86/50 and 5.8/200. The total of the external and internal fractions is

$$\frac{1\,\text{rem}}{5\,\text{rem}} + \frac{0.86\,\mu\text{Ci}}{50\,\mu\text{Ci}} + \frac{5.8\,\mu\text{Ci}}{200\,\mu\text{Ci}} = 0.246$$

or approximately one-fourth of the limit. In this particular case, the expected hazard is lower than by the older method.

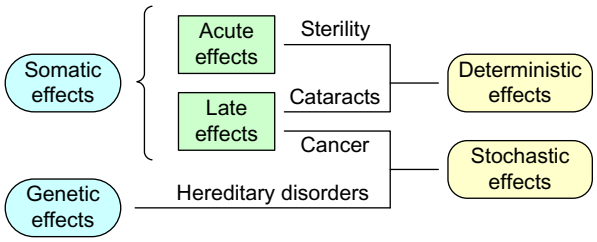

FIG. 11.6

Relationship between radiation effects terminology.

Other features of the new rule are separate limits on exposures (1) of body extremities—hands, forearms, feet, lower legs; (2) of the lens of the eye; and (3) of an embryo and fetus. The risk to the whole body per rem of dosage is 1 in 6000. For the limit of 5 rem, the annual risk is 8×10^{-4}, which is approximately eight times acceptable rates in "safe" industries. The figure is to be compared with the lifetime risk of cancer from all causes of approximately 1 in 6.

Dose limits for individual members of the public (0.1 rem/y) are quite a bit lower than those working with radionuclides (5 rem/y). In calculating concentrations of radionuclides in air released to an unrestricted area, differences in time of exposure, breathing rate, and average age are accounted for by dividing worker DAC values by 300 for inhalation or 219 for submersion.

EXAMPLE 11.14

Determine the concentration release limits for the general public for Xe-133 and Cs-137. Using Table 11.7, DACs for gaseous Xe-133 submersion and Cs-137 inhalation along with the proper divisors leads to

$$\mathrm{Xe-133}: \left(1 \times 10^{-4}\,\mu\mathrm{Ci/mL}\right)/219 = 5 \times 10^{-7}\,\mu\mathrm{Ci/mL}$$

$$\mathrm{Cs-137}: \left(6 \times 10^{-8}\,\mu\mathrm{Ci/mL}\right)/300 = 2 \times 10^{-10}\,\mu\mathrm{Ci/mL}$$

11.9 SUMMARY

Radiation protection of living organisms requires control of sources, barriers between source and living being, or removal of the target entity. Calculations required to evaluate external hazard include the dose as it depends on flux and energy, material, and time; the inverse square geometric spreading effect; and the exponential attenuation in shielding materials. Internal hazard depends on many physical and biological factors. Maximum permissible concentrations of radioisotopes in air and water can be deduced from the properties of the emitter and the dose limits. Application of the principle of ALARA is designed to reduce exposure to levels that are as low as reasonably achievable. There are many biological pathways that transport radioactive materials. New dose limit rules are based on the total effects of radiation—external and internal—on all parts of the body.

11.10 EXERCISES

11.1 What is the dose rate in mrem/y corresponding to a continuous (a) 0.5 MeV, (b) 2 MeV, and (c) 0.1 MeV gamma-ray flux of 100/(cm^2 s)? What dose equivalent would be received by a person who worked 40 h/wk throughout the year in such a flux?

11.2 A Co-60 source is to be selected to test radiation detectors for operability. Assuming that the source can be kept at least 1 m from the body, what is the largest strength acceptable (in μCi) to assure an exposure rate of less than 500 mrem/y? (Recall that ^{60}Co emits two gammas of energy 1.17 and 1.33 MeV.)

11.3 Similar to the Kr-85 analysis, estimate the MPC in air for (a) tritium and (b) argon-41, having average beta particle energy of 6 and 459 keV, respectively.

11.4 The nuclear reactions resulting from thermal neutron absorption in boron and cadmium are

$$\begin{aligned} {}^{10}_{5}\mathrm{B} + {}^{1}_{0}\mathrm{n} &\rightarrow {}^{7}_{3}\mathrm{Li} + {}^{4}_{2}\mathrm{He} \\ {}^{113}_{48}\mathrm{Cd} + {}^{1}_{0}\mathrm{n} &\rightarrow {}^{114}_{48}\mathrm{Cd} + \gamma[5\,\mathrm{MeV}] \end{aligned} \tag{11.19}$$

Which material would you select for a radiation shield? Explain.

11.5 Find the uncollided gamma ray flux at the surface of a spherical lead shield of radius 12 cm surrounding a very small source of 200 mCi of 1 MeV gammas.

11.6 Effluent concentration limits of some radionuclides in water released to the public, according to 10CFR20 in the old and new versions, are listed here. Calculate the new/old ratio for each radionuclide.

	Concentration Limits (μCi/mL)	
Radionuclide	**Old**	**New**
Tritium (H-3)	3×10^{-3}	1×10^{-3}
Cobalt-60	3×10^{-5}	3×10^{-6}
Strontium-90	3×10^{-7}	5×10^{-7}
Iodine-131	3×10^{-7}	1×10^{-6}
Cesium-137	2×10^{-5}	1×10^{-6}

11.7 Water discharged from a nuclear plant contains in solution traces of strontium-90, cerium-144, and cesium-137. Assuming that the concentrations of each isotope are proportional to their fission yields, find the allowed activities per mL of each. Note the following data:

Isotope	Half-life	Yield	Limit (μCi/mL)
^{90}Sr	29.1 y	0.0575	5×10^{-7}
^{144}Ce	284.6 d	0.0545	3×10^{-6}
^{137}Cs	30.1 y	0.0611	1×10^{-6}

11.8 A 50-year exposure time is assumed in deriving the dose factors listed in Section 11.8. These account for the radioisotope's physical half-life t_H and also its biological half-life t_B. (a) Find the effective half-life t_E for these three cases cited by Eichholz (1985):

Radionuclide	t_H	t_B
Iodine-131	8.04 d	138 d
Cobalt-60	5.27 y	99.5 d
Cesium-137	30.1 y	70 d

(b) If t_H and t_B are greatly different from each other, what can be said about the size of t_E?

11.9 The activities of U-238, Ra-226, and Rn-222 in a closed system are approximately equal, in accord with the principle of secular equilibrium. Assuming that the natural uranium content of soil is 10 ppm (parts per million), calculate the specific activities of the isotopes in microcuries per gram of soil (Table 3.2 gives the needed half-lives).

11.10 For the conditions in Example 11.11, determine the annual dose to (a) an infant's kidney, (b) a child's bones, (c) a teenager's liver, and (d) an adult's GI tract.

11.11 Over the course of six 10-h working days, an employee receives an external dose of 200 mrem and inhales air consisting of 1.3×10^{-8} μCi/mL of I-131 and 7.3×10^{-8} μCi/mL of Cs-137. Compute the ratio of the dose received to the annual effective dose equivalent limit.

11.12 What are the release limits (in Bq/mL) for the general public for gaseous (a) Kr-85 and (b) I-131?

11.13 Using range relations from Chapter 5, determine the flux resulting in a 0.1 rem/y dose from (a) 1 MeV maximum energy betas, (b) 1 MeV electrons, and (c) 1 MeV alphas. Recall that the average beta energy is about one-third of the maximum.

11.14 Identify the three places in the gamma-ray flux formula that r appears, pursuant to the statement of Example 11.9.

11.15 Calculate the specific gamma-ray dose constant for (a) Cs-137 and (b) Na-24.

11.16 Use the Γ value from the previous exercise to determine the distance from an 8-mCi Cs-137 point source at which the dose rate is 5 mrem/h.

11.17 To study the impact of neglecting air attenuation, calculate and graph the flux for distances of 0.1–5 m from (a) a Co-60 and (b) a Cs-137 point source emitting 10^8 photons/s with and without air attenuation.

11.18 Determine the alpha particle energy corresponding to the 0.1-rem/y flux of $10^{-5}/(\text{cm}^2\,\text{s})$ given in Table 11.1.

11.11 COMPUTER EXERCISES

11.A Program EXPOSO looks up gamma ray attenuation coefficients and buildup factors on data tables for several shield materials, and finds the radiation exposure at a distance from a point source. (a) Verify that the flux at 10 cm from a point millicurie 1-MeV gamma ray source in lead is 39.2/(cm^2 s). (b) Use the program to find the distance through Pb from a millicurie 1-MeV source that yields 5 mrem/y, to within 1 mm. (c) Check the neutron flux found for a reactor in space (Example 11.4) with the shield option 7 (none). (d) Compute the gamma dose from the reactor if seven photons of 1 MeV each are produced from each fission and 20% escape.

11.B A small research reactor core is located near the bottom of a deep pool of water. The water serves as moderator, coolant, and shield. (a) With a power of 10 MW and a fission neutron leakage fraction of 0.3, estimate, with the point source version of the computer program NEUTSHLD, the uncollided flux of fast neutrons at a distance of 20 ft from the core, treated as a point source. (b) Samples to be irradiated are placed near the core, the dimensions of which are 30 cm × 30 cm × 60 cm high. Assuming that the neutron source strength per unit area is uniform, calculate, with the plane version of NEUTSHLD, the fast neutron flux at 10 cm from the center of a large face of the core. (c) Compare the H scattering cross-section and fission spectrum graphs from NEUTSHLD to those of Figs. 4.7 and 6.6, respectively.

11.C To improve the uniformity of irradiation of large objects in a water pool, a set of five Co-60 point sources (average gamma ray energy 1.25 MeV) are arranged in a plane at coordinates in centimeters (0, 0), (20, 20), (20, −20), (−20, −20), and (−20, 20). (a) Explore the variation of total gamma flux over a parallel plane 10 cm away with computer program EXPOSO to calculate contributions of each source. (b) Compare with results in a case where all five sources are concentrated near the point (0, 0).

11.D A room with concrete walls is constructed of sand with a small uranium content, such that the concentration of radium-226 (1600 y) is 10^6 atoms per cm^3. Normally, the room is well ventilated so the gaseous radon-222 (3.82 d) is continually removed, but during a holiday, the room is closed up. With the parent-daughter computer program RADIOGEN (Chapter 3), calculate the trend in air activity caused by Rn-222 over a 1-week period, assuming that half the radon enters the room. Data on the room: 10 ft × 10 ft × 10 ft, walls 3 in. thick. Does the radon concentration warrant action according to the EPA criterion?

REFERENCES

Eichholz, G.G., 1985. Environmental Aspects of Nuclear Power. Lewis Publishers, Chelsea.

Evans, R.D., 1982. The Atomic Nucleus. Krieger, New York.

International Commission on Radiological Protection (ICRP), 1960. ICRP Publication 2: Recommendations of the International Commission on Radiological Protection, Report of Committee II on Permissible Dose for Internal Radiation. Pergamon Press, Oxford Also appears in Health Physics 3 (1), 1–380.

Lewis, R.K., 2006. A history of radon-1470 to 1984. In: National Radon Meeting, Council of Radiation Control Protection Directors. Frankford, KY.

Thompson, D.F., Church, C.O., 2001. Prussian blue for treatment of radiocesium poisoning. Pharmacotherapy 21 (11), 1364–1367.
Trubey, D.K., 1988. New Gamma-Ray Buildup Factor Data for Point Kernel Calculations: ANS-6.4.3 Standard Reference data, Oak Ridge National Laboratory, ORNL/RSIC-49.
U.S. Environmental Protection Agency (EPA), 1986. EPA J. 12 (6). xi–15. Nearly every article addresses radon.
U.S. Nuclear Regulatory Commission (NRC), 1977. Regulatory Guide 1.109 Calculation of Annual Doses to Man From Routine Releases of Reactor Effluents for the Purpose of Evaluating Compliance With 10CFR Part 50 Appendix I. October.
U.S. Nuclear Regulatory Commission (NRC), 1986. Standards for protection against radiation. Fed. Regist. 51 (6), 1092–1210. January 9.
U.S. Nuclear Regulatory Commission (NRC), 1991. Fed. Regis. 56 (98), 23360–23474. May 21. The Introduction contains useful reading on the history of dose regulations in the United States.
U.S. Nuclear Regulatory Commission (NRC), Standards for Protection Against Radiation, Part 20 of the Code of Federal Regulations—Energy, 10CFR20. http://www.nrc.gov/reading-rm/doc-collections/cfr/part020. to each subpart (e.g., C: Occupational Dose Limits, and D: Radiation Dose Limits for Individual Members of the Public).
Unger, L.M., Trubey, D.K., 1982. Specific Gamma-Ray Dose Constants for Nuclides Important to Dosimetry and Radiological Assessment. ORNL/RSIC-45/R1. Oak Ridge National Laboratory.

FURTHER READING

Bevelacqua, J.J., 1995. Contemporary Health Physics: Problems and Solutions. Wiley, New York.
Bevelacqua, J.J., 1999. Basic Health Physics: Problems and Solutions. Wiley, New York. Helpful in preparing for certified health physicist exam.
Brill, A.B., Becker, D.V., Donahoe, K., Goldsmith, S.J., Greenspan, B., Kase, K., Royal, H., Silberstein, E.B., Webster, E.W., 1994. Radon update: facts concerning environmental radon: levels, mitigation strategies, dosimetry, effects and guidelines. J. Nucl. Med. 35 (2), 368–385.
Cember, H., Johnson, T.E., 1999. The Health Physics Solutions Manual. PS&E Publications, Silver Spring, MD.
Cember, H., Johnson, T.E., 2009. Introduction to Health Physics, fourth ed. McGraw-Hill, New York.
Dowd, S.B., Tilson, E.R. (Eds.), 1999. Practical Radiation Protection and Applied Radiobiology. W.B. Saunders Co., Philadelphia. All about radiation, its effects, and protection, from a nuclear medicine viewpoint.
Eremenko, V.A., Droppo, J.G., 2006. A personal experience reducing radiation exposures: protecting family in Kiev during the first two weeks after Chernobyl. Health Phys. 91 (2), S39–S46.
Faw, R.E., Shultis, J.K., 1999. Radiological Assessment: Sources and Doses. American Nuclear Society, La Grange Park, IL. Fundamentals and extensive data; reprint with a few changes of a 1991 book published by Prentice-Hall.
International Atomic Energy Agency (IAEA), 2004. International Basic Safety Standards for Protection Against Ionizing Radiation and for the Safety of Radiation Sources. Safety Series No. 115, Vienna.
Miller, K.L., Weidner, W.A., 1986. CRC Handbook of Management of Radiation Protection Programs. CRC Press, Boca Raton, FL. An assortment of material not found conveniently elsewhere, including radiation lawsuit history, the responsibilities of health physics professionals, information about state radiological protection agencies, and emergency planning.
National Council of Radiation Protection and Measurements (NCRP), 1991. Radon Exposure of the United States Population—Status of the Problem. NCRP Commentary No. 6. Bethesda, MD.
National Research Council, Committee on Health Effects of Exposure to Radon, 1999. Health Effects of Exposure to Radon (BEIR VI). National Academies Press, Washington, DC. Conclusion: new information needs to be considered and improved models developed.

National Research Council, Committee on the Biological Effects of Ionizing Radiations, 1988. Health Risks of Radon and Other Internally Deposited Alpha-Emitters, BEIR IV. National Academies Press, Washington, DC. Emphasizes lung cancer and the relationship of smoking and radon.

Rockwell III, T., 1956. Reactor Shielding Design Manual. McGraw-Hill, New York. Classic book on shielding calculations that remains a valuable reference.

Shleien, B., Slayback Jr., L.A., Birky, B.K. (Eds.), 1998. Handbook of Health Physics and Radiological Health. third ed. Williams & Wilkins, Baltimore, MD. A greatly expanded version of a classic document of 1970.

Shultis, J.K., Faw, R.E., 1996. Radiation Shielding. Prentice-Hall, Upper Saddle River, NJ.

Till, J.E., Meyer, H.R. (Eds.), 1983. Radiological Assessment, A Textbook on Environmental Dose Analysis. Nuclear Regulatory Commission, NUREG/CR-3332, Washington, DC.

Turner, J.E., 2007. Atoms, Radiation, and Radiation Protection, third ed. Wiley, New York.

U.S. Environmental Protection Agency (EPA), Radiation Protection. http://www.epa.gov/radiation. Select from a variety of links.

U.S. Nuclear Regulatory Commission (NRC), 1977. Regulatory Guide 1.111 methods for estimation of atmospheric transport and dispersion of gaseous effluents in routine releases from light-water-cooled reactors. Washington, DC.

U.S. Nuclear Regulatory Commission (NRC), 1978. Select Division 8, Occupational Health, 8.8 Information Relevant to Ensuring that Occupational Radiation Exposures at Nuclear Power Stations Will Be as Low as is Reasonably Achievable June. 1978.

Wood, J., 1982. Computational Methods in Reactor Shielding. Pergamon Press, Oxford.

Hubbell, J.H., Seltzer, S.M., 2004. Tables of X-Ray Mass Attenuation Coefficients and Mass Energy-Absorption Coefficients. National Institute of Standards and Technology, Gaithersburg, MD. http://physics.nist.gove/xaamdi.

CHAPTER

RADIATION DETECTORS 12

CHAPTER OUTLINE

Measurement of radiation is required in all facets of nuclear energy: in scientific studies, in the operation of reactors for the production of electric power, and for protection from radiation hazards. Detectors are used to identify the radioactive products of nuclear reactions and to measure neutron flux. Instruments determine the amount of radioisotopes in the air we breathe and the water we drink, or the uptake of a sample of radioactive material administered to the human body for diagnosis. In recent years, detectors have become indispensable for thwarting terrorism.

The kind of detector used depends on the particles to be observed, whether electrons, gamma rays, neutrons, ions such as fission fragments, or combinations. It depends on the energy of the particles. It also depends on the radiation environment in which the detector is to be used—at one end of the scale is a minute trace of a radioactive material and at the other a source of large radiation exposure. The type of measuring device, as in all applications, is chosen for the intended purpose and the accuracy desired.

The demands on the detector are related to what it is we wish to know:

(a) Whether there is a radiation field present.
(b) The number of nuclear particles that strike a surface per second or some other specified period of time.

Nuclear Energy. https://doi.org/10.1016/B978-0-12-812881-7.00012-5

(c) The type of particles present, and, if there are several types, the relative number of each.
(d) The energy of the individual particles.
(e) The instant a particle arrives at the detector.

From the measurement of radiation, we can deduce properties of the radiation such as ability to penetrate matter and to produce ionization. We can also determine properties of a radioactive source, including decay rate, half-life, and amount of material.

In this chapter, we describe the important features of a few popular types of detectors. Most of them are based on the ionization produced by incoming radiation. The instrument may operate in one of two modes: (1) current, in which an average electrical flow is measured, as with an ammeter, and (2) pulse, in which the electrical signals produced by individual particles or rays are amplified and counted. A detector operating in this latter mode is known as a *counter*.

Because none of the five human senses will measure nuclear radiation, a detector serves as a sixth sense. A detector also makes it possible to reveal the existence of amounts of material much smaller than can be found by ordinary chemical tests.

12.1 DETECTOR CHARACTERISTICS

Radiation detectors employ a variety of physical effects to convert radiation into a readable output. Sensing methods include electrical, chemical, and light-based approaches. Certain descriptors apply to radiation measuring instruments regardless of the sensing mechanism. A key metric is the *efficiency* ε by which radiation is detected

$$\varepsilon = \frac{\text{Radiation emissions counted by detector}}{\text{Radiation emissions from the source}} = \frac{R}{S} = \varepsilon_g \varepsilon_i \tag{12.1}$$

Sensing ineffectiveness is the consequence of geometric and radiation detection limitations expressed in terms of geometric ε_g and intrinsic ε_i efficiencies, respectively.

First, the geometry should be favorable for adequate amounts of radiation to reach the detector. Fig. 12.1 depicts two common situations for radiation measurements: surveys using hand-held instruments and laboratory radiation counting with fixed equipment. Radiation sensing by the survey instrument is limited by the combination of the source strength and the distance from the survey meter to the source, whereas in the laboratory the sample is placed directly adjacent to the detector. In the latter

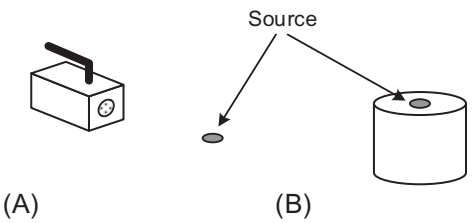

FIG. 12.1

Two typical applications of radiation measuring instruments: (A) a survey meter and (B) a laboratory detector.

case, roughly half the emissions would enter the detector material if the sample is a thin disc. A detector configuration that completely surrounds the sample is termed as 4π geometry.

Second, the detector must interact with the radiation in some manner; otherwise, the radiation may simply pass through the detector's active volume without any impact. Furthermore, if an interaction occurs, the consequence must be significant and long-lasting enough that the desired signal is generated.

EXAMPLE 12.1

A health physicist is searching for a 1-μCi Cs-137 sealed source dropped in a 15 m × 15 m classroom. The worst geometric efficiency encountered during the measurement would occur if the survey meter and misplaced source were located at opposite corners of the room, such that the source-to-detector distance is $15\sqrt{2}$m. Table 3.2 reveals that Cs-137 emits a 0.662 MeV gamma 85.1% of the time such that the source strength is

$$S = fA = (0.851\gamma/\text{decay})(1\,\mu\text{Ci})\left(3.7\times10^4\,\text{Bq}/\mu\text{Ci}\right) = 3.15\times10^4\gamma/\text{s}$$

At this distance, the Cs-137 betas are inconsequential. The point source relation, Eq. (11.6), shows that from S source emissions, the radiation flux incident to the detector is

$$\phi = S/\left(4\pi r^2\right) = \left(3.15\times10^4\gamma/\text{s}\right)/\left[4\pi\left(15\sqrt{2}\times100\text{cm}\right)^2\right] = 5.6\times10^{-4}\gamma/\left(\text{cm}^2\,\text{s}\right)$$

If the detector surface area normal to the gamma flux is $A_d = 10\,\text{cm}^2$, then the geometric efficiency is

$$\varepsilon_g = \phi A_d/S = A_d/\left(4\pi r^2\right) = \left(10\text{cm}^2\right)/\left[4\pi\left(15\sqrt{2}\times100\text{cm}\right)^2\right] = 1.8\times10^{-7}$$

Assuming a perfect detector intrinsic efficiency ($\varepsilon_i = 1$ count per incident photon), the count rate is

$$R = \varepsilon_g\varepsilon_i S = \left(1.8\times10^{-7}\right)(1\text{count}/\gamma)\left(3.15\times10^4\gamma/\text{s}\right) = 0.0057\text{count}/\text{s}$$

This unfavorable geometry leads to an essentially zero count rate such that the health physicist must move about the room to reduce the distance between the source and survey instrument in order to achieve a measurable count rate, especially because background radiation is already contributing to a nonzero reading.

12.2 GAS COUNTERS

Picture a gas-filled chamber with a central electrode (*anode*, electrically positive) and a conducting wall (*cathode*, negative). They are maintained at different voltage potential, as shown in Fig. 12.2. If a charged particle or gamma ray is allowed to enter the chamber, it may produce a certain amount of ionization in the gas. The resultant positive ions and electrons are attracted toward the negative and positive surfaces, respectively. A charge moves in the local electric field $\mathscr{E}$ with a drift velocity $v_D = \mu\mathscr{E}$, where the mobility μ depends on the time between collisions and the mean free path (see Sections 4.5 and 4.7). If a magnetic field is present, charges tend to execute circular paths interrupted by collisions. When the voltage across the tube is low, the charges merely migrate through the gas, they are collected, and a current of short duration (a pulse) passes through the resistor R and the meter. More generally, amplifying circuits are required. The number of current pulses is a measure of the number of incident particles that enter the detector, which is designated as an *ionization chamber* when operated in this mode.

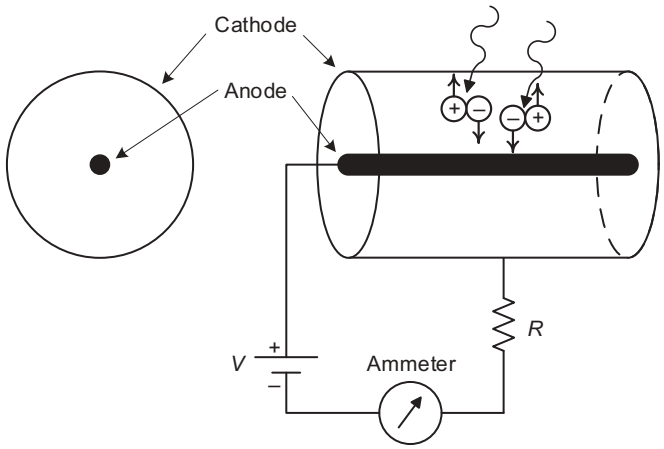

FIG. 12.2

Basic gas-filled detector.

If the applied voltage is then increased sufficiently, electrons produced by the incident radiation through ionization are able to gain enough speed to cause further (secondary) ionization in the gas. Most of this action occurs near the central electrode, where the electric field is highest (see Exercise 12.4). The current pulses are much larger than in the ionization chamber because of the amplification effect. The current is proportional to the original number of electrons produced by the incoming radiation, and the detector is now called a *proportional counter*. One may distinguish between the passage of beta particles and alpha particles, which have a widely different ability to ionize. The time for collection is very short, of the order of microseconds.

If the voltage on the tube is raised still higher, a particle or ray of any energy will set off a discharge in which the secondary charges are so great in number that they dominate the process. The discharge stops of its own accord because of the generation near the anode of positive ions, which reduce the electric field there to such an extent that electrons are not able to cause further ionization. The current pulses are then of the same size, regardless of the event that initiated them. In this mode of operation, the detector is called a *Geiger-Müller* (GM) counter. Unlike the proportional counter, the magnitude of the pulses produced by a GM counter is independent of the original number of electrons released by the ionizing radiation. Therefore, the counter provides no information about the type or energy of the radiation. There is a short period, the *dead time*, in which the detector will not count other incoming radiation. If the radiation level is very high, a correction of the observed counts to yield the true counts must be made to account for the dead time τ. In particular, for a measured count rate of R_M, the true count rate is

$$R_C = R_M/(1 - R_M\tau) \tag{12.2}$$

In some gases, such as argon, there is a tendency for the electric discharge to be sustained, and it is necessary to include external circuitry or a small amount of foreign gas or vapor (e.g., alcohol or halogen) to quench the discharge.

EXAMPLE 12.2

If a GM detector with a 75-μs dead time records 25,000 counts per min (cpm), the actual count rate is

$$R_C = \frac{R_M}{1 - R_M\tau} = \frac{25{,}000\text{cpm}}{1 - (25{,}000\text{cpm})(75 \times 10^{-6}\text{s})(1\,\text{min}/60\text{s})} = 25{,}800\text{cpm}$$

This corrected count rate is about 3% higher than that measured by the meter.

A qualitative distinction between the preceding three types of counters is displayed graphically in Fig. 12.3, which is a semilogarithmic plot of the charge collected as a function of applied voltage. We note that the current varies over several orders of magnitude.

Many instruments, especially those employing gas chambers, display the radiation field in terms of the classic exposure unit of roentgen (R), which is defined as 2.58×10^{-4} C/kg (originally, an R was defined in terms of the now-obsolete electrostatic unit). In this context, *exposure* specifically refers to

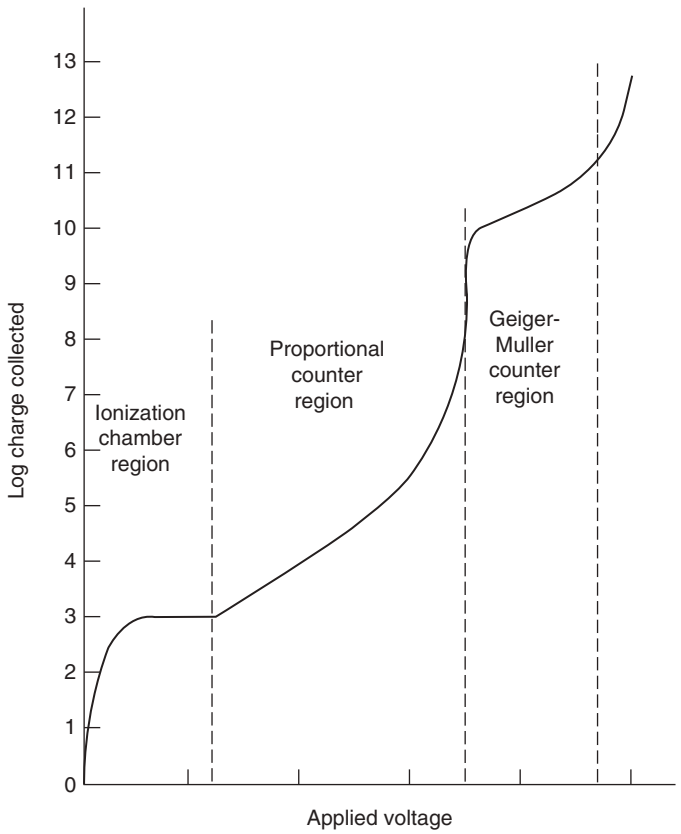

FIG. 12.3

Collection of charge in gas counters.

the charge imparted (ΔQ) to air mass m by photons and is mathematically expressed in a form very similar to dose

$$X = \Delta Q/m \tag{12.3}$$

With such narrow applicability, the scientific community prefers the units rad and rem, and their SI equivalents; however, the continued usage of R to measure radiation compels its inclusion here.

EXAMPLE 12.3

For convenience, we determine the equivalent energy deposition for a roentgen of charge imparted. Because about 34 eV is needed to create an ion pair in air, then

$$1\,\mathrm{R} = \frac{(2.58\times10^{-4}\,\mathrm{C/kg})(34\,\mathrm{eV/ip})}{(1.602\times10^{-19}\,\mathrm{C/ip})(10^{6}\,\mathrm{eV/MeV})} = 5.48\times10^{10}\,\mathrm{MeV/kg}$$

With a unity quality factor for photons, a meter reading 15 mR/h equates to

$$\dot{H} = \dot{D}\,QF = \frac{(15\,\mathrm{mR/h})(1\,\mathrm{rad}/0.01\,\mathrm{J/kg})(1\,\mathrm{rem/rad})}{(1\,\mathrm{R}/5.48\times10^{10}\,\mathrm{MeV/kg})(1\,\mathrm{MeV}/1.602\times10^{-13}\,\mathrm{J})} = 13\ \mathrm{mrem/h}$$

Then approximately, $1\,\mathrm{R} \approx 1\,\mathrm{rad} = 1\,\mathrm{rem}$ when measuring gamma and X-rays.

Many smoke detectors operate on essentially the same principle as an ionization chamber. The smoke alarm contains about 1 μCi (37 kBq) of Am-241, which emits alpha particles that ionize the nearby air. Smoke particles tend to neutralize the ionized air, thereby interrupting the detector current, and thus sounding the fire alarm.

12.3 NEUTRON DETECTORS

To detect neutrons, which do not create ionization directly, it is necessary to provide a means for generating the charges that can ionize a gas. Advantage may be taken of the nuclear reaction involving neutron absorption in boron

$${}^{1}_{0}\mathrm{n} + {}^{10}_{5}\mathrm{B} \rightarrow {}^{4}_{2}\mathrm{He} + {}^{7}_{3}\mathrm{Li} \tag{12.4}$$

where the helium and lithium atoms are released as ions. One form of *boron counter* is filled with the gas boron trifluoride (BF_3) and operated as an ionization chamber or a proportional counter. It is especially useful for the detection of thermal neutrons because the cross-section of B-10 at 0.0253 eV is large, 3837 barns, as noted in Table 4.2. Most of the 2.8 MeV energy release goes to the kinetic energy of the product nuclei. The reaction rate of neutrons with the boron in BF_3 gas is independent of the thermal neutron velocity distribution (see Exercise 12.10), as can be seen by forming the product

$$R_\mathrm{a} = nvN\sigma_\mathrm{a} \tag{12.5}$$

where σ_a varies as $1/v$. The detector thus measures the number density n of an incident neutron beam rather than the flux. Alternatively, the metal electrodes of a counter may be coated with a layer of boron that is thin enough to allow the alpha particles to escape into the gas. The counting rate in a boron-lined chamber depends on the surface area exposed to the neutron flux.

The *fission chamber* is often used for slow neutron detection. A thin layer of U-235, with a large thermal neutron fission cross-section, is deposited on the cathode of the chamber. Energetic fission fragments produced by neutron absorption traverse the detector and give the necessary ionization. Uranium-238 is avoided because it is not fissionable with slow neutrons and because of its stopping effect on fragments from U-235 fission.

Neutrons in the thermal range can be detected by the radioactivity induced in a substance in the form of small foil or thin wire. Examples are manganese $^{55}_{25}$Mn with a 13.3 barn cross-section at 2200 m/s, which becomes $^{56}_{25}$Mn with half-life 2.58 h; and dysprosium $^{164}_{66}$Dy, 1.7×10^3 barns, becoming $^{165}_{66}$Dy, half-life 2.33 h. For detection of neutrons slightly above thermal energy, materials with a high resonance cross-section are used (e.g., indium with a peak at 1.45 eV). To separate the effects of thermal neutron capture and resonance capture, comparisons are made between measurements taken with thin activation foils of indium and those of indium covered with cadmium. The Cd cover screens out low-energy neutrons (below 0.5 eV) and passes those of higher energy (see Fig. 4.6).

EXAMPLE 12.4

The thermal and resonance activation cross-sections of indium are 145 b and 2640 b, respectively (Price, 1964). If two identical In foils with and without a Cd cover are exposed to a low-energy neutron flux for sufficient time to achieve a saturated activity level (see Eq. 3.17), the activities of the foils are

$$A_{\text{In-bare}} = N_{\text{In}}\left(\sigma^{\text{In}}_{\text{therm}}\phi_{\text{therm}} + \sigma^{\text{In}}_{\text{reson}}\phi_{\text{reson}}\right)$$
$$A_{\text{In-Cd}} = N_{\text{In}}\sigma^{\text{In}}_{\text{reson}}\phi_{\text{reson}}$$

We recognize that the count rate is proportional to activity, $R = \varepsilon A$. If measurements of 1800 counts per second (cps) and 1500 cps are recorded for the bare and Cd-covered foils, the ratio of the thermal to resonance fluxes is obtained from

$$\frac{\phi_{\text{therm}}}{\phi_{\text{reson}}} = \frac{\sigma_{\text{reson}}}{\sigma_{\text{therm}}}\left(\frac{R_{\text{In-bare}}}{R_{\text{In-Cd}}} - 1\right) = \frac{2640\,\text{b}}{145\,\text{b}}\left(\frac{1800\,\text{cps}}{1500\,\text{cps}} - 1\right) = 3.6$$

For the detection of fast neutrons, up in the MeV range, the *proton recoil* method may be used. We recall from Section 4.7 that the scattering of a neutron by hydrogen results in an energy loss, which is an energy gain for the proton. Thus a hydrogenous material such as methane (CH_4) or H_2 itself may serve as the counter gas. The energetic protons play the same role as alpha particles and fission fragments in the counters discussed previously. Nuclear reactions such as ^{3}He(n, p)^{3}H and ^{6}Li(n, α)^{3}H can also be used to obtain detectable charged particles. Fig. 12.4 reveals that ^{3}He and ^{10}B have similar neutron cross-sections below 100 keV whereas ^{6}Li is about an order of magnitude smaller. To exploit the larger cross-sections at lower energy, the detector may be surrounded by a hydrogenous medium, such as polyethylene (e.g., a Bonner sphere), to thermalize the fast neutrons.

12.4 SCINTILLATION COUNTERS

The name of this detector comes from the fact that the interaction of a particle with some materials gives rise to a scintillation or flash of light. The basic phenomenon is familiar: many substances can be stimulated to glow visibly on exposure to ultraviolet light, and the images on a CRT (cathode

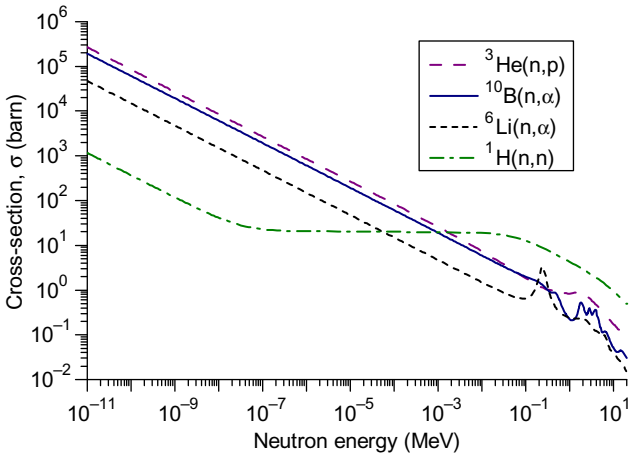

FIG. 12.4

Cross-sections of neutron detecting materials.

Data from ENDF/B-VII.1 (Chadwick, M.B., Herman, M., Obložinský, P., Dunn, M.E., Danon, Y., Kahler, A.C., et al., 2011. ENDF/B-VII.1 Nuclear data for science and technology: cross-sections, covariances, fission product yields and decay data. Nucl. Data Sheets 112(12), 2887–2996).

ray tube) display are the result of electron bombardment. Molecules of materials classed as phosphors are excited by radiation such as charged particles and subsequently emit pulses of light. The substances used in the scintillation detector are inorganic (e.g., sodium iodide or lithium iodide) or organic, in one of various forms: crystalline, plastic, liquid, or gas. Example scintillators include ZnS(Ag) for alpha particles and NaI(Tl) for gamma rays.

The amount of light released when a particle strikes a phosphor is often proportional to the energy deposited, and thus makes the detector especially useful for the determination of particle energies. Because charged particles have a short range, most of their energy appears in the substance. Gamma rays also give rise to an energy deposition through electron recoil in both the photoelectric effect and Compton scattering, and through the pair production-annihilation process. A schematic diagram of a detector system is shown in Fig. 12.5. Some of the light released in the phosphor is collected in the

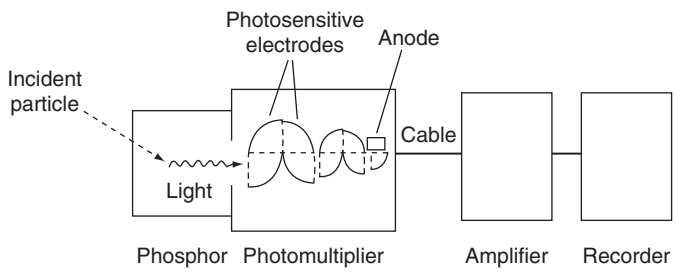

FIG. 12.5

Scintillation detection system.

photomultiplier tube, which consists of a set of electrodes with photosensitive surfaces. When a light photon strikes the surface, an electron is emitted by the photoelectric effect, it is accelerated to the next surface where it dislodges more electrons, and so on, and a multiplication of current is achieved. An amplifier then increases the electrical signal to a level convenient for counting or recording.

Imagine a beam of photons incident to the scintillator face of Fig. 12.5. For flawless light-to-electrical signal conversion, the intrinsic efficiency can be estimated from the fraction of gamma rays interacting in the detector, specifically

$$\varepsilon_i = 1 - e^{-\mu d} \tag{12.6}$$

where d is the thickness of the detector parallel with the beam.

EXAMPLE 12.5

Consider a cesium iodide (CsI) crystal ($\rho = 4.51\,\text{g/cm}^3$) with a mass attenuation coefficient of $2.035\,\text{cm}^2/\text{g}$ at 0.1 MeV. The corresponding intrinsic efficiency for a 1-cm thick detector is

$$\varepsilon_i = 1 - e^{-\mu d} = 1 - \exp\left[-\left(2.035\,\text{cm}^2/\text{g}\right)\left(4.51\,\text{g/cm}^3\right)(1\,\text{cm})\right] = 0.9999$$

Utilizing a solid versus a gas leads to higher intrinsic efficiency.

12.5 PERSONNEL DOSIMETRY

Radiation workers are required to wear personal detectors called *dosimeters* to determine the amount of exposure to X-rays or gamma rays, beta particles, and neutrons. Traditional dosimeters include the pen-size self-reading ionization chambers pictured in Fig. 12.6A. Modern solid-state meters incorporate silicon diode detectors and typically have a liquid crystal display (LCD). Audible warning signals based on cumulative dose and dose rate are available on some instruments. For a more permanent

FIG. 12.6

Common personnel dosimetry. (A) Ionization-type self-reading pocket dosimeter. (B) Four-element thermoluminescent dosimeter (TLD), elements 1 and 2 composed of $^{n}Li_2B_4O_7$, elements 3 and 4 of $CaSO_4$.

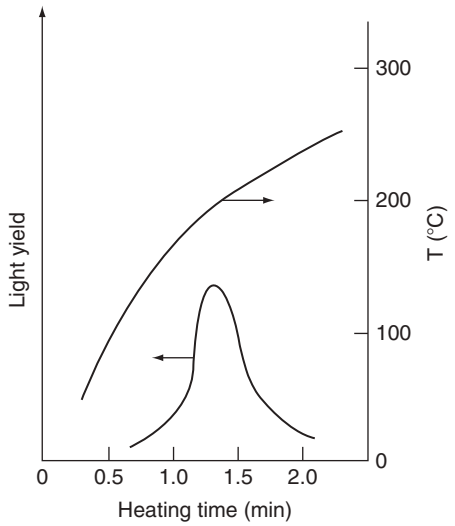

FIG. 12.7

Glow curve of the phosphor CaF_2.

record, a film badge or thermoluminescent dosimeter (TLD), such as that displayed in Fig. 12.6B, is worn. Film badges consist of several photographic films of different sensitivity, with shields to select radiation types. They are developed periodically, and if significant exposure is noted, individuals are relieved of future work in areas with potential radiation hazards for a suitable length of time. An emerging technology is optically stimulated luminescence dosimetry.

Among the most reliable and accurate personal dosimeters is the TLD, which measures the energy of radiation absorbed. It contains crystalline materials such as CaF_2 or LiF that store energy in excited states of the lattice called traps. When the substance is heated, it releases light in a typical *glow curve* as shown in Fig. 12.7. The dosimeter reader consists of a small vacuum tube with a coated cylinder that can be heated by a built-in filament when the tube is plugged into a voltage supply. A photomultiplier reads the peak of the glow curve and gives values of the accumulated energy absorbed (i.e., the dose). The device is linear in its response over a very wide range of exposures; it can be used repeatedly with little change in behavior.

EXAMPLE 12.6

The first element of the TLD shown in Fig. 12.6B uses a thin plastic window that filters radiation by $14\,\text{mg/cm}^2$ to record skin dose. Using the Katz-Penfold formula of Eq. (5.2), that is,

$$0.014\,\text{g/cm}^2 = 0.412\,E^{1.265-0.0954\,\ln(E)}$$

and employing a numerical solution technique reveals that beta particles below 84 keV are stopped from reaching the TLD material.

12.6 SOLID STATE DETECTORS

The use of a solid rather than a gas in a detector has the advantage of compactness because of the short range of charged particles. Furthermore, when the solid is a semiconductor, great accuracy in measurement of energy and arrival time is possible. The mechanism of ion motion in a solid detector is unique. Visualize a crystal semiconductor, such as silicon or germanium, as a regular array of fixed atoms with their complement of electrons. An incident charged particle can dislodge an electron and cause it to leave the vicinity, which leaves a vacancy or *hole* that acts effectively as a positive charge. The electron-hole pair produced is analogous to negative and positive ions in a gas. Electrons can migrate through the material or be carried along by an electric field, while the holes move more slowly as electrons are successively exchanged with neighboring atoms. Thus, electrons and holes are negative and positive charge carriers, respectively.

The electrical conductivity of a semiconductor is very sensitive to the presence of certain impurities. Consider silicon, chemical valence 4 (with four electrons in the outer shell); see Fig. 2.1. Introduction of a small amount of valence 5 material such as phosphorus or arsenic gives an excess of negative carriers, and the new material is called *n*-type silicon. If instead a valence 3 material such as boron or gallium is added, there is an excess of positive carriers, and the substance is called *p*-type silicon. When two layers of *n*-type and *p*-type materials are put in contact and a voltage is applied, as in Fig. 12.8, electrons are drawn one way and holes the other, leaving a neutral or depleted region. Most of the voltage drop occurs over that zone, which is very sensitive to radiation. An incident particle creates electron-hole pairs that are swept out by the internal electric field to register as a current pulse. High accuracy in measurement by an *n*-*p* junction comes from the fact that a low energy (W) is needed to create an electron-hole pair. For Si and Ge at 77 K, W is only 3.86 and 2.97 eV, respectively, per pair versus 34 eV for an ion pair in a gas (Srdoč et al., 1995). Thus, a 100 keV photon creates a very large number of pairs, giving high statistical accuracy. The collection time is very short, approximately a billionth of a second, allowing precise time measurements.

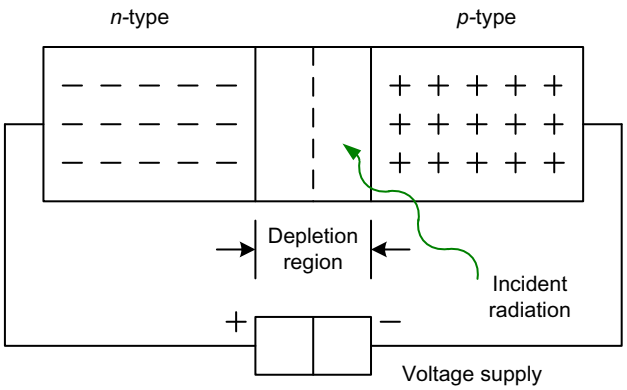

FIG. 12.8

Solid-state *n*-*p* junction detector.

Statistical fluctuations in the detector system are manifest as variations in the particle energy recorded. A metric of solid state and scintillation detectors employed for spectroscopy is their *energy resolution* defined as

$$E_R = \Delta E/E \tag{12.7}$$

where ΔE is the full width at half maximum (FWHM) of the energy peak at E. Smaller resolution manifests as thinner spectral lines (see Fig. 13.4), thereby permitting more accurate radionuclide identification.

EXAMPLE 12.7

A germanium detector has an energy resolution of 0.2% at 1 MeV. A peak at that energy would have a FWHM of $\Delta E = (0.2\%/100\%)(1000\,\text{keV}) = 2\,\text{keV}$.

One way to produce a semiconductor detector with a large active volume is to introduce lithium on one surface of a heated crystal and apply an electric field. This drifts the Li through the volume that compensates residual *p*-type impurities. This detector must be kept permanently at liquid nitrogen temperature (77 K) to prevent redistribution of the lithium; examples include Si(Li) and Ge(Li) detectors for X-ray and gamma-ray measurements, respectively. A preferable detector for many applications is made of an ultrahigh-purity (intrinsic) germanium (HPGe), with impurity atoms reduced to 1 in approximately 10^{12}. A simple diode arrangement gives depletion depths of several centimeters. Such HPGe detectors still require liquid N_2 for operation, but they can be stored at room temperature. In contrast, cadmium telluride (CdTe) and cadmium zinc telluride (CZT) detectors can be operated at room temperature, but their energy resolution is poorer than Ge detectors.

12.7 STATISTICS OF COUNTING

The measurement of radiation has some degree of uncertainty because the basic processes, such as radioactive decay, are random in nature. From the radioactive decay law, Section 3.3, we can say that *on average* in a time interval t a given atom in a large collection of atoms has a chance $\exp(-\lambda t)$ of not decaying, and thus it has a probability $p = 1 - \exp(-\lambda t)$ of decaying. Because of the statistical nature of radioactivity, however, more or less than these numbers will actually be observed in a certain time interval. There is actually a small probability that either none or all would decay. In a series of identical measurements, there will be a spread in the number of counts. Statistical methods may be applied to the data to estimate the degree of uncertainty or error. The laws of probability may be applied. As discussed in texts on statistics and radiation detection (see Knoll, 2010; Tsoulfanidis and Landsberger, 2015), the most rigorous expression is the binomial distribution (see Exercise 12.6), which must be used to interpret the decay of isotopes of very short half-life. In the radioactive decay of a population of n atoms (representing the number of trials), the mean number of decays during period t is $\bar{x} = pn$.

A simple approximation to the binomial is the Poisson distribution (see Exercise 12.7), required for the study of low-level environmental radioactivity in which the probability of decay is small

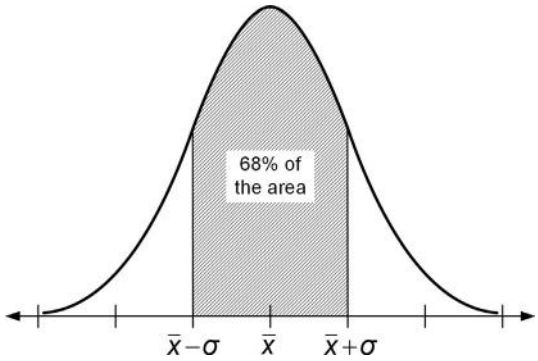

FIG. 12.9

Gaussian distribution. The area between the limits $\bar{x} \pm \sigma$ is 68% of the total.

($p \ll 1$). A further approximation when the number of successes becomes large ($\bar{x} \gtrsim 20$) is the widely used normal or Gaussian distribution, shown in Fig. 12.9. Measured values of the number of counts x in repeated trials tend to fit the formula,

$$P(x) = \left(1/\sqrt{2\pi\sigma^2}\right) \exp\left[-(x-\bar{x})^2/(2\sigma^2)\right] \tag{12.8}$$

where $P(x)$ is the probability of being in a unit range at x, and $\bar{x}$ is the mean value of the counts. A measure of the width of the curve is the standard deviation, σ. The area under the curve between $\bar{x} - \sigma$ and $\bar{x} + \sigma$ is 68% of the total, which indicates that the chance is 0.68 that a given measurement will lie in that range. The figure for 95% is $\pm 2\sigma$, and for 99.7% is $\pm 3\sigma$.

For the Poisson distribution $\sigma = \sqrt{\bar{x}}$, therefore the radiation counting result for a sample is $\bar{x}_S \pm \sqrt{\bar{x}_S}$ (counts). As the sample is counted for a specified period (T), the corresponding count rate is

$$R_S = \frac{\bar{x}_S}{T} \pm \frac{\sqrt{\bar{x}_S}}{T} \tag{12.9}$$

The results are reported in units of inverse time, for example, counts per minute (cpm). It can be shown (Exercise 12.14) that the fractional error in count rate is inversely proportional to the square root of the total number of counts. When the ambient radiation level is not negligible, a background count ($\bar{x}_B$) is performed and subtracted from the gross sample count to yield the net sample count rate of

$$R_N = \frac{\bar{x}_S - \bar{x}_B}{T} \pm \frac{\sqrt{\bar{x}_S + \bar{x}_B}}{T} \tag{12.10}$$

In low-level radiation counting, the statistical distributions lead to situations in which confidence levels must be stated as to whether radioactivity qualitatively exists in a sample, and if so, whether the radiation can be quantitatively measured. Detection thresholds based on the background radiation level are established considering the distributions of both the sample and background counts. For instance, the lower limit of detection using the approach of Pasternack and Harley (1971) for a 5% confidence for

both a false positive (false alarm) and a false negative (missed alarm) indication of the presence of sample radioactivity is

$$\text{LLD} \cong 4.66\sqrt{\bar{x}_B} \tag{12.11}$$

Background count rates are reduced in laboratory settings through the use of shielding.

The program STAT, used in Computer Exercises 12.A–12.D, is provided to calculate binomial, Poisson, and Gaussian statistics. Also, program EXPOIS generates simulated counting data for study by use of the Poisson distribution.

EXAMPLE 12.8

A detector with a 32% efficiency is used to count a radioactive sample for 200 min, yielding 3050 counts. Immediately thereafter, a 2000-count background measurement is recorded for the same duration. The net sample count rate is

$$\begin{aligned} R_N &= \left[(\bar{x}_S - \bar{x}_B) \pm \sqrt{\bar{x}_S + \bar{x}_B}\right]/T \\ &= \left[(3050 - 2000) \pm \sqrt{3050 + 2000}\right] \text{counts}/(200\,\text{min}) \\ &= 5.25 \pm 0.36\,\text{cpm} \end{aligned}$$

The efficiency provides the means to calculate the sample activity

$$A = R_N/\varepsilon = (5.25 \pm 0.36\,\text{cpm})(1\,\text{min}/60\,\text{s})/(0.32\ \text{count/decay}) = 0.27 \pm 0.02\,\text{Bq}$$

The lower limit of detection in terms of activity is

$$\text{LLD} \cong \frac{4.66\sqrt{\bar{x}_B}}{\varepsilon T} = \frac{(4.66\sqrt{2000}\,\text{counts})(1\,\text{min}/60\,\text{s})}{(0.32\,\text{count/decay})(200\,\text{min})} = 0.05\,\text{Bq}$$

As the recorded activity is noticeably greater than the LLD, the sample is radioactive.

12.8 PULSE HEIGHT ANALYSIS

The determination of the energy distribution or spectrum of nuclear particles and rays is important for identifying radioactive species. If an incoming particle deposits all its energy in the detector, the resulting voltage signal in the external electric circuit of Fig. 12.10A can be used as a measure of particle energy. The particle ionizes the medium, a charge Q is produced, and a current flows, giving a time-varying voltage. If the time constant $\tau = RC$ of the circuit is short compared with the collection time, the voltage rises, plateaus briefly, and then drops quickly to zero, as in Fig. 12.10B. If τ is large, however, the voltage rises to a peak value $V_m = Q/C$, where C is the capacitance, and then because of the circuit characteristics declines slowly, as in Fig. 12.10C. The particle energy, proportional to charge, is thus obtained by a voltage measurement.

Suppose that there are two types of particles entering the detector, for instance alpha particles of 4 MeV and beta particles of 1 MeV. By application of a voltage bias, the pulses caused by beta particles can be eliminated, and the remaining counts represent the number of alpha particles. The circuit that performs that separation is called a *discriminator*.

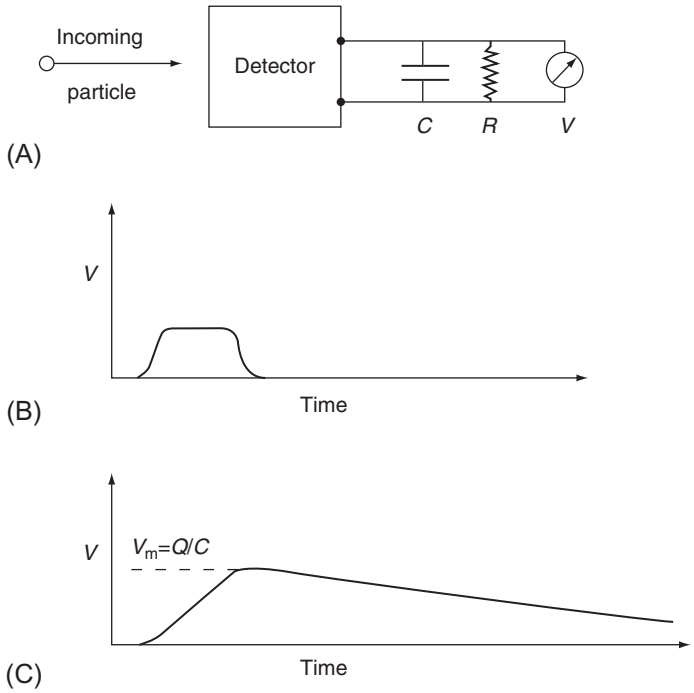

FIG. 12.10

Effect of circuit on pulse. (A) Detector and electronic circuit, (B) voltage variation with short time constant, and (C) voltage variation with long time constant.

Based on Knoll, G.F., 2010. Radiation Detection and Measurement, fourth ed. Wiley. (A very comprehensive, modern, and readable text that should be in every nuclear engineer's library).

EXAMPLE 12.9

The aforementioned alpha and beta particles will liberate a charge of $Q=E_K/W$ where W is the energy required to create each ion pair. In air the charge deposition by each is

$$Q_\alpha = \left[\left(4\times10^6\,\text{eV}\right)/\left(34\,\text{eV/ip}\right)\right]\left(1.6\times10^{-19}\,\text{C/ip}\right) = 1.9\times10^{-14}\,\text{C}$$

$$Q_\beta = \left[\left(1\times10^6\,\text{eV}\right)/\left(34\,\text{eV/ip}\right)\right]\left(1.6\times10^{-19}\,\text{C/ip}\right) = 0.5\times10^{-14}\,\text{C}$$

Because the capacitance of the detector is independent of the entering particle, the voltage output ($V=Q/C$) from these alpha particles is four times larger than that produced by the betas.

The radiation from a given source will have some variation in particle energy, and thus a series of pulses caused by successive particles will have a variety of heights. To find the energy distribution, a *single-channel analyzer* can be used. This consists of two adjustable discriminators and a circuit that

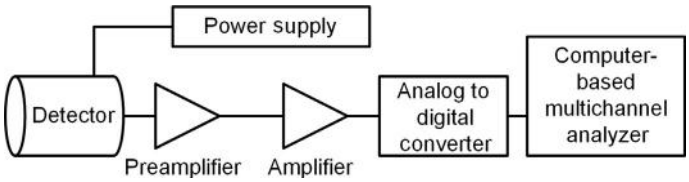

FIG. 12.11

Block diagram for spectroscopy equipment setup.

passes pulses within a range of energy. The *multichannel analyzer* (MCA) is a much more efficient and accurate device for evaluating an entire energy spectrum in a short time. Successive pulses are manipulated electronically and the signals are stored in computer memory according to energy. The radiation energy distribution is graphically displayed by a computer that also typically includes automatic spectra processing software for radionuclide identification and quantification. Fig. 12.11 depicts the equipment connections for spectroscopy.

EXAMPLE 12.10

A 4096-channel gamma spectroscopy system has an energy resolution of 50 keV. If the range of the MCA is 0–3 MeV, each channel spans (3000 keV)/(4096 channels) = 0.73 keV.

12.9 ADVANCED DETECTORS

A number of specialized instruments have been developed in addition to basic detectors. They are used for precise measurements of the products of high-energy nuclear collisions. Examples are:

(a) Nuclear emulsion track detectors, originally used for cosmic ray studies. By application of the energy loss formula (see Section 5.3), information is obtained on particle energy, mass, and charge. Special etching techniques are used and the counting of tracks with a microscope is automated.
(b) Cherenkov counters, which measure the light produced when a particle has a speed higher than that of light in the medium. Cherenkov radiation gives the blue glow seen near a pool reactor core (see Exercise 12.17).
(c) Hadron calorimeters, which measure showers of hadrons—baryons (such as protons and neutrons) and mesons—produced by bombardment of materials of particles in the GeV range.
(d) Neutrino detectors, consisting of large volumes of liquid or metal in which the rare collisions resulting in a scintillation occur.

These specialized devices are discussed in the book by Kleinknecht (1998).

12.10 DETECTORS AND COUNTERTERRORISM

Radiation detectors play a vital role in protecting against terrorist action. Of greatest importance is the screening of shipments at their point of origin and on their arrival at a domestic port. X-rays are helpful in finding well-shielded items in large shipping containers, prompting further inspection. Portable X-ray generators powered with batteries are available, giving 150-keV rays that can penetrate half an inch of steel.

To check for the presence of fissionable materials—enriched uranium or plutonium—several techniques are available. One involves an intense beam of 14 MeV neutrons from a D-T generator (see Chapter 7). Pulses of very short duration are introduced to cause fission and neutron release. Silicon carbide (SiC) semiconductor detectors measure the fission neutrons very quickly. Devices used in research are considered suitable for commercial production.

An alternative method to detect fissionable materials uses a pulsed photonuclear neutron detector. It consists of a portable accelerator that produces energetic photons. These cause fission, which releases neutrons that are detected externally. In tests, a sample vial shielded by wood, polyethylene, and lead was quickly and readily identified. Distinctions between enrichments of uranium or fissionable elements were achieved by use of different photon energies.

According to the International Atomic Energy Agency (International Atomic Energy Agency (IAEA), 2002), quantities of weapons material that are significant are 25 kg for high enriched uranium and 8 kg for plutonium. The half-lives of U-235 and U-238 are too long for their inherent radiation to be detected. For the radiological dispersal device, the so-called dirty bomb, there is direct detection of their radiation. Isotopes that are likely to be used are cobalt-60, half-life 5.27 y, average 1.25 MeV gammas, and cesium-137, half-life 30.1 y, 0.662 MeV gammas. Other candidate radioisotopes are americium-241, californium-252, iridium-192, and strontium-90. Californium is a neutron emitter with half-life of 2.65 y. In the case of Sr-90, the beta particles are readily shielded, but the *bremsstrahlung* emitted as the electrons decelerate in matter can be detected. All these isotopes have commercial applications, which makes them vulnerable to theft.

Nuclear forensics involves a signature method, the determination of the origin of radioactivity whether it is from a dirty bomb or from the explosion of a nuclear assembly. Search algorithms are developed that correlate the time dependence of isotope decay with reactor type and neutron irradiation history.

Research continues on the problem of finding the radiation dosage to individuals in emergencies. Plans are being developed for the handling of a large number of people who are irradiated or contaminated.

Tracer studies in Manhattan are used to develop models for the dispersal of radioactivity in a city with streets between skyscrapers (Kiess, 2006).

In methods that use or produce neutrons, consideration must be given to the *neutron ship effect*. When muons in cosmic rays bombard iron, as in bridges or ships, there is a release of neutrons, which constitutes a competing background.

Much of the R&D on detectors is sponsored and supported by the Department of Homeland Security (DHS), formed in the wake of the terrorist attacks of September 11, 2001. The Domestic Nuclear Detection Office of DHS has the goal of improving the nation's capability to thwart attempts to use nuclear or radiological materials against the United States. The principal emphasis is on detection that

reduces vulnerability. The agency has a mammoth task in providing radiation detection equipment at the 1205 seaports and airports. The US Government Accountability Office (GAO) has reported gaps and vulnerabilities (U.S. Government Accountability Office (GAO), 2009).

12.11 SUMMARY

The detection of radiation and the measurement of its properties are required in all aspects of the nuclear field. In gas counters, the ionization produced by incoming radiation is collected. Depending on the voltage between electrodes, counters detect all particles or distinguish between types of particles. Neutrons are detected indirectly by the products of nuclear reactions—for slow neutrons by absorption in boron or uranium-235, for fast neutrons by scattering in hydrogen. Scintillation counters release measurable light on bombardment by charged particles or gamma rays. Solid-state detectors generate a signal from the motion of electron-hole pairs created by ionizing radiation. Pulse-height analysis yields energy distributions of particles. Statistical methods are used to estimate the uncertainty in measured counting rates. Advanced specialized detectors are used in high-energy physics research. Detectors of nuclear radiation play a crucial role in counterterrorism programs.

12.12 EXERCISES

12.1 Find the required number density of molecules of BF_3 in a detector of 2.54-cm diameter to ensure that 90% of the thermal neutrons incident along a diameter are caught (σ_a for natural boron is 760 barns). (b) How does this compare with the number density for the gas at atmospheric pressure, with density 3.0×10^{-3} g/cm^3? (c) Suggest ways to achieve the high efficiency desired.

12.2 An incident particle ionizes helium to produce an electron and a He^{2+} ion halfway between two parallel plates with potential difference between them. If the gas pressure is very low, estimate the ratio of the times elapsed until the charges are collected. Discuss the effect of collisions on the collection time.

12.3 We collect a sample of gas suspected of containing a small amount of radioiodine, half-life 8 d. If we observe in a period of 1 d a total count of 50,000 in a counter that detects all radiation emitted, how many atoms were initially present?

12.4 In a gas counter, the potential difference at any point r between a central wire of radius r_1 and a concentric wall of radius r_2 is given by

$$V = V_0 \frac{\ln(r/r_1)}{\ln(r_2/r_1)} \tag{12.12}$$

where V_0 is the voltage across the tube. If $r_1 = 1$ mm and $r_2 = 1$ cm, what fraction of the potential difference exists within 1 mm of the wire?

12.5 How many electrodes would be required in a photomultiplier tube to achieve a multiplication of 1 million if one electron releases four electrons at each electrode?

12.6 The probability of x successful events in n trials, each of which has a chance p, is given by the binomial distribution formula,

$$P(x) = n!p^x\,(1-p)^{n-x}/[(n-x)!x!] \tag{12.13}$$

(a) Apply to flipping a coin one, two, and three times, finding the number of times the result is heads, including zero. Check by simple logic. (b) Apply to throwing a single die one or two times, finding the number of sixes. Check. (c) Repeat the preceding calculations with program STAT (see Computer Exercise 12.A).

12.7 For a situation in which the chance of success p is much smaller than 1, the probability of x successes in n trials in the binomial formula of Exercise 12.6 is well approximated by the Poisson formula

$$P(x) \cong (\bar{x}^x/x!)\exp(-\bar{x}) \tag{12.14}$$

where $\bar{x} = pn$ is the mean value of x. What is the value of p in throwing a single die? Find $\bar{x}$ for one or two throws of a die and calculate $P(x)$ for each case.

12.8 Counts are taken for a minute from a microcurie source of Cs-137, half-life 30.1 y. (a) Assuming one count for each 50 decays, find the expected counting rate and the number of counts for the interval. (b) Find the standard deviation in the counting rate. (c) Find the probability of decay of a given atom of cesium in the 1-min interval.

12.9 A pair of dice is thrown $n = 10$ times. (a) Verify that the chance on one throw of getting a seven is $p = 1/6$. (b) By use of the binomial distribution, find out the chance of getting a seven exactly $x = 2$ times out of the 10. (c) Repeat with the Poisson distribution.

12.10 The cross-section for absorption for low-energy neutrons of nuclides such as B-10 varies as $1/v$, as discussed in Section 4.6. Formally, we may write $\sigma_a = \sigma_{a0}v_0/v$ where σ_{a0} is the cross-section at $v_0 = 2200$ m/s. A boron neutron detector is placed in a neutron speed distribution $n(v)$, with n_0 as the total number of neutrons per cm^3 and N as the number of boron nuclei per cm^3. Form the total reaction rate per cm^3 by integrating over the distribution, as a generalization of Eq. (12.5). Discuss the result in terms of what is being measured by the detector.

12.11 Determine the new intrinsic efficiency for photons if the CsI crystal of Example 12.4 is replaced with (a) an HPGe detector and (b) an air gas-based detector. For Ge at 0.1 MeV, μ is 2.95/cm.

12.12 (a) Repeat the calculation of Example 12.1 at a distance of 1 m. (b) Also determine the photon dose rate experienced by the health physicist at this distance.

12.13 Compute the Q value for the following neutron detecting reactions: (a) ^{10}B(n, α)^{7}Li and (b) ^{3}He(n, p)^{3}H. What type of reactions are these according to the Q value?

12.14 Using Eq. (12.9), prove that the fractional error in count rate is inversely proportional to the square root of the total number of counts.

12.15 (a) Determine the energy resolution of a NaI detector having a FWHM of 80 keV at the gamma emission energy of Cs-137. (b) What is the resolution of an HPGe detector with a FWHM of 1 keV at that energy?

12.16 What electron energies are prevented from reaching the second and third elements of the TLD in Fig. 12.6B, which are shielded by 160 mg/cm^2 of plastic?

12.17 Charged particles traveling at $0.75c$ within water are capable of producing Cherenkov radiation. Determine the minimum electron energy needed to produce the bluish glow in a pool type reactor.

12.18 (a) Verify the ^{10}B(n, α) reaction energy of 2.8 MeV. (b) Using methods developed in Chapter 4, determine the energy distribution to each reaction product, if the incident neutron has negligible energy.

12.19 (a) Estimate the dose rate which should be measured by a radiation detector that is 1 m below a 1-μCi Am-241 source in a smoke detector. (b) How often would the Am-241 source need to be replaced in a smoke alarm?

12.13 COMPUTER EXERCISES

12.A Program STAT calculates the probability distribution $P(x)$ with a choice of the binomial, Poisson, or Gaussian formulas. (a) What is the value of p for throwing a six with a single die? (b) Run the program with $n = 1$, 2, 5, and 10 trials, and note the probabilities of finding 0, 1, 2, …, n sixes for each run. (c) Assuming that binomial is exact, comment on the apparent accuracy of the other two methods.

12.B An alpha particle detector for surface contamination is counted for thirty 1-minute intervals, with a total of 225 counts. (a) What is the value of p? (b) With the binomial and Poisson distributions in the computer program STAT, calculate $P(x)$ for $x = 0$, 1, 2, …, 30. (c) How accurate is the Poisson formula?

12.C (a) What is the chance that any given person's birthday is today? (b) If we select 1000 people at random, with the Poisson distribution in program STAT, what is the probability that none has a birthday today? (c) Calculate $P(x)$ for $x = 0$–10 and plot a bar graph of the results. What is the most likely number that has a birthday today and what is the mean value? (d) Run STAT in binomial mode for 23 people at a party and show that the chance of two people having the same birthday is about one-half.

12.D Computer program EXPOIS simulates particle-counting data that can be analyzed by Poisson statistics. (a) Run the program for 10–30 one-minute counting periods. (b) Compare the results graphically with Poisson data produced by the program STAT (Computer Exercise 12.A).

12.E To gain an appreciation for the challenges in discriminating low-level radioactivity from background, use the COMPDIST program to superimpose the two Gaussian distributions for the gross sample count and a background count. Specifically, compare three gross sample measurements of (a) 200, (b) 150, and (c) 120 counts each. In all cases, assume an average background count of 100.

REFERENCES

International Atomic Energy Agency (IAEA), 2002. IAEA Safeguards Glossary. International Nuclear Verification Series No. 3, p. 23.

Kiess, T.E., 2006. Results and characteristics of the homeland security office of research and development radiological and nuclear countermeasures program. Trans. Am. Nucl. Soc. 95, 9.

Kleinknecht, K., 1998. Detectors for Particle Radiation, second ed. Cambridge University Press, Cambridge.

Knoll, G.F., 2010. Radiation Detection and Measurement, fourth ed. Wiley, Hoboken A very comprehensive, modern, and readable text that should be in every nuclear engineer's library.

Pasternack, B.S., Harley, N.H., 1971. Detection limits for radionuclides in the analysis of multi-component gamma ray spectrometer data. Nucl. Instr. Meth. 91 (3), 533–540.

Price, W.J., 1964. Nuclear Radiation Detection, second ed. McGraw-Hill, New York.

Srdoč, D., Inokuti, M., Krajcar-Bronić, I., 1995. Yields of ionization and excitation in irradiated matter. In: Atomic and Molecular Data for Radiotherapy and Radiation Research. IAEA-TECDOC-799.

Tsoulfanidis, N., Landsberger, S., 2015. Measurement and Detection of Radiation, fourth ed. CRC Press, Boca Raton.

U.S. Government Accountability Office (GAO), 2009. Nuclear Detection. GAO-09-257.

FURTHER READING

Bevington, P.R., Robinson, D.K., 1992. Data Reduction and Error Analysis for the Physical Sciences, second ed. McGraw-Hill, New York.

Chadwick, M.B., Herman, M., Obložinský, P., Dunn, M.E., Danon, Y., Kahler, A.C., et al., 2011. ENDF/B-VII. 1 Nuclear data for science and technology: cross-sections, covariances, fission product yields and decay data. Nucl. Data Sheets 112 (12), 2887–2996.

Eichholz, G.G., Poston, J.W., 1979. Principles of Nuclear Radiation Detection. Ann Arbor Science, Ann Arbor, MI.

Evans, R.D., 1982. The Atomic Nucleus. Krieger, New York. Excellent treatment of statistical distributions; reprint of the McGraw-Hill 1955 classic advanced book.

Fleischer, R.L., 1998. Tracks to Innovation: Nuclear Tracks in Science and Technology. Springer-Verlag, New York.

Frame, P.W., 2005. A history of radiation detection instrumentation. Health Phys. 88 (6), 613–637.

Ku, H.H. (Ed.), 1969. Precision Measurement and Calibration—Statistical Concepts and Procedures. vol. 1. National Bureau of Standards Publication 300, Washington, DC.

L'Annunziata, M.F. (Ed.), 2012. Handbook of Radioactivity Analysis. third ed. Academic Press, San Diego, CA.

Moody, K.J., Hutcheon, I.D., Grant, P.M., 2005. Nuclear Forensic Analysis. Taylor & Francis, Boca Raton, FL.

Wackerly, D.D., Mendenhall III, W., Schaeffer, R.L., 2001. Mathematical Statistics with Applications, sixth ed. Cengage Learning, Stanford.

CHAPTER

INFORMATION FROM ISOTOPES 13

CHAPTER OUTLINE

The applications of nuclear processes can be divided into three basic classes: military, power, and radiation. In a conference shortly after the end of World War II, the famous physicist Enrico Fermi discussed potential applications of radioisotopes (Fermi, 1946). He then said, "It would not be very surprising if the stimulus that these new techniques will give to science were to have an outcome more spectacular than an economic and convenient energy source or the fearful destructiveness of the atomic bomb."

Perhaps Fermi would be surprised to see the extent to which radioisotopes have become a part of research, medicine, and industry, as described in the following sections.

Many important economic and social benefits are derived from the use of isotopes and radiation. The discoveries of modern nuclear physics have led to new ways to observe and measure physical, chemical, and biological processes, providing strengthened understanding for human survival and progress. The ability to isolate and identify isotopes gives additional versatility, supplementing techniques involving electrical, optical, and mechanical devices.

Radioisotopes have become even more prominent in the wake of terrorist threats and acts such as the September 11, 2001 attack on the World Trade Center in New York. Detection of potential hazards has become a high priority of the US Department of Homeland Security.

Nuclear Energy. https://doi.org/10.1016/B978-0-12-812881-7.00013-7

Special isotopes of an element are distinguishable and thus traceable by virtue of their unique mass or their radioactivity while essentially behaving chemically as do the other isotopes of the element. Thus, it is possible to measure amounts of the element or its compounds and trace movement and reactions.

When one considers the thousands of stable and radioactive isotopes available and the many fields of science and technology that require knowledge of process details, it is clear that a catalog of possible isotope uses would be voluminous. Here we will only be able to compare the merits of stable and radioactive species, to describe some of the special techniques, and to mention a few interesting or important applications of isotopes.

13.1 STABLE AND RADIOACTIVE ISOTOPES

Stable isotopes, as their name suggests, do not undergo radioactive decay. Most of the isotopes found in nature are in this category and appear in the element as a mixture. The principal methods of separation, according to isotopic mass, that have been used are electromagnetic (as in the large-scale mass spectrograph) and thermal-mechanical (as in the distillation or gaseous centrifuge processes); see Chapter 15. Important examples are isotopes of elements involved in biological processes (e.g., deuterium and oxygen-18). The main advantages of stable isotopes are the absence of radiation effects in the specimens under study, the availability of an isotope of a chemical for which a radioactive species would not be suitable, and freedom from necessity for speed in making measurements because the isotope does not decay in time. Their disadvantage is the difficulty of detection.

Radioactive isotopes, or *radioisotopes*, are available with a great variety of half-lives, types of radiation, and energy. They come from three main sources: charged particle reactions in an accelerator, neutron bombardment in a reactor, and separated fission products. Among the principal sources of stable and longer-lived isotopes are the US Department of Energy (DOE), MDS Nordion of Canada, and Russia. A number of cyclotrons that generate radioisotopes are located at hospitals. The main advantages of the use of radioisotopes are ease of detection of their presence through the emanations and the uniqueness of identifying the half-lives and radiation properties. Potential shortage is a perennial problem for users of radioisotopes. The number of reactor sources is limited and some are being shut down. In an American Nuclear Society position statement (American Nuclear Society (ANS), 2004), a strong recommendation is made, stating, "There is no present US policy for the purpose of maintaining reliable sources of radioisotope supplies crucial for both medical and industrial applications."

13.2 TRACER TECHNIQUES

We will now describe several special methods involving radioisotopes and illustrate their use. The tracer method consists of the introduction of a small amount of an isotope and the observation of its progress as time goes on. For instance, the best way to apply fertilizer containing phosphorus to a plant may be found by including minute amounts of the radioisotope phosphorus-32, half-life 14.28 d, emitting 1.7 MeV beta particles. Measurements of the radiation at various times and locations in the plant by a detector or photographic film provide accurate information on the rate of phosphorus intake and deposition. Similarly, circulation of blood in the human body can be traced by the injection of a harmless solution of radioactive sodium, Na-24, half-life 14.96 h. For purposes of medical diagnosis, it is desirable to administer enough radioactive material to provide the needed data, but not so much that the patient is harmed.

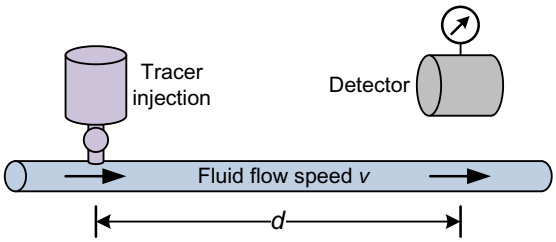

FIG. 13.1

Tracer measurement of flow rate.

The flow rate of many materials can be found by observing the passage of admixed radioisotopes. The concept is the same for flows as diverse as blood in the body, oil in a pipeline, or pollution discharged into a river. As shown in Fig. 13.1, a small amount of radioactive material is injected at a point, the stream carries it along, and its passage at a distance d away at time t is noted. In the simplest situation, the average fluid speed is

$$v = d/t \tag{13.1}$$

It is clear that the half-life of the tracer must be long enough for detectable amounts to be present at the point of observation but not so long that the fluid remains contaminated by radioactive material.

EXAMPLE 13.1

To verify the flow rate of sewage sludge, a radioisotope with a 20-min half-life is to be added to the sludge entering a pipe. The sewage travels 0.5 km and is believed to move at between 0.1 and 0.5 m/s. The detector at the pipe outlet has an efficiency of 5% and requires a minimum count rate of 60 cpm to discriminate from background radiation. Our goal is to determine the minimum amount of radioactivity to carry out this measurement. To ensure that the experiment need be performed only once, we must solve using the minimum speed, such that the expected delay time is maximized at

$$t = d/v = (500\text{m})/(0.1\text{m/s}) = 5000\text{s} = 83.3\text{ min}$$

To be detectable, the activity reaching the outlet detector needs to be at least

$$A(t) = R/\varepsilon = (1\text{count/s})/(0.05\text{count/decay}) = 20\text{Bq}$$

The activity introduced into the sludge must be at least

$$A(0) = A(t)\Big/\left(\frac{1}{2}\right)^{t/t_H} = (20\text{Bq})/(0.5)^{(83.3\,\text{min})/(20\,\text{min})} = 359\text{Bq}$$

Realistically, the activity will need to be larger due to sewage mixing and nonuniform flow rates.

In many tracer measurements for biological or engineering purposes, the effect of removing the isotope by other means besides radioactive decay must be considered. Suppose, as in Fig. 13.2, that liquid flows in and out of a tank of volume V (cm^3) at a rate G (cm^3/s). A tracer of initial amount N_0 atoms is injected and assumed to be uniformly mixed with the contents. Each second, the fraction of fluid (and isotope) removed from the tank is G/V, which serves as a flow decay constant λ_F for the isotope. If radioactive decay were small, the counting rate from a detector would decrease with time as $\exp(-\lambda_F t)$. From this trend, one can deduce either the speed of flow or volume of fluid, if the other quantity is known. If both radioactive decay (λ) and flow decay (λ_F) occur, the exponential formula

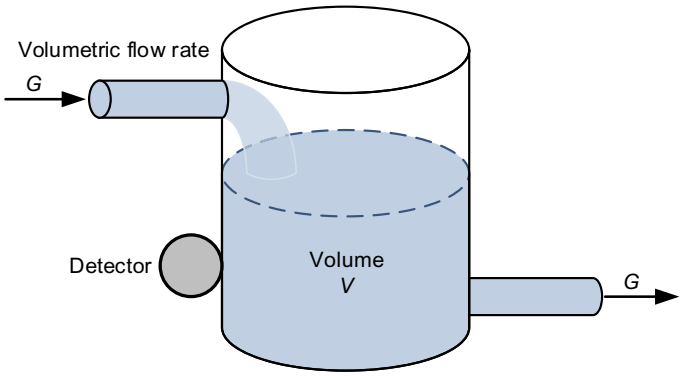

FIG. 13.2

Flow decay.

may also be used, but with the effective decay constant $\lambda_E = \lambda + \lambda_F$. The composite effective half-life then can be found from the relationship

$$1/t_E = 1/t_H + 1/t_F \tag{13.2}$$

This formula is seen to be of the same form as Eq. (10.3) developed in Section 10.1 for radioactive materials in the body. Here, the flow half-life takes the place of the biological half-life.

Soon after Watson and Crick (1953) explained the structure of DNA, tracers P-32 and S-35 were used to prove that genes were associated with DNA molecules. Tritium-labeled thymidine, involved in the cell cycle, was synthesized. The field of molecular biology has expanded greatly since then, leading to the Human Genome Project, an international effort to map the complete genetic structure of human beings, involving chromosomes, DNA, genes, and protein molecules. Its purpose was to find which genes cause various diseases and to enable gene therapy to be applied. Part of the complex process of mapping is hybridization, in which a radioactive or fluorescent label marks a particular point on the DNA molecule.

An outgrowth of genetic research is DNA fingerprinting, a method of identifying individual persons, each of which (except for rare chimera) has a unique DNA structure as even the DNA of identical twins can diverge with age. In one of the techniques (restriction fragment length polymorphism or RFLP), the procedure involves treating samples of blood, skin, or hair with an enzyme that splits DNA into fragments. The membrane containing them is exposed to a radioactive probe and dark bands appear on an X-ray film. The method is accurate but requires a large sample and a long exposure of film. An alternate method (polymerase chain reaction-short tandem repeat or PCR-STR) is more popular, and involves making multiple copies of DNA. The processes are used in crime investigation and court cases to help establish guilt or innocence and to give evidence in paternity disputes.

13.3 RADIOPHARMACEUTICALS

Radionuclides prepared for medical diagnosis and therapy are called *radiopharmaceuticals*. They include a great variety of chemical species and isotopes with half-lives ranging from minutes to weeks,

Table 13.1 Radiopharmaceuticals Used in Medical Diagnosis

Radionuclide	Compound	Use
Technetium-99m	Sodium pertechnetate	Brain scanning
Hydrogen-3	Tritiated water	Body water
Iodine-131	Sodium iodide	Thyroid scanning
Gold-198	Colloidal gold	Liver scanning
Chromium-51	Serum albumin	Gastrointestinal
Mercury-203	Chlormerodrin	Kidney scanning
Selenium-75	Selenomethionine	Pancreas scanning
Strontium-85	Strontium nitrate	Bone scanning

depending on the application. They are generally beta or gamma-ray emitters. Prominent examples are technetium-99m (6.01 h), iodine-131 (8.04 d), and phosphorus-32 (14.28 d). Table 13.1 illustrates the variety of radionuclides used, their chemical forms, and the organs studied.

A radionuclide generator is a long-lived isotope that decays into a short-lived nuclide used for diagnosis. The advantage over the use of the short-lived isotope directly is that speed or reliability of shipment is not a factor. As needed, the daughter isotope is extracted from the parent isotope. The earliest example of such a generator was radium-226 (1600 y), decaying into radon-222 (3.82 d). The most widely used generator is molybdenum-99 (65.98 h) decaying to technetium-99m (6.01 h). The Tc-99m is said to be "milked" from the Mo-99 "cow." Tc-99m is the most widely used radioisotope in nuclear medicine because of its favorable radiations and half-life. The parent isotope Mo-99 originates predominately from research reactors located internationally (National Academy of Sciences (NAS), 2016). If for any reason the US borders were closed to imports of radioactive materials, innumerable medical tests would cease.

Several iodine isotopes are used. One produced by a cyclotron is I-123 (13.2 h). The accompanying isotopes I-124 (4.18 d) and I-126 (13.0 d) are undesirable impurities because of their excessively energetic gamma rays. Two fission products are I-125 (59.4 d) and I-131 (8.04 d). The beta emissions from I-131 are used in the treatment of hyperthyroidism.

Specialists in radiopharmaceuticals are called radiopharmacists. They are concerned with the purity, suitability, toxicity, and radiative characteristics of the radioactive drugs they prepare.

EXAMPLE 13.2

From the data forming Fig. 6.5, there is a 6.1% yield (y) of Mo-99 from U-235 fission. The number of fissions to produce 1 μg of ^{99}Mo is

$$n_f = \frac{m_{99} N_A}{y M_{99}} = \frac{(10^{-6}\,\text{g})(6.02 \times 10^{23}\,\text{atom/mol})}{(0.061\,\text{atom/fission})(99\,\text{g/mol})} = 1.0 \times 10^{17}\,\text{fissions}$$

The ^{235}U mass required when considering material loss by neutron capture also is

$$m_{235} = \frac{n_f M_{235}}{N_A} \frac{\sigma_a}{\sigma_f} = \frac{(10^{17}\,\text{fissions})(235\,\text{g/mol})(582.6 + 98.8)}{(6.02 \times 10^{23}\,\text{atom/mol})(582.6)} = 46\,\mu\text{g}$$

Thus, a foil of highly enriched uranium can be placed in a reactor temporarily to create Mo-99.

13.4 MEDICAL IMAGING

Administering a suitable radiopharmaceutical to a patient results in a selective deposit of the radioactive material in the tissue or organ under study. The use of these radionuclides to diagnose malfunctions or disease is called *medical imaging*. Millions of diagnostic nuclear medicine studies are performed each year in the United States. In imaging, a photographic screen or a detector (array) examines the adjacent area of the body and receives an image of the organ, revealing the nature of some medical problem. A scanner consists of a sodium iodide crystal detector, movable in two directions, a collimator to define the radiation, and a recorder that registers counts in the sequence of the points it observes. In contrast, an Anger scintillation camera is stationary, with a number of photomultiplier tubes receiving gamma rays through a collimator with many holes, and an electronic data-processing circuit.

The Anger camera provides a view of activity in the form of a plane. The introduction of computer technology has made possible more sophisticated displays, including three-dimensional images. Such a process is called *tomography*, of which there are several types. The first is single photon emission computed tomography (SPECT), which has a rotating camera that takes a series of planar pictures of the region containing a radionuclide. A sodium iodide crystal detects uncollided photons from the radioactive source and produces electric signals. Data from 180 different angles are processed by a computer to give two- and three-dimensional views of the organ. SPECT is used especially for diagnosis of the heart, liver, and brain. The second is positron emission tomography (PET), in which a positron-emitting radiopharmaceutical is used. Three important examples are oxygen-15 (2 min), nitrogen-13 (10 min), and carbon-11 (20 min). They are isotopes of elements found in all organic molecules, allowing them to be used for many biological studies and medical applications, especially heart disease. A fourth, fluorine-18 (110 min), is especially important in brain studies, in which there is difficulty getting most chemicals through what is called the blood-brain barrier. In contrast, F-18 forms a compound that acts like glucose, which can penetrate brain tissue and show the location of a disease such as stroke or cancer. The isotopes are produced by a cyclotron on the hospital site, and the targets are quickly processed chemically to achieve the desired labeled compound. The gamma rays released in the annihilation of the positron and an electron are detected, taking advantage of the simultaneous emission (coincidences) of the two gammas and their motion in opposite directions. The data are analyzed by a computer to give high-resolution displays. PET scans are analogous to X-ray computerized axial tomography (CT) scans, but better for some purposes. Fig. 13.3 compares the ability of CT and PET to locate a brain tumor.

EXAMPLE 13.3

A blood flow radiotracer using ^{99m}Tc ($t_H = 6\,h$) for SPECT has a biological half-life of 11 h. The effective half-life is

$$t_E = (1/t_H + 1/t_B)^{-1} = [1/(6h) + 1/(11h)]^{-1} = 3.9h$$

Applying Eq. (11.14), only 1% of the radionuclide remains in the body after a period of

$$t = \frac{-t_E}{\ln(2)} \ln\left(\frac{N(t)}{N_0}\right) = \frac{-3.9h}{\ln(2)} \ln(0.01) = 26h$$

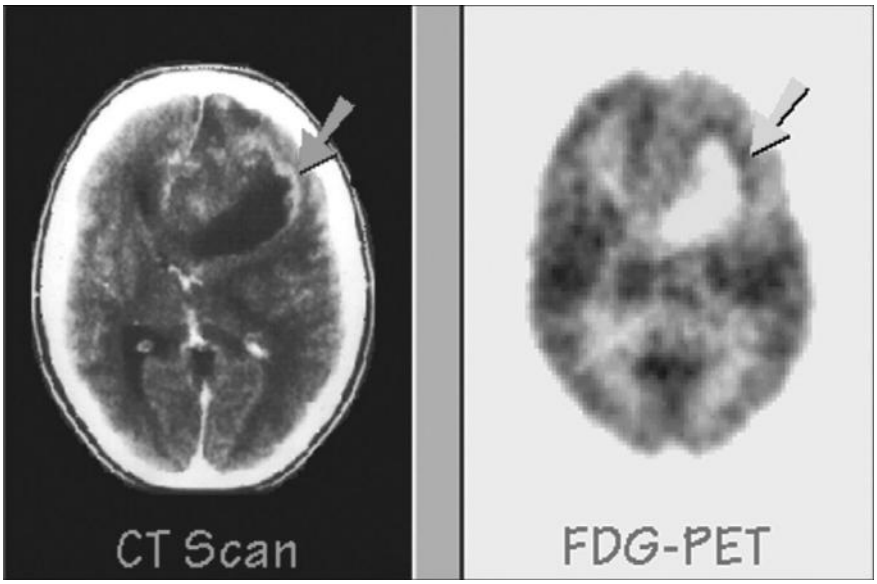

FIG. 13.3

CT and PET scans of a brain tumor.

Courtesy Lawrence Berkeley National Laboratory.

An alternate diagnostic method that is very popular and does not involve radioactivity is magnetic resonance imaging (MRI). It takes advantage of the magnetic properties of atoms in cells. Formerly it was called nuclear magnetic resonance (NMR), but physicians adopted the new name to avoid the association with anything "nuclear." (The interested reader is directed to Further Reading at the end of this chapter.)

13.5 RADIOIMMUNOASSAY

Radioimmunoassay, discovered by Yalow and Berson (1960), is a chemical procedure that uses radionuclides to find the concentration of biological materials very accurately in parts per billion and less. It was developed in connection with studies of the human body's immune system. In that system, a protective substance (antibody) is produced when a foreign protein (antigen) is introduced. The method makes use of the fact that antigens and antibodies also react. Such reactions are involved in vaccinations, immunizations, and skin tests for allergies.

The goal is to measure the amount of an antigen present in a sample containing an antibody. The latter has been produced previously by repeatedly immunizing a rabbit or guinea pig and extracting the antiserum. A small amount of the radioactively labeled antigen is added to the solution. There is competition between the two antigens, known and unknown, to react with the antibody. For that reason, the method is also called competitive binding assay. A chemical separation is performed, and the

radioactivity in the products is compared with those in a standard reaction. The method has been extended to many other substances, including hormones, enzymes, and drugs. It is said that the amounts of almost any chemical can be measured very accurately because it can be coupled chemically to an antigen.

The method has been extended to allow medical imaging of body tissues and organs. Radiolabeled antibodies that go to specific types of body tissue provide the source of radiation. As noted in Section 14.1, the same idea applies to radiation treatment. The field has expanded to include many other diagnostic techniques not involving radioactivity (see Further Reading at the end of this chapter).

13.6 RADIOMETRIC DATING

There would seem to be no relationship between nuclear energy and the humanities such as history, archaeology, and anthropology. There are, however, several interesting examples in which nuclear methods establish dates of events. The carbon dating technique of Arnold and Libby (1949) is being used regularly to determine the age of ancient artifacts. The technique is based on the fact that carbon-14 is and has been produced by cosmic rays in the atmosphere. Cosmic rays yield neutrons which in turn react with nitrogen

$$ {}^{1}_{0}\mathrm{n} + {}^{14}_{7}\mathrm{N} \rightarrow {}^{14}_{6}\mathrm{C} + {}^{1}_{1}\mathrm{p} \tag{13.3} $$

Plants take up CO_2 and deposit C-14, and animals eat the plants. At equilibrium conditions, the $^{14}C/^{12}C$ ratio is about 10^{-12}. At the death of either, the supply of radiocarbon obviously stops and the C-14 that is present decays, with half-life 5700 y. By measurement of the radioactivity, the age within approximately 50 y can be found. This method was used to determine the age of the Dead Sea Scrolls as approximately 2000 y, making measurements on the linen made from flax; to date documents found at Stonehenge in England, by use of pieces of charcoal; and to verify that prehistoric people lived in the United States as long ago as 9000 y, from the C-14 content of rope sandals discovered in an Oregon cave. Carbon dating proved that the famous Shroud of Turin was made from flax in the fourteenth century.

EXAMPLE 13.4

A bone is found to have a $^{14}C/^{12}C$ ratio of $R = 10^{-13}$. Applying the radioactive decay law to the ratio yields

$$ R(t) = N_{\mathrm{C-14}}(t)/N_{\mathrm{C-12}} = R(0)\left(\frac{1}{2}\right)^{t/t_H} $$

The time since death is

$$ t = t_{\mathrm{H}}\frac{\log\left(R(t)/R(0)\right)}{\log(0.5)} = (5700\mathrm{y})\frac{\log\left(10^{-13}/10^{-12}\right)}{\log(0.5)} = 19{,}000\mathrm{y} $$

Even greater accuracy in dating biological artifacts can be obtained by direct detection of carbon-14 atoms. Molecular ions formed from ^{14}C are accelerated in electric and magnetic fields and then slowed

by passage through thin layers of material. This sorting process can measure three atoms of ^{14}C out of 10^{16} atoms of ^{12}C.

The age of minerals in the Earth, in meteorites, or from the moon can be obtained by a comparison of their uranium and lead contents. Because Pb-206 is the final product of the decay chain starting with U-238, half-life 4.47×10^9 y (see Fig. 3.8), the number of lead atoms now present is equal to the loss in uranium atoms, that is,

$$N_{Pb}(t) = N_U(0) - N_U(t) \tag{13.4}$$

where

$$N_U(t) = N_U(0)e^{-\lambda t} \tag{13.5}$$

Elimination of the original number of uranium atoms $N_U(0)$ from these two formulas gives a relationship between time and the ratio N_{Pb}/N_U:

$$t = \ln[1 + (N_{Pb}(t)/N_U(t))]/\lambda \tag{13.6}$$

Using this radiometric dating method, Patterson (1956) estimated the age of the Earth as 4.55 billion years.

For intermediate ages, thermoluminescence (heat and light) is used. Radiation shifts electrons in atoms to higher orbits (Section 2.3), whereas heating causes electrons to drop back. Thus, the firing of clay in ancient pottery starts the clock. Over the years, traces of radioactive U and Th cause a cumulative shifting, which is measured by heating and observing the light emitted. Jespersen and Fitz-Randolph (1996) provide an elementary but entertaining account of the applications of this technique.

For the determination of ages ranging from 50,000 y to a few million years, an argon method can be used. It is derived from the fact that the potassium isotope K-40 (half-life 1.25×10^9 y) crystallizes in materials of volcanic origin and decays into the stable argon isotope Ar-40. An improved approach makes use of neutron bombardment of samples to convert K-39, a stable isotope of potassium, into Ar-39. This provides a substitute for measuring the content of K. These techniques, described by Taylor and Aitken (1997), are of special interest in relation to the possible collision of an asteroid with the Earth 65 million years ago and the establishment of the date of the first appearance of man. Dating methods are used in conjunction with activation analysis described in the next section.

13.7 NEUTRON ACTIVATION ANALYSIS

Neutron activation analysis (NAA) is an analytical method that will reveal the presence and amount of minute impurities. A sample of material that may contain traces of a certain element is irradiated with neutrons, as in a reactor. The gamma rays emitted by the product radioisotope have unique energies and relative intensities, in analogy to spectral lines from a luminous gas. Measurements and interpretation of the gamma-ray spectra, with data from standard samples for comparison, provide information on the amount of the original impurity.

Let us consider a practical example. Reactor design engineers may be concerned with the possibility that some stainless steel to be used in moving parts in a reactor contains traces of cobalt, which would yield undesirable long-lived activity if exposed to neutrons ($^{59}Co + n \rightarrow {}^{60}Co$). To check on this possibility, a small sample of the stainless steel is irradiated in a test reactor to produce Co-60, and gamma

radiation from the Co-60 is compared with that of a piece known to contain the radioactive isotope. The "unknown" is placed on a Pb-shielded large-volume lithium-drifted germanium Ge(Li) detector used in gamma-ray spectroscopy, as noted in Section 12.3. Gamma rays from the decay of the 5.27-y Co-60 give rise to electrons by photoelectric absorption, Compton scattering, and pair production. The electrons produced by photoelectric absorption then give rise to electrical signals in the detector that are approximately proportional to the energy of the gamma rays. If all the pulses produced by gamma rays of a single energy were equal in height, the observed counting rate would consist of two perfectly sharp peaks at energy 1.17 and 1.33 MeV. Various effects cause the response to be broadened somewhat, as shown in Fig. 13.4. The location of the peaks clearly shows the presence of the isotope Co-60 and the heights tell how much of the isotope is present in the sample. Modern electronic circuits can process a large amount of data at one time. The multichannel analyzer accepts counts caused by photons of all energy and displays the entire spectrum graphically. When neutron activation analysis is applied to a mixture of materials, it is necessary after irradiation to allow time to elapse for the decay of certain isotopes whose radiation would compete with that of the isotope of interest. In some cases, prior chemical separation is required to eliminate interfering isotope effects.

Compton scattering within the detector used for spectroscopy can give rise to additional features besides photopeaks. Using Eq. (5.9), the final energy of a backscattered ($\theta = 180°$) photon is

$$E' = \frac{E}{1 + 2E/(m_e c^2)} \tag{13.7}$$

Therefore, the maximum energy imparted to a Compton electron is

$$E^e_{K,\max} = E - E' = E\{1 - 1/[1 + 2E/(m_e c^2)]\} \tag{13.8}$$

This limiting energy creates a *Compton edge*, which is the maximum energy in the Compton continuum, of the gamma spectrum. Other artifacts include single and double escape peaks from positron-negatron annihilation within the detector subsequent to pair production.

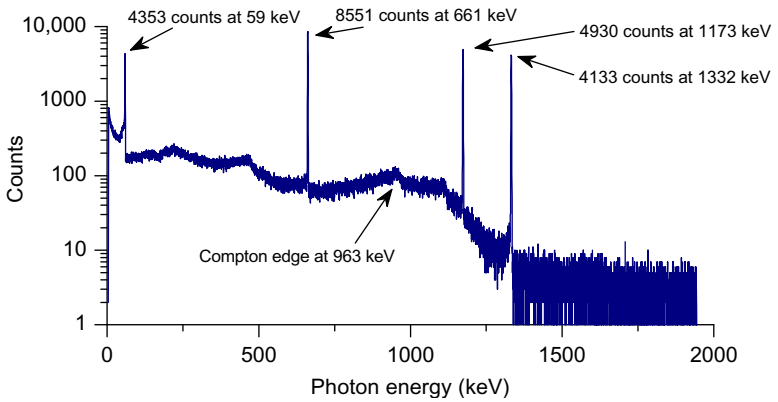

FIG. 13.4

Gamma ray spectra for a sample containing cobalt-60. The 15-min measurement was made using a solid-state germanium detector.

EXAMPLE 13.5

For the 1173 keV gamma ray from ^{60}Co, the Compton edge occurs at

$$E^{e}_{K,\max} = (1173\,\text{keV})\{1 - 1/[1 + 2(1173\,\text{keV})/(511\,\text{keV})]\} = 963\,\text{keV}$$

which is annotated in Fig. 13.4.

The activation analysis method is of particular value for the identification of chemical elements that have an isotope of adequate neutron absorption cross-section and for which the products yield a suitable radiation type and energy. Not all elements meet these specifications, of course, which means that activation analysis supplements other techniques. For example, neutron absorption in the most abundant naturally occurring isotopes of carbon, hydrogen, oxygen, and nitrogen produces stable isotopes. This is fortunate, however, in that organic materials including biological tissue are composed of those very elements, and the absence of competing radiation makes the measurement of trace contaminants easier. The sensitivity of activation analysis is remarkably high for many elements. It is possible to detect quantities as low as a millionth of a gram in 76 elements, a billionth of a gram in 53, or even as low as a trillionth in 11.

EXAMPLE 13.6

A 5-g sample of steel is irradiated in a thermal reactor with a fluence of 10^{15} n/cm^2. Immediately thereafter, the net area under one of the Co-60 photopeaks is 140 counts from a 1-min measurement in a 3% efficient detector. Because ^{60}Co emits 1 photon at each energy, its activity is

$$A_{\text{Co}-60} = R/\varepsilon = (140\,\text{count})/[(60\,\text{s})(0.03\,\text{count/decay})] = 78\,\text{Bq}$$

The ^{59}Co(n, γ) reaction produces the ^{60}Co in an amount of $n_{\text{Co-60}} = n_{\text{Co-59}}\sigma_{\gamma}^{\text{Co-59}}\Phi$. From the measured activity, the original number of ^{59}Co atoms in the sample was

$$n_{\text{Co}-59} = \frac{A_{\text{Co}-60}}{\lambda_{\text{Co}-60}\sigma_{\gamma}^{\text{Co}-59}\Phi} = \frac{A_{\text{Co}-60}t_H^{\text{Co}-60}}{\ln(2)\sigma_{\gamma}^{\text{Co}-59}\Phi} =$$

$$= \frac{(78\,\text{decay/s})(5.271\,\text{y})\left(3.1558\times10^{7}\,\text{s/y}\right)}{\ln(2)\left(20.4\times10^{-24}\,\text{cm}^2\right)\left(10^{15}\,\text{n/cm}^2\right)} = 9.2\times10^{17}\,\text{atom}$$

Assuming for a moment that all the steel is iron, the original number of atoms in the sample was

$$n_{\text{Fe}} = \frac{mN_{\text{A}}}{M} = \frac{(5\,\text{g})\left(6.022\times10^{23}\,\text{atom/mol}\right)}{(55.85\,\text{g/mol})} = 5.39\times10^{22}\,\text{atom}$$

This equates to a Co impurity of about $n_{\text{Co-59}}/n_{\text{Fe}} = 17$ ppm (parts per million).

Prompt gamma neutron activation analysis (PGNAA) is a variant on the method just described. PGNAA measures the capture gamma ray from the original (n, γ) reaction resulting from neutron absorption in the element or isotope of interest, instead of measuring gammas from new radioactive species formed in the reaction. The distinction between NAA and PGNAA is presented in Fig. 13.5, which shows the series of reactions that can result from a single neutron.

Because the reaction rate depends on the neutron cross-section, only a relatively small number of elements can be detected in trace amounts. The detection limits in ppm are smallest for B, Cd, Sm, and

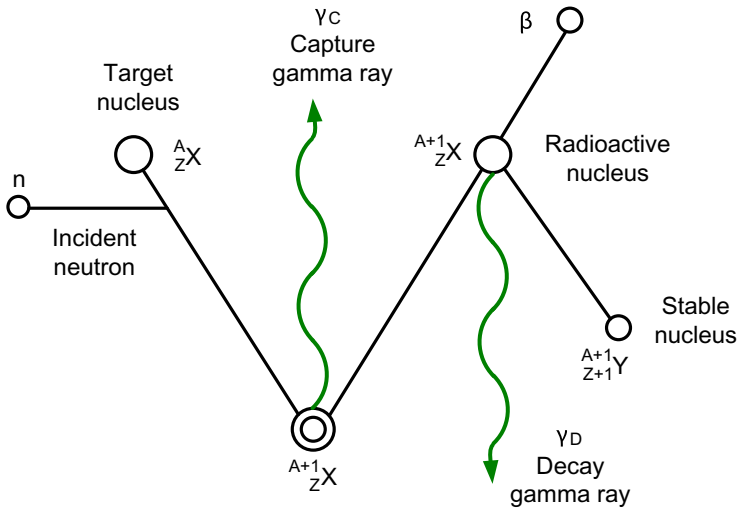

FIG. 13.5

Nuclear reactions involved in neutron activation analysis (PGNAA).

Courtesy of Institute of Physics.

Gd (0.01–0.1), and somewhat higher for Cl, Mn, In, Nd, and Hg (1–10). Components that can readily be measured are those often present in large quantities such as N, Na, Al, Si, Ca, K, and Fe. The method depends on the fact that each element has its unique prompt gamma-ray spectrum. The advantages of PGNAA are that it is nondestructive, it gives low residual radioactivity, and the results are immediate.

A few of the many applications of neutron activation analysis include:

(a) *Textile manufacturing*. In the production of synthetic fibers, certain chemicals such as fluorine are applied to improve textile characteristics, such as the ability to repel water or stains. Activation analysis is used to check on inferior imitations by comparison of the content of fluorine or other deliberately added trace elements.

(b) *Petroleum processing*. The cracking process for refining oil involves an expensive catalyst that is easily poisoned by small amounts of vanadium, which is a natural constituent of crude oil. Activation analysis provides a means for verifying the effectiveness of the initial distillation of the oil.

(c) *Crime investigation*. The process of connecting a suspect with a crime involves physical evidence that often can be accurately obtained by NAA. Examples of forensic applications are the comparison of paint flakes found at the scene of an automobile accident with paint from a hit-and-run driver's car; the determination of the geographical sources of drugs by comparison of trace element content with that of soils in which plants are grown; verification of theft of copper wire by use of differences in content of wire from various manufacturers; distinguishing between murder and suicide by measurement of barium or antimony on hands; and tests for poison in a victim's body. The classic example of the latter is the verification of the hypothesis that Napoleon was poisoned, by activation analysis of arsenic in hair samples.

(d) *Authentication of artwork*. The probable age of a painting can be found by testing a small speck of paint. Over the centuries the proportions of elements such as chromium and zinc used in pigment have changed, so forgeries of the work of old masters can be detected. An alternate method of examination involves irradiation of a painting briefly with neutrons from a reactor. The radioactivity induced produces an autoradiograph in a photographic film, so that hidden underpainting can be revealed. It was desired to determine the authenticity of some metal medical instruments, said to be from Pompeii, the city buried by the eruption of Vesuvius in AD 79. PGNAA was applied, and by use of the fact that the zinc content of true Roman artifacts was low, the instruments were shown to be of modern origin.

(e) *Diagnosis of disease*. Medical applications (Wagner Jr., 1969) include accurate measurements of the normal and abnormal amounts of trace elements in the blood and tissue as indicators of specific diseases. Other examples are the determination of sodium content of children's fingernails and the very sensitive measurement of the iodide uptake by the thyroid gland.

(f) *Pesticide investigation*. The amounts of residues of pesticides such as DDT (dichlorodiphenyltrichloroethane) or methyl bromide in crops, foods, and animals are found by analysis of the bromine and chlorine content.

(g) *Mercury in the environment*. The heavy element mercury is a serious poison for animals and human beings, even at low concentrations. It appears in rivers as the result of certain manufacturing waste discharges. By the use of activation analysis, the Hg contamination in water or tissues of fish or land animals can be measured, thus helping to establish the ecological pathways.

(h) *Astronomical studies*. Measurement by NAA of the variation in the minute amounts of iridium (parts per billion) in geological deposits led to some startling conclusions about the extinction of the dinosaurs some 65 million years ago (Alvarez et al., 1980). A large meteorite, 6 km in diameter, is believed to have struck the Earth and to have caused atmospheric dust that reduced the sunlight needed by plants eaten by the dinosaurs. The theory is based on the fact that meteorites have higher iridium content than the Earth. The sensitivity of NAA for Ir was vividly demonstrated by the discovery that contact of a technician's wedding ring with a sample for only 2 s was sufficient to invalidate results. Evidence is mounting for the correctness of the idea. Large impact craters and buried formations have been discovered in Yucatan and Iowa. They are surrounded by geological debris, the age of which can be measured by the K-Ar method (see Section 13.6).

(i) *Geological applications of PGNAA*. Oil and mineral exploration *in situ* of large-tonnage, low-grade deposits far below the surface has been found to yield better results than extracting small samples. In another example, measurements were made on the ash on the ground and particles in the atmosphere from the 1980 Mount St. Helens volcano eruption. Elemental composition was found to vary with distance along the ground and with altitude. Many other examples of the use of PGNAA are found in the literature (see Alfassi and Chung, 1995; Molnar, 2004).

An alternative and supplement to NAA and PGNAA is X-ray fluorescence spectrometry. It is more accurate for measuring trace amounts of some materials. The method consists of irradiating a sample with an intense X-ray beam to cause target elements to emit characteristic line spectra (i.e., to fluoresce). Identification is accomplished by either (1) measurements of the wavelengths by diffraction with a single crystal, comparison with a standard, and analysis by a computer, or (2) use of a commercial low-energy photon spectrometer, a semiconductor detector. The sensitivity of the method varies with the element irradiated, being lower than 20 ppm for all elements with atomic number above 15. The time required is much shorter than for wet chemical analyses, making the method useful when a large number of measurements are required.

13.8 RADIOGRAPHY

The oldest and most familiar beneficial use of radiation is for medical diagnosis by X-rays. These consist of high-frequency electromagnetic radiation produced by electron bombardment of a heavy-metal target. As is well known, X-rays penetrate body tissue to different degrees depending on material density, and shadows of bones and other dense materials appear on the photographic film. The term *radiography* includes the investigation of the internal composition of living organisms or inanimate objects by use of X-rays, gamma rays, or neutrons.

Fig. 13.6 illustrates the production of X-rays. Using a few volts, the cathode filament is heated to over 2200°C to initiate thermionic emission of electrons. The high voltage (kV) between the electrodes draws the electrons through the vacuum to the tungsten (W) anode where X-rays are generated via bremsstrahlung and characteristic X-ray emission, the latter from the high-energy electrons removing inner shell electrons from the W anode. The high-Z tungsten not only produces X-rays more effectively but W also has a high melting point (3420°C). The monoenergetic electron beam produces a continuum of X-ray energies with a maximum equal to the beam energy. A collimator, formed of material with a large absorption coefficient, may be used to confine the X-ray beam.

EXAMPLE 13.7

Consider an X-ray tube operating at 100 mA and 75 kV, and therefore a power of $P = IV = (0.1\,\text{A})(75\,\text{kV}) = 7.5\,\text{kW}$. Use of Eq. (5.1) reveals that $<1\%$ of the electron beam energy is converted to X-rays at the tungsten anode

$$f_e = 10^{-3}\,ZE_e = \left(10^{-3}\right)(74)(0.075\,\text{MeV}) = 0.0056$$

The remaining electron kinetic energy is converted to heat within the anode. Let us assume a focal point for the beam encompassing a volume of 1 mm^3. Modifying Eq. (1.3) provides a relation for the temperature increase rate of the W metal

$$\frac{dT}{dt} = \frac{\dot{Q}}{mc_p} = \frac{(1-f_e)P}{\rho V c_p} = \frac{(1-0.0056)\left(7.5\times10^3\,\text{J/s}\right)}{(19.3\,\text{g/cm}^3)\left(10^{-3}\,\text{cm}^3\right)(0.134\,\text{J/(gK)})} = 2.9\times10^6\,\text{K/s}$$

Even with heat transfer to other regions of the anode, these results motivate mitigation approaches such as limiting the exposure (i.e., beam on) times and rapidly rotating the target (e.g., thousands of rpm) to prevent excessive tungsten temperatures.

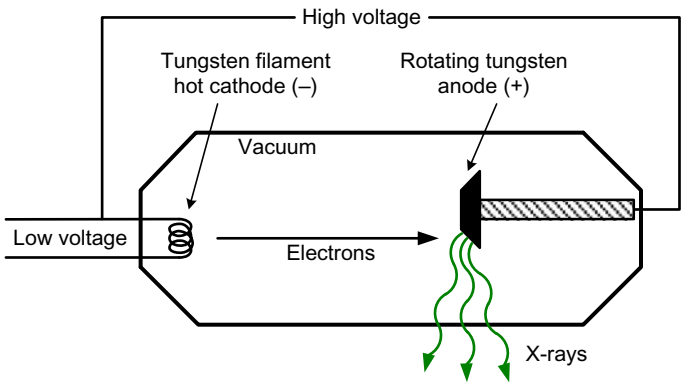

FIG. 13.6

X-ray production.

For both medical and industrial use, the isotope cobalt-60, produced from Co-59 by neutron absorption, is an important alternative to the X-ray tube. Co-60 emits gamma rays of energy 1.17 and 1.33 MeV, which are especially useful for examination of flaws in metals. Internal cracks, defects in welds, and nonmetallic inclusions are revealed by scanning with a cobalt radiographic unit. Advantages include small size and portability, and freedom from the requirement of an electrical power supply. The half-life of 5.27 y permits use of the device for a long time without need for replenishing the source. On the other hand, the energy of the rays is fixed and the intensity cannot be varied, as is possible with the X-ray machine.

Other isotopes that are useful for gamma-ray radiography are: (1) iridium-192, half-life 73.8 d, photon energy approximately 0.4 MeV, for thin specimens; (2) cesium-137 (30.1 y), because of its long half-life and 0.662 MeV gamma ray; and (3) thulium-170, half-life 128.6 d, emitting low-energy gammas (0.052, 0.084, 0.16 MeV), useful for thin steel and light alloys because of the high cross-section of the soft radiation.

The purpose of radiography that uses neutrons is the same as that which uses X-rays, namely to examine the interior of an opaque object. There are some important differences in the mechanisms involved, however. X-rays interact principally with the electrons in atoms and molecules, and thus are scattered best by heavy high-Z elements. Neutrons interact with nuclei and are scattered according to the isotopic composition of the target. Hydrogen atoms have a particularly large scattering cross-section. In addition, some isotopes have very high capture cross-section (e.g., cadmium, boron, and gadolinium). Such materials are useful in detectors as well. Fig. 13.7 shows the schematic arrangement of a thermal neutron radiography unit, where the source can be a nuclear reactor, a particle accelerator, or a radioisotope. Exposure times are shortest for the reactor source because of the large supply of neutrons; they are longest for the isotopic source. A typical accelerator reaction that uses neutrons is the (d, n) reaction on tritium or beryllium.

Several of the radioisotopes sources use the (γ, n) reaction in beryllium-9, with gamma rays from antimony-124 (60.20 d), or the (α, n) reaction with alpha particles from americium-241 (432 y) or curium-242 (163 d). An isotope of the artificial element 98, californium-252, is especially useful as a neutron source. It decays usually (96.9%) by alpha particle emission, but the other part (3.1%)

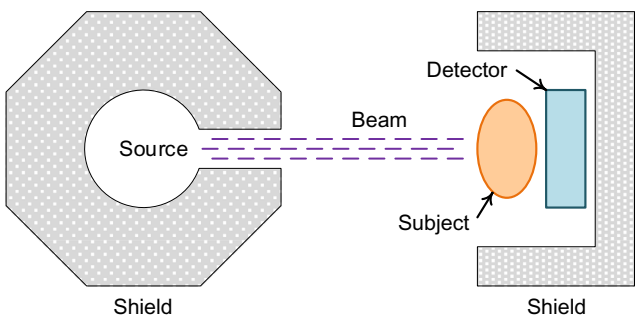

FIG. 13.7

Schematic diagram of a thermal neutron radiography unit. Source can be an accelerator, a reactor, or a radioisotope.

undergoes spontaneous fission, releasing approximately 3.76 neutrons on average. The half-lives for the two processes are 2.73 and 85.5 y, respectively. An extremely small mass of Cf-252 serves as an abundant source of neutrons. These fast neutron sources must be surrounded by a light-element moderator to thermalize the neutrons.

Detection of transmitted neutrons is by the small number of elements that have a high thermal neutron cross-section and which emit secondary radiation that readily affects a photographic film that records the images. Examples are boron, indium, dysprosium, gadolinium, and lithium. Several neutron energy ranges may be used: thermal, fast and epithermal, and cold neutrons, obtained by passing a beam through a guide tube with reflecting walls that select the lowest energy neutrons of a thermal distribution.

Examples of the use of neutron radiography are:

(a) Inspection prior to operation of reactor fuel assemblies for defects such as enrichment differences, odd-sized pellets, and cracks.
(b) Examination of used fuel rods to determine radiation and thermal damage.
(c) Inspection for flaws in explosive devices used in the US space program. The devices served to separate booster stages and to trigger release of reentry parachutes. Items are rejected or reworked based on any 1 of 10 different types of defects.
(d) Study of seed germination and root growth of plants in soils. The method allows continued study of the root system without disturbance. Root diameters down to ⅓ mm can be discerned, but better resolution is needed to observe root hairs.
(e) Real-time observations of a helicopter gas turbine engine at Rolls-Royce, Ltd. Oil flow patterns that use cold neutrons are observable, and bubbles, oil droplets, and voids are distinguishable from normal density oil.

13.9 RADIATION GAUGES

Some physical properties of materials are difficult to ascertain by ordinary methods but can be measured easily by observing how radiation interacts with the substance. For example, the thickness of a layer of plastic or paper can be found by measuring the transmitted number of beta particles from a radioactive source. The separated fission product isotopes strontium-90 (29.1 y, 0.546-MeV beta particle) and cesium-137 (30.1 y, 0.514-MeV beta particle) are widely used for such gauging.

The density of a liquid flowing in a pipe can be measured externally by detection of the gamma rays that pass through the substance. The liquid in the pipe serves as a shield for the radiation and attenuation of the beam dependent on μ and thus particle number density.

The level of liquid in an opaque container can be measured readily without the need for sight glasses or electric contacts. A detector outside the vessel measures the radiation from a radioactive source mounted on a float in the liquid. Alternatively, an external source transmits radiation through the tank walls and media to a detector, as diagrammed in Fig. 13.8. Such fixed gauges incorporate a movable radiation shield, called a shutter, to protect personnel during maintenance procedures.

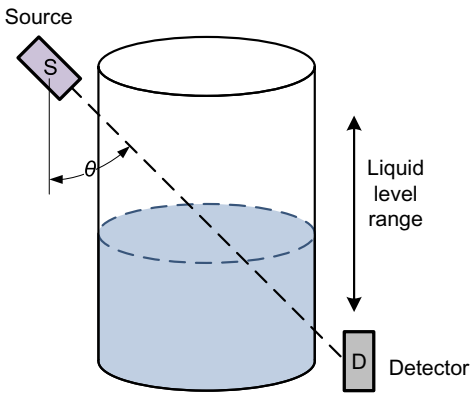

FIG. 13.8

Radiation gauge for tank level measurement.

EXAMPLE 13.8

Water level in a tank with $H=0.5$ m height and $D=0.25$ m inside-diameter is to be measured using an externally mounted 50 mCi ^{137}Cs source, such that $\theta=\arctan(1/2)=26.6°$ according to Fig. 13.8, and the source emission rate is

$$S=(50\text{mCi})\left(3.7\times10^{7}\text{Bq/mCi}\right)(0.851\,\text{gamma/decay})=1.6\times10^{9}\gamma/\text{s}$$

The 0.662-MeV radiation beam is always attenuated by the 2 $d=0.5$ cm thick iron tank walls, which in terms of mean free paths (mfp) of travel is

$$(\mu r)_{\text{Fe}}=\mu 2d/\sin(\theta)=\left(0.07392\text{cm}^2/\text{g}\right)\left(7.874\text{g/cm}^3\right)(2)(0.5\text{cm})/\sin(26.6°)=1.30\text{mfp}$$

When the tank is empty, the uncollided flux (neglecting air attenuation) at the detector is

$$\phi_u=\frac{S\exp\left[-(\mu r)_{\text{Fe}}\right]}{4\pi\left[H^2+(D+2d)^2\right]}=\frac{\left(1.6\times10^{9}\gamma/\text{s}\right)\exp(-1.3)}{4\pi\left[(50\text{cm})^2+(25+1\text{cm})^2\right]}=1.1\times10^{4}\gamma/\left(\text{cm}^2\,\text{s}\right)$$

The attenuation from water is maximally

$$(\mu r)_{\text{W}}=\mu D/\sin(\theta)=\left(0.08618\text{cm}^2/\text{g}\right)\left(1\,\text{g/cm}^3\right)(25\text{cm})/\sin(26.6°)=4.8\text{mfp}$$

When the tank is full of water, the uncollided flux to be measured is only

$$\phi_u=\frac{S\exp\left[-(\mu r)_{\text{Fe}}-(\mu r)_{\text{W}}\right]}{4\pi\left[H^2+(D+2d)^2\right]}=\frac{\left(1.6\times10^{9}\gamma/\text{s}\right)\exp(-1.3-4.8)}{4\pi\left[(50\text{cm})^2+(26\text{cm})^2\right]}=90\gamma/\left(\text{cm}^2\,\text{s}\right)$$

Without exposure buildup, the present source may lack the requisite water level measurement accuracy due to low count rates. The uncollided flux varies with the water level (Exercise 13.22).

Portable gauges for measurement of both moisture and density are available commercially with typical source strengths of 40 mCi (1.5 GBq) ^{241}AmBe for neutrons and 8 mCi (300 MBq) ^{137}Cs for gammas. A rechargeable battery provides power for the electronics involving a microprocessor. Gamma rays for density measurements in materials such as soil or asphalt paving are supplied by a

Cs-137 source. For operation in the direct-transmission mode, a hole is punched into the material being tested and a probe rod with radioactive source in its end is inserted. A Geiger-Müller gamma ray detector is located at the base of the instrument, as shown in Fig. 13.9. A typical calibration curve for the instrument is also shown. Standard blocks of test material with various amounts of magnesium and aluminum are used to determine the constants in an empirical formula that relates density to counting rate. If the source is retracted to the surface, measurements in the back-scattering mode can be made. The precision of density measurements is 0.4% or better.

For moisture measurements by the instrument, neutrons of average energy 4.5 MeV are provided by an americium-beryllium source. Particles of approximately 5 MeV from Am-241, half-life 432 y, bombard Be-9 to produce the reaction $^{9}Be(\alpha, n)^{12}C$ (see Eq. 8.1). Neutrons from the source, located in the center of the gauge base, migrate through the material and slow down, primarily with collisions with the hydrogen atoms in the contained moisture. The more water that is present, the larger the thermal neutron flux is in the vicinity of the gauge. The flux is measured by a thermal-neutron detector consisting

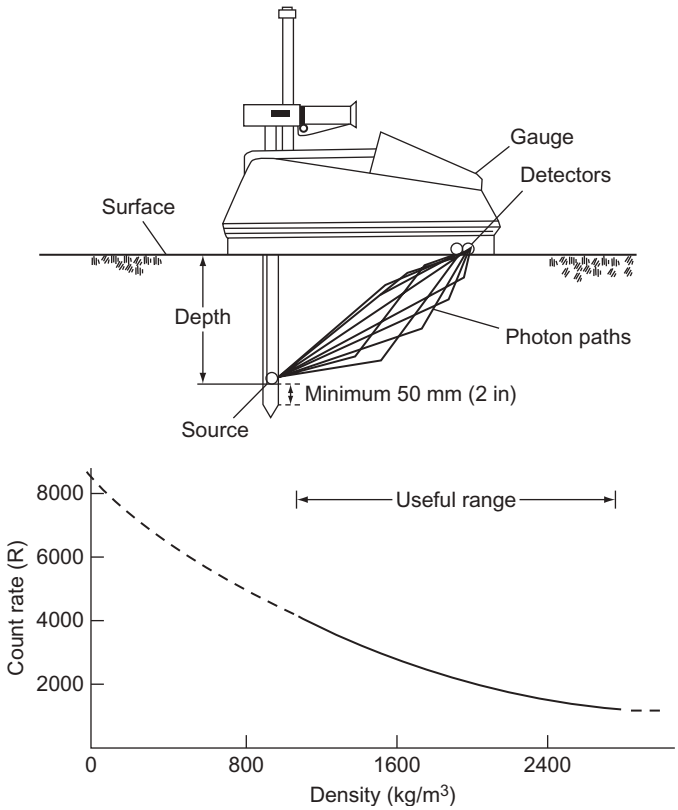

FIG. 13.9

Direct-transmission radiation gauge to measure soil density.

Courtesy of Troxler Electronic Laboratories, Inc.

of a helium-3 proportional counter, in which the ionization is created by the products of the reaction ^{3}He(n, p)^{3}H ($\sigma_a = 5333$ barns). Protons and tritons create the ionization measured in the detector. The gauge is calibrated by use of laminated sheets of the hydrocarbon polyethylene and of magnesium. The moisture content can be measured to approximately 5% in normal soil. The device requires correction if there are significant amounts of absorbers such as iron, chlorine, or boron in the ground or if there are hydrogenous materials other than water present.

Several nuclear techniques are used in the petroleum industry. In well drilling, the logging process involves the study of geological features. One method consists of the measurement of natural gamma radiation. When the detector is moved from a region of ordinary radioactive rock to one containing oil or another liquid, the signal is reduced. A neutron moisture gauge is adapted to determine the presence of oil, which contains hydrogen. Neutron activation analysis of chemical composition is performed by lowering a neutron source and a gamma ray detector into the well.

13.10 SUMMARY

Radioisotopes provide a great deal of information for human benefit. The characteristic radiations permit the tracing of processes such as fluid flow. Radiopharmaceuticals are radioactively tagged chemicals used in hospitals for diagnosis. Scanners detect the distribution of radioactivity in the body and form images of diseased tissue. Radioimmunoassay measures minute amounts of biological materials. The dates of archaeological artifacts and of rock formations can be found from carbon-14 decay data and the ratios of uranium to lead and of potassium to argon. The irradiation of materials with neutrons gives rise to unique prompt gamma rays and radioactive decay products, allowing measurement of trace elements for many applications. Radiography uses gamma rays from cobalt-60 or neutrons from a reactor, accelerator, or californium-252. Radiation gauges measure density, thickness, ground moisture, water/cement ratios, and oil deposits.

13.11 EXERCISES

13.1 A radioisotope is to be selected to provide the signal for arrival of a new grade of oil in an 800-km-long pipeline in which the fluid speed is 1.5 m/s. Some of the candidates are:

Isotope	Half-Life	Particle, Energy (MeV)
Na-24	14.96 h	β, 1.389; γ, 1.369, 2.754
S-35	87.2 d	β, 0.167
Co-60	5.27 y	β, 0.315; γ, 1.173, 1.332
Fe-59	44.5 d	β, 0.273, 0.466; γ, 1.099, 1.292

Which would you pick? On what basis did you eliminate the others?

13.2 The radioisotope F-18, half-life 1.83 h, is used for tumor diagnosis. It is produced by bombarding lithium carbonate (Li_2CO_3) with neutrons, with tritium as an intermediate particle. Deduce the two nuclear reactions.

13.3 The range of beta particles of energy 0.53 MeV in metals is 170 mg/cm^2. What is the maximum thickness of aluminum sheet, density 2.7 g/cm^3, that would be practical to measure with a Sr-90 or Cs-137 gauge?

13.4 The amount of environmental pollution by mercury is to be measured with neutron activation analysis. Neutron absorption in the mercury isotope Hg-196, present with 0.15% abundance, activation cross-section 3×10^3 barns, produces the radioactive species Hg-197, half-life 2.67 d. The smallest activity for which the resulting photons can be accurately analyzed in a sample of river water is 10 Bq. If a reactor neutron flux of 10^{12}/(cm^2 s) is available, how long an irradiation is required to be able to measure mercury contamination of 20 ppm (μg/g) in a 4-mL water test sample?

13.5 The ratio of numbers of atoms of Pb-206 and U-238 in a certain moon rock is found to be 0.05. What is the probable age of the sample?

13.6 The activity of C-14 in a wooden figure found in a cave is only three-fourths of today's value. Estimate the date the figure was carved.

13.7 Examine the possibility of adapting the uranium-lead dating analysis to the potassium-argon method. What would be the ratio of Ar-40 to K-40 if a deposit were 1 million years old? Note that only 10.86% of K-40 decay yields Ar-40, the rest going into Ca-40.

13.8 The age of minerals containing rubidium can be found from the ratio of radioactive Rb-87 to its daughter Sr-87. Develop a formula relating this ratio to time.

13.9 It has been proposed that radioactive krypton-85 gas of 10.76 y half-life be used in conjunction with film for detecting small flaws in materials. Discuss the concept, including possible techniques, advantages, and disadvantages.

13.10 A krypton isotope $^{81m}_{36}Kr$ of half-life 13.1 s is prepared by charged particle bombardment. It gives off a gamma ray of 0.19 MeV energy. Discuss the application of the isotope to the diagnosis of emphysema and black lung disease. Consider production, transportation, hazards, and other factors.

13.11 Tritium (^3H) has a physical half-life of 12.32 y, but when taken into the human body as water, it has a biological half-life of 12.0 d. Calculate the effective half-life of tritium for purposes of radiation exposure. Comment on the result.

13.12 With the half-life relationship as given in Section 13.8, calculate the overall effective half-life of californium-252 from the spontaneous fission and alpha decay processes.

13.13 The spontaneous fission half-life of Cf-252 is 85.6 y. Assuming that it releases 3.76 neutrons per fission, how much of the isotope in micrograms is needed to provide a source of strength of 10^7 neutrons per second? What would be the diameter of the source in the form of a sphere if the Cf-252 had a density as pure metal of 20 g/cm^3?

13.14 Three different isotopic sources are to be used in radiography of steel in ships as follows:

Isotope	Half-Life	Gamma Energy (MeV)
Co-60	5.27 y	1.25 (average)
Ir-192	73.8 d	0.4 (average)
Cs-137	30.1 y	0.66

Which isotope would be best for insertion in pipes of small diameter and wall thickness? For finding flaws in large castings? For more permanent installations? Explain.

13.15 The number of atoms of a parent isotope in a radionuclide generator such as Mo-Tc is given by $N_P = N_{P0} \exp(-\lambda_P t)$ with N_{P0} as the initial number of atoms. The number of daughter atoms for zero initially is

$$N_D = f\lambda_P N_{P0} [\exp(-\lambda_P t) - \exp(-\lambda_D t)]/(\lambda_D - \lambda_P)$$

where f is the fraction of parents that decay into daughters. (a) Find the ratio of Tc-99m atoms to Mo-99 atoms for very long times, with $f = 0.87$. (b) What is the percent error in the use of the ratio found in (a) if it takes one half-life of the parent to ship the fresh isotope to a laboratory for use?

13.16 Pharmaceuticals containing carbon-14 (5700 y) and tritium (12.32 y) are both used in a biological research laboratory. To avoid an error of greater than 10% in counting beta particles as a result of accidental contamination of C-14 by H-3, what must be the upper limit on the fraction of atoms of tritium in the sample? Assume that all betas are counted, regardless of energy.

13.17 The atom fraction of C-14 in carbon was approximately 1.2×10^{-12} before bomb tests. How many counts per minute would be expected from a 1-g sample of carbon? Discuss the implications of that number.

13.18 Determine half-thickness in the body for gamma rays produced by positron annihilation.

13.19 Use Table 3.2 to determine the radioisotopes causing the first two photopeaks in Fig. 13.4.

13.20 Compute the Compton edge for (a) a 661-keV and (b) a 1332-keV photon. Verify your result using Fig. 13.4.

13.21 Because the Cs-137 of Example 13.8 results in a low flux when the tank is filled, someone has suggested switching to 50 mCi of Co-60 because of its more prolific and energetic gamma emissions. (a) Determine the uncollided flux at the detector when the tank is full of water. (b) Compute the total flux when buildup is included. (c) Do you foresee any disadvantage to the use of Co-60 compared to Cs-137?

13.22 Plot the calibration curve, that is, the uncollided flux versus water level, for the tank and measurement system of Example 13.8. Is the curve linear?

13.23 For what time period should the U-235 foil of Example 13.2 be exposed to neutrons in a reactor to maximize the Mo-99 production?

13.12 COMPUTER EXERCISES

13.A Recall the computer program RADIOGEN (see Computer Exercise 3.C) giving activities of parent and daughter isotopes. (a) Apply to the radionuclide generator of Section 13.3 by use of half-lives 65.98 h for Mo-99 and 6.01 h for Tc-99 m, with $f = 0.87$. (b) From the formula in Exercise 13.15, show that the ratio of activities of daughter to parent at very long times is

$$A_D/A_P = f/(1 - \lambda_P/\lambda_D)$$

(c) Find out how much error there is with the formula of (b), rather than the ratio calculated by RADIOGEN, if it takes exactly one half-life of Mo-99 to ship the generator to a laboratory for use.

13.B Use the EXPOSO program to continue Example 13.8 by determining the buildup factors in the iron and water. Then include photon buildup to calculate the total flux at the detector when the tank is (a) empty and (b) full of water. (c) What is the maximum dose rate at the detector?

REFERENCES

Alfassi, Z., Chung, C. (Eds.), 1995. Prompt Gamma Neutron Activation Analysis. CRC Press. Boca Raton. Includes in vivo measurements of elements in the human body and in situ well-logging in the petroleum industry.

Alvarez, L.W., Alvares, W., Asaro, F., Michel, H.V., 1980. Extraterrestrial cause for the cretaceous-tertiary extinction. Science 208 (4448), 1098–1108.

American Nuclear Society (ANS), 2004. United States Radioisotope Supply. ANS Position Statement No. 30, http://www.ans.org/pi/ps/.

Arnold, J.R., Libby, W.F., 1949. Age determinations by radiocarbon content: checks with samples of known age. Science 110 (2869), 678–680.

Fermi, E., 1946. Atomic energy for power. In: Hill, A.V. (Ed.), Science and Civilization, The Future of Atomic Energy. McGraw-Hill, New York.

Jespersen, J., Fitz-Randolph, J., 1996. Mummies, Dinosaurs, Moon Rocks: How We Know How Old Things Are. Atheneum Books for Young Readers, New York.

Molnar, G. (Ed.), 2004. Handbook of Prompt Gamma Activation Analysis with Neutron Beams. Kluwer, Dordrecht.

National Academy of Sciences (NAS), 2016. Molybdenum-99 for Medical Imaging. National Academies Press, Washington, DC.

Patterson, C., 1956. Age of meteorites and the earth. Geochim. Cosmochim. Acta 10 (4), 230–237.

Taylor, R.E., Aitken, M.J. (Eds.), 1997. Chronometric Dating in Archaeology. Plenum Press. New York. Principle, history, and current research for a number of dating techniques; articles are written by experts in the methods.

Wagner Jr., H.N. (Ed.), 1969. Principles of Nuclear Medicine. W.B. Saunders Co., Philadelphia

Watson, J.D., Crick, F.H.C., 1953. Molecular structure of nucleic acids: a structure for deoxyribose nucleic acid. Nature 171 (4356), 737–738.

Yalow, R.S., Berson, S.A., 1960. Immunoassay of endogenous plasma insulin in man. J. Clin. Invest. 39, 1157–1175.

FURTHER READING

Adelstein, S.J., Manning, F.J. (Eds.), 1995. Isotopes for Medicine and the Life Sciences. National Academies Press, Washington. Describes sources of stable and radioactive isotopes and recommends a national dedicated accelerator.

Bowman, S. (Ed.), 1991. Science and the Past. University of Toronto Press, Toronto. Qualitative technical treatment of dating with emphasis on the artifacts.

Brucer, M., 1990. A Chronology of Nuclear Medicine 1600–1989. Heritage Publications, St. Louis. Interesting and informative discussion with abundant references.

Chandra, R., 2004. Nuclear Medicine Physics: The Basics. Lippincott Williams & Wilkins, Philadelphia. Intended for resident physicians; covers scintillation cameras and computer tomography.

Chard, T., 1995. An Introduction to Radioimmunoassay and Related Techniques. Elsevier, Amsterdam. Concept, principles, and laboratory techniques; immunoassays in general, labeling techniques, and commercial services.

Choppin, G., Liljenzin, J.-O., Rydberg, J., 2002. Radiochemistry and Nuclear Chemistry, third ed. Butterworth-Heinemann, Oxford. Includes chapters on isotope uses in chemistry and on nuclear energy.

Dance, D.R., Christofides, S., Maidment, A.D.A., McLean, I.D., Ng, K.H., 2014. Diagnostic Radiology Physics: A Handbook for Teachers and Students. International Atomic Energy Agency (IAEA), Vienna.

Domanus, J.C. (Ed.), 1992. Practical Neutron Radiography. Kluwer, Dordrecht. Sources, collimation, imaging, and applications (e.g., nuclear fuel).

Halmshaw, R., 1995. Industrial Radiology, Theory and Practice, second ed. Chapman & Hall, London. Principles and equipment using X-rays, gamma-rays, neutrons, and other particles; computers and automation in quality control and nondestructive testing.

Harbert, J., da Rocha, A.F.G., 1984. Textbook of Nuclear Medicine, second ed. Lea & Febiger, Philadelphia. Volume I: Basic Science, Volume II: Clinical Applications. Volume I contains good descriptions of radionuclide production, imaging, radionuclide generators, radiopharmaceutical chemistry, and other subjects; Volume II gives applications to organs.

Harms, A.A., Wyman, D.R., 1986. Mathematics and Physics of Neutron Radiography. 1986. Dordrecht, Holland. Highly technical reference.

Hendee, W.R., Ritenour, E.R., 2002. Medical Imaging Physics, fourth ed. Wiley-Liss, New York.

Heydorn, K., 1984. Neutron Activation Analysis for Clinical Trace Element Research. vols. I & II. CRC Press, Boca Raton, FL.

Hornak, J.P., 2017. The Basics of MRI. http://www.cis.rit.edu/htbooks/mri. Comprehensive treatment.

Human Genome Project Information, http://genomics.energy.gov/. Comprehensive information.

Idaho National Laboratory (INL), Gamma-Ray Spectrometry Center. http://www4vip.inl.gov/gammaray/. Display of spectra and decay schemes.

International Atomic Energy Agency (IAEA), 1990. Guidebook on Radioisotope Tracers in Industry. IAEA, Vienna. Methodology, case studies, and trends.

Jones, P., 2004. DNA Forensics: From RFLP and PCR-STR and Beyond. http://www.forensicmag.com/article/dna-forensics-rflp-pcr-str-and-beyond. September. Comparison of DNA fingerprinting methods.

Knoche, H.W., 1991. Radioisotopic Methods for Biological and Medical Research. Oxford University Press, New York. Includes mathematics of radioimmunoassay and isotope dilution.

Krawczak, M., Schmidtke, J., 1998. DNA Fingerprinting, second ed. Springer-Verlag, New York. Genetics background, applications to forensics, and legal and ethical aspects.

Mettler Jr., F.A., Guiberteau, M.J., 2005. Essentials of Nuclear Medicine Imaging, fifth ed. W.B. Saunders Co., Philadelphia. After presenting background on radioactivity, instruments, and computers, the book describes the methods used to diagnose and treat different tissues, organs, and systems of the body.

National Isotope Development Center, http://www.isotopes.gov/. Catalog of stable and radioactive isotopes.

Ponto, J.A., 1998. Radiopharmaceuticals. Radiographics 18 (6), 1395–1404.

Price, C.P., Newman, D.J. (Eds.), 1991. Principles and Practices of Immunoassay. Stockton Press, New York. A great variety of immunoassay techniques.

Saha, G.B., 2005. Fundamentals of Nuclear Pharmacy, fifth ed. Springer, New York. Instruments, isotope production, and diagnostic and therapeutic uses of radiopharmaceuticals. Reflects the continued growth of the field.

Troxler Labs, Nuclear Gauges. http://troxlerlabs.com. Details on company's products.

Vaughan, D., 1997. A Vital Legacy: Biological and Environmental Research in the Atomic Age. U.S. Department of Energy (DOE), Office of Science, Office of Scientific and Technical Information. September. https://www.osti.gov/scitech/servlets/purl/305940.

Wilson, M.A., 1998. Textbook of Nuclear Medicine. Lippincott Williams & Wilkins, Philadelphia, PA.

CHAPTER

USEFUL RADIATION EFFECTS 14

CHAPTER OUTLINE

Radiation in the form of gamma rays, beta particles, and neutrons is being used in science and industry to achieve desirable changes. Radiation doses control offending organisms, including cancer cells and harmful bacteria, and sterilize insects. Local energy deposition can also stimulate chemical reactions and modify the structure of plastics and semiconductors. Neutrons and X-rays are used to investigate basic physical and biological processes. In this chapter, we will briefly describe some of these interesting and important applications of radiation. For additional information on the uses around the world, the proceedings of international conferences can be consulted.

14.1 MEDICAL TREATMENT

The use of radiation for medical therapy has increased greatly in recent years, with millions of treatments given to patients annually. The radiation comes from teletherapy units in which the source is at some distance from the target, from isotopes in sealed containers implanted in the body, or from ingested solutions of radionuclides. Table 14.1 shows some of the radionuclides used in treatment.

Nuclear Energy. https://doi.org/10.1016/B978-0-12-812881-7.00014-9

Table 14.1 Radionuclides Used in Therapy

Radionuclide	Disease Treated
P-32	Leukemia
Y-90	Cancer
I-131	Hyperthyroidism Thyroid cancer
Sm-153 and Re-186	Bone cancer pain
Re-188 and Au-198	Ovarian cancer

The mechanism of the effects of radiation is known qualitatively. Abnormal cells that divide and multiply rapidly are more sensitive to radiation than normal cells. Although both types are damaged by radiation, the abnormal cells recover less effectively. Radiation is more effective if the dosage is fractionated (i.e., split into parts and administered at different times, allowing recovery of normal tissue to proceed).

Use of excess oxygen is helpful. Combinations of radiation, chemotherapy, and surgery are applied as appropriate to the particular organ or system affected. The ability to control cancer has improved over the years, but a cure based on better knowledge of cell biology is yet to come.

Doses of radiation are found to be effective in the treatment of diseases such as cancer. In early times, X-rays were used, but they were supplanted by cobalt-60 gamma rays because the high-energy (1.17 and 1.33 MeV) photons penetrated tissue better and could deliver doses deep inside the body, with a minimum of skin reaction. In modern nuclear medicine, there is increasing use of accelerator-produced radiation in the range of 4–35 MeV for cancer treatment. Doses for diagnostic procedures, of course, are much less than those for medical therapy. For instance, a typical administered activity of sodium iodide (^{131}I) for thyroid imaging is 1.9–3.7 MBq whereas for treating hyperthyroidism the dose is 185–1221 MBq (UNSCEAR, 2008).

Treatment of disease by temporary or permanent implantation of a radionuclide is called interstitial brachytherapy (*brachys* is Greek for short). A small radioactive capsule or "seed" is imbedded in the organ, producing local gamma irradiation. The radionuclides are chosen to provide the correct dose. In earlier times, the only material available for such implantation was alpha-emitting radium-226 (1600 y). Most frequently used today are iridium-192 (73.8 d), iodine-125 (59.4 d), and palladium-103 (17.0 d). Examples of tumor locations where this method is successful are the head and neck, breast, lung, and prostate gland. Other isotopes sometimes used are cobalt-60, cesium-137, tantalum-182, and gold-198. Intense fast neutron sources are provided by californium-252. For treatment of the prostate, 40–100 rice-sized seeds (4.5-mm long and 0.81-mm diameter) containing a soft-gamma emitter, Pd-103, are implanted via thin hollow needles (Garnick and Fair, 1998). Computerized tomography (CT) and ultrasound aid in the implantation.

One sophisticated device for administering cancer treatment uses a pneumatically controlled string of glass beads impregnated with cesium-137 that are encapsulated in stainless steel of only 2.5-mm diameter. Tubes containing the beads are inserted in the bronchus, larynx, and cervix.

Success in treatment of abnormal pituitary glands is obtained by charged particles from an accelerator, and beneficial results have come from slow neutron bombardment of tumors in which a boron solution is injected. Selective absorption of chemicals makes possible the treatment of cancers of certain types by administering the proper radionuclides. Examples are iodine-125 or iodine-131 for the

thyroid gland and phosphorus-32 for the bone. However, there is concern in medical circles that use of iodine-131 to treat hyperthyroidism could cause thyroid carcinoma, especially in children.

EXAMPLE 14.1

A patient ingests 155 mCi of I-131 to destroy remnant tissue after surgical removal of the thyroid. Before releasing the patient, the measured dose rate at 1 m should be less than 7 mrem/h (per NUREG-1556 Appendix U (Howe et al., 2008)). Focusing on the more penetrating, and correspondingly longer range, gamma ray emissions, as listed in Table 3.2, yields a dose rate at 1 m of

$$\begin{aligned}\dot{H} &= \frac{S}{4\pi r^2}[E_1(\mu_{en}/\rho)+E_2(\mu_{en}/\rho)+E_3(\mu_{en}/\rho)]QF \\ &= \frac{(155\,\text{mCi})\left(3.7\times10^7\,\text{decay/s/mCi}\right)}{4\pi(100\,\text{cm})^2}\left[(0.284\,\text{MeV})(0.061\,\gamma/\text{decay})\left(0.03156\,\text{cm}^2/\text{g}\right)+\right. \\ &\quad \left.(0.364\,\text{MeV})(0.815\,\gamma/\text{decay})\left(0.03248\,\text{cm}^2/\text{g}\right)+(0.637\,\text{MeV})(0.072\,\gamma/\text{decay})\left(0.03270\,\text{cm}^2/\text{g}\right)\right] \\ &\quad \left(1.602\times10^{-13}\,\text{J/MeV}\right)(1000\,\text{g/kg})\left(10^5\,\text{mrad/(J/kg)}\right)(3600\,\text{s/h})(1\,\text{mrem/mrad}) \\ &= 31\,\text{mrem/h}\end{aligned}$$

where we have conservatively neglected any attenuation by the body. With an effective half-life of 0.76 d, the exponential decay behavior leads to a projected patient discharge delay time of

$$t = \frac{-t_E}{\ln(2)}\ln\left(\frac{\dot{H}(t)}{\dot{H}_0}\right) = \frac{-0.76\,\text{d}}{\ln(2)}\ln\left(\frac{7\,\text{mrem/h}}{31\,\text{mrem/h}}\right) = 1.6\,\text{d} = 39\,\text{h}$$

Note that this calculation does not incorporate an *occupancy factor*, which reduces the estimated dose to other individuals by considering the interaction time with and distance from the patient.

Patients discharged after therapeutic doses of administered radionuclides have been known to activate radiation detectors installed for security purposes. A strong residual radioactivity in a patient represents not only an external dose source to others, but also a potential internal exposure contamination pathway via, for example, saliva.

Relief from rheumatoid arthritis is obtained by irradiation with beta particles. The radionuclide dysprosium-165 (2.33 h) is mixed with ferric hydroxide, which serves as a carrier. The radiation from the injected radionuclide reduces the inflammation of the lining of joints.

A great deal of medical research is an outgrowth of radioimmunoassay (see Section 13.5). It involves monoclonal antibodies (MAbs), which are radiolabeled substances that have an affinity for particular types of cancer, such as those of the skin and lymph glands. The diseased cells are irradiated without damage to neighboring normal tissue. The steps in this complex procedure start with the injection into mice of human cancer cells as antigens. The mouse spleen, a part of the immune system, produces antibodies through the lymphocyte cells. These cells are removed and blended with myeloma cancer cells to form new cells called hybridoma. In a culture, the hybridoma clones itself to produce the MAb. Finally, a beta-emitting radionuclide such as yttrium-90 is chemically bonded to the antibody.

A promising treatment for cancer is boron neutron capture therapy (BNCT) (Moss, 2014). A boron compound that has an affinity for diseased tissue is injected, and the patient is irradiated with neutrons from a reactor. Boron-10, with abundance of 20% in natural boron, strongly absorbs thermal neutrons to release lithium-7 and helium-4 ions. An energy of more than 2 MeV is deposited locally because of the short range of the particles. Brookhaven National Laboratory pioneered the technique in the 1950s, but the program was suspended from 1961 to 1994 and terminated in 1999. Research is continuing at other locations, however (Barth et al., 2005). A compound, Bisphenol A (BPA), was found that localized boron better, and thermal neutrons were replaced by intermediate energy neutrons, with favorable

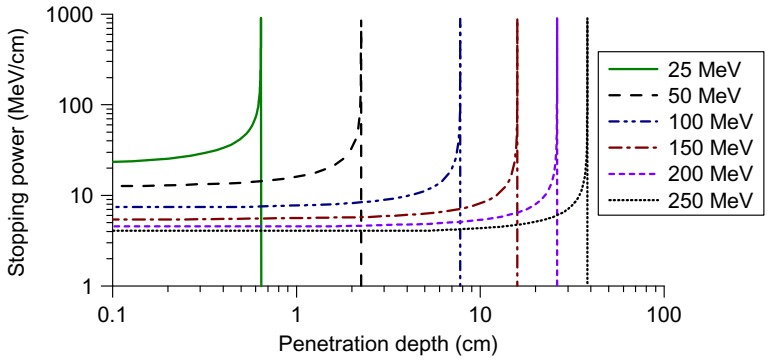

FIG. 14.1

Bragg curves for proton passage through ICRU four-component soft tissue. Data generated using the Monte Carlo radiation transport code MCNP6 (Goorley et al., 2012).

results. A single treatment with BNCT is as effective as many conventional radiation-chemotherapy sessions. The method has been found to be effective in treatment of malignancies such as melanoma (skin) and glioblastoma multiforme (brain). The discovery of monoclonal antibodies opens up new possibilities for large-scale use of BNCT.

Cancer treatment is also being undertaken using accelerator-delivered proton beams. Judicious selection of the proton energy permits determining the depth at which most of the particle energy deposits. The Bragg curve graphs the charged particle energy loss as a function of penetration depth into a material (Bragg and Kleeman, 1904). An ionization peak—referred to as a Bragg peak—occurs near the end of the particle path, thus giving rise to a greater local dose at that point. Fig. 14.1 shows the concentration of linear energy transfer for protons within tissue. Modulation of the beam energy achieves a spread out Bragg peak. Moreover, compared to an electron, the more massive proton undergoes less angular deflections. The advantage then of proton beam therapy lies in the ability to target cancerous cells more precisely while preserving the normal tissue. Proton treatment is seen as especially suited for children in order to avoid radiogenic-caused second cancers later in their lifetime (Levin et al., 2005; Eaton et al., 2015).

14.2 RADIATION PRESERVATION OF FOOD

The ability of radiation treatment to eliminate insects and microorganisms from food has been known for many years. Significant benefits to the world's food supply are beginning to be realized, as a number of countries build irradiation facilities. Such application in the United States has been slow because of fears related to anything involving radiation.

Spoilage of food before it reaches the table is due to a variety of effects: sprouting as in potatoes, rotting caused by bacteria as in fruit, and insect infestation as in wheat and flour. Certain diseases stem from microorganisms that contaminate food. Examples are the bacteria *Salmonella*, found in many poultry products, and the parasite trichinae that infest some pork. The Centers for Disease Control and Prevention (CDC) state that foodborne illnesses affect millions of people in the United States each year, causing thousands of deaths (Scallan et al., 2011).

Various treatments are conventionally applied to preserve food, including drying, pickling, salting, freezing, canning, pasteurization, sterilization, the use of food additives such as nitrites, and—until they were banned—the application of fumigants such as ethylene dibromide (EDB). Each treatment method has its advantages, but nitrites and EDB are believed to have harmful physiological effects.

On the other hand, research has shown that gamma radiation processing can serve as an economical, safe, and effective substitute and supplement for existing treatments. The shelf life of certain foods can be extended from days to weeks, allowing adequate time for transportation and distribution. It has been estimated that 20%–50% of the food supplied to certain countries is wasted by spoilage that could be prevented by radiation treatment. The radiation dosages required to achieve certain goals are listed in Table 14.2. The principal sources of ionizing radiation suitable for food processing are X-rays, electrons from an accelerator, and gamma rays from a radionuclide. Much experience has been gained from the use of cobalt-60, half-life 5.27 y, with its two gamma rays of energy 1.17 and 1.33 MeV. The largest supplier of Co-60 is a Canadian firm, MDS Nordion, formerly part of Atomic Energy of Canada, Ltd. The isotope is prepared by irradiating pure cobalt-59 target pellets with neutrons in CANDU and RBMK reactors (see Section 18.5 and Section 21.8). The targets are disassembled and shipped for processing into double-layer capsules of approximately 10 Ci (370 GBq) each. Another attractive isotope is cesium-137, gamma ray 0.662 MeV, because of its longer half-life of 30.1 y and its potential availability as a fission product. A considerable amount of Cs-137 has been separated at Hanford, Washington, as a part of the radioactive waste management strategy. Arrangements for loans of capsules from the Department of Energy (DOE) to industrial firms have been made. Additional Cs-137 could be obtained through limited reprocessing of spent reactor fuel.

Many people are concerned about the use of irradiated products because of the association with nuclear processes. The first worry is that the food might become radioactive. The concern is unfounded, because there is no detectable increase in radioactivity at the dosages and particle energies of the electrons, X-rays, or gamma rays used. Even at higher dosages than are planned, the induced radioactivity would be less than that from natural amounts of potassium-40 or carbon-14 in foods. Another fear is that hazardous chemicals may be produced via radiolysis. Research shows that the amounts of unique radiolytic products (URP) are small, less than those produced by cooking or canning, and similar to natural food constituents. No indication of health hazard has been found, but scientists recommend continuing monitoring of the process. A third concern is that there would be a loss in nutritional value. Some loss in vitamin content occurs, just as it does in ordinary cooking. Research is continuing on the effects of radiation on nutritional value. It seems that the loss is minor at the low dose levels used. On various food products, there are certain organoleptic effects (changes in taste, smell, color, texture), but these are a matter of personal reaction, not of health. Even these effects can be eliminated by operating

Table 14.2 Doses to Achieve Beneficial Effects

Effect	Dose (Gy)
Inhibit sprouting of potatoes and onions	60–150
Eliminate trichinae in pork	200–300
Kill insects and eggs in fruits	200–500
Disinfect grain, prolong berry life	200–1000
Delay ripening of fruit	250–350
Eliminate salmonella from poultry	1000–3000

the targets at reduced temperatures. The astronauts of the Apollo missions and the space shuttle have dined regularly on treated foods while in orbit. They were enthusiastic about the irradiated bread and meats. Many years ago, some scientists in India reported that consumption of irradiated wheat caused polyploidy, an increase in cell chromosomes. Extensive studies elsewhere disproved the finding.

Finally, it has been suggested that radiation might induce resistance of organisms, just as with pesticides and antibiotics, but the effect seems not to occur. The difference is attributed to the fact that there is a broad effect on enzymes and compounds.

The main components of a multiproduct irradiation facility that can be used for food irradiation on a commercial basis are shown in Fig. 14.2. Important parts are:

a. Transfer equipment, involving conveyors for pallets, which are portable platforms on which boxes of food can be loaded.
b. An intense gamma ray source with a strength of approximately 1 million curies consisting of doubly encapsulated pellets of Co-60.
c. Water tanks for storage of the source, with a cooling and purification system.
d. A concrete biological shield, approximately 2 m thick.

In the operation of the facility, a rack of cobalt rods is raised out of the water pool, and the food boxes are exposed as they pass by the gamma source. Commercial firms providing irradiation equipment and carrying out irradiations, mainly for sterilization of medical supplies, are MDS Nordion of Ontario, Canada; Food Technology Service, Inc. of Mulberry, Florida; STERIS of Whippany, New Jersey; and Sterigenics International of Oak Brook, Illinois, which has facilities around the world. Among

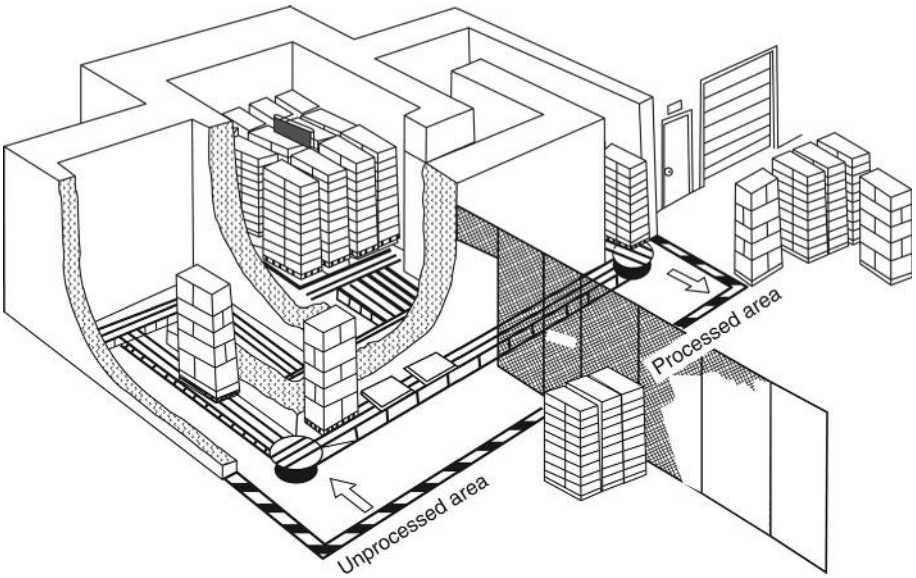

FIG. 14.2

Gamma irradiation of Sterigenics International, at Haw River, North Carolina. Pallets containing boxes of products move on a computer-controlled conveyor through a concrete maze past a gamma-emitting screen.

services provided is mold remediation in books, documents, and records with gamma rays. A fruit company, Pa'ina Hawaii, operates a Co-60 irradiator at Honolulu for phytosanitary treatment of exotic fruits such as papayas before shipment to the continental United States and foreign markets.

EXAMPLE 14.2

To understand the use of 2 m of concrete for a 1-MCi source of Co-60, the dose outside this shielding is computed. Conservatively assume that the source is directly encased in the concrete such that the uncollided flux is obtained from Eq. (11.9)

$$\phi_u = \frac{S\exp(-\mu r)}{4\pi r^2} = \frac{(10^6\,\text{Ci})\exp[-(0.05807\,\text{cm}^2/\text{g})(2.3\,\text{g/cm}^3)(200\,\text{cm})]}{4\pi(200\,\text{cm})^2(1\,\text{Ci}/3.7\times10^{10}\,\text{Bq})(1\,\text{decay}/2\,\text{photons})} = 0.37\,\text{photons}/(\text{cm}^2\,\text{s})$$

However for $\mu r = 27$ mean free paths, the buildup factor in concrete is about 70 such that the actual flux is $\phi = B\phi_u = (70)(0.37\,\gamma/\text{cm}^2\,\text{s}) = 26\,\gamma/(\text{cm}^2\,\text{s})$. Therefore, the dose rate is

$$\dot{D} = \phi E_\gamma \mu_{en}/\rho = \frac{(26\gamma/(\text{cm}^2\,\text{s}))(1.25\,\text{MeV}/\gamma)(0.02965\,\text{cm}^2/\text{g})}{(1\,\text{MeV}/1.6\times10^{-13}\,\text{J})(1\,\text{kg}/1000\,\text{g})}$$
$$= (1.5\times10^{-10}\,\text{Gy/s})(3.1558\times10^7\,\text{s/y})(10^5\,\text{mrad/Gy}) = 490\,\text{mrad/y}$$

The actual dose rate is lower because the material being irradiated is also absorbing gamma energy and the concrete must be at sufficient distance from the source to permit passage of this material.

A number of experimental facilities and irradiation pilot plants have been built and used in some 70 countries. Some of the items irradiated have been grain, onions, potatoes, fish, fruit, and spices. The most active countries in the development of large-scale irradiators have been the United States, Canada, Japan, and the former USSR.

Table 14.3 shows the approvals for irradiation as issued by the US Food and Drug Administration (FDA). Limitations are typically set on dosages to foodstuffs of 1 kGy (100 krad) except for dried spices, not to exceed 30 kGy (3 Mrad). Final rules on red meat irradiation as a food additive were issued by the FDA (1997) in December 1997 and by the US Department of Agriculture (USDA, 1999) in December 1999. The action was prompted in part by the discovery of the bacteria *Escherichia coli* contamination of hamburger by an Arkansas supplier (Henkel, 1998). Some 25 million pounds of meat were recalled and destroyed. That rule cites statistics on outbreaks of disease and numbers of deaths related to beef. Maximum permitted doses for meat are 4.5 kGy (450 krad) as refrigerated and 7.0 kGy (700 krad) as frozen. More than 80 technical references are cited by the FDA (1997) on all aspects of the subject.

Labeling of the packages to indicate special treatment is required by use of a phrase such as "treated with radiation." In addition, packages will exhibit the international logo, called a *radura*, shown in Fig. 14.3. The symbol's two petals signify food; the solid circle represents an energy source; the breaks in the outer circle mean rays from the energy source. The radura label is required for shipment to the first purchaser, not for a consumer in a restaurant. Labeling of radiation-treated food is obviously a factor in acceptance by the public.

Approval to irradiate does not guarantee that it actually will be done, however. Many large food processors and grocery chains tend to shy away from the use of irradiated food products, believing that the public will be afraid of all their products. Obviously, people will not have much opportunity to find treated foods acceptable if there are few products on the market. Antiirradiation activists, who claim

Table 14.3 Approvals by the US Food and Drug Administration for Use of Irradiated Substances

Product	Irradiation Purpose	Maximum Dose (kGy)
Fresh pork	Control *Trichinella spiralis*	0.3–1
Fresh foods	Growth and maturation inhibition	1
All foods	Arthropod pest disinfestation	1
Enzyme preparations	Microbial disinfection	10
Spices, seasonings	Microbial disinfection	30
Poultry	Foodborne pathogen control	Nonfrozen: 4.5; frozen: 7.0
Beef, lamb, pork, goat	Control of foodborne pathogens and extension of shelf life	Nonfrozen: 4.5; frozen: 7.0
Fresh shell eggs	Control of *Salmonella*	3.0
Seeds for sprouting	Control of microbial pathogens	8.0
Molluscan shellfish	Control of *Vibrio* bacteria and other foodborne microorganisms	5.5
Iceberg lettuce, spinach	Control of foodborne pathogens and extension of shelf life	4.0
Crustaceans	Control of foodborne pathogens and extension of shelf life	6.0

Data from U.S. Food and Drug Administration (FDA), 2017. Ionizing Radiation for the Treatment of Food. 21CFR179.26; Komolprasert, V., Bailey, A., Machuga, E., 2007. Regulatory report: irradiation of food packaging materials. Food Safety Mag., December 2007–January 2008.

FIG. 14.3

International logo (radura) to appear on irradiated food (USDA version).

that the nuclear irradiation process is unsafe, have taken advantage of that reluctance. In contrast, enthusiastic endorsement of food irradiation is provided by groups such as the World Health Organization, the American Medical Association, the American Dietetic Association, the International Atomic Energy Agency, the Grocery Manufacturers of America, and many others.

At the First World Congress on Food Irradiation, held in 2003, a number of facts were reported. The 2002 Food Bill specified that irradiated food should be made available to the National School Lunch Program; regulation of facilities was developed by an International Consultative Group on Food Irradiation (ICGFI) and adopted worldwide; consumers are generally aware of beef irradiation (68%) and favor marketing irradiated ground beef (78%).

14.3 STERILIZATION OF MEDICAL SUPPLIES

Ever since the germ theory of disease was discovered, increasingly effective methods of sterilizing medical products have been sought. Example items are medical instruments, plastic gloves, sutures, dressings, needles, and syringes. Traditional methods of killing bacteria include dry heat, steam under pressure, and strong chemicals such as carbolic acid and gaseous ethylene oxide. Some of the chemicals are too harsh for equipment that is to be reused, and often the substances themselves are hazardous. Most of the previous methods are batch processes, difficult to scale up to handle the production needed. More recently, accelerator-produced electron beams have been introduced and preferred for some applications.

The special virtue of Co-60 gamma-ray sterilization is that the rays penetrate matter effectively. The item can be sealed in plastic and then irradiated, assuring freedom from microbes until the time it is needed in the hospital. Although the radioactive material is expensive, the system is simple and reliable, consisting principally of the source, the shield, and the conveyor. A typical automated plant requires a source of approximately 1 MCi (37 PBq).

The *decimal reduction dose*, D_{10}, quantifies the radiation resistance of a microorganism. D_{10} is defined as the absorbed dose needed to reduce the microbial population by a factor of 10. For example, D_{10} for *Salmonella* and *Streptococcus* is 1.0 and 5.5 kGy (Marciniec and Dettlaff, 2008), respectively, whereas for *Deinococcus radiodurans* it is 13 kGy (Daly, 2009). The sterility assurance level (SAL) describes the probability of the presence of a viable microorganism on a product after sterilization.

EXAMPLE 14.3

To achieve a SAL of 10^{-6} for an initial bioburden of 1000 microorganisms per mL requires 9 (=3+6) orders of magnitude reduction in the population. For a D_{10} of 2.8 kGy, the required sterilization dose is $D = 9\ D_{10} = (9)(2.8\,\text{kGy}) = 25\,\text{kGy}$.

14.4 PATHOGEN REDUCTION

In the operation of public sewage treatment systems, enormous amounts of solid residues are produced. In the United States alone, annual production of sewage sludge amounts to about 6.5 million dry metric tons (Venkatesan et al., 2015). Typical methods of disposal are by incineration, burial at sea, placement in landfills, and application to cropland. In all these, there is some hazard caused by pathogens—disease-causing organisms such a parasites, fungi, bacteria, and viruses. Experimental tests of pathogen reduction by Co-60 or Cs-137 gamma irradiation have been conducted in Germany and the United States. The program in the United States was part of the Department of Energy's studies of beneficial

uses of fission product wastes and was carried out at Sandia National Laboratories and the University of New Mexico. Tests of the effectiveness of radiation were made, and the treated sludge was found to be suitable as a feed supplement for livestock, with favorable economics. However, no use of those results was made in the United States. Apparently, the only large-scale application of sewage sludge irradiation is in Argentina, in the large city of Tucuman (IAEA, 1997a). It is conceivable that the time is not yet ripe in the United States and Europe for such application of radiation. It took a number of years to adopt recycling of household wastes.

Irradiation has also been touted as a means of neutralizing viral agents that could be used in biowarfare or bioterrorism (Lowy, 2005). In the aftermath of the anthrax (*Bacillus anthracis*)-laden letters sent through the postal mail in fall 2001, the US Postal Service decontaminated mail in the affected facilities using 56 kGy of electron beam irradiation (Helfinstine et al., 2005).

14.5 CROP MUTATIONS

Beneficial changes in agricultural products are obtained through mutations caused by radiation. Seeds or cuttings from plants are irradiated with charged particles, X-rays, gamma rays, or neutrons, or chemical mutagens are applied. Genetic effects have been created in a large number of crops in many countries. The science of crop breeding has been practiced for many years. Unusual plants are selected and crossed with others to obtain permanent and reproducible hybrids. However, a wider choice of stock to work with is provided by mutant species. In biological terms, genetic variability is required.

Features that can be enhanced are larger yield, higher nutritional content, better resistance to disease, and adaptability to new environments, including higher or lower temperature of climate. New species can be brought into cultivation, opening up sources of income and improving health.

The leading numbers of mutant varieties of food plants that have been developed are as follows: rice, 28; barley, 25; bread wheat, 12; sugar cane, 8; and soybeans, 6. Many mutations of ornamental plants and flowers have also been produced, improving the income of small farmers and horticulturists in developing countries. For example, there are 98 varieties of chrysanthemum. The International Atomic Energy Agency (IAEA), since its creation in 1957, has fostered mutation breeding through training, research support, and information transfer. The improvement of food is regarded by the IAEA as a high-priority endeavor in light of the expanding population of the world.

More recently, the application of genetic engineering to improve crops and foodstuffs has drawn a great deal of criticism, especially in Europe, and a deep-seated conflict with the United States over use of biotechnology will be difficult to resolve.

14.6 INSECT CONTROL

To suppress the population of certain insect pests, the sterile insect technique (SIT) has been applied successfully. The standard method is to breed large numbers of male insects in the laboratory, sterilize them with gamma rays, and release them for mating in the infested area. Competition of sterile males with native males results in a rapid reduction in the population.

The classic case was the eradication of the screwworm fly from Curaçao, Puerto Rico, and the southwestern United States. The flies lay eggs in wounds of animals and the larvae feed on living flesh

and can kill the animal if untreated. After the numbers were reduced in the early 1960s, flies came up from Mexico, requiring a repeat operation. As many as 350 million sterile flies were released each week, bringing the infestations from 100,000 to 0. The annual savings to the livestock industry was approximately $100 million.

The rearing of large numbers of flies is a complex process, involving choice of food, egg treatment, and control of the irradiation process to provide sterilization without causing body damage. Cobalt-60 gamma rays are typically used to give doses (e.g., 5 krad) that are several times the amounts that would kill a human being. The dose must be optimized, as the mating competitiveness of the sterile male insects is generally lower than that of native fertile males.

EXAMPLE 14.4

The LD 50/30 for humans is approximately 4 Gy (see Section 10.2) while the dose to sterilize 95% of the male tsetse flies is around 90 Gy. In contrast, the dose equivalent to the testes causing temporary and permanent sterility in an adult human is 0.15 and 3.5 Sv, respectively (NCRP, 1989).

SIT has been used against several species of mosquito in the United States and India and stopped the infestation of the Mediterranean fruit fly in California in 1980.

The discovery of a screwworm infestation in Libya in 1988 prompted international emergency action by the United Nations Food and Agriculture Organization, the International Atomic Energy Agency, and others (Lindquist and Abusowa, 1992; Van der Vloedt and Butt, 1990). Arrangements were made for the fly factory in Mexico to supply millions of radiation-sterilized males to Libya. There, light aircraft dropped them in a grid pattern, starting in 1990. Within 5 months, the screwworm was eradicated, thus protecting Libyan wildlife as a whole.

The technique was effective on the island of Zanzibar, part of Tanzania, in combating the tsetse fly (see IAEA, 1997b; FAO, 1998; Vreysen et al., 2014). The insect is a carrier of trypanosomiasis, a livestock disease, and of sleeping sickness, which affects humans. Prior pesticide use made SIT feasible, and within 2 y, by 1996, there were no flies left. Unfortunately, vast areas of Africa are infested with tsetse flies, and the fly-free zones are overloaded.

SIT can potentially control *Heliothis* (American bollworm, tobacco budworm, and corn earworm) and other pests such as ticks and the gypsy moth. Other related techniques include genetic breeding that will automatically yield sterile males. Another potential SIT application is the control of mosquitoes carrying the Zika virus.

Some of the organizations providing gamma-ray insect irradiation are ceasing operations for fear of terrorist action. An alternative is the use of X-rays.

14.7 APPLICATIONS IN CHEMISTRY

Radiation chemistry refers to the effect of high-energy radiation on matter, with particular emphasis on chemical reactions. Examples are ion-molecule reactions, capture of an electron that leads to dissociation, and charge transfer without a chemical reaction when an ion strikes a molecule. Many reactions have been studied in the laboratory, and a few have been used on a commercial scale. For a number of years, Dow Chemical used Co-60 radiation in the production of ethyl bromide (CH_3CH_2Br), a volatile

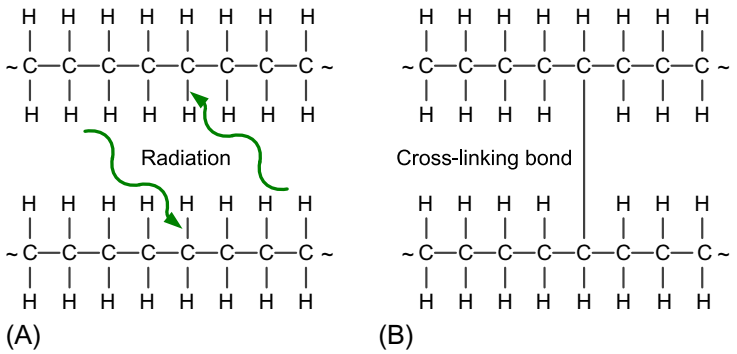

FIG. 14.4

Radiation-induced cross-linking in long chains of polyethylene. (A) Radiation breaks original bonds and (B) single bond cross-links chain.

organic liquid used as an intermediate compound in the synthesis of organic materials. The application was terminated for reasons of cost and safety. As catalysts, gamma rays have been found to be superior in many cases to chemicals, to the application of ultraviolet light, and to electron bombardment.

Various properties of polymers such as polyethylene are changed by electron or gamma ray irradiation. The original material consists of long parallel chains of molecules, and radiation damage causes chains to be connected in a process called *cross-linking*, as depicted in Fig. 14.4. Irradiated polyethylene has better resistance to heat and serves as a good insulating coating for electrical wires. Fabrics can be made soil-resistant by radiation bonding of a suitable polymer to a fiber base.

Highly wear-resistant wood flooring is produced commercially by gamma irradiation. Wood is soaked in a monomer plastic, encased in aluminum, and placed in a water pool containing a cesium-137 source of 661 keV photons. The process of polymerization takes place throughout the wood. The molecular structure is changed so that the surface cannot be scratched or burned.

A related process has been applied in France to the preservation of artistic or historic objects of wood or stone. The artifact is soaked in a liquid monomer and transferred to a Co-60 gamma cell where the monomer is polymerized into a solid resin.

The chemical yield from radiation is described using G values, which quantify the number of moles transformed per energy absorbed. For example, G is 0.047 μmol/J for the production of H_2 from liquid water exposed to gamma rays and electrons (Choppin et al., 2002).

14.8 TRANSMUTATION DOPING OF SEMICONDUCTORS

Semiconductor materials are used in a host of modern electrical and electronic devices. Their functioning depends on the presence of small amounts of impurities such as phosphorus in the basic crystal element silicon. The process of adding impurities is called doping. For some semiconductors, impurities can be introduced in the amounts and locations needed by use of neutron irradiation to create an isotope that decays into the desired material.

The process is relatively simple. A pure silicon monocrystal is placed in a research or experimental reactor of several megawatts power level. The sample is irradiated with a previously calibrated thermal neutron flux for a specified time. This converts one of the silicon isotopes into a stable phosphorus isotope by the reactions

$$\begin{aligned} {}^{1}_{0}\mathrm{n} + {}^{30}_{14}\mathrm{Si} &\rightarrow {}^{31}_{14}\mathrm{Si} + \gamma \\ {}^{31}_{14}\mathrm{Si} &\rightarrow {}^{31}_{15}\mathrm{P} + {}^{0}_{-1}\mathrm{e} \end{aligned} \tag{14.1}$$

where the abundance of Si-30 is 3.1% and the half-life of Si-31 is 2.62 h. After irradiation, the silicon resistivity is too high because of radiation damage caused by the fast neutron component of the flux. Heat treatment is required before fabrication to anneal out the defects.

The principal application of neutron transmutation doping (NTD) has been in the manufacture of power thyristors, which are high-voltage, high-current semiconductor rectifiers (Baliga, 1982), so named because they replaced the thyratron, a vacuum tube. The virtue of NTD compared with other methods is that it provides a uniform resistivity over the large area of the device. Annual yields of the product material are more than 50 tons, with a considerable income to the reactor facilities involved in the work. NTD is expected to become even more important in the future for household and automotive devices. The doping method is also applicable to other substances besides silicon (e.g., germanium and gallium arsenide).

EXAMPLE 14.5

In a constant neutron flux, Si-31 is generated at a rate of $g = \Sigma_\gamma \phi$ such that Eq. (4.36) describes the ^{31}Si atomic density while the silicon is being irradiated

$$N_{\text{Si-31}}(t) = \left(\Sigma_\gamma^{\text{Si-30}} \phi / \lambda\right)\left(1 - e^{-\lambda t}\right) \quad \text{for } t \le t_{\text{I}} \tag{14.2}$$

After an irradiation period of t_{I}, the production of ^{31}Si ceases and only decay occurs such that

$$N_{\text{Si-31}}(t) = \left(\Sigma_\gamma^{\text{Si-30}} \phi / \lambda\right)\left(1 - e^{-\lambda t_{\text{I}}}\right) e^{-\lambda (t - t_{\text{I}})} \quad \text{for } t \ge t_{\text{I}} \tag{14.3}$$

The P-31 dopant accrues from the decay of ^{31}Si at a rate of $\lambda N_{\text{Si-31}}(t)$. If sufficient time passes for essentially all the radioactive ^{31}Si atoms to decay, we reason that the total dopant concentration is simply equal to the number of neutron captures

$$N_{\text{P-31}} = \Sigma_\gamma^{\text{Si-30}} \phi t_{\text{I}} \tag{14.4}$$

The formal mathematical steps for arriving at the above relation are left as Exercise 14.10.

14.9 NEUTRONS IN FUNDAMENTAL PHYSICS

Intense neutron beams produced in a research reactor serve as powerful tools for investigation in physics. Three properties of the neutron are important in this work: (1) the lack of electrical charge, which allows a neutron to penetrate atomic matter readily until it collides with a nucleus; (2) a magnetic moment, resulting in special interaction with magnetic materials; and (3) its wave character, causing beams to exhibit diffraction and interference effects.

Measurements of neutron cross-sections of nuclei for scattering, capture, and fission are necessary for reactor analysis, design, and operation. An area of study that goes beyond those needs is called inelastic neutron scattering. It is based on the fact that the energy of thermal neutrons, 0.0253 eV, is comparable to the energy of lattice vibrations in a solid or liquid. Observations of changes in the energy of bombarding neutrons provide information on the interatomic forces in materials, including the effects of impurities in a crystal, which is of interest in semiconductor research. Additionally, inelastic scattering yields understanding of microscopic magnetic phenomena and the properties of molecular gases.

We recall that the magnetic moment of a bar magnet is the product of its length s and the pole strength p. For charges moving in a circle of radius r, the magnetic moment is the product of the area πr^2 and the current i. Circulating and spinning electrons in atoms and molecules also give rise to magnetic moments. Even though the neutron is uncharged, it has an intrinsic magnetic moment. Thus, the neutron interacts differently with materials according to their magnetic properties. If the materials are paramagnetic, with randomly oriented atomic moments, no special effect occurs. Ferromagnetic materials such as iron and manganese have unpaired electrons, and moments are all aligned in one direction. Antiferromagnetic materials have aligned moments in each of two directions. Observations of scattered neutrons lead to understanding of the microscopic structure of such materials.

The wavelength of a particle of mass m and speed v according to the theory of wave mechanics is

$$\lambda = h/(mv) \tag{14.5}$$

where h is Planck's constant, 6.64×10^{-34} J s.

EXAMPLE 14.6

For neutrons of mass 1.67×10^{-27} kg, at the thermal energy 0.0253 eV, speed 2200 m/s, the wavelength is readily calculated to be

$$\lambda = h/(mv) = \left(6.64 \times 10^{-34}\,\text{J s}\right)/\left[\left(1.67 \times 10^{-27}\,\text{kg}\right)(2200\,\text{m/s})\right] = 1.8 \times 10^{-10}\,\text{m}$$

This is fairly close to d, the spacing of atoms in a lattice; for example, in silicon d is 3.135×10^{-10} m.

The wave property is involved in the process of neutron diffraction, in analogy to X-ray and optical diffraction, but the properties of the materials that are seen by the rays differ considerably. Whereas X-rays interact with atomic electrons and thus diffraction depends strongly on atomic number Z, neutrons interact with nuclei according to their scattering lengths, which are unique to the isotope, and are rather independent of Z. Scattering lengths, labeled a, resemble radii of nuclei but have both magnitude and sign. For nearby isotopes, a values and the corresponding cross-sections $\sigma = \pi r^2$ differ greatly. For example, the approximate σ_s values of three nickel isotopes are: Ni-58, 26 b; Ni-60, 1 b; and Ni-62, 10 b (Sears, 1992). In neutron diffraction one applies the Bragg formula $\lambda = 2d \sin(\theta)$, where d is the lattice spacing and θ is the scattering angle. Various isotopes, elements, and compounds have been investigated by neutron diffraction, as discussed by Bacon (1975).

A still more modern and sophisticated application of neutrons is *interferometry* in which neutron waves from a nuclear reactor source are split and then recombined. We can describe the essential equipment needed. A perfect silicon crystal is machined very accurately in the form of the letter E, making sure the planes are parallel. A neutron beam entering the splitter passes through a mirror plate and analyzer. Reflection, refraction, and interference take place, giving rise to a periodic variation of observed

intensity. Insertion of a test sample causes changes in the pattern. The method has been used to measure accurately the scattering lengths of many materials. Images of objects are obtained in *phase topography*, so named because the introduction of the sample causes a change in phase in the neutron waves in an amount dependent on thickness, allowing observation of surface features. Interference fringes have been observed for neutrons passing through slightly different paths in the Earth's magnetic field. This suggests the possibility of studying the relationship of gravity, relativity, and cosmology.

In the Spallation Neutron Source (SNS) (in Section 9.7), wavelengths and energies of neutrons produced match the size and energy scales of many materials of interest. Its enhanced neutron beams allow higher resolution images of biological materials. Of special benefit in the SNS is the ability to locate hydrogen atoms in complex molecules. Neutron crystallography studies will lead to more effective drugs (ORNL, 2001).

The broad scope of research with SNS can be appreciated by a listing of areas adapted from the Oak Ridge National Laboratory (ORNL) website:[1]

Chemistry. Use of neutron scattering to study microstructures in chemical products.
Complex fluids. Investigation of new time-release drug-delivery systems targeting specific parts of the human body.
Crystalline materials. Research on ways to tailor structures and properties of new materials.
Disordered materials. Study of proteins of interest to biological industries.
Engineering. Knowledge on material failures and substitutes.
Magnetism and superconductivity. Understanding leading to improved devices.
Polymers. Small-angle scattering to reveal behavior of molecular chains.
Structural biology. Neutrons as complement to X-rays for studying vitally important chemicals.

14.10 NEUTRONS IN BIOLOGICAL STUDIES

One of the purposes of research in molecular biology is to describe living organisms by physical and chemical laws. Thus, finding sizes, shapes, and locations of components of biological structures is the first step in understanding. Neutron scattering provides a useful tool for this purpose. The radiation does not destroy the specimen; cross-sections of materials of interest are of the same order for all nuclei so that heavier elements are not favored, as in the case of X-rays; long wavelength neutrons needed to study the large biological entities are readily obtained from a reactor. Of special importance is the fact that scattering lengths for hydrogen (3.8×10^{-15} m) and deuterium (6.5×10^{-15} m) are quite different, so that the neutron scattering patterns from the two isotopes can be readily distinguished.

An example is the investigation of the ribosome. It is a particle approximately 25 nm in diameter that is part of a cell and helps manufacture proteins. The *E. coli* ribosome is composed of two subunits, one with 34 protein molecules and two RNA molecules, the other with 21 proteins and one RNA. The proteins are quite large, with molecular weight as high as 65,000. Study with X-rays or an electron microscope is difficult because of the size of the ribosome. For the neutron experiment, two of the 21 proteins are stained with deuterium (i.e., they are prepared by growing bacteria in D_2O rather than H_2O).

[1] http://neutrons.ornl.gov

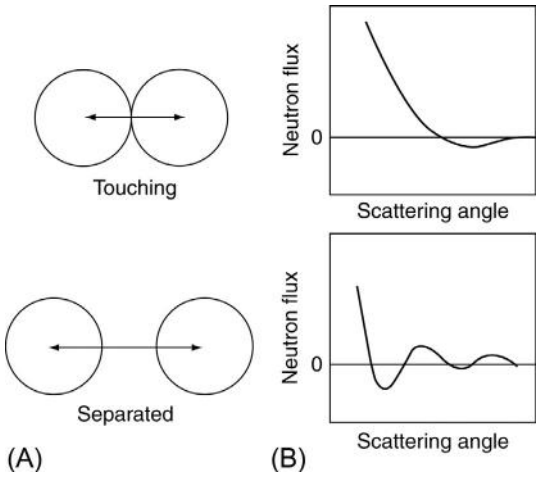

FIG. 14.5

Interference patterns for the ribosome, a particle in the cell. Estimates of size and spacing are a start toward understanding biological structures. (A) Geometric arrangement of protein pairs, and (B) interference curves.

Early research on ribosomes was performed at the Brookhaven National Laboratory High Flux Beam Reactor (now shut down). A beam of neutrons was scattered from a graphite crystal that selected neutrons of a narrow energy range at wavelength 2.37×10^{-10}m. The specimen to be studied was placed in the beam in front of a helium-3 detector, which counted the number of neutrons as a function of scattering angle. The neutron wave, when scattered by a protein molecule, exhibited interference patterns similar to those of ordinary light. A distinct difference in pattern would be expected depending on whether the two molecules are touching or separated, as shown in Fig. 14.5. For the ribosome, the distance between centers of molecules was deduced to be 35×10^{-10}m. Tentative maps of the ribosome subunit were developed as well.

14.11 RESEARCH WITH SYNCHROTRON X-RAYS

Knowledge of the structure of molecules is made possible by the use of synchrotron X-rays because of their high intensity and sharp focus. Studies are faster and less damaging than those with conventional X-rays. Materials in crystalline form are bombarded with photons, and the diffraction patterns are produced on a sensitive screen. The patterns are analyzed by computer by use of the Fourier transform to determine electron densities and thus atom locations. Suitable manipulations yield 3D data. Knowing molecular structure provides information on how chemicals work and helps find better drugs and treatments for disease. A classic example of a synchrotron X-ray study result was the determination of the structure of the rhinovirus HRV14, the cause of the common cold. The crystals were very sensitive to radiation and would cease to diffract before data were obtained by ordinary X-rays. Many other macromolecular proteins, enzymes, hormones, and viruses have been investigated. It is possible to observe chemical processes as they occur (e.g., photodissociation of hydrocarbons and of ozone). Information for improvement of industrial processes and products is also made available.

14.12 SUMMARY

Many examples of the use of radiation for beneficial purposes can be cited. Diseases such as cancer can be treated by gamma rays. Food spoilage is reduced considerably by irradiation. Medical supplies are rendered sterile within plastic containers. Sewage sludge can be disinfected by irradiation. New and improved crops are produced by radiation mutations. The sterile insect technique has controlled insect pests in many areas of the world. Radiation serves as a catalyst in the production of certain chemicals. Properties of fibers and wood are enhanced by radiation treatment. Desirable impurities can be induced in semiconductor materials by neutron bombardment. The scattering by neutrons provides information on magnetic materials, and interference of neutron beams is used to examine surfaces. Scattered neutrons yield estimations of location and size of minute biological structures. Synchrotron X-rays are required for detailed study of biological molecules.

14.13 EXERCISES

14.1 Thyroid cancer is treated successfully by the use of iodine-131, half-life 8.04 d, energy release approximately 0.5 MeV. The biological half-life of I-131 for the thyroid is 4 d. Estimate the number of millicuries of the isotope that should be administered to obtain a dose of 25,000 rad to the 20-g thyroid gland.

14.2 The disease polycythemia vera (PV) is characterized by an excess of red blood cells. Treatment by chemotherapy and radiation is often successful. In the latter, the patient is injected with a solution of sodium phosphate containing phosphorus-32, half-life 14.28 d, average beta energy 0.69 MeV. Estimate the dose in rad resulting from the administration of an initial 10 mCi of P-32, of which 10% goes to the 3-kg bone marrow. Suggestion: Neglect biological elimination of the isotope.

14.3 A company supplying Co-60 to build and replenish radiation sources for food processing uses a reactor with thermal flux $10^{14}/(\text{cm}^2\,\text{s})$. To meet the demand of a megacurie per month, how many kilograms of Co-59 must be inserted in the reactor? Note that the density of Co-59 is $8.9\,\text{g/cm}^3$ and the thermal neutron capture cross-section is 37 barns.

14.4 A cobalt source is to be used for irradiation of potatoes to inhibit sprouting. What strength in curies is needed to process 250,000 kg of potatoes per day, providing a dose of 10,000 rad? Recall that the two gammas from Co-60 total approximately 2.5-MeV energy. What is the amount of isotopic power? Discuss the practicality of absorbing all the gamma energy in the potatoes.

14.5 Transmutation of silicon to phosphorus is to be achieved in a research reactor. The capture cross-section of silicon-30, abundance 3.1%, is 0.108 barns. How large must the thermal flux be to produce an impurity content of 10 parts per billion in a day's irradiation?

14.6 Natural silicon consists of three stable isotopes: ^{28}Si, ^{29}Si, and ^{30}Si. Eq. (14.1) shows the production of an *n*-type (negative type) dopant from the ^{30}Si(n, γ) reaction. How do the corresponding (n, γ) reactions in the other two Si isotopes impact the doped material produced?

14.7 A patient is being treated for skin cancer using a monoenergetic beam of 4-MeV electrons incident to the patient's nose. To protect the patient's eyes, an aluminum shield is to be placed over the eyes. Calculate the minimum thickness of Al needed to stop all the electrons.

14.8 A conveyer system travels a 250-m serpentine path in a food irradiation facility in which the average dose rate is 3.5 Gy/min. Compute the conveyer speed to achieve a dose of 300 Gy.

14.9 A laboratory study with *Staphylococcus aureus* has found that a dose of 15 kGy reduces the initial population of 1 million bacteria down to 500. Determine the D_{10} value.

14.10 (a) Integrate the decay of Si-31 in Example 14.5 to show that the P-31 dopant concentration over time is

$$N_{\text{P-31}}(t) = \begin{cases} \Sigma_{\gamma}^{\text{Si-30}}\phi\left(t + \dfrac{e^{-\lambda t}}{\lambda} - \dfrac{1}{\lambda}\right) & \text{for } t \le t_{\text{I}} \\ \Sigma_{\gamma}^{\text{Si-30}}\phi\left[t_{\text{I}} + \dfrac{e^{-\lambda t}}{\lambda} - \dfrac{e^{-\lambda(t-t_{\text{I}})}}{\lambda}\right] & \text{for } t \ge t_{\text{I}} \end{cases} \tag{14.6}$$

(b) Confirm Eq. (14.4).

14.14 COMPUTER EXERCISES

14.A The classic predator-prey balance equations simulate interacting populations such as foxes and rabbits. Run the program PREDPREY to see trends with time. Study the impact of changing the Lotka-Volterra equation parameters (α, β, γ, and δ).

14.B An adaptation of the predator-prey equations can be used to analyze the control of the screw-worm fly by the sterile male technique. Using the program ERADIC (eradicate), study the trend in population under different initial conditions and sterile male introduction rates. In particular, find the number of generations required to reduce the population to less than one fly.

REFERENCES

Bacon, G.E., 1975. Neutron Diffraction, third ed. Clarendon Press, Oxford.

Baliga, B.J., 1982–1984. Neutron transmutation doping of semiconductor materials. In: Larrabee, R.D. (Ed.), Proceedings of the Fourth Neutron Transmutation Doping Conference. Plenum Press, New York, pp. 167–180.

Barth, R.F., Coderre, J.A., Vicente, M.G.H., Blue, T.E., 2005. Boron neutron capture therapy of cancer: current status and future prospects. Clin. Cancer Res. 11 (6), 3987–4002.

Bragg, W.H., Kleeman, R., 1904. On the ionization curves of radium. Philos. Mag. 8 (48), 726–738.

Choppin, G., Liljenzin, J.-O., Rydberg, J., 2002. Radiochemistry and Nuclear Chemistry, third ed. Butterworth-Heinemann, Woburn.

Daly, M.J., 2009. A new perspective on radiation resistance based on Deinococcus radiodurans. Nat. Rev. Microbiol. 7 (3), 237–239.
der Vloedt, V., Butt, B., 1990. The New World Screwworm eradication programme in North Africa. IAEA Bull. 32 (4), 35–41.
Eaton, B.R., MacDonald, S.M., Yock, T.I., Tarbell, N.J., 2015. Secondary malignancy risk following proton radiation therapy. Front. Oncol. 5, article 261.
Food and Agriculture Organization of the United Nations (FAO), 1998. Tsetse Fly Eradicated on the Island of Zanzibar. http://www.fao.org/NEWS/1998/980505-e.htm.
Garnick, M.B., Fair, W.R., 1998. Combatting prostate cancer. Sci. Am. 279 (6), 74–83.
Goorley, T., James, M., Booth, T., Brown, F., Bull, J., Cox, L.J., et al., 2012. Initial MCNP6 release overview. Nucl. Technol. 180 (3), 298–315.
Helfinstine, S.L., Vargas-Aburto, C., Uribe, R.M., Woolverton, C.J., 2005. Inactivation of Bacillus endospores in envelopes by electron beam irradiation. Appl. Environ. Microbiol. 71 (11), 7029–7032.
Henkel, J., 1998. Irradiation: a safe measure for safer food. FDA Consum. 32 (May–June), 12–17.
Howe, D.B., Beardsley, M., Bakhsh, S., 2008. Consolidated Guidance About Material Licenses: Program-Specific Guidance about Medical Use Licenses; 2008. NUREG-1556, vol. 9, rev. 2. Nuclear Regulatory Commission.
International Atomic Energy Agency (IAEA), 1997a. Argentina irradiates urban sludge. INSIDE Tech. Cooperat. 3 (1), 2–3.
International Atomic Energy Agency (IAEA), 1997b. Eradicating the Tsetse Fly on Zanzibar Island. https://www.iaea.org/technicalcooperation/documents/Factsheets/archive/tsetse2.pdf.
Levin, W.P., Kooy, H., Loeffler, J.S., DeLaney, T.F., 2005. Proton beam therapy. Br. J. Cancer 93 (8), 849–854.
Lindquist, D.A., Abusowa, M., 1992. Eradicating the New World Screwworm from the Libyan Arab Jamahiriya. IAEA Bull. 34 (4), 17–24.
Lowy, R.J., 2005. Ionizing radiation inactivation of medically relevant viruses. In: Gazsó, L.G., Ponta, C.C. (Eds.), Radiation Inactivation of Bioterrorism Agents. IOS Press, Amsterdam, pp. 175–186.
Marciniec, B., Dettlaff, K., 2008. Radiation sterilization of drugs. In: Trends in Radiation Sterilization of Health Care Products. International Atomic Energy Agency (IAEA), Vienna STI/PUB/1313.
Moss, R.L., 2014. Critical review, with an optimistic outlook, on Boron Neutron Capture Therapy (BNCT). Appl. Radiat. Isot. 88, 2–11.
National Council on Radiation Protection and Measurements (NCRP), 1989. Guidance on Radiation Received in Space Activities; 1989. NCRP Report No. 98. Bethesda.
Oak Ridge National Laboratory (ORNL), 2001. SNS and biological research. ORNL Rev. 34 (1), 24–25.
Scallan, E., Griffin, P.M., Angulo, F.J., Tauxe, R.V., Hoekstra, R.M., 2011. Foodborne illness acquired in the United States—unspecified agents. Emerg. Infect. Dis. 17 (1), 16–22.
Sears, V.F., 1992. Neutron scattering lengths and cross-sections. Neutron News 3 (3), 26–37.
U.S. Department of Agriculture (USDA), 1999. Irradiation of meat products, final rule. Fed. Regist. 64 (246), 72149–72166. December 23.
U.S. Food and Drug Administration (FDA), 1997. Irradiation in production processing and handling of food. Fed. Regist. 62 (232), 64107–64121. December 3.
United Nations Scientific Committee on the Effects of Atomic Radiation (UNSCEAR), 2008. Sources and Effects of Ionizing Radiation; 2008. Vol. I: Sources.
Venkatesan, A.K., Done, H.Y., Halden, R.U., 2015. United States national sewage sludge repository at Arizona State University—a new resource and research tool for environmental scientists, engineers, and epidemiologists. Environ. Sci. Pollut. Res. Int. 22 (3), 1577–1586.
Vreysen, M.J.B., Saleh, K., Mramba, F., Parker, A., Feldman, U., Dyck, V.A., Msangi, A., Bouyer, J., 2014. Sterile insects to enhance agricultural development: the case of sustainable tsetse eradication on Unguja Island, Zanzibar, using an area-wide integrated pest management approach. PLoS Negl. Trop. Dis. 8 (5), 1–5.

FURTHER READING

Altarelli, M., Schlacter, F., Cross, J., 1998. Making ultrabright X-rays. Sci. Am. 279 (6), 66–73.

American Nuclear Society (ANS), 2012. Major advances in nuclear medicine diagnosis and treatment. http://www.ans.org/pi/np/diagnosis. Data on remission rates with cell-targeted therapy.

Anderson, L.L., Interstitial Collaborative Working Group, 1990. Interstitial Brachytherapy: Physical, Biological, and Clinical Considerations. Raven Press, New York.

Anon, 2007. FDA seeks to ease labeling requirements for food that has been irradiated. Nucl. News 50 (6), 61.

Bailey, D.L., Humm, J.L., Todd-Pokropek, A., van Aswegen, A., 2014. Nuclear Medicine Physics: A Handbook for Teachers and Students. International Atomic Energy Agency, Vienna.

D'Amico, K.L., Terminello, L.J., Shuh, D.K., 1996. Synchrotron Radiation Techniques in Industrial, Chemical, and Materials Science. Plenum Press, New York.

Ehmann, W.D., Vance, D.E., 1991. Radiochemistry and Nuclear Methods of Analysis. Wiley, New York.

Foldiak, G. (Ed.), 1986. Industrial Applications of Radioisotopes. Elsevier, Amsterdam.

Hatanaka, H., Sweet, W.H., Sano, K., Ellis, F., 1991. The present status of boron-neutron capture therapy for tumors. Pure Appl. Chem. 63 (3), 373–374.

Helliwell, J.R., Rentzepis, P.M. (Eds.), 1997. Time-Resolved Diffraction. Oxford University Press, Oxford. Research on time-dependent structural changes by use of X-rays (including synchrotron radiation), electrons, and neutrons.

Hofmann, A., 2004. The Physics of Synchrotron Radiation. Cambridge University Press, New York.

Idaho State University, 2011. Radiation Information Network: Food Irradiation. http://www.physics.isu.edu/radinf/food.htm. Extensive discussion, references, and links.

International Atomic Energy Agency (IAEA), 1991. IAEA Bull. 33 (1). The issue features nuclear medicine.

International Atomic Energy Agency (IAEA), 2006. Nuclear Medicine Resource Manual. STI/PUB/1198. IAEA, Vienna. Guide for establishing nuclear medicine service.

International Atomic Energy Agency (IAEA), 2008. Trends in radiation sterilization of health care products; 2008. IAEA Publication 1313.

International Atomic Energy Agency (IAEA), 2017. Insect Pest Control. http://www-naweb.iaea.org/nafa/ipc/index.html.

Komolprasert, V., Bailey, A., Machuga, E., 2007. Regulatory report: irradiation of food packaging materials. Food Safety Mag. December 2007–January 2008.

Mason, T.E., Abernathy, D., Anderson, I., Ankner, J., Egami, T., Ehlers, G., et al., 2006. The spallation neutron source in Oak Ridge: a powerful tool for materials research. Physica B 385–386 (2), 955–960.

Michal, R., 2003. Irradiated food, good; foodborne pathogens, bad. Nucl. News 46 (8), 62. 69–71.

Morehouse, K.M., Komolprasert, V., 2004. Irradiation of food and packaging: an overview. In: Irradiation of Food and Packaging. ACS Symposium Series, 875, American Chemical Society, Washington, DC, pp. 1–11.

Murano, E.A. (Ed.), 1995. Food Irradiation: A Sourcebook. Iowa State University Press, Ames, IA. Processing, microbiology, food quality, consumer acceptance, and economics.

Theragenics, Brachytherapy. http://www.theragenics.com. Commercial supplier of radioactive particles; select Products.

U.S. Department of Agriculture (USDA), National Agricultural Library, 2000. STOP Screwworms. http://www.nal.usda.gov/speccoll/collect/screwworm/. History of screwworm eradication; discovery and application of sterile male technique.

U.S. Food and Drug Administration, 2016. Irradiation of food & packaging. https://www.fda.gov/food/ingredientspackaginglabeling/irradiatedfoodpackaging/.

U.S. Food and Drug Administration (FDA), 2017. Ionizing Radiation for the Treatment of Food. 2017. 21CFR179.26.

Wilkinson, V.M., Gould, G.W., 1996. Food Irradiation: A Reference Guide. Butterworth-Heinemann, Oxford. Topics, definitions, and discussion with references to all relevant terms.

Woods, R.J., Pikaev, A.K., 1994. Applied Radiation Chemistry: Radiation Processing. Wiley, New York. Includes synthesis, polymerization, sterilization, and food irradiation.

PART

NUCLEAR POWER III

The main focus of the remainder of the book is electricity generation via fission reactors. Today's power plants primarily employ low-enriched uranium produced from an isotope separation scheme. The operation of nuclear reactors requires understanding the neutronics and heat removal processes. Nuclear reactor theory describes both the static and dynamic behaviors of the reactor. Nuclear power plants are built in several different configurations, such as boiling and pressurized water reactors. Nuclear safety is paramount, and valuable lessons can be found from the negative experiences of Three Mile Island, Chernobyl, and Fukushima. Although an entire fuel cycle surrounds the nuclear fuel utilization, controversy endures over the final disposition of radioactive waste produced from fission reactors. Besides electricity production, nuclear energy utilization also includes propulsion and small-scale radioisotopic power sources. Future uses of nuclear power include desalination, but the power may eventually be derived from either breeder or fusion reactors. Finally, this last part of the book concludes with an examination of atomic weapons, which are dramatically different from nuclear reactors, although both exploit the energy within the nucleus.

CHAPTER

ISOTOPE SEPARATORS 15

CHAPTER OUTLINE

All our technology is based on materials in various forms: elements, compounds, alloys, and mixtures. Ordinary chemical and mechanical processes can be used to separate many materials into components. In the nuclear field, however, individual isotopes such as U-235, H-2 (deuterium), B-10, and Li-7 are required. Because isotopes of a given element have the same atomic number Z, they are essentially identical chemically, and thus a physical method must be found that distinguishes among particles based on mass number A. In this chapter, we will describe several methods by which isotopes of uranium and other elements are separated. Four methods that depend on differences in A are: (1) ion motion in a magnetic field, (2) diffusion of particles through a membrane, (3) motion with centrifugal force, and (4) atomic response to a laser beam. Calculations on the amounts of material that must be processed to obtain nuclear fuel will be presented, and estimates of costs will be given.

15.1 MASS SPECTROGRAPH

We recall from Section 9.1 that a particle of mass m, charge q, and speed v will move in a circular path of radius r if injected perpendicular to a magnetic field of strength B, according to the relation

$$r = mv/(qB) \tag{15.1}$$

Nuclear Energy. https://doi.org/10.1016/B978-0-12-812881-7.00015-0

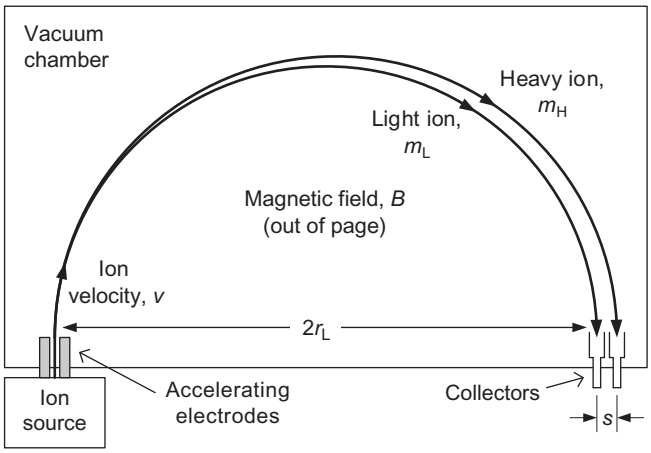

FIG. 15.1

Mass spectrograph.

In the mass spectrograph (Fig. 15.1), ions of the element whose isotopes are to be separated are produced in an electrical discharge and accelerated through a potential difference V to provide a kinetic energy

$$\frac{1}{2}mv^2 = qV \tag{15.2}$$

The charges move freely in a chamber maintained at very low gas pressure, guided in semicircular paths by the magnetic field. The heavier ions have a larger radius of motion than the lighter ions, and the two may be collected separately. It is found (see Exercise 15.1) that the distance s between the points at which ions are collected is proportional to the difference in the square roots of the masses. The spectrograph can be used to measure masses with some accuracy, to determine the relative abundance of isotopes in a sample, or to enrich an element in a certain desired isotope.

The electromagnetic process was used on uranium during World War II to obtain weapons material, using the *calutron* (named after the University of California at Berkeley, where it was developed). A total of 1152 units in the Alpha and Beta processes were operated at the Y-12 Plant at Oak Ridge, producing the enriched uranium for one atomic bomb by 1945. Because the cost of electrical power for the process is large, alternative processes such as gaseous diffusion and centrifugation are used to produce reactor fuels. In 1945, the Y-12 plant had a rated peak demand rate of 200 MW while for the Oak Ridge K-25 gaseous diffusion plant, the rating was 80 MW (Jones, 1985). However, for more than 50 years, a few calutrons were maintained at Oak Ridge. These separated light-stable isotopes in small quantities needed for research and for targets for accelerator-produced radioisotopes. The system was shut down permanently in 1999 (ORNL, 1999).

15.2 GASEOUS DIFFUSION SEPARATOR

The principle of this process can be illustrated by a simple experiment (Fig. 15.2). A container is divided into two parts by a porous membrane, and air is introduced on both sides. Recall that air is a mixture by volume of 79% nitrogen, $A = 14$, and 21% oxygen, $A = 16$. If the pressure on one side is

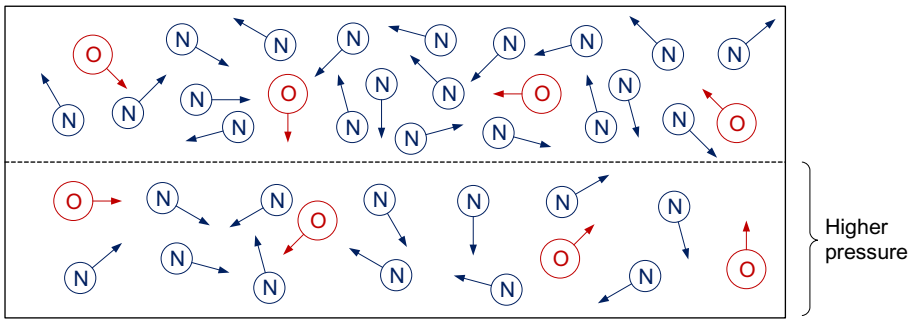

FIG. 15.2

Gaseous diffusion separation of nitrogen and oxygen.

raised, the relative proportion of nitrogen on the other side increases. The separation effect can be explained on the basis of particle speeds. The average kinetic energies of the heavy (H) and light (L) molecules in the gas mixture are the same, $E_H = E_L$, but because the masses are different, the typical particle speeds bear a ratio

$$\frac{v_L}{v_H} = \sqrt{\frac{m_H}{m_L}} \tag{15.3}$$

The number of molecules of a given type that hit the membrane each second is proportional to nv in analogy to neutron motion discussed in Section 4.4. Those with higher speed thus have a higher probability of passing through the holes in the porous membrane, called the barrier.

The physical arrangement of one processing unit of a gaseous diffusion plant for the separation of uranium isotopes U-235 and U-238 is shown in Fig. 15.3. A thin nickel alloy serves as the barrier material. In this stage, gas in the form of the compound uranium hexafluoride (UF_6) is pumped in as feed and removed as two streams. One is enriched and one depleted in the compound $^{235}UF_6$, with corresponding changes in $^{238}UF_6$. Because of the very small mass difference of particles of molecular weight 349 and 352, the amount of separation is small, and many stages in series are required in what is called a *cascade*. At atmospheric pressure, UF_6 undergoes sublimation (i.e., direct transformation from solid to

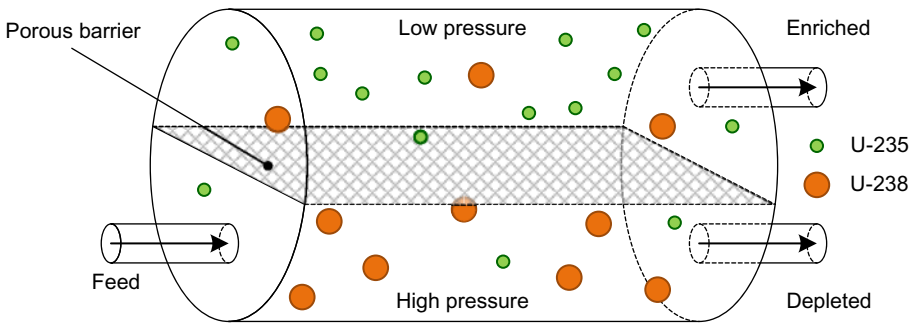

FIG. 15.3

Gaseous diffusion stage.

gas) at a temperature of 56.5°C (134°F). The chemically reactive nature of UF_6 led to employing Teflon in the compressor seals.

Natural uranium has a small U-234 component, atom fraction 0.000055. For simplicity, we will ignore its effect except for Exercise 15.11.

Any isotope separation process causes a change in the relative numbers of molecules of the two species. Let n_H and n_L be the number of molecules in a sample of gas. Their abundance ratio is defined as

$$R = n_L/n_H \tag{15.4}$$

EXAMPLE 15.1

For gases, volume fraction and atom fraction are identical; therefore, in ordinary air, the abundance ratio of N_2 to O_2 is $R = n_N/n_O = 79/21 = 3.76$.

The effectiveness of an isotope separation process depends on a quantity called the *separation factor* α. If we supply gas at an abundance ratio R, the ratio R' on the low-pressure side of the barrier is given by

$$R' = \alpha R \tag{15.5}$$

If only a very small amount of gas is allowed to diffuse through the barrier, the ideal separation factor for this process is given by

$$\alpha = \sqrt{m_H/m_L} \tag{15.6}$$

which for UF_6 is $\sqrt{(238+6(19))/(235+6(19))} = 1.0043$. However, for a more practical case, in which half the gas goes through the membrane, the separation factor is smaller, 1.0030 (see Exercise 15.2).

EXAMPLE 15.2

Let us calculate the effect of one stage on natural uranium, 0.711% by weight of ^{235}U, corresponding to a U-235 atom fraction of 0.00720. Considering just ^{235}U and ^{238}U, the abundance ratio is $R = n_{235}/n_{238} = 0.00720/0.99274 = 0.00725$. Now

$$R' = \alpha R = (1.0030)(0.00725) = 0.00727$$

The amount of enrichment is very small. By processing the gas in a series of S stages, each one of which provides a factor α, the abundance ratio is increased by a factor α^S. If R_F and R_P refer to feed and product, respectively,

$$R_P = \alpha^S R_F \tag{15.7}$$

EXAMPLE 15.3

For $\alpha = 1.0030$, we can easily show that 2378 enriching stages are needed to go from $R_F = 0.00725$ to highly enriched 90% U-235. First, the product abundance ratio is

$$R_P = \frac{n_{235}}{n_{238}} = \frac{0.9}{1-0.9} = 9$$

Rearranging Eq. (15.7), the number of stages required is

$$S = \frac{\log(R_P/R_F)}{\log(\alpha)} = \frac{\log(9/0.00725)}{\log(1.0030)} = 2378$$

Fig. 15.4 illustrates the arrangement of several stages in an elementary cascade, and indicates the value of R at various points. The feed is natural uranium, the product is enriched in U-235, and the waste is depleted in U-235.

A gaseous diffusion uranium isotope separation facility is very expensive, of the order of a billion dollars, because of the size and number of components such as separators (see Fig. 15.5), pumps, valves, and controls, but the process is basically simple. The plant runs continuously with a small

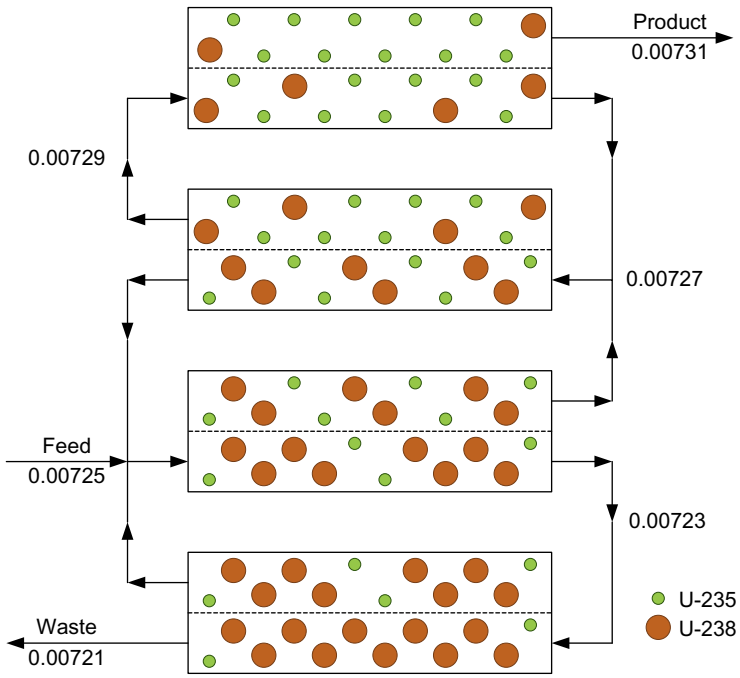

FIG. 15.4

Gaseous diffusion cascade with U-235 abundance indicated.

FIG. 15.5

Gaseous diffusion process, circa 1972.

Courtesy United States Department of Energy.

number of operating personnel. The principal operating cost is for the electrical power to provide the pressure differences and to perform work on the gas. The gaseous diffusion plants at Paducah, Kentucky, and Piketon, Ohio, operated from 1952 and 1954 until 2013 and 2001, respectively, before being retired due to being uneconomical.

15.3 GAS CENTRIFUGE

This device for separating isotopes, also called the ultracentrifuge because of the very high speeds involved, has been known since the 1940s. It was tested and abandoned during World War II because materials that would withstand high rotation speeds were not available and existing bearings gave large power losses. Developments since have made centrifuges practical and economical.

The centrifuge consists of a cylindrical chamber—the rotor—turning at very high speed in a vacuum, as shown in Fig. 15.6. The rotor is driven and supported magnetically. Gas is supplied and centrifugal force tends to compress it in the outer region, but thermal agitation tends to redistribute the gas molecules throughout the whole volume. Light molecules are favored in this effect, and their concentration is higher near the center axis. By mechanical or thermal means, a countercurrent flow of UF_6 gas is established that tends to carry the heavy and light isotopes to opposite ends of the rotor. Scoop pipes withdraw depleted and enriched streams of gas, as shown schematically in Fig. 15.6. Olander (1978) provides diagrams that are more detailed.

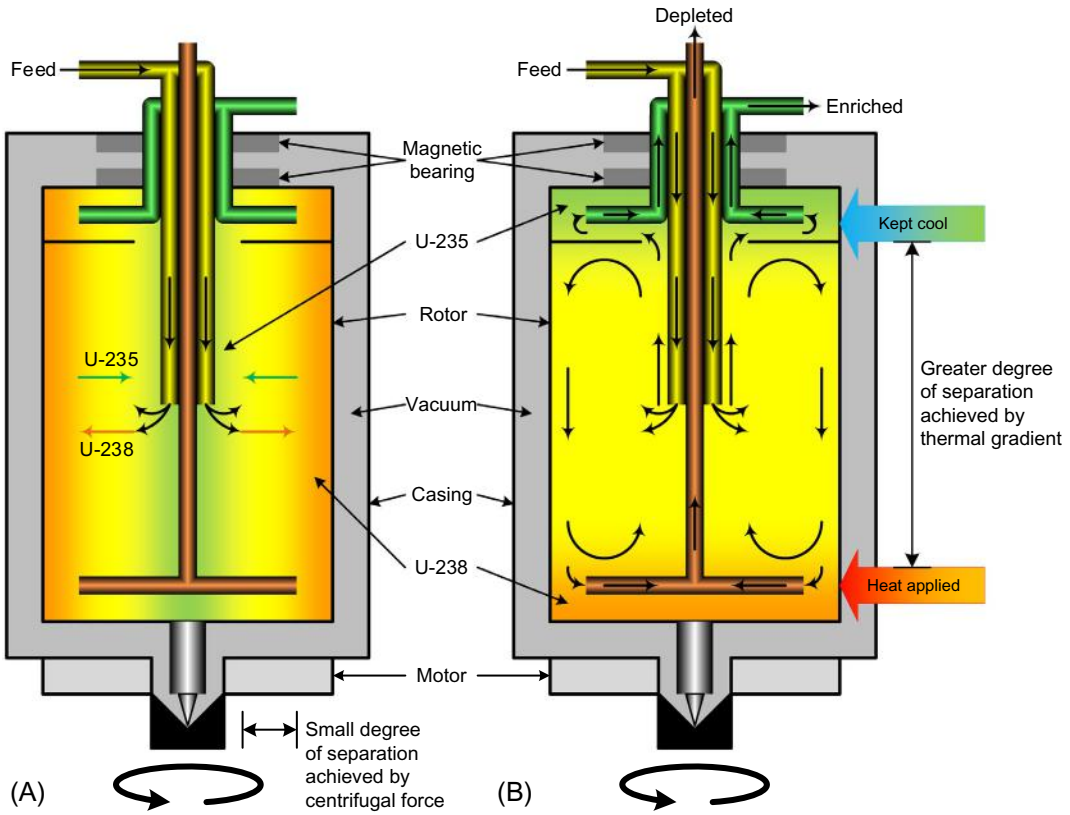

FIG. 15.6

Gas centrifuge: (A) Centrifugal force only and (B) centrifugal force and heat. With centrifugal force only as in (A), a small degree of separation is achieved, whereas with the addition of a thermal gradient as in (B), a greater amount of separation occurs.

The theory of separation by centrifugal force starts with the formula for the gas density distribution in a gravitational field,

$$N = N_0 \exp(-mgh) \tag{15.8}$$

where the potential energy is mgh. Adapt the expression to a rotating gas, with kinetic energy at radius r being

$$E_K = \frac{1}{2}mv^2 = \frac{1}{2}m\omega^2 r^2 \tag{15.9}$$

where ω is the angular velocity, v/r. Apply to two gases of masses m_H and m_L to obtain the abundance ratio as a function of distance

$$R = R_0 \exp\left[(m_H - m_L)\,\omega^2 r^2/(2kT)\right] \tag{15.10}$$

Table 15.1 Design Features of Centrifuges

Machine	Date	Rotor Characteristics				Separative Power (kg-SWU/y)
		Material	Diameter (cm)	Length (m)	Speed (m/s)	
Zippe	1960	Aluminum	7.4	0.3	350	0.44
SNOR/CNOR	1960s–70s	Aluminum	10	2.0	350	2–3
G-2	1960s–70s	Maraging steel[a]	15	1.0	485	5–6
SLM (TC-10)	Late 1980s	Maraging steel	15	3.2	500	21
AC100	2008	Carbon fiber composite	60	12	900	330

[a]*Maraging steels are strong with low carbon content and up to 25% nickel.*
Data from Glaser, A., 2008. Characteristics of the gas centrifuge for uranium enrichment and their relevance for nuclear weapon proliferation. Sci. Glob. Secur. 16(1–2), 1–25; Kemp, R.S., 2009. Gas centrifuge theory and development: a review of U.S. programs. Sci. Glob. Secur. 17(1), 1–19.

Note that separation depends on the difference in masses rather than on their square roots as for gaseous diffusion.

Zippe obtained separation factors of 1.1 or better with centrifuges approximately 30 cm long, rotating at a rate such that the rotor surface speed is 350 m/s (Villani, 1976). Table 15.1 shows that technology advances have resulted in higher speeds and greater separative power.

EXAMPLE 15.4

Composite rotor materials permit higher rotation speeds. The separation factor for a carbon fiber composition that has a peripheral speed of 600 m/s is

$$\alpha = R/R_0 = \exp\left[(m_H - m_L)v^2/(2kT)\right] = \exp\left[\frac{(352-349\text{u})\left(1.66\times10^{-27}\text{kg/u}\right)(600\text{m/s})^2}{2\left(1.38\times10^{-23}\text{J/K}\right)(57+273\text{K})}\right] = 1.22$$

The flow rate per stage of a centrifuge is much lower than that of gaseous diffusion, requiring large numbers of units in parallel. However, the electrical power consumption for a given capacity is lower by an order of magnitude, giving a lower operating cost. Furthermore, the capital cost of a centrifuge plant is lower than that of a gaseous diffusion plant. European countries have taken advantage of the lower costs of centrifuge separation to challenge the former monopoly on enrichment services by the United States. In fact, several American utilities buy fuel from Europe. Examples of facilities are plants of Urenco, Ltd. at Capenhurst in the United Kingdom, at Almelo in The Netherlands, and at Gronau in West Germany (IPFM, 2015).

A centrifuge-based uranium enrichment plant, known as the URENCO USA facility, is located near Eunice, New Mexico. This plant, managed by Louisiana Energy Services (a project in Louisiana was abandoned), began operations in June 2010, with additional capacity planned. In 2016, Centrus Energy

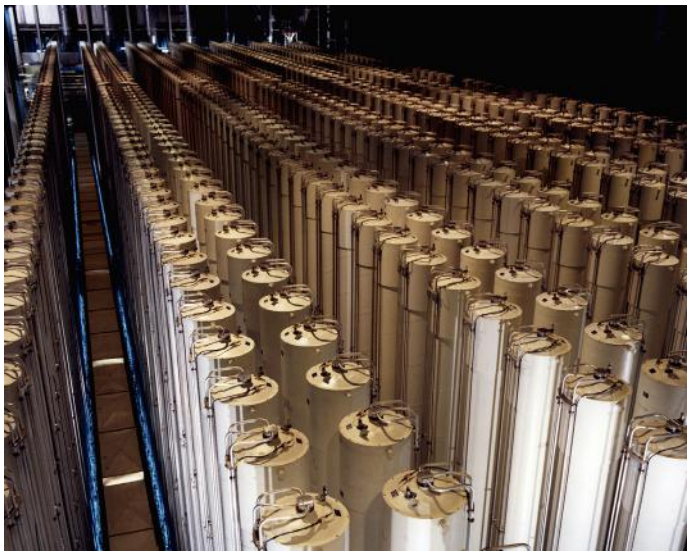

FIG. 15.7

Cascade of gas centrifuges at the Piketon, Ohio plant in 1984.

Courtesy of the NRC under Creative Commons license BY 2.0.

completed testing of the domestically developed American Centrifuge demonstration cascade (see Fig. 15.7) at the Piketon, Ohio, enrichment facility, where a gaseous diffusion plant was previously in operation.

15.4 URANIUM ENRICHMENT

Both gaseous diffusion and gas centrifuge separation processes require multiple units connected in parallel and series. The flow of UF_6 and thus uranium through either individual stages or the whole plant can be analyzed by the use of material balances. One could keep track of the number of particles, moles, or kilograms because the flow is continuous. It will be convenient to use kilograms per day as the unit of uranium flow for three streams: feed (F), product (P), and waste (W), also called *tails*. The overall uranium mass balance is

$$F = P + W \tag{15.11}$$

Letting x stand for the U-235 weight fractions in the flows, the balance for the light isotope is

$$x_F F = x_P P + x_W W \tag{15.12}$$

A similar equation could be written for U-238, but it would contain no additional information. The two equations can be solved to obtain the ratio of feed and product mass rates. Eliminating W yields

$$\frac{F}{P} = \frac{x_P - x_W}{x_F - x_W} \tag{15.13}$$

The use of mass fractions in the formulas of this section leads to the convention of *enrichment* being defined in terms of U-235 weight percent rather than atom percent. The abbreviation "w/o" typically denotes weight percent. The product-to-feed mass ratio is termed the unit "cut."

EXAMPLE 15.5

Let us find the required feed of natural uranium to obtain 1 kg/d of product containing 3 w/o U-235. Assume that the waste is at 0.3 w/o. Now

$$\frac{F}{P}=\frac{x_P-x_W}{x_F-x_W}=\frac{0.03-0.003}{0.00711-0.003}=6.57$$

Thus, the feed is $F=6.57$ $P=6.57$ kg/d. We note that $W=F-P=5.57$ kg/d, which shows that large amounts of depleted uranium tails must be stored for each kilogram of U-235 produced. With a density greater than lead, depleted uranium is used for antitank munitions, but this practice has been controversial (Bem and Bou-Rabee, 2004). The U-235 content of the tails is too low for use in conventional reactors, but the breeder reactor can convert the U-238 into plutonium, as will be discussed in Chapter 25.

The cost of enrichment depends in part on the energy expended, which is measured in *separative work units* (SWU, pronounced "swoo"). The energy intensive nature of the gas diffusion process is revealed by its electricity use of around 2400 kWh/kg-SWU, whereas the gas centrifuge can be 95% more efficient (Whitaker, 2005). Regardless of the technology, the separative work required is

$$SWU=PV(x_P)+WV(x_W)-FV(x_F) \tag{15.14}$$

with typical units of kg-SWU, and in which the U-shaped value function is

$$V(x)=(1-2x)\ \ln[(1-x)/x] \tag{15.15}$$

By encoding these relations into a program called ENRICH, Table 15.2 was developed. The feed was taken as 0.711 w/o, corresponding to an atom percent of 0.720, and the tails were set to 0.3 w/o U-235.

Table 15.2 Nuclear Fuel Enrichment Data

Product (*P*) Weight Percent U-235	Ratio of Feed to Product (*F*/*P*)	Separative Work Per Product, *SWU*/*P* (SWU)
0.711	1.000	0
0.8	1.217	0.070
1.0	1.703	0.269
2.0	4.136	1.697
3.0	6.569	3.425
4.0	9.002	5.276
5.0	11.436	7.198
10.0	23.601	17.284
20.0	47.932	38.315
90.0	218.248	192.938

Feed of 0.711 w/o and tails of 0.3 w/o U-235.

As the price of uranium increases, financial considerations encourage extracting more of the U-235, which correspondingly decreases the tails assay.

EXAMPLE 15.6

Let us find the amount of uranium fuel needed and its cost to a utility. Assume that the uranium is to be enriched to 3 w/o. Thus, each kg of fuel (product, P) contains 30 g of U-235 and 970 g of U-238. From Table 15.2 the F/P ratio is 6.569, and therefore the natural uranium feed required for the isotope separation process is 6.569 kg. Uranium ore is typically extracted from the earth as U_3O_8 (uranium oxide). It is easy to show (Exercise 15.8) that the weight fraction of uranium in U_3O_8 is 0.848. Hence our feed becomes $6.569/0.848 = 7.75$ kg of the oxide. The price of U_3O_8 varies, but we assume \$44/kg, giving \$341 as the cost of the uranium material itself.

In addition to the expense of the mined ore, there is a cost to convert U_3O_8 into UF_6 for use in the enrichment process. Assuming \$10/kg-U, this amounts to \$66. The third column of Table 15.2 gives the SWU/P value of 3.425 SWU, and by use of a reasonable enrichment charge of \$100/kg-SWU, the cost is \$343. For instance, a fuel element fabrication cost of \$275/kg adds for the 1 kg a sum of \$275. Excluding transportation cost, Table 15.3 shows that the preceding numbers total to \$1025/kg. To fuel a nuclear reactor rated at 1000 MWe, an electric utility may need approximately 27,200 kg/y giving an annual fuel cost (F_C) of \$27.88 million. However with a capacity factor (CF) of 85% (a formal definition of CF is given in Section 18.3) over the 8760 h in a year, the unit produces a total annual electric energy of

$$E = P\,CF\,T = \left(1000 \times 10^3\,\text{kW}\right)(0.85)(8760\text{h}) = 7.45 \times 10^9\,k\text{Wh}$$

Table 15.3 Summary of Nuclear Fuel Costs for Example 15.6

Item Description	Unit Cost	Quantity	Item Cost
Mined ore	\$44/kg-U_3O_8	7.75 kg-U_3O_8	\$341
Conversion	\$10/kg-U	6.569 kg-U	\$66
Enrichment	\$100/kg-SWU	3.425 kg-SWU	\$343
Fabrication	\$275/kg-U	1 kg-U	\$275
Subtotal			\$1025
Reactor fuel requirements	\$1025/kg-U	27,200 kg/y	\$27.88 million

The basic fuel cost is thus $F_C/E = 0.37$ cents/kWh. The total cost of producing electricity would also include capital charges and operating and maintenance (O&M) expenses.

The world picture on uranium enrichment has been changing in recent years, as more suppliers have appeared and United States utilities have diversified their sources. In 2014, 94% of the natural uranium used in the United States originated from other countries, with Australia and Canada supplying 38%, and Kazakhstan, Russia, and Uzbekistan accounting for 39% (NEA, 2016). Presently, the sole operating enrichment facility in the United States is the gaseous centrifuge plant at Eunice, New Mexico, with a capacity of 3.7 million kg-SWU/y (IPFM, 2015). Fig. 15.8 shows that the Earth has considerable uranium resources, but the production cost (e.g., mining, transportation, and processing the ore) can vary significantly. In 2016, US civilian nuclear power plants paid an average price of \$131 per SWU for enrichment (DOE, 2017).

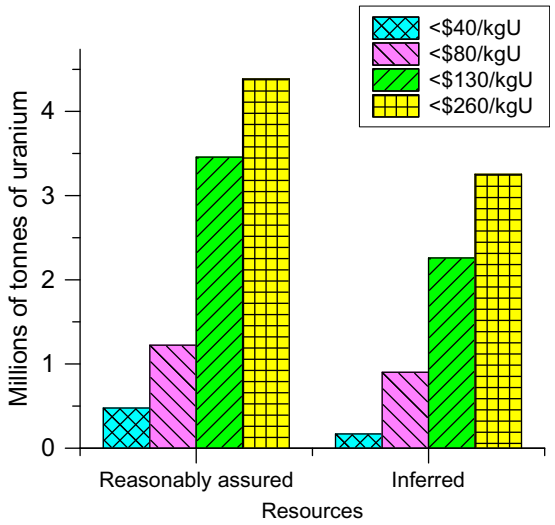

FIG. 15.8

Global uranium resources in terms of recovery cost.

Data from Nuclear Energy Agency (NEA), 2016. Uranium 2016: Resources, Production and Demand. NEA No. 7301. Boulogne-Billancourt, France.

15.5 LASER ISOTOPE SEPARATION[1]

A different technique for separating uranium isotopes uses laser light (see Section 2.4) to selectively photoionize U-235 atoms, which can be drawn away from U-238 atoms. There are two variants of laser isotope separation: atomic and molecular.

Lawrence Livermore National Laboratory and Oak Ridge National Laboratory cooperated in research and development on the atomic vapor laser isotope separation (AVLIS) process. AVLIS was regarded as promising, but the United States Enrichment Corporation (now Centrus Energy Corp.) determined that it was less economic than gaseous diffusion or centrifuge separators. That R&D program was terminated in 1999. The French carried out tests with SILVA (AVLIS backward), obtaining 200 kg of low-enrichment uranium and a tonne of depleted uranium. However, they concluded that the method would be useful only sometime in the future.

An element such as uranium has a well-defined set of electron orbits, similar to those described in Section 2.3, but much more complex because it has 92 electrons. The difference in masses of the nuclei of U-235 and U-238 results in subtle differences in the electronic orbit structure and corresponding energies required to excite or to ionize the two isotopes.

A laser can supply intense light of precise frequencies, and a fine-tuned laser beam can provide photons that ionize the U-235 and leave the U-238 unchanged. The ionization potential for U-235 is 6.1 eV. The method performs resonance stepwise excitation of an atom. In the AVLIS technique, three photons of approximately 2 eV achieve the ionization.

[1]Thanks are due to James I. Davis of Lawrence Livermore National Laboratory and N. Haberman of the Department of Energy (DOE) for some of the information in this section.

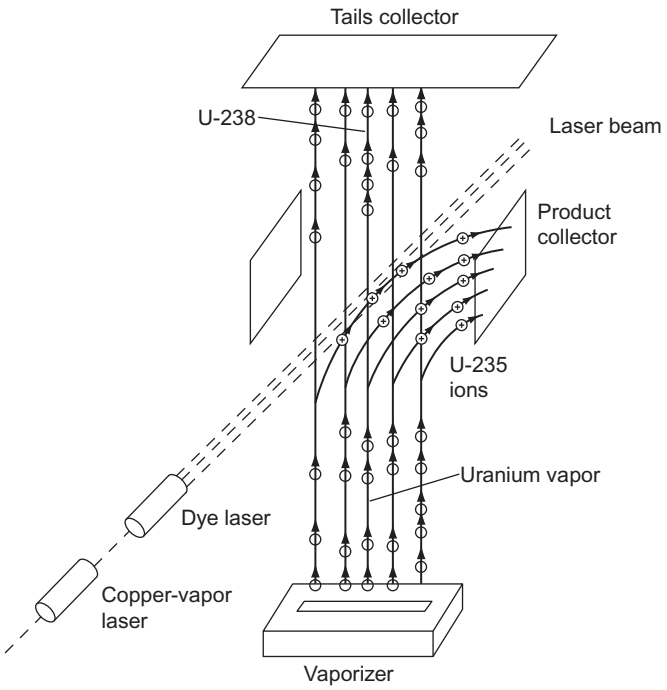

FIG. 15.9

Atomic vapor laser isotopic separation.

The virtue of the method is the almost perfect selection of the desired isotope. Of 100,000 atoms ionized by a laser beam, all but one are U-235. This permits enrichment from 0.7% to 3% in a single stage rather than thousands as with gaseous diffusion. One kilogram of enriched product comes from 6 kg of natural uranium. The metallic uranium is vaporized by a stream of electrons, as in Fig. 15.9. A yellow-green laser energizes ("pumps") a second orange-red laser. This irradiates the uranium vapor, with selective ionization of uranium-235 atoms. An electric field draws those ions off to condense on product collector plates. U-238 atoms pass through the laser beam and condense on the walls of the chamber to be removed as tails.

EXAMPLE 15.7

Estimate the separation factor required for a single-step atomic laser enrichment from natural to 3.0 a/o uranium. Using the input (R) and output (R') abundance ratios, the separation factor is

$$\alpha = \frac{R'}{R} = \frac{n'_{235}/n'_{238}}{n_{235}/n_{238}} = \frac{0.03/0.97}{0.00720/0.99274} = 4.3$$

In the mid-1990s, the Australian company Silex developed a molecular laser enrichment process using UF_6. Since 2008, a General Electric subsidiary has continued the development by successfully

implementing a test loop. In September 2012, the Nuclear Regulatory Commission (NRC) issued a license for a pilot plant that may be built in Wilmington, North Carolina, though more recent plans call for the plant to be constructed at Paducah, Kentucky. Deployment of the proprietary (and classified) separation of isotopes by laser excitation (SILEX) process has been controversial, as some have expressed legitimate proliferation concerns. It is noteworthy that this third-generation technique has the potential to use existing stocks of depleted uranium as feed material.

15.6 SEPARATION OF DEUTERIUM

The heavy isotope of hydrogen ^{2}H, deuterium, has two principal nuclear applications: (1) as a low-absorption moderator for reactors, especially those that use natural uranium, and (2) as a reactant in the fusion process. The differences between the chemical properties of light water and heavy water (D_2O) are slight (see Table 15.4), but sufficient to permit separation of ^{1}H and ^{2}H by several methods. Among these are electrolysis, in which the H_2O tends to be more readily dissociated; fractional distillation, which takes advantage of the fact that D_2O has a boiling point approximately 1°C higher than that of H_2O; and catalytic exchange, involving the passage of HD gas through H_2O to produce HDO and light hydrogen gas.

15.7 SUMMARY

The separation of isotopes requires a physical process that depends on mass. In the electromagnetic method, as used in a mass spectrograph, ions to be separated travel in circles of different radii. In the gaseous diffusion process, light molecules of a gas diffuse through a membrane more readily than do heavy molecules. The amount of enrichment in gaseous diffusion depends on the square root of the ratio of the masses and is small per stage, requiring a large number of stages. An alternative separation device is the gas centrifuge, in which gases diffuse against the centrifugal forces produced by high speeds of rotation. By the use of material balance equations, the amount of feed can be computed, and by the use of tables of separative work, costs of enriching uranium for reactor fuel can be found. Laser isotope separation involves the selective excitation of uranium atoms by lasers to produce chemical reactions. Several methods of separating deuterium from ordinary hydrogen are available.

Table 15.4 Comparison of Water and Heavy Water Properties

Property	Water (H_2O)	Heavy Water (D_2O)
Density (g/cm^3)	0.9970	1.1044
Melting point (°C)	0.00	3.82
Boiling point (°C)	99.974	101.42

Data from Rumble, J.R., (Ed.), 2018. CRC Handbook of Chemistry and Physics, ninety-eighth ed. CRC Press, Boca Raton, FL.

15.8 EXERCISES

15.1 Show that the radius of motion of an ion in a mass spectrograph is given by

$$r = \sqrt{\frac{2mV}{qB^2}}$$

(b) If the masses of heavy (H) and light (L) ions are m_H and m_L, show that their separation s at the plane of collection in a mass spectrograph is proportional to $\sqrt{m_H} - \sqrt{m_L}$.

15.2 A practical separation factor for a gaseous diffusion stage with a cut of one-half is

$$\alpha = 1 + \ln(2)\left(\sqrt{m_H/m_L} - 1\right)$$

Compute its value for $^{235}UF_6$ and $^{238}UF_6$, noting that $A = 19$ for fluorine.

15.3 (a) Verify that for particles of masses m_H and m_L the atom fraction γ_L of the light particle is related to the weight fractions ω_H and ω_L by

$$\gamma_L = \frac{n_L}{n_L + n_H} = \frac{1}{1 + \omega_H m_L/(\omega_L m_H)}$$

(b) Show that the abundance ratio of numbers of particles is either

$$R = \frac{n_L}{n_H} = \frac{\gamma_L}{1 - \gamma_L} \quad \text{or} \quad \frac{\omega_L/m_L}{\omega_H/m_H}$$

Calculate the atom fraction and abundance ratio for uranium metal that is (c) 3%, (d) 20%, and (e) 90% U-235 by weight.

15.4 The total fuel loading of a new research reactor is 2000 kg of uranium at 20 w/o U-235. From Table 15.2, find the amount of natural uranium feed and the SWUs required to fuel the reactor, assuming tails of 0.3 w/o.

15.5 A typical reactor that uses product uranium from an isotope separator at 3% enrichment burns 75% of the U-235 and 2.5% of the U-238. What percentage of the mined uranium is actually used for electrical power generation?

15.6 Find the amount of natural uranium feed (0.711% by weight) required to produce 1 kg/d of highly enriched uranium (90% by weight), if the waste concentration is 0.25% by weight. Assume that the uranium is in the form of UF_6.

15.7 How many gaseous diffusion enriching stages with $\alpha = 1.0030$ are required to produce uranium that is (a) 3%, (b) 5%, and (c) 20% by weight by use of natural UF_6 feed? Let the waste be 0.2%.

15.8 By use of the atomic weights of uranium and oxygen in Table A.4, verify that the weight fraction of U in U_3O_8 is 0.848.

15.9 The number density of molecules as the result of loss through a barrier can be expressed as $n = n_0 \exp(-cvt)$ where c is a constant, v is the particle speed, and n_0 and n are values before

and after an elapsed time t. If half the heavy isotope is allowed to pass through, find the abundance ratio $R'/R = \alpha$ in the enriched gas as a function of the ratio of molecular masses. Test the derived formula for the separation of uranium isotopes.

15.10 Depleted uranium (0.3% U-235) is processed by laser separation to yield natural uranium (0.711%). If the feed rate is 1 kg/d and all the U-235 goes into the product, what amounts of product and waste are produced per day?

15.11 By use of natural uranium isotope fractions and atomic masses for U-238, U-235, and U-234 given in Table A.5, calculate the atomic mass of natural U and the weight percent of each isotope. *Suggestion*: make a table of numbers.

15.12 A utility plans to increase the enrichment of its nuclear fuel from 3 w/o to either (a) 4 w/o or (b) 5 w/o, achieving an increase in capacity factor from 0.70 to either (i) 0.80 or (ii) 0.90, respectively, as the result of longer operating cycles. Using data from Example 15.6, estimate fuel costs in the two cases and determine whether there is a net financial gain or loss compared to the reference case, assuming that electricity is worth approximately 4 cents/kWh.

15.13 A certain country covertly builds production mass spectrographs to separate uranium isotopes. The objective is to obtain 50 kg of highly enriched uranium for a nuclear weapon in 1 year of continuous operation. (a) Assuming optimistically that separation is perfect, what current of U^+ ions would be required? (b) Neglecting power needed for heating and magnets, what amount of electrical power at 50 kV is required? (c) Would the power source be difficult to conceal?

15.14 (a) Calculate the centrifugal acceleration $a = v^2/r$ in a centrifuge at radius $r = 0.1$ m with an angular speed of 5000 rad/s. By what factor is a larger than the acceleration of Earth's gravity, g_0? (b) Find the ratio R/R_0 for UF_6 of molecular weights 349 and 352 at 330 K.

15.15 For gas centrifuges operating with separation factors of (a) 1.1 and (b) 1.25, determine the number of stages needed to enrich natural U to HEU.

15.16 A 1000-MWe nuclear unit operating with a capacity factor of 90% requires about 100,000 kg-SWU worth of fuel annually. For enrichment from gaseous diffusion, what fraction of the power plant output is effectively needed to produce its fuel in this manner?

15.17 From a nuclear characteristics viewpoint, why is the use of UF_6 more advantageous over that of UCl_6 in gaseous diffusion and centrifuge enrichment processes?

15.18 For atomic laser enrichment with a separation factor of 4, estimate the product enrichment in weight percent from a single stage using (a) a natural and (b) a depleted (0.2 w/o) uranium feed.

15.9 COMPUTER EXERCISES

15.A The tails concentration of a gaseous diffusion separation process is typically 0.3 w/o. For a fixed product (e.g., 1 kg of 3 w/o fuel) graph the feed, enrichment, and their total costs versus tails concentrations from 0.1 to 0.65, with (i) computer program ENRICH and some separate calculations, or (ii) by adapting ENRICH to calculate costs.

15.B Adapt computer program ENRICH to calculate costs in addition to flows and SWU. Then, graph the cost per gram of U-235 and cost per kilogram of U for the product enrichments from 1 to 10 w/o. Keep a constant tails assay of 0.3 w/o.

REFERENCES

Bem, H., Bou-Rabee, F., 2004. Environmental and health consequences of depleted uranium use in the 1991 Gulf War. Environ. Int. 30 (1), 123–134.

International Panel on Fissile Materials (IPFM), 2015. Global Fissile Material Report 2015. IPFM, Princeton, NJ. http://fissilematerials.org.

Jones, V.C., 1985. Manhattan: The Army and the Atomic Bomb. CMH Pub. 11-10, United States Army, Washington, DC, p. 391.

Nuclear Energy Agency (NEA), 2016. Uranium 2016: Resources, Production and Demand. 2016. NEA No. 7301. Boulogne-Billancourt, France.

Oak Ridge National Laboratory (ORNL), 1999. ORNL's calutrons wrap up historic half-century of isotopes. ORNL Reporter 1. March.

Olander, D.R., 1978. The gas centrifuge. Sci. Am. 239 (2), 37–43.

U.S. Department of Energy (DOE), Energy Information Administration (EIA), 2017. 2016 Uranium Marketing Annual Report, 2017. DOE EIA.

Villani, S., 1976. Isotope Separation. American Nuclear Society, La Grange Park, IL. Monograph that describes most of the techniques for separating isotopes, including theory, equipment, and data.

Whitaker, J.M., 2005. Uranium enrichment plant characteristics–a training manual for the IAEA. ORNL/TM-2005/43. Oak Ridge National Laboratory.

FURTHER READING

Benedict, M., Pigford, T.H., Levi, H.W., 1981. Nuclear Chemical Engineering, second ed. McGraw-Hill, New York.

Glaser, A., 2008. Characteristics of the gas centrifuge for uranium enrichment and their relevance for nuclear weapon proliferation. Sci. Glob. Secur. 16 (1–2), 1–25.

Kemp, R.S., 2009. Gas centrifuge theory and development: a review of U.S. programs. Sci. Glob. Secur. 17 (1), 1–19.

Lyman, J.L., 2005. Enrichment separative capacity for SILEX. LA-UR-05-3786, Los Alamos National Laboratory.

Parkins, W.E., 2005. The uranium bomb, the Calutron, and the space charge problem. Phys. Today 58 (5), 45–51.

Physical constants of inorganic compounds. Rumble, J.R. (Ed.), 2018. CRC Handbook of Chemistry and Physics. ninety-eighth ed. CRC Press, Boca Raton, FL.

Smyth, H.D., 1945. Atomic Energy for Military Purposes. Princeton University Press, Princeton (also known as the "Smyth Report"; republished in *Reviews of Modern Physics* **17** (4), 351–471).

U.S. Department of Energy (DOE), Energy Information Administration (EIA), Nuclear & Uranium. http://www.eia.gov/nuclear/.

Urenco-Areva, Centrifuge Technology. http://www.enritec.com.

World Information Service on Energy (WISE), Uranium Enrichment Calculator. http://www.wise-uranium.org/nfcue.html. Reproduces calculations in Section 15.4.

World Nuclear Association (WNA), 2017. Uranium Enrichment. http://www.world-nuclear.org/information-library/nuclear-fuel-cycle/conversion-enrichment-and-fabrication/uranium-enrichment.aspx.

Zare, R.N., 1977. Laser separation of isotopes. Sci. Am. 236 (2), 86–98.

CHAPTER

NEUTRON CHAIN REACTIONS 16

CHAPTER OUTLINE

The possibility of a chain reaction involving neutrons in a mass of nuclear fuel such as uranium depends on (1) nuclear properties such as cross-sections and neutrons produced per absorption, and (2) the size, shape, and arrangement of the materials.

16.1 CRITICALITY AND MULTIPLICATION

To achieve a self-sustaining chain reaction, one needing no external neutron supply, a critical mass of fuel must be collected. To appreciate this requirement, we visualize the simplest nuclear reactor, consisting of a sphere of uranium-235 metal. Suppose that it consists of only one atom of U-235. If it absorbs a neutron and fissions, the resultant neutrons do nothing further, there being no more fuel. If instead we have a small chunk of uranium, for instance a few grams, the introduction of a neutron might set off a chain of several fission reactions, producing more neutrons, but most of them would escape through the surface of the body—a process called *leakage*. Such an amount of fuel is said to be *subcritical*. Now if we bring together approximately 50 kg of U-235 metal, the neutron production balances the leakage losses, and the system is self-sustaining or *critical*. The physical size is the critical volume and the amount of fuel is the critical mass. Neutrons had to be introduced to start the chain reaction, but the number of neutrons is maintained without further additions. The term *critical mass* has become popular to describe any collection of entities large enough to operate independently.

Nuclear Energy. https://doi.org/10.1016/B978-0-12-812881-7.00016-2

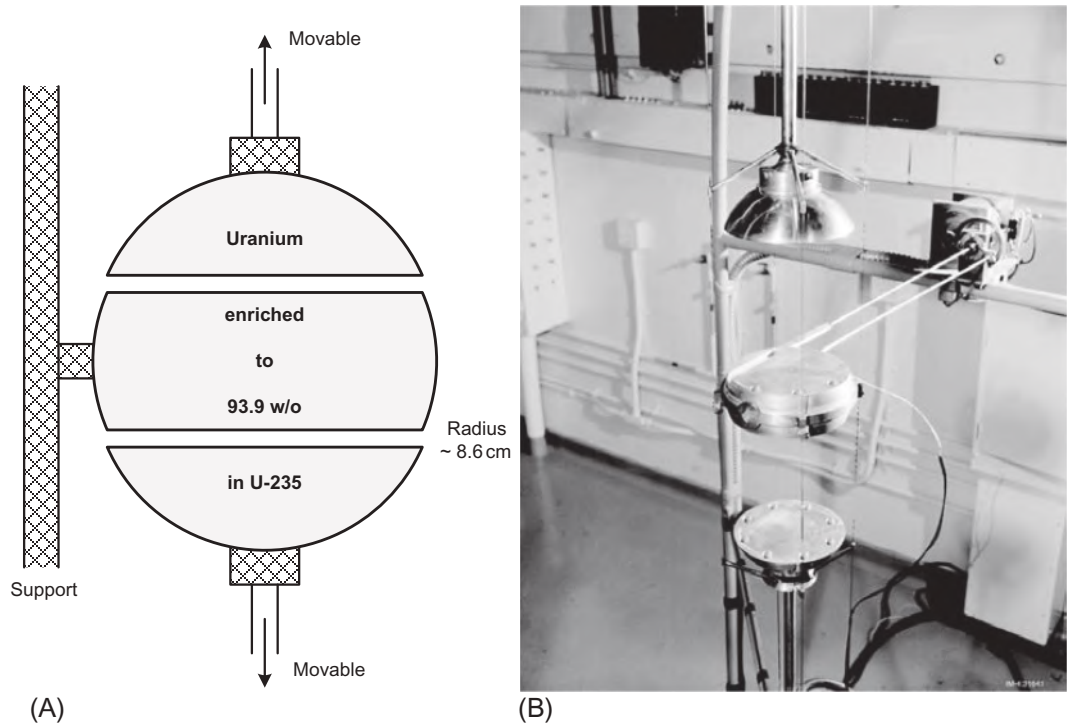

FIG. 16.1

Fast metal assemblies: (A) Lady Godiva and (B) Jezebel. The upper and lower thirds of the spherical reactors can be withdrawn for subcriticality.

(B) Courtesy of Los Alamos National Laboratory.

Table 16.1 Bare Metal Fast Assemblies

Assembly	Material	Density (g/cm^3)	Critical Mass (kg)
Godiva	93.9% U-235	18.75	48.8
Jezebel	Pu-239	15.44	16.28

Data from Argonne National Laboratory (ANL), 1963. Reactor Physics Constants, ANL-5800, second ed.

Fig. 16.1A shows the highly enriched (in U-235) metal assembly Lady Godiva, so named because it was bare (i.e., it had no surrounding materials such as a neutron reflector). Godiva and Jezebel (Fig. 16.1B) were used for test purposes for a number of years at Los Alamos (Paxton, 1983). As specialized reactors, such critical assemblies (see Table 16.1) are typically tasked to carry out low-power physics experiments. If we add still more uranium to the 50 kg required for criticality, more neutrons are produced than are lost, the neutron population increases, and the reactor is *supercritical*. Early nuclear weapons involved the use of such masses in which the rapid growth of neutrons and resulting fission heat caused a violent explosion.

16.2 MULTIPLICATION FACTORS

The behavior of neutrons in a nuclear reactor can be understood through analogy with populations of living organisms, for example, human beings. There are two ways to look at changes in numbers of people: as individuals and as a group. A human is born and throughout life has various chances of fatal illness or accident. The life expectancy at birth might be 75 years on average, according to statistical data. A person may die without an heir, with one, or with many children. If on average there is exactly one offspring per individual, the population is constant. From the other viewpoint, if the rates of birth and death are the same in a group of people, the population is again steady. If there are more births than deaths by 1% per year, the population will grow accordingly. This approach emphasizes the competition of process rates.

The same ideas apply to neutrons in a multiplying assembly. We can focus attention on a typical neutron that was born in fission and has various chances of dropping out of the cycle because of leakage and absorption in other materials besides fuel. On the other hand, we can compare the reaction rates for the processes of neutron absorption, fission, and leakage to determine whether the number of neutrons is increasing, steady, or decreasing. Each of the methods has its merits for purposes of discussion, analysis, and calculation.

For any arrangement of nuclear fuel and other materials, a single number k expresses the net number of neutrons generated per initial neutron, accounting for all losses and reproduction by fission. The state of the system can be summarized by this *multiplication factor* as:

$$k\begin{cases} >1 & \text{supercritical} \\ =1 & \text{critical} \\ <1 & \text{subcritical} \end{cases} \tag{16.1}$$

The design and operation of all reactors is focused on k or on related quantities such as $\delta k = k - 1$, called delta-k, or $\delta k/k$, called *reactivity*, symbolized by

$$\rho = \frac{\delta k}{k} = \frac{k-1}{k} \tag{16.2}$$

The choice of materials and size is made to assure that k has the desired value. For safe storage of fissionable material, k should be well below 1. In the critical experiment—a process of bringing materials together with a neutron source present—observations on neutron flux are used to yield estimates of k. During operation, variations in k are executed as needed by adjustments of neutron-absorbing rods or dispersed chemicals. Eventually, in the operation of the reactor, enough fuel is consumed to bring k below 1 regardless of adjustments in control materials, and the reactor must shut down for refueling.

Two different multiplication factors are commonly utilized to evaluate the system criticality. The *infinite multiplication factor* k_∞ is employed to assess the potential for achieving criticality in the reactor materials alone. Once the materials are arranged in a finite geometry, the *effective multiplication factor* k_{eff} describes the neutron population growth, including the impact of neutrons leaking from the system

$$k_{\text{eff}} = \frac{\text{Rate of neutron production}}{\text{Rate of neutron absorption} + \text{rate of neutron leakage}} \tag{16.3}$$

The context in which the multiplication factor is spoken of differentiates as to which k is being referred to because Eqs. (16.1) and (16.2) are applicable to both k_∞ and k_{eff}.

EXAMPLE 16.1

An assembly is producing 5.2×10^5 n/s while 4.9×10^5 n/s are being absorbed and 6.0×10^4 n/s are leaking out of the reactor. Whereas the infinite multiplication factor is

$$k_\infty = \frac{\text{Neutron production}}{\text{Neutron absorption}} = \frac{5.2\times10^5\,\text{n/s}}{4.9\times10^5\,\text{n/s}} = 1.06$$

and indicates that the material alone is supercritical, the effective multiplication factor denotes an overall subcritical condition

$$k_{\text{eff}} = \frac{\text{Neutron production}}{\text{Neutron absorption and leakage}} = \frac{5.2\times10^5\,\text{n/s}}{(4.9\times10^5+6.0\times10^4)\,\text{n/s}} = 0.95$$

The corresponding reactivity of the reactor is $\rho=(k_{\text{eff}}-1)/k_{\text{eff}}=(0.95-1)/0.95=-0.053$ (unitless).

16.3 FAST REACTOR CRITICALITY

We can develop a formula for k for the uranium metal assembly with the statistical approach. As in Fig. 16.2A, a neutron may escape on first flight from the sphere because mean free paths for fast neutrons are rather long (see Exercise 16.12). Another neutron (Fig. 16.2B) may make one scattering collision and then escape. Other neutrons may collide and be absorbed either (Fig. 16.2C) to form U-236 or (Fig. 16.2D) to cause fission, the latter yielding three new neutrons in this case. Still other neutrons may make several scattering collisions before leakage or absorption takes place. The statistical nature of the process is revealed by the application of Computer Exercise 16.B, which involves the program SLOWINGS in which scattering, absorption, and escape are simulated with a Monte Carlo technique.

A flow diagram as in Fig. 16.3 is useful to describe the various fates. The boxes represent processes; the circles represent the numbers of neutrons at each stage. The fractions of absorbed neutrons that form U-236 and that cause fission, respectively, are the ratios of the cross-section for capture σ_γ and fission σ_f

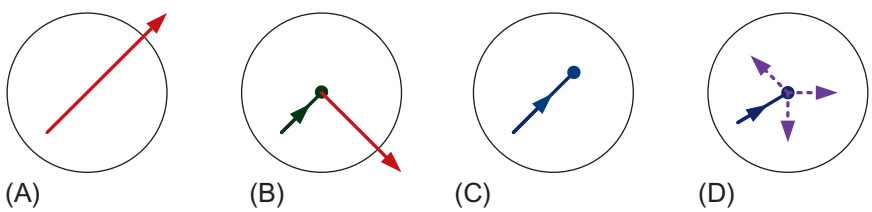

FIG. 16.2

Neutron histories after birth. (A) Escape in the first flight; (B) Escape after one collision; (C) Absorption in U-235 to form U-236; (D) Absorption with neutron production.

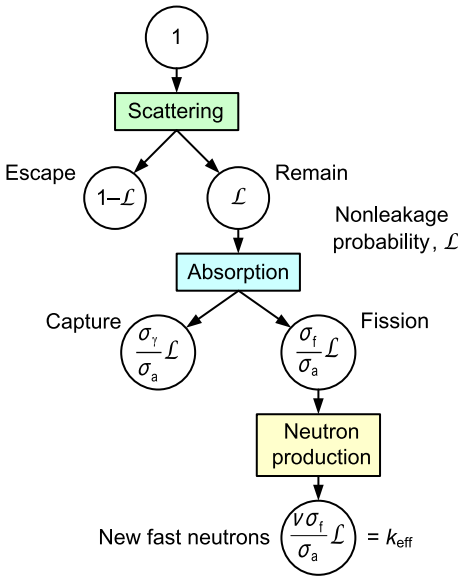

FIG. 16.3

Neutron cycle in fast metal reactor.

to that for absorption σ_a. The average number of neutrons produced by fission is ν. We recall (from Section 6.3) that the reproduction factor η is the number of neutrons emitted per absorption in the fuel

$$\eta = \nu\sigma_f/\sigma_a \tag{16.4}$$

Thus letting $\mathcal{L}$ be the fraction *not* escaping by leakage,

$$k_{eff} = \eta\mathcal{L} \tag{16.5}$$

EXAMPLE 16.2

A system is critical if $k_{eff} = 1$, or $\eta\mathcal{L} = 1$. Measurements show that η is approximately 2.2 for fission caused by fast neutrons, thus $\mathcal{L}$ must be $1/\eta = 1/(2.2) = 0.45$, which says that as many as 45% of the neutrons must remain in the sphere, whereas no more than 55% escape through its boundary for criticality.

Let us now examine more closely $\mathcal{L}$, the nonleakage factor, coming from the process of neutron loss through the surface of a reactor core without a reflector. Leakage depends on scattering collisions and on the size and shape of the core. We would expect that the amount of neutron leakage depends on the ratio of surface to volume because production occurs within the core and losses occur at the boundary. For a sphere, for example, the volume is $V = (4/3)\pi R^3$ and the surface area is $S = 4\pi R^2$, so the ratio is $S/V = 3/R$. As it turns out from the theory of neutron diffusion (see Chapter 19), the parameter that actually applies is $B_g = \pi/R$, the square of which, B_g^2, is called the *geometric buckling*. It is also logical that leakage should be larger, the greater the transport mean free path (recall Section 4.7) and the

Table 16.2 Geometric Buckling

Geometry	Dimensions	Geometric Buckling, B_g^2
Sphere	Radius, R	$(\pi/R)^2$
Right cylinder	Radius, R Height, H	$(\pi/H)^2+(j_0/R)^2$ where $j_0=2.40483$
Rectangular parallelepiped	$L\times W\times H$	$(\pi/L)^2+(\pi/W)^2+(\pi/H)^2$

smaller the absorption cross-section (Section 4.4). This is indeed the case, involving the use of the diffusion length, $L=\sqrt{D/\Sigma_a}$ as introduced in Section 4.7, but for fast neutrons here. The *nonleakage probability* for one neutron energy group in a bare reactor is thus

$$\mathcal{L}=1/\left(1+L^2B_g^2\right) \tag{16.6}$$

Table 16.2 lists the geometric buckling for three important shapes.

EXAMPLE 16.3

If Godiva were purely composed of U-235 with a density of $19\,g/cm^3$, the fuel concentration is readily found as $N=\rho N_A/M=4.87\times10^{22}\,atom/cm^3$. To estimate the *diffusion area* L^2 in the assembly, we combine Eqs. (4.54) and (4.55), and substitute U-235 cross-sections from Table 16.3 to yield

$$L^2=D/\Sigma_a=1/(3\Sigma_{tr}\Sigma_a)=1/\left(3N^2\sigma_{tr}\sigma_a\right)=1/\left[3N^2\sigma_{tr}\left(\sigma_f+\sigma_\gamma\right)\right]$$
$$=1/\left[(3)\left(4.87\times10^{22}/cm^3\right)^2(6.8b)(1.4+0.25b)\left(10^{-24}cm^2/b\right)^2\right]=12.5cm^2$$

According to Fig. 16.1, the assembly radius is ~8.6 cm such that the geometric buckling is

$$B_g^2=(\pi/R)^2=[\pi/(8.6cm)]^2=0.13/cm^2$$

The nonleakage probability is therefore

$$\mathcal{L}=1/\left(1+L^2B_g^2\right)=1/\left[1+\left(12.5cm^2\right)\left(0.13/cm^2\right)\right]=0.38$$

Table 16.3 Nuclear Reactor Fast Group Constants

Material	ν	σ_f	σ_γ	σ_{tr}
U-235	2.6	1.4	0.25	6.8
U-238	2.6	0.095	0.16	6.9
Pu-239	2.98	1.85	0.26	6.8
Na	–	–	0.0008	3.3

Data from Argonne National Laboratory (ANL), 1963. Reactor Physics Constants, ANL-5800, second ed.

Critical conditions for more complex situations, including mixtures of fuels, can be analyzed by use of the program CRITICAL, discussed in Computer Exercise 16.A. The key to such analysis is to recall that macroscopic cross-sections are summed for mixtures; see Example 4.7.

16.4 THERMAL REACTOR CRITICALITY

The presence of large amounts of neutron-moderating material such as water in a reactor greatly changes the neutron distribution in energy. Fast neutrons slow down by means of collisions with light nuclei, with the result that low-energy (thermal) neutrons produce most of the fissions. Such a system is called a *thermal* reactor in contrast with a system without moderator, a *fast* reactor, operating principally with fast neutrons. The cross-sections for the two energy ranges are widely different, as can be seen in Fig. 16.4. Furthermore, the neutrons are subject to being removed from the multiplication cycle during the slowing process by strong resonance absorption in nuclides such as U-238. Finally, there is competition for the neutrons between fuel, coolant, structural materials, fission products, and control absorbers.

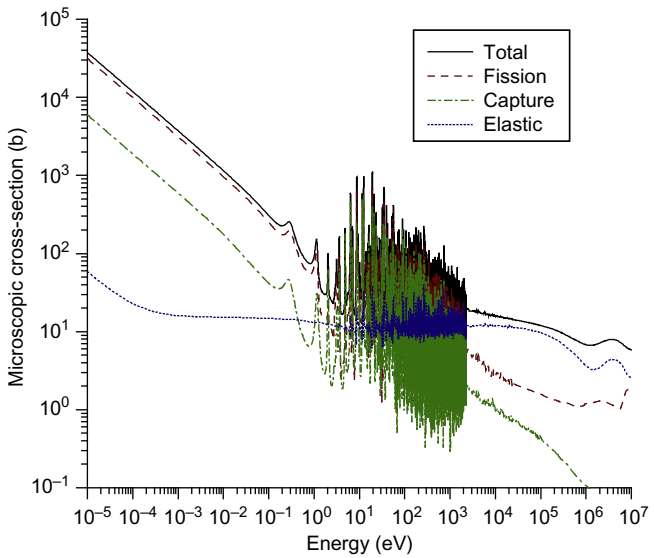

FIG. 16.4

U-235 microscopic cross-sections.

Data from ENDF/B-VII.1 (Chadwick, M.B., Herman, M., Obložinský, P., Dunn, M.E., Danon, Y., Kahler, A.C., et al., 2011. ENDF/B-VII.1 Nuclear data for science and technology: cross-sections, covariances, fission product yields and decay data. Nucl. Data Sheets 112 (12), 2887–2996).

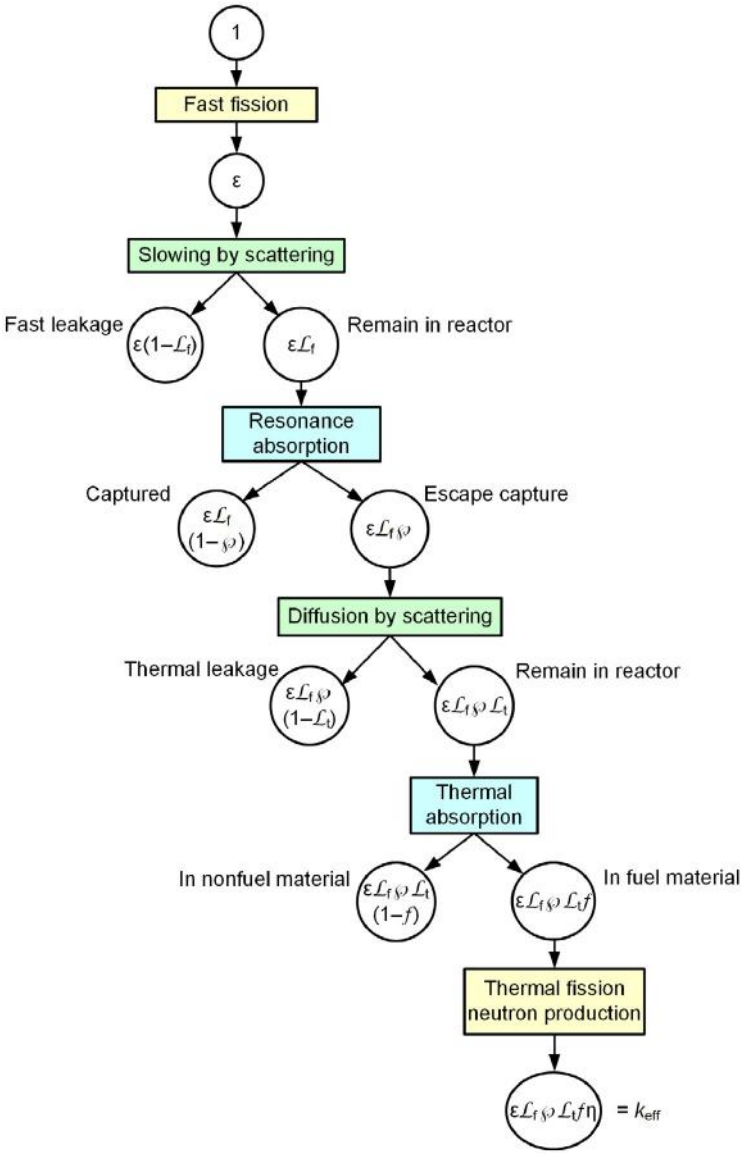

FIG. 16.5

Neutron cycle in thermal reactor.

The description of the multiplication cycle for a thermal reactor, as seen in Fig. 16.5, is somewhat more complicated than that for a fast metal assembly. The set of reactor parameters is:

(1) Fast fission factor ε (epsilon), representing the immediate multiplication because of fission at high neutron energy, mainly in U-238.
(2) Fast nonleakage probability $\mathcal{L}_f$, being the fraction remaining in the core during neutron slowing.

(3) Resonance escape probability $\wp$, the fraction of neutrons not captured during slowing.
(4) Thermal nonleakage probability $\mathcal{L}_t$, the fraction of neutrons remaining in the core during diffusion at thermal energy.
(5) Thermal utilization f, the fraction of thermal neutrons absorbed in fuel.
(6) Reproduction factor η, as the number of new fission neutrons per absorption in fuel.

At the end of the cycle starting with one fission neutron, the number of fast neutrons produced is seen to be $\varepsilon\wp f\,\eta\mathcal{L}_f\mathcal{L}_t$, which may be also labeled k_{eff}, the effective multiplication factor. It is convenient to group four of the factors to form the so-called infinite multiplication factor that would be identical to k_{eff} if the medium were infinite in extent, without leakage

$$k_\infty = \eta f \varepsilon \wp \tag{16.7}$$

This relation is known as the *four-factor formula*. If we form a composite nonleakage probability $\mathcal{L} = \mathcal{L}_f\mathcal{L}_t$, then we may write

$$k_{eff} = k_\infty \mathcal{L} \tag{16.8}$$

For a reactor to be critical, k_{eff} must equal 1, as before. Combining the above relations gives the six-factor formula of

$$k_{eff} = k_\infty \mathcal{L} = \eta f \varepsilon \wp \mathcal{L}_f \mathcal{L}_t \tag{16.9}$$

EXAMPLE 16.4

To provide some appreciation of the sizes of various factors, let us calculate the values of the composite quantities for a thermal reactor, for which $\varepsilon = 1.03$, $\wp = 0.71$, $\mathcal{L}_f = 0.97$, $\mathcal{L}_t = 0.99$, $f = 0.79$, and $\eta = 1.8$. Now, these values lead to

$$k_\infty = \eta f \varepsilon \wp = (1.8)(0.79)(1.03)(0.71) = 1.04$$

$$\mathcal{L} = \mathcal{L}_f\mathcal{L}_t = (0.97)(0.99) = 0.96$$

$$k_{eff} = k_\infty \mathcal{L} = (1.04)(0.96) = 1.00$$

For this example, the various parameters yield a critical system. In Section 18.1, we will describe the physical construction of typical thermal reactors.

16.5 FOUR-FACTOR FORMULA PARAMETERS

Actual reactors are comprised of multiple materials, thereby necessitating the ability to calculate the four factors in Eq. (16.7) for a variety of situations. The four-factor formula can be further envisioned by overlaying a cross-section plot with the progression of events in the life of a neutron, as shown in Fig. 16.6. Within a low enrichment core, the neutron birth at ~2 MeV leads to ample opportunities for the neutron to interact with the abundant U-238 atoms; however, as Table 16.3 shows, the fast fission cross-section is small (0.095 b). Although the fast fission factor is readily defined in words as

$$\varepsilon = \frac{\text{Total fission neutrons from thermal and fast fission}}{\text{Fission neutrons from thermal fission}} \tag{16.10}$$

the calculation of ε is far more complex. For our purposes, we simply note that ε is roughly 1.04.

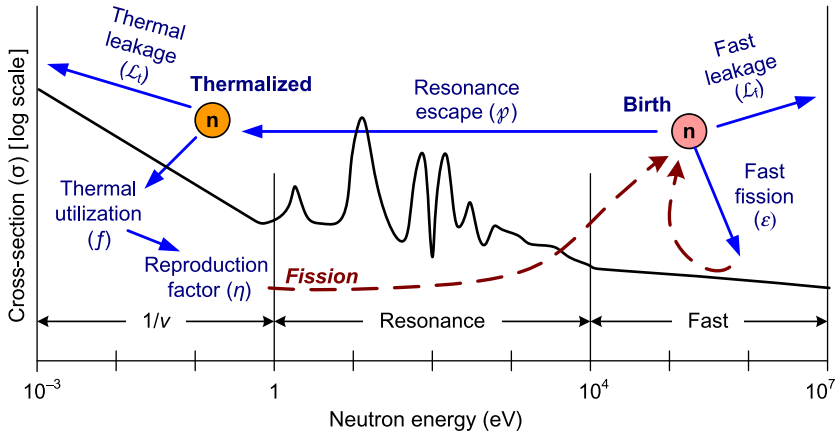

FIG. 16.6

Neutron lifecycle superimposed on cross-section graph.

While the moderator endeavors to slow the neutron down to thermal energy, the fuel (F) presents large resonance cross-sections that attempt to absorb it. The competing mechanisms of resonance capture, primarily by U-238, and moderator (M) thermalization are expressed in a formulation for the resonance escape probability

$$\wp = \exp\left[-(NI)_F / \left(\xi \Sigma_{\text{s,epi}}\right)_M\right] \tag{16.11}$$

in which I is the fuel *resonance integral* for absorption, and the product $\xi\Sigma_{\text{s, epi}}$ is the *moderating power* using the scattering cross-section in the epithermal energy range and ξ as defined in Section 4.7. The resonance escape probability usually varies approximately from 0.6 to 0.9.

A thermal neutron that does not leak from the system will be absorbed by one of the materials present. Reactors contain not only fuel and moderator, but also structural (S) materials, such as steel and cladding, as well as neutron absorbers for control (C). The thermal, or fuel, utilization is the ratio of neutron absorption in the fuel to the total (T) in all the materials. This competition for neutrons is quantified by

$$f = \frac{\Sigma_a^F}{\Sigma_a^T} = \frac{\Sigma_a^F}{\Sigma_a^F + \Sigma_a^M + \Sigma_a^S + \Sigma_a^C + \cdots} \tag{16.12}$$

Although the fuel utilization can range from zero to unity, f should be nearer to 1 to avoid parasitic loss of neutrons.

EXAMPLE 16.5

A fast reactor fueled with U-235 is cooled with sodium. To overcome leakage and maintain criticality, k_∞ must be greater than 1.2. Determine the maximum sodium to fuel (N_{Na}/N_{235}) ratio. For this fast reactor, the product $\wp\varepsilon$ is not applicable; hence, $k_\infty = \eta f$. From Example 16.2, $\eta = 2.2$ such that $f = k_\infty/\eta = 1.2/(2.2) = 0.55$. The fuel utilization may be written as

$$f = \frac{\Sigma_a^{235}}{\Sigma_a^{235} + \Sigma_a^{\text{Na}}} = \frac{N_{235}\sigma_a^{235}}{N_{235}\sigma_a^{235} + N_{\text{Na}}\sigma_a^{\text{Na}}} = \frac{\sigma_a^{235}}{\sigma_a^{235} + (N_{\text{Na}}/N_{235})\sigma_a^{\text{Na}}}$$

Rearranging this expression algebraically gives

$$\frac{N_{Na}}{N_{235}}=\frac{\sigma_a^{235}}{\sigma_a^{Na}}\left(\frac{1}{f}-1\right)=\frac{(1.4+0.25)\text{b}}{0.0008\text{b}}\left(\frac{1}{0.55}-1\right)=1700$$

This result indicates that the fuel concentration can be rather small and nonetheless criticality is achieved.

The reproduction factor embodies the efficacy at which the fuel produces more neutrons for each neutron it absorbs. In the case of multiple fuel nuclides, η must account for neutrons produced by each constituent

$$\eta=\frac{\nu_1\Sigma_f^1+\nu_2\Sigma_f^2+\nu_3\Sigma_f^3+\cdots}{\Sigma_a^1+\Sigma_a^2+\Sigma_a^3+\cdots} \tag{16.13}$$

For both η and f, the demarcation of "fuel" is at the discretion of the analyst so long as consistency is maintained—meaning that fuel could be uranium dioxide (UO_2), just the uranium, or only the U-235.

EXAMPLE 16.6

Determine η at thermal energies for UO_2 composed of natural uranium. The atomic densities of the fuel materials are related via $N_O=2N_U$, $N_{235}=0.0072N_U$, and $N_{238}=0.9927N_U$. Taking cross-sections from Table 4.2 and assuming that all oxygen is O-16 yields

$$\eta=\frac{\nu_{235}\Sigma_f^{235}}{\Sigma_a^{235}+\Sigma_a^{238}+\Sigma_a^{O}}=\frac{\nu_{235}N_{235}\sigma_f^{235}}{N_{235}\sigma_a^{235}+N_{238}\sigma_a^{238}+N_O\sigma_a^{O}}$$

$$=\frac{(2.4355)(0.0072)(582.6\text{b})}{(0.0072)(98.3+582.6\text{b})+(0.9927)(2.683\text{b})+(2)(0.00019\text{b})}=1.35$$

where ν_{235} was obtained from Table 6.2.

16.6 NEUTRON FLUX AND REACTOR POWER

The thermal power developed by a reactor is a quantity of great interest for practical reasons. Reactor power is related to the neutron population and to the mass of fissionable material present. First, let us look at a typical cubic centimeter of the reactor, containing N fuel nuclei, each with cross-section for fission σ_f at the typical neutron energy of the reactor, corresponding to neutron speed v. Suppose that there are n neutrons in the volume. The rate (fissions/(s cm^3)) at which the fission reaction occurs is thus

$$R_f=nvN\sigma_f \tag{16.14}$$

If each fission produces an energy w, then the power per unit volume is $q'''=wR_f$. For the whole reactor, of volume V, the rate of production of thermal energy is $P=q'''V$. If we have an average flux $\phi_{avg}=nv$ and a total number of fuel atoms $n_F=NV$, the total reactor power is seen to be

$$P=\phi_{avg}n_F\sigma_f w \tag{16.15}$$

From Section 6.4, $w=190$ MeV/fission or $1/w=3.29\times10^{16}$ fissions/(MW s).

Thus, we see that the power depends on the product of the number of neutrons and the number of fuel atoms. A high flux is required if the reactor contains a small amount of fuel, and vice versa. All other things equal, a reactor with a large fission cross-section can produce a required power with less fuel than one with small σ_f. We recall that σ_f decreases with increasing neutron energy. Thus for given power P, a fast reactor, operating with neutron energies principally in the vicinity of 1 MeV, requires either a much larger flux or a larger fissionable fuel mass than does the thermal reactor, with neutrons of energy less than 0.1 eV.

The power developed by most familiar devices is closely related to fuel consumption. For example, a large car generally has a higher gasoline consumption rate than a small car, and more gasoline is used in operation at high speed than at low speed. In a reactor, it is necessary to add fuel very infrequently because of the very large energy yield per unit mass, and the fuel content remains essentially constant. From Eq. (16.15) relating power, flux, and fuel, we observe that the power can be readily raised or lowered by changing the flux. By manipulation of control rods, the neutron population is allowed to increase or decrease to the proper level.

Power reactors used to generate electricity produce approximately 3000 megawatts of thermal power (MWt) and, with an efficiency of approximately one-third (33%), supply 1000 MW of electrical power (MWe).

EXAMPLE 16.7

The reactor in a 1000-MWe power plant is composed of 100 MTU (metric tons of uranium) of 3 w/o fuel. Therefore, the number of U-235 fuel atoms is

$$n_F = \frac{m_{235} N_A}{M_{235}} = \frac{(100 \times 10^6\,\text{g})(0.03)(6.022 \times 10^{23}\,\text{atom/mol})}{(235\,\text{g/mol})} = 7.69 \times 10^{27}\,\text{atoms}$$

To generate the requisite thermal power, the needed thermal flux is

$$\phi_{avg} = \frac{P}{n_F \sigma_f w} = \frac{(3000\,\text{MWt})(3.29 \times 10^{16}\,\text{fissions/(MWs)})}{(7.69 \times 10^{27}\,\text{atom})(582.6 \times 10^{-24}\,\text{cm}^2)} = 2.2 \times 10^{13}\,\text{n/(cm}^2\text{s)}$$

The flux and criticality are separate descriptors of the reactor condition. The difference can be explained by using an automobile as an analogy. The multiplication factor is akin to vehicle acceleration while the flux is comparable to car speed. Hence, a critical reactor can be operated at many flux, or equivalently power, levels.

16.7 THE NATURAL REACTOR

Until the 1970s, it had been assumed that Enrico Fermi and his associates put the first nuclear reactor into operation in 1942. It seems, however, that a natural chain reaction involving neutrons and uranium took place in the African state of Gabon, near Oklo, some 2 billion years ago (Cowan, 1976). At that time, the isotope concentration of U-235 in natural uranium was higher than it is now because of the differences in half-lives: U-235, 7.04×10^8 y; U-238, 4.47×10^9 y. The water content in a rich vein of

ore was sufficient to moderate neutrons to thermal energy. It is believed that this natural reactor operated off and on for thousands of years at power levels of the order of kilowatts. The discovery of the Oklo phenomenon resulted from the observations of an unusually low U-235 abundance in the mined uranium. The effect was confirmed by the presence of fission products.

16.8 SUMMARY

A self-sustaining chain reaction involving neutrons and fission is possible if a critical mass of fuel is accumulated. The value of the multiplication factor k indicates whether a reactor is subcritical (<1), critical ($=1$), or supercritical (>1). The reactor power, which is proportional to the product of flux and the number of fuel atoms, is readily adjustable. A thermal reactor contains a moderator and operates on slowed neutrons. Approximately 2 billion years ago, deposits of uranium in Africa had a high enough concentration of U-235 to become natural chain reactors.

16.9 EXERCISES

16.1 Calculate the reproduction factor η for fast neutrons for (a) U-235, (b) U-238, and (c) Pu-239.

16.2 If a power of 100 W is developed by (a) the Godiva-type reactor of mass 50 kg (93.9 w/o enrichment) or (b) the Jezebel-type reactor of mass 17 kg, what is the average flux within each respective assembly?

16.3 (a) Find the multiplication factors k_∞ and k_{eff} for a thermal reactor with $\varepsilon = 1.05$, $\wp = 0.75$, $\mathcal{L}_f = 0.90$, $\mathcal{L}_t = 0.98$, $f = 0.85$, and $\eta = 1.75$. (b) Evaluate the reactivity ρ.

16.4 The value of the reproduction factor η in uranium containing both U-235 (1) and U-238 (2) is given by

$$\eta = \frac{\nu_1 N_1 \sigma_f^1 + \nu_2 N_2 \sigma_f^2}{N_1 \sigma_a^1 + N_2 \sigma_a^2}$$

Calculate η for three reactors (a) thermal, with 3% U-235, $N_1/N_2 = 0.0315$; (b) fast, with the same fuel; and (c) fast, with pure U-235. Comment on the results. For the thermal constants, see tables in Chapter 6.

16.5 (a) Using thermal neutron values, find η for uranium dioxide in which the U-235 atom fraction is 0.2, regarded as a practical lower limit for nuclear weapons material. (b) Would the fuel be suitable for a research reactor?

16.6 Determine the reactivity values corresponding to supercriticality, criticality, and subcriticality.

16.7 Find the ratio of weight percentages of U-235 and U-238 at a time 1.9 billion years ago, assuming the present 0.711/99.3 ratio.

16.8 Constants for a spherical fast uranium-235 metal assembly are: diffusion coefficient $D = 1.02\,\text{cm}$; macroscopic absorption cross-section $\Sigma_a = 0.0795/\text{cm}$; effective radius $R = 10\,\text{cm}$. Calculate (a) the diffusion length L, (b) the geometric buckling B^2, and (c) the nonleakage factor $\mathcal{L}$.

16.9 Using the Lady Godiva specifications in Table 16.1, determine (a) the diffusion area and (b) the nonleakage probability.

16.10 Compute the geometric buckling for (a) a parallelepiped $25\,\text{cm} \times 35\,\text{cm} \times 40\,\text{cm}$, and (b) a cylinder with radius 25 cm and height 50 cm. If these cores are bare metal reactors of fully enriched uranium with density $19\,\text{g/cm}^3$, what is the nonleakage probability for each?

16.11 Calculate the resonance escape probability for a homogeneous uranium-graphite mixture in which the ratio of moderator-to-fuel atoms is 450. The resonance integral of the uranium is 277 b, and the epithermal scattering cross-section of carbon is 4.66 b.

16.12 Show that $\sigma_{tr} = \sigma_t - \overline{\mu}\sigma_s \cong \sigma_t$ for heavy nuclides (recall Eq. 4.50).

16.13 Estimate and compare the total mean free paths for fast and thermal neutrons in the (a) Godiva and (b) Jezebel assemblies. (See results of preceding exercise.)

16.14 Using the nuclear data of Table 16.3, estimate the critical radius for (a) Godiva and (b) Jezebel. What is the percentage error between the estimated radius and the actual radius obtained using data from Table 16.1.

16.15 A homogeneous thermal reactor is comprised by volume of 99% moderator and 1% natural uranium. Determine the thermal utilization if the moderator is (a) light water, (b) heavy water, and (c) graphite.

16.10 COMPUTER EXERCISES

16.A The evaluation of critical conditions for a variety of spherical metal assemblies can be made with the program CRITICAL. It uses a one-neutron group model with cross-sections deduced from early critical experiments related to weapons. CRITICAL can handle any combination of uranium and plutonium. Run the program, choosing U enrichment and Pu content. Suggested configurations: (a) pure U-235; (b) Godiva (Table 16.1); (c) Jezebel (Table 16.1); (d) natural U (0.0072 atom fraction U-235, should not be possible to be made critical); (e) depleted U (0.003 atom fraction U-235); (f) elementary breeder reactor (Pu-239 volume 10%, depleted U).

16.B Competition among three neutron processes—scattering, absorption, and leakage—is illustrated by the program SLOWINGS. It simulates the release of a series of neutrons at the center of a carbon sphere and, by use of slowing theory and random numbers, finds the number of neutrons absorbed and escaping, and displays their paths in three dimensions. (a) Run the program several times to note statistical variations. (b) Increase the absorption cross-section by a factor of 200 as if considerable boron were added to the sphere, and note the effect.

REFERENCES

Cowan, G.A., 1976. A natural fission reactor. Sci. Am. 234 (1), 36–47.
Paxton, H.C., 1983. A History of Critical Experiments at Pajarito Site. LA-9685-H, Los Alamos National Laboratory.

FURTHER READING

Argonne National Laboratory (ANL), 1963. Reactor Physics Constants, ANL-5800, second ed.
Chadwick, M.B., Herman, M., Obložinský, P., Dunn, M.E., Danon, Y., Kahler, A.C., et al., 2011. ENDF/B-VII.1 Nuclear data for science and technology: cross-sections, covariances, fission product yields and decay data. Nucl. Data Sheets 112 (12), 2887–2996.
Glasstone, S., Sesonske, A., 1994. Nuclear Reactor Engineering, fourth ed. vol. 1, Reactor Design Basics, vol. 2, Reactor Systems EngineeringChapman and Hall, New York.
Jarvis, G.A., Linenberger, G.A., Orndoff, J.D., Paxton, H.C., 1960. Two plutonium-metal critical assemblies. Nucl. Sci. Eng. 8 (6), 525–531.
Karam, A., 2005. The Natural Reactor at Oklo. www.physics.isu.edu/radinf/Files/Okloreactor.pdf. A comparison with modern nuclear reactors.
Meshik, A.P., 2005. The workings of an ancient nuclear reactor. Sci. Am. 293 (5), 82–91.
Peterson, R.E., Newby, G.A., 1956. An unreflected U-235 critical assembly. Nucl. Sci. Eng. 1 (2), 112–125 Description of Godiva.

CHAPTER

NUCLEAR HEAT ENERGY 17

CHAPTER OUTLINE

Most of the energy released in fission appears as kinetic energy of a few high-speed particles. As these pass through matter, they slow down by multiple collisions and impart thermal energy to the medium. The purpose of this chapter is to examine the means by which this energy is transferred to a cooling agent and transported to devices that convert mechanical energy into electrical energy. Methods for dealing with the large amounts of waste heat generated are also discussed.

17.1 METHODS OF HEAT TRANSMISSION

We learned in basic science that heat, as one form of energy, is transmitted by three methods: conduction, convection, and radiation. The physical processes for the methods are different. In *conduction*, molecular motion in a substance at a point at which the temperature is high causes motion of adjacent molecules, and a flow of energy toward a region of low temperature takes place. The rate of heat flow is proportional to the slope of the temperature (i.e., the temperature gradient). In *convection*, molecules of a cooling agent such as air or water strike a heated surface, gain energy, and return to raise the bulk temperature of the coolant. The rate of heat removal is proportional to the difference between the surface temperature and that of the surrounding medium and also depends on the amount of circulation of the coolant near the surface. In *radiation*, molecules of a heated object emit and receive electromagnetic radiations, with a net transfer of energy that depends on the temperatures of the body and the adjacent regions, specifically on the difference between the temperatures raised to the fourth power. For reactors, this third mode of heat transfer is generally of less importance than the former two.

Nuclear Energy. https://doi.org/10.1016/B978-0-12-812881-7.00017-4

Before examining heat generation and removal from the reactor core, it is useful to establish the common nomenclature when addressing the heat transfer processes. Taking q as heat flow in watts, three variants of this quantity are:

1. q': linear power density—the heat generation per unit length [W/cm].
2. q'': heat flux—the heat flow per unit area [W/cm^2].
3. q''': power density—the volumetric heat generation rate [W/cm^3].

Notice that the number of prime marks for all four heat terms is the exponent to which the length unit in the denominator is raised.

17.2 FUEL ELEMENT CONDUCTION AND CONVECTION

The transfer of heat by *conduction* in a flat plate (insulated on its edges) is first reviewed. If the plate has a thickness Δx and cross-sectional area A, and the temperature difference between its faces is ΔT, the rate of heat flow through the plate, q, is given by Fourier's law of heat conduction

$$q = kA\frac{\Delta T}{\Delta x} \tag{17.1}$$

where k is the *thermal conductivity*, with typical units W/(cm °C). For the plate, the slope of the temperature is the same everywhere. In a more general case, the slope may vary with position, and the rate of heat flow per unit area $q'' = q/A$ is proportional to the slope or gradient written as dT/dx.

The conductivity k varies somewhat with temperature, but we treat k as constant for the following analysis of conduction in a single fuel rod of a reactor. Let the production rate of thermal energy by fission be uniform throughout the rod. If the rod is long in comparison with its radius R, or if it is composed of a stack of pellets, most of the heat flow is in the radial direction. If the surface is maintained at a temperature T_S by the flow of coolant, the center of the rod must be at some higher temperature T_0. For a unit length of rod with volume πr^2, the heat generation rate is $\pi r^2 q'''$. The amount of energy produced within a region of radius r must flow out across the boundary of surface area $2\pi r$ with flow rate $-k(dT/dr)2\pi r$, that is

$$\pi r^2 q''' = -k2\pi r\, dT/dr \tag{17.2}$$

We can integrate this expression from $r = 0$, where $T = T_0$, to an arbitrary radial position to yield the fuel temperature profile of

$$T_F(r) = T_0 - q'''r^2/(4k) \tag{17.3}$$

Thus, the fuel temperature distribution T_F is in the shape of a parabola within the rod, as shown in Fig. 17.1.

At the surface $T_S = T_F(R) = T_0 - q'''R^2/(4k)$, such that the temperature change across the fuel pellet is

$$\Delta T_F = T_0 - T_S = \frac{q'}{4\pi k} \tag{17.4}$$

As expected, the temperature difference is large if the rate of heat generation per unit volume q''' or the rate of heat generation per unit length q' is large. For a fuel rod of height H, the overall heat production can be written as

$$q = q'H = q''2\pi RH = q'''\pi R^2 H \tag{17.5}$$

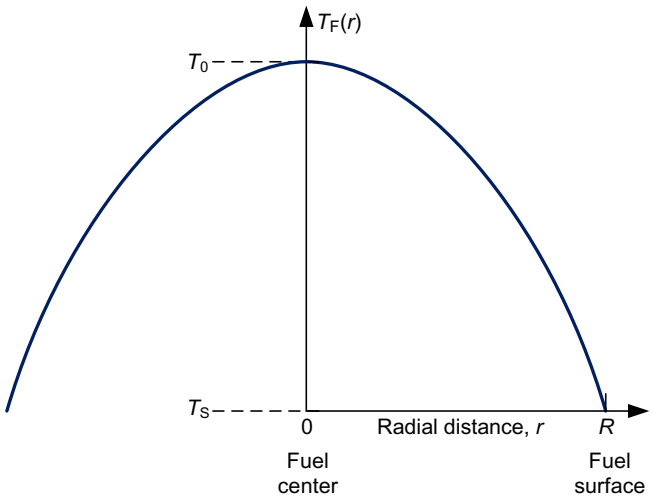

FIG. 17.1

Temperature distribution in a fuel pellet.

EXAMPLE 17.1

Let us calculate the temperature difference ΔT_F for a reactor fuel rod of radius 0.5 cm, at a point where the power density is $q''' = 200\,\text{W/cm}^3$. This corresponds to a linear heat rate

$$q' = \pi R^2 q''' = \pi(0.5\text{cm})^2\left(200\text{W/cm}^3\right) = 157\text{W/cm}\,(\text{or}\,4.8\text{kW/ft})$$

Letting the thermal conductivity of UO_2 be $k = 0.062\,\text{W/(cm °C)}$, we find

$$\Delta T_F = \frac{q'}{4\pi k} = \frac{157\text{W/cm}}{4\pi(0.062\text{W/(cm°C)})} = 200°\text{C} = 360°\text{F}$$

If we wish to keep the temperature low along the centerline of the fuel to avoid structural changes or melting, the conductivity k should be high, the rod diameter small, or the reactor power level low. The UO_2 ceramic fuel melts at 5080°F (2800°C), but the melting temperature decreases with fuel burnup. In a typical reactor, there is a small gap between the fuel pellet and the inside surface of the cladding. During operation, this gap contains gases (e.g., helium and fission product gases), which are poor heat conductors and thus cause a rather large temperature drop across the gap. A smaller drop will occur across the cladding, which is thin and has a high thermal conductivity.

We have so far assumed that the thermal conductivity is constant. It actually varies with temperature and thus with position in the fuel pin. A more general calculation of k is possible with the program CONDUCT utilized in Computer Exercise 17.A, and the temperature distribution may be found with a program TEMPPLOT in Computer Exercise 17.B.

Convective cooling depends on many factors such as the fluid speed, the size and shape of the flow passage, and the thermal properties of the coolant as well as the area exposed and the *film temperature*

difference between surface and coolant $\Delta T_S = T_S - T_C$. Experimental measurements yield the *heat transfer coefficient h*, appearing in Newton's law of cooling describing the rate of heat transfer q across the surface of area S

$$q = hS\,(T_S - T_C) \tag{17.6}$$

where the fuel rod surface area is $S = 2\pi RH$. The most common usage of the heat flux is to describe conditions at the cladding surface because $q'' = h\Delta T_S$.

The units of h are typically W/(cm^2 °C). To keep the surface temperature low to avoid melting of the metal cladding of the fuel or to avoid boiling if the coolant is a liquid, a large surface area is needed or the heat transfer coefficient must be large, a low-viscosity coolant of good thermal conductivity is required, and the flow speed must be high.

EXAMPLE 17.2

Using data from the prior example, we can estimate a representative surface heat transfer coefficient value for a fuel rod. If the film temperature difference ΔT_S is 15°C, then

$$h = \frac{q}{S(T_S - T_C)} = \frac{q'''R}{2\Delta T_S} = \frac{(200\,\mathrm{W/cm^3})(0.5\,\mathrm{cm})}{2(15°\mathrm{C})} = 3.3\,\mathrm{W/(cm^2\,°C)}$$

17.3 TEMPERATURE DISTRIBUTIONS THROUGH A REACTOR

As coolant flows along the many channels surrounding fuel rods in a reactor, it absorbs thermal energy and rises in temperature. Because it is the reactor power that is being extracted, we may apply the principle of conservation of energy. If the coolant of specific heat c_p enters the reactor at temperature $T_{C,in}$ and leaves at $T_{C,out}$, with a mass flow rate $\dot{m}_R$, then the reactor thermal power Q_R is

$$Q_R = \dot{m}_R c_p\,(T_{C,out} - T_{C,in}) = \dot{m}_R c_p \Delta T_C \tag{17.7}$$

This relation is valid so long as the coolant does not change state (e.g., within pressurized water reactors [PWRs] and high-temperature, gas-cooled reactors [HTGRs]); however, if bulk boiling occurs, then the enthalpy change must be utilized to correctly describe the situation.

EXAMPLE 17.3

Let us find the amount of circulating water flow to cool a reactor that produces 3000 MW of thermal power. Let the water enter at 300°C (572°F) and leave at 325°C (617°F). Assuming the water is at PWR conditions of 140 bar (2000 psia, pounds per square inch absolute) and 316°C, the specific heat is 6.06 kJ/(kg °C) and the density is 687 kg/m^3. Thus the mass flow rate is

$$\dot{m}_R = \frac{Q_R}{c_p(T_{C,out} - T_{C,in})} = \frac{3000 \times 10^6\,\mathrm{W}}{\left(6.06 \times 10^3\,\mathrm{J/(kg°C)}\right)(325 - 300°\mathrm{C})} = 19{,}800\,\mathrm{kg/s}$$

This corresponds to a volumetric flow rate of

$$\dot{V} = \frac{\dot{m}_R}{\rho} = \frac{19{,}800\,\text{kg/s}}{687\,\text{kg/m}^3} = 28.8\,\text{m}^3/\text{s} = 1.73 \times 10^6\,\text{L/min}$$

To appreciate the magnitude of this flow, we can compare it with that from a garden hose of 40 L/min. The water for cooling a reactor is not wasted, of course, because it is circulated in a closed loop.

The temperature of a coolant as it moves along any channel of the reactor can also be found by application of the preceding energy conservation relation. In general, the power produced per unit length of fuel rod varies with position in the reactor because of the variation in neutron flux shape. In particular, the volumetric heat generation rate is related to the nuclear fission process via

$$q''' = w\Sigma_f\phi \tag{17.8}$$

Reactor thermal analyses may be carried out considering the entire core, or often by simply using a representative fuel rod and coolant channel. In the latter case, heat production and coolant flow are relative to the number of fuel rods N_R. For instance, the coolant mass flow rate associated with each fuel rod is $\dot{m} = \dot{m}_R/N_R$.

For a special case of a *uniform* power along the z-axis with origin at the core midplane as in Fig. 17.2A, the power per unit length is $q' = (Q_R/N_R)/H$. The temperature rise of a nonboiling coolant at z is then

$$T_C(z) = T_{C,in} + \frac{(z + H/2)\,q'}{\dot{m}c_p} \quad \frac{-H}{2} \le z \le \frac{H}{2} \tag{17.9}$$

This shows that the temperature increases linearly with distance along the channel, as graphed in Fig. 17.2B. The temperature difference between coolant and fuel surface is the same at all points along the channel for this constant power distribution, and the temperature difference between the fuel center and fuel surface is also uniform. We can plot these as in Fig. 17.2C. The highest temperatures in this case are at the reactor coolant exit.

If instead, the axial power were shaped as a cosine function, see Fig. 17.3A, with $q'(z) = q'_{max}\cos(\pi z/H)$, the application of the relations for conduction and convection would yield temperature curves as shown in Fig. 17.3B. The fuel surface and center temperatures are obtained using Eqs. (17.4) and (17.6) in conjunction with the coolant temperature distribution

$$T_C(z) = T_{C,in} + \frac{q'_{max}H}{\pi\dot{m}c_p}\left[1 + \sin\left(\frac{\pi z}{H}\right)\right] \quad \frac{-H}{2} \le z \le \frac{H}{2} \tag{17.10}$$

For this case, the highest temperatures of fuel surface and fuel center occur between the halfway point and the coolant exit. In the design of a reactor, a great deal of attention is given to the determination of which channels have the highest coolant temperature and at which points on the fuel rods *hot spots* occur. Ultimately, the power of the reactor is limited by conditions at these channels and points.

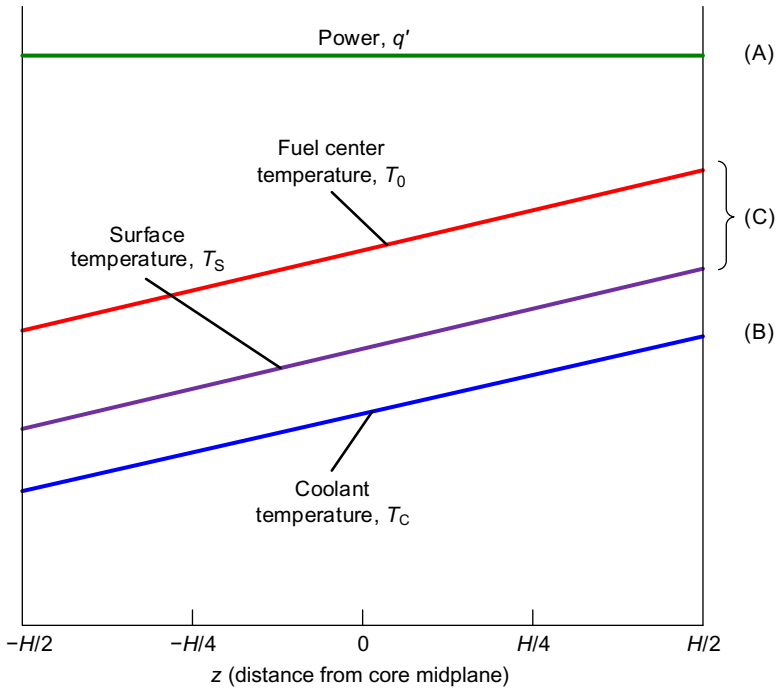

FIG. 17.2

Temperature distributions along axis of reactor with uniform power.

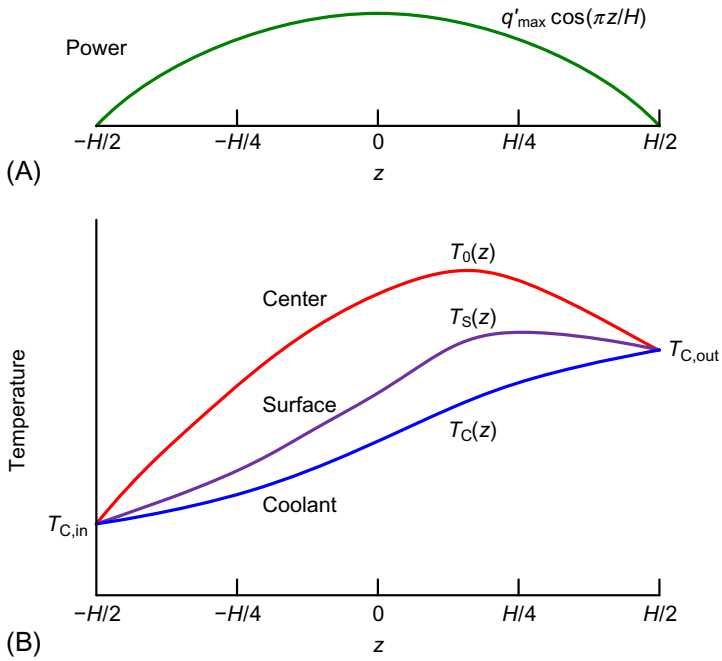

FIG. 17.3

Temperature distributions (B) along channel with sinusoidal power profile (A).

EXAMPLE 17.4

Using data from prior examples in this chapter, we shall determine the fuel centerline temperature at three-quarters of its height for the sinusoidal power distribution. If the average heat generation rate q'_{avg} is 157 W/cm, then the maximum is (see Exercise 17.12)

$$q'_{\max} = q'_{\text{avg}}\pi/2 = (157\,\text{W/cm})(\pi/2) = 247\,\text{W/cm}$$

With a core height of 3.6 m, the number of fuel rods is

$$N_{\text{R}} = \frac{Q_{\text{R}}}{q} = \frac{Q_{\text{R}}}{q'_{\text{avg}}H} = \frac{(3000\times 10^6\,\text{W})}{(157\,\text{W/cm})(360\,\text{cm})} = 53{,}080\,\text{rods}$$

Therefore, the coolant flow through each channel is

$$\dot{m} = \dot{m}_{\text{R}}/N_{\text{R}} = (19{,}800\,\text{kg/s})/(53{,}080\,\text{rods}) = 0.373\,\text{kg/s}$$

The coolant temperature at the location of interest, $z = H/4$, is

$$\begin{aligned} T_{\text{C}}(H/4) &= T_{\text{C,in}} + \frac{q'_{\max}H}{\pi\dot{m}c_{\text{p}}}[1+\sin(\pi/4)] \\ &= 300^\circ\text{C} + \frac{(247\,\text{W/cm})(360\,\text{cm})(1.707)}{\pi(0.373\,\text{kg/s})\left(6.06\times 10^3\,\text{J/(kg°C)}\right)} = 321^\circ\text{C} \end{aligned}$$

At this axial position, the linear power density is

$$q'(z) = q'_{\max}\cos(\pi z/H) = (247\,\text{W/cm})\cos(\pi/4) = 175\,\text{W/cm}$$

Thus, the film temperature difference at the fuel cladding surface is

$$\Delta T_{\text{S}} = \frac{q''(z)}{h} = \frac{q'(z)}{2\pi Rh} = \frac{175\,\text{W/cm}}{2\pi(0.5\,\text{cm})(3.3\,\text{W/(cm}^2\text{°C))}} = 17^\circ\text{C}$$

The temperature rise across the fuel pellet is

$$\Delta T_{\text{F}} = \frac{q'(z)}{4\pi k} = \frac{175\,\text{W/cm}}{4\pi(0.062\,\text{W/(cm°C)})} = 225^\circ\text{C}$$

Overall, the fuel center temperature at this position is found from

$$T_0 = T_{\text{C}} + \Delta T_{\text{S}} + \Delta T_{\text{F}} = 321 + 17 + 225^\circ\text{C} = 563^\circ\text{C}$$

In comparison, the uniform distribution yields a lower fuel centerline temperature of 534°C at this location (see Exercise 17.13).

The mechanism of heat transfer from metal surfaces to water is quite sensitive to the film temperature difference. As the latter ΔT_{S} increases, ordinary convection gives way to *nucleate boiling*, in which bubbles form at points on the surface, and eventually *film boiling* can occur, in which a blanket of vapor creates an insulating layer, thereby reducing heat transfer and allowing hazardous melting. The value of the heat flux q'' at which film boiling begins is called the *critical heat flux*. A parameter called the *departure from nucleate boiling ratio* (DNBR) is used to indicate how close the heat flux is to the critical value. For example, a DNBR of 1.3 implies a safety margin of 30%. Fig. 17.4 indicates maximum temperature values for a typical PWR.

Achieving a water temperature of 620°F (approximately 327°C) requires that a very high pressure be applied to the water coolant-moderator. Fig. 17.5 shows the behavior of water in the liquid and vapor phases. The curve that separates the two phase regions describes what are called saturated conditions.

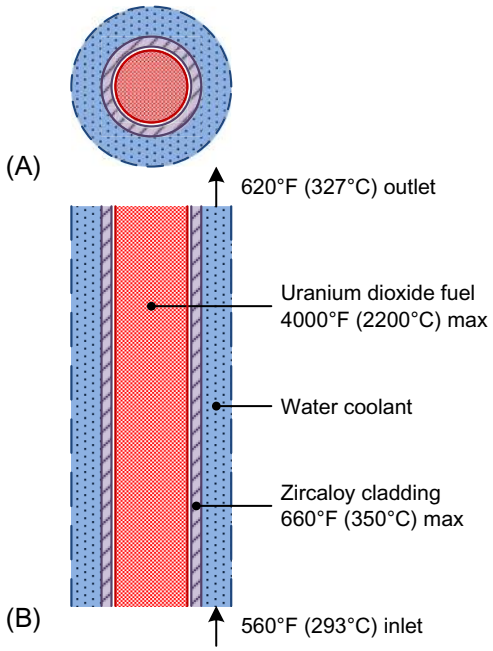

FIG. 17.4

Reactor channel heat removal. (A) Top view and (B) side view.

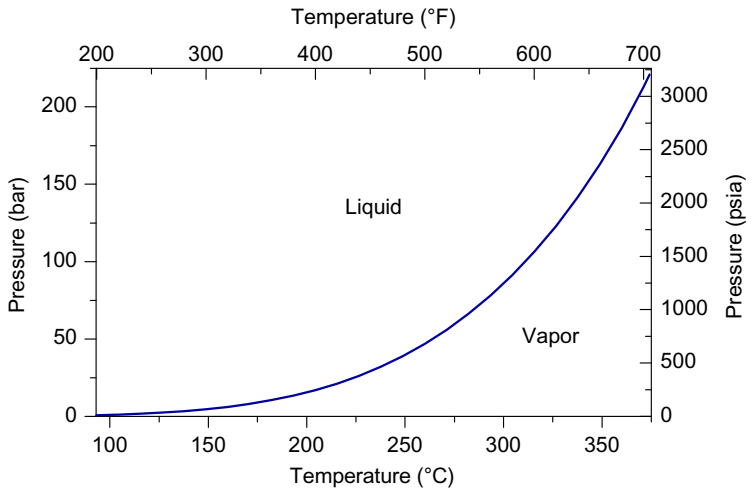

FIG. 17.5

Relationship of pressure and temperature for saturated water.

Suppose that the pressure vessel of the reactor contains water at 2000 psia and 600°F and the temperature is raised to 650°F. The result will be considerable steam formation (flashing) within the liquid. The two-phase condition could lead to inadequate cooling of the reactor fuel. If instead, the pressure was allowed to drop to 1200 psia, for example, the vapor region is again entered and flashing would occur. However, it should be noted that deliberate two-phase flow conditions are used in boiling water reactors (BWRs), providing efficient and safe cooling.

17.4 STEAM GENERATION AND ELECTRICAL POWER PRODUCTION

The original development of nuclear power plants made prudent use of the considerable experience previously acquired with fossil generating stations, the basic strategy being to replace the combustion-based heat source with a nuclear reactor. Thus, the heat absorbed by the reactor coolant is converted to steam for use in a traditional steam turbine. The turbine is shaft-connected to an electric generator that produces the alternating current (ac) power. The ac current is carried through high-voltage transmission lines to the electric loads, such as cities and large industrial facilities.

A boiling water reactor pipes its steam directly to the turbine, whereas the pressurized water reactor utilizes steam generators to produce the water vapor. In general, for those reactor types that do not vaporize the water directly, thermal energy in the circulating reactor coolant is transferred to a separate working fluid such as steam by means of a heat exchanger or steam generator. To avoid confusion, the water flowing through the reactor system is referred to as *primary coolant* while the water that is converted into steam is part of the secondary system. In the case of a BWR, the radioactive primary water is permitted to pass through the turbine while this is not the situation in a PWR.

The PWR vendors deployed two types of steam generators. Fig. 17.6A depicts a recirculating, or U-tube, steam generator. In simplest construction, this steam generator consists of a vessel partly filled with liquid water through which pass thousands of inverted U-shaped tubes containing heated water from the reactor. Moisture separators and steam dryers serve to ensure that only vapor is allowed to exit the steam generator. Steam from the steam generator flows to a turbine while the primary coolant returns to the reactor. Fig. 17.6B illustrates the once-through steam generator that has the distinction of being able to produce superheated steam, but it has little water inventory to accommodate certain transient situations.

At a number of nuclear plants, the steam generator has failed prematurely because of corrosion that created holes in tubes, requiring plugging or repair. In some cases, replacement of the steam generator was required, with corresponding outage, cost, and loss of revenue. Details on the problem appear in a Nuclear Regulatory Commission Technical Issue Paper (NRC, 2014).

The conversion of thermal energy of steam into mechanical energy of rotation of a turbine and then to electrical energy from a generator is achieved by conventional means. Steam at high pressure and temperature strikes the blades of the turbine, which drives the electric generator. The exhaust steam is passed through another heat exchanger that serves as the *condenser*, and the condensate is returned to the nuclear steam supply system as feedwater. The condenser is a shell-and-tube heat exchanger in which the steam condenses on the outside of the tubes that carry liquid water. This cooling water for the condenser is pumped from a nearby body of water or cooling tower, as discussed in the next section. The condenser cooling water forms yet another isolated fluid circuit from that of either the primary or the secondary closed loops. The water in these latter closed loops is continuously recycled

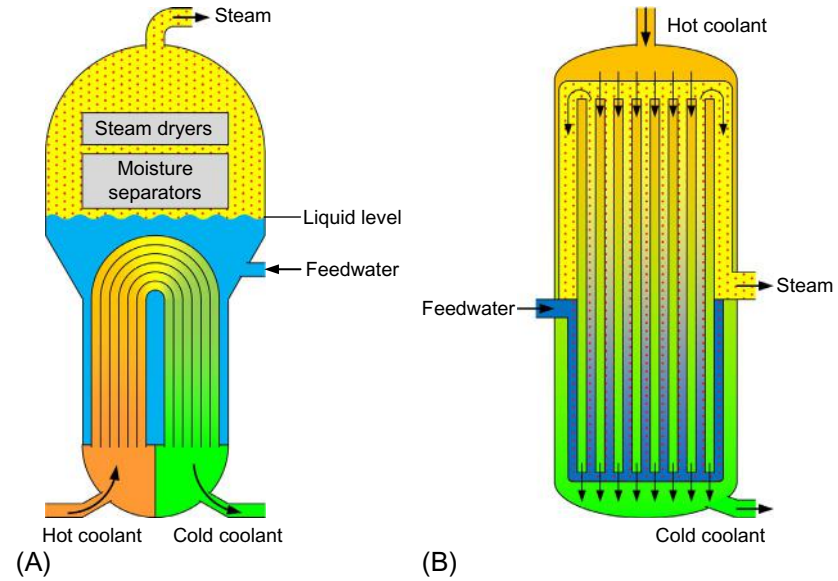

FIG. 17.6

Heat exchanger or steam generator. (A) U-tube and (B) once-through steam generators.

and considerable effort is expended to maintain a water chemistry that is compatible with the cooling system materials.

The large synchronous electric generators at nuclear power plants typically have rotor speeds of 1800 revolutions per minute to produce 60 Hz, 25 kV alternating current. A nearby step-up transformer increases the voltage to several hundred kilovolts while proportionately decreasing the output current, which is sent to the plant switchyard for connection to the transmission system of the electric grid.

The thermal efficiency η_{th} allows calculating the plant electric power output P_e from the reactor thermal power Q_R via

$$P_e = \eta_{th} Q_R \tag{17.11}$$

Hence, the thermal efficiency η_{th} is the ratio of net work performed to thermal energy supplied. For any thermal conversion process, the efficiency is limited by the temperatures at which the system operates. According to the second law of thermodynamics, an ideal (Carnot) cycle has the highest efficiency value,

$$\eta_C = 1 - T_L/T_H \tag{17.12}$$

in which T_L and T_H are the lowest and highest absolute temperatures (Kelvin, °C+273; Rankine, °F+460), specifically, the temperatures at which heat is rejected from and added to the cycle, respectively. For a nuclear power plant, the high and low temperatures of the thermal cycle are found in the steam and condensate, respectively.

EXAMPLE 17.5

Suppose the steam generator produces steam at 300°C and cooling water for the condenser comes from a source at 20°C. To ensure heat transfer in the condenser, assume that the condensate temperature is about 15°C higher than the inlet cooling water, such that we find a maximum (Carnot) cycle efficiency of

$$\eta_C = 1 - \frac{T_L}{T_H} = 1 - \frac{20 + 15 + 273\,\text{K}}{300 + 273\,\text{K}} = 0.46$$

The overall efficiency of the plant is lower than this because of heat loss in piping, pumps, and other equipment. The thermal efficiency of a typical nuclear power plant is approximately 0.33. Coal-fired plants can operate at higher steam temperatures, giving overall efficiencies of approximately 0.40.

17.5 WASTE HEAT REJECTION

The generation of electric power by consumption of any fuel is accompanied by the release of large amounts of waste heat. While fossil plants can emit heat via the flue gas stack, nuclear units must dissipate the waste heat solely via the condenser cooling water. By conservation of energy and referring to Fig. 17.7, the plant condenser must reject a waste power of

$$Q_W = Q_R - P_e \tag{17.13}$$

Because nuclear plants have a thermal efficiency of 33%, about twice as much energy is rejected as is converted into useful electrical energy.

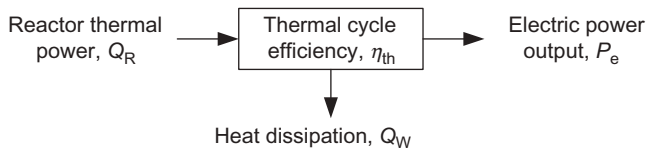

FIG. 17.7

Power plant energy balance.

EXAMPLE 17.6

A nuclear plant operating at electrical power 1000 MWe would have a reactor thermal power of

$$Q_R = P_e/\eta_{th} = (1000\,\text{MWe})/0.33 = 3030\,\text{MWt}$$

which means that η_{th} has implicit units of MWe per MWt, or similar. The waste power is

$$Q_W = Q_R - P_e = 3030 - 1000 = 2030\,\text{MWt}$$

We can calculate the condenser cooling water mass flow rate $\dot{m}_C$ required to limit the temperature rise to a typical figure of $\Delta T = 12°C$ with a specific heat of $c_p = 4.18 \times 10^3$ J/(kg °C) for ambient environmental conditions

$$\dot{m}_C = \frac{Q_W}{c_p \Delta T} = \frac{2.03 \times 10^9 \text{ W}}{(4.18 \times 10^3 \text{ J/(kg°C)})(12°C)} = 4.05 \times 10^4 \text{ kg/s}$$

This corresponds to a flow of 925 million gallons (3.5×10^9 L) per day.

Smaller power plants in past years were able to use the run of the river (i.e., to take water from a stream, pass it through the condenser, and discharge heated water downstream). Stream flows of the order of a billion gallons per day are rare, and the larger power plants must typically dissipate heat by use of a large lake or cooling towers. Either method involves some environmental effects.

If a lake is used, the temperature of the water at the discharge point may be too high for certain organisms. It is common knowledge, however, that fishing is especially good where the heated water emerges. Means by which heat is removed from the surface of a lake are evaporation, radiation, and convection due to air currents. Regulations of the Environmental Protection Agency (EPA, 1986) limit the rise in temperature in bodies of water. Clearly, the larger the lake and the wider the dispersal of heated water, the easier it is to meet requirements. When the thermal discharge goes into a lake, the ecological effects are frequently called *thermal pollution*, especially when the elevated temperatures damage plants and animals. Other effects are the deaths of aquatic animals by striking screens, or passing through the system, or being poisoned by chemicals used to control the growth of undesirable algae. However, the environmental effects are mixed. Warm water is attractive to various fish and favors growth in their population.

Many nuclear plants have had to adopt the cooling tower for disposal of waste heat into the atmosphere. In fact, the hyperboloid shape (see Fig. 17.8) is so common that many people mistake it for the reactor. A cooling tower is basically a large heat exchanger with airflow provided by natural convection or by mechanical blowers. In a *wet* type (see Fig. 17.8A), the interior surfaces are kept saturated with moisture, and evaporation provides cooling. Water demands by this model may be excessive. In a *dry* type (see Fig. 17.8B), analogous to an automobile radiator, the cooling is by convection and requires more surface area and airflow. It is therefore larger and more expensive. A hybrid wet/dry cooling tower is used to minimize the effects of vapor plumes in cold weather and to conserve water in hot weather. The rising value of water will likely move industry increasingly toward greater utilization of dry cooling technology. The relationship of methods of reactor cooling is highlighted by the problem faced by Dominion Energy as it considered an additional reactor at North Anna, Virginia. The water drawn from and returned to a lake—a once-through system—would be too warm for wildlife, so one or more cooling towers will be required. Because water is lost by evaporation, reactors in areas experiencing drought may have to cut back on power.

EXAMPLE 17.7

Let us determine the water loss, or makeup requirement, for a 1000-MWe nuclear unit employing wet cooling. From Section 1.4, the latent heat of vaporization h_{fg} is 2258 J/g. Because around 80% of the heat removal in wet cooling towers occurs through evaporative cooling, the water loss to the atmosphere is

$$\dot{m}_L = \frac{0.8 Q_W}{h_{fg}} = \frac{(0.8)(2.03 \times 10^9 \text{ W})}{(2258 \text{ W s/g})(10^3 \text{ g/kg})} = 719 \text{ kg/s}$$

This represents 1.8% of the condenser cooling water flow of 4.05×10^4 kg/s from the prior example.

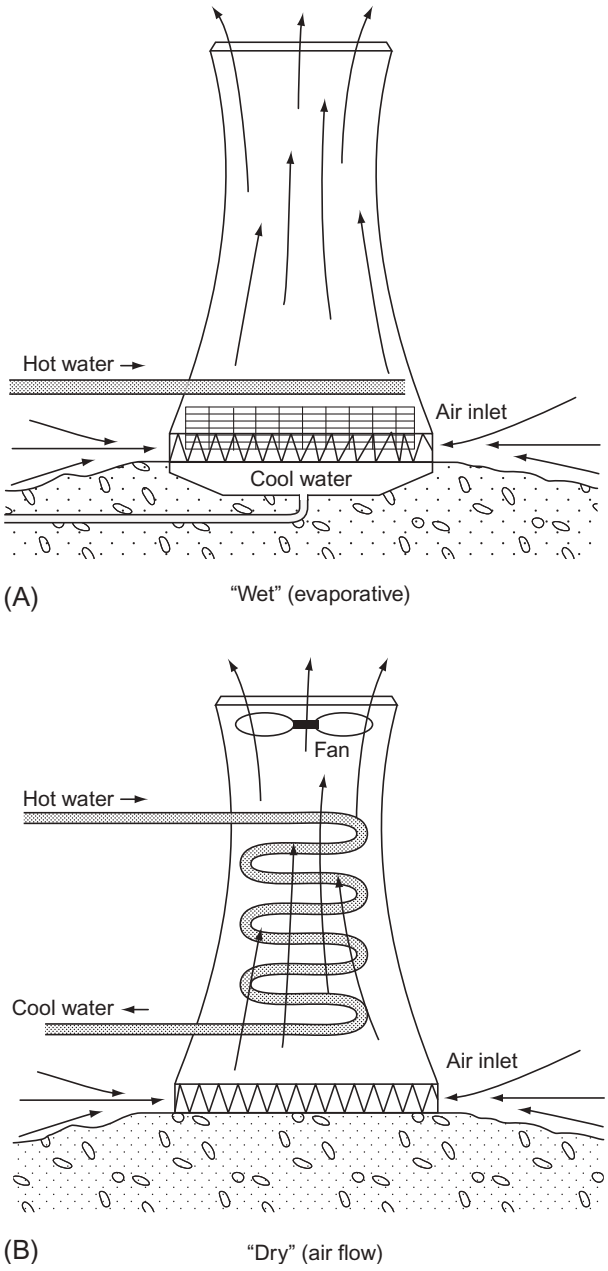

FIG. 17.8

Cooling towers: (A) wet (evaporative) and (B) dry (air flow).

From Clark, J.R., 1969. Thermal pollution and aquatic life. Sci. Am. 220(3), 18–27.

Waste heat can be viewed as a valuable resource. If it can be used in any way, it reduces the need for oil and other fuels. Some of the actual or potential beneficial uses of waste heat are the following (Oesterwind, 1978; Margen, 1978; IAEA, 1987):

- District heating: Homes, business offices, and factories of whole towns in Europe are heated in this way.
- Production of fish: Warm water can be used to stimulate growth of the food fish need.
- Extension of plant growth season: For colder climates, use of water to warm the soil in early spring would allow crops to be grown for a longer period.
- Biological treatment: Higher temperatures may benefit water treatment and waste digestion.
- Desalination: Removal of salt from seawater or brackish water (see Section 24.8 for details).
- Production of hydrogen gas: Use of a dedicated reactor or combined heat and electricity source to isolate H_2 (see Section 24.9 for details).

Each of these applications has merit, but there are two problems: (1) the need for heat is seasonal, so the systems must be capable of being bypassed in summer or, if buildings are involved, they must be designed to permit air conditioning; and (2) the amount of heat is far greater than any reasonable use that can be found. It has been said that the waste heat from electrical plants was sufficient to heat all the homes in the United States. If all homes within practical distances of power plants were so heated, there still would be a large amount of unused waste heat.

A few reactors around the world have been designed or adapted to produce both electrical power and useful heat for space heating or process steam. For example, the Beznau plant in Switzerland provides 81 MWt of district heating to 15,000 residents in 11 nearby municipalities via a main piping network of 31 km. The abbreviation CHP for combined heat and power is applied to these systems. It can be shown (see Exercise 17.11) that if half the turbine steam of a reactor with thermal efficiency 1/3 is diverted to useful purposes, the efficiency is doubled, neglecting any adjustment in operating conditions.

A similar practice, called *cogeneration*, has been promoted for facilities already producing steam for in-plant use. In particular, a boiler used for producing steam is connected to a turbine to generate electricity while continuing to provide process heat. Typical steam users are refineries, chemical plants, and paper mills. In general, cogeneration is any simultaneous production of electrical or mechanical energy and useful thermal energy, but it is regarded as a way to save fuel. For example, an oil-fired system uses 1 barrel (bbl) of oil to produce 750 kWh of electricity, and a process-steam system uses 2 bbl of oil to give 8700 lbm (3950 kg) of steam, but cogeneration requires only 2.4 bbl to provide both products.

17.6 SUMMARY

The principal modes by which fission energy is transferred in a reactor are conduction and convection. The radial temperature distribution in a fuel pellet is approximately parabolic. The rate of heat transfer from fuel surface to coolant by convection is directly proportional to the temperature difference. The allowed power level of a reactor is governed by the temperatures at local hot spots. Coolant flow along channels extracts thermal energy and delivers it to an external circuit consisting of a heat exchanger (PWR), a steam turbine that drives an electric generator, a steam condenser, and various pumps. Electric power plants discharge large amounts of waste heat because of inherent limits on efficiency.

Typically, a billion gallons of water per day must flow through the steam condenser to limit the temperature rise of the environment. When rivers and lakes are not available or adequate, waste heat is dissipated by cooling towers. Potential beneficial uses of the waste thermal energy include space heating and desalination. Some nuclear facilities produce and distribute both steam and electricity.

17.7 EXERCISES

17.1 Show that the temperature varies with radial distance in a fuel pellet of radius R according to

$$T_F(r) = T_S + (T_0 - T_S)\left[1 - (r/R)^2\right]$$

where the center and surface temperatures are T_0 and T_S, respectively. Verify that the formula gives the correct results at $r = 0$ and $r = R$.

17.2 Explain the advantage of a circulating fuel reactor in which fuel is dissolved in the coolant. What disadvantages are there?

17.3 If the power density of a uranium oxide fuel pin, of radius 0.6 cm, is 500 W/cm^3, what is the heat flux across the fuel rod surface? If the temperatures of rod surface and coolant are 300°C and 250°C, respectively, what must the heat transfer coefficient h be?

17.4 A PWR operates at thermal power of 2500 MW, with water coolant mass flow rate of 15,000 kg/s. (a) If the coolant inlet temperature is 275°C, what is the outlet temperature? (b) If bulk boiling occurs at 336°C, at what reactor power would this take place?

17.5 A power reactor is operating with coolant temperature 500°F and pressure 1500 psia. A leak develops and the pressure falls to 500 psia. By how much must the coolant temperature be reduced to avoid flashing?

17.6 The thermal efficiencies of a PWR converter reactor and a fast breeder reactor are 0.33 and 0.40, respectively. (a) What are the amounts of waste heat for a 900 MWe reactor? (b) What percentage reduction in waste heat is achieved by going to the breeder?

17.7 As shown here, water is drawn from a cooling pond and returned at a temperature 14°C higher to extract 1500 MW of waste heat. All the heat is dissipated by water evaporation from the pond with an absorption of 2258 J/g. (a) How many kilograms per second of makeup water must be supplied from an adjacent river? (b) What percentage is this of the circulating flow to the condenser?

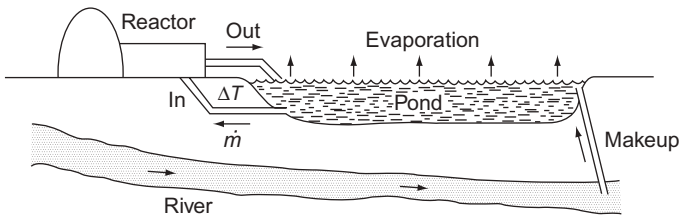

17.8 As a rough rule of thumb, it takes 1–2 acres of cooling lake per megawatt of installed electrical capacity. (a) If one conservatively uses the latter value, what is the area for a 1000-MWe plant? (b) Assuming 35% efficiency, how much energy in joules is dissipated per square meter per hour from the water?

17.9 How many gallons of water must be evaporated each day to dissipate 100% of the waste thermal power of 2030 MWt from a reactor?

17.10 Verify that approximately 1.6 kg of water must be evaporated to dissipate 1 kWh of energy.

17.11 A plant produces power both as useful steam, S, and electricity, E, from an input heat Q. (a) Develop a formula for the overall efficiency η', expressed in terms of the ordinary efficiency $\eta = E/Q$ and x, the fraction of waste heat used for steam. (b) Show that η' is 2/3 if $\eta = 1/3$ and $x = 1/2$. (c) Find η' for $\eta = 0.4$ and $x = 0.6$.

17.12 Show that the ratio $q'_{\max}/q'_{\text{avg}}$ for the sinusoidal power distribution is $\pi/2$.

17.13 For a uniform power distribution, determine the fuel centerline temperature three-quarters of the way through the reactor. Use reactor data from Examples 17.1–17.3.

17.14 Calculate the volumetric heat generation rate in a thermal reactor fueled with naturally enriched UO_2 of density 10 g/cm^3 and which is exposed to a flux of 10^{14} n/(cm^2 s).

17.15 (a) Perform the necessary integration on Eq. (17.2) to yield Eq. (17.3). (b) Repeat the integration across the entire fuel pellet to show that if the fuel thermal conductivity is a function of temperature, that

$$q' = 4\pi \int_{T_s}^{T_0} k\,dT \tag{17.14}$$

17.16 Derive Eq. (17.10) from the differential energy balance relation of $q'(z)\,dz = \dot{m} c_p\,dT$ for a PWR coolant channel.

17.8 COMPUTER EXERCISES

17.A If the thermal conductivity of UO_2 used as reactor fuel pins varies with temperature, Eq. (17.14) shows that the linear heat rate q' is 4π times the integral of k with respect to temperature T. (a) With computer program CONDUCT, which calculates the integral from 0 to T, verify that the integral is approximately 93 W/cm when T is the melting point of UO_2, 2800°C. (b) Find the linear heat rate with the maximum temperature $T_m = 2800$°C and surface temperature $T_s = 315$°C.

17.B The temperature distribution within a reactor fuel rod for variable thermal conductivity can be calculated with the integrals of k over temperature (Computer Exercise 17.A). In the program TEMPPLOT, by specifying maximum allowed center temperature and the expected surface temperature for a fuel pellet of radius R_0, the linear heat rate is calculated and used to obtain values of radius R as a function of temperature T. Test the program with typical inputs such as $R_0 = 0.5$ cm, $T_m = 2300$°C, and $T_s = 300$°C, plotting the resulting temperature distribution.

REFERENCES

International Atomic Energy Agency (IAEA), 1987. Low-Temperature Nuclear Heat Applications: Nuclear Power Plants for District Heating. IAEA-TECDOC-431. Vienna.

Margen, P., 1978. Summary—low-temperature nuclear heat. Nucl. Technol. 38 (2), 321–330.

Oesterwind, D., 1978. Economics and potential use of low-temperature nuclear heat. Nucl. Technol. 38 (1), 11–18.

U.S. Environmental Protection Agency (EPA), 1986. Quality Criteria for Water. EPA 440/5-86-001. (Known as the Gold Book).

U.S. Nuclear Regulatory Commission (NRC), 2014. Backgrounder on steam generator tube issues. https://www.nrc.gov/reading-rm/doc-collections/fact-sheets/steam-gen.html.

FURTHER READING

Becher, B., Becher, H., 2006. Cooling Towers. MIT Press, Cambridge, MA.

Becker, M., 1986. Heat Transfer: A Modern Approach. Plenum Press, New York.

Cheremisinoff, N.P., Cheremisinoff, P.N., 1981. Cooling Towers: Selection, Design and Practice. Ann Arbor Science, Ann Arbor, MI.

Clark, J.R., 1969. Thermal pollution and aquatic life. Sci. Am. 220 (3), 18–27.

El-Wakil, M.M., 1978. Nuclear Heat Transport. American Nuclear Society, La Grange Park, IL.

Hill, G.B., Pring, E.J., Osborn, P.D., 1990. Cooling Towers: Principles and Practice, third ed. Butterworth-Heinemann, London.

Incropera, F.P., DeWitt, D.P., 2001. Introduction to Heat Transfer, fourth ed. Wiley, New York.

Kays, W.M., Crawford, M.E., 2005. Convective Heat and Mass Transfer, fourth ed. McGraw-Hill, New York.

Keenan, J.H., Keyes, F.G., Hill, P.G., Moore, J.G., 1992. Steam Tables: Thermodynamic Properties of Water Including Vapor, Liquid, and Solid Phases With Charts. Krieger Publishing Co., Malabar, FL. Reprint of a classic work.

Lahey, R.T., Moody, F.J., 1993. The Thermal-Hydraulics of a Boiling Water Nuclear Reactor, second ed. American Nuclear Society, La Grange Park, IL. Emphasizes understanding of physical phenomena.

Minkowycz, W.J., Sparrow, E.M., Murthy, J.Y., 2006. Handbook of Numerical Heat Transfer. Wiley, Hoboken, NJ.

Todreas, M.E., Kazimi, M.S., 1990. Nuclear Systems I: Thermal Hydraulic Fundamentals; Nuclear Systems II: Elements of Thermal Hydraulic Design. Hemisphere Publishing Corp., New York. Advanced but understandable texts on thermal analysis; comprehensive coverage with many numerical examples.

Tong, L.S., Weisman, J., 1996. Thermal Analysis of Pressurized Water Reactors, third ed. American Nuclear Society, La Grange Park, IL. Graduate level book with principles, engineering data, and new information.

U.S. Nuclear Regulatory Commission (NRC), Steam Generator Tube Issues. http://www.nrc.gov/reading-rm/doc-collections/fact-sheets/steam-gen.html. Background information from the NRC.

CHAPTER

NUCLEAR POWER PLANTS 18

CHAPTER OUTLINE

Nuclear power plants convert the reactor-produced heat into electricity. As conventional steam turbines are utilized to drive the electric generator, the reactor in conjunction with other equipment constitutes a nuclear steam supply system (NSSS). The non-NSSS equipment, such as the turbine-generator and condenser, comprise the balance of a plant. In this chapter, we first identify important reactor features, compare several concepts, and then focus attention on the components and configurations of specific power reactor types.

18.1 REACTOR TYPES

Although the only requirement for a neutron chain reaction is a sufficient amount of a fissile nuclide, many combinations of materials and arrangements can be used to construct an operable nuclear reactor. Several different types or concepts have been devised and tested since 1942, when the first reactor started operation, just as various kinds of engines have been used: steam, internal combustion, reciprocating, rotary, jet, and so on. Experience with individual reactor concepts has led to the selection of a few that are most suitable by use of criteria such as economy, reliability, and ability to meet performance demands.

A general classification scheme for reactors has evolved that is related to the distinguishing features of the reactor types. These features are listed in the following paragraphs.

Nuclear Energy. https://doi.org/10.1016/B978-0-12-812881-7.00018-6

Purpose: Most reactors in operation or under construction are purposed for the generation of large blocks of commercial electric power. Others serve training or radiation research needs, and many provide propulsion power for ships and submarines. At various stages of development of a new concept, such as the breeder reactor, there will be constructed both a prototype reactor (for testing feasibility) and a demonstration reactor (for evaluating commercial possibilities).

Neutron Energy: A fast reactor is one in which most of the neutrons are in the energy range of 0.1–1 MeV, below but near the energy of neutrons released in fission. The neutrons remain at high energy because there is relatively little material present to cause them to slow down. In contrast, the thermal reactor contains a good neutron-moderating material, and the bulk of the neutrons have energy less than 0.1 eV.

Moderator and Coolant: In some reactors, one substance serves two functions: to assist in neutron slowing and to remove the produced heat. Others employ one material for moderator and another for coolant. The most frequently used materials are as follows:

Moderators	Coolants
Light water	Light water
Heavy water	Carbon dioxide
Graphite	Helium
Beryllium	Liquid sodium

The condition of the coolant serves as a further identification. The *pressurized water reactor* provides high-temperature water to a heat exchanger that generates steam, whereas the *boiling water reactor* supplies steam directly.

Materials within the reactor environment undergo radiation damage. For instance, water experiences both radiolysis and neutron-induced radioactivity. The former mechanism due to beta particles and gamma rays was investigated in Section 5.6. Water flowing through or near the reactor is subject to neutron exposure.

EXAMPLE 18.1

The isotopic abundance of O-16 is 99.8%, and the $^{16}O(n,p)^{16}N$ reaction has an average fast cross-section of 0.02 mb. According to Table 3.2, N-16 emits powerful 6.1 and 7.1 MeV gamma rays.

$$\begin{aligned} {}^{16}_{8}\mathrm{O} + {}^{1}_{0}\mathrm{n} &\rightarrow {}^{1}_{1}\mathrm{p} + {}^{16}_{7}\mathrm{N} \\ {}^{16}_{7}\mathrm{N} &\xrightarrow{7.1\,\mathrm{s}} {}^{0}_{-1}\beta + {}^{16}_{8}\mathrm{O} + \gamma \end{aligned} \tag{18.1}$$

With the penetrating gamma emissions delayed by the ^{16}N half-life of 7.1 s, the water becomes a photon source away from the reactor itself. In addition, the beta particles can cause radiolysis.

Fuel: Uranium with U-235 content varying from natural uranium ($\cong$0.7%) to slightly enriched ($\cong$3%–5%) to highly enriched ($\cong$90%) is used in various reactors, with the enrichment depending on what other absorbing materials are present. The fissile isotope Pu-239 is produced and consumed in reactors containing significant amounts of U-238. Plutonium serves as fuel for fast breeder reactors and can be recycled as fuel for thermal reactors. A few reactors have been built with fertile Th-232, producing fissile U-233.

Table 18.1 Reactor Fuel Properties

Material	Density (g/cm^3)	Thermal Conductivity, k (Btu/(h ft °F))	Specific Heat, c_p (Btu/(lbm °F))	Melting Temperature (°F)
U (metal)	19.0	~20	0.04	2070
UC	13.0	~12	0.035	4200
UO_2	10.5	~2	0.059	4980
ThO_2	10.0	~3	0.058	5970

Data from El-Wakil, M.M., 1978. Nuclear Heat Transport. American Nuclear Society, La Grange Park, IL.

The fuel may have various physical forms—a metal, or an alloy with a metal such as aluminum, or a compound such as the oxide UO_2 or carbide UC. Table 18.1 compares the properties of several fuels. While uranium metal boasts the highest thermal conductivity k, which leads to smaller temperature drops through the fuel, it has the lowest melting temperature. In addition, U metal undergoes metallurgical phase changes at 1234°F (α-β) and 1425°F (β-γ) (El-Wakil, 1978), making it unsuitable for use in power reactors. UC has the next highest thermal conductivity, but carbides are very reactive with water should fuel cladding fail. In contrast, the oxides exhibit good resistance to aqueous corrosion. Although the low k of the oxides causes higher temperatures, the melting points of these ceramic fuels are the highest.

Arrangement: In most modern reactors, the fuel is isolated from the coolant in what is called a *heterogeneous* arrangement. The alternative is a homogeneous mixture of fuel and moderator or fuel and coolant. The molten salt reactor exemplifies the latter.

Structural Materials: The functions of support, retention of fission products, and heat conduction are provided by various metals. The main examples are aluminum, stainless steel, and Zircaloy. Zircaloy-2 and -4 are alloys of zirconium with tin, iron, chromium, and in the case of Zircaloy-2, nickel (Scott, 1965).

18.2 POWER REACTORS

By placing emphasis on one or more of the preceding features, reactor concepts are identified. Some of the more widely used or promising power reactor types are the following:

(a) Pressurized water reactor (PWR), a thermal reactor with light water at high pressure (2200 psi, 150 bar) and temperature (610°F, 320°C) serving as moderator-coolant, and a heterogeneous arrangement of slightly enriched uranium fuel.
(b) Boiling water reactor (BWR), similar to the PWR except that the coolant pressure and temperature are lower (1000 psi, 70 bar and 550°F, 290°C).
(c) High temperature gas-cooled reactor (HTGR), which uses graphite moderator and helium coolant (1400°F, 760°C and 600 psi, 40 bar).
(d) Canadian deuterium uranium (CANDU), which uses heavy-water moderator and natural uranium fuel that can be loaded and discharged during operation.
(e) Liquid metal fast breeder reactor (LMFBR), with no moderator, liquid sodium coolant, and plutonium fuel, surrounded by natural or depleted uranium.

Table 18.2 amplifies the principal features of the preceding five main power reactor concepts. This chapter emphasizes the light water reactors (LWRs) such as the PWR and BWR. A description of the RBMK, exemplified by the ill-fated Chernobyl-4 reactor, appears in Section 21.8. Other reactors include the Magnox and advanced gas-cooled reactor (AGR) of the United Kingdom and several concepts that were tested but abandoned (Holbert, 2017).

Argonne National Laboratory has described the evolution of power reactors in terms of four generations. The early prototype reactors (pre-1965), such as Shippingport, Dresden, Fermi I, and Magnox comprise the first generation. The bulk of today's plants consist of the second-generation commercial power reactors (1965–95), including the BWRs, PWRs, CANDU, and the Russian RBMK and VVER (a PWR design). Generation III (1995–2030) comprises advanced LWRs and evolutionary designs such as the ABWR, ACR1000 (an advanced CANDU), AP600/1000, EPR (European or evolutionary passive reactor), and ESBWR (economic simplified BWR). The Generation IV (post-2030) reactors are revolutionary in nature and are intended to offer significant advances in sustainability, safety, reliability, and economics.

Table 18.3 gives the present global makeup of power reactors. In the United States, there are 65 PWRs and 34 BWRs operating with Watts Bar Unit 2, which entered service in October 2016, becoming the first new power reactor completed since 1996, when Watts Bar Unit 1 went online. All the operating gas-cooled reactors are located in the United Kingdom while all the graphite-moderated reactors and the two LMFBRs are in Russia. For data on individual reactors, see ANS (2018), IAEA (2018), and University of New Mexico (n.d.). Fig. 18.1 shows the Watts Bar Nuclear Plant operated by the Tennessee Valley Authority. These two four-loop Westinghouse PWRs have a net power output of almost 1200 MWe each.

Compliance with licensing rules plays an important role in the operation of any nuclear facility. A power reactor is designed to withstand the effects of high temperature, erosion by moving coolant, and nuclear radiation. The materials of construction are chosen for their favorable properties. Fabrication, testing, and operation are governed by strict procedures.

Table 18.2 Power Reactor Materials

	Pressurized Water (PWR)	Boiling Water (BWR)	Natural U Heavy Water (CANDU)	High Temp. Gas-cooled (HTGR)	Liquid Metal Fast Breeder (LMFBR)
Fuel form	UO_2	UO_2	UO_2	UC, ThC_2	PuO_2, UO_2
Enrichment	3% U-235	2.5% U-235	0.7% U-235	~10% U-235	15 wt. % Pu-239
Moderator	Water	Water	Heavy water	Graphite	None
Coolant	Water	Water	Light water or heavy water	Helium gas	Liquid sodium
Cladding	Zircaloy	Zircaloy	Zircaloy	Graphite	Stainless steel
Control	B_4C or Ag-In-Cd rods	B_4C blades	Moderator level	B_4C rods	Tantalum or B_4C rods
Vessel	Steel	Steel	Steel	Prestressed concrete	Steel

Table 18.3 Power Reactors Worldwide

Reactor Type	In Operation		Forthcoming	
	No. of Units	Net MWe	No. of Units	Net MWe
Pressurized light water	291	274,975	79	86,951
Boiling light water	75	73,816	6	7950
Gas cooled	14	7685	1	200
Heavy water	49	24,596	8	5240
Graphite moderated	15	10,219	0	0
Liquid metal cooled	2	1349	3	590
Total	446	392,640	97	100,931

Data from American Nuclear Society (ANS), 2018. 20th annual reference issue. Nucl. News 61(3), 39–61.

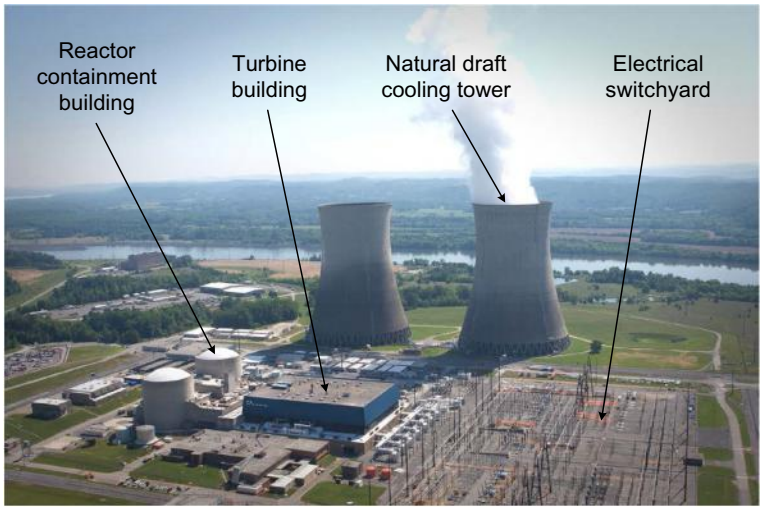

FIG. 18.1

The Watts Bar Nuclear Plant comprises two pressurized water reactors.

Courtesy Tennessee Valley Authority.

The instrumentation and control (I&C) system of a power reactor (1) provides continuous information on status, including neutron flux, power level, power distribution, temperatures, water level, and control rod position; (2) provides commands to trip the reactor if preset limits are exceeded; and (3) reports deviations from normal or failures of components. Traditionally, the I&C systems were of the analog type, involving a sensor, a feedback circuit, and a display device. Obsolescence is motivating the industry to convert to digital I&C, which consists of computer software and microprocessor-based hardware.

18.3 POWER PLANT ECONOMICS

Nuclear power plants are almost exclusively employed to meet the base load of the electric power system, that is, the grid. Electricity generation costs can be divided into three components and normalized to a per kilowatt-hour (kWh) basis. First, capital costs are those required to construct the facility, including equipment, land, and interest payments on the loaned money to build. Operating and maintenance (O&M) expenses, such as wages, insurance, taxes, and consumables, are sustained throughout the life of the plant. Finally, there are nuclear fuel costs comprised of the uranium itself, enrichment, and assembly fabrication (see Section 15.4). Nuclear plants are well known to incur high capital costs and low fuel costs relative to other electricity production technologies. Exclusively in the case of nuclear plants, the US government additionally collects 0.1 cents/kWh that is destined to cover spent fuel disposal (USC, 1983).

Both the plant thermal efficiency η_{th} and the fuel expense F_{C} [\$/kg] directly impact the fuel cost of electricity

$$e_{\text{F}} = F_{\text{C}}/(\eta_{\text{th}} B) \tag{18.2}$$

where B is the fuel burnup. This *specific burnup* describes the thermal energy release from the fuel expressed as megawatt-days per metric ton of uranium (or heavy metal), or simply MWD/MTU.

O&M costs consist of fixed and variable expenses. Equipment maintenance and consumables are examples of variable costs that are proportional to electric energy production while employee wages and overhead comprise fixed expenses. The capital costs F_B are prorated on an annual basis using a levelized fixed charge rate I. If the annual O&M costs [\$/y] are known, then the total electricity generation cost is

$$e = \frac{F_{\text{B}} I + \text{O\&M}}{P_{\text{e}} CF(8760\text{h/y})} + \frac{F_{\text{C}}}{\eta_{\text{th}} B} \tag{18.3}$$

where CF is the plant capacity factor. The ratio $F_{\text{B}}/P_{\text{e}}$ [\$/kWe] is a common metric for comparing the (overnight) cost of building a power plant.

EXAMPLE 18.2

A 1000-MWe nuclear unit built for \$2 billion achieves a capacity factor of 90% with a burnup of 30,000 MWD/MTU. Fuel costs are \$1025/kg, and O&M expenses are \$60 million/y. Using Eq. (18.3), the electricity generation cost for a levelized fixed charge rate of 17%/y is

$$e = \frac{(\$2\times10^9)(0.17/\text{y}) + (\$60\times10^6/\text{y})}{(1000\times10^3\,\text{kWe})(0.9)(8760\text{h/y})} + \frac{(\$1025/\text{kg})(10^3\,\text{kg/MT})(1\text{d}/24\text{h})}{(0.33)(30,000\times10^3\,\text{kWD/MTU})}$$
$$= 0.0431\,\$/\text{kWh} + 0.0076\,\$/\text{kWh} + 0.0043\,\$/\text{kWh} = 5.5\,¢/\text{kWh}$$

This breakdown of the total cost into its three components demonstrates that the capital portion is highest and the fuel part is the lowest.

The capacity factor is an important parameter in the performance of a power reactor and the electric power industry as a whole. The *capacity factor* is the ratio of electric energy produced during some time interval to that which could have been produced at net rated power P_{e} during the same period T,

$$CF = \int_0^T P(t)dt/(P_e T) \tag{18.4}$$

Included in its calculation are the outage for refueling and any other shutdown time. The median *CF* for 3-year periods in the United States has risen from 61% in 1975–77 to 90% in 2002–16 (Blake, 2017). A similar metric, the *availability factor*, quantifies the fraction of time that a plant is operable.

EXAMPLE 18.3

A 1-GWe nuclear plant operates for 6 months at 90% power, and then is offline for a month of maintenance. Afterward, the plant returns to 100% power for the remainder of the year. The capacity factor for this year is

$$CF = \frac{(6 \text{ months})(0.9P_e) + (5 \text{ months})P_e}{(12 \text{ months})P_e} = 0.867 \text{ (or } 87\%)$$

For this plant, the availability factor for that year was

$$AF = (6 \text{ months} + 5 \text{ months})/(12 \text{ months}) = 0.917 \text{ (or } 92\%)$$

Here, as in all situations, $AF \geq CF$.

18.4 LIGHT WATER REACTORS

The large-scale reactors used for the production of thermal energy that is converted to electrical energy are much more complex than the Godiva fast assembly described in Section 16.1. To illustrate, we can identify the components and their functions in a modern PWR. Fig. 18.2 gives some indication of the sizes of the various parts. The fresh fuel installed in a typical PWR consists of cylindrical pellets of slightly enriched (3% U-235) uranium oxide (UO_2) of diameter approximately 3/8 inch (~1 cm) and length approximately 0.6 in. (~1.5 cm). Sintering, which is a high temperature-high pressure process, compacts the UO_2 powder to achieve a density of approximately 95% theoretical in the pellets. A Zircaloy tube of wall thickness 0.025 in. (~0.6 mm) is filled with the pellets to an active length of 12 ft (~360 cm), backfilled with pressurized helium, and sealed to form a *fuel rod* (or pin). The metal tube serves to provide support for the column of pellets, to provide cladding that retains radioactive fission products, and to protect the fuel from interaction with the coolant. Approximately 200 of the fuel pins are grouped in a bundle called a *fuel element* or *fuel assembly* of roughly 8 in. (~20 cm) on a side (see Fig. 18.3), and around 180 elements are assembled in an almost cylindrical array to form the *reactor core*. This structure is mounted on supports in a steel *pressure vessel* of outside diameter approximately 16 ft (~5 m), height 40 ft (~12 m), and walls up to 12 in. (~30 cm) thick.

Control rods consisting of boron carbide or an alloy of cadmium, silver, and indium provide the ability to change the amount of neutron absorption. For PWRs, the control rods are inserted in some vacant guide tubes and magnetically connected to drive mechanisms. On interruption of magnet current, the rods enter the core through the force of gravity. The pressure vessel is filled with light water, which serves as the neutron moderator, as coolant to remove fission heat, and as a *reflector*, a layer of material surrounding the core that helps prevent neutron escape. The water also contains in solution the compound boric acid, H_3BO_3, which strongly absorbs neutrons in proportion to the number of boron

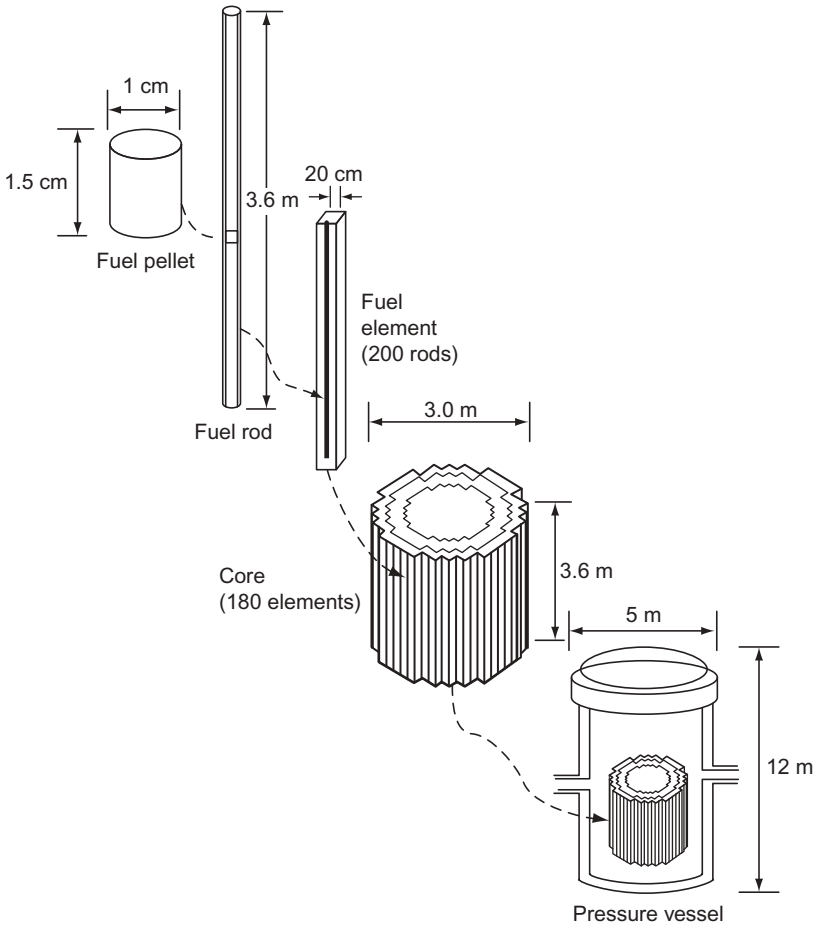

FIG. 18.2

Reactor construction.

atoms and thus inhibits neutron multiplication (i.e., "poisons" the reactor). The term *soluble poison* is often used to identify this material, the concentration of which can be adjusted during reactor operation. To keep the reactor critical as fuel is consumed, the boron content is gradually reduced (see Section 20.6). A *biological shield* of concrete surrounds the pressure vessel and other equipment to provide workers protection against neutrons and gamma rays from the nuclear reactions. The shield also serves as an additional barrier to the release of radioactive materials.

We have mentioned only the main components, which distinguish a nuclear reactor from other heat sources such as a furnace burning coal. An actual system is much more complex than described earlier. As the reactor vessel diagram of Fig. 18.4 reveals, a power reactor contains equipment such as spacers (see Fig. 18.3) to hold the many fuel rods apart; core support structures; baffles to direct coolant flow effectively; guides, seals, and motors for the control rods; guide tubes and electrical leads for

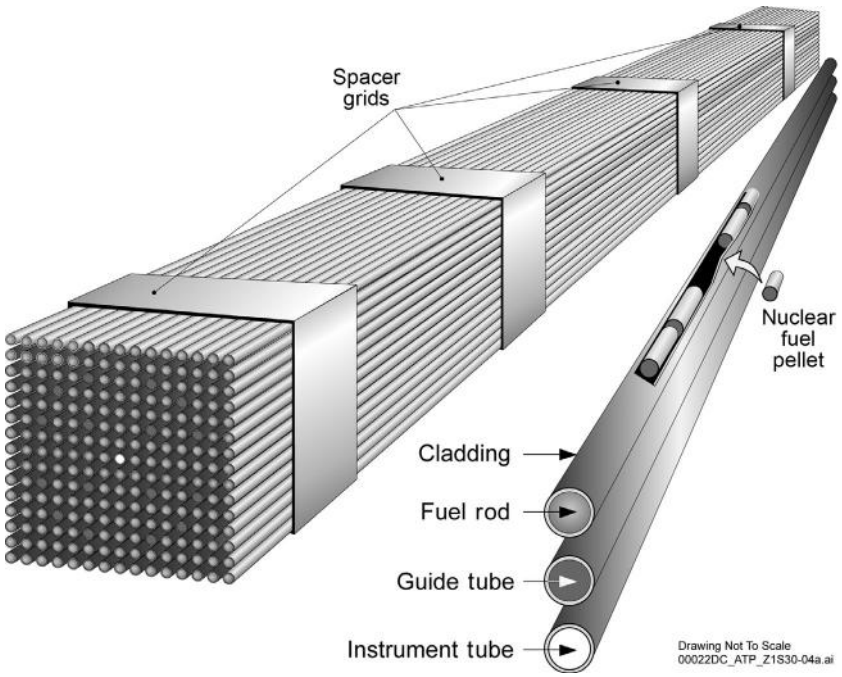

FIG. 18.3

PWR fuel assembly.

Courtesy US DOE Office of Civilian Radioactive Waste Management.

neutron-detecting instruments, brought through the bottom of the pressure vessel and up into certain fuel assemblies; and bolts to hold down the vessel head and maintain the high operating pressure.

Fig. 18.5 presents the flow diagram for a PWR-type reactor system. Primary coolant flows into the reactor pressure vessel (RPV) via an inlet nozzle, and then is immediately redirected downward such that the water enters the core at its base. After absorbing the fission-produced heat, the coolant exits the RPV and reaches the steam generator via the hot leg piping. Once the heat is transferred to the secondary system water to make steam, a reactor coolant system (RCS) pump returns the primary water to the RPV through the cold leg. A power plant NSSS consists of multiple primary loops such that each reactor is paired with two, three, or four steam generators and RCS pumps. Each RCS pump draws a few MWe of power, which during startup serves to gradually heat the coolant to operating temperatures prior to criticality. In the PWR, a single *pressurizer* maintains the pressure in the system at the desired value to prevent bulk boiling in the core. It uses a combination of immersion electric heaters and a water spray system to control the pressure. A concrete containment building designed to prevent the release of radioactivity to the environment encloses the RCS.

The BWR core is similar to that of the PWR; exceptions include the fuel assembly configuration and the control elements. As illustrated in Fig. 18.6, the BWR canned fuel assemblies contain about one-fourth of the fuel rods of a PWR assembly and are separated by cruciform-shaped control blades that are hydraulically driven in from the bottom of the core upward. After passing through the core,

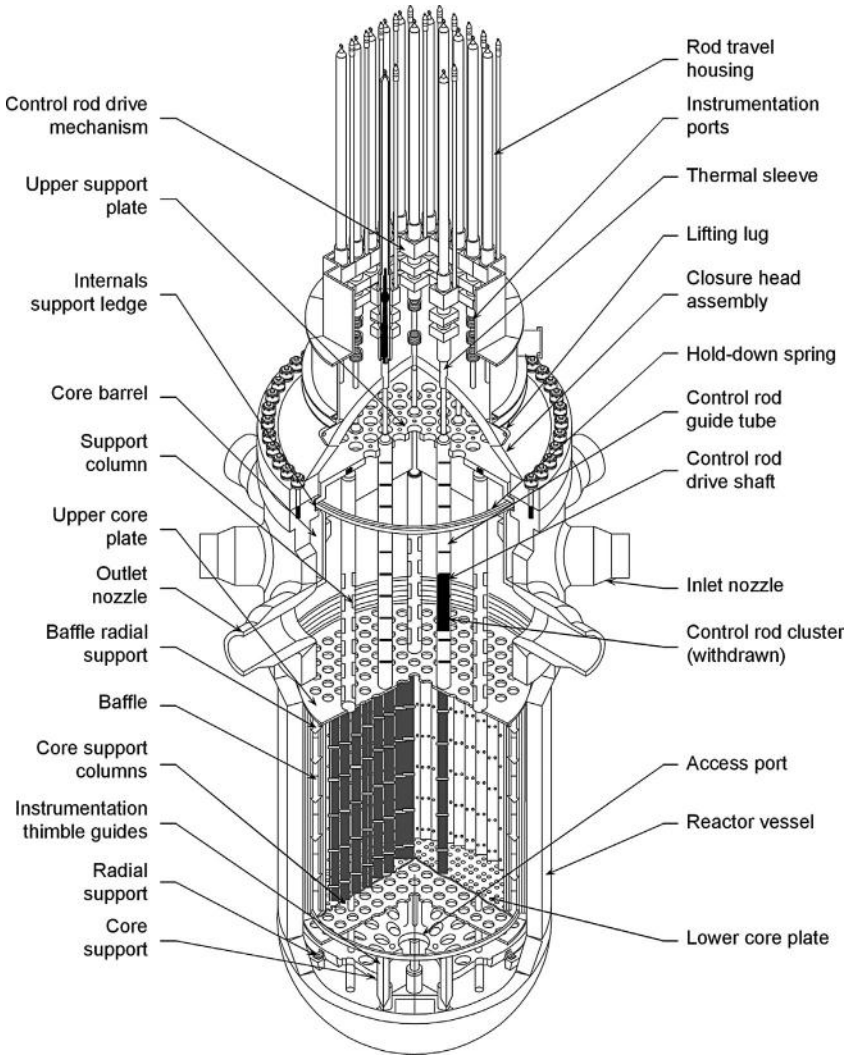

FIG. 18.4

PWR reactor vessel.

Courtesy US NRC.

water that has not been vaporized must be recirculated back to the bottom of the core. This is accomplished by means of physical recirculation pumps that feed multiple jet nozzles located on the interior periphery of the reactor pressure vessel.

Fig. 18.7 provides a flow diagram for a BWR-type reactor system. Feedwater enters the RPV at a height above the top of the core. The combined effects of the recirculation and jet pumps force liquid water into the reactor core from the bottom. The saturated steam is processed by steam separators and

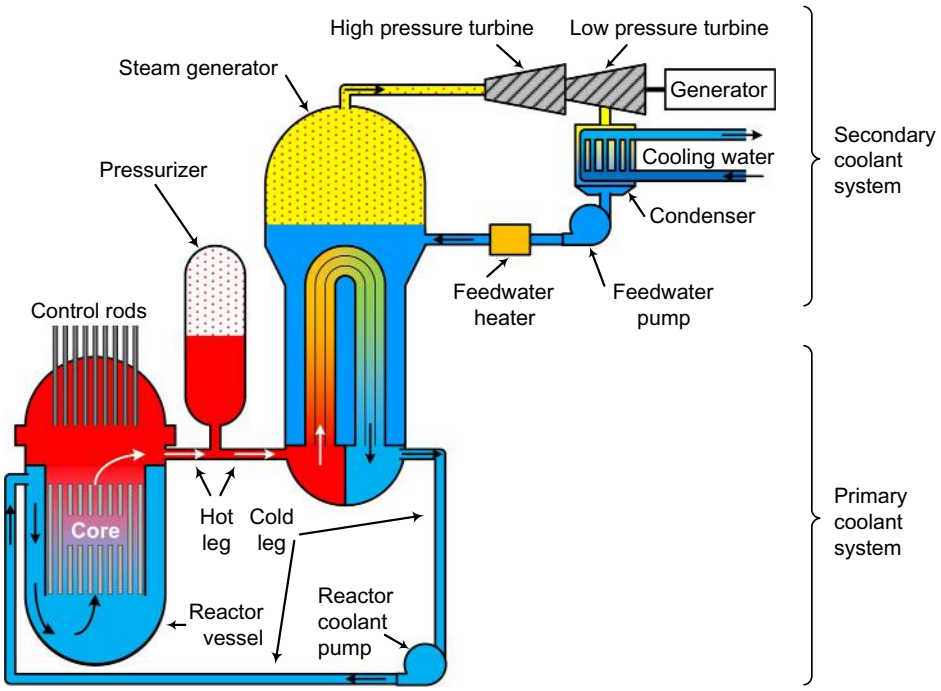

FIG. 18.5

PWR system flow diagram.

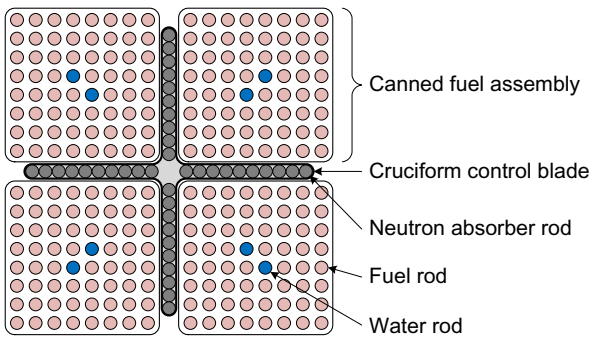

FIG. 18.6

Four BWR canned fuel assemblies with central control blade.

dryers located above the core to remove moisture from the vapor that is sent to the high-pressure turbine. This equipment above the core is one reason that the control blades enter the core at its base. The other motivation is that the lower density steam in the upper portion provides less moderation compared to the liquid water in the lower regions of the core.

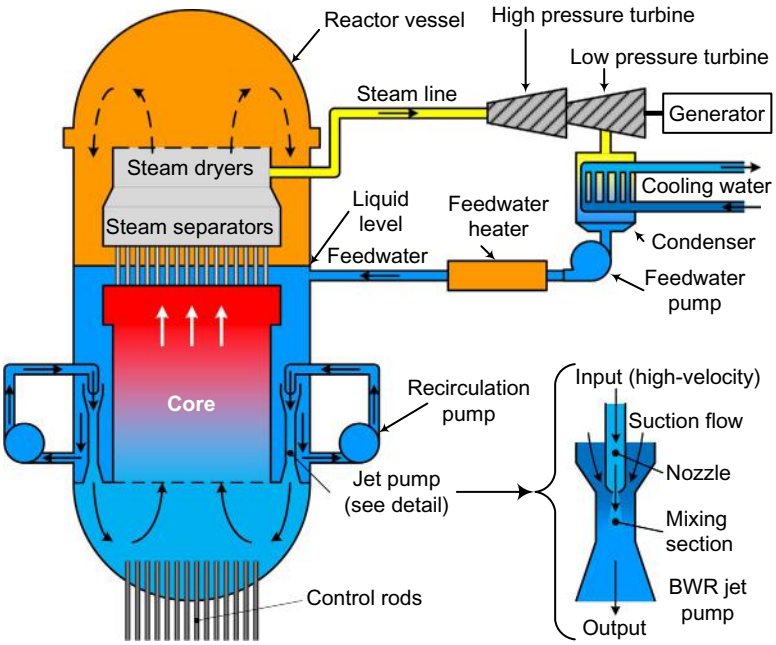

FIG. 18.7

BWR system flow diagram.

With PWRs and BWRs being the mainstay of nuclear power plants today, Table 18.4 compares representative values of these two reactors. The BWR core and reactor pressure vessel are larger, but the PWR enjoys higher power density. This core *power density* is not the volumetric heat generation rate q''' but rather is relative to the active core volume, V_R,

$$PD = Q_R / V_R \tag{18.5}$$

Another related quantity is the *specific power*, which is the ratio of reactor power to fuel metal mass m_U, that is,

$$SP = Q_R / m_U \tag{18.6}$$

EXAMPLE 18.4

Using the data of Table 18.4, the PWR core life can be estimated from the burnup

$$T = \frac{Bm_U}{Q_R} = \frac{(35,000\,\text{MWD/MTU})(96,000\,\text{kg})}{(3600\,\text{MW})(1000\,\text{kg/MT})} = 933\ \text{days}$$

Although this might imply continuous operation for 2.5 y, we shall see in Section 20.6 that fuel assemblies are utilized over multiple fuel cycles of shorter duration.

Table 18.4 Light Water Reactor Comparison

Characteristic	PWR	BWR
Power: thermal/electric (MW)	3600/1200	3600/1200
Reactor vessel: height/diameter (ft)	45/15	73/21
Active core height/diameter (in.)	145/139	148/144
Active core volume (L)	36,000	64,000
Number of fuel assemblies	200	800
Fuel element array	17×17	8×8
Fuel mass (kg-U)	96,000	138,000
Fuel burnup (MWD/MTU)	35,000	28,000
Reactor coolant flow rate (lbm/h)	135×10^6	100×10^6
Reactor coolant pressure (psia)	2250	1040
Coolant temperature: core inlet/outlet (°F)	555/620	530/547
Average linear power density (kWt/ft)	5.4	6.1
Average core power density (kWt/L)	100	56
Average heat flux (Btu/(h ft^2))	190,000	160,000
Specific power (kWt/kg-U)	37.5	26.1
Maximum cladding temperature (°F)	655	560
Maximum fuel centerline temperature (°F)	3500	3400

18.5 OTHER GENERATION II REACTORS

Table 18.3 has revealed that although LWRs dominate the worldwide reactor population, there are significant numbers of heavy water reactors. During the initial years of nuclear power development, enrichment facilities were uncommon, although the capacity of a single enrichment plant in those days far exceeded the needs of one nuclear unit. For nations having domestic uranium resources but without enrichment technology, this state of affairs motivated the deployment of reactors using natural uranium. However, achieving criticality with natural uranium requires a heavy water or graphite moderator. The Canadians, in particular, responded to this world market need.

Canada has established a heavy water industry and uses uranium mined within the country. The government corporation Atomic Energy Canada Ltd. (AECL) provided heavy water reactors (HWRs) for domestic deployment and export. The heavy-water moderated reactors of Canada have operated very successfully for many years. The CANDU uses natural or very slightly enriched uranium in pressure tubes that permit refueling during operation. Very high capacity factors are thus possible. The CANDU primary system resembles a PWR in that heavy or light water coolant at high pressure transfers heat from the reactor to a U-tube steam generator, as shown in Fig. 18.8. However, the cylindrical fuel bundles are markedly different as they are placed inside the pressure tubes through which the heavy (or light) water coolant flows. Surrounding the pressure tubes is a large horizontal tank, referred to as the *calandria*, containing the heavy water moderator. Because the moderator is kept at low pressure, the calandria does not require the specialized manufacturing facilities needed for producing PWR-type reactor pressure vessels.

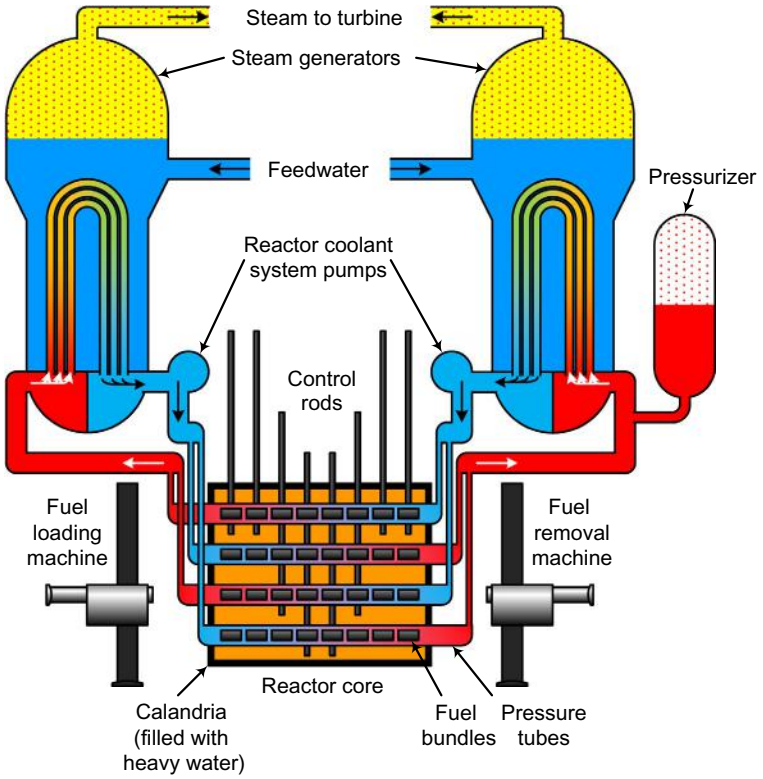

FIG. 18.8

CANDU system flow diagram.

The United Kingdom has a long history of the use of gas-cooled reactors (GCRs) for commercial electricity. In fact, a Magnox reactor at Calder Hall was the world's first full-scale electric generating station, delivering 60 MWe to the grid beginning in 1956. However, the Calder Hall reactors served a dual purpose: electricity generation and plutonium production. Deriving their name from the magnesium cladding alloy, the Magnox series of reactors employed carbon dioxide coolant at pressures of 100–400 psi (7 – 27 bar), graphite moderator, and natural uranium. To achieve higher operating temperatures, the next generation of AGRs utilized a stainless steel cladding, which necessitated using enriched uranium. While the earlier GCRs utilized CO_2, operation at high temperatures required switching to a coolant such as helium that did not decompose at elevated temperature.

In the United States, two high temperature gas reactors (HTGRs) were designed by General Atomics and built (Agnew, 1981). Peach Bottom 1 was a 40 MWe prototype that operated from 1966 to 1974. The Fort St. Vrain demonstration plant utilized newer technology and was scaled up to 330 MWe. The thorium and fully enriched uranium fuel spheres were coated and placed within drilled holes in the hexagonal graphite blocks. Reactor heat was transferred to 12 steam generators. The helium coolant circulators experienced seal leakage that contributed significantly to the dismal availability factor for the plant. Noteworthy is that the 39% thermal efficiency and 100,000 MWD/MTU burnup are noticeably larger than the other reactors described earlier.

EXAMPLE 18.5

Let us determine coolant flow in a 1200-MWe HTGR using the same core inlet and exit temperatures as the Fort St. Vrain reactor, that is, 406°C and 785°C, respectively. For a 39% efficient plant, the required reactor power is

$$Q_R = P_e/\eta_{th} = (1200\text{MWe})/(0.39) = 3077\text{MWt}$$

Using the specific heat c_p of 5.19 kJ/(kg °C) for He, the coolant flow rate is

$$\dot{m}_R = \frac{Q_R}{c_p(T_{C,out} - T_{C,in})} = \frac{(3077\text{MW})(1000\text{kJ/(MWs)})}{(5.19\text{kJ/(kg°C)})(785°\text{C} - 406°\text{C})} = 1564\text{kg/s}$$

This equates to 12.4×10^6 lbm/h, which is an order of magnitude smaller compared to the LWRs delivering an equivalent P_e.

18.6 GENERATION III(+) REACTORS

A Strategic Plan for Building New Nuclear Power Plants was published two decades ago by the Nuclear Energy Institute (NEI, 1998). The document served to highlight the industry's commitment to encouraging new plant orders. The plan identified a number of building blocks for accomplishing goals. Among these were continued plant safety and reliability, stable licensing including NRC design certification, well-defined utility requirements, successful first-of-a-kind engineering, progress in disposal of high-level and low-level wastes, adequate fuel supply, enhanced government support, and improved public acceptance.

The first major step in carrying out the plan was the development of an Advanced Light Water Reactor Utility Requirements Document (EPRI, 1999). It provided policy statements about key features such as simplification of systems, margins of safety, attention to human factors, design for constructability and maintainability, and favorable economics.

Two different concepts were specified: (1) a large-output (1300 MWe) evolutionary design that benefits from current designs, and (2) a mid-sized output (600 MWe) passive design that depends more on natural processes for safety instead of mechanical-electrical devices. Numerical specifications included completion in 5 y, low worker radiation exposure (less than 100 mrem/y), refueling on a 24-month basis, and an ambitious 87% average availability over a 60-y design life. A thorough analysis was made of the means by which standardization could be achieved in design, maintenance, and operation, along with the benefits that accrue:

(a) A reduction in construction time and costs comes from the use of common practices.
(b) Use of identical equipment in several plants favors both economy and safety.
(c) Standardized management, training, and operating procedures lead to greater efficiency and productivity.

Advanced reactor designs intended to meet the US nuclear industry objectives were developed. Some of the principal contenders are presented in the remainder of this section.

General Electric has an advanced boiling water reactor (ABWR) design of 1300 MWe (Wolfe and Wilkins, 1989). The ABWR circulates coolant by internal pumps to reduce piping penetrations into the RPV. Other passive safety features include containment cooling that uses natural convection. Analysis

of the plant by probabilistic risk assessment (PRA) indicates a negligible hazard to the public. The 3900-MWt ABWR design received initial certification from the NRC in May 1997. Four ABWRs have been built in Japan.

Westinghouse designed an advanced passive (AP) reactor with a lower power level of 600 MWe (Tower et al., 1988), that is, the AP600. The principal design goals were simplicity and enhanced safety. The numbers of pipes, valves, pumps, and cables were greatly reduced in this design. The AP600 has a number of passive processes for safety, including the uses of gravity, convection, condensation, and evaporation. Examples are a large water storage reservoir for emergency cooling and another one for containment wall cooling. Later, the AP600 design was scaled up with changes limited to those required for a higher output power. Modular construction is utilized to minimize costs and time. The estimated core damage frequency is smaller than NRC requirements by a factor of 250. Some of the key parameters of the two-loop Westinghouse design (Schulz, 2006) are as follows:

Net electrical/thermal output	1117 MWe/3400 MWt
Number of 17×17 fuel assemblies	157
Peak coolant temperature	321°C (610°F)
Reactor vessel ID	39 cm (157 in.)
Operating cost	3.5 cents/kWh

Westinghouse ownership has gone through phases, including purchase by British Nuclear Fuels (BNFL), which sold the company to the Japanese firm Toshiba.

A consensus developed in the United States that it was time to expand nuclear power. The reactor concept being adopted early in the nuclear revival is the AP1000, for which the NRC has issued design preapproval. That approval greatly simplifies the application by a nuclear company for a construction and operating license (COL). As of early 2018, six units are scheduled for commercial start by 2021 in China and two (Vogtle 3 and 4) in the United States. Construction costs escalated, causing Westinghouse to declare bankruptcy in March 2017, leading to the cancellation of two units (Summer 2 and 3) in South Carolina.

Building upon the French nuclear power experience, the Areva entry is the 1600-MWe evolutionary power reactor (EPR), formerly the European pressurized reactor. Besides a slightly higher thermal efficiency than traditional PWRs, the EPR can utilize a core completely composed of mixed oxide (MOX) fuel. In compliance with European regulators, the EPR employs a molten core catcher under the RPV. Because France generates more than 75% of its electricity from nuclear plants, the EPR is to have unique load-following capability. From 25% to 60% power, a power increase rate of 2.5% P_e per min is touted, and $0.05 P_e$/min above 60%. Four EPRs are under construction: two in China, one in Finland, and one in France, with commercial operation expected in the 2018–19 timeframe.

EXAMPLE 18.6

Let us determine the time for the EPR to move from 25% to 100% full power. Using the maximum ramp rate for the two power ranges gives

$$t = \frac{60\% - 25\%}{2.5\%/\text{min}} + \frac{100\% - 60\%}{5\%/\text{min}} = 22\,\text{min}$$

Even though the plant is capable of such performance, it is conceivable that frequent cycling may cause fatigue that reduces the expected lifetime of some components.

The economic simplified boiling water reactor (ESBWR) from GE-Hitachi uses natural circulation for the 4500 MWt reactor (Hinds and Maslak, 2006). The NRC certified this design in 2014. Other Generation III+ designs include the US-APWR from Mitsubishi Heavy Industries and the Korean Advanced Power Reactor 1400 (APR-1400). KOPEC has completed one APR-1400 unit in South Korea, and is constructing three more APR-1400 units in Korea and four units in the United Arab Emirates. The APR-1400 evolved from Combustion Engineering's System 80+ NSSS.

18.7 SMALL MODULAR REACTORS

Although the original prototypes as well as naval reactors were small, the heyday of commercial power development experienced rapid size increases. Renewed interest in small modular reactors (SMRs) is taking place for a variety of reasons. Small-scale reactors are envisioned as being manufactured in a dedicated facility, transported to the plant site, and installed in power blocks consisting of one or more units for flexibility. They would be simple, safe, long-lived, and proliferation-resistant. SMRs would also be able to supply heat applications such as district heating and desalination.

Larger reactors have traditionally benefited from *economy of scale* considerations, which means that the net electric rating P_e in the denominator of Eq. (18.3) is increased so as to reduce the overall electricity cost. Smaller reactors, however, represent a reduced investment by a utility and provide the capability of adding smaller increments of power-generation capacity. For instance, SMRs may be more suitable for remote sites and nations with emerging economies whose needs are not in the 1-GWe range. In addition, SMRs are more compatible with the environment after the Great Recession of 2008 in which electricity growth rates have been stymied and the availability of investment capital is lower.

Several conceptual SMR designs are vying for deployment. With power outputs under about 300 MWe, a common characteristic of many is their configuration as an integral PWR (iPWR). An iPWR seeks to position the entire reactor coolant system within the confines of the RPV, as shown in Fig. 18.9. These tall RPVs locate the core at the bottom and the steam generators near the top in order to set up natural circulation cooling capability. Natural circulation can be achieved using the chimney effect in which the reactor heating reduces the density of the coolant such that it rises, and then once the heat is removed in the steam generator, the increased density causes the coolant to gravitate down to the core inlet. The upper dome of the RPV serves as the pressurizer.

Toshiba-Westinghouse has taken a different approach with its 4S (super-safe, small, and simple) design, which is a sodium-cooled fast reactor. A unique feature of the 4S is that no onsite refueling would be needed for 30 years. Another variation on the SMR approach is the Russian plan to construct 30-MWe ship-borne PWRs, so-called floating nuclear power plants that can be anchored at locations requiring power.

A contender was the Babcock & Wilcox (B&W) 530-MWt mPower module. In April 2013, the Department of Energy (DOE) signed a cooperative agreement to provide $226 million in cost-shared funding over 5 years for development and licensing of the mPower SMR. The Tennessee Valley Authority (TVA), as a potential host utility, identified a site on the Clinch River for construction of up to four reactors. The mPower reactor was slated to use 5% enriched fuel for a better than 4-y core life. The reactor coolant pressure was to be kept at 2050 psi (14.1 MPa) within the iPWR vessel of diameter 13 ft (4.0 m) and height 83 ft (25 m). The steam production at 825 psi (5.69 MPa) was proposed to

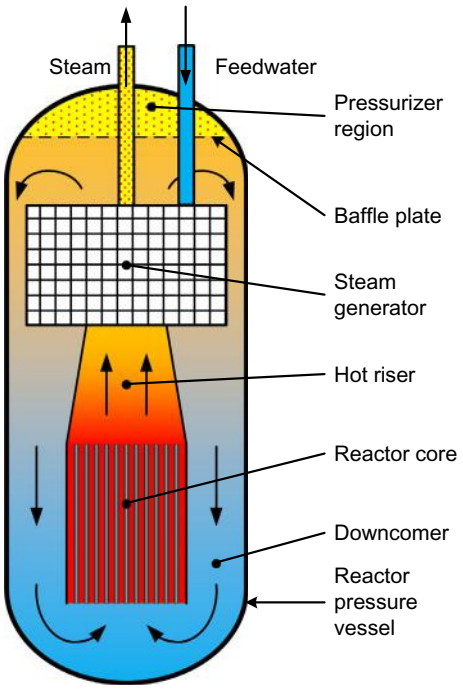

FIG. 18.9

Small modular reactor configured as an iPWR.

include 50°F (28°C) of superheat. The anticipated unit electric output was 155 or 180 MWe for air versus water condenser cooling, respectively. B&W discontinued the reactor development in 2017.

The DOE also partially funded the NuScale Power iPWR that employs natural circulation. The NuScale design is an extension of the multiapplication small light water reactor developed at Oregon State University (Reyes and Lorenzini, 2010). Multiple 160-MWt SMR modules would comprise a complete power plant, which could also provide heat for desalination (Ingersoll et al., 2014). The reactor utilizes standard 17×17 fuel assemblies with a length of 2 m and an enrichment of $<5\%$. The NRC began review of the NuScale design certification application in early 2017.

EXAMPLE 18.7

We compare the thermal efficiency for the air and water condenser cooling models of the mPower module:

$$\text{Air cooled}: \eta_{\text{th}} = (155\,\text{MWe})/(530\,\text{MWt}) = 0.29$$

$$\text{Water cooled}: \eta_{\text{th}} = (180\,\text{MWe})/(530\,\text{MWt}) = 0.34$$

A notable increase in efficiency is recorded with water cooling, but with the concomitant usage of water.

18.8 GENERATION IV REACTORS

Looking toward further improvements in reactor technology, the US DOE initiated a study of new nuclear designs titled Generation IV. Contributing to the study is the Generation IV International Forum (GIF), a consortium of presently 13 countries comprising Argentina, Australia, Brazil, Canada, China, France, Japan, Republic of Korea, Russian Federation, South Africa, Switzerland, United Kingdom, and the United States, plus the European Union. A 2002 report titled, "Technology Roadmap for Generation IV Nuclear Energy Systems," (DOE/GIF, 2002) describes the long-term goals as:

(1) *Sustainable nuclear energy*, which focuses on waste management and resource utilization.
(2) *Competitive nuclear energy*, which seeks low-cost electricity and other products such as hydrogen.
(3) *Safe and reliable systems*, which implies both prevention and responses to accidents.
(4) *Proliferation resistance and physical protection*, which means control of materials and prevention of terrorist action.

Of a large group of reactor systems, six were identified as prospects for research and development, as follows:

(1) Gas-cooled fast reactor (GFR): Helium cooled, fast neutron spectrum, closed fuel cycle for actinide burnup.
(2) Lead-cooled fast reactor (LFR): Lead or Pb-Bi coolant, fast neutron spectrum, closed fuel cycle, metal fuel, long core life.
(3) Molten salt reactor (MSR): Circulating coolant of molten Na-Zr-U fluorides that allows actinide feeds, graphite moderator, thermal spectrum.
(4) Sodium-cooled fast reactor (SFR): Na coolant, fast neutron spectrum, closed pyrometallurgical fuel cycle, MOX fuel.
(5) Supercritical-water-cooled reactor (SCWR): Fast or thermal spectrum, operation above the critical point for water (22 MPa, 374°C), high thermal efficiency.
(6) Very-high-temperature reactor (VHTR): Thermal spectrum, once-through cycle, either HTGR or pebble-bed type, high efficiency, useful for process heat.

The nuclear power field in the United States has come full circle in the choice of reactor type. Graphite served as the moderator for reactors at Chicago, Hanford, Oak Ridge, and Brookhaven. Except for reactors at Peach Bottom and Fort St. Vrain, light water reactors have dominated since. However, for the future, graphite-moderated reactors seem promising.

Two concepts have recently been studied for the United States. Both make use of coated particles as fuel, with uranium oxide and layers of silicon carbide and carbon to retain fission products. Each uses helium gas as the coolant and operates at high temperatures.

The first is the pebble bed modular reactor (PBMR), initiated by the South African company Eskom (Koster et al., 2003). In the PBMR, the coated particles are held in spheres of approximately 6 cm diameter. The reactor core would contain some 450,000 of such spheres, which would flow through the reactor vessel and be irradiated.

The second is the gas turbine modular helium reactor (GT-MHR), designed by General Atomics. The core consists of hexagonal graphite blocks of 36 cm across flats. The prisms are pierced by holes

that contain 1.25-cm diameter rods of coated particles mixed with a carbon binder and have holes for the helium coolant. LaBar and others (2003) provide a complete description of the reactor.

The Energy Policy Act of 2005 called for the establishment of the next-generation nuclear plant (NGNP), specifying that the NGNP should be located at the Idaho National Laboratory and be capable of producing hydrogen (see Section 24.9). An independent technology review group (ITRG) was assigned the task of selecting the most promising reactor concept and assessing the requirements for R&D leading to a prototype reactor. The type selected out of an initial group of six was the VHTR, which is said to satisfy all requirements on safety, economics, proliferation resistance, waste reduction, and fuel use. In early 2012, the prismatic block core was chosen over the pebble bed based on a business case.

The ITRG noted several needs: (1) to develop a high-temperature H_2 facility; (2) to address the role of an intermediate heat exchanger to isolate the reactor from the hydrogen unit; (3) to determine the proper dynamic coupling of the two components; (4) to achieve successful fabrication of fuel kernels; and (5) to develop a high-performance helium turbine. Fig. 18.10 shows the coupled reactor and hydrogen unit. The coated particle fuel elements must perform at the 900°C–950°C helium temperatures needed for hydrogen production. Some of the preliminary design features are as follows:

Coolant inlet/outlet temperatures	640°C/1000°C
Thermal power	600 MW
Efficiency	>50%
Helium flow rate	320 kg/s
Average power density	6–10 MWt/m^3

Since 2012, the preferred VHTR choice for the NGNP is the prismatic core (Fütterer et al., 2014). Additional details are found in the original roadmap (DOE/GIF, 2002) and the updated roadmap (GIF, 2014), and in an assessment of features and uncertainties by the ITRG (2004).

EXAMPLE 18.8

Using the VHTR design data and Eq. (18.5), the core volume is around

$$V_R = Q_R/PD = (600\text{MW})/\left(8\text{MW/m}^3\right) = 75\text{m}^3$$

Assuming that Fig. 18.10 is to scale, the core height is about three times the diameter such that

$$V_R = \pi(D/2)^2 H = \pi(D/2)^2 3D$$
$$D = \sqrt[3]{4V_R/(3\pi)} = \sqrt[3]{4(75\text{m}^3)/(3\pi)} = 3.2\text{m}$$

And the core height then is $H = 3D = 9.6\,\text{m}$, which is significantly taller than the LWR core sizes of Table 18.4.

Completion of tests of fuel integrity for the VHTR is expected around the year 2020. If the tests are successful, a number of these reactors could be in operation for hydrogen generation by the middle of the 21st century. In addition to avoiding oil use, the reactors would contribute significantly to a reduction in emissions of greenhouse gases and help alleviate global climate change.

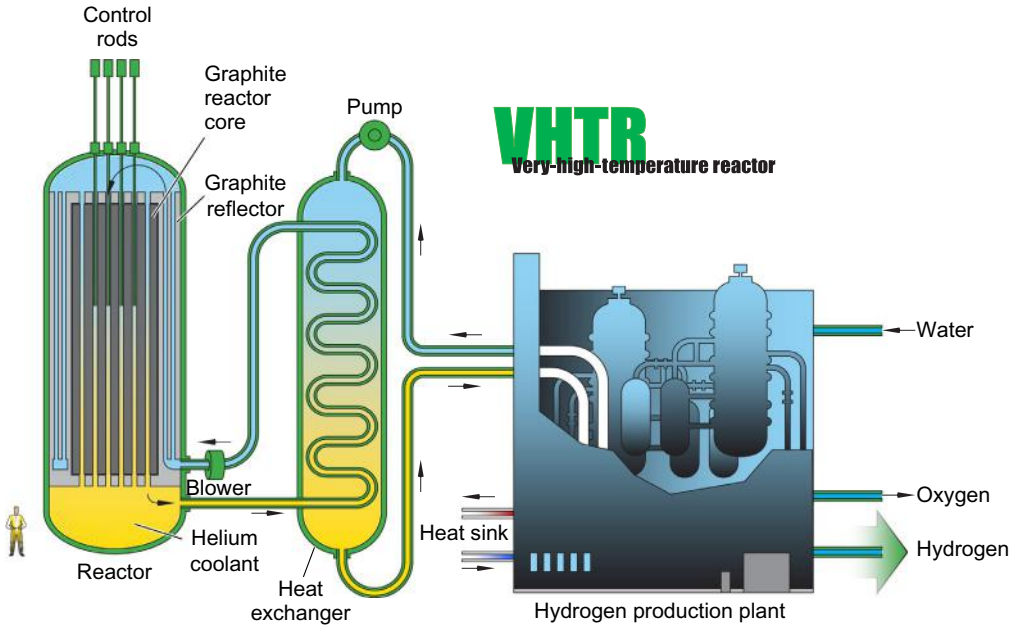

FIG. 18.10

Very-high-temperature reactor with hydrogen processing unit.

Courtesy U.S. Department of Energy (DOE)/Generation IV International Forum (GIF), 2002. A technology roadmap for generation IV Nuclear energy systems. DOE report. http://www.gen-4.org/Technology/roadmap.htm.

18.9 SUMMARY

Reactors are classified according to purpose, neutron energy, moderator and coolant, fuel, arrangement, and structural material. Principal power reactor types include the PWR, the BWR, the HWR, the HTGR, and the LMFBR. As of the end of 2017, there were 99 operating power reactors in the United States and 446 total globally. Several evolutionary reactor concepts, such as the AP1000, are vying for today's market. Small modular reactors with lower upfront costs are also in the competition. The very-high-temperature reactor is regarded as the best candidate for the next-generation nuclear system.

18.10 EXERCISES

18.1 Calculate the threshold energy of the (a) $^{16}O(n, p)^{16}N$ and (b) $^{17}O(n, p)^{17}N$ reactions.

18.2 For a water inventory of 15,000 kg in the core and a fast flux of 10^{16} n/(cm^2 s), compute the steady-state production rate of (a) ^{16}N and (b) ^{17}N. The fission-spectrum averaged cross-sections for the reactions of the preceding exercise are 0.020 and 0.007 mb, respectively (Stephenson, 1958).

18.3 Using an external technical reference, determine the emissions from the decay of N-17, which is produced from the $^{17}O(n, p)$ reaction. Why is this reaction in water of perhaps less concern than that of $^{16}O(n, p)$?

18.4 A 2200-MWe advanced nuclear plant has an expected construction cost of $5,000/kWe and estimated annual O&M expenses of $89/kWe. If the projected fuel charge is $2/(MWe h), compute the electricity generation cost for an annual levelized fixed charge rate of 15% and anticipated capacity factor of 92%.

18.5 Find the yearly savings of oil by use of uranium in a nuclear reactor, with rated power 1000 MWe, efficiency 0.33, and capacity factor 0.8. Note that the burning of one barrel of oil per day corresponds to 71 kW of heat power (see Exercise 24.3). At $90 per barrel, how much is the annual dollar savings of oil?

18.6 (a) How many individual fuel pellets are there in the PWR reactor described in Section 18.4? (b) Assuming a density of uranium oxide of 10 g/cm^3, estimate the total mass of uranium and U-235 in the core in kilograms. (c) Using Table 15.3 data, what is the initial fuel cost?

18.7 The core of a PWR contains 180 square fuel assemblies of length 4 m, width 0.2 m. (a) Find the core volume and radius of an equivalent cylinder. (b) If there are 200 fuel rods per assembly with pellets of diameter 0.9 cm, what is the approximate UO_2 volume fraction of the core?

18.8 For an HTGR with a thermal efficiency of 50%, what is the percentage savings in fuel mass as compared to a Generation II LWR with an identical burnup?

18.9 Over the course of 3 years, a nuclear unit was shut down twice for refueling outages lasting 32 and 45 days, respectively, but was otherwise operating at full power. Determine the capacity factor for this 3-year period.

18.10 Compute a predicted core lifetime for the BWR of Table 18.4.

18.11 Using data from Table 18.4, estimate the number of fuel rods in (a) the PWR and (b) the BWR.

18.12 If the theoretical density of UO_2 is 10.97 g/cm^3, determine the atomic density of U-235 in a typical sintered fuel pellet enriched to 3.5 w/o.

18.13 By what percentage is the fuel cost of electricity from an air-cooled mPower module larger than that using water cooling?

18.14 Using the Table 18.4 data, estimate the average thermal neutron flux in the active core volume of the (a) PWR and (b) BWR for fuel enrichments of 2.6 and 1.9 w/o, respectively.

18.15 Considering the spontaneous fission in the U-238 within the reactor of Exercise 18.6, calculate the number of neutrons emitted per second.

18.16 For the 6.1 MeV gamma rays emitted from N-16, compute the corresponding half-thickness in (a) lead, (b) iron, and (c) concrete.

REFERENCES

Agnew, H.M., 1981. Gas-cooled nuclear power reactors. Sci. Am. 244 (6), 55–63.
American Nuclear Society (ANS), 2018. 20th annual reference issue. Nucl. News 61 (3), 39–61.
Blake, E.M., 2017. U.S. capacity factors: close to a new peak. Nucl. News 60 (6), 24–30.
Electric Power Research Institute (EPRI), 1999. Advanced Light Water Reactor Utility Requirements Document. vols. 1–3, EPRI, Palo Alto, CA.
El-Wakil, M.M., 1978. Nuclear Heat Transport. American Nuclear Society, La Grange Park, IL.
Fütterer, M.A., Fu, L., Sink, C., de Groot, S., Pouchon, M., Kim, Y.W., Carré, F., Tachibana, Y., 2014. Status of the very high temperature reactor system. Prog. Nucl. Energy 77, 266–281.
Generation IV International Forum (GIF), 2014. Technology roadmap update for generation iv nuclear energy systems. OECD Nuclear Energy Agency.www.gen-4.org.
Hinds, D., Maslak, C., 2006. Next-generation nuclear energy: the ESBWR. Nucl. News 49 (1), 35–40.
Holbert, K.E., 2017. Nuclear reactors. In: Seidel, A. (Ed.), Kirk-Othmer Encyclopedia of Chemical Technology. Wiley, New York.
Independent Technology Review Group (ITRG), 2004. Design Features and Technology Uncertainties for the Next Generation Nuclear Plant. Idaho National Laboratory, Idaho Falls.
Ingersoll, D.T., Houghton, Z.J., Bromm, R., Desportes, C., 2014. NuScale small modular reactor for co-generation of electricity and water. Desalination 340, 84–93.
International Atomic Energy Agency (IAEA), 2018. Nuclear Power Reactors in the World. IAEA, Vienna.
Koster, A., Matzner, H.D., Nicholsi, D.R., 2003. PBMR design for the future. Nucl. Eng. Des. 222 (2-3), 231–245.
LaBar, M.P., Shenoy, A.S., Simon, W.A., Campbell, E.M., 2003. The gas turbine-modular helium reactor. Nucl. News 46 (11), 28–37.
Nuclear Energy Institute (NEI), 1998. Strategic Plan for Building New Nuclear Power Plants. NEI, Washington, DC.
Reyes, J.N., Lorenzini, P., 2010. NuScale power: a modular, scalable approach to commercial nuclear power. Nucl. News 53 (7), 97–104.
Schulz, T.L., 2006. Westinghouse AP1000 advanced passive plant. Nucl. Eng. Des. 236, 1547–1557.
Scott, D.B., 1965. Physical and mechanical properties of Zircaloy 2 and 4. Report WCAP-3269-41, Westinghouse Electric Corp., Pittsburgh, PA.
Stephenson, R., 1958. Introduction to Nuclear Engineering, second ed. McGraw-Hill, New York, pp. 277–278.
Tower, S.N., Schulz, T.L., Vijuk, R.P., 1988. Passive and simplified system features for the advanced Westinghouse 600 MWe PWR. Nucl. Eng. Des. 109, 147–154.
U.S. Code (USC), 1983. Nuclear waste fund. 42 U.S.C. § 10222(a).
U.S. Department of Energy (DOE)/Generation IV International Forum (GIF), 2002. A technology roadmap for generation IV Nuclear energy systems. DOE report, http://www.gen-4.org/Technology/roadmap.htm.
University of New Mexico, (n.d.). Nuclear Engineering Wall Charts. http://econtent.unm.edu/cdm/search/collection/nuceng. Nuclear power plant diagrams from the famous *Nuclear Engineering International* series of wall charts.
Wolfe, B., Wilkins, D.R., 1989. Future directions in boiling water reactor design. Nucl. Eng. Des. 115, 281–288.

FURTHER READING

CANTEACH, https://canteach.candu.org/. Comprehensive educational and reference library on CANDU technology.
Cochran, R.G., Tsoulfanidis, N., Miller, W.F., 1993. Nuclear Fuel Cycle: Analysis and Management, second ed. American Nuclear Society, La Grange Park, IL.
Foster, A.R., Wright, R.L., 1983. Basic Nuclear Engineering, fourth ed. Allyn and Bacon, Boston.

General Electric Co., 1980. BWR/6 General Description of a Boiling Water Reactor. General Electric Co., San Jose, CA.

Karady, G.G., Holbert, K.E., 2013. Electrical Energy Conversion and Transport: An Interactive Computer-Based Approach, second ed. Wiley, Hoboken.

Knief, R.A., 1992. Nuclear Engineering: Theory and Technology of Commercial Nuclear Power, second ed. Taylor & Francis, Bristol, PA.

Lish, K.C., 1972. Nuclear Power Plant Systems and Equipment. Industrial Press, New York.

Nero Jr., A.V., 1979. A Guidebook to Nuclear Reactors. University of California Press, Berkeley.

Pebble Bed Modular Reactor, http://www.pbmr.co.za/ Use "Read more" features for details of the program.

Westinghouse Electric Corp, 1984. The Westinghouse Pressurized Water Reactor Nuclear Power Plant. Westinghouse Electric Corp, Pittsburgh, PA.

World Nuclear Association (WNA), Information Library. http://www.world-nuclear.org/. Information on present and future reactor concepts worldwide.

CHAPTER

REACTOR THEORY INTRODUCTION

19

CHAPTER OUTLINE

Detailed treatment of neutron behavior provides a means to design reactors more effectively. After deriving the neutron diffusion equation, we shall demonstrate its application to three-dimensional reactor shapes of interest. The linkage between the diffusion equation and reactor criticality is quantified. The fact that reactor configurations physically separate the fuel and moderator is found to increase the multiplication factor. Design of next-generation and small modular reactors motivates a renewed interest in these topics. Here we focus on steady-state conditions, with time-dependent behavior being the forte of the next chapter.

19.1 THE DIFFUSION EQUATION

As budgeting and conserving neutrons are of great importance in reactor design, we begin by counting neutrons. Similar to radioactive decay, the basic neutron balance is

$$\text{Rate of change} = \text{Production} - \text{Losses} \tag{19.1}$$

Production is from a neutron source, such as fission; the losses arise from absorption and leakage such that Eq. (19.1) can be rewritten in terms of the change in neutron concentration

$$dn/dt = \text{Production} - \text{Absorption} - \text{Leakage} \tag{19.2}$$

Besides fulfilling thermal-hydraulic and safety constraints, reactor design seeks to minimize neutron leakage and absorption by nonfuel materials, and maximize neutron generation from fission.

Nuclear Energy. https://doi.org/10.1016/B978-0-12-812881-7.00019-8

The neutron absorption rate is simply $\Sigma_a\phi$. The production rate depends on the physical situation, meaning that neutrons may be generated by some arbitrary neutron source, S, such as Cf-252. Within an operating reactor, the source term is inevitably fission; hence, the neutron production rate is $\nu\Sigma_f\phi$. For a single coordinate system problem, the leakage rate is the derivative of the neutron current with respect to position, that is, dj/dx. Substituting for each of the three terms and confining to steady-state conditions when $dn/dt = 0$ provides an expression for neutron continuity

$$0 = \nu\Sigma_f\phi - \Sigma_a\phi - dj/dx \tag{19.3}$$

Unfortunately, this relation has two dependent variables: neutron flux ϕ and current density j. To resolve this we utilize Fick's Law.

Recall from Section 4.7 that Fick's Law describes how neutrons diffuse from a region of high concentration to that of low density. In one-dimensional geometry, Fick's law relates the neutron current density and flux via

$$j = -D\, d\phi/dx \tag{19.4}$$

in which D is the diffusion coefficient, $D = \lambda_{tr}/3$. The diffusion process is physically accomplished through the preferential forward scattering of neutrons.

Incorporating Fick's Law into the relation for neutron continuity yields the *neutron diffusion equation*

$$\frac{d^2\phi}{dx^2} + \frac{\nu\Sigma_f - \Sigma_a}{D}\phi = 0 \tag{19.5}$$

To simplify writing the expression, we denote the coefficient to the flux as B^2. Owing to a similarity of this second-order linear differential equation to the form of that found in the loading of a vertical column for strength analysis, the coefficient is termed the *buckling*. This particular rendition of B^2 is called the *material buckling,* as it may be computed purely using quantities describing the reactor composition.

$$B_m^2 = (\nu\Sigma_f - \Sigma_a)/D \tag{19.6}$$

In the case of a general neutron source S, the diffusion equation may be written as

$$\frac{d^2\phi}{dx^2} - \frac{\Sigma_a}{D}\phi = \frac{-S}{D} \tag{19.7}$$

This formulation can also be employed to study neutron diffusion in the absence of a source ($S = 0$). In particular, the ratio D/Σ_a is the neutron diffusion area L^2. The *diffusion area* has physical significance, as L^2 is one-sixth of the average of the crow-flight distance squared that is traveled by a neutron from origination to absorption $\left(\overline{r^2} = 6L^2\right)$. More often, we refer to the diffusion length

$$L = \sqrt{D/\Sigma_a} \tag{19.8}$$

EXAMPLE 19.1

Compare the neutron mean free path in C-12 to the diffusion length. Using results from Example 4.8, the diffusion coefficient of graphite is approximately

$$D = \lambda_{tr}/3 = (2.72\text{cm})/3 = 0.91\text{cm}$$

With the cross-sections from Table 4.2 and $N_{\text{C-12}} = 8.3 \times 10^{22}/\text{cm}^3$, relevant macroscopic cross-sections are

$$\Sigma_s = N\sigma_s = \left(8.3 \times 10^{22}/\text{cm}^3\right)\left(4.7 \times 10^{-24}\,\text{cm}^2\right) = 0.39/\text{cm}$$

$$\Sigma_a = N\sigma_a = \left(8.3 \times 10^{22}/\text{cm}^3\right)\left(0.0035 \times 10^{-24}\,\text{cm}^2\right) = 0.00029/\text{cm}$$

The scattering reaction dominates in carbon such that the mean free path (mfp) is

$$\lambda = 1/\Sigma_s = 1/(0.39/\text{cm}) = 2.6\,\text{cm}$$

In contrast, the diffusion length of a thermal neutron is

$$L = \sqrt{D/\Sigma_a} = \sqrt{(0.91\,\text{cm})/(0.00029/\text{cm})} = 56\,\text{cm}$$

The root-mean-square crow-flight distance travelled by the neutron can be roughly appraised from $r \approx L\sqrt{6} = (56\text{cm})\sqrt{6} = 140\text{cm}$. The ratio of the scattering to absorption cross-sections supplies an estimate of the number of scatters that a neutron undergoes before absorption, specifically in this case, $\Sigma_s/\Sigma_a = (0.39/\text{cm})/(0.00029/\text{cm}) = 1340$. This implies that the neutron diffuses by scattering a total path length of $1340\lambda = 3480\,\text{cm}$. Hence, the mfp permits calculating the total path length traversed, whereas the diffusion length offers an assessment of the net vector distance travelled by a neutron from its origin.

19.2 DIFFUSION EQUATION SOLUTIONS

The derived diffusion equation permits determining the flux distribution throughout the reactor. Although we know that neutrons with energies from eV to MeV exist within the reactor, to keep the situation readily solvable by analytical techniques, we generally treat all the neutrons as belonging to a single energy group. In the case of a thermal reactor, the neutrons are assumed to be at low energy (<0.1 eV) while all the neutrons of a fast reactor would be considered as high energy (0.1–1 MeV).

Let us consider an infinite slab of fissionable material placed in a vacuum, such as that drawn in Fig. 19.1A. Logically speaking, one would expect the highest concentration of neutrons to occur at the center of the slab because neutrons leaking from the sides cannot be scattered back into the slab given the absence of material in the vacuum. This also means that the neutron flux would be approximately equal to zero at the edges of the slab. More precisely, we set the flux equal to zero at the extrapolation distance d beyond the slab edges (see Fig. 19.1B), where from transport theory

$$d = 0.7104\,\lambda_{\text{tr}} \tag{19.9}$$

Hence, two boundary conditions are established:

(1) Flux at the center ($x = 0$) is maximal: $\phi(0) = \phi_{\max}$.
(2) Flux at the extrapolated edges ($x = -\tilde{a}/2, \tilde{a}/2$) is zero: $\phi(-\tilde{a}/2) = 0 = \phi(\tilde{a}/2)$ where $\tilde{a} = a + 2d$.

These boundary conditions can be applied to the one-speed diffusion equation for a one-dimensional slab geometry

$$d^2\phi/dx^2 + B^2\phi(x) = 0 \tag{19.10}$$

The astute reader will recognize that the solution to this ordinary differential equation is the cosine function, that is, $\phi(x) = \phi_{\max}\cos(Bx)$. Using the boundary conditions reveals that $B = \pi/\tilde{a}$. When B^2 depends only on the physical dimensions of the system, it is called the *geometric buckling* B_g^2.

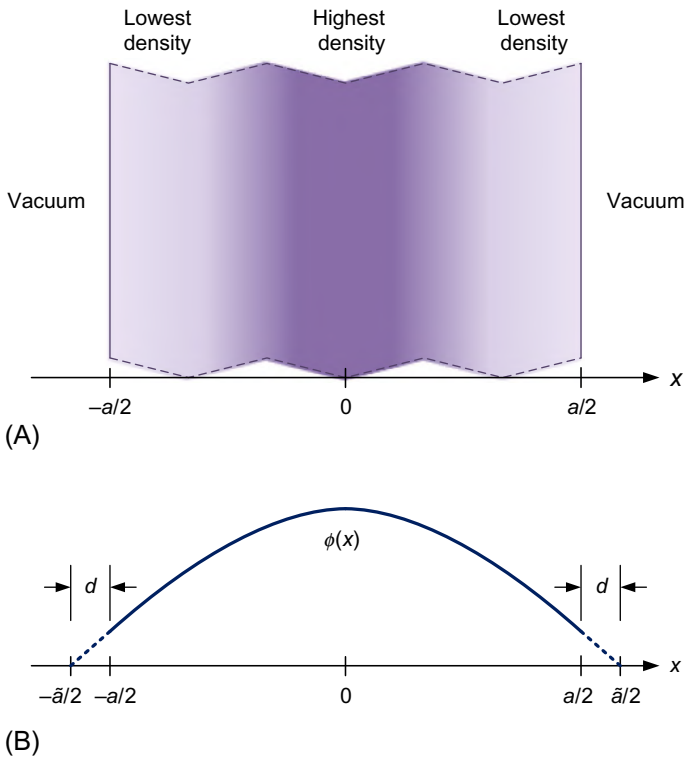

FIG. 19.1

Fissionable material in infinite slab geometry. (A) Slab and (B) flux.

A similar but more involved derivation leads to the same functional form for the axial flux behavior in a cylindrically shaped reactor, and hence, the reason for the use of the cosine function in describing the axial power distribution earlier in the text (for example, see Fig. 17.3).

The one-dimensional slab results can be extended to the three-dimensional rectangular shape such that its flux distribution is

$$\phi(x,y,z)=\phi_C\cos(\pi x/\tilde{a})\cos\left(\pi y/\tilde{b}\right)\cos(\pi z/\tilde{c}) \tag{19.11}$$

where $-a/2\le x\le a/2$, $-b/2\le y\le b/2$, and $-c/2\le z\le c/2$. Substituting the midpoint (origin) values in each direction reveals that the flux at the center ϕ_C is also the maximum value ϕ_{max}. The cosinusoidal flux profile for the y-direction of the rectangular parallelepiped is drawn in Fig. 19.2. Solving the *reactor equation*, $\nabla^2\phi+B^2\phi=0$, for the sphere and cylinder yields the results listed in Table 19.1. As most reactors may be approximated as a right cylinder, we emphasize that shape primarily, although spherical and cuboid forms are not uncommon.

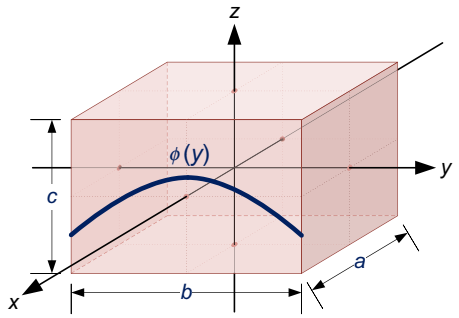

FIG. 19.2

Rectangular parallelepiped reactor shape with cosinusoidal flux profile.

Table 19.1 Bare Reactor Characteristics

Geometry (Dimensions)	Flux Profile (With Coordinate System Origin at the Center of the Shape)	Geometric Buckling, B_g^2
Rectangular parallelepiped ($a \times b \times c$)	$\phi(x,y,z) = \phi_C \cos\left(\frac{\pi x}{\tilde{a}}\right) \cos\left(\frac{\pi y}{\tilde{b}}\right) \cos\left(\frac{\pi z}{\tilde{c}}\right)$	$\left(\frac{\pi}{\tilde{a}}\right)^2 + \left(\frac{\pi}{\tilde{b}}\right)^2 + \left(\frac{\pi}{\tilde{c}}\right)^2$
Sphere (radius, R)	$\phi(r) = \frac{\phi_C \tilde{R}}{\pi r} \sin\left(\frac{\pi r}{\tilde{R}}\right);\ 0 \le r \le R$	$\left(\frac{\pi}{\tilde{R}}\right)^2$
Right cylinder (radius, R; height, H)	$\phi(r,z) = \phi_C \cos\left(\frac{\pi z}{\tilde{H}}\right) J_0\left(\frac{2.405r}{\tilde{R}}\right)$	$\left(\frac{\pi}{\tilde{H}}\right)^2 + \left(\frac{2.405}{\tilde{R}}\right)^2$

Where J_0 is the Bessel function of the first kind of order zero.

EXAMPLE 19.2

Compare the maximum flux in a cylindrical reactor to that at the position a quarter of the height and half the radius. Using the coordinate system specified in Table 19.1 and neglecting the extrapolation distance, the flux at $r = R/2$, $z = -H/4$ is

$$\phi(R/2, -H/4) = \phi_{max} \cos(-\pi/4)\, J_0(2.405/2) = 0.474\, \phi_{max}$$

in which the value of the Bessel function J_0 was found using a built-in function within spreadsheet software.

These flux (or power) distributions are for bare reactors, for which a vacuum or sparse substance such as air surrounds the core. Without material directly adjacent to the core, neutrons leaking from the reactor are lost. Actual light-water reactors include a variety of other structural elements such as those illustrated in Fig. 19.3. The metallic components, such as the core barrel and thermal shield, surrounding the core serve to scatter the leaking fast neutrons back into the reactor. Lighter elements such as the incoming coolant that traverses down the inside of the reactor vessel tend to scatter the leaking thermal neutrons back toward the core. In both cases, the material functions as a neutron *reflector*.

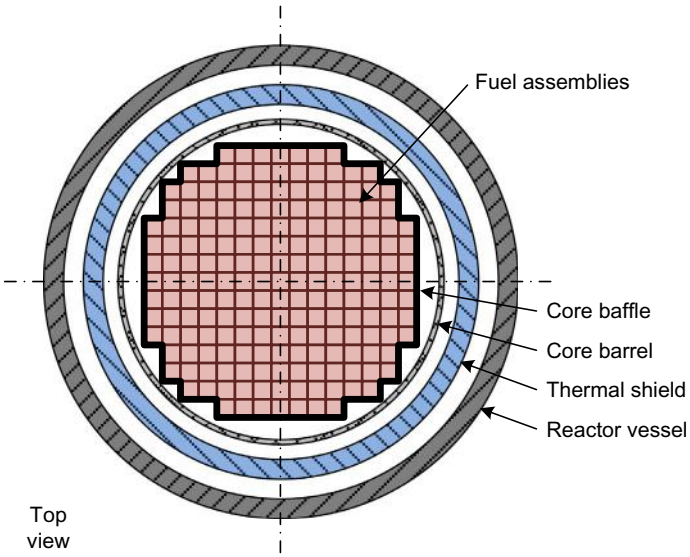

FIG. 19.3

Top view of a pressurized water reactor (PWR) core layout.

Not only does the reflector conserve neutrons, it also assists in achieving a more uniform power distribution across the core compared to the cosinusoidal profile. Instead of a reflector, breeder reactors place a *blanket* of fertile material at the core periphery in order to produce more fissile material from the otherwise leaking neutrons.

Considering the formula for the nonleakage probability (i.e., Eq. 16.6) and the definition of the diffusion area leads to

$$\mathcal{L} = \frac{1}{1 + L^2 B^2} = \frac{\Sigma_a}{\Sigma_a + DB^2} \tag{19.12}$$

According to Eq. (19.10), the buckling is numerically proportional to the second derivative, that is, $d^2\phi/dx^2 = -B^2\,\phi$. Hence, the one-group diffusion equation can be written as

$$-DB^2\phi + (\nu\Sigma_f - \Sigma_a)\,\phi = 0 \tag{19.13}$$

in which the terms from left to right represent leakage, production, and absorption. Comparing this expression to the nonleakage probability discloses that $\mathcal{L}$ is the ratio

$$\mathcal{L} = \frac{\text{Neutron absorption}}{\text{Neutron absorption and leakage}} \tag{19.14}$$

A simple algebraic rearrangement furnishes a relation between leakage and absorption

$$\frac{\text{Neutron leakage}}{\text{Neutron absorption}} = \frac{1 - \mathcal{L}}{\mathcal{L}} = \frac{DB^2}{\Sigma_a} = L^2 B^2 \tag{19.15}$$

For dilute fuel concentrations in the moderator, the diffusion coefficient and Fermi age τ of the homogeneous mixture are essentially those of the moderator because it dominates the scattering interactions. The absorption cross-section is substantially impacted by the fuel, and the diffusion area is (see Exercise 19.7)

$$L^2 = L_M^2(1-f) \tag{19.16}$$

where L_M is the diffusion length of the pure moderator and f is the fuel utilization.

EXAMPLE 19.3

Here we determine the neutron leakage from a 200-kW cubical reactor of 1-m sides. The reactor is composed of the graphite from Example 19.1 with U-235 randomly impregnated throughout to a density of $N_{235} = N_C/1000$. The macroscopic absorption cross-section of the fuel is

$$\Sigma_a^F = N_{235}\sigma_a^{235} = \left(8.3\times10^{19}/\text{cm}^3\right)\left(680.9\times10^{-24}\,\text{cm}^2\right) = 0.0565/\text{cm}$$

Using D for carbon, the diffusion area of the mixture is

$$L^2 = \frac{D}{\Sigma_a^F + \Sigma_a^M} = \frac{0.9\,\text{cm}}{(0.0565+0.00029)/\text{cm}} = 16\,\text{cm}^2$$

By use of Table 19.1 with $d=0$, the cubical reactor has a geometric buckling of

$$B_g^2 = 3(\pi/a)^2 = 3(\pi/100\text{cm})^2 = 0.0030/\text{cm}^2$$

The average flux may be obtained from the thermal power

$$\phi_{avg} = \frac{P}{w\Sigma_f V} = \frac{\left(200\times10^3\,\text{W}\right)\left(3.29\times10^{10}\,\text{fission}/(\text{W s})\right)}{\left(8.3\times10^{19}/\text{cm}^3\right)\left(582.6\times10^{-24}\,\text{cm}^2\right)(100\text{cm})^3} = 1.36\times10^{11}\,\text{n}/\left(\text{cm}^2\,\text{s}\right)$$

The total neutron absorption rate across the core is

$$R_a = \Sigma_a\phi_{avg}V = (0.0565+0.00029/\text{cm})\left(1.36\times10^{11}\,\text{n}/\left(\text{cm}^2\,\text{s}\right)\right)(100\text{cm})^3 = 7.7\times10^{15}\,\text{n/s}$$

Using Eq. (19.15), the neutron leakage rate is

$$R_L = R_aL^2B_g^2 = \left(7.7\times10^{15}\,\text{n/s}\right)\left(16\text{cm}^2\right)\left(0.0030/\text{cm}^2\right) = 3.7\times10^{14}\,\text{n/s}$$

19.3 REACTOR CRITICALITY

While the diffusion equation describes the neutron flux throughout the core, for criticality the following condition from Chapter 16 must still be satisfied

$$k_{eff} = k_\infty\mathcal{L} = k_\infty/\left(1+L^2B^2\right) \tag{19.17}$$

Manipulating this algebraically and solving for the buckling yields

$$B^2 = \frac{1}{L^2}\left(\frac{k_\infty}{k_{eff}}-1\right) \tag{19.18}$$

The classic two-parameter representation for k_∞ can be expanded as

$$k_\infty = \eta f = \frac{\nu\Sigma_f^F}{\Sigma_a^F}\frac{\Sigma_a^F}{\Sigma_a^T} = \frac{\nu\Sigma_f}{\Sigma_a} \tag{19.19}$$

in which the fuel (F) and total (T) superscripts have been removed in the rightmost expression because fuel is undoubtedly the fissionable material and Σ_a clearly denotes all absorbing material. The buckling can now be written as

$$B^2 = \frac{1}{L^2}\left(\frac{k_\infty}{k_{\text{eff}}} - 1\right) = \frac{\Sigma_a}{D}\left(\frac{\nu\Sigma_f/\Sigma_a}{k_{\text{eff}}} - 1\right) \tag{19.20}$$

Earlier versions of the diffusion equation assumed that criticality exists. To account for the criticality condition, the effective multiplication factor can be incorporated into the steady-state diffusion equation using the buckling relation in Eq. (19.20)

$$\frac{d^2\phi}{dx^2} + \frac{\nu\Sigma_f/k_{\text{eff}} - \Sigma_a}{D}\phi = 0 \tag{19.21}$$

These results are based upon all the neutrons being of similar energy such that k_∞ may be represented as ηf. Therefore, for a thermal reactor, the coefficients such as D and L^2 would be computed from cross-sections at low energy while these parameters are acquired around 1 MeV for a fast reactor.

The relationship between geometric and material buckling provides an alternative means by which the criticality of a system may be assessed

$$\begin{aligned} &\text{Subcritical } (k_{\text{eff}} < 1): && B_g^2 > B_m^2 \\ &\text{Critical } (k_{\text{eff}} = 1): && B_g^2 = B_m^2 \\ &\text{Supercritical } (k_{\text{eff}} > 1): && B_g^2 < B_m^2 \end{aligned} \tag{19.22}$$

At first, supercritical may sound ominous, but unless k_{eff} initially exceeds unity, criticality would cease after a short operational period as fuel is consumed.

EXAMPLE 19.4

The minimum critical volume is a function of the buckling. For instance, consider a sphere, for which $B_g^2 = (\pi/R)^2$ neglecting the extrapolation distance; hence, the critical radius is $R = \pi/B$. The minimum critical volume for a spherical core is

$$V_{\min} = \frac{4}{3}\pi R^3 = \frac{4}{3}\pi\left(\frac{\pi}{B}\right)^3 = \frac{130}{B^3}$$

Similar expressions can be derived for the cylinder and cube (Exercise 19.10). Although the derivation is beyond the scope of this textbook, the minimum-sized cylindrical reactor for criticality has a height-to-diameter (H/D) ratio of 0.924.

EXAMPLE 19.5

Let's revisit the Example 16.3 calculation of the nonleakage probability for the Godiva fast metal assembly if the extrapolation distance is considered. The extrapolated radius of the sphere is

$$\begin{aligned} \widetilde{R} &= R + d = R + 0.7104\lambda_{\text{tr}} = R + 0.7104/\Sigma_{\text{tr}} = R + 0.7104/(N\sigma_{\text{tr}}) \\ &= 8.6\text{cm} + (0.7104)/\left[\left(4.87\times10^{22}/\text{cm}^3\right)\left(6.8\times10^{-24}\,\text{cm}^2\right)\right] = 10.7\text{cm} \end{aligned}$$

The geometric buckling becomes

$$B_g^2 = \left(\pi/\tilde{R}\right)^2 = [\pi/(10.7\,\text{cm})]^2 = 0.086/\text{cm}^2$$

with the corresponding fast neutron nonleakage probability increasing from its original value of 0.38 to

$$\mathcal{L} = 1/\left(1 + L^2 B_g^2\right) = 1/\left[1 + \left(12.5\,\text{cm}^2\right)\left(0.086/\text{cm}^2\right)\right] = 0.48$$

Inclusion of d in the computation provides a more accurate result. Utilization of the extrapolation distance is of greater importance in the analysis of small-sized cores compared to large commercial power reactors.

For more accurate estimation in thermal reactors, the material buckling may be computed using the migration area M^2 rather than L^2. The *migration area* combines the neutron crow-flight distances travelled during slowing down and diffusion

$$M^2 = L^2 + \tau = L_M^2(1 - f) + \tau \tag{19.23}$$

Besides using M^2 to calculate B_m, a single expression appears to represent the combined effects of fast and thermal leakage, such that the overall nonleakage probability is

$$\mathcal{L} = \mathcal{L}_t \mathcal{L}_f \cong \frac{1}{1 + M^2 B_g^2} \tag{19.24}$$

These substitutions are known as modified one-group theory, which is especially appropriate when $\tau > L^2$ such as with a water-moderated reactor.

EXAMPLE 19.6

We can use the preceding formulas to determine the criticality condition of the reactor of Example 19.3. For the fully enriched core, the two-parameter representation for k_∞ is sufficient

$$k_\infty = \eta f = \frac{\nu\Sigma_f}{\Sigma_a} = \frac{(2.42)\left(8.3 \times 10^{19}/\text{cm}^3\right)\left(582.6 \times 10^{-24}\,\text{cm}^2\right)}{(0.0565 + 0.00029)/\text{cm}} = 2.06$$

This large multiplication factor demonstrates the efficacy of such a dilute concentration of fissile material. By replacing L^2 in Eq. (19.34) with the migration area of Eq. (19.23), the material buckling for modified one-group theory becomes

$$B_m^2 = \frac{k_\infty - 1}{M^2} = \frac{k_\infty - 1}{L^2 + \tau} = \frac{2.06 - 1}{16\,\text{cm}^2 + 364\,\text{cm}^2} = 0.0028/\text{cm}^2$$

in which the Fermi age is obtained from Table 4.4. Because $B_m^2 < B_g^2$, this reactor is subcritical. The reader is challenged in Exercise 19.8 to find the critical size.

19.4 HETEROGENEOUS REACTOR

Although reactor theory is more easily applied to homogenous mixtures of fuel and moderator, most reactors physically separate the two, and sometimes even the coolant. Heterogeneous reactors are exemplified by light-water reactors (LWRs) in which moderator–coolant flows on the outside of the cladding-encased fuel pellets. Fuel element configurations are typically of either the hexagonal,

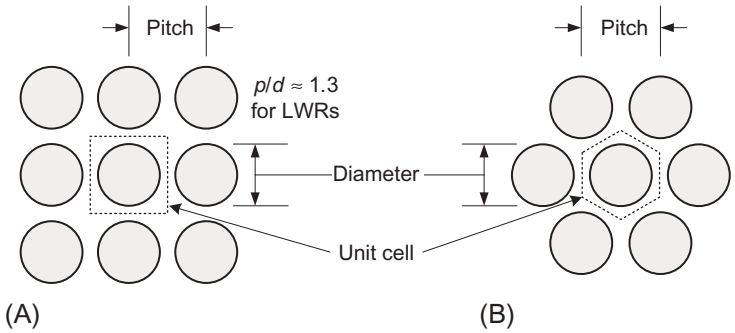

FIG. 19.4

Reactor heterogeneous lattice configurations. (A) Square and (B) hexagonal.

sometimes referred to as triangular, or square arrangements, as drawn in Fig. 19.4. The pitch-to-diameter ratio (p/d) is important to analyses of both the neutronics and the thermal-hydraulics of the reactor.

As one might expect, there is an optimum moderator-to-fuel ratio in terms of achieving the largest multiplication factor. The p/d ratio is a direct means by which the number of moderator-to-fuel atoms can be manipulated. As p/d increases beyond the value at which k_{eff} is maximum, the reactor is said to be *overmoderated*, and similarly, smaller p/d values provide an *undermoderated* reactor. Reactors are designed to be undermoderated for stability reasons, specifically to achieve a negative reactivity feedback coefficient, which is a subject of the next chapter.

EXAMPLE 19.7

As the primary moderating material in water is hydrogen, let's find the hydrogen-to-uranium atom ratio for a square lattice with $p/d = 1.32$. Referring to the square *unit cell* in Fig. 19.4A, the moderator-to-fuel volume ratio for a single fuel rod and its associated coolant is

$$\frac{V_{\text{M}}}{V_{\text{F}}} = \frac{p^2 - \pi(d/2)^2}{\pi(d/2)^2} = \frac{4}{\pi}\left(\frac{p}{d}\right)^2 - 1 = \frac{4}{\pi}(1.32)^2 - 1 = 1.22$$

For a fuel rod of atomic density $N_{\text{F}} = 2.3 \times 10^{22}/\text{cm}^3$ surrounded by water of density $N_M = 3.3 \times 10^{22}/\text{cm}^3$, the H/U atom ratio is

$$\frac{n_{\text{H}}}{n_{\text{U}}} = \frac{2N_{\text{M}}V_{\text{M}}}{N_{\text{F}}V_{\text{F}}} = \frac{(2)\left(3.3 \times 10^{22}/\text{cm}^3\right)}{\left(2.3 \times 10^{22}/\text{cm}^3\right)}(1.22) = 3.5$$

Fuel heterogeneity tends to increase the multiplication factor of the system. This effect can be explained using the four-factor formula of Eq. (16.7) with the assistance of Fig. 19.5. The diagram enumerates the interactions a neutron has while at fast, resonance, and thermal energy levels as well as delineating where these interactions happen. The important changes due to heterogeneity occur in the thermal utilization f, fast fission factor ε, and resonance escape probability $\wp$.

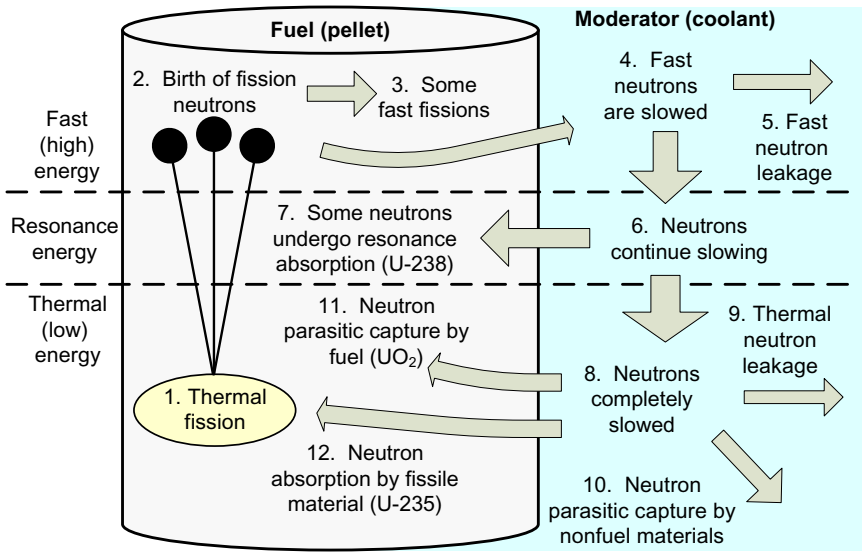

FIG. 19.5

Depiction of four-factor formula in heterogeneous LWR fuel.

The thermal utilization describes the neutron absorption in fuel as compared to total absorption. With the strong thermal neutron absorption within the fuel pellet, the average low-energy neutron flux in the fuel ϕ_F is smaller than that in the moderator ϕ_M. This disparity gives rise to the notion of a *thermal disadvantage factor*, $\zeta = \phi_M/\phi_F$. The thermal utilization for a heterogeneous configuration is

$$f_{het} = \frac{\Sigma_a^F \phi_F V_M}{\Sigma_a^F \phi_F V_F + \Sigma_a^M \phi_M V_M} = \frac{\Sigma_a^F}{\Sigma_a^F + \Sigma_a^M \varsigma (V_M/V_F)} \tag{19.25}$$

For a homogeneous fuel-moderator mixture, $f_{hom} = \Sigma_a^F/(\Sigma_a^F + \Sigma_a^M)$. Therefore, the fuel utilization decreases ($f_{het} < f_{hom}$) for the heterogeneous arrangement because $\phi_M > \phi_F$.

The fast fission factor accounts for the extra fissions caused by high-energy neutrons. In a homogeneous reactor, the dilute fuel concentration means that the fast neutrons born are more likely to initially interact with a moderator atom and be slowed before contacting another fuel atom. In contrast, a newly liberated fast neutron in a fuel pellet is released into a region that is rich with fissionable material, and thus can induce fast fission before the external moderator slows the neutron. Hence, a heterogeneous configuration increases the fast fission factor ($\varepsilon_{het} > \varepsilon_{hom}$).

The most significant impact of heterogeneity is the increase afforded the resonance escape probability. Fig. 19.5 provides understanding of the *self-shielding* effect of the heterogeneous fuel. The slowing of the neutrons in the moderator means that neutron energy decreases while physically separate from the fuel, thereby resulting in a higher probability that the neutron is not absorbed by the resonance cross-sections. Furthermore, even if a neutron at resonance energy would scatter into

the fuel, only the fuel on the pellet edge contributes to the absorption such that resonance capture occurs in only a small fraction of the fuel atoms. In contrast, in the homogeneous case, all the fuel can partake in resonance capture. Thus, the heterogeneous structure considerably improves the resonance escape probability ($\wp_{het} > \wp_{hom}$).

Overall, the multiplication factor benefits from a heterogeneous design ($k_{\infty,het} > k_{\infty,hom}$). As a case in point, if the natural uranium and graphite of the Chicago Pile (see Section 8.3) had been a homogeneous mixture, the CP-1 would not have been able to achieve criticality. In calculations, the heterogeneous unit cell of Fig. 19.4 can be converted into a round *equivalent cell* having the same physical volume fractions (V_M and V_F), and even homogenized such that the neutronic characteristics are maintained.

EXAMPLE 19.8

Divide the hexagon of Fig. 19.4B into six equilateral triangles with height $h = p/2$. Because the length of each side of an equilateral triangle is $b = 2h/\sqrt{3}$, the triangle area is

$$A_t = bh/2 = h^2/\sqrt{3} = p^2/\left(4\sqrt{3}\right)$$

With the hexagon area being $A_h = 6A_t$, the circular cell with an equivalent area has a radius of

$$r = \sqrt{A_h/\pi} = 0.525p$$

19.5 MULTIGROUP DIFFUSION THEORY

For scoping studies, one-group diffusion theory provides a reasonable depiction of reactor neutronics. A more accurate representation may be obtained for the thermal reactor using two-group diffusion theory in which one equation describes the thermal neutrons and a second relation represents the fast neutrons. As illustrated in Fig. 19.6, the source of fast neutrons is thermal neutron-induced fission, and the thermal neutron group source is the moderated fast neutrons. The most significant alteration in deriving the diffusion equations for two groups is accounting for neutron scattering between groups. At steady-state conditions, the coupled set of differential equations is

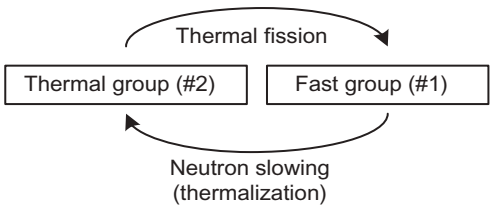

FIG. 19.6

Interchange within two-group diffusion theory.

$$\begin{aligned} &\underbrace{D_1 d^2\phi_1/dx^2}_{\text{fast neutron leakage}} + \underbrace{\nu\Sigma_{f,2}\phi_2}_{\text{thermal fission}} - \underbrace{\Sigma_{a,1}\phi_1}_{\text{fast absorption}} - \underbrace{\Sigma_{s,1\to 2}\phi_1}_{\text{fast to thermal downscattering}} = 0 \\ &\underbrace{D_2 d^2\phi_2/dx^2}_{\text{thermal neutron leakage}} + \underbrace{\Sigma_{s,1\to 2}\phi_1}_{\text{fast to thermal downscattering}} - \underbrace{\Sigma_{a,2}\phi_2}_{\text{thermal absorption}} = 0 \end{aligned} \tag{19.26}$$

in which "1" and "2" signify the fast and thermal group variables, respectively. The likelihood of upscattering from the thermal group to the fast group is negligible. The downscattering cross-section is called the *slowing down* cross-section.

Two-group theory also has the capability of incorporating all the parameters of the four-factor formula and the nonleakage probabilities. The fast fission factor ε and resonance escape probability $\wp$ were omitted previously from the one-speed diffusion equation. The effects of resonance capture reduce the thermal neutron source term, which originates from the slowing down of fast neutrons. Similarly, the fast neutron source term, which originates from thermal fission, can be augmented by including fast neutron-induced fissions. Neglecting the small fast absorption, the two-group diffusion equations become

$$\begin{aligned} D_1 d^2\phi_1/dx^2 - \Sigma_{s,1\to 2}\phi_1 &= -\varepsilon\nu\Sigma_{f,2}\phi_2 \\ D_2 d^2\phi_2/dx^2 - \Sigma_{a,2}\phi_2 &= -\wp\Sigma_{s,1\to 2}\phi_1 \end{aligned} \tag{19.27}$$

where the source terms have been intentionally moved to the right side of the equations for emphasis.

EXAMPLE 19.9

Show that the two-group theory formulation provides a complete criticality relation. First, from Eq. (19.10), the numerical value of the second-order derivative is $-B^2\phi$, and the $\nu\Sigma_{f,2}$ term can be replaced with $\eta f\Sigma_{a,2}$. Placing the two-group diffusion equations into a matrix formulation gives

$$\begin{bmatrix} D_1B^2 + \Sigma_{s,1\to 2} & -\varepsilon\eta f\Sigma_{a,2} \\ -\wp\Sigma_{s,1\to 2} & D_2B^2 + \Sigma_{a,2} \end{bmatrix} \begin{bmatrix} \phi_1 \\ \phi_2 \end{bmatrix} = \begin{bmatrix} 0 \\ 0 \end{bmatrix} \tag{19.28}$$

The matrix determinant, which must be zero for nontrivial solutions, yields

$$1 = \frac{\eta f\varepsilon\Sigma_{a,2}\wp\Sigma_{s,1\to 2}}{(D_1B^2 + \Sigma_{s,1\to 2})(D_2B^2 + \Sigma_{a,2})}$$

With recognition that the Fermi age τ is represented by an expression similar to that for the diffusion area, specifically $\tau = D_1/\Sigma_{s,1\to 2}$, the criticality relation appears

$$k_{\text{eff}} = 1 = \frac{\eta f\varepsilon\wp}{(1+\tau B^2)(1+L^2B^2)} = k_\infty \mathcal{L}_f \mathcal{L}_t \tag{19.29}$$

The process of increasing the number of describing equations leads to multigroup diffusion theory. Like two-group theory, a diffusion equation must be written for each energy group while considering that neutrons may scatter into or out of a group such that the balance equation is

$$dn/dt = \text{Production} + \text{Inscatter} - \text{Outscatter} - \text{Absorption} - \text{Leakage} \tag{19.30}$$

The neutrons are placed into G discrete energy intervals with a reverse indexing scheme such that the first group includes those neutrons at the highest energies. For steady-state conditions and neglecting upscattering, the diffusion equation for group g is

$$\underbrace{D_g \nabla^2 \phi_g}_{\text{leakage}} - \underbrace{\Sigma_{a,g}\phi_g}_{\text{absorption}} - \sum_{h=g+1}^{G} \underbrace{\Sigma_{s,g\to h}\phi_g}_{\substack{\text{downscatter}\\ \text{from group } g \text{ to } h}} + \sum_{h=1}^{g-1} \underbrace{\Sigma_{s,h\to g}\phi_h}_{\substack{\text{downscatter}\\ \text{from group } h \text{ to } g}} + \chi_g \sum_{h=1}^{G} \underbrace{\nu_h \Sigma_{f,h}\phi_h}_{\text{fission}} = 0 \tag{19.31}$$

in which χ_g is the probability that a neutron is born with an energy within group g; see Eq. (6.6). After placing the G equations into a matrix formulation, the computational power of computers is brought to bear on the problem.

A challenge to analytically solving multigroup equations occurs in dealing with the spatial derivative term. Inclusion of the derivative $d^2\phi/dx^2$ involves dividing the shape into discrete points, for example, $x_0, x_1, x_2, \ldots, x_N$ with equal spacing of Δx. A Taylor series expansion of the flux at those points adjacent to the position of interest x_i can be taken

$$\begin{aligned} \phi(x_{i+1}) &= \phi(x_i) + \Delta x \left.\frac{d\phi}{dx}\right|_{x_i} + \frac{(\Delta x)^2}{2}\left.\frac{d^2\phi}{dx^2}\right|_{x_i} + \cdots \\ \phi(x_{i-1}) &= \phi(x_i) - \Delta x \left.\frac{d\phi}{dx}\right|_{x_i} + \frac{(\Delta x)^2}{2}\left.\frac{d^2\phi}{dx^2}\right|_{x_i} - \cdots \end{aligned} \tag{19.32}$$

Adding the two expressions within Eq. (19.32) yields a formula for the required second derivative of the flux

$$\left.\frac{d^2\phi}{dx^2}\right|_{x_i} \cong \frac{\phi(x_{i+1}) - 2\phi(x_i) + \phi(x_{i-1})}{(\Delta x)^2} \tag{19.33}$$

Such an approach creates a coupled finite difference equation at each x_i location. Between the multiple energy groups and the chosen number of spatial positions, the resultant set of algebraic equations forms an increasingly large matrix to be solved numerically.

Computer Exercise 19.A employs the program MPDQ, which utilizes two neutron energy groups, to illustrate the effect of flux variation with position.

EXAMPLE 19.10

Four energy groups ($G = 4$) are to be utilized in describing a one-dimensional slab geometry problem. The slab is divided into $N = 10$ equal-width segments such that the 1st and 11th points lie on the slab edges. If the flux on the edges is set to zero, that is, $\phi(x_0) = 0 = \phi(x_{10})$, then there are $N - 1 = 9$ positions for which a finite difference relation is written. The total matrix size is therefore $G(N-1)$ squared, that is, 36×36 in this case.

19.6 SUMMARY

The diffusion equation is obtained from a neutron balance and the application of Fick's Law. With appropriate boundary conditions, the flux distribution for a bare reactor can be found using the diffusion equation. Comparing geometric and material bucklings provides a means by which the criticality condition can be determined. Greater precision is obtained with diffusion theory by increasing the number of energy groups into which neutrons are clustered.

19.7 EXERCISES

19.1 Complete the steps required to derive the neutron diffusion Eq. (19.5) from the continuity (19.3) and Fick's Law (19.4) relations.

19.2 Verify that $\phi(x) = \phi_{\max} \cos(Bx)$ is the solution to the diffusion equation for slab geometry by finding the second derivative of $\phi(x)$ and then substituting into Eq. (19.10).

19.3 Use L'Hopital's Rule to show that the maximum flux at the center of a bare spherical reactor is ϕ_C.

19.4 In a simple core such as a bare uranium metal sphere of radius R, the neutron flux varies with position, as given in Table 19.1. Calculate and plot the flux distribution for a core with $R = 10\,\text{cm}$, $d = 0$ and central flux $\phi_C = 5 \times 10^{11}/(\text{cm}^2\,\text{s})$.

19.5 Show that the material buckling given by Eq. (19.6) can be represented by

$$B_m^2 = (k_\infty - 1)/L^2 \tag{19.34}$$

19.6 Calculate the moderator-to-fuel volume ratio in a (a) hexagonal and (b) square lattice in which $p/d = 1.1$.

19.7 Show that the diffusion area for a homogeneous fuel-moderator mixture is represented by Eq. (19.16).

19.8 For the graphite-uranium mixture of Example 19.3, determine the minimum physical size and the minimum fuel mass for criticality for (a) a cube, (b) a sphere, and (c) a cylinder. Assume that the extrapolation distance is negligible.

19.9 While neglecting the extrapolation distance(s), compute the maximum-to-average volumetric heat generation rate $q'''_{\max}/q'''_{\text{avg}}$ in (a) a rectangular parallelepiped and (b) a sphere. Note that the differential volume in spherical coordinates is $4\pi r^2 dr$.

19.10 Derive an expression for the minimum critical volume as a function of the geometric buckling (with $d = 0$) for (a) a cube and (b) a cylinder.

19.11 Using data from Table 4.4, calculate the migration area for (a) light water, (b) heavy water, (c) graphite, and (d) beryllium.

19.12 Compare the nonleakage probabilities for (a) a small 550-MWt core and (b) a large 3500-MWt power reactor with power densities of 80 kW/L and 100 kW/L, respectively. Each cylindrical reactor has the optimal H/D ratio and $L^2 = 1.9\,\text{cm}^2$.

19.13 Find the radius of an equivalent cell for a square lattice with pitch p.

19.14 Determine the matrix size for a diffusion theory calculation using five energy groups with 12 intervals along each axis in (a) one-dimensional, (b) two-dimensional, and (c) three-dimensional rectangular geometry.

19.15 Repeat Exercise 16.14 while including the extrapolation distance. Does including d improve the estimated radius?

19.8 COMPUTER EXERCISE

19.A A miniature version of a classic computer code PDQ (Bilodeau et al., 1957) is called MPDQ. By solution of difference equations, it finds the amount of uniform control rod absorber required to achieve criticality in a core of the form of an unreflected slab. Run the program and compare the results of choosing a linear or sine trial fast flux function.

REFERENCE

Bilodeau, G.G., Cadwell, W.R., Dorsey, J.P., Fairey, J.G., Varga, R.S., 1957. PDQ—An IBM-704 Code to Solve the Two-dimensional Few-Group Neutron-Diffusion Equations. WAPD-TM-70. Westinghouse Electric Corporation Bettis Plant, Pittsburgh, PA.

FURTHER READING

Duderstadt, J.J., Hamilton, L.J., 1976. Nuclear Reactor Analysis. Wiley, New York A thorough treatment.

El-Wakil, M.M., 1962. Nuclear Power Engineering. McGraw-Hill, New York.

Faw, R.E., Shultis, J.K., 2008. Fundamentals of Nuclear Science and Engineering, second ed. CRC Press, Boca Raton, FL.

Glasstone, S., Sesonske, A., 1994. Nuclear Reactor Engineering, fourth ed. vol. 1. Chapman and Hall, New York Reactor Design Basics.

Graves, H.W., 1979. Nuclear Fuel Management. Wiley, New York.

Lamarsh, J.R., Baratta, A.J., 2018. Introduction to Nuclear Engineering, fourth ed. Pearson, Hoboken.

Stacey, W.M., 2001. Nuclear Reactor Physics. Wiley, New York.

CHAPTER

TIME DEPENDENT REACTOR BEHAVIOR

20

CHAPTER OUTLINE

Reactor operations involve changes in power level and concomitant transients in state variables. Initially, we describe the dependence of numbers of neutrons and reactor power on the multiplication factor, which is in turn affected by temperature and control rod absorbers. We then examine the processes of fuel consumption, fission product poisoning, and control in a power reactor. This chapter is arranged such that the fastest-acting mechanisms are presented first, and then phenomena of longer duration are examined.

20.1 NEUTRON POPULATION GROWTH

The reproduction of neutrons in a reactor can be described by the multiplication factor k, as presented in Section 16.2. The introduction of one neutron produces k neutrons; they in turn produce k^2, and so on. Such a behavior tends to be analogous to the increase in principal with compound interest or the exponential growth of the human population. The fact that k can be less than, equal to, or greater than 1 results in significant differences, however.

The total number of reactor neutrons is the sum of the geometric series $1+k+k^2+\ldots$. For $k<1$ this is finite, equal to $1/(1-k)$. For $k>1$ the sum is infinite (i.e., neutrons multiply indefinitely). We thus see that knowledge of the effective multiplication factor of any arrangement of fuel and other material is needed to assure safety. A classic measurement involves the stepwise addition of small amounts of fuel with a neutron source present to ensure adequate count rates. The thermal neutron flux without the

Nuclear Energy. https://doi.org/10.1016/B978-0-12-812881-7.00020-4

additional fuel ϕ_0 and with more fuel ϕ is measured at each stage. Ideally, for a subcritical system with a nonfission source of neutrons in place, in a steady-state condition, the multiplication factor k appears in the relation

$$\phi/\phi_0 = 1/(1-k) \tag{20.1}$$

As k approaches 1, the critical condition, the flux increases greatly. On the other hand, the reciprocal ratio

$$\phi_0/\phi = 1-k \tag{20.2}$$

reaches zero as k attains unity. Plotting this measured flux ratio as it depends on the mass of uranium or the number of fuel assemblies allows increasingly accurate predictions of the point at which criticality occurs, as shown in Fig. 20.1. Fuel additions are always intended to be less than the amount expected to bring the system to criticality.

EXAMPLE 20.1

With 30 and 40 fuel assemblies loaded, the flux ratio ϕ_0/ϕ is measured to be 0.226 and 0.101, respectively, as plotted in Fig. 20.1. The slope between these two most recent loading steps is first determined as

$$m = \frac{\phi_{40}/\phi_0 - \phi_{30}/\phi_0}{N_{40} - N_{30}} = \frac{0.101 - 0.226}{40 - 30} = -0.0125$$

Extrapolating a line from these two measurements to the horizontal axis provides an estimate of the total number of assemblies required to reach criticality

$$N_C = N_{40} - (\phi_{40}/\phi_0)/m = 40 - (0.101)/(-0.0125) = 48$$

Hence, eight (i.e., 48 – 40) or fewer assemblies should be added at the next step, rather than the typical 10 assemblies as for prior loadings.

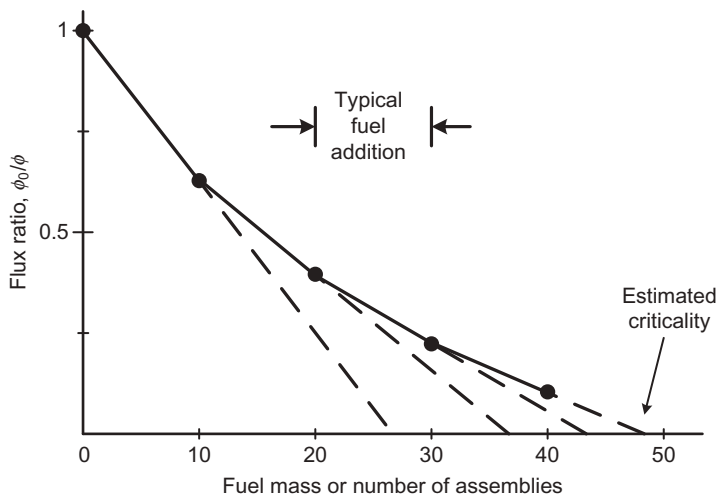

FIG. 20.1

Approach to criticality experiment.

20.2 REACTOR KINETICS

Let us now examine the time-dependent response of a reactor to changes in multiplication. For each neutron, the gain in the number of neutrons during a lifecycle of time length ℓ is $\delta k = k - 1$. Thus for n neutrons in an infinitesimal time dt, the gain is

$$dn = \delta k \, n \, dt/\ell \tag{20.3}$$

This can be treated as a differential equation. For constant δk the solution is

$$n = n_0 \exp(t/T) \tag{20.4}$$

where T is the *reactor period*, the time for the population to increase by a factor $e = 2.718\ldots$, given by

$$T = \ell/\delta k \tag{20.5}$$

When applied to people, the formula states that the population grows more rapidly the more frequently reproduction occurs and the more abundant the progeny. Because flux and power are proportional to neutron concentration (i.e., $\phi = nv$ and $P = w\Sigma_f V\phi$), they also exhibit the same $e^{t/T}$ response from their initial condition.

A typical lifetime ℓ_p for prompt neutrons in a thermal reactor is very short, approximately 10^{-5} s, so that a δk as small as 0.02 would give a very short period of 0.0005 s. The growth according to the formula would be exceedingly rapid and, if sustained, would consume all the atoms of fuel in a fraction of a second. In a thermal reactor, a fast neutron slows rapidly such that a neutron spends most of its lifetime in the diffusion process. Hence, the neutron lifetime in an infinite reactor can be estimated from its velocity v and absorption mean free path λ_a using

$$\ell_\infty = \frac{\lambda_a}{v} = \frac{1}{v\Sigma_a} \tag{20.6}$$

A finite reactor reduces this lifetime by the nonleakage probability, leading to the *prompt neutron lifetime* of

$$\ell_p = \ell_\infty \mathcal{L} = \frac{1}{v\left(\Sigma_a + DB_g^2\right)} \tag{20.7}$$

EXAMPLE 20.2

For a certain large light water reactor (LWR), the macroscopic cross-section of the water is 0.022/cm. At 20°C, the neutron lifetime in the moderator is

$$\ell_\infty = \frac{1}{v\Sigma_{a,M}} = \frac{1}{(2.2 \times 10^5 \text{ cm/s})(0.022/\text{cm})} = 2.1 \times 10^{-4} \text{ s}$$

For a large core, the nonleakage probability is near unity.

A peculiar and fortunate fact of nature provides an inherent reactor control for small values of δk in the range of 0 to approximately 0.0065 for U-235. Recall that approximately 2.5 neutrons are released from fission. Of these, some 0.65% appear later as the result of radioactive decay of certain fission products and are thus called *delayed neutrons*. Quite a few different radionuclides contribute these, but usually six groups are identified by their different fractions and half-lives. Table 20.1 lists

Table 20.1 Delayed Neutron Yields From Fission of U-235 and Pu-239

	U-235		Pu-239	
Group i	**Fraction β_i**	**Half-Life $t_{H,i}$ (s)**	**Fraction β_i**	**Half-Life $t_{H,i}$ (s)**
1	0.000247	54.51	0.0000798	53.75
2	0.001385	21.84	0.0005880	22.29
3	0.001222	6.00	0.0004536	5.19
4	0.002645	2.23	0.0006888	2.09
5	0.000832	0.496	0.0002163	0.549
6	0.000169	0.179	0.0000735	0.216

Data from Keepin, G.R., Wimett, T.F., 1958. Reactor kinetic functions. Nucleonics 16(10), 86–90.

commonly used fractions and half-lives of the nuclides that are delayed neutron emitters for fission in U-235 and Pu-239. The average half-life of the isotopes from which they come, taking into account their yields, is approximately 8.8 s for U-235 (see Exercise 20.1). Using Eq. (3.13), this corresponds to a mean life

$$\tau = t_H / \ln(2) = (8.8\,\text{s}) / \ln(2) = 12.7\,\text{s}$$

as the average length of time required for a radioactive isotope to decay. Although there are very few delayed neutrons, their presence extends the cycle time greatly and slows the growth rate of the neutron population. The effect of delayed neutrons on reactor transients has an analogy to the growth of principal in an investment, for instance at a bank. Imagine that the daily interest was mailed out to a client, who had to reinvest by sending the interest back. This "check is in the mail" process would cause principal to increase at a slower rate.

Then, to understand the mathematics of this effect, let β_T be the fraction of all neutrons that are delayed, a value 0.0065 for U-235; $1-\beta_T$ is the fraction of those emitted instantly as *prompt neutrons*. They take only a very short time ℓ_p to appear, whereas the delayed neutrons take a time $\ell_p+\tau$. The average delay is thus

$$\ell_{eff} = (1-\beta_T)\,\ell_p + \beta_T\,(\ell_p + \tau) = \ell_p + \beta_T \tau \tag{20.8}$$

Now because $\beta_T = 0.0065$ and $\tau = 12.7$ s, their product of 0.083 s greatly exceeds the multiplication cycle time, which is only 10^{-5} s. The delay time can thus be regarded as the *effective lifetime*,

$$\ell_{eff} \cong \beta_T\,\tau \tag{20.9}$$

This approximation holds for values of δk much less than β_T.

EXAMPLE 20.3

Let $\delta k = 0.001$, and use $\ell_{eff} = 0.083$ s; thus the reactor period is

$$T = \ell_{eff}/\delta k = (0.083\,\text{s})/0.001 = 83\,\text{s}$$

Utilizing the exponential formula, a very slight neutron population increase occurs in one second according to

$$n(1\,\text{s})/n_0 = \exp(t/T) = \exp[(1\,\text{s})/(83\,\text{s})] = 1.01$$

Without the delayed neutrons, the reactor period would have been only $T = \ell_p/\delta k = (10^{-5}\,\text{s})/(0.001) = 0.01\,\text{s}$, and after 1 s, the neutron population would have been multiplied by $\exp[(1\,\text{s})/(0.01\,\text{s})] = 2.7 \times 10^{43}$!

On the other hand, if δk is greater than β_T, we still find very rapid responses, even with delayed neutrons. If all neutrons were prompt, one neutron would give a gain of δk, but because the delayed neutrons actually appear much later, they cannot contribute to the immediate response. The apparent δk is then $\delta k - \beta_T$, and the cycle time is ℓ_p. We can summarize by listing the reactor period T for the two regions

$$T \cong \begin{cases} \dfrac{\beta_T \tau}{\delta k} & |\delta k| << \beta_T \\ \dfrac{\ell_p}{\delta k - \beta_T} & \delta k > \beta_T \end{cases} \tag{20.10}$$

However, for a large negative reactivity insertion ($\delta k \ll -\beta_T$), such as occurs during a reactor trip (scram), the period is approximately $-80\,\text{s}$ (see Exercise 20.17).

Even though the *delayed neutron fraction* β_T is a small number, it is conventional to consider δk small only if it is less than β_T but large if it is greater. Fig. 20.2 shows the growth in reactor power for several different values of reactivity ρ, defined as $\delta k/k$ (see Eq. 16.2). These curves were generated with the full set of delayed neutron emitters. Because k is close to 1, $\rho \cong \delta k$. We conclude that the rate of growth of the neutron population or reactor power is very much smaller than expected, so long as δk is kept well below the value β_T, but rapid growth will take place if δk is larger than β_T. With the reactor response directly depending on β_T, reactivity is often expressed in terms of dollars and cents by taking the ratio ρ/β_T, where \$1 occurs when $\rho = \beta_T$. With typical reactivity values being rather small, another commonly employed unit is percent millirho (pcm), obtained by multiplying ρ by 10^5.

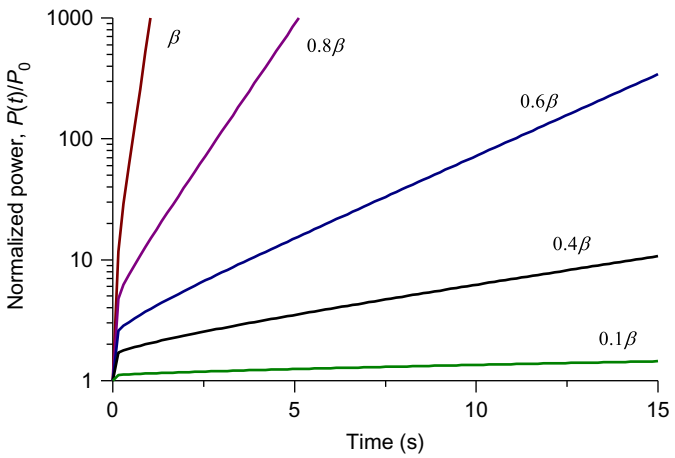

FIG. 20.2

Effect of delayed neutrons.

EXAMPLE 20.4

Two cents of negative reactivity ($\rho = -2\,¢$) are introduced into a critical U-235 reactor operating at 150 MWt. This reactivity insertion equates to $\rho = -0.02\,\beta_T = (-0.02)(0.0065) = -0.00013$, which corresponds to -13 pcm. The resultant reactor period is

$$T = \frac{\beta_T \tau}{\rho} = \frac{\beta_T \tau}{-0.02\beta_T} = \frac{12.7\,\text{s}}{-0.02} = -635\,\text{s}$$

After 5 min, the reactor power has reduced to

$$P(t) = P(0)\, e^{t/T} = (150\text{MW})\, \exp[(300\text{s})/(-635\text{s})] = 93.5\text{MW}$$

We have used the value of β_T for U-235 for illustration but should note that its effective value depends on reactor size and type of fuel (e.g., β_T for Pu-239 is only 0.0021). Also, the value of the neutron cycle time depends on the energy of the predominant neutrons. The ℓ_p for a fast reactor is much shorter than that for a thermal reactor.

A more precise description of the neutron concentration is accomplished with the point kinetics equations. A simplified version of this analysis of neutron population growth is obtained from the one-delayed-group model. The six delayed neutron precursors listed in Table 20.1 are replaced by a single emitter with total fraction of

$$\beta_T = \sum_{i=1}^{6} \beta_i \tag{20.11}$$

and a decay constant obtained from

$$\frac{1}{\lambda} = \frac{1}{\beta_T} \sum_{i=1}^{6} \frac{\beta_i}{\lambda_i} \tag{20.12}$$

Differential equations for the neutron population n and the delayed emitter concentration C are written:

$$\begin{aligned} dn/dt &= n(\rho - \beta_T)/\Lambda + \lambda C \\ dC/dt &= n\beta_T/\Lambda - \lambda C \end{aligned} \tag{20.13}$$

which utilizes the neutron generation time $\Lambda = \ell_p/k_{\text{eff}}$. In Computer Exercises 20.A and 20.B, we demonstrate the growth with time of the neutron population as it depends on reactivity. One equivalent delayed neutron group is used in Computer Exercise 20.A; six groups are employed in Computer Exercise 20.B. The widely spaced time constants, or eigenvalues, in the solution favor numerical methods for *stiff systems*.

20.3 REACTIVITY FEEDBACK

The inherent nuclear control provided by delayed neutrons is aided by proper design of the reactor to favor certain negative feedback effects. These are reductions in the neutron multiplication factor resulting from increases in reactor power. With additional heat input the temperature increases, and the negative reactivity tends to shut the reactor down. Design choices include the size and spacing of fuel rods and the soluble boron content of the cooling water. Among the most important reactivity feedback

mechanisms are the effects of fuel and moderator temperature. The reactivity feedback should be negative for stable reactor operations.

One of the temperature effects is simple thermal expansion. The moderator heats up, it expands, the density of atoms is reduced, and neutron mean free paths and leakage increase, whereas thermal absorption decreases. In early homogeneous aqueous reactors, this was a dominant effect to provide shutdown safety. In heterogeneous reactors utilizing a chemical shim for control (such as PWRs), it tends to have the opposite effect in that reductions in dissolved boron concentration accompany reduction in water density. Thus, some other effect is needed to override moderator expansion effects.

The process of Doppler broadening of resonances provides the needed feedback. Fig. 20.3 illustrates a feedback loop. An increase in the fuel temperature causes greater motion of the uranium atoms, which effectively broadens the neutron resonance cross-section as shown in Fig. 20.4 using the lowest energy U-238 capture cross-section. For fuel containing a high fraction of U-238, the multiplication decreases (due to the reduction in the resonance escape probability $\wp$) as the temperature increases. The Doppler effect is prompt in that it responds to the fuel temperature, whereas the moderator effect is delayed as heat is transferred from fuel to coolant. The use of the term Doppler comes from the analogy with frequency changes in sound or light when there is relative motion between the source and observer.

The amounts of these effects can be expressed by formulas such as

$$\rho = \alpha \Delta T \tag{20.14}$$

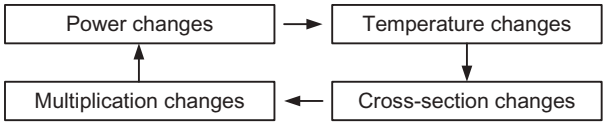

FIG. 20.3

Reactivity feedback loop.

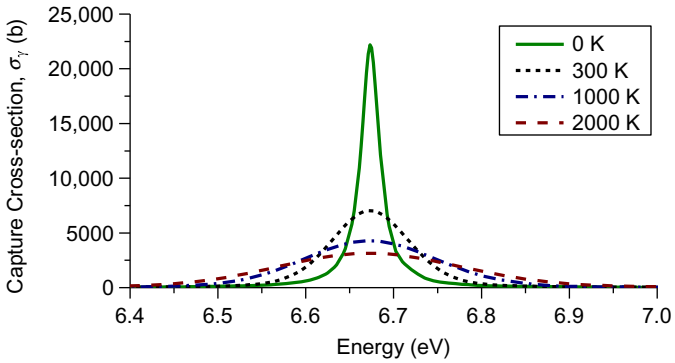

FIG. 20.4

Doppler broadening with temperature of a U-238 radiative capture cross-section resonance. ENDF/B-VII.1 data (Chadwick et al., 2011) processed by author with NJOY2016 (MacFarlane et al., 2016).

in which the reactivity ρ is proportional to the temperature change ΔT, with a temperature coefficient α that should be a negative number. Another relationship is

$$\rho = \alpha_P \Delta P/P \tag{20.15}$$

with a negative power coefficient α_P and fractional change in power $\Delta P/P$.

EXAMPLE 20.5

If the value of the reactivity feedback coefficient α is $-10^{-5}/°C$, a temperature rise of 20°C would give a reactivity of

$$\rho = \alpha \Delta T = (-10^{-5}/°C)(20°C) = -0.0002$$

In a pressurized water reactor if $\alpha_P = -0.012$, a 2% change in power would give a reactivity of

$$\rho = \alpha_P \Delta P/P = (-0.012)(0.02) = -0.00024$$

Temperature effects cause significant differences in the response of a reactor to disturbances. The effects were ignored in Fig. 20.2, and the population grew exponentially, but if the fuel and moderator reactivity feedback effects are included, as in Fig. 20.5, the power flattens out and becomes constant.

Computer Exercise 20.C provides the opportunity to explore the effect of temperature reactivity feedback on the transient behavior of a reactor.

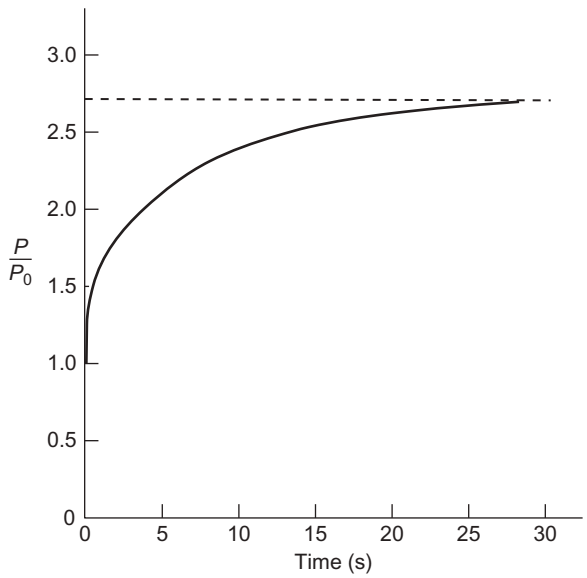

FIG. 20.5

Effect of temperature on power.

20.4 REACTOR CONTROL

Even though a reactor is relatively insensitive to increases in multiplication in the region $\delta k < \beta_T$, and temperature rises furnish stability through feedback, additional protection is provided in reactor design and operating practices. As described in Section 18.4, part of the control of a reactor of the PWR type is provided by a boron solution (H_3BO_3). This *chemical shim* balances the excess fuel loading and is adjusted gradually as fuel is consumed during reactor life; such long-term control is addressed in Section 20.6. In addition, rods composed of burnable poisons, such as boron carbide (B_4C) and gadolinium oxide (gadolinia, Gd_2O_3), control excess reactivity at the beginning of the core life and reduce the initial chemical shim requirements.

Reactors are also provided with several groups of movable rods of neutron-absorbing material, as depicted in Fig. 20.6. The rods serve three main purposes: (1) to permit temporary increases in multiplication that bring the reactor up to the desired power level or to make adjustments in power; (2) to cause changes in the flux and power shape in the core, usually striving for uniformity; and (3) to shut down the reactor manually or automatically in the event of unusual behavior. To ensure effectiveness of the shutdown role, even if the control rod cluster of greatest reactivity worth is fully withdrawn, the reactor will be subcritical. In the PWR, they are supported by electromagnets that release the rods on interruption of current, whereas in the boiling water reactor (BWR) they are driven in from the bottom of the vessel by hydraulic means.

The reactivity worth of control and safety rods as a function of depth of insertion into the core can be measured by a comparison technique. Suppose a control rod in a critical reactor is withdrawn slightly by a distance δz and a measurement is made of the resulting period T of the rise in neutron population.

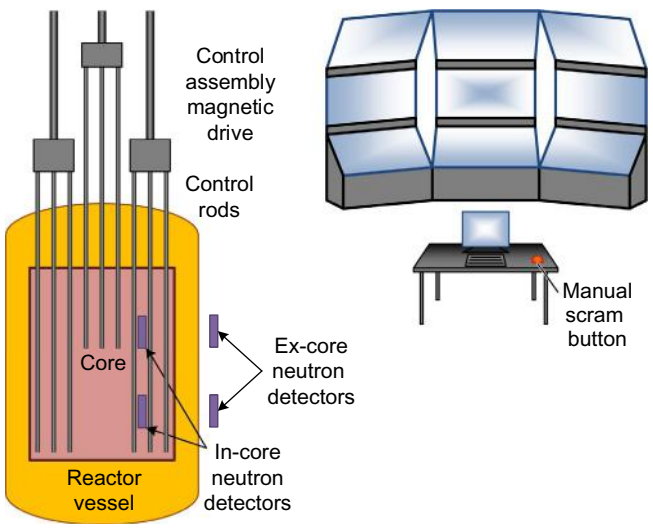

FIG. 20.6

Reactor control.

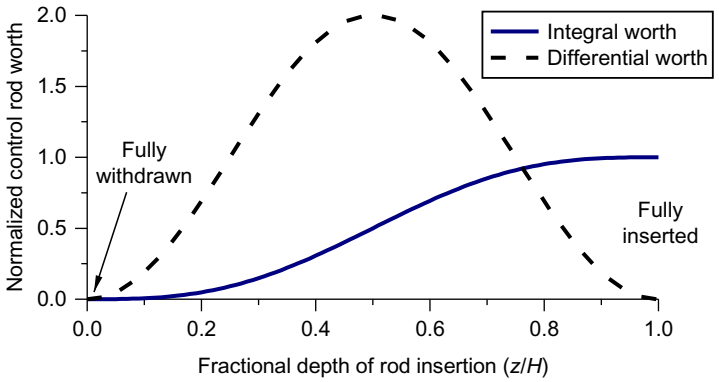

FIG. 20.7

Control rod worth as it depends on amount of insertion in an unreflected reactor core. The integral worth is normalized to the total rod worth ρ_T, the differential worth to its average value ρ_T/H.

By use of the approximate formula $T \cong \beta_T \tau/\delta k$, we deduce the relation of δk to δz. The reactor is brought back to critical by an adjustment of the soluble boron concentration. Then the operation is repeated with an additional shift in rod position. The experiment serves to find both the reactivity worth of the rod as a function of position and, by summation, the total worth of the rod ρ_T. Fig. 20.7 shows the calibration curves of a control rod in an idealized case of a core without end reflectors. It is noted that the effect of a rod movement in a reactor depends strongly on the location of the tip. The integral rod worth as a function of total insertion depth z into the core is

$$\rho(z) = \rho_T \left[\frac{z}{H} - \frac{1}{2\pi} \sin\left(\frac{2\pi z}{H}\right) \right] \quad 0 \le z \le H \tag{20.16}$$

The basis for the S-shaped curve of Fig. 20.7 is found in reactor theory, which tells us that the reactivity effect of an added absorber sample to a reactor is approximately dependent on the square of the thermal flux that is disturbed (Murray, 1954). Thus if a rod is fully inserted or fully removed, such that the tip moves in a region of low flux, the change in multiplication is practically zero. At the center of the reactor, movement makes a large effect. The differential worth when the rod tip is near the center of the core is twice the average in this simple case, that is,

$$(\delta\rho/\delta z)_{z=H/2} = 2(\delta\rho/\delta z)_{\text{avg}} \tag{20.17}$$

EXAMPLE 20.6

A particular cluster of control rods has a total worth of \$1.5. The control rods, which are initially positioned 35% into the core, are moved to a depth of 42% full insertion. This adjustment equates to a reactivity of

$$\begin{aligned}
\Delta\rho &= \rho(z_{\text{initial}}) - \rho(z_{\text{final}}) = \rho(0.35H) - \rho(0.42H) \\
&= \rho_T \left\{ \left[\frac{0.35H}{H} - \frac{1}{2\pi} \sin\left(\frac{2\pi 0.35H}{H}\right) \right] - \left[\frac{0.42H}{H} - \frac{1}{2\pi} \sin\left(\frac{2\pi 0.42H}{H}\right) \right] \right\} \\
&= (\$1.5)(0.221 - 0.343) = -\$0.18
\end{aligned}$$

A deeper insertion of control rods results in a negative reactivity change to the core.

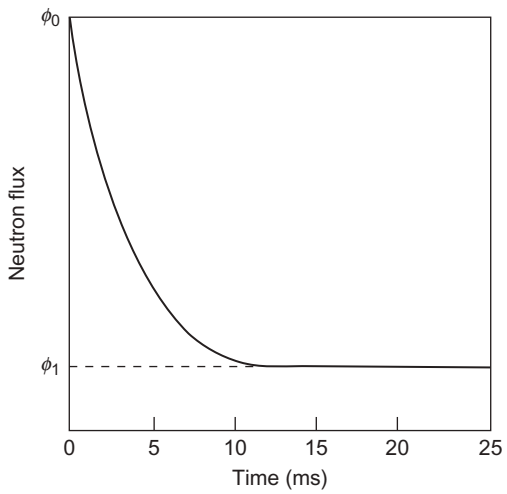

FIG. 20.8

Neutron flux variation with time in the rod-drop method of measuring reactivity.

Estimates of total reactivity worth can also be made by the rod-drop technique. A control rod is allowed to fall from a position outside the core to a full-in position. The very rapid change of neutron flux from an initial value ϕ_0 to a final value ϕ_1 is shown in Fig. 20.8. Then the reactivity worth is calculated from the formula

$$\rho/\beta_T = (\phi_0/\phi_1) - 1 \tag{20.18}$$

The result somewhat depends on the location of the detector.

An instrumentation system is provided to detect an excessive neutron flux and thus power level to provide signals calling for a trip or *scram* of the reactor. As sketched in Fig. 20.6, independent detectors are located both inside the core and outside the reactor vessel. A computer processes data from core detectors to determine whether power distributions are acceptable. This scram, or protection, logic is independent from the control system, as required by Criterion 24 of 10CFR50 Appendix A.

A PWR control program typically seeks to maintain a reasonably constant average reactor coolant system temperature to maintain a constant coolant volume and avoid having to compensate for reactivity fluctuations due to moderator temperature changes. In contrast to the PWR that institutes short-term reactivity adjustments using only control rods, the BWR can also utilize changes in the recirculation flow to maneuver the power.

20.5 FISSION PRODUCT POISONS

During normal reactor operation, fission products begin to build up as fuel is burned. Neutron absorption in the fission products has an effect on control requirements. The most important fission product poison is a radioactive isotope of xenon, Xe-135, which has a cross-section at 0.0253 eV of 2.65 *million* barns. A fission product of secondary importance is samarium-149 with $\sigma_a = 41{,}000$ b. These nuclei act

as poisons in the reactor, thereby reducing the core multiplication factor. Fission product poisoning transpires over a longer period (∼hours) compared to the fuel and moderator temperature effects.

Xe-135 is generated directly from fission as well as from the decay of Te-135 and I-135, which are themselves fission products. The short half-life of Te-135 ($t_H = 19\,s$) permits its inclusion with I-135 for which $t_H = 6.57\,h$. The total I-135 yield in fission is high, $\gamma_I = 0.061$, meaning that for each fission, one obtains 6.1% as many atoms of I-135. Taking fission production, radioactive decay, and neutron absorption into account, the rate of change in the Xe-135 and I-135 concentrations can be described as

$$\begin{aligned} dN_X/dt &= \left(\gamma_X\Sigma_f - \sigma_a^X N_X\right)\phi + \lambda_I N_I - \lambda_X N_X \\ dN_I/dt &= \gamma_I\Sigma_f\phi - \lambda_I N_I \end{aligned} \tag{20.19}$$

where $\gamma_X = 0.003$.

The negative reactivity introduced by the fission product poison is

$$\rho_X = \frac{-\Sigma_a^X}{\Sigma_a^F + \Sigma_a^M} = \frac{-\Sigma_a^X f}{\Sigma_a^F} \tag{20.20}$$

In steady operation at high neutron flux, the production rate of Xe-135 is equal to its consumption by neutron absorption, if its decay is neglected. Hence

$$N_X\sigma_a^X = N_F\sigma_f^F(\gamma_I + \gamma_X) \tag{20.21}$$

EXAMPLE 20.7

With the ratio σ_f/σ_a for U-235 of 0.86, we see that the absorption rate of Xe-135 is 0.055 times that of the fuel itself:

$$\frac{R_a^X}{R_a^F} = \frac{\phi_{avg}N_X\sigma_a^X}{\phi_{avg}N_F\sigma_a^F} = \frac{N_F\sigma_f^F(\gamma_I+\gamma_X)}{N_F\sigma_a^F} = \frac{\sigma_f^F(\gamma_I+\gamma_X)}{\sigma_a^F} = (0.86)(0.061+0.003) = 0.055$$

This factor is approximately 0.04 if the radioactive decay ($t_H = 9.14\,h$) of xenon-135 is included (see Exercise 20.7). Either value leads to the conclusion that a large negative reactivity insertion accompanies the Xe-135 production. Using the latter value and assuming a thermal utilization of 0.7, the xenon reactivity worth is

$$\rho_X = \frac{-\Sigma_a^X f}{\Sigma_a^F} = \frac{-R_a^X f}{R_a^F} = -(0.04)(0.7) = -0.028$$

This equates to $-0.028/0.0065 = -\$4.3$, which is a significant amount of reactivity!

The time-dependent variation of neutron absorption in xenon-135 is the subject of Computer Exercise 20.D, which utilizes the program XETR.

20.6 FUEL BURNUP

The generation of energy from nuclear fuels is unique in that a rather large amount of fuel must be present at all times for the chain reaction to continue. In contrast, an automobile will operate even though its gasoline tank is practically empty. There is a subtle relationship between reactor fuel and other quantities such as consumption, power, neutron flux, criticality, and control.

The first and most important consideration is the energy production, which is directly related to fuel consumption. Let us simplify the situation by assuming that the only fuel consumed is U-235 and that the reactor operates continuously and steadily at a definite power level. Because each atom burned has an accompanying energy release, we can find the amount of fuel that must be consumed (i.e., converted into either U-236 or fission products by neutron absorption) in a given period. The power level in a reactor was shown in Eq. (16.15) to be proportional to neutron flux (i.e., $P = \phi_{avg} n_F \sigma_f w$). However, in a reactor that experiences fuel consumption, the flux must increase with time because the power is proportional also to the fuel content n_F.

EXAMPLE 20.8

Let us examine the fuel utilization in a simplified PWR that uses 20 w/o fuel and operates at 100 MWe or 300 MWt, as in a test reactor or a propulsion reactor. The initial fuel loading into a single zone is 1000 kg U. We apply the rule of thumb that 1.3 g of U-235 is consumed for each megawatt-day of thermal energy, assuming that all fissions are due to U-235. In 1 year, the amount of U-235 consumed is

$$m_C = (1.30\,\text{g}/(\text{MWtd}))(300\,\text{MWt})(365\,\text{d}) = 142\,\text{kg}$$

while the U-235 burned is

$$m_B = (1.11\,\text{g}/(\text{MWtd}))(300\,\text{MWt})(365\,\text{d}) = 122\,\text{kg}$$

We see that a great deal of the original 200 kg of U-235 has been consumed, but the U-235 undergoing capture remains uranium in the form of U-236 ($t_H = 2.342 \times 10^7$ y) such that the final enrichment is 6.6 w/o:

$$\omega = \frac{m_{235}}{m_U} = \frac{200 - m_C}{1000 - m_B} = \frac{200 - 142\,\text{kg}}{1000 - 122\,\text{kg}} = 0.066$$

Note that the loss of U-238 to absorption is ignored but amounts to about 2 kg (Exercise 20.20) in this case. Let us assume that a completely new core is installed at the end of a year's operation. If we carry out the calculations as in Section 15.4, the fuel cost excluding fabrication and transport is

$$(1000\,\text{kg-U})\,[(\$44/\text{kg-U}_3\text{O}_8)(47.932)/(0.848\,\text{kg-U/kg-U}_3\text{O}_8) + (\$10/\text{kg-U}) + (\$100/\text{kg-SWU})$$
$$(38.315\,\text{kg-SWU})] = \$6.33\,\text{million}$$

Most of that expense is for enrichment. The electricity produced is

$$E_e = P_e T = (10^5\,\text{kW})(8760\,\text{h/y}) = 8.76 \times 10^8\,\text{kWh}$$

This makes the unit cost of fuel $(\$6.33 \times 10^6)/(8.76 \times 10^8\,\text{kWh}) = \$0.0072/\text{kWh}$ or approximately seven-tenths of a cent per kWh.

The fuel assemblies in a large power reactor are grouped into several zones with different enrichments, as illustrated in Fig. 20.9. The reactor is shut down periodically to remove, rearrange, and install fuel. Each operating period, termed a *fuel cycle*, typically lasts from 18 to 24 months. At the periodic shutdowns for fuel replacement and shuffling, a great deal of maintenance work is done. There is an economic premium for careful and thorough outage management to minimize the time the reactor is not producing power. Down times as low as 3 weeks have been achieved. Replacement of large equipment such as a steam generator requires several months. Power plant operators strive to stagger the reactor outages at a multiunit site.

Because no fuel is added during the operating cycle of most reactors, the amount to be burned must be installed at the beginning. First, the amount of uranium needed to achieve criticality is loaded into

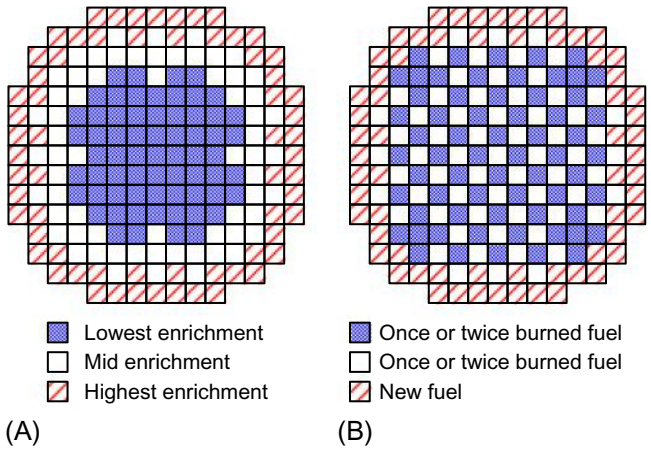

FIG. 20.9

Fuel assembly loading pattern in core. (A) Annular zonal pattern and (B) a combination arrangement of interior scatter (checkerboard) and annular on periphery.

the reactor. If excess fuel is then added, it is clear that the reactor would be supercritical unless some compensating action were taken. In the PWR, the excess fuel reactivity is reduced by the inclusion of control rods, boron solution, and burnable poison rods. The amount of control absorber required at the beginning of the cycle is proportional to the amount of excess fuel added to permit burnup for power production.

EXAMPLE 20.9

If the fuel is expected to go from 3% to 1.5% U-235, an initial boron atomic number density in the moderator is approximately $0.0001 \times 10^{24}/\text{cm}^3$. For comparison, the number of water molecules per cubic centimeter is 0.0334×10^{24}. The boron content is usually expressed in parts per million, ppm (i.e., micrograms of an additive per gram of diluent). With 10.8 and 18.0 as the molecular weights of boron and water, respectively, the required B concentration is

$$\frac{m_B}{m_{H_2O}} = \frac{N_B M_B V/N_A}{N_{H_2O} M_{H_2O} V/N_A} = \frac{(0.0001/\text{cm}^3)(10.8\,\text{g/mol})}{(0.0334/\text{cm}^3)(18.0\,\text{g/mol})}\left(\frac{\text{ppm}}{\text{per } 10^6}\right) = 1800\text{ppm}$$

A reactor is brought to full power, operating temperature, and pressure by means of control rod position adjustments. Then, as the reactor operates and fuel begins to burn out, the concentration of boron is reduced. By the end of the cycle, the extra fuel is gone, all the available control absorption has been removed, and the reactor is shut down for refueling. The trends in fuel and boron are shown in Fig. 20.10, neglecting the effects of certain fission product absorption and plutonium production. The graph represents a case in which the power is kept constant. The fuel content thus linearly decreases with time. Such operation characterizes a reactor that supplies a *base load* in an electric power system that also includes fossil fuel plants and hydroelectric stations.

It might appear from Fig. 20.10 that the reactor cycle could be increased to as long a time as desired merely by adding more U-235 at the beginning. There are limits to such additions, however. First, the

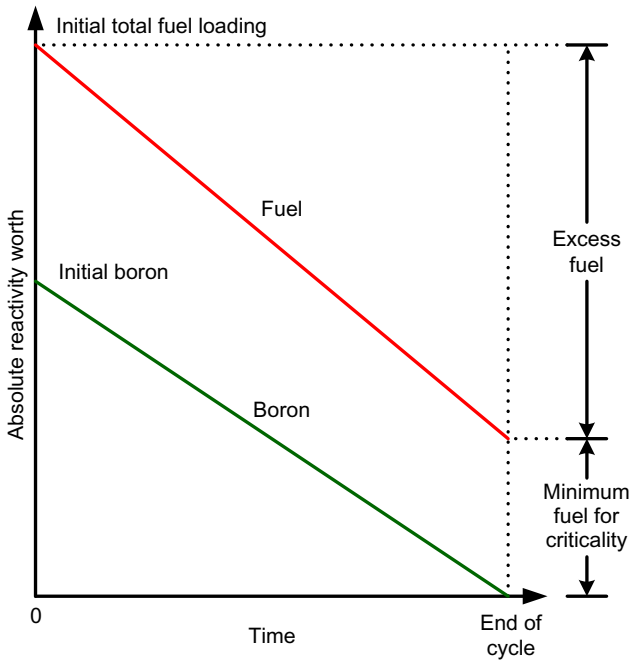

FIG. 20.10

Reactor control during fuel consumption in power reactor.

more the excess fuel that is added, the greater must be the control by rods or soluble poison. Second, radiation and thermal effects on fuel and cladding materials increase with life. The total thermal energy E extracted from the initial uranium mass m_U, including all fissionable isotopes, is the *specific burnup* expressed as the number of megawatt-days per metric ton of uranium or heavy metal (MW d/tonne)

$$B = E/m_U \tag{20.22}$$

EXAMPLE 20.10

We can calculate the burnup value for 1 year's operation of a 3000-MWt power reactor with an initial U-235 fuel loading of 2800 kg. With an enrichment of 0.03, the *uranium* content was 2800/0.03 = 93,000 kg or 93 tonnes. With the energy yield of (3000 MW)(365 d) ≅ 1,100,000 MW d, we find a burnup of

$$B = \frac{E}{m_U} = \frac{1.1 \times 10^6 \text{ MW d}}{93 \text{ tonne}} = 12{,}000 \text{ MW d/tonne}$$

If a reactor is fueled with natural uranium or slightly enriched uranium, the generation of plutonium tends to extend the cycle time. The fissile Pu-239 helps maintain criticality and provides part of the power. Small amounts of higher plutonium isotopes are also formed: Pu-240, fissile Pu-241 (14.4 y half-life), and Pu-242. These isotopes and those of elements of higher Z are called *transuranic* materials

or *actinides*, see Fig. 2.1. They are important as fuels, poisons, or nuclear wastes (see Exercise 20.13). Accounting for plutonium and the management of fuel in the core, a typical average exposure is actually 30,000 MW d/tonne. It is desirable to seek larger values of this quantity to prolong the cycle and thus minimize the costs of fuel, reprocessing, and fabrication.

As shown in Fig. 20.9, modern power reactor cores consist of several regions. At the start of an operating cycle, a reactor core will contain fresh and partially burned fuel; at the end, partially and fully burned fuel. For a reactor core with n zones, let k_i be the multiplication constant of fuel in zone i and assume nearly equal power over the core. Then the average k is

$$k = \frac{1}{n}\sum_{i=1}^{n} k_i \tag{20.23}$$

It has been found that k_i varies with burnup B according to (Graves, 1979)

$$k_i = k_0 - aB \tag{20.24}$$

where k_0 is the initial multiplication constant, and a is a constant.

The amount of control absorber required to keep the reactor critical is a measure of the average k of the core. Fig. 20.11 shows its variation with time for different numbers of zones. As noted, the larger is n, the smaller is the initial control absorber.

A little algebra shows us (see Exercise 20.15) that the discharge burnup of fuel depends on the number of zones. Letting $B(1)$ be that for one zone, the burnup for n zones is

$$B(n) = (2n/(n+1))\,B(1) \tag{20.25}$$

Thus $B(2) = (4/3)B(1)$, $B(3) = (3/2)B(1)$, and so on. For very large n, corresponding to continuous refueling as in the Canadian reactors, the burnup turns out to be twice $B(1)$.

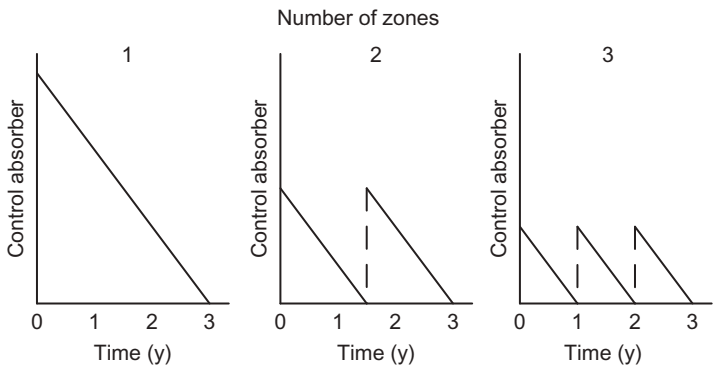

FIG. 20.11

Reactor operation with different numbers of fuel zones. The initial control absorber varies inversely with the number of regions.

20.7 SUMMARY

The importance of delayed neutrons to the controllability of the reactor cannot be overstated. Inherent reactor control is provided by negative reactivity feedback mechanisms. Control rods permit rapid shutdown. Excess fuel is added to a reactor initially to compensate for burning during the operating cycle, with adjustable control absorbers maintaining criticality. Account must be taken of fission product absorbers such as Xe-135 and of limitations related to thermal and radiation effects.

20.8 EXERCISES

20.1 Using Table 20.1 for (a) U-235 and (b) Pu-239, calculate the total delayed neutron fraction β_T and the weighted average half-life t_H for each fuel.

20.2 (a) If the total number of neutrons from fission by thermal neutrons absorbed in U-235 is 2.42, how many are delayed and how many are prompt? (b) A reactor is said to be *prompt critical* if it has a positive reactivity of β_T or more. Explain the meaning of the phrase. (c) What is the period for a reactor with prompt neutron lifetime 5×10^{-6} s if the reactivity is 0.013? (d) What is the reactor period if instead the reactivity is 0.0013?

20.3 A U-235 fueled reactor is operating at a power level of 250 MWe. Control rods are removed to give a reactivity of 0.0005. Noting that this is much less than β_T, calculate the time required to go to a power of 300 MWe, neglecting any temperature feedback.

20.4 Measurements of the fast neutron cycle time ℓ were made on EBR-I, the first reactor to produce electricity. Calculate its value in two different ways:[1] (a) With the ratio β_T/ℓ, called the Rossi-α, with a value of 1.74×10^5/s and β_T of 0.0068; (b) With a rough formula $\ell = 1/(v\Sigma_a)$ with an average energy of 500 keV neutrons. At that energy, $\sigma_\gamma = 0.12$ barn and $\sigma_f = 0.62$ barn. Note $N_U = 0.054 \times 10^{24}/\text{cm}^3$, and $v = 2200$ m/s for $E = 0.0253$ eV.

20.5 During a critical experiment in which fuel is initially loaded into a reactor, a fuel element of reactivity worth 0.0036 is suddenly dropped into a core that is already critical. If the temperature coefficient is -9×10^{-5}/°C, how high will the temperature of the system go above room temperature before the positive reactivity is canceled out?

20.6 A reactivity of −0.0025 caused by the Doppler effect results when the thermal power goes from 2500 to 2800 MW. Estimate the contribution of this effect on the power coefficient for the reactor.

20.7 (a) Taking account of Xe-135 production, absorption, and decay, show that the balance equation is

$$N_X\left(\phi\sigma_a^X + \lambda_X\right) = \phi N_F \sigma_f^F (\gamma_I + \gamma_X)$$

(b) Calculate λ_X and the ratio of absorption rates in Xe-135 and fuel if ϕ is $2 \times 10^{13}/(\text{cm}^2\ \text{s})$.

[1] Thanks are due Professor Robert Busch for this exercise and its answers.

20.8 The initial concentration of boron in a 10,000-ft^3 reactor coolant system is 1500 ppm. What volume of solution of concentration 8000 ppm should be added to achieve a new value of 1600 ppm?

20.9 An adjustment of boron content from 1500 to 1400 ppm is made in the reactor described in Exercise 20.8. Pure water is pumped in, and then mixed coolant and poison are pumped out in two separate steps. How long should the 500 ft^3/min pump operate in each of the operations?

20.10 Counting rates for several fuel addition steps in a critical experiment are listed as follows:

Number of Fuel Assemblies	Counting Rate (counts/min)
0	200
50	350
100	800
125	1600
140	6600
150	20,000

At the end of each fuel addition, what is the estimated critical number of assemblies? Was the addition always less than the amount expected to make the array critical?

20.11 When a control rod is withdrawn 4 cm from its position with its tip at the center of a critical reactor, the power rises on a period of 200 s. (a) With a value $\beta_T = 0.008$ and $\tau = 13$ s, estimate the δk produced by the rod shift and the slope of the calibration curve $\Delta k/\Delta z$. (b) Estimate the rod worth if the core height is 300 cm.

20.12 Measurements are made of the periods of power rise in a research reactor of height 24 in. for shifts in control rod positions from fully inserted ($z = 0$) to fully withdrawn ($z = 24$ in.). From the periods, values are obtained for the slope of the reactivity $\Delta\rho_i/\Delta z_i$, with units percent per inch, listed as follows:

i	$z_i \rightarrow z_{i+1}$ (in.)	$\Delta\rho_i/\Delta z_i$	i	$z_i \rightarrow z_{i+1}$ (in.)	$\Delta\rho_i/\Delta z_i$
1	$0 \rightarrow 3$	0.02	9	$12 \rightarrow 12.5$	1.02
2	$3 \rightarrow 5.5$	0.16	10	$12.5 \rightarrow 13$	1.03
3	$5.5 \rightarrow 7.5$	0.38	11	$13 \rightarrow 14$	1.08
4	$7.5 \rightarrow 9$	0.68	12	$14 \rightarrow 15$	1.02
5	$9 \rightarrow 10$	0.83	13	$15 \rightarrow 16.5$	0.95
6	$10 \rightarrow 11$	0.89	14	$16.5 \rightarrow 18.5$	0.77
7	$11 \rightarrow 11.5$	0.96	15	$18.5 \rightarrow 21$	0.40
8	$11.5 \rightarrow 12$	0.98	16	$21 \rightarrow 24$	0.11

(a) Plot the differential worth against average position $\overline{z_i} = (z_{i+1} + z_i)/2$. (b) Use simple numerical integration to graph the integral worth versus z. (c) Estimate the rod integral worth when the tip is at $z = 16$ in.

20.13 A reactor is loaded with 90,000 kg of U at 3 w/o U-235. It operates for a year at 75% of its rated 3000-MWt capacity. (a) Apply the rule of thumb 1.3 g/(MWt d) to find the consumption of U-235. What is the final enrichment of the fuel? (b) If instead one-third of the energy came from plutonium, what would the final U-235 enrichment be?

20.14 (a) Show that a megawatt per tonne is the same as a watt per gram. (b) Because most nuclear power plants are base loaded, the power is constant and the product of the flux and fissile atom concentration is likewise. Show that the burnup is given by the formulas

$$B = w\sigma_f N_{235}(0)\phi_0 t/\rho_U = w\sigma_f N_{235}(0)N_A\phi_0 t/(N_U M_U)$$

(c) Calculate B for a three-year fuel cycle having an initial atomic enrichment $N_{235}(0)/N_U = 0.03$ and flux ϕ_0 of $2 \times 10^{13}/(\text{cm}^2\ \text{s})$.

20.15 To remain critical at the end of a cycle of operation, a power reactor must have an average multiplication factor k_F. For a one-zone core, this is related to the burnup B by

$$k_F = k_0 - aB$$

where a is a constant, so that the discharge burnup is

$$B(1) = (k_0 - k_F)/a$$

For a two-zone core, we have

$$k_F = (k_0 - aB)/2 + (k_0 - 2aB)/2 = k_0 - (3/2)aB$$

The discharge burnup is $2B$ or $B(2) = (4/3)\,B(1)$. Continue the analysis to find $B(3)$ and $B(4)$. Check the results against the formulas quoted in the text.

20.16 For a constant neutron source S, show that the number of neutrons in a subcritical multiplying medium is $S/(1-k)$.

20.17 By negating the reciprocal of the decay constant of the longest-lived delayed neutron precursor of U-235, estimate the reactor period for a large negative reactivity insertion, i.e., $T = -1/\lambda_1$.

20.18 Starting with Eq. (20.16), derive the following formula for the differential rod worth

$$\frac{d\rho}{dz} = \frac{\rho_T}{H}\left[1 - \cos\left(\frac{2\pi z}{H}\right)\right] \tag{20.26}$$

20.19 A safety rod having a worth of 75 cents is positioned 110 cm into a 1.5-m tall core. Determine the reactivity change and subsequent reactor period if the rod is (a) withdrawn 15 cm or (b) inserted 15 cm from its original depth in the critical reactor.

20.20 Determine the mass of U-238 undergoing absorption in Example 20.8.

20.9 COMPUTER EXERCISES

20.A To solve the one-group point kinetics equations, the program OGRE (One Group Reactor Kinetics) is used. (a) Plot the time responses of the neutron population for various reactivity values such as 0.0001, 0.0005, and 0.001. (b) Change differential equation solver from "ode45" to "ode15s," and retry the reactivity value of 0.0001. Explain the difference in the results.

20.B The program KINETICS solves the time-dependent equations for neutrons and delayed emitters, yielding the neutron population as a function of time. Six emitters are used, and feedback is neglected. Try various input reactivity values: positive, negative, and zero; small and large with respect to $\beta = 0.0065$.

20.C The effect of temperature feedback on the time response of a reactor can be estimated by use of the program RTF (Reactor Transient with Feedback). RTF solves simple differential equations that express the rates of change with time of power and temperature. There is a negative temperature coefficient of reactivity, and power is extracted according to a temperature difference. (a) Run the program RTF to see how the power, temperature, and reactivity vary with time for the sample problem using uranium. (b) Examine the effect of changing the reactor fuel from uranium to plutonium. Pu has an effective neutron lifetime of only 0.04 s compared with the value for U of 0.083 s. Let all other factors be the same as in (a).

20.D The amount of xenon in a reactor varies with time, especially when large changes in neutron flux occur, as at startup or shutdown. Program XETR (Xenon Transient) solves differential equations for the content of iodine-135 and xenon-135. (a) Run the program and study the trends in the concentrations and the reactivity ρ versus time for a startup. (b) Use the concentrations of I-135 and Xe-135 calculated for long times after startup in part (a) as initial concentrations, and set the flux equal to zero to simulate a sudden shutdown of the reactor. Note and discuss the trend in xenon with time.

REFERENCES

Chadwick, M.B., Herman, M., Obložinský, P., Dunn, M.E., Danon, Y., Kahler, A.C., et al., 2011. ENDF/B-VII.1 Nuclear data for science and technology: cross-sections, covariances, fission product yields and decay data. Nucl. Data Sheets 112 (12), 2887–2996.

Graves, H.W., 1979. Nuclear Fuel Management. Wiley, New York.

MacFarlane, R.E., Muir, D.W., Boicourt, R.M., Kahler, A.C., Conlin, J.L., 2016. The NJOY Nuclear Data Processing System, Version 2016. Los Alamos National Laboratory, Los Alamos.

Murray, R.L., 1954. Introduction to Nuclear Engineering. Prentice-Hall, Englewood Cliffs.

FURTHER READING

Duderstadt, J.J., Hamilton, L.J., 1976. Nuclear Reactor Analysis. Wiley, New York.

Glasstone, S., Sesonske, A., 1994. Nuclear Reactor Engineering, fourth ed. Reactor Design Basics, vol. 1. Chapman and Hall, New York.
Keepin, G.R., Wimett, T.F., 1958. Reactor kinetic functions. Nucleonics 16 (10), 86–90.
Lamarsh, J.R., Baratta, A.J., 2018. Introduction to Nuclear Engineering, fourth ed. Pearson, Hoboken.
Weaver, L.E., 1976. Reactor control. In: Rust, J.H., Weaver, L.E. (Eds.), Nuclear Power Safety. Pergamon Press, New York.

CHAPTER

REACTOR SAFETY AND SECURITY

21

CHAPTER OUTLINE

It is well known that the accumulated fission products in a reactor that has been operating for some time constitute a potential radiation hazard. Assurance is needed that the fuel integrity is maintained throughout the operating cycle, with negligible release of radioactive materials. This implies limitations on power level, temperature, and adequacy of cooling under all conditions. Fortunately, physical features of the fission chain reaction provide inherent safety. In addition, the choice of materials, their arrangement, and restrictions on modes of operation give a second level of protection. Devices and structures that minimize the chance of accident and the extent of radiation release in the event of accident are a third line of defense. Finally, nuclear plant location at a distance from centers of high population density results in further protection.

We will examine the precautions taken to prevent release of radioactive materials to the surroundings and discuss the philosophy of safety. This chapter then examines three well-known nuclear power plant accidents: Three Mile Island (TMI), Chernobyl, and Fukushima. While TMI is deemed an "accident with wider consequences" (Level 5) on the International Nuclear and Radiological Event Scale (INES), the last two are categorized as "major accidents" (Level 7).

Nuclear Energy. https://doi.org/10.1016/B978-0-12-812881-7.00021-6

Although this chapter focuses upon safety related to reactors, the INES also includes radiological events. A variety of incidents have occurred with industrial and medical radioactive sources. For instance, an INES Level 5 accident occurred in 1987 at Goiânia, Brazil, where a 1375 Ci Cs-137 radiotherapy unit from a hospital was improperly secured. Upon its theft, it was dismantled, eventually causing four fatalities (IAEA, 1988).

21.1 SAFETY CONSIDERATIONS

Simply stated, the discipline of reactor safety endeavors to minimize the negative impact of nuclear power plant operations on individuals and society. Preventing the release of radioactive material then becomes a fundamental goal. As the majority of the radionuclides are present within the fuel, the basic strategy is to preclude fuel overheating. Preventing fuel from melting is not the sole consideration. In water-cooled reactors, elevated temperatures can lead to phenomena such as the exothermic zirc-water reaction

$$Zr + 2\,H_2O \rightarrow ZrO_2 + 2\,H_2 \tag{21.1}$$

Beginning around 1600 °F, this cladding oxidation turns the ductile Zr into a brittle ZrO_2. For each kg of Zr, the reaction yields 0.5 m^3 of H_2 and 6500 kJ of heat (Pershagen, 1989). The 10CFR50.46 acceptance criteria for emergency core cooling systems for light-water reactors (LWRs) states, "the calculated maximum fuel element cladding temperature shall not exceed 2200 °F."

Reactor designers contemplate a variety of circumstances in which controls on radioactive material might be compromised. Accidents can be initiated due to uncontrolled positive reactivity insertion, cooling system failure, and site-induced phenomena. The latter mostly includes natural phenomena such as winds, floods, tornadoes, and earthquakes.

Accidental criticality is prevented in a number of situations: (1) chemical processing of enriched uranium or plutonium, (2) storage of fuel in arrays of containers or of fuel assemblies, and (3) initial loading of fuel assemblies at time of startup of a reactor.

In the many hundreds of critical experiments and manipulations of nuclear fuel in processing plants, there have been serious criticality accidents involving radiation exposure as well as several deaths. In the early days, fewer precautions were taken (Koponen, 1999; McLaughlin et al., 2000). Even as late as 1999, an accident at the Tokaimura plant in Japan resulted from the addition of an excess of enriched uranium to a process vessel. An unrestrained fission reaction ensued for almost a day, with two workers quickly receiving fatal doses (IAEA, 1999).

EXAMPLE 21.1

Measured neutron and gamma dose rates at the Tokaimura site boundary were around 4.0 and 0.84 mSv/h, respectively. The US nonoccupational limit of 100 mrem would have been reached in

$$t = \frac{D}{\dot{D}} = \frac{(100\text{ mrem})(1\text{ mSv}/100\text{ mrem})}{4.0\text{ mSv/h} + 0.84\text{ mSv/h}} = 0.2\,\text{h} = 12\,\text{min}$$

21.2 ASSURANCE OF SAFETY

The systems by which safety is assured can be categorized into three types:

(a) Inherent: Based on intrinsic physics principles.
(b) Passive: Does not require active initiation or power but can have components that may fail, thereby making the approach ineffective.
(c) Engineered: Power operated and must be activated.

Examples of these safety mechanisms include negative reactivity feedback (inherent), natural circulation and gravity-fed cooling (passive), and digital reactor protection systems and emergency diesel generators (engineered). To enhance safety, newer reactor designs have sought to replace engineered systems with inherent and passive features.

Because almost all the radioactivity generated by a reactor appears in the fuel elements, great precautions are adopted to ensure the integrity of the fuel. Care is taken in fuel fabrication plants to produce fuel pellets that are identical chemically, of the same size and shape, and of common U-235 concentration. If one or more pellets of unusually high fissile material content were used in a reactor, excessive local power production and temperature would result. The metal tubes that contain the fuel pellets are made sufficiently thick to stop the fission fragments, to provide the necessary mechanical strength to support the column of pellets, and to withstand erosion by water flow or corrosion by water at high temperatures. In addition, the tube must sustain a variable pressure difference caused by moderator–coolant outside and fission product gases inside. The cladding material usually selected for low neutron absorption and for resistance to chemical action, melting, and radiation damage in thermal reactors is Zircaloy, an alloy that is approximately 98% zirconium with small amounts of tin, iron, nickel, and chromium. The tube is formed by an extrusion process that eliminates seams, and special fabrication and inspection techniques are used to ensure that there are no defects such as deposits, scratches, holes, or cracks.

Each reactor has a set of specified limits on operating parameters to ensure protection against events that could cause hazard. Typical of these is the upper limit on total reactor power, which determines temperatures throughout the core. Another is the ratio of peak power to average power that is related to hot spots and fuel integrity. Protection is provided by limiting the allowed control rod position, reactor imbalance (the difference between power in the bottom half of the core and the top half), reactor tilt (departure from symmetry of power across the core), maximum reactor coolant temperature, minimum coolant flow, and maximum and minimum primary system pressure. Exceeding a limit causes the control and/or safety rods to be inserted to trip the reactor. Maintenance of chemical purity of the coolant to minimize corrosion, limitation on allowed leakage rate from the primary cooling system, and continual observations on the level of radioactivity in the coolant serve as further precautions against release of radioactive materials.

Protection of fuel against failure that would release fission products into the coolant is thus an important constraint in the operation of a reactor. Correct choices must be made of the enrichment of U-235, the operating power level, the length of time between refuelings, and the arrangement of new and partially burned fuel, all with consideration of cost.

In the foregoing paragraphs, we have alluded to a few of the physical features and procedures used in the interests of safety. These have evolved from experience over a number of years, and much of the design and operating experience has been translated into widely used *standards*, which are descriptions

of acceptable engineering practices. Professional technical societies, industrial organizations, and the federal government cooperate in the development of these useful documents. They represent general agreement, arrived at by careful study, writing, review, and discussion by qualified practitioners. Many hundreds of scientists and engineers participate in standards development.

The American National Standards Institute (ANSI) provides an umbrella under which standards are written and published for use by reactor designers, manufacturers, constructors, utilities, and regulators. Some of the societies that are active in standards development are the American Nuclear Society (ANS), the Health Physics Society (HPS), the American Society of Mechanical Engineers (ASME), the IEEE (formerly the Institute of Electrical and Electronics Engineers), and the American Society for Testing and Materials (ASTM).

Throughout the analysis, design, fabrication, construction, testing, and operation of a nuclear facility, adequate *quality control* (QC) is required. This consists of a careful, documented inspection of all steps in the sequence. In addition, a *quality assurance* (QA) program that verifies that quality control is being exercised properly is imposed. Licensing by the Nuclear Regulatory Commission (NRC) is possible only if the QA program has satisfactorily performed its function. During the life of the plant, periodic inspections of the operation are made by the NRC to ascertain whether the owner is in compliance with safety regulations, including commitments made in plant technical specifications and the safety analysis report. An exhaustive testing program of components and systems is carried out at the plant.

Furthermore, in the United States, requirements related to safety have a legal status because all safety aspects of nuclear systems are rigorously regulated by federal law and administered by the NRC.

21.3 THE NUCLEAR REGULATORY COMMISSION

The federal government through the NRC has the authority to license and regulate nuclear facilities of all types, from a multireactor power station down to isotope research in an individual laboratory. The Office of Nuclear Reactor Regulation of the NRC requires an applicant for a reactor license to submit a voluminous and detailed safety analysis report and an environmental report. In the old two-step licensing process, codified in 10CFR50, these documents provide the basis for issuance of a construction permit and later, when the plant is completed, an operating license. To streamline and eliminate uncertainty in the process, the new 10CFR52 approach uses a combined construction permit and operating licensing procedure for which a single hearing is held for the combined license, on the basis of standardized designs. In both cases, the licensing process involves several steps: review of the application by the NRC staff; an independent safety evaluation by the Advisory Committee on Reactor Safeguards (ACRS); the holding of public hearings in the vicinity of the proposed plant by an Atomic Safety and Licensing Board Panel (ASLBP); and the testing of qualifications of the people who will operate the plant. In addition to completing a written examination, operators are tested on the plant simulator and on their knowledge of the location and operation of equipment. The NRC and the Federal Emergency Management Agency (FEMA) collaborate in setting criteria for emergency response programs that are developed by the utilities, state government, and local government. The five NRC commissioners make the final decision on license issuance and facility operation.

Once a plant is licensed, the Office of Nuclear Reactor Regulation has oversight. The nuclear operations are subject to continual scrutiny by the resident inspectors and periodic inspection by teams

Table 21.1 Emergency Classification Levels

Event Classification	Level of Safety	Radioactivity Release
Notification of unusual event	Potential degradation	None expected
Alert	Actual or potential substantial degradation	Limited to small fraction of PAGs
Site area emergency	Actual or likely major failures of plant functions	Not expected to exceed PAGs except near site boundary
General emergency	Actual or imminent core	Expected to exceed PAGs

PAGs, Environmental Protection Agency protective action guides.

from the regional NRC office. Training of operating personnel goes on continuously, with one shift in training while other shifts run the plant. Periodic exercises of the emergency plan for the plume exposure pathway zone, which encompasses an approximately 10-mile (16-km) radius around the plant, are conducted. Nuclear stations are required to report unusual events to the NRC promptly. Table 21.1 lists the NRC emergency classification levels, which are defined in relation to public risk and radioactivity release. The NRC maintains a nuclear engineer on duty at all times to receive calls and take action as needed. The staff routinely reviews all incidents. For a number of years, the NRC administered a program called Systematic Assessment of Licensee Performance (SALP). A new substitute is the Reactor Oversight Process, which involves monitoring performance in three areas: reactor safety, radiation safety, and safeguards (against security threats). The process gives attention to human performance, safety culture, and corrective actions. Plants provide reports to the NRC on a set of performance indicators. Companies are subject to fines for lack of compliance with regulations, and if necessary, the NRC can shut a plant down.

The principal reference is the *Code of Federal Regulations Title 10, Energy*. Key sections of that annually updated book are: Part 20, Standards for Protection Against Radiation; Part 50, Domestic Licensing of Production and Utilization Facilities; Part 60, Disposal of High-Level Radioactive Wastes in Geological Repositories; Part 61, Licensing Requirements for Land Disposal of Radioactive Waste; Part 71, Packaging and Transportation of Radioactive Material; and Part 100, Reactor Site Criteria. Part 50 has a number of appendices covering criteria for general design, quality assurance, emergency plans, emergency core cooling system, and fire protection. Standards for NRC-licensed facilities and DOE sites in 10CFR61.41 include annual dose limits of 25 mrem (250 μSv) to the whole body or 75 mrem to the thyroid or 25 mrem to any other organ of members of the public. Other NRC references are the Regulatory Guides (Reg. Guides), each consisting of many pages of instructions. Reg. Guides do not carry the weight of law but rather provide direction for satisfying legal requirements.

The NRC's policies and practices underwent a transition. Traditionally, evaluation of compliance was based on deterministic design information that involved engineering data and analysis. It also was prescriptive in nature, in which specific instructions to nuclear facilities were provided (e.g., Appendix A of 10CFR50, which covers general design criteria). In 1995, the NRC adopted risk-informed regulation. Probabilistic risk assessment (PRA, see Section 21.5) was to be used to decide the most important areas for attention in terms of safety. The NRC also endorsed the idea of performance-based regulation, in which goals of performance are provided, but the utilities are able to decide how to

achieve the goals. The combination of approaches is designated as Risk-Informed Performance-Based Regulation. Definitions and discussion of the various approaches to regulation appear in a 1999 NRC white paper (NRC, 1999).

An example of regulation that required much effort to implement was the Maintenance Rule, a brief statement by the NRC in 1996 of expectations on monitoring the performance of structures, systems, and components (SSC) with respect to maintenance. PRA was not mandated, but needed to define the scope of safety significance. The nuclear industry responded with detailed guidance documents.

The NRC can delegate some of its authority to individual states by negotiation. An Agreement State can develop its own regulations for users of radiation and radioactive material (i.e., facilities other than those of the nuclear fuel cycle). However, the regulations must be compatible with, and no less strict than, those of the NRC.

In addition to its licensing and regulatory activities, the NRC carries out an extensive research program related to radiation protection, nuclear safety, and radioactive waste disposal. Part of the research is in-house and part is through contractors to the NRC. The workload of the NRC has increased greatly as many nuclear power plants seek license extension and as applications for licenses of new reactors have been received.

The Office of Nuclear Material Safety and Safeguards has responsibility for interaction with, and reporting to, the International Atomic Energy Agency on fissionable material for safeguard purposes.

21.4 EMERGENCY CORE COOLING AND CONTAINMENT

The design features and operating procedures for a reactor are such that under normal conditions, a negligible amount of radioactivity will infiltrate the coolant and find its way out of the primary loop. Knowing that abnormal conditions can exist, the worst possible events, called *design basis accidents*, are postulated. The engineered safety features, such as core cooling, containment, and control room habitability systems, consist of backup protection equipment provided to render the effect of an accident negligible. A loss of coolant accident (LOCA) is one condition typically assumed, in which the main coolant piping somehow breaks and thus the pumps cannot circulate coolant through the core. Although in such a situation the reactor power would be reduced immediately by use of control rods, there is a continuing supply of heat from the decaying fission products that would tend to increase temperatures above the melting point of the fuel and cladding. In a severe situation, the fuel tubes would be damaged and a considerable amount of fission products released. To prevent melting, an emergency core cooling system (ECCS) is provided for water-moderated reactors, consisting of auxiliary pumps that inject and circulate cooling water to keep temperatures down. Detailed analysis of heat generation and transfer is required in an application to the NRC for a license to operate a nuclear power plant (see 10CFR50 Appendix K). The operation of a typical ECCS can be understood by examining some schematic diagrams.

The basic pressurized water reactor (PWR) system (Fig. 21.1) includes the reactor vessel, the primary coolant pump, and the steam generator, all located within the containment building. The system usually has more than one steam generator and pump (these are not shown for ease in visualization). We show in Fig. 21.2 some of the equipment that constitutes the engineered safety features. First is the

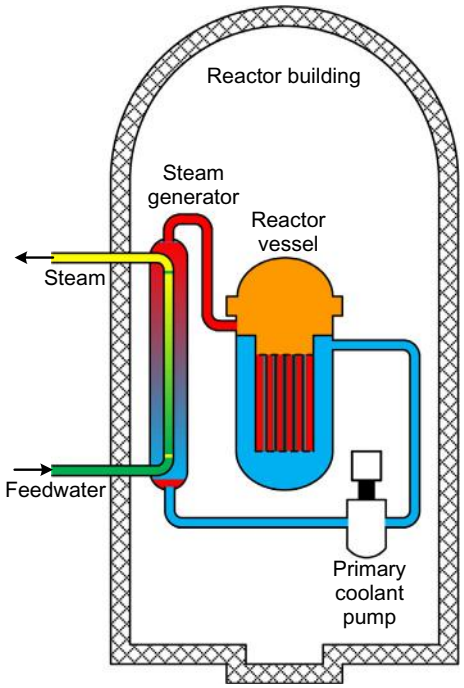

FIG. 21.1

Pressurized water reactor containment.

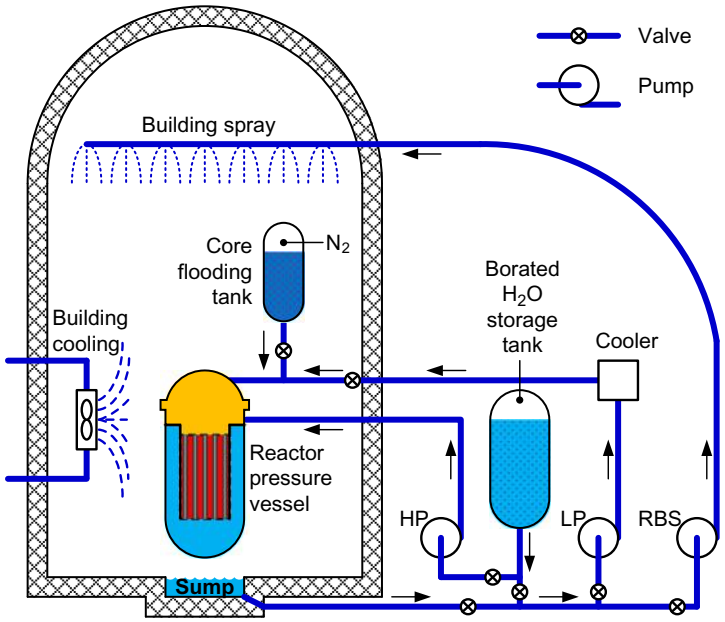

FIG. 21.2

Emergency core cooling systems, including high pressure (HP), low pressure (LP), and reactor building spray (RBS).

high-pressure injection system, which goes into operation if the vessel pressure drops from a normal value of approximately 2250 psi (155 bar) to approximately 1500 psi (100 bar) as the result of a small leak. Water is taken from the borated water storage tank and introduced to the reactor through the inlet cooling line. Next is the *core flooding tank*, also called the safety injection tank, which delivers borated water to the reactor through separate nozzles in the event a large pipe break occurs. Such a rupture would cause a reduction in vessel pressure and an increase in building pressure. When the vessel pressure becomes approximately 600 psi (40 bar), the tank check valve opens and water is forced into the core through nitrogen pressure in the tank. Then if the primary loop pressure falls to approximately 500 psi (35 bar), the *low-pressure injection* pumps start to transfer water from the borated water storage tank to the reactor. The refueling water storage tank typically serves as a large reservoir of borated water. When this tank is nearly empty, the pumps take spilled water from the building sump as a source and continue the flow through coolers that remove the decay heat generated from fission products. Another feature, the containment spray system, also goes into operation if the building gauge pressure increases above approximately 4 psi (0.3 bar). It takes water from the borated water storage tank or the sump and discharges it from a set of nozzles located above the reactor to provide a means for condensing steam in the containment atmosphere. At the same time, the emergency cooling units of the reactor building are operated to reduce the temperature and pressure of any released vapor, and reactor containment isolation valves are closed on unnecessary piping to prevent the spread of radioactive materials outside the structure.

We can estimate the magnitude of the problem of removing fission-product heat. The actual decay heat rate is an ensemble of the decaying exponentials for a multitude of radioactive fission fragments (recall Fig. 6.5). For times between 10 s and 100 d after fission, Way and Wigner (1946) give a rule of thumb that the emission rate of combined beta and gamma ray energy per fission is

$$E_f = 2.66\, t^{-1.2}\ [\text{MeV}/(\text{s fission})] \tag{21.2}$$

with t in seconds. Consider that a reactor is operated at constant power P_0 for a period T and then shut down, as graphed in Fig. 21.3. We know from Eq. (6.12) that the fission rate during power operations is $R_f = P_0/w$. At some time t after shutdown, the total decay energy release from the accumulated fission products is found by totaling the differential contributions ($R_f E_f d\tau$) from fissions occurring throughout the operation period

$$\begin{aligned} P_f(t) &= \int_t^{t+T} \left(\frac{P_0}{190\ \text{MeV/fission}}\right) \frac{2.66\ \text{MeV}}{\text{s fission}} \tau^{-1.2} d\tau \\ &= P_0\, 0.070 \left[t^{-0.2} - (t+T)^{-0.2}\right] \end{aligned} \tag{21.3}$$

If T is large, then the latter term is negligible, such that

$$P_f(t) = P_0\, 0.070\, t^{-0.2} \tag{21.4}$$

This function is graphed in Fig. 21.4.

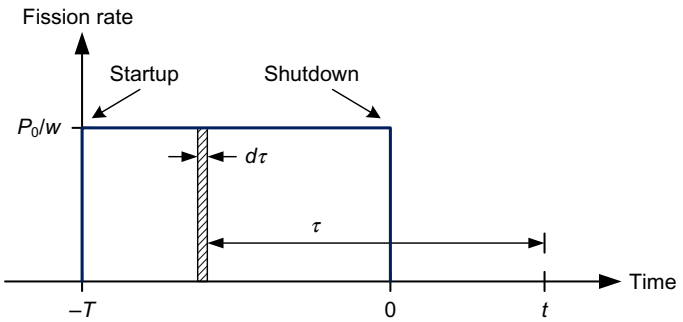

FIG. 21.3

Constant power operation followed by shutdown.

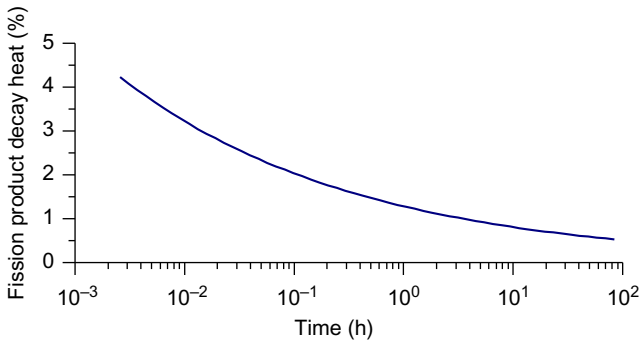

FIG. 21.4

Reactor fission product decay heat rate after shutdown following an infinite operating time.

EXAMPLE 21.2

After operating for an extended period before shutdown, we find that at 10 s the fission product-generated heat is 4.4% of the reactor power:

$$P_f(10\text{s}) = P_0\,(0.070)\,t^{-0.2} = P_0(0.070)(10)^{-0.2} = 0.044\,P_0$$

By the end of a day, it has dropped to 0.72%, which still corresponds to a sizable power. For instance, the total decay heat rate for a 3000-MWt reactor is

$$P_f(1\text{d}) = 0.0072\,P_0 = (0.0072)(3000\ \text{MWt}) = 22\ \text{MWt}$$

The ECCS must be capable of limiting the surface temperature of the Zircaloy cladding to specified values (e.g., 2200 °F), of preventing significant chemical reaction, and of maintaining cooling over the long term after the postulated accident.

The role of the steel-reinforced concrete reactor building is to provide containment of fission products that might be released from the reactor. It is designed to withstand internal pressures and to have a

very small leak rate. The reactor building is located within a zone called an *exclusion area*, of radius of the order of half a kilometer, and the nuclear plant site is several kilometers from any population center.

A series of experiments called loss of fluid tests (LOFT) were performed at Idaho Falls to check the adequacy of mathematical models and computer codes related to LOCA/ECCS. A double-ended coolant pipe break was introduced and the ability to inject water against flow reversal and water vapor determined. Tests showed that peak temperatures reached were lower than predicted, indicating conservatism in the calculation methods.

21.5 PROBABILISTIC RISK ASSESSMENT

The results of an extensive investigation of reactor safety were published in 1975. The document is variously called *Reactor Safety Study*, WASH-1400, or the Rasmussen Report, after its principal author. This study (NRC, 1975) involved 60 scientists and cost several million dollars. The technique used was probabilistic risk analysis (PRA), a formal method of analyzing reactor systems. The objective was to find the chance of an undesired event such as core damage, breach of containment or release of radioactivity, and to determine potential causes. The first step is to investigate all the possible faults in the equipment or processes. Flow diagrams of fluid systems and circuit diagrams of electrical systems serve as reference. *Event trees* are logic diagrams relating an initiating event to either successful mitigation or failure. Fig. 21.5 shows a simple event tree. Probabilities of success and failure at each branch are applied. The principal logic diagrams are the *fault trees*, which trace causes and effects mathematically by use of Boolean algebra, a form of set theory. Fig. 21.6A shows a simple high-pressure injection system to which we can apply the concept for illustration. The failure of both pumps and/or the valve prevents cooling water from reaching the reactor. In Fig. 21.6B, the fault tree diagram shows two gate types: the AND ($\cap$) that requires two or more events to result in failure, and the OR ($\cup$)

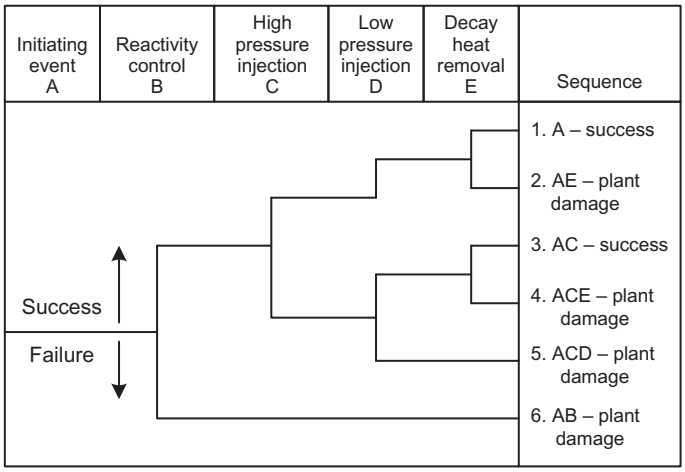

FIG. 21.5

Simple event tree.

Modified from Breeding, R.J., Leahy, T.J., Young, J., 1985. Probabilistic Risk Assessment Course Documentation. vol. 1: PRA Fundamentals, NUREG/CR-4350/1; SAND-85-1495/1.

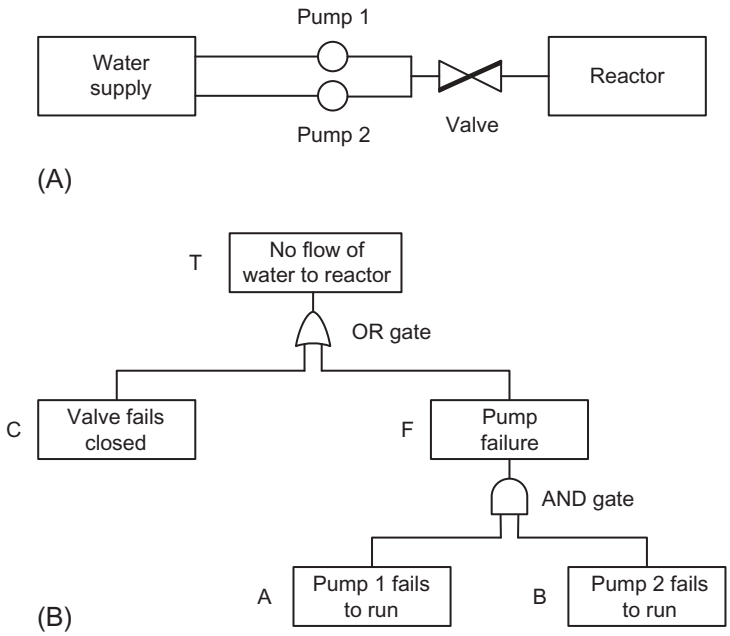

FIG. 21.6

Simple example of PRA diagrams. (A) Physical arrangement of pumping system and (B) fault tree.

Based on Vesely, W.E., Goldberg, F.F., Roberts, N.H., Haasl, D.F., 1981. Fault Tree Handbook, NUREG-0492. Nuclear Regulatory Commission, Washington, DC. http://www.nrc.gov/reading-rm/doc-collections/nuregs/staff/sr0492.

that requires only one event. We have attached symbols A, B, C, F, and T to the various events for use in the mathematical manipulation. Note that F occurs if both A *and* B occur, expressed in Boolean algebra as an intersection

$$\mathrm{F} = \mathrm{A} \cap \mathrm{B} \tag{21.5}$$

Also, the top event T occurs if either C *or* F occurs, expressed as a union

$$\mathrm{T} = \mathrm{C} \cup \mathrm{F} \tag{21.6}$$

Theory (e.g., WASH-1400 Appendix: NRC, 1975) tells us what the probability of T is in terms of C and F, namely,

$$P(\mathrm{T}) = P(\mathrm{C}) + P(\mathrm{F}) - P(\mathrm{C} \cap \mathrm{F}) \tag{21.7}$$

Insert the formula for F and note that because A, B, and C are independent events, the joint probabilities $P(\mathrm{A} \cap \mathrm{B})$ and $P(\mathrm{C} \cap \mathrm{A} \cap \mathrm{B})$ are simply products of the separate probabilities. Thus,

$$P(\mathrm{T}) = P(\mathrm{C}) + P(\mathrm{A})\,P(\mathrm{B}) - P(\mathrm{A})\,P(\mathrm{B})\,P(\mathrm{C}) \tag{21.8}$$

The virtue of Boolean algebra is seen by comparison of this formula with the statement in words that the probability of failure of the high-pressure injection system is the sum of the probabilities of individual failures of the valve and the pumps less the probability of failure of both valves and pumps, which was included already.

EXAMPLE 21.3

To illustrate numerically, let event probabilities $P(\mathrm{A})$ and $P(\mathrm{B})$ be 10^{-3} for pump failure and P(C) be 10^{-4} for valve failure. Inserting numbers,

$$P(\mathrm{T}) = 10^{-4} + \left(10^{-3}\right)^2 - \left(10^{-3}\right)^2\left(10^{-4}\right) \cong 1.01 \times 10^{-4}$$

This shows that the top event is dominated by the possibility of valve failure. The product of three probabilities can be neglected assuming rare events. The numerical result illustrates two ideas: that fault trees can reveal potential vulnerabilities and that redundancy in safety equipment is beneficial. The figure calculated can be included in the simple event tree of Fig. 21.5.

Although duplicate systems render nuclear power plants more expensive, redundant equipment is employed extensively because safety considerations are paramount. For instance, per Criterion 26 of 10CFR50 Appendix A, each nuclear reactor must be outfitted with two independent systems to shut the reactor down and one of the two systems must use control rods.

Several good books on fault trees are listed in the Further Reading section at the end of this chapter. Among important topics discussed in those references are Venn diagrams, used to visualize relationships of intersections and unions; conditional probability, related to sequences of events; the Bayes theorem, a technique for updating failure probability data; and *common mode* failures, those in which several components can fail from a single cause such as environment, design, and manufacturing.

The ultimate objective of PRA is to estimate risks to people, calculated by use of a principle most simply stated as

$$\text{Risk} = \text{Frequency} \times \text{Consequences} \tag{21.9}$$

For reactors, *frequency* means the number of times per year of operation of a reactor that the incident is expected to occur, and *consequences* include the number of injuries or fatalities, either immediate or latent, as well as property damage. The technique of PRA is used to determine which changes in equipment or operation are most important to ensure safety and also give guidance on emergency plans.

EXAMPLE 21.4

For 2009, the US Census Bureau reports 10.8 million motor vehicle accidents with 35,900 resultant deaths. The number of deaths per accident is

$$\text{Consequence} = \frac{\text{Risk}}{\text{Frequency}} = \frac{35{,}900\,\text{deaths/y}}{10.8 \times 10^6\,\text{accidents/y}} = 0.00332\,\text{death/accident}$$

For a national population of 306.8 million, the individual risk becomes

$$\frac{35{,}900\,\text{deaths/y}}{306.8 \times 10^6\,\text{individuals}} = 1.17 \times 10^{-4}\,\text{deaths/(person year)}$$

Two main conclusions from WASH-1400 were (1) reactor accident consequences are no larger than those from nonnuclear accidents, and (2) reactor accident likelihood is smaller than those from nonnuclear for the same consequence. While WASH-1400 studied only two reactors (a BWR and a PWR),

the later updated study of NUREG-1150 (NRC, 1990) examined five reactors (two BWRs and three PWRs), including the original reactors in WASH-1400.

In recent years, the regulation of nuclear activities, including reactor operation and handling of radioisotopes, has changed. Currently, regulations are risk-informed and performance-based in contrast with previous prescriptive approaches. As discussed in an American Nuclear Society position statement (ANS, 2004), "risk-informed" implies use of probability in prioritizing challenges to safety, and "performance-based" makes use of measurable safety parameters. Fuller explanations are found in a publication of the NRC (NRC, 1999; Apostolakis et al., 2012).

If an incident occurring at a nuclear plant has the potential of releasing radioactivity to the atmosphere, a chain of reactions to alert or warn the public is set in motion. In the United States, the NRC and FEMA cooperate in providing requirements and in monitoring tests of readiness. Each nuclear station and the state in which it is located are required to have emergency plans in place and to hold drills periodically, resembling action to be taken in a real accident situation. In such exercises, state and local officials are notified, and an emergency team made up of many organizations undertakes a coordinated response. Included are radiation protection staff, police and fire departments, highway patrol, public health officers, and medical response personnel. Command posts are set up; weather observations are correlated with radiation conditions to evaluate the possible radiation exposure of the public. Advisories are sent out by radio and television, sirens are sounded, and the public is advised to take shelter in homes or other buildings. In extreme cases, people would be urged to evacuate the affected area.

In case of an actual accident involving reactors or transportation of fuel or waste, members of the public who suffer a loss can be compensated. In 1957, Congress passed the Price-Anderson Act to provide rules about nuclear insurance that were favorable to the development of the nuclear industry. The act was renewed in 2005 for 20 y. Nuclear plants are required to take out insurance from private companies in the amount of $300 million. In the event of an accident, all reactors would be assessed to bring the total liability to approximately $10 billion. The act has been criticized as unfairly benefiting the nuclear industry because any excess cost would be borne by government and thus taxpayers.

21.6 THE THREE MILE ISLAND ACCIDENT AND LESSONS LEARNED

At 4 a.m. on March 28, 1979, an accident occurred in the Three Mile Island (TMI) Unit 2 reactor near Harrisburg, Pennsylvania. A small amount of radioactivity was released, causing great alarm throughout the region. As the reactor had been in operation for only three months, the fission product inventory was substantially below the maximum. We briefly review with Fig. 21.7 what happened at TMI and the resultant improvements in reactor safety.

TMI-2, an 880-MWe B&W PWR, was operating at 97% power when the steam generator main feedwater system malfunctioned, causing the turbine-generator to trip. The backup feedwater system failed to operate because a block valve to the steam generator had been left closed. The once-through steam generator dried of secondary water, causing the primary water coolant temperature and pressure to increase due to the loss of a heat sink. High pressure appropriately triggered a pilot-operated relief valve (PORV) on top of the pressurizer to open, discharging vapor and liquid to a quench tank inside the containment building. The high reactor coolant system (RCS) pressure also scrammed the reactor, with control rods being inserted into the core to stop the fission reaction and reduce power. The RCS

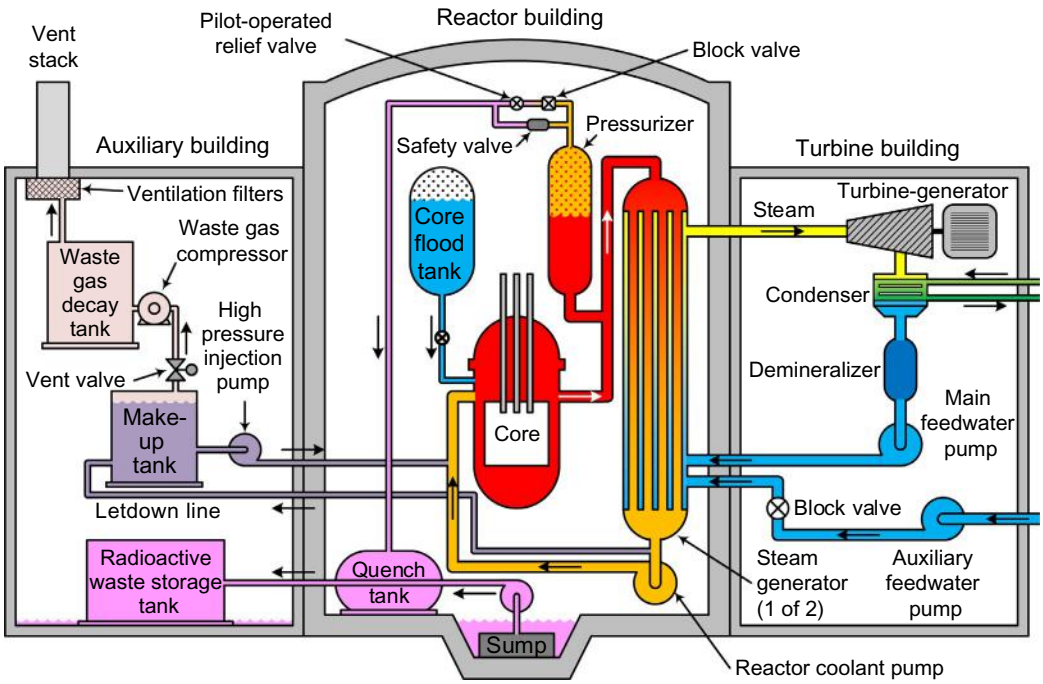

FIG. 21.7

Three Mile Island PWR nuclear power plant, after NUREG/CR-1250 (Rogovin and Frampton, 1980) and Pershagen (1989).

pressure dropped to normal within about 13 s and the PORV should have closed, but instead it stuck open and remained so for 142 min, thereby constituting a small LOCA. Unfortunately, the reactor operators were unaware that the PORV remained open, as an indicator on the control panel implied it had closed. The escaping primary coolant eventually filled the quench tank that in turn released radioactive water to the containment building floor.

About 2 min into the accident, the high-pressure ECCS actuated due to the reduced RCS pressure. Operators thought the pressurizer was filling with water (i.e., "going solid") and they manually reduced the ECCS flow dramatically—2–3 min later. The core heated up and became uncovered as the primary coolant boiled away. Boiling within the core exacerbated operator confusion because steam bubble formation displaced water into the pressurizer, thus increasing the pressurizer level and giving the appearance of adequate coolant inventory. Decay heat caused major fuel damage, including melting and hydrogen production. With the RCS at saturation conditions, the reactor coolant pumps were shut off for lack of liquid water. The water released from the quench tank collected in the building sump and about 8000 gallons were pumped to the auxiliary building, where the radioactive waste tank filled to the point that the rupture disk was blown and water was spilled onto the floor, releasing radioactive gases. A second release point was the dissolved gases in the primary coolant, which was removed through the letdown line and placed in the makeup tank. The gases in the makeup tank were transferred to the waste gas tank system that had leaks.

Radioactive xenon and krypton (noble gases) as well as a small amount of radioactive iodine passed through ventilation filters and were detected outside the containment building. The radiation dosage to anyone was estimated to be less than 100 mrem (1 mSv). This was based on assumed continuous exposure outdoors at the site boundary for 11 d. The average exposure to people within 50 miles (80 km) was estimated to be only 1.5 mrem (15 μSv), noted to be less than that caused by a medical X-ray. Because of a warning by the governor of Pennsylvania, many people, especially pregnant women, left the area for several days. These estimates (Battist et al., 1979) indicate that the exposure over the lifetimes of the 2 million people in the region there would be statistically only one additional cancer death (of 325,000 from other causes).

The TMI accident was due to a combination of (1) design deficiency—inadequate control of water and insufficient instrumentation, (2) equipment failure—the stuck pressurizer valve, and (3) operator error—especially turning off the ECCS and the pumps. Some would view the event as proof that reactors are unsafe; others would note that even with core damage little radioactivity was released. Two weeks before the TMI-2 accident, the movie *China Syndrome* had been released. It focused on a hypothetical accident in which the whole core is assumed to melt its way through the reactor vessel and go on in the earth toward China. No such scenario is valid, but public fears were aroused.

A recovery program for TMI was initiated. The interior of the reactor pressure vessel was examined by use of miniature video cameras attached to the ends of long cables inserted from the top. The damage, as illustrated in Fig. 21.8, was greater than originally thought. A significant region of the core, the upper 5 ft (1.5 m), was missing, having slumped into the portion below, and solidified molten fuel was found in the lower part of the vessel. Special handling tools were devised to extract the damaged fuel. Care was taken by measurements and analysis to ensure that the debris would not go critical during recovery. The fuel was transferred to a series of always-safe canisters for storage and shipment.

US President Jimmy Carter took a keen interest in the accident. He created the President's Commission on the Accident at Three Mile Island (called the Kemeny Commission after its chairperson, John Kemeny, president of Dartmouth College). It was composed of qualified people without nuclear industry connections. A number of recommendations were made in its report (Kemeny et al., 1979), including the need for the nuclear industry to enhance operator and supervisor training, to set its own standards of excellence, and to conduct performance evaluations. Insights on the Kemeny Commission are found in Eytchison (2004). In cooperation with utility leaders, many of the recommendations were implemented. One of the most significant outcomes of the TMI accident was the formation by the industry of the Institute of Nuclear Power Operations (INPO). This organization reviews all aspects of the performance of US nuclear power plants and provides recommendations for improvements. Details of the function of INPO are found in the next section. Shortly after the TMI-2 accident, the NRC requested that utilities take a number of corrective actions to improve safety. In anticipation of the NRC's expectations, the industry conducted a study called Industry Degraded Core Rulemaking (IDCOR). Its purpose was to provide well-documented databases on reactor safety. It was concluded that fission product releases would be much lower than those predicted by WASH-1400 (Section 21.5). This discrepancy prompted new studies of the *source term*, the radioactive release in case of accident.

A second study sponsored by the NRC was described in report BMI-2104 (Gieseke et al., 1983/1984). New computer codes by Battelle Memorial Institute were applied to all processes, giving an improvement over the *Reactor Safety Study*. Risks were found to be dependent on containment design. Other studies were made by the American Nuclear Society and by the American Physical Society. The general conclusion was that source terms were lower because of particle retention at the containment wall.

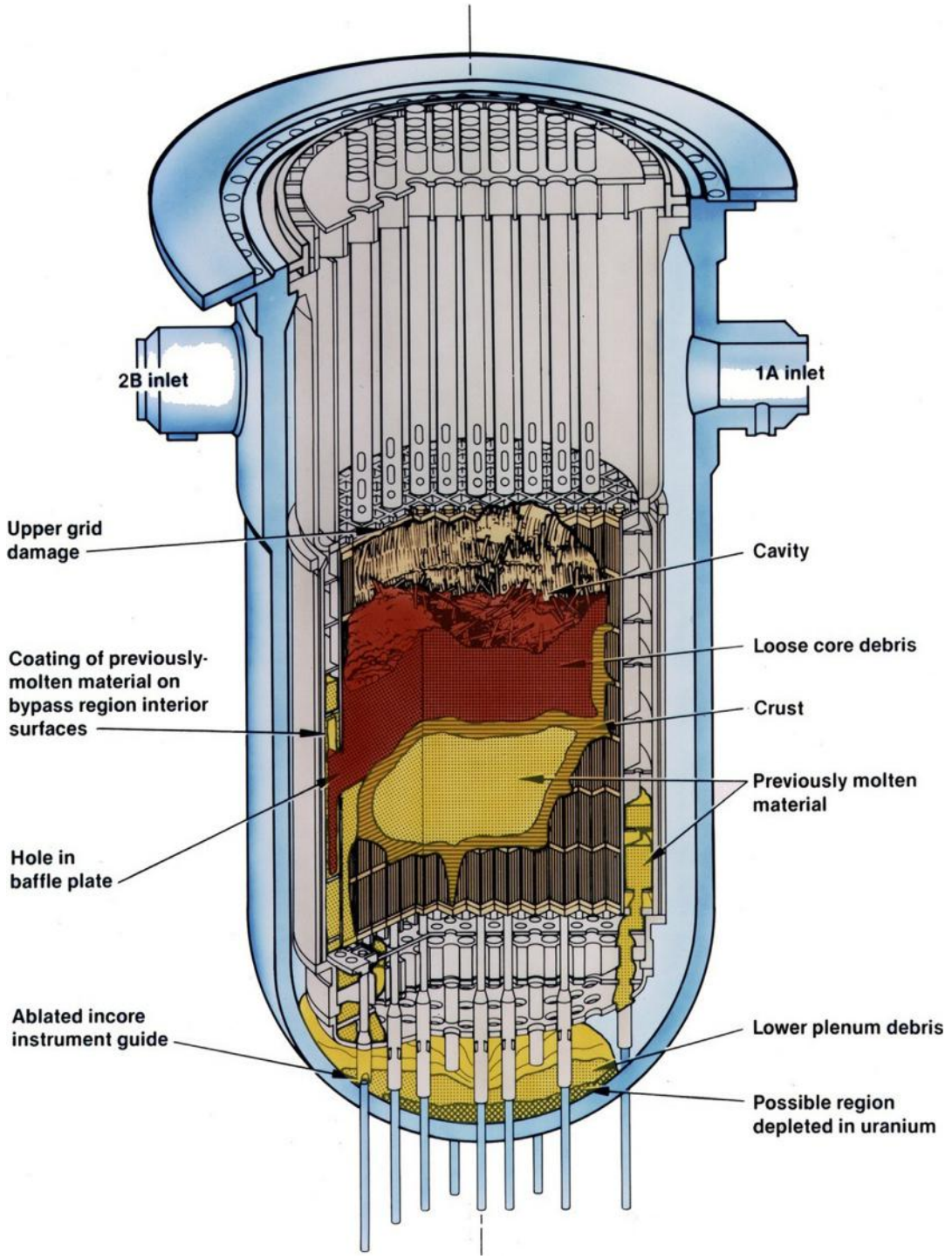

FIG. 21.8

TMI-2 reactor core end-state configuration.

Courtesy US NRC.

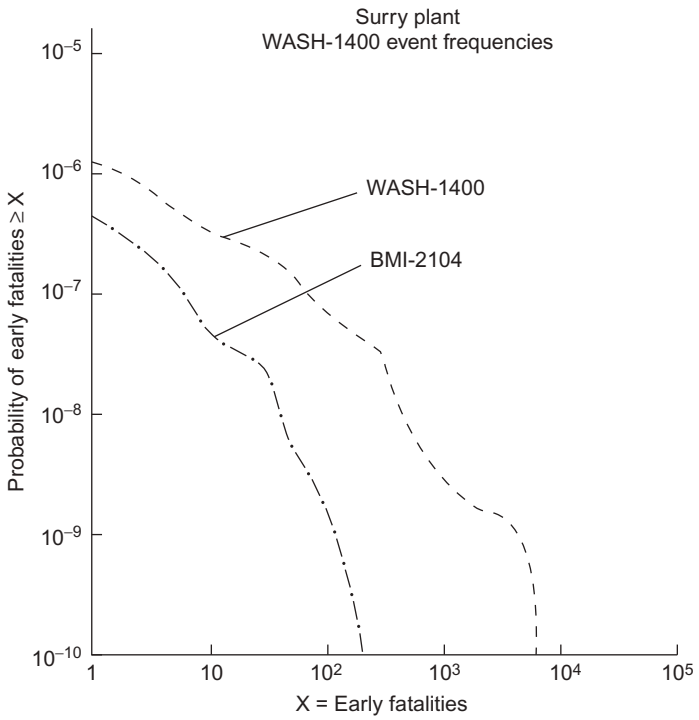

FIG. 21.9

Distribution function for the Surry, Virginia, plant. The probabilities for various numbers of early fatalities are shown.

Adapted from Silberberg, M., Mitchell, J.A., Meyer, R.O., Ryder, C.P., 1986. Reassessment of the Technical Bases for Estimating Source Terms, NUREG-0956.

Fig. 21.9 illustrates the improvement in going from WASH-1400 to BMI-2104 for one example reactor, the Surry Nuclear Station. The interpretation of the lower curve is as follows: the chance for as many as *one* early fatality is about 5×10^{-7} per reactor year. However, the chance of latent cancer fatalities is quoted to be larger, 3.4×10^{-3} per reactor year. This still corresponds to a prediction of less than one death per year for the nearly 100 US reactors. Many misunderstand the terminology used by reactor safety analysts (e.g., "a 10^{-6} chance per year of harm"). Norman Rasmussen, after whom the report (Section 21.5) was named, remarks, "For most people, a rare event is one that occurs once in a lifetime, like Halley's Comet, frequency 10^{-2}. Once in 100 lifetimes is 10^{-4}, that's getting hard to believe."

EXAMPLE 21.5

If one selects a larger number of fatalities, for example 200, then the probability is 10^{-10} per reactor year due to the Surry plant, according to Fig. 21.9. Compared to the single death probability, the chance has dropped by a factor of approximately $(5 \times 10^{-7})/10^{-10} = 5000$.

When the findings on source term are used in establishing emergency plans, evacuation of people from a large area surrounding a damaged plant would be an inappropriate action. Over the period 1985–2001, the NRC carried out a program called Individual Plant Examination (IPE) to seek out vulnerabilities and report them. PRA was the only way to accomplish that. No significant problems were uncovered.

21.7 INSTITUTE OF NUCLEAR POWER OPERATIONS[1]

Many organizations contribute to the safety and effectiveness of nuclear power generation, not the least of which are the operating companies themselves. One organization, however, provides a broad stimulus to excellence that warrants special attention. The Institute of Nuclear Power Operations (INPO) is the industry's self-regulation organization. Its objective is to promote the highest level of safety and reliability in the operation of nuclear electric generating plants.

Based in Atlanta, Georgia, INPO was founded by the electric utilities operating nuclear plants and has a number of employees who are on loan from industry. Corporate leaders saw the need for the utilities to be actively responsible for safety rather than merely complying with NRC regulations. All utilities that have nuclear plants are members of INPO as a private nonprofit organization. Its programs embrace nuclear systems vendors and utilities outside the United States. In its work to promote excellence in safety and reliability of operation of nuclear electric generating plants, it has four cornerstone programs. It evaluates the operational performance of utilities, analyzes plant events and distributes lessons-learned information, evaluates training and provides accreditation, and assists member companies. INPO has no role as an advocate of nuclear power but recognizes that excellent performance is vital to public confidence.

Teams of INPO staff members and personnel from other utilities perform evaluations regularly. They visit a facility for two weeks: reviewing, observing, and discussing activities. Day-to-day operations and maintenance programs are examined, along with management practices. Candid interactions lead to an evaluation report that identifies both strengths and areas needing improvement. Such evaluations are shared only with the utility for its use in improving performance. This ability to communicate freely is regarded as very important.

Data on operational events are obtained by the INPO program called Significant Event Evaluation and Information Network (SEE-IN), established in 1980. It is designed to share experiences. INPO receives reports from the utilities and other sources, studies them for possible precursors of severe problems, and sends out information on a computer-based communication system called NUCLEAR NETWORK. INPO also prepares formal documents including Significant Event Reports (SERs) that describe the most important occurrences, and Significant Operating Experience Reports (SOERs) that are comprehensive reviews of key topics. The latter documents provide recommendations for solutions in areas such as radiological protection, training, and maintenance practices.

An enormous amount of information on nuclear power plant equipment has been collected and put into INPO's database, the Equipment Performance Information Exchange (EPIX). Events and incidents involving equipment failure are reported and analyzed for root causes and ways to prevent future problems. A continuous flow of information to and from INPO keeps the industry up to date on

[1]Thanks are due to Philip McCullough for helpful information on INPO.

equipment performance. Of special value is the ability of a utility to quickly obtain information on the solution of an equipment problem by access to EPIX.

In the area of personnel training, INPO administers the National Academy for Nuclear Training. The Academy's objective is to assure ample knowledge and skill on the part of nuclear personnel and to promote professionalism among nuclear workers. INPO issues guidelines on training in classes and on simulators. It reviews the training programs set up by utilities for supervisors, shift technical advisors, operators, maintenance personnel, and technicians. It also manages the accreditation done by the independent National Nuclear Accrediting Board. The Academy provides workshops, meetings, training courses, and reports, all aimed at the improvement of performance by workers, supervisors, and management.

Assistance programs that continually evolve to meet the changing needs of the nuclear industry help member utilities improve nuclear operations. Through assistance visits, working meetings, workshops, technical documents, and loan of personnel, INPO fosters comparison and exchange of successful methods among members. INPO carefully watches a set of performance indicators, which are quantified trends that measure success in achieving excellence. Examples are plant availability to produce electricity, industrial safety, safety system performance, fuel reliability, unplanned automatic scrams, radiation exposure, and volume of radioactive waste. With input from its Board of Directors and Advisory Council, INPO assists in setting target goals for the industry, with distinctions between pressurized water reactors (PWRs) and boiling water reactors (BWRs) as appropriate.

The organization welcomes utilities from other countries as participants who receive the benefits of information exchange but are not subject to evaluations or accreditations. Other countries often assign liaison engineers to the INPO staff. International cooperation on nuclear power is stimulated by an allied organization called the World Association of Nuclear Operators (WANO), with centers in Atlanta, Paris, Moscow, and Tokyo, and a coordinating center in London. It establishes the performance indicators and facilitates communication, comparison, and emulation among organizations in many countries. INPO is the US representative to WANO and makes its information capabilities available worldwide. The WANO-Atlanta Center is colocated with INPO. Whenever possible, WANO helps maintain stable nuclear power operations in countries that have economic and social problems.

INPO's activities are recognized as independent and supplementary to those of the NRC. The industry supports and oversees INPO but gives it authority to enforce its recommendations, thus providing self-regulation by peer review. It is widely accepted that the activities of INPO have significantly contributed to the improvement in the level of safety in the United States and abroad.

21.8 THE CHERNOBYL ACCIDENT

At 1:23 a.m. on April 26, 1986, a very serious reactor accident occurred at the Chernobyl[2] Unit 4 reactor near Kiev in Ukraine in the Soviet Union. An explosion took place that blew a hole in the roof of the building housing the reactor and a large amount of radioactive material from the damaged nuclear fuel was released into the atmosphere. The amount of radiation exposure to workers and the public is not precisely known, but the doses exceeded the fallout from earlier weapons tests. A number of workers were killed, nearby towns were contaminated, and it is estimated that the collective dose to the public

[2]Ukraine prefers the spelling "Chornobyl" but we will use the more familiar Russian form.

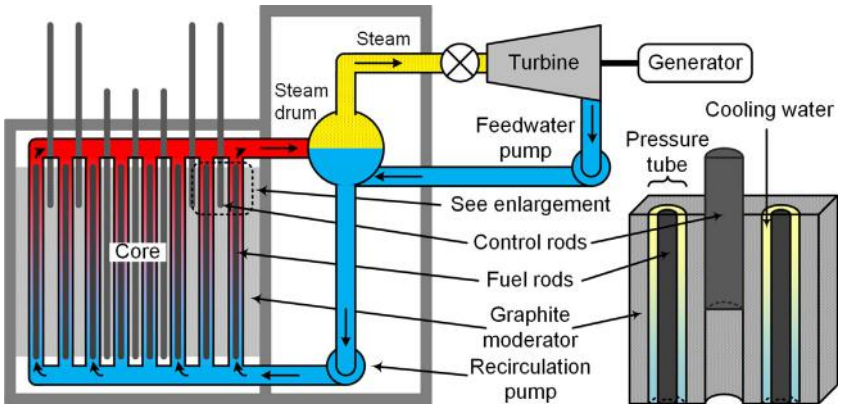

FIG. 21.10

The Chernobyl RBMK graphite-moderated light-water-cooled reactor.

increased the cancer risk. A number of people were evacuated from the nearby town of Pripyat. Agriculture was disrupted in the Soviet Union, and a ban on food imports was imposed by several European countries.

The Chernobyl reactors were of the type designated RBMK-1000. Fig. 21.10 shows the reactor system, which was housed in a normal industrial building (not shown) rather than a dedicated containment structure. This RBMK design, having evolved from Russian defense reactors, possessed online refueling capability. The core was cylindrical, 7 m high, 12 m diameter. Moderator graphite blocks were pierced by vertical holes to hold 8.8-cm diameter pressure tubes. Each tube contained multiple slightly (2%) enriched UO_2 fuel rods and ordinary water coolant that underwent boiling. Similar to many coal-fired power plants, a steam drum separated vapor from the coolant exiting the core and recirculated the liquid component back to the reactor.

An experiment related to the capability of the turbines to supply electricity during coast down in an emergency was being performed. A separate group had planned the experiment. Operators were under pressure to complete the test because the next available maintenance period was more than a year away. The power was to be reduced from 3200 MWt to approximately 700 MWt, but the operators allowed it to drop to 30 MWt. At that point, the neutron flux was too low to burn out accumulated Xe-135. The buildup of this absorber made it very difficult to raise the power, and only 200 MWt could be reached. In violation of rules, most of the control rods were pulled out to maintain criticality. Coolant flow was reduced to a value at which steam voids were created. The steam bubble formation decreased the water mass in the core region, thereby lessening neutron absorption by the water and concomitantly raising the neutron flux. Thus, the overmoderated RBMK had a *positive* void coefficient of reactivity, in contrast with that of light-water reactors (LWRs) in which the reduced coolant mass would have meant less moderator present too. The positive reactivity feedback initiated by steam void formation caused the power to flash up to 30,000 MWt—10 times the operating level. The power could not be reduced because the control rods were too far out to have an effect. About one minute passed from the start of the experiment to the runaway reaction. The large energy release caused physical disassembly of the core, thereby terminating the fission chain reaction.

EXAMPLE 21.6

The Chernobyl reactor experienced two peak powers during the accident. The first peak was stopped by the Doppler fuel temperature coefficient, $\alpha_F = -1.2 \times 10^{-5}/°C$ (NRC, 1987). Using the delayed neutron fraction β of 0.0048, the fuel temperature increase may be estimated from the compensation for the positive reactivity insertion of \$2.5 via

$$\Delta T_F = \frac{\rho}{\alpha_F} = \frac{-(2.5)(0.0048)}{-1.2 \times 10^{-5}/°C} = 1000°C$$

The excess energy pulverized fuel, caused steam pressure to build, and ruptured coolant tubes. Chemical reactions involved steam, graphite, zirconium, and fuel, creating heat that vaporized fuel. The steam and hydrogen explosions blew off the roof of the building housing the reactor and released some 13 EBq (360 MCi) (NEA, 2002) of activity, including Cs-137, I-131, noble gases, and other fission products. A radioactive cloud passed over several countries of Europe, but activity was detected worldwide. Food crops had to be discarded because of contamination.

A total of 237 operating personnel, firefighters, and emergency workers were initially hospitalized with radiation sickness; 28 of them died from acute radiation syndrome (UNSCEAR, 2000). Their exposures ranged from 2.2 Gy to as high as 16 Gy (1600 rad). Thousands of people were evacuated, many of whom were permanently relocated with great cost and undoubtedly much distress. About 116,000 people were evacuated, including 49,000 from the town of Pripyat. The average internal and external doses to those in the evacuation zone were 1 and 2 rem (10 and 20 mSv), respectively; however, the average dose to the thyroid from I-131 was 50 rad (0.5 Gy) with children receiving the highest averages. Those children who were exposed are experiencing a significantly higher incidence of thyroid cancer. In contrast, the general population that was exposed has not shown increased risk of leukemia. The exposure outside the USSR was considerably less, being only several times natural background radiation. The United Nations Scientific Committee on the Effects of Atomic Radiations (UNSCEAR) continues to assess the radiation effects from the Chernobyl accident. For an enthralling personal experience of radiation protection in Kiev after the accident, see (Eremenko and Droppo, 2006).

By the end of 1986, a structure called a sarcophagus was erected around the damaged reactor in an effort to prevent future releases of radioactivity. In late 2016, a new arch-shaped shelter was slid over the existing sarcophagus to better confine the remains of the reactor.

Several implications of the accident were noted:

(a) The RBMK reactor type is inherently unsafe and should be phased out.
(b) Reactor safety philosophy and practice need to be revised with greater attention to human factors and safety systems.
(c) International cooperation and information exchange should be strengthened.
(d) Reactor accidents have global significance.
(e) Users of LWRs need to examine equipment and practices, even though the reactors are far safer with their negative power coefficients and strong containment buildings.
(f) The consequences of the Chernobyl accident should continue to be monitored.

One consequence of the accident was the formation of a set of joint research projects between the United States and the Russian Federation. These emphasized databases, computer codes, and the

development of a plan for Russian nuclear safety research. Similar to the formation of INPO after TMI, WANO was established in response to Chernobyl.

21.9 THE FUKUSHIMA DAIICHI ACCIDENT

On March 11, 2011, a multiunit accident occurred at the Fukushima Daiichi plant on the northeastern coastline of Japan. At 2:46 p.m., the Great East Japan Earthquake—a seismic event registering 9.0 on the moment magnitude scale (MMS)—struck 70 km off the eastern coast, resulting in an automatic shutdown of Units 1, 2, and 3, which were operating at rated power at the time (Units 4, 5, and 6 were in outages). The earthquake caused damage to the nearby electric power system resulting in the loss of offsite power, but onsite diesel generators were started to supply equipment such as decay heat removal systems for these three BWRs, which began operations in the 1970s.

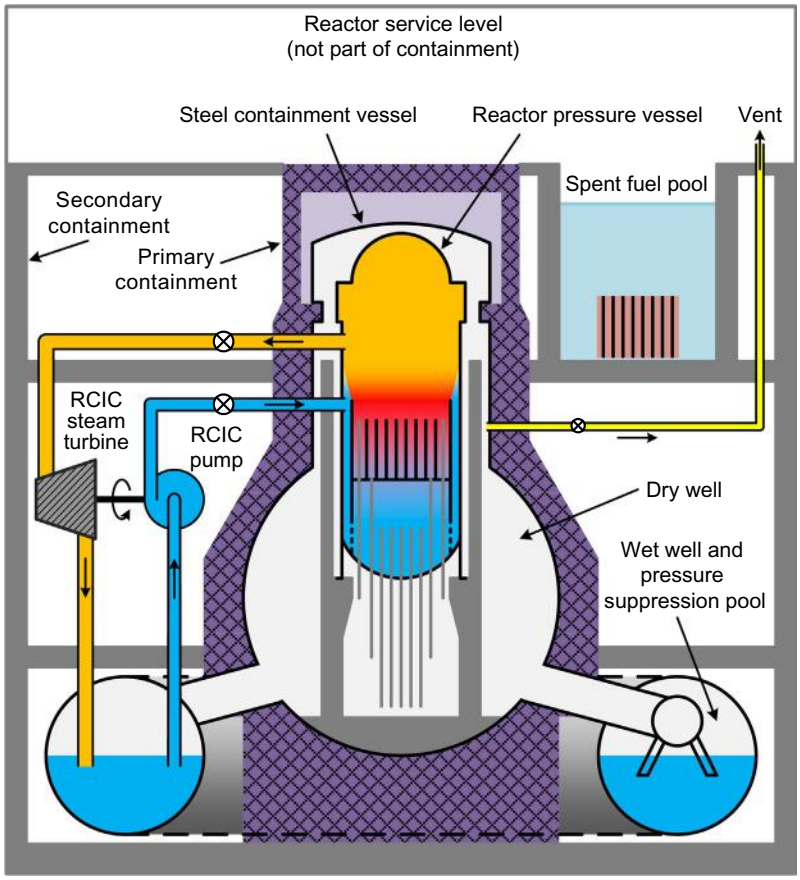

FIG. 21.11

Fukushima General Electric BWR with Mark I containment and reactor core isolation cooling (RCIC) system.

Approximately an hour after the earthquake, a tsunami of about 13 m in height inundated the plant site. The resulting flooding rendered the emergency diesel generators and other required electrical switchgear inoperable. Thus, the plant experienced a *station blackout*, which is the loss of both onsite and offsite alternating current (ac) power. At this point, only the Unit 3 dc batteries were supplying its instrumentation and control systems, but sufficient power was not available for large equipment such as pumps. Although the fission process had ceased when the plant scrammed, the fission product decay heat requires large heat removal systems. The details and timing of the following events differ from unit to unit but the overall loss of cooling sequence is similar.

Fig. 21.11 depicts the inverted light bulb shaped primary containment for the BWR systems in Units 1–4. Unit 1 incorporated a passive isolation condenser (IC) system, but it was turned off prior to the arrival of the tsunami. Units 2 and 3 featured a reactor core isolation cooling (RCIC) system. The RCIC pump is driven by steam from the reactor to provide makeup water when the normal cooling water supply is unavailable. Liquid water from the toroidal wetwell is pumped into the reactor while the vapor exiting the reactor through the RCIC turbine is condensed in the wetwell to suppress pressure. However, the requisite batteries for this system to function will eventually be depleted. In addition, this closed system has no capability of dissipating its heat beyond ambient heat loss mechanisms.

Without heat dissipation (e.g., when the reactor isolation pump stops), the coolant pressure in the reactor increased as decay heat continued to produce steam. Relief valves opened to discharge steam into the wetwell and reduce reactor pressure. Without the introduction of more water into the reactor, the liquid level in the vessel descended and the top of the core was no longer submerged in liquid. Thus, the cladding and fuel began to overheat, releasing gaseous fission products and hydrogen into the reactor vessel, which eventually passed into the wetwell and later the drywell atmosphere. Over the next few days, core damage occurred to reactors 1, 3, and 2 (in order).

The steam and released gases drove up pressure within the primary containment. Rather than allow the containment to rupture, the operators partially depressurized the system, which resulted in the venting of radioactive fission products and H_2 into the upper floor of the reactor building. The flammable H_2 exploded, thereby destroying the steel frame structure of the Unit 1, 3, and 4 reactor service levels; the Unit 3 H_2 gas underwent backflow, thereby migrating to Unit 4, which was defueled previously.

EXAMPLE 21.7

The earliest time at which fuel melting began in Fukushima Unit 1 can be estimated from the thermal energy needed to raise the UO_2 fuel temperature from about 300 °C to 2800 °C. Using the UO_2 fuel mass of 77 tonnes and specific heat of 0.25 kJ/(kg °C), the heat required is

$$Q = mc_p\Delta T = \left(77\times10^3\,\text{kg}\right)\left(0.25\text{kJ}/(\text{kg°C})\right)(2800-300\text{°C}) = 4.8\times10^7\,\text{kJ}$$

Integrating Eq. (21.4) provides the total heat produced for some period after shutdown following an infinite operating period, which conservatively leads to the greatest heat generation rate. Assuming cooling of the 1380-MWt reactor ceased about an hour after the earthquake, the onset of fuel melt occurs at

$$Q = \int_{1\,\text{h}}^{t} P_f(\tau)d\tau = \int_{3600\ \text{s}}^{t} P_0\,0.070\,\tau^{-0.2}d\tau = \frac{0.070}{0.8}P_0\left(t^{0.8}-3600^{0.8}\right)$$

Equating the two preceding expressions for thermal energy leads to a time t of 6316 s. Thus, there was more than 0.75 h after the tsunami to restore core cooling before fuel damage. We note that this calculation has neglected the other materials (e.g., cladding) in the reactor vessel, which would also absorb heat.

The Fukushima Nuclear Accident Independent Investigation Commission (NAIIC, 2012) deplored the conduct of the government, regulators, and electric utility, going so far as to deem the accident a manmade disaster. Dose rates of 12 mSv/h (1.2 rem/h) were measured 1 km from the units during releases (INPO, 2011). Overall, radioactive material discharges from Fukushima were about an order of magnitude smaller than those at Chernobyl. Residents within 20 km of the plant site were evacuated. In May 2013, the United Nations Scientific Committee on the Effect of Atomic Radiation concluded (UNIS, 2013), "Radiation exposure following the nuclear accident at Fukushima-Daiichi did not cause any immediate health effects. It is unlikely to be able to attribute any health effects in the future among the general public and the vast majority of workers." However, the World Health Organization (WHO, 2013) states, "The lifetime risk for some cancers may be somewhat elevated above baseline rates in certain age and sex groups that were in the areas most affected."

In response to the accident at Fukushima and NRC Order EA-12-049, the US nuclear power industry developed FLEX. FLEX provides additional backup power and equipment for nationwide dispatch to cope with a beyond-design-basis external event that simultaneously causes an extended loss of ac power (ELAP) and loss of normal access to the ultimate heat sink (LUHS).

EXAMPLE 21.8

Let us consider evolutionary design changes that decrease the possibility of a Fukushima-type accident. Even before Fukushima, designers of the ESBWR elevated the wetwell water inventory above the reactor core, which enables cooling water to be gravity fed in the event of power loss. This is an example of replacing active pumping with a passive approach.

21.10 PHILOSOPHY OF SAFETY

The subject of safety is a subtle combination of technical and psychological factors. Regardless of the precautions that are provided in the design, construction, and operation of any device or process, the question can be raised "Is it safe?" The answer cannot be a categorical "yes" or "no" but must be expressed in more ambiguous terms related to the chance of malfunction or accident, the nature of protective systems, and the consequences of failure. This leads to more philosophical questions such as "How safe is safe?" and "How safe do we want to be?"

In an attempt to answer such questions, the NRC (1986) adopted what are called *safety goals*. These are intended to free neighbors of nuclear plants from worry. Regulations are "… providing reasonable assurance … that a severe core damage accident will not occur at a US nuclear power plant." Design and operation are to be such that risks of death from a nuclear accident are no greater than a thousandth of known and accepted risks. The comparison is to be made with other common accidents for those people living within 1 mile (1.6 km) of the plant and with cancer from all causes for those living within 10 miles.

Every human endeavor is accompanied by a certain risk of loss, damage, or hazard to individuals. In the act of driving an automobile on the highways, or in turning on an electrical appliance in the home, or even in the process of taking a bath, one is subject to a certain danger. Everyone agrees that the consumer deserves protection against hazard outside his or her personal control, but it is not at all clear as to

what lengths it is necessary to go. In the absurd limit, for instance, a complete ban on all mechanical conveyances would ensure that no one would be killed in accidents involving cars, trains, airplanes, boats, or spacecraft. Few would accept the restrictions thus implied. It is easy to say that reasonable protection should be provided, but the word "reasonable" has different meanings among people. The concept that the benefit must outweigh the risk is appealing, except that it is very difficult to assess the risk of an innovation for which no experience or statistical data are available or for which the number of accidents is so low that many years would be required for adequate statistics to be accumulated. Nor can the benefit be clearly defined. A classic example is the use of a pesticide that ensures protection of the food supply for many, with finite danger to certain sensitive individuals. To the person affected adversely, the risk completely overshadows the benefit. The addition of safety measures is inevitably accompanied by increased cost of the device or product, and the ability or willingness to pay for the increased protection varies widely among people.

It is thus clear that the subject of safety falls within the scope of the socioeconomic political structure and processes, and is intimately related to the fundamental conflict of individual freedoms and public protection by control measures. It is presumptuous to demand that every action possible should be taken to provide safety, just as it is negligent to contend that because of evident utility, no effort to improve safety is required. Between these extreme views lies an opportunity to arrive at satisfactory solutions, applying technical skill accompanied by responsibility to assess consequences. It is most important to provide understandable information on which the public and its representatives can base judgments and make wise decisions as to the proper level of investment of effort and funds.

Recognizing that operations and maintenance (O&M) costs are a major expenditure to produce electricity, utilities have increased attention to efficiency in the maintenance and repair process. They have concentrated on reduction in the time required for refueling outages and eliminated unscheduled reactor trips to enhance capacity factors. Such actions had to be taken with care that safety was not jeopardized. It is clear that every additional monitoring device, safety equipment, or special procedure intended to enhance safety adds to the product cost. As performance improves, it becomes more difficult to find areas for further improvement. But it is difficult for a regulator, from either government or industry, to refrain from recommending new safety initiatives. In the limit, the industry could be put out of business by escalating costs. From another point of view, the addition of excessive complexity to a facility can be counterproductive to safety. This suggests that greater attention be given to establishing priorities and to reducing costs in other areas besides those that are safety-sensitive. A more important goal still is the achievement of a uniform level of excellence in every nuclear unit in the country.

EXAMPLE 21.9

The human perception of risk can be illustrated. In 2008 within the United States, there were 1.3 traffic accident-related deaths per 100 million vehicle miles, while worldwide there were 0.01 fatalities per 100 million air passenger-kilometers (USCB, 2011). In fact, only 439 people perished globally in air transport operations whereas 37,400 died in the United States from motor vehicle accidents. The fact that a single incident such as an airplane crash can cause a large number of causalities becomes more noteworthy for the media. Subsequently, individuals perceive a higher risk of traveling by air even though the chance of dying is far less.

21.11 NUCLEAR SECURITY

Protection of nuclear facilities from adverse actions has always been regarded as important, but the terrorist attacks on the United States on September 11, 2001 (9/11), prompted a need for significant enhancement of security.

In 1979, the NRC defined the *design basis threat* (DBT), which involves the number of attackers, their weapons capability, and probable mode of action on the basis of intelligence gathered; see 10CFR73.1 (NRC, n.d.). A ground-based threat is assumed to be by a well-armed, well-trained, suicidal group that uses vehicles and explosives.

The nuclear industry spent well over a billion dollars to extend security at power plants. Included were improved training and arming of security guards, additional physical barriers, better intrusion surveillance and detection, stronger access controls, institution of protection of plant computer systems, and improved background checks of plant employees.

An innovation called *force-on-force* exercises was required by the NRC. At a plant, the roles of attacker and responder are played, with reviews of performance. At nuclear plants in the United States, some 8000 security officers are available to counter a ground threat. Physical barriers are erected between three zones labeled owner-controlled, protected, and vital, as illustrated in Fig. 21.12. The *owner-controlled area* usually corresponds to the power plant site boundary as delimited by an outer fence. Access to the *protected area* around the plant itself is further limited by double fencing. The innermost zone is the *vital area*, including as a minimum the reactor control room and spent fuel pool. The exclusion area size of Section 21.4 is based upon dosimetry considerations whereas these three zones are defined in terms of physical protection.

After the events of September 11, 2001, concern was expressed about the possibility of an aircraft attack on nuclear facilities. The Electric Power Research Institute (EPRI) prepared a report (NEI, 2002) on the effects. The selected aircraft was the Boeing 767 with wing span 170 ft (52 m), larger than the diameter of a typical containment building of 140 ft (43 m). A low speed of 350 mph (560 km/h) was assumed because of the difficulty in precision flying near the ground. The containment was composed of steel-reinforced concrete approximately 4 ft (1.2 m) thick, designed to be impervious to natural disasters such as hurricanes, tornadoes, earthquakes, and floods. Its curved surface prevents a full impact of the airplane. Conservative assumptions were made to give the maximum force. The result of the

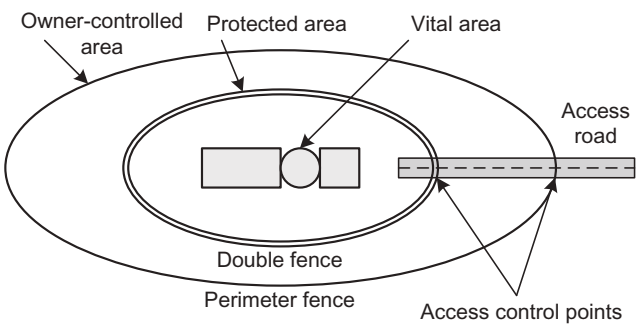

FIG. 21.12

Physical protection zones for a nuclear facility.

analyses was that the containment was not breached, so no parts of the plane entered the building. The report also concluded that fuel storage pools, dry storage units, and shipping casks would be safe against air attack. The targets would be very near the ground, requiring a sharp dive of the airplane, with only a glancing blow.

A new challenge to many industries is cybersecurity. Ubiquitous Internet connections can permit hackers to gain entry into distant systems. Nuclear power plants must protect the digital computer and communications systems from malicious attack.

21.12 SUMMARY

Prevention of release of radioactive fission products and fuel isotopes is the ultimate purpose of safety features. Reactor components are designed and constructed to minimize the chance of failure. Emergency core cooling equipment is installed to reduce the hazard in the event of an accident. Licensing is administered by the Nuclear Regulatory Commission, which expects plants to use probabilistic safety risk analysis (PRA).

An accident at Three Mile Island Unit 2 in 1979 resulted in considerable damage to the reactor core, but little radioactive material was released. The event stimulated the nuclear industry to make many changes that enhance reactor safety.

A serious accident occurred in 1986 at Chernobyl in the Soviet Union. As a result of an unauthorized experiment, there was an explosion and fire, accompanied by the release of a great deal of radioactivity. Nearby cities were evacuated, a number of people were killed, and many received significant dosage.

A multireactor meltdown occurred at the Fukushima Daiichi, Japan, plant in 2011. Caused by a station blackout due to an earthquake and the resulting tsunami, the release of radioactivity was significant but long-term health impact is predicted to be less than that from Chernobyl.

Eventually, people will appreciate the fact that no technology is entirely risk-free, as dams break and wind turbines fail. Even the production of materials for solar energy collectors and their installation result in fatalities.

Security at nuclear plants was greatly enhanced after the terrorist attacks of September 11, 2001. A study indicates that terrorist aircraft do not pose a problem.

21.13 EXERCISES

21.1 How has the safety of modern PWR vessels (see Fig. 18.4) improved over the 1950s era Shippingport RPV (see Fig. 8.3)?

21.2 Confirm that the oxidation of 1 kg of Zr produces 0.5 m^3 of H_2.

21.3 From a safety standpoint, which containment building design is more desirable: cylindrical or spherical?

21.4 Indicate the type of safety (active, inherent, or passive) exemplified by each of the following: (a) diesel generator, (b) high-pressure coolant injection, (c) low-pressure coolant

injection, (d) natural water circulation, (e) power-operated relief valve, and (f) negative reactivity feedback coefficient.

21.5 How long will it take for a fully withdrawn control rod in a reactor of height 4 m to drop into a reactor core, neglecting all friction and buoyancy effects? (Recall $s = g_0 t^2/2$ with $g_0 = 9.81\,\text{m/s}^2$.)

21.6 Using Eq. (21.4), calculate the ratio of fission product power to reactor power for: (a) 1 day, (b) 1 week, (c) 1 month, and (d) 1 year after shutdown.

21.7 Expand the PRA for Fig. 21.6A by considering the possibility that the tank holding the water supply fails. (a) Draw the fault tree. (b) Compute the probability that the top event occurs if the probability the tank fails is 10^{-5}.

21.8 Assuming a probability of reactor core meltdown of 3×10^{-4} per reactor year, calculate the chance of one meltdown for 100 reactors in a period of 20 y.

21.9 For the second power excursion experienced by the Chernobyl-4 reactor, the power ramped up at a roughly constant rate from 200 MWt to 1300 GWt over 0.2 s. (a) Compute the energy deposition per unit mass within the UO_2 fuel composed of 190 tonnes of uranium. (b) If the specific heat and heat of fusion for UO_2 are 350 J/(kg °C) and 245 kJ/kg, respectively, does the fuel melt?

21.10 When a large positive reactivity is added to a fast reactor assembly, the power rises to a peak value and then drops, crossing the initial power level. In this response, which is the result of a negative temperature effect, the times required for the rise and fall are about the same. If the neutron lifetime is 4×10^{-6} s, what would be the approximate duration of an energy pulse resulting from a reactivity of 0.0165, if the peak power is 10^3 times the initial power? See figure.

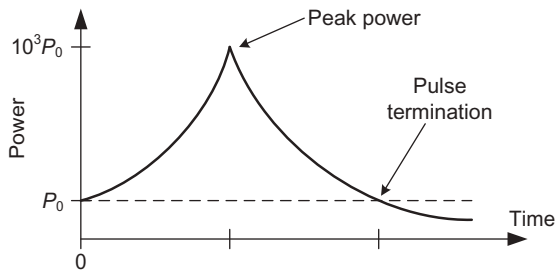

21.11 On a single graph, plot (i) the maximum fission product decay heat generation rate and (ii) the fission power for the first 10 min after a 3000-MWt reactor is scrammed.

21.12 On a conservative basis, calculate the total decay heat produced during (a) the first 2.5 h of the TMI-2 accident, and (b) the first 4 h after shutdown of the Unit 1 reactor at Fukushima.

21.13 If the probability of a main coolant pipe failure is 3 in 10,000 operating years, how many total failures might be expected to occur over a 40-y lifetime of the LWR and heavy-water reactor (HWR) plants in operation worldwide (see Table 18.3)?

21.14 For a flux of 10^{16} n/(cm^2 s), compute the neutron absorption rate by 1 cm^3 of (a) liquid water ($\rho = 0.75$ g/cm^3), (b) vaporized water ($\rho = 0.033$ g/cm^3), and (c) solid graphite.

21.15 Expand the PRA for Fig. 21.6A by replacing the single valve with two valves in parallel. (a) Draw the fault tree. (b) Compute the probability of the top event occurring if the probability that each valve fails in the closed position is 5×10^{-4}. (c) Repeat the analyses in (a) and (b) for the case of placing the two valves in series instead.

21.16 Estimate the earliest time after shutdown for fuel melting in the 2381-MWt Fukushima Unit 3 reactor, which had a UO_2 mass of 107 tonnes.

REFERENCES

American Nuclear Society (ANS), 2004. Risk-Informed and Performance-Based Regulations for Nuclear Power Plants. American Nuclear Society Position Statement.

Apostolakis, G., Cunningham, M., Lui, C., Pangburn, G., Reckley, W., 2012. A Proposed Risk Management Regulatory Framework, NUREG-2150. U.S. Nuclear Regulatory Commission.

Battist, L., Buchanan, J., Congel, F., Nelson, C., Nelson, M., Peterson, H., Rosenstein, M., 1979. Population Dose and Health Impact of the Accident at the Three Mile Island Nuclear Station. NUREG-0558. Nuclear Regulatory Commission.

Eremenko, V.A., Droppo Jr., J.G., 2006. A personal experience reducing radiation exposures: protecting family in Kiev during the first two weeks after Chernobyl. Health Phys. 91 (5), S39–S46.

Eytchison, R.M., 2004. Memories of the Kemeny commission. Nucl. News 47 (3), 61–62.

Gieseke, J.A., Cybulskis, P., Denningm, R.S., Kuhlman, M.R., Lee, K.W., Chen, H., 1983/1984. Radionuclide Release Under Specific LWR Accident Conditions, BMI-2104. Vols. I–III. Battelle Columbus Laboratories, Columbus.

Institute of Nuclear Power Operations (INPO), 2011. Special report on the nuclear accident at the Fukushima Daiichi nuclear power station. INPO Report 11-005.

International Atomic Energy Agency (IAEA), 1988. The Radiological Accident in Goiânia. STI/PUB/815.

International Atomic Energy Agency (IAEA), 1999. Report on the preliminary fact finding mission following the accident at the nuclear fuel processing facility in Tokaimura, Japan.

Kemeny, J., Babbitt, B., Haggerty, P.E., Lewis, C., Marks, P.A., Marrett, C.B., et al., 1979. The Need for Change: The Legacy of TMI. Report of the President's Commission on the Accident at Three Mile Island. Washington, DC.

Koponen, B.L. (Ed.), 1999. Nuclear Criticality Safety Experiments, Calculations, and Analyses—1958 to 1998: Compilation of Papers from the Transactions of the American Nuclear Society. Golden Valley Publications, Livermore, CA.

McLaughlin, T.P., Monahan, S.P., Pruvost, N.L., Frolov, V.V., Ryazanov, B.G., Sviridov, V.I., 2000. A Review of Criticality Accidents 2000 Revision. LA-13638, Los Alamos National Laboratory.

Nuclear Accident Independent Investigation Commission (NAIIC), 2012. Official Report of The Fukushima Nuclear Accident Independent Investigation Commission. National Diet of Japan.

Nuclear Energy Agency (NEA), 2002. Chernobyl: Assessment of radiological and Health Impacts. 2002 Update of Chernobyl Ten Years On. Organization for Economic Cooperation and Development, Paris.

Nuclear Energy Institute (NEI), 2002. Deterring Terrorism: Aircraft Crash Impact Analyses Demonstrate Nuclear Power Plant's Structural Strength. http://www.nei.org/corporatesite/media/filefolder/EPRI_Nuclear_Plant_Structural_Study_2002.pdf. Summary of EPRI study; conclusion that fuel is protected.

Pershagen, B., 1989. Light Water Reactor Safety. Pergamon Press, Oxford.

Rogovin, M., Frampton Jr., G.T., 1980. Three Mile Island: a report to the commissioners and the public, Vol. I and II. Nuclear Regulatory Commission, NUREG/CR-1250.

U.S. Census Bureau (USCB), 2011. Statistical Abstract of the United States: 2012. U.S. Department of Commerce.
U.S. Nuclear Regulatory Commission (NRC), 1975. Reactor Safety Study: An Assessment of Accident Risks in U.S. Commercial Nuclear Power. WASH-1400 (NUREG-75/014). Often called the Rasmussen Report after the project director, Norman Rasmussen; the first extensive use of probabilistic risk assessment in the nuclear field.
U.S. Nuclear Regulatory Commission (NRC), 1986. Safety goals for the operations of nuclear power plants. Fed. Regist. 51 (162), 30028–30033.
U.S. Nuclear Regulatory Commission (NRC), 1987. Report on the Accident at the Chernobyl Nuclear Station. NUREG-1250. Compilation of information obtained by DOE, EPRI, EPA, FEMA, INPO, and NRC.
U.S. Nuclear Regulatory Commission (NRC), 1990. Severe Accident Risks: An Assessment for Five U.S. Nuclear Power Plants. NUREG-1150.
U.S. Nuclear Regulatory Commission (NRC), 1999. Risk-Informed and Performance-Based Regulation. NRC White Paper, SRM 1998-144.
U.S. Nuclear Regulatory Commission (NRC), Physical Protection of Plants and Materials, Part 73 of the Code of Federal Regulations. 10CFR73.1, https://www.nrc.gov/reading-rm/doc-collections/cfr/part073/part073-0001.html.
United Nations Information Service, 2013. No Immediate Health Risks from Fukushima Nuclear Accident Says UN Expert Science Panel. UNIS/INF/475, http://www.unis.unvienna.org/unis/en/pressrels/2013/unisinf475.html.
United Nations Scientific Committee on the Effects of Atomic Radiations (UNSCEAR), 2000. Sources and Effects of Ionizing Radiation. Report to the General Assembly. New York.
Way, K., Wigner, E.P., 1946. Radiation from Fission Products. MDDC-48. U.S. Atomic Energy Commission.
World Health Organization (WHO), 2013. Health Risk Assessment from the Nuclear Accident After the 2011 Great East Japan Earthquake and Tsunami Based on a Preliminary Dose estimation.

FURTHER READING

Breeding, R.J., Leahy, T.J., Young, J., 1985. Probabilistic Risk Assessment Course Documentation. PRA Fundamentals, vol. 1. NUREG/CR-4350/1; SAND-85-1495/1.
Dickinson College's Three Mile Island website, http://tmi.dickinson.edu/.
Eisenbud, M., Gesell, T., 1997. Environmental Radioactivity: From Natural, Industrial, and Military Sources, fourth ed. Academic Press, San Diego, CA.
Farmer, F.R., 1977. Nuclear Reactor Safety. Academic Press, New York.
Fullwood, R.R., Hall, R.E., 1988. Probabilistic Risk Assessment in the Nuclear Power Industry: Fundamentals and Applications. Pergamon Press, Oxford.
Golding, D., Kasperson, J.X., Kasperson, R.E., 1995. Preparing for Nuclear Power Plant Accidents. Westview Press, Boulder, CO.
Hatamura, Y., Abe, S., Fuchigami, M., Kasahara, N., 2015. The 2011 Fukushima Nuclear Power Plant Accident: How and Why it Happened. Woodhead Publishing, Cambridge.
Henley, E.J., Kumamoto, H., 1992. Probabilistic Risk Assessment. IEEE Press, New York.
International Atomic Energy Agency (IAEA), Consequences of the Chernobyl Accident. http://www-ns.iaea.org/appraisals/chernobyl.htm.
International Atomic Energy Agency (IAEA), In Focus Chernobyl. http://www.iaea.org/NewsCenter/Focus/Chernobyl. Status and recommended actions.
Knief, R.A., 1985. Nuclear Criticality Safety: Theory and Practice. American Nuclear Society, La Grange Park, IL. Methods of protection against inadvertent criticality, with an appendix on the Three Mile Island recovery program.
Lewis, E.E., 1977. Nuclear Power Reactor Safety. Wiley, New York.

Lewis, E.E., 1996. Introduction to Reliability Engineering. Wiley, New York.
Marples, D.R., 1986. Chernobyl and Nuclear Power in the USSR. St. Martin's Press, New York.
Mazuzan, G.T., Walker, J.S., 1984. Controlling the Atom: The Beginnings of Nuclear Regulation 1946–1962. California University Press, Berkeley and Los Angeles.
McCormick, N.J., 1981. Reliability and Risk Analysis: Method and Nuclear Power Applications. Academic Press, New York.
National Research Council, 2014. Lessons Learned from the Fukushima Nuclear Accident for Improving Safety of U.S. Nuclear Plants. National Academies Press, Washington, DC.
Nénotm, J.-C., 2009. Radiation accidents over the last 60 years. J. Radiol. Prot. 29 (3), 301–320.
News, N., 2002. Nuclear plant damage from air attacks not likely. Nucl. News 45 (8), 21.
Nuclear Energy Institute (NEI), Safety & Security. http://www.nei.org.
Pennsylvania State University Library, TMI-2 Recovery and Decontamination Collection. http://www.libraries.psu.edu/tmi. TMI-2 Cleanup Highlights Program (24-min QuickTime video).
Petrangeli, G., 2006. Nuclear Safety. Butterworth-Heinemann, Amsterdam.
Randerson, D. (Ed.), 1984. Atmospheric Science and Power Production. U.S. Department of Energy.
Silberberg, M., Mitchell, J.A., Meyer, R.O., Ryder, C.P., 1986. Reassessment of the Technical Bases for Estimating Source Terms. NUREG-0956. U.S. Nuclear Regulatory Commission.
Technology for Energy Corp, 1984. IDCOR Nuclear Power Plant Response to Serious Accidents. Technology for Energy Corp., Knoxville, TN.
U.S. Government Printing Office, Code of Federal Regulations, Energy, Title 10, Parts 0–199. United States Government Printing Office, Washington, DC. (annual revision). All rules of the Nuclear Regulatory Commission appear in this publication.
U.S. Nuclear Regulatory Commission (NRC), 1983. PRA Procedures Guide: A Guide to the Performance of Probabilistic Risk Assessments for Nuclear Power Plants. vols. 1 and 2. NUREG/CR-2300. A comprehensive 936-page report prepared by the American Nuclear Society and the IEEE; issued after the Three Mile Island accident, it serves as a primary source of training and practice.
U.S. Nuclear Regulatory Commission (NRC), Backgrounder on the Three Mile Island 2 Accident. http://www.nrc.gov/reading-rm/doc-collections/fact-sheets/3mile-isle.html. Account of the accident with diagram, references, and glossary by NRC.
U.S. Nuclear Regulatory Commission (NRC), NRC Regulatory Guides. http://www.nrc.gov/reading-rm/doc-collections/reg-guides. select from list of ten divisions.
U.S. Nuclear Regulatory Commission (NRC), 10 CFR Part 50—Domestic Licensing of Production and Utilization Facilities. http://www.nrc.gov/reading-rm/doc-collections/cfr/part050.
Walker, J.S., 2004. Three Mile Island: A Nuclear Crisis in Historical Perspective. University of California Press, Berkeley, CA. The most authoritative book on the accident; a scholarly but gripping account, it details the accident, the crisis situation, the heroic role of Harold Denton, the aftermath, and the implications.
Vesely, W.E., Goldberg, F.F., Roberts, N.H., Haasl, D.F., 1981. Fault Tree Handbook, NUREG-0492. Nuclear Regulatory Commission, Washington, DC. http://www.nrc.gov/reading-rm/doc-collections/nuregs/staff/sr0492. A frequently cited tutorial containing fundamentals and many sample analyses.
Wolfson, R., 1993. Nuclear Choices: A Citizen's Guide to Nuclear Technology. MIT Press, Cambridge. Nuclear power and nuclear weapons, with comments on the accidents at TMI and Chernobyl.
Wood, M.S., Schultz, S.M., 1988. Three Mile Island: A Selectively Annotated Bibliography. Greenwood Press, New York.
World Association of Nuclear Operators (WANO), http://www.wano.info/.

CHAPTER

NUCLEAR PROPULSION AND REMOTE POWER

22

CHAPTER OUTLINE

Nuclear processes are logical choices for compact energy sources in vehicles that must travel long distances without refueling. The most successful application is in the propulsion of naval vessels, especially submarines and aircraft carriers. Research and development has been done on reactors for aircraft and rockets, and reactors may be used in future space missions. Besides employing reactors for large-scale electric power generation, radioisotopes can be utilized to supply smaller power needs and basic thermal heating. Thermoelectric generators that use the isotope plutonium-238 provide reliable electric power for interplanetary spacecraft.

22.1 REACTORS FOR NAVAL PROPULSION

The discovery of fission stimulated interest on the part of the US Navy in the possible use of nuclear power for submarine propulsion. The development of the present fleet of nuclear ships was due largely to Admiral H.G. Rickover, a legendary figure because of his reputation for determination, insistence on quality, and personalized management methods. The team that then-Captain Rickover brought to Oak Ridge in 1946 to learn nuclear technology supervised the building of the land-based prototype, Submarine Thermal Reactor Mark I (STR-I, later designated S1W), at Idaho Falls and the first nuclear submarine, U.S.S. *Nautilus* (STR-II, S2W). As noted by historians for the project, the name had been used for submarines before, including Jules Verne's fictional ship (Hewlett and Duncan, 1974). These efforts inaugurated the development of pressurized water reactors (PWRs).

Nuclear Energy. https://doi.org/10.1016/B978-0-12-812881-7.00022-8

The principal virtue of a nuclear-powered submarine is its ability to travel long distances at high speed without refueling. It can remain submerged because the reactor power plant does not require oxygen. Argonne National Laboratory conducted research on the Submarine Thermal Reactor, and the development was carried out at the Bettis Laboratory of Westinghouse Electric Corporation.

The power plant for the *Nautilus* was a water-moderated, highly enriched uranium core with zirconium-clad plates. The submarine's first sea trials were made in 1955. Some of its feats were a 1400-mile (2250-km) trip with an average speed of 20 knots (37 km/h), the first underwater crossing of the Arctic ice cap, and traveling a distance of more than 62,000 miles (100,000 km) on its first core loading. Subsequently, the U.S.S. *Triton*, which demonstrated a twin-reactor propulsion system, reproduced Magellan's trip around the world, but completely submerged. Decommissioned in 1980, the *Nautilus* is now in a museum at Groton, Connecticut.

The US nuclear fleet was built up during the years of the Cold War (1947–91), with more than 100 nuclear-powered submarines, a number of aircraft carriers, and a few cruisers. The first of the aircraft carriers was the U.S.S. *Enterprise*, deployed in 1961 and deactivated in 2012. It had 8 reactors (2 for each of 4 propeller shafts), 85 aircraft, and 5830 men. Fig. 22.1 shows the carrier with Einstein's

FIG. 22.1

The first entirely nuclear-powered task force, including the aircraft carrier U.S.S. *Enterprise*. Sailors in formation on the flight deck spell out Einstein's formula. The accompanying ships are the cruiser U.S.S. *Long Beach* (center) and the frigate U.S.S. *Bainbridge* (top), powered by two reactors each.

Courtesy U.S. Navy (1964).

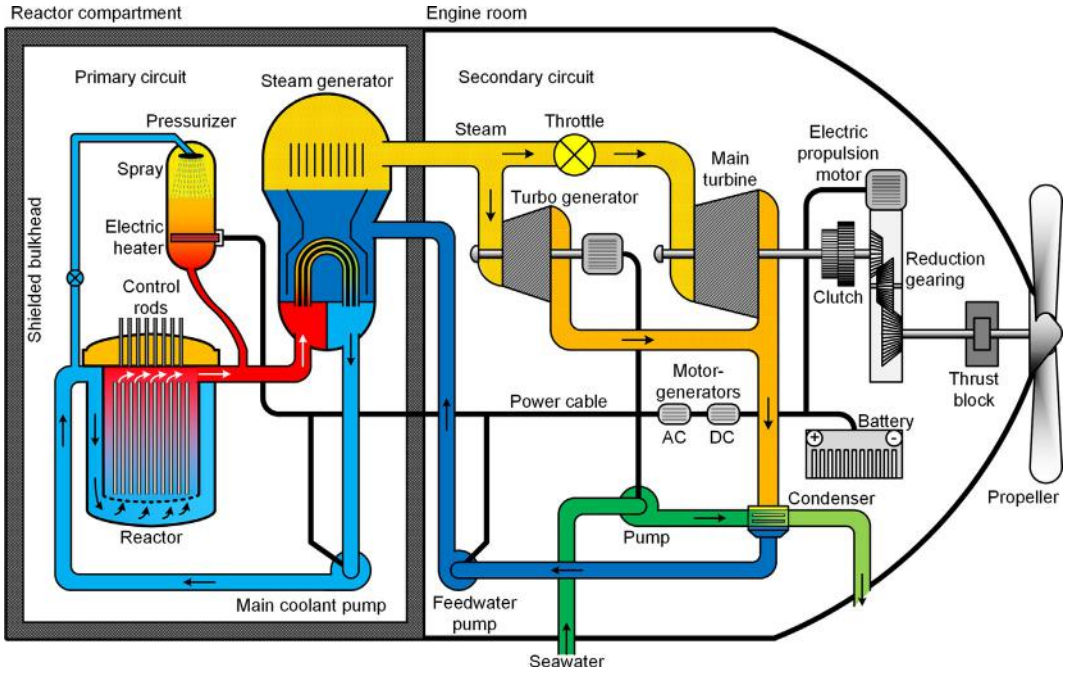

FIG. 22.2

Generic naval propulsion system.

familiar formula spelled out on the deck by members of the crew. Since then, more than 10 additional carriers have been built, but with only two reactors per ship.

Attack submarines are designed to seek and destroy enemy submarines and surface ships. The *Seawolf* and *Virginia* class submarines are powered with one reactor and armed with Tomahawk cruise missiles. Ballistic missile submarines are designed as deterrents to international conflict. Examples are the *Ohio* class submarines, which carry 24 long-range Trident strategic missiles. These weapons can be ejected by compressed air while the vessel is underwater, with the rocket motors starting when the missile clears the surface. The number of US nuclear-powered naval vessels is gradually being reduced by obsolescence as well as reductions in strategic weapons (see Section 27.3).

The nuclear steam supply system of a vessel can be configured in multiple ways, as depicted in Fig. 22.2. The steam can directly drive the propeller through gearing connected to the turbine. Alternatively, turbine-generator supplied electric power can be fed to a motor that turns the propeller, to battery storage, and to equipment such as pumps.

EXAMPLE 22.1

The *Nautilus* boasted an installed mechanical shaft power P_m of 13,400 hp (horsepower). Assuming the submarine averaged a speed of 17 knots, the first core loading encompassed an operational period of

$$T = d/v = (62{,}000\,\text{mi})/[(17\,\text{knot})(1.15\,\text{mi/h/knot})] = 3170\,\text{h}$$

If the thermal efficiency η_{th} was 22%, the ^{235}U fuel consumption over the 132 days was

$$m_C = (P_m/\eta_{th})T(1.30\,g/(MW\,d))$$
$$= \frac{(13,400\,hp)(132\,d)(1.30\,g/(MW\,d))}{(0.22)(1\,hp/745.7\,W)(10^6\,W/MW)} = 7.8\,kg$$

Commercial nuclear power has benefited in two ways from the Navy's nuclear program. First, industry received a demonstration of the effectiveness of the PWR. Second, utilities and vendors have obtained the talents of a large number of highly skilled professionals who are retired officers and enlisted men.

The United States built only one commercial nuclear vessel, the merchant ship N.S. *Savannah*. Babcock & Wilcox Company designed its 74-MWt reactor. The core was fueled with UO_2 having an average enrichment of 4.4% in type 304 stainless steel tubes, operating at 1730 psig (119 bar) (FASTI, 1968). Carrying both cargo and passengers, it successfully operated for several years in the 1960s, making a goodwill voyage to many countries (MARAD, 2017). After being on display at a naval museum in South Carolina, the N.S. *Savannah* was moved in 1994 to Virginia as a national landmark.

Japan launched an experimental nuclear-powered merchant ship *Mutsu* in 1972. It successfully passed several rigorous sea trials, performing well in rough seas caused by a typhoon. However, excessive fast neutron leakage prompted modifications of the radiation shielding (Freire and de Andrade, 2015). Ishida et al. (1993) noted that the reactor system of a nuclear-powered ship must be designed to accommodate more severe load changes than land-based systems. In 1995, the ship was decommissioned and placed in a museum; its experience served as the basis for the design of two other vessels.

Several icebreakers powered by nuclear reactors have been built by the former USSR and continue to be used in the far north for expedition cruises. The most recent Russian icebreaker is the *50 Years Since Victory*, which was commissioned in 2006. The *Arktika*—the first of three larger nuclear icebreakers, powered by two 175 MWt reactors each—is to be placed in service in 2019.

22.2 ENERGY CONVERSION METHODS

Besides using nuclear energy, remote power generation can be accomplished with chemical and solar energy sources. For instance, chemical fuels serve to launch and return space vehicles. Fig. 22.3 shows that for long-duration missions requiring kilowatts of electric power, nuclear reactors are the energy source of choice while for lower power requirements, photovoltaic and radioisotopic sources are in competition. However, deep space probes cannot exploit solar energy due to the faintness of sunlight.

Reactors and radioisotopes both produce heat, but if electricity is the desired energy form, then a means to convert thermal energy to electrical energy must be employed. Terrestrial reactors utilize dynamic heat engines such as the Rankine (vapor) and Brayton (gas) power cycles, which are also options for space reactors. Alternatively, static power conversion methods such as thermoelectrics and thermionics may be used. Thermoelectrics rely upon the Seebeck effect in which two dissimilar materials generate a voltage potential when their junctions are at different temperatures. This phenomenon is the principle upon which temperature-measuring thermocouples are based. For example,

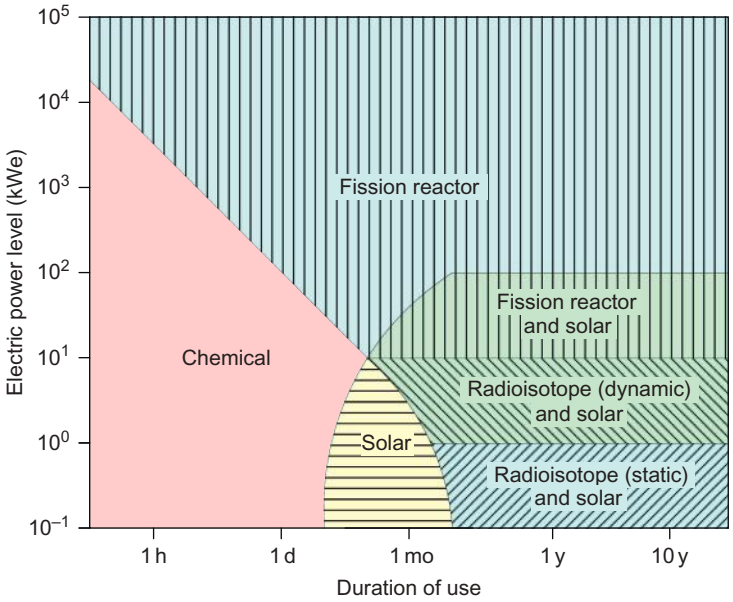

FIG. 22.3

Relative regimes of applicability for remote power generation by various energy sources.

thermocouples placed at the top of light water reactor cores measure the coolant exit temperature. Traditional Type K thermocouple materials are chromel-alumel, whereas lead-telluride (PbTe) and silicon-germanium (SiGe) typically comprise the thermoelectrics used for electricity production. Both reactors and radioisotopes have exploited thermoelectric materials to accomplish electricity generation.

While the efficiencies of the thermoelectric and thermionic conversion processes are Carnot cycle limited (see Eq. 17.12), some other direct energy conversion schemes, such as betavoltaics and fission cells, do not suffer from such restrictions. Commercial betavoltaic batteries using tritium are available for use in terrestrial applications. For instance, NanoTritium batteries like that shown in Fig. 22.4 can produce 50–350 nA at an open circuit voltage of 0.8–2.4 V. The small current output can continuously (trickle) charge a second battery. The pure beta emitter H-3, 12.32-y half-life, has been utilized in other devices such as exit signs.

EXAMPLE 22.2

If the conversion efficiency of a 1-μW betavoltaic unit employing H-3 is 3%, compute the electric power output of the unit when it is 10 years old. Since the power generation is proportional to the activity ($P \propto A$), the radioactive decay relation may be applied directly

$$P(t) = P_0\left(\frac{1}{2}\right)^{t/t_H} = (1\ \mu\text{W})\left(\frac{1}{2}\right)^{(10\ \text{y})/(12.32\ \text{y})} = 0.57\ \mu\text{W}$$

FIG. 22.4

Betavoltaic battery as a dual in-line package using tritium.

Courtesy City Labs, Inc.

22.3 SPACE REACTORS

Many years before the advent of the space program, an attempt was made to develop an aircraft reactor. The US Air Force started a project with the acronym NEPA (Nuclear Energy for the Propulsion of Aircraft) at Oak Ridge in 1946. The basis for the program was that nuclear weapon delivery would require supersonic long-range (12,000 miles) bombers not needing refueling. As part of this effort, Heat Transfer Reactor Experiment (HTRE) 1, 2, and 3 were carried out at the NRTS in Idaho. An important technical question that still exists is how to shield a crew without incurring excessive weight. As described by Hewlett and Duncan (1972), the program suffered from much uncertainty, changes of management, and frequent redirection. It was transferred from Oak Ridge to Cincinnati under General Electric as the Aircraft Nuclear Propulsion (ANP) program. The $1 billion effort was terminated in 1961 for several reasons: (1) the need for a much larger airplane than expected, (2) improvements in performance of chemically fueled jet engines, and (3) the selection of intercontinental ballistic missiles to carry nuclear weapons. Some useful technical information had been gained, but the project never came close to its objective.

The space program was given new impetus in 1961 with US President John F. Kennedy's goal of a manned lunar landing. Other missions visualized were manned exploration of the planets and ultimately colonization of space. For such long voyages requiring high power, the light weight of nuclear fuel made reactors a logical choice for both electrical power and propulsion. One concept that was studied extensively was ion propulsion, with a reactor supplying the electric energy needed to

accelerate the ions that give thrust. A second approach involved a gaseous core reactor in which a mixture of uranium and a gas would be heated by the fission reaction and expelled as propellant. Another more exotic idea, known as nuclear pulse propulsion, was to explode a number of small nuclear weapons external to a plate mounted on the space vehicle, with the reaction to the explosion giving a repetitive thrust (Schmidt et al., 2002).

Fission reactors with thermoelectric conversion systems were developed in the period 1955–70 by the Atomic Energy Commission. Its contractor, Atomics International, conducted the Systems for Nuclear Auxiliary Power (SNAP) program. The most successful of these was SNAP-10A, which was the first and only US reactor to be flown in space (Voss, 1984). Two systems were built: one tested on Earth, the other put in orbit. Their fuel was an alloy of highly enriched uranium and zirconium hydride (^{235}U-ZrH) to operate at high temperatures (810 K). The coolant was liquid sodium-potassium (NaK) for efficient heat transfer. The NaK was circulated through the reactor and a thermoelectric converter system that produced 580 W of electrical power. The total weight of one system, shown in Fig. 22.5, was 435 kg. The space version was launched in 1965 by an Agena rocket and started up by remote control. It operated smoothly in orbit for 43 d until it was accidentally shut down by an electric failure

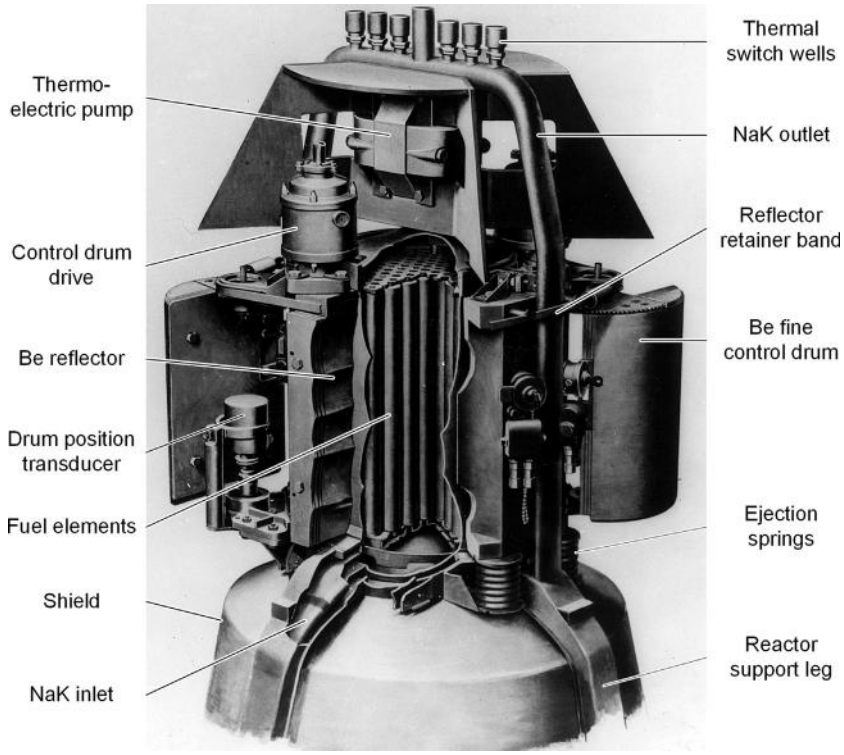

FIG. 22.5

The SNAP-10A reactor.

Courtesy US Department of Energy.

in the spacecraft. The ground version operated satisfactorily for 10,000 h. Bennett (1989) provides further details. Another successful reactor, SNAP-8, used mercury as a coolant with conversion to 50 kW of electric power in a Rankine cycle. Further details of these reactors appear in the book by Angelo and Buden (1985).

Unlike terrestrial power stations that typically dissipate condenser heat to nearby bodies of water, space-based systems radiate waste heat into outer space. The Stefan-Boltzmann law describes the heat rejection by thermal radiation

$$Q_W = \sigma \varepsilon A \left(T_r^4 - T_s^4\right) \tag{22.1}$$

in which σ is the Stefan-Boltzmann constant; ε and A are the emissivity and area of the radiator surface, respectively; and T_r and T_s are the temperatures of the radiator and outer space, respectively. Such thermal radiators, which are used for both thermoelectric converters and thermodynamic cycles, tend to be large due to the low thermal efficiencies and must be designed to withstand meteoroids.

EXAMPLE 22.3

Let us estimate the radiator surface area required for the SNAP-10A reactor. Using Eq. (17.13) and the results of Exercise 22.5, the waste heat is

$$Q_W = Q_R - P_e = 36{,}300\,\text{W} - 580\,\text{W} = 35{,}700\,\text{W}$$

For an emissivity of 0.9 and radiator temperature of 321°C, the needed surface area would be

$$A = \frac{Q_W}{\sigma \varepsilon \left(T_r^4 - T_s^4\right)} = \frac{35{,}700\,\text{W}}{\left(5.67 \times 10^{-8}\,\text{W}/\left(\text{m}^2\,\text{K}^4\right)\right)(0.9)\left[(321 + 273\,\text{K}) - 0\right]^4} = 5.62\,\text{m}^2$$

where the temperature of space is set to zero, even though in orbit, the Earth presents a nearby warm body.

The nuclear system that received the most attention in the space program was the solid core nuclear rocket. The nuclear thermal rocket shown in Fig. 22.6 is a relatively simple device. Hydrogen propellant is stored in a tank as a liquid. Liquid hydrogen would be heated to a high temperature as gas on

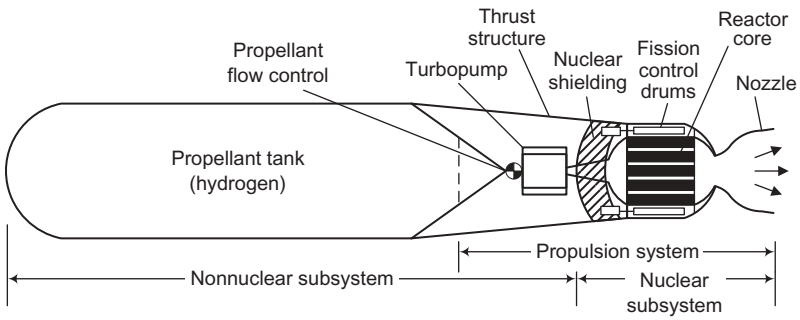

FIG. 22.6

Nuclear-thermal rocket system. Hydrogen stored in liquid form is heated in the solid core and expelled as propellant.

Courtesy Gary Bennett.

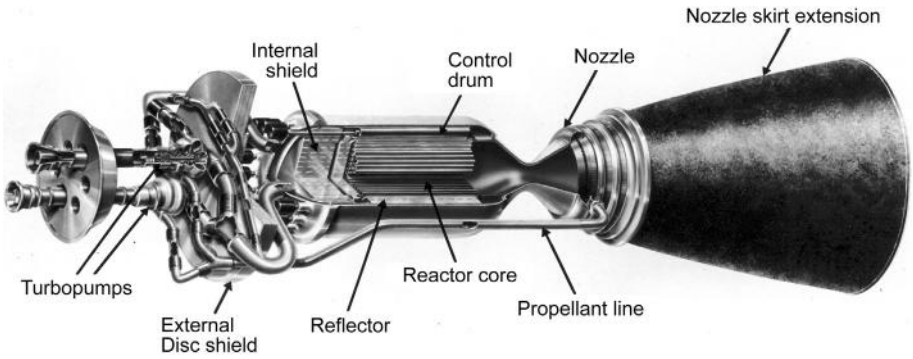

FIG. 22.7

NERVA thermodynamic nuclear rocket engine.

Courtesy NASA.

passing through holes in a reactor with a graphite moderator and highly enriched uranium fuel. In the proposed vehicle, the hydrogen would be exhausted as propellant through a nozzle.

The Rover project at Los Alamos was initiated in 1955 with a manned mission to Mars intended. Hydrogen propellant would minimize flight time because its specific impulse would be approximately twice that of typical chemical fuels. A series of reactors named Kiwi, NRX, Pewee, Phoebus, and XE-Prime were built and tested at the Nuclear Rocket Development Station in Nevada. The systems used uranium carbide fuel, a graphite moderator, and once-through hydrogen coolant, entering as a liquid and leaving as a gas. The best performance obtained in the Nuclear Engine for Rocket Vehicle Application (NERVA) program was a power of 4000 MW for 12 min (Angelo and Buden, 1985). Fig. 22.7 depicts the liquid H_2 injection into the regeneratively cooled nozzle from which the H_2 travels to the core inlet for heating. The control drums are comprised of a beryllium neutron reflector that can be rotated outward to reduce the power level (Esselman, 1965). The program was a technical success but was terminated in 1973 because of a change in National Aeronautics and Space Administration (NASA) plans. After the lunar landing in the Apollo program, a decision was made not to have a manned Mars flight. It was judged that radioisotope generators and solar power would be adequate for all future space needs.

Various R&D programs on space reactors to provide electric power were initiated subsequently (e.g., the SP-100, which was to be a reactor in the 100-kW to 1-MW range). Most of the projects were eventually canceled. Long-range missions for the 21st century planned by NASA include a manned Mars mission, which will likely require a nuclear power supply. It is noteworthy that the reactors developed for rocket propulsion were of much greater power than those constructed for electricity generation.

22.4 RADIOISOTOPIC POWER

The SNAP program included reactors, which were the even-numbered units, and devices that relied upon radioisotopes, which were the odd-numbered units. Table 22.1 lists characteristics of radionuclides that might be suitable as standalone power sources. Selection criteria include the half-life, which

Table 22.1 Practical Radioisotopes for Power

Radioisotope	Half-Life (y)	Chemical Form	Typical Specific Power (W/g)	Unshielded Dose Rate (mrem/h)[a]	
				Gammas	Neutrons
^{60}Co	5.271	Metal	1.7	7×10^7	–
^{90}Sr	28.79	$SrTiO_3$	0.23	2×10^6	–
^{137}Cs	30.08	Glass	0.067	6×10^7	–
^{144}Ce	0.780	Ce_2O_3	1.0	8×10^6	–
^{147}Pm	2.6234	Pm_2O_3	0.27	4×10^4	–
^{170}Tm	0.3521	Tm_2O_3	1.2	1.2×10^6	–
^{210}Po	0.3789	GdPo	81.5	150	2.5
^{238}Pu	87.7	PuO_2	0.39	2.0	80
^{242}Cm	0.4457	Cm_2O_3	98	90	300
^{244}Cm	18.1	Cm_2O_3	2.27	150	3000

[a]*From a 1-kW source at a distance of 1 m.*
Data from Lubarsky, B., 1969. Nuclear power systems for space applications. In: Advances in Nuclear Science and Technology, vol. 5, pp. 223–323.

needs to be appropriate to the mission duration. The radioisotope generally manifests as a compound, thereby increasing the deployed mass and decreasing the typical specific power. The *specific power* of a radioisotope may be determined from

$$SP = SA\,E_d \tag{22.2}$$

in which SA is its specific activity defined in Eq. (3.14), and E_d is the energy release per decay. As the alpha and beta particle emissions of these radionuclides constitute the majority of the harnessed energy, any gamma ray and neutron emissions, which originate from spontaneous fission and (α, n) reactions, must be managed. Radioisotopes used in the SNAP generators include strontium-90, cerium-144, polonium-210, plutonium-238, and curium-242.

EXAMPLE 22.4

Per Table 3.2, Co-60 releases a 0.318-MeV beta and two gammas of total energy 2.505 MeV. With an average β energy of approximately one-third the maximum, the energy per decay is $E_d \cong (0.318\,\text{MeV})/3 + 2.505\,\text{MeV} = 2.611\,\text{MeV}$. Using the specific activity found in Example 3.4, the specific power of Co-60 is

$$SP = SA\,E_d = \left(4.19 \times 10^{13}\,\text{Bq/g}\right)\left(2.611\,\text{MeV/decay}\right)\left(1.602 \times 10^{-13}\,\text{J/MeV}\right) = 17.52\,\text{W/g}$$

Depending on the energy conversion method, not all this energy may be recoverable, for instance, the gamma rays penetrate thin materials.

While reactors can produce large amounts of power, the output of radionuclide-based units is more limited. Besides systems designed for space, radioisotopes have served as the power source for navigation buoys (SNAP-7A), remote weather stations (SNAP-7D), and cardiac pacemakers. The annual

radiation dose to the spouse of an individual outfitted with a ^{238}Pu-powered pacemaker has been estimated at approximately 10 mrem (0.1 mSv) (McKee et al., 1974). When the use of a chemical-fueled power unit is not possible because of problems in fuel delivery or operability, an isotopic source is very practical even for terrestrial applications, despite the high cost.

For long missions such as interplanetary exploration, in which it is necessary to supply electric power to control and communication equipment for years, nuclear power is needed. The radioisotope thermoelectric generator (RTG) has been developed and used successfully for many missions. It uses a long-lived radionuclide to supply heat that is converted into electricity. The power source has many desirable features:

(a) Lightness and compactness, to fit within the spacecraft readily.
(b) Long service life.
(c) Continuous power production.
(d) Resistance to environmental effects such as the cold of space, radiation, and meteorites.
(e) Independence from the sun, permitting visits to distant planets.

The isotope used to power the RTGs is Pu-238, half-life 87.74 y, which emits alpha particles of 5.5 MeV. The high-energy alpha particles and the relatively short half-life of Pu-238 give the isotope the high specific activity of 17 Ci/g (0.63 TBq/g) and the favorable power-to-weight ratio quoted to be 0.555 W/g (Exercise 22.1). The radionuclide is produced by reactor neutron irradiation of the almost-stable isotope Np-237, half-life 2.14×10^6 y.

$$\begin{aligned} {}^{237}_{93}\mathrm{Np} + {}^{1}_{0}\mathrm{n} &\rightarrow {}^{238}_{93}\mathrm{Np} \\ {}^{238}_{93}\mathrm{Np} &\rightarrow {}^{238}_{94}\mathrm{Pu} + {}^{0}_{-1}\mathrm{e}^{-1} \end{aligned} \tag{22.3}$$

The Np-237 is a decay product of U-237, a 6.75-d beta emitter that arises from neutron capture in U-236 or by (n, 2n) and (γ, n) reactions with U-238. Presently, the available supply of Pu-238 is dwindling (National Research Council, 2009).

To help maintain proper temperatures for sensitive electronic components, small (2.7 g, 1 W) Pu-238 sources—radioisotope heating units (RHUs)—are sometimes provided. These were used in the missions to distant planets and also in the Sojourner minirover that explored the surface of Mars as well as the Spirit and Opportunity rovers, which carried eight RHUs each (Bennett, 2008).

Other isotopes that can be used for remote unattended heat sources are the fission products strontium-90 in the form of SrF_2 and cesium-137 as CsCl. If the two isotopes were extracted by fuel reprocessing to reduce the heat and radiation in radioactive waste, many applications would surely materialize.

The earliest ^{238}Pu use for supplying electric power was in the Transit navigation satellites of the early 1960s. Subsequent use included Pioneer 10, launched in 1972, and Pioneer 11, launched in 1973; these missions were to explore Jupiter. The last radio signal from Pioneer 10 was received on January 22, 2003. The spacecraft was then 7.6 billion miles from Earth, after more than 30 y in space. It was powered by an RTG of initial power 160 W along with several one-watt RHUs. These two spacecraft have departed the solar system.

Typical of the RTGs is the one sent to the moon in the Apollo 12 mission. It powered a group of scientific instruments called Apollo Lunar Surface Experimental Package (ALSEP), which measured magnetic fields, dust, the solar wind, ions, and earthquake activity. The generator is shown

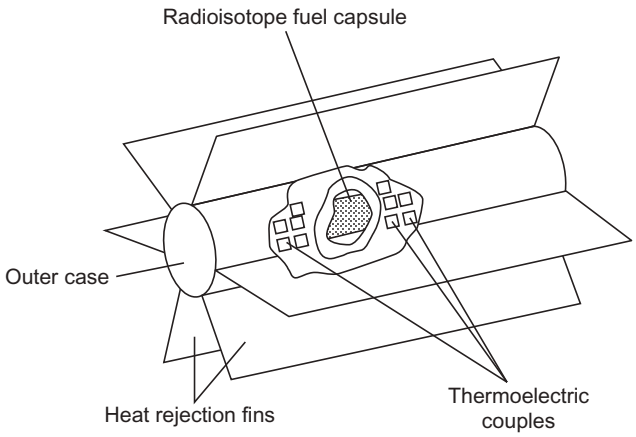

FIG. 22.8

Radioisotopic electrical power generator (SNAP-27 used in Apollo 12 mission).

Table 22.2 Radioisotope Thermoelectric Generator SNAP-27	
System mass 20 kg	Thermal power 1480 W
Pu-238 mass 2.6 kg	Electrical power 74 W
Activity 44,500 Ci	Electrical voltage 16 V
Capsule temperature 732°C	Operating range −173°C to 121°C

schematically in Fig. 22.8. Lead-telluride thermoelectric couples were placed between the PuO_2 and the beryllium case. Data on the generator, called SNAP-27, are listed in Table 22.2.

EXAMPLE 22.5

Using Table 22.2 data, the thermal-to-electric efficiency of the SNAP-27 generator is

$$\eta_{th} = P_e/Q_{th} = (74\,\text{W})/(1480\,\text{W}) = 0.05$$

This 5% efficiency pales in comparison to that of a nuclear power plant, but radioisotopic-powered units need to be compact and equipment mass must be limited for space-borne applications.

The SNAP-27 generator was also used in several other Apollo missions, and data were returned to Earth for the period 1969–77. For the 1975 Viking mission, the somewhat smaller SNAP-19 powered the Mars landers, which sent back pictures of the surface of that planet.

An advanced model, called multihundred watt (MHW), provided all electrical power for the two Voyager spacecraft, designed and operated by the Jet Propulsion Laboratory of NASA. They were launched in the summer of 1977 and reached Jupiter in 1979 and Saturn in late 1980 and early 1981, sending back pictures of Saturn's moons and rings. Voyager 1 was then sent out of the solar system to deep space. Taking advantage of a rare alignment of three planets, Voyager 2 was redirected

to visit Uranus in January 1986. The reliability of the power source after 9 y in space was crucial to the mission. Because of limited light at 2.9 billion kilometers from the sun, long exposure times of photographs and thus great stability of the spacecraft were needed. By sending radio signals to Voyager 2, the onboard computers were reprogrammed to allow very small corrective thrusts (Laeser et al., 1986). Several new moons of Uranus were discovered, including some whose gravity stabilizes the planet's rings. Voyager 2 arrived at Neptune in 1989; it then went on to outer space. The MHW generator used silicon-germanium as thermoelectric material rather than lead-telluride; each generator was heavier and more powerful than SNAP-27. Similar power supplies were used for the Lincoln Experimental Satellites (LES 8/9), which communicated with each other and with ships and aircraft.

A still larger supply, called General Purpose Heat Source (GPHS), was used in the Galileo spacecraft sent out in October 1990 toward Jupiter. On its way, it photographed the asteroids Gaspra and Ida, viewed the impacts of the Shoemaker-Levy 9 comet on the surface of Jupiter, and made flybys of moons Io and Europa. A battery-powered instrumented probe was sent down through Jupiter's atmosphere. Studies of this distant planet complement those made of nearby Venus by the solar-powered Magellan. Pictures of the moon Europa indicate an icy surface of a liquid ocean. The mission ended when the spacecraft entered Jupiter's heavy atmosphere.

The spacecraft Ulysses, launched in November 1990, was also powered by a GPHS. It was a cooperative mission between the United States and Europe to study the solar wind—a stream of particles from the Sun—and the star's magnetic field. Ulysses had to rendezvous with Jupiter to use the planet's gravity to take the spacecraft out of the ecliptic (the plane in which the planets move) to pass through the Sun's poles.

The Cassini spacecraft, launched in 1997 toward Saturn and its moon Titan, contained three RTGs to power instruments and computers, each with approximately 10.9 kg of PuO_2. The total power was initially 888 We. In addition to radio power, RTGs were used to keep the electronic components warm. Unusual views of the planet's rings were obtained. The accompanying Huygens probe landed on Titan.

The spacecraft New Horizons with a 246-We GPHS-RTG was launched in 2006 to go past Jupiter to Pluto in 2015 and the Kuiper Belt in 2019. There, many planetary objects will be encountered.

Power supplies planned for missions of the more distant future will be in the multikilowatt range, have high efficiency, and make use of a different principle. In the dynamic isotope power system (DIPS), the isotopic source heats the organic fluid Dowtherm A, the working fluid for a Rankine thermodynamic cycle, with the vapor driving a turbine connected to an electric generator. In a ground test, the DIPS operated continuously for 2000 h without failure. Angelo and Buden (1985) give details of all these RTGs.

Success with power sources for space applications prompted a program to develop a nuclear-powered artificial heart (Mott, 1975). It involved a Pu-238 heat source, a piston engine, and a mechanical pump. The research program was suspended and is unlikely to be revived, with the advent of battery-powered implantable artificial hearts.

22.5 FUTURE NUCLEAR SPACE APPLICATIONS

The extent to which nuclear processes are used in space depends on the degree of commitment to a space program. Over the years, enthusiasm for space programs has varied greatly in the United States. The Russian Sputnik satellite of 1957 prompted a flurry of activity; Kennedy's proposal to put a man on

the moon gave the space effort new impetus. NASA programs are inevitably affected by the priorities of the presidential administration and Congress.

In 1989, US President George H.W. Bush announced a new program called Space Exploration Initiative (SEI), involving returning to the moon and establishing a base there, then a manned trip to the planet Mars. A report by the Synthesis Group (1991) discussed justification and strategies. One nuclear aspect of the project was the possibility of mining helium-3 from the surface of the moon for use in fusion reactors, as discussed in Section 26.5. Congress did not accept the proposed SEI program, and more modest NASA activities involving unmanned spacecraft such as Mars Pathfinder took its place. The exploration of the surface of Mars by the remotely controlled Sojourner minirover was viewed on television by millions of people.

US President George W. Bush revived prospects for a Mars mission. The first step would be to return to the moon. The objective would be exploration for scientific knowledge, to prepare for a base there, and to gain experience relevant to a human visit to Mars. The method by which travel would be made has not been firmly decided. Originally, a nuclear rocket of the NERVA type was considered. Later, electric propulsion with ions providing thrust was proposed, and still later, matter-antimatter annihilation energy generation was suggested. However, NASA has indicated that a Mars mission would be sometime in the 2030s. Some believe that a manned trip to an asteroid would be easier and less expensive.

Whatever the mode of transport to Mars, it is presumed that an initial unmanned vehicle would carry cargo, including a habitat and reactor for power on the planet's surface. Both timing and duration are important factors for a manned mission. Travel to Mars would take approximately 160 d, allowing 550 d for exploration, until the planets are in correct position for return, which would take 160 d again. Only nuclear power is available for such a schedule. For the descent and ascent between Mars orbit and the planet's surface, chemical rockets would be needed. Studies of geology and microbiology would be carried out, investigating further the possibility of life forms. The fuel produced on Mars—methane (CH_4) and liquid oxygen—would come from the thin CO_2 atmosphere and the supply of H_2 brought from Earth.

For power to process materials on the moon, a small reactor might be used. Potential resources include water, oxygen, and hydrogen. With adequate heat, the fine dust (regolith) that covers the surface could be formed into bulk solids for construction and radiation shielding. Helium-3 as a fuel for a fusion reactor could be recovered for return to Earth. Presently, NASA and the Department of Energy are developing a fission reactor that generates up to 10 kW of electrical power by using heat pipe technology coupled to Stirling engines.

The reason space travel by nuclear rocket is advantageous can be seen from the mechanics of propulsion. In deep space, a spacecraft is free of gravitational and atmospheric drag forces acting upon it. Applying conservation of linear momentum, the instantaneous thrust of the rocket is

$$T = \dot{m}_p v_p = ma \tag{22.4}$$

where $\dot{m}_p$ is the propellant flow rate; v_p is the speed of the exhaust gases relative to the rocket; and m and a are the rocket mass and acceleration. The *specific impulse* I_{sp}, which is a measure of rocket efficiency in terms of the delivered thrust provided by a given exhaust gas flow rate, is the propellant exhaust velocity, that is,

$$I_{sp} \equiv T/\dot{m}_p = v_p \tag{22.5}$$

The corresponding power requirement is $Tv_p/2$.

Integrating the earlier expression for thrust yields the Tsiolkovsky rocket equation relating increased spacecraft velocity Δv to the initial and final masses m_i and m_f of the rocket

$$\Delta v = v_f - v_i = v_p \ln(m_i/m_f) \tag{22.6}$$

with the mass of exhausted fuel being $m_i - m_f$.

Drawing upon Section 2.2, the exhaust velocity is related to the gas absolute temperature T_p and its molecular mass M_p via $v_p \propto \sqrt{T_p/M_p}$. The burning products of a chemical system are relatively heavy molecules; for example, the combustion of hydrogen forms water with $M_p = 18$. In comparison, a nuclear reactor can heat light hydrogen gas ($M_p = 2$). Thus for a given temperature, v_p is much larger for a nuclear system and m_f is closer to m_i (i.e., less fuel is needed).

To escape from the Earth or from an orbit around the Earth requires work to be done on the spacecraft against the force of gravity. The escape velocity v_e for vertical flight is

$$v_e = \sqrt{2 g_0 r_E} \tag{22.7}$$

in which g_0 is the acceleration of gravity at the Earth's surface, 32.174 ft/s^2 or 9.80665 m/s^2, and r_E is the radius of the Earth, approximately 3959 miles or 6371 km.

Calculations of trajectory can be made with the program ORBIT, described in Computer Exercise 22.A.

EXAMPLE 22.6

Inserting numbers for Earth into Eq. (22.7), we find the escape velocity to be

$$v_e = \sqrt{2 g_0 r_E} = \sqrt{(2)(9.807 \times 10^{-3}\,\text{km/s}^2)(6371\,\text{km})} = 11.2\,\text{km/s}$$

This is approximately 36,700 ft/s or 25,000 mi/h.

The Challenger shuttle accident in 1986 resulted in increased attention to safety. It also raised the question as to the desirability of the use of robots for missions instead of human beings. The benefit is protection of people from harm; the disadvantage is loss of capability to cope with unusual situations. Among the hazards experienced by astronauts are high levels of cosmic radiation outside the Earth's atmosphere, possible impacts of small meteorites on the spacecraft, debilitating effects of long periods of weightlessness, and in the case of a nuclear-powered vehicle, radiation from the reactor. If a reactor were used for transport, to avoid the possibility of contamination of the atmosphere with fission products if the mission is aborted, the reactor would be started only when it is safely in Earth orbit.

For power supplies that use radioisotopes, encapsulation of the Pu-238 with iridium and enclosing the system with graphite fiber reduce the possibility of radioactivity release. For space missions, risk analyses analogous to those for power reactors are carried out.

Sometime in the distant future, electric propulsion may be used. Charged particles are discharged backward to give a forward thrust. Its virtue is the low mass of propellant that is needed to permit a larger payload or a shorter travel time. Several possible technologies exist:

(1) Electrothermal, including arcjets and resistojets (in which a propellant is heated electrically).
(2) Electrostatic, which uses an ion accelerator.
(3) Electromagnetic, such as a coaxial magnetic plasma device.

The distinction between electric propulsion and thermal propulsion is in the ratio of thrust and flow rate of propellant, which is the specific impulse, I_{sp}. For example, the shuttle launcher has a high thrust but also a high flow rate, and its I_{sp} is approximately 450 s. Electric propulsion has a low thrust but a very low flow rate, giving an I_{sp} of some 4000 s.

Prospects for nuclear power for space propulsion have waxed and waned over many decades. Project Prometheus was designed to use a nuclear reactor as a power source, driving an ion engine that expels xenon ions for its thrust. The engine was successfully tested on the ground in 2003. Speeds were expected to be up to 200,000 miles per hour (300,000 km/h), 10 times that of the space shuttle. The system was originally intended for an exploration of Jupiter's icy moons, but the mission was shifted to the Earth's moon. A decision was then made to suspend or possibly abandon Prometheus in favor of some other approach. The ion engine concept will be retained, however. The spacecraft Dawn, launched in 2007 toward asteroids Vesta and Ceres, has solar-powered ion engines rather than an RTG, but its detectors are unique. The 21 sensors measure cosmic ray gammas and neutrons that bounce off the asteroids, providing information about composition.

Looking into the very distant future, some scientists contemplate the terraforming of Mars by the introduction of chemicals that change the atmosphere and ultimately permit the normal existence of life forms. Finally, the vision is always present of manned interstellar travel, paving the way for colonization of planets outside our solar system. The discovery of a number of stars with planets has given encouragement to that idea.

What the future of nuclear applications in space will be depends on the accomplishments and aspirations of humanity in space. The urge to investigate and understand is a strong and natural aspect of the human psyche, and some say it is desirable or necessary to plan for interplanetary colonization. Supporters of space exploration cite its many spinoff benefits. Others remind us that there are many serious problems on Earth that need attention and money. How to balance these views remains an issue to be resolved by the political process.

22.6 SUMMARY

Nuclear reactors serve as the power source for the propulsion of submarines and aircraft carriers. Tests of reactors for aircraft and for rockets have been made, and reactors are being considered for future space missions. Thermoelectric generators that use Pu-238 provided electric power for lunar exploration in the Apollo program and for interplanetary travel of the spacecrafts Voyager, Galileo, Ulysses, and Cassini.

22.7 EXERCISES

22.1 Using decay data from Table 3.2, verify that plutonium-238 yields a specific activity of 17 Ci/g and a specific power of 0.555 W/g. (b) Determine the plutonium mass and activity needed for a 200-μW heart pacemaker having an efficiency of 0.5%.

22.2 Note that the force of gravity varies inversely with R^2 and that centrifugal acceleration balances gravitational attraction for an object of mass m and velocity v orbiting a second object of mass M, that is,

$$mv^2/R = GmM/R^2$$

where G is the gravitational constant. (a) Show that the velocity of a satellite at height h above the Earth is,

$$v_s = r_E\sqrt{g_0/(r_E + h)}$$

where g_0 is the acceleration of gravity at the surface of the Earth, of radius r_E. (b) Calculate the velocity of a spacecraft in orbit at 100 miles above the Earth. (c) Derive a formula and calculate h in miles and kilometers for a geosynchronous (24 h) communications satellite.

22.3 If the exhaust velocity of rocket propellant is 11,000 ft/s (3.3528 km/s), what percent of the initial mass must be fuel for vertical escape from the Earth?

22.4 Assuming that only the beta energy is recoverable, compute the specific power of (a) Co-60, (b) Cs-137, and (c) Sr-90 with Y-90 in secular equilibrium.

22.5 The overall efficiency of the SNAP-10A power system was 1.6% (Voss, 1984). Determine: (a) the reactor power, and (b) the specific power for a total uranium mass of 5.173 kg. Note that the specific power for a reactor is computed differently from that of a radioisotope.

22.6 The solar constant, which is the amount of solar radiation just outside the Earth's atmosphere, is 1.353 kW/m^2. If the Earth is $r_E = 150 \times 10^6$ km from the Sun, find the corresponding sunlight intensity at (a) Mars ($r_M = 228 \times 10^6$ km), (b) Saturn ($r_S = 1.43 \times 10^9$ km), (c) Uranus ($r_U = 2.87 \times 10^9$ km), and (d) Neptune ($r_N = 4.50 \times 10^9$ km).

22.7 Calculate the thermal-to-electric efficiency of the Cassini power system.

22.8 An RTG employing Pu-238 is required to supply 100 W of electric power for a 24-y mission. For a conversion efficiency of 4%, determine the initial loading (a) activity of Pu and (b) mass of PuO_2.

22.9 The N.S. *Savannah* had a range of 560,000 km at a speed of 20 knots for a single fuel loading. (a) Compute the U-235 mass consumed for these specifications. (b) Calculate the volume of diesel fuel required to provide the same power, if a barrel of oil releases 5.8×10^6 Btu.

22.10 Determine the total buildup of helium from the decay of a 2.7 g ^{238}Pu fueled RHU after 5 y (without venting).

22.8 COMPUTER EXERCISES

22.A The initial velocity of a rocket ship determines whether it falls back to Earth, goes into orbit about the Earth, or escapes into outer space. The program ORBIT calculates the position of a spacecraft and its distance from the center of the Earth for various input values of the starting point and tangential velocity. (a) Try 100 and 290 miles per minute. (b) Explore various starting points and velocities. Comment on the results.

22.B A trip to Mars will probably be made in a spacecraft assembled in orbit around the Earth at altitude of, for instance, 100 miles (160.9 km). (a) Find its initial speed with the formula for v_S in Exercise 22.2. What is its period, as the time for one revolution? (b) With computer program ALBERT from Chapter 1, find the fractional increase of mass of the ship (and the astronauts) at that speed.

REFERENCES

Angelo Jr., J.A., Buden, D., 1985. Space Nuclear Power. Orbit Book Co., Malabar, FL. A definitive textbook.

Bennett, G.L., 1989. Historical overview of the US use of space nuclear power. Space Power 8 (3), 259–284.

Bennett, G.L., 2008. Mission interplanetary: using radioisotope power to explore the solar system. Energy Convers. Manag. 49 (3), 382–392.

Esselman, W.H., 1965. The NERVA nuclear rocket reactor program. Westinghouse Eng. 25 (3), 66–75.

First Atomic Ship Transport Inc. (FASTI), 1968. NS Savannah Safety Assessment, Rev III; 1968.

Freire, L.O., de Andrade, D.A., 2015. Historic survey on nuclear merchant ships. Nucl. Eng. Des. 293, 176–186.

Hewlett, R.G., Duncan, F., 1972. A History of the United States Atomic Energy Commission: Atomic Shield, 1947/1952. vol II. U.S. Atomic Energy Commission (AEC), Washington, DC.

Hewlett, R.G., Duncan, F., 1974. Nuclear Navy 1946–1962. University of Chicago Press, Chicago.

Ishida, T., Kusunoki, T., Ochial, M., Tanaka, Y., Yao, T., Inoue, K., 1993. Response to severe changes of load on the reactor system of nuclear ship Mutsu. J. Nucl. Sci. Technol. 30 (2), 116–130.

Laeser, R.P., McLaughlin, W.I., Wolff, D.M., 1986. Engineering Voyager 2's encounter with Uranus. Sci. Am. 255 (5), 36–45. Discusses the power problem caused by decay of Pu-238 in RTGs.

Maritime Administration (MARAD), 2017. N.S. Savannah Program. www.marad.dot.gov/ships-and-shipping/n-s-savannah-program-home/ https://voa.marad.dot.gov/Programs/NSSavannah/Library.aspx?m=1. U.S. Department of Transportation.

McKee, R.W., Clark, L.L., Cole, B.M., Libby, R.A., 1974. Dose-to-the-population estimates for use of radioisotope powered cardiac pacemakers. BNWL-1858, Pacific Northwest Laboratories, Richland, Washington.

Mott, W.E., 1975. Nuclear power for the artificial heart. Biomater. Med. Devices Artif. Organs 3 (2), 181–191.

National Research Council, 2009. Radioisotope Power Systems: An Imperative for Maintaining U.S. Leadership in Space Exploration. National Academies Press, Washington, DC.

Schmidt, G.R., Bonometti, J.A., Irvine, C.A., 2002. Project Orion and future prospects for nuclear pulse propulsion. J. Propuls. Power 18 (3), 497–504.

Synthesis Group, 1991. America at the Threshold: Report of the Synthesis Group on America's Space Exploration Initiative. NASA, Arlington, VA. An illustrated description of the proposed goals and plans for the space trips to the Moon and Mars.

Voss, S.S., 1984. SNAP reactor overview, AFWL-TN-84-14. Air Force Weapons Laboratory, Kirtland Air Force Base, NM.

FURTHER READING

Adams, R., 2011. Why did the NS Savannah fail? Can she really be called a failure? Atomic Insights. http://www.atomicinsights.com (search for article using title). Additional information on N.S. *Savannah*.

Anderson, U.S.N., Commander, W.R., Blair Jr., C., 1959. Nautilus-90-North. World Publishing, Cleveland. An account by the chief officer of the nuclear submarine *Nautilus* of the trip to the North Pole.

Angelo Jr., J.A., 2001. Encyclopedia of Space and Astronomy. Facts on File, New York.

Bukharin, O., 2006. Russia's nuclear icebreaker fleet. Sci. Glob. Secur. 14 (1), 25–31.
El-Genk, M.S. (Ed.), 1994. A Critical Review of Space Nuclear Power and Propulsion, 1984–1993. AIP Press, New York Includes papers on radioisotope generators and nuclear thermal propulsion.
El-Wakil, M.M., 1982. Nuclear Energy Conversion. American Nuclear Society, La Grange Park.
Lubarsky, B., 1969. Nuclear power systems for space applications. In: Advances in Nuclear Science and Technology. vol. 5. Academic Press, New York, pp. 223–323.
Nautilus Museum, http://www.ussnautilus.org. History, tour, and links.
NavSource Naval History, Photographic History of the U.S. Navy. http://navsource.org/. Specifications, histories, and photographs.
Nuclear Engineering and Design Nucl. Eng. Des. 10 (2), 123-258. (June 1969 issue with ten papers about the N.S. Mutsu).
Rockwell, T., 1992. The Rickover Effect: How One Man Made a Difference. Naval Institute Press, Annapolis. Describes the key role Admiral Rickover had in the United States Navy's nuclear submarine program and the first nuclear power plant.
Simpson, J.W., 1995. Nuclear Power from Underseas to Outer Space. American Nuclear Society, La Grange Park, IL. History of the development of the nuclear submarine *Nautilus*, the first commercial nuclear power plant at Shippingport, and the nuclear thermal rocket engine, NERVA.
U.S. Department of Energy (DOE), 2011. DOE/NE-0071, Nuclear Power in Space; 2011. Review of all missions by Department of Energy.
U.S. Department of Energy (DOE), Office of Science, RTG History. http://www.osti.gov/accomplishments/rtg.html. Links to many documents.

CHAPTER

RADIOACTIVE WASTE DISPOSAL

23

CHAPTER OUTLINE

Materials that contain radioactive atoms and that are deemed to be of no value are classed as radioactive wastes. They may be natural substances, such as uranium ore residues with isotopes of radium and radon, products of neutron capture with isotopes such as those of cobalt and plutonium, or fission products with a great variety of radionuclides. Wastes may be generated as byproducts of national defense efforts, of the operation of commercial electric power plants and their supporting fuel cycle, or of research and medical application at various institutions. The radioactive components of the waste may emit alpha particles, beta particles, gamma rays, and in some cases neutrons, with half-lives of concern from the standpoint of storage and disposal ranging from several days to thousands of years.

Because it is very difficult to render the radioactive atoms inert, we face the fact that the use of nuclear processes must be accompanied by continuing safe management of materials that are potentially hazardous to workers and the public. The means by which this essential task is accomplished is the subject of this chapter.

Nuclear Energy. https://doi.org/10.1016/B978-0-12-812881-7.00023-X

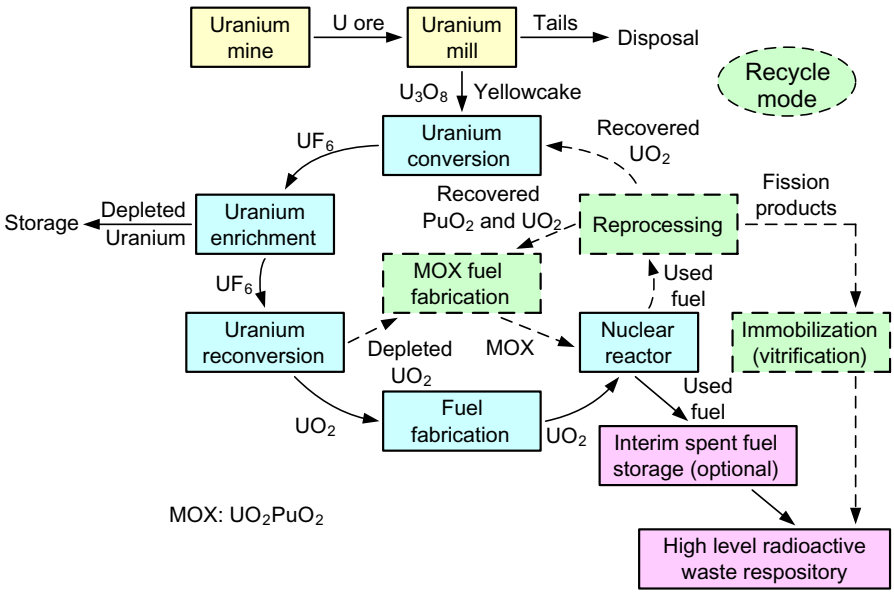

FIG. 23.1

Nuclear fuel cycles: the once-through cycle, delineated by solid lines, is used in the United States; the recycle steps, indicated by dashed lines, are used in some other countries to close the back end of the fuel cycle.

23.1 THE NUCLEAR FUEL CYCLE

Radioactive wastes are produced throughout the nuclear fuel cycle shown in Fig. 23.1. This diagram is a flowchart of the processes that start with mining and end with disposal of wastes. Two alternative modes are shown: once-through and recycle, which are sometimes referred to as open and closed cycles, respectively, although this categorization is not entirely precise.

Uranium ore contains very little of the element uranium, approximately 0.1% by weight. The ore is treated at processing plants known as mills, where mechanical and chemical treatment yields *yellowcake*, which is mainly U_3O_8 (triuranium octaoxide), and large residues called *mill tailings*. These tailings still have the daughter products of the uranium decay chain (see Fig. 3.8), especially radium-226 (1600 y), radon-222 (3.82 d), and some polonium isotopes. Tailings are disposed of in large piles near the mills, with an earth cover to reduce the rate of release of the noble radon gas and thus prevent excessive air contamination. Strictly speaking, the tailings are waste, but they are treated separately.

EXAMPLE 23.1

To realize 100 kg of U from an ore grade G of 6% U_3O_8 requires mining an ore mass of

$$m_{\text{ore}} = \frac{m_{U_3O_8}}{G} = \frac{m_U}{G}\left(\frac{3M_U + 8M_O}{3M_U}\right)$$
$$= \frac{(100\text{kg-U})[3(238) + 8(16)\ \text{kg-}U_3O_8]}{(0.06\text{kg-}U_3O_8/\text{kg-ore})[3(238\text{kg-U})]} = 1965\text{kg}$$

The corresponding mass of mill tailings is

$$m_{\text{tail}} = m_{\text{ore}} - m_{U_3O_8} = m_{\text{ore}}(1 - G) = (1965\text{kg})(1 - 0.06) = 1847\text{kg}$$

Conversion of U_3O_8 into uranium hexafluoride, UF_6, for use in isotope enrichment plants produces relatively small amounts of slightly radioactive material. The separation process, which brings the uranium-235 concentration from 0.7 to 3–5 w/o, also has little waste. It does generate large amounts of depleted uranium, known as *tails*, at approximately 0.2–0.3 w/o U-235. Depleted uranium is stored and could be used as fertile material for future breeder reactors. The fuel fabrication operation, involving the conversion of UF_6 to UO_2 and the manufacture of fuel assemblies, yields considerable waste despite recycling practices. Because U-235 has a shorter half-life than U-238, the slightly enriched fuel is more radioactive than natural uranium (see Exercise 23.1).

The operation of reactors gives rise to liquids and solids that contain radioactive materials from two sources. One is activation of metals by neutrons, producing isotopes of iron, cobalt, and nickel. The other is fission products that escape from the fuel tubes or are produced from uranium residue on their surfaces.

Spent fuel, resulting from neutron irradiation in the reactor, contains the highly radioactive fission products and various plutonium isotopes, along with the sizeable residue of uranium that is near natural concentration. According to current US practice, the used fuel will be stored, packaged, and disposed of by burial.

In some countries other than the United States, the spent fuel from commercial reactors is being reprocessed. As demarcated by dashed lines in Fig. 23.1, the recovered uranium is returned to the isotope separation facility for reenrichment, and the plutonium is combined with slightly enriched or depleted uranium fuel to produce mixed-oxide (MOX) fuel of UO_2-PuO_2. Only the fission products are subject to disposal.

23.2 WASTE CLASSIFICATION

For purposes of management and regulation, classification schemes for radioactive wastes have evolved. The first contrasts defense and nondefense wastes. The original wastes were from the Hanford reactors used in World War II to produce weapons material. The wastes were stored in moist form in large underground tanks. Over subsequent years, part of these defense wastes have been processed for two reasons: (1) to fix the wastes in stable form and (2) to separate out the two intermediate half-life isotopes, strontium-90 (29.1 y) and cesium-137 (30.1 y), leaving a relatively inert residue. Additional defense wastes were generated by reactor operation over the years for the stockpile of plutonium and tritium for nuclear weapons, and the spent fuel from submarine reactors was reprocessed.

Nondefense wastes include those produced in the commercial nuclear fuel cycle as described previously, by industry and by institutions. Industrial wastes come from manufacturers who use isotopes and from pharmaceutical companies. Institutions include universities, hospitals, and research laboratories.

Another way to classify wastes is according to the type of material and the level of radioactivity. The first class is high-level waste (HLW) from reactor operations. These are the fission products that have been separated from other materials in spent fuel by reprocessing. They are characterized by their very high radioactivity; hence the name.

A second category is spent fuel, which really should not be called a waste because of its residual fissile isotopes. However, in common use, because such used fuel in the United States is to be disposed of in a high-level waste repository, it is often thought of as HLW.

A third category is transuranic wastes, abbreviated TRU, which are wastes that contain plutonium and heavier artificial isotopes. Any material having an activity greater than 100 nanocuries per gram (3.7 kBq/g) caused by alpha-emitting transuranic isotopes with half-lives greater than 20 y is classed as TRU (40CFR191.02). The main source is nuclear weapon fabrication plants.

Mill tailings are the residue from processing uranium ore. The main radioactive elements other than residual uranium are radium-226 (1600 y) and thorium (7.54×10^4 y). Nuclear Regulatory Commission (NRC) regulations (10CFR40 Appendix A) call for covers of tailings piles to prevent the release of radon gas.

EXAMPLE 23.2

We can attempt to estimate the activity of Ra-226 within a tonne of 5% grade U_3O_8 ore. First, the mass of U-238 present in the ore is

$$\begin{aligned} m_{238} &= \omega_{238} m_{\text{ore}} G[3M_{\text{U}}/(3M_{\text{U}} + 8M_{\text{O}})] \\ &= (0.9928)(1\,\text{tonne})(0.05)\{(3)(238)/[(3)(238) + (8)(16)]\} \\ &= 0.0421\,\text{tonne} = 42.1\,\text{kg} \end{aligned}$$

in which the U-238 weight fraction ω_{238} is obtained from Exercise 15.11. If secular equilibrium exists between the U-238 and Ra-226, then the radium activity is

$$A_{226} = A_{238} = (\lambda n)_{238} = \frac{\ln(2)}{t_{H,238}} \frac{m_{238} N_{\text{A}}}{M_{238}}$$

$$= \frac{\ln(2)\left(42.1 \times 10^3\,\text{g}\right)\left(6.022 \times 10^{23}\,\text{atom/mol}\right)}{\left(4.468 \times 10^9\,\text{y}\right)\left(3.1558 \times 10^7\,\text{s/y}\right)(238\,\text{g/mol})} = 5.24 \times 10^8\,\text{Bq}$$

Geochemistry and nuclide migration differences within the uranium deposit will upset the secular equilibrium.

Another important category is low-level waste (LLW), which officially is defined as material that does not fall into any other class. LLW has a small amount of radioactivity in a large volume of inert material and is generally subject to placement in a near-surface disposal site. The name low-level waste is misleading in that some LLW can have an activity content comparable to that of some old high-level waste.

Two other categories are (1) NARM, that is, naturally occurring or accelerator-produced radioactive materials; and (2) its subset NORM, that is, naturally occurring radioactive materials that have been technologically enhanced (TENORM), such as byproducts of phosphate mining and hydraulic fracturing. Both have slight radioactivity, but are not regulated by the NRC.

Still other categories are used for certain purposes, for example, remedial action wastes, coming from the cleanup of formerly used facilities of the Department of Energy (DOE). A category called mixed LLW has the characteristics of LLW but also contains hazardous organic chemicals or heavy metals such as lead or mercury.

For a number of years, the category below regulatory concern (BRC) referred to wastes having trivial amounts of activity and subject to unrestricted release. The NRC was unsuccessful in obtaining consensus on the subject and abandoned the category around 1990.

Some perspective of the fuel cycle and nuclear wastes can be gained from Table 23.1. The 19.1–27.6 tonnes of spent fuel is to be compared with the burning of 3 million tonnes of coal with a release of 7 million tonnes of CO_2 (see Example 24.3).

Table 23.1 Typical Annual Material Balances 1000 MWe Reactor		
Fuel Enrichment (w/o)	4.5%	5%
Burnup (MW d/tonne)	45,000	65,000
Fuel supplied (UO_2) and discharged (tonne)	27.6	19.1
Enriched uranium (tonne)	24.3	16.85
Enriched UF_6 (tonne)	35.9	25
Depleted UF_6 (tonne)	276	216
Uranium ore and tailings (tonne)	20,000–400,000	

Data from World Nuclear Association, 2017. The nuclear fuel cycle. http://world-nuclear.org/information-library/nuclear-fuel-cycle/introduction/nuclear-fuel-cycle-overview.aspx.

23.3 SPENT FUEL STORAGE

The management of spent fuel at a reactor involves a great deal of care in mechanical handling to avoid physical damage to the assemblies and to minimize exposure of personnel to radiation. At the end of a typical operating period of 18–24 months for a pressurized water reactor (PWR), the head of the reactor vessel is removed and set aside. The whole space above the vessel is filled with borated water to allow fuel assemblies to be removed while immersed. The radiation levels at the surface of an unshielded assembly are millions of rem per hour. By use of movable hoists, the individual assemblies weighing approximately 600 kg (1320 lb) are extracted from the core and transferred to a water-filled storage pool in an adjacent building. Fig. 23.2 shows the arrangement of fuel assembly racks in the bottom of the spent fuel storage pool. Approximately a third of the core is removed; the fuel remaining in the core is rearranged to achieve the desired power distribution in the next cycle; and fresh fuel assemblies are inserted into the vacant spaces. The water in the 40-ft (12-m) deep storage pool serves as a shielding and cooling medium to remove the fission product residual heat. To ensure integrity of the fuel, the purity of the water in the spent fuel pool is controlled by filters and demineralizers, and the temperature of the water is maintained by use of coolers.

EXAMPLE 23.3

We may apply the decay heat formula from Section 21.4 to estimate the energy release and source strength of the used fuel. Three months (7.9×10^6 s) after shutdown, the maximum decay power from all the spent fuel of a 3000-MWt reactor is

$$P = 0.070\,P_0\,t^{-0.2} = (3000\,\text{MWt})(0.070)\left(7.9 \times 10^6\right)^{-0.2} = 8.76\,\text{MWt}$$

If we assume that the typical particles released have an energy of 1 MeV, this corresponds to an activity of 1.5 billion curies:

$$A = \frac{P}{E_d} = \frac{\left(8.76 \times 10^6\,\text{J/s}\right)}{(1\,\text{MeV/decay})\left(1.602 \times 10^{-13}\,\text{J/MeV}\right)} = 5.5 \times 10^{19}\,\text{Bq}$$

The storage facilities consist of vertical stainless steel racks that support and separate fuel assemblies to prevent criticality because the multiplication factor k of a single assembly is rather close to unity. When most reactors were designed, it was expected that fuel would be held for radioactive

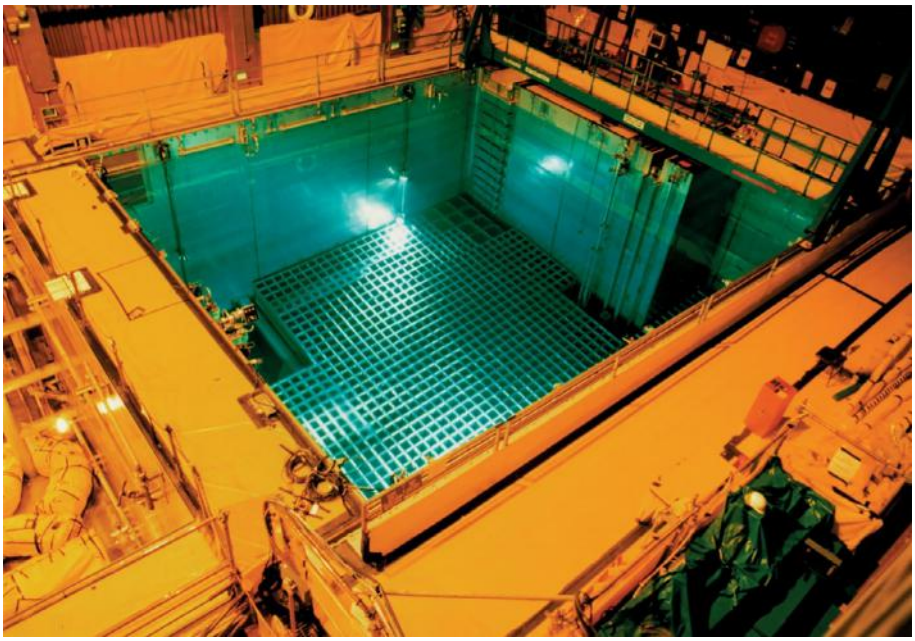

FIG. 23.2

Spent fuel pool at the San Onofre Nuclear Generating Station.

Courtesy of the NRC under Creative Commons license BY 2.0.

"cooling" for only a few months, after which time the assemblies would be shipped to a reprocessing plant. Capacity was provided for only about two full cores, with the possibility of having to unload all fuel from the reactor for repairs.

The abandonment of reprocessing by the United States in 1977 required utilities to store all spent fuel on site, awaiting acceptance of fuel for disposal by the federal government in accordance with the Nuclear Waste Policy Act of 1982 (NWPA). Reracking of the storage pool was the first action taken. Spacing between assemblies was reduced, and neutron-absorbing materials were added to inhibit neutron multiplication. For some reactors, this was not an adequate solution for the problem of fuel accumulation, and thus alternative storage methods were investigated. There were several choices. The first was to ship spent fuel to a pool of a newer plant in the utility's system. The second was for the plant to add more water basins or for a commercial organization to build basins at another central location. The third was to use storage at government facilities, a limited amount of which was promised in the NWPA. The fourth was rod consolidation, in which the bundle of fuel rods is collapsed and put in a container, again to go into a pool. A volume reduction of about two can be achieved. A fifth was to store a number of dry assemblies in large casks sealed to prevent access by water. A variant is the storage of intact assemblies in dry form in a large vault. Dry storage is the favored alternative. An ideal solution would be to use the same container for storage, shipment, and disposal. A combination of methods may instead be adopted as the DOE accepts spent fuel.

EXAMPLE 23.4

The amount of material in spent fuel to be disposed of annually can be shown to be surprisingly small. Dimensions in meters of a typical PWR fuel assembly are $0.214 \times 0.214 \times 4.06$, giving a volume of $0.186\,m^3$. If 60 assemblies are discharged from a typical reactor, the annual volume of spent fuel is $11.2\,m^3$ or $394\,ft^3$. For 100 US reactors, this would be $39{,}400\,ft^3$, which would fill a standard football field ($300\,ft \times 160\,ft$) to a depth of less than 10 in. assuming that the fuel assemblies could be packed closely.

EXAMPLE 23.5

The amount of fission products can be estimated by letting their mass be equal to the mass of fuel fissioned, which is 1.11 g/MW d of thermal energy (see Section 6.4). For a reactor operating at 3000 MWt, this implies 3.3 kg/d or on an annual basis

$$\dot{m}_{FP} = (1.11\,g/(MWtd))(3000\,MWt)(365\,d/y) = 1200\,kg/y$$

If the density is taken to be $10^4\,kg/m^3$ ($=10\,g/cm^3$), the annual volume is

$$\dot{V}_{FP} = \dot{m}_{FP}/\rho = (1200\,kg/y)/\left(10^4\,kg/m^3\right) = 0.12\,m^3/y$$

This corresponds to a cube 50 cm per side. This figure is the origin of the claim that the wastes from a year's operation of a reactor would fit under an office desk. Even with reprocessing, the actual volume would be considerably larger than this.

The detailed composition of a spent fuel assembly is determined by the number of MW d/tonne of exposure it has received. A burnup of 33,000 MW d/tonne corresponds to a 3-y operation in an average thermal neutron flux of $2.9 \times 10^{13}/(cm^2\,s)$ (Cohen, 1977). Fig. 23.3 shows the fuel composition before and after irradiation. The fissile material content has only been changed from 3.3% to 1.43%, and the U-238 content is reduced only slightly. The fact that fuel consumption has reduced the U-235 composition from 3.3% to 0.81% (a loss of only 2.5% of the uranium) while there are 3.5% fission products implies that plutonium contributes significantly to the fission process (see Exercise 23.7).

23.4 TRANSPORTATION

The US Department of Transportation and the NRC provide regulations on radioactive material transportation (10CFR71). Container construction, records, and radiation limits are among the specifications. Three principles used are:

(a) Packaging is to provide protection.
(b) The greater the hazard, the stronger the package must be.
(c) Design analysis and performance tests assure safety.

A classification scheme for containers has been developed to span levels of radioactivity from exempt amounts to that of spent nuclear fuel. For LLW coming from processing reactor water, the cask consists of an outer steel cylinder, a lead lining, and an inner sealed container. For spent fuel, protection is required against (1) direct radiation exposure of workers and the public, (2) release of radioactive fluids, (3) excessive heating of internals, and (4) criticality. The General Electric IF-300 shipping cask shown in Fig. 23.4 consists of a steel tank of length 5 m (16.5 ft) and diameter 1.6 m (5 ft). When fully loaded

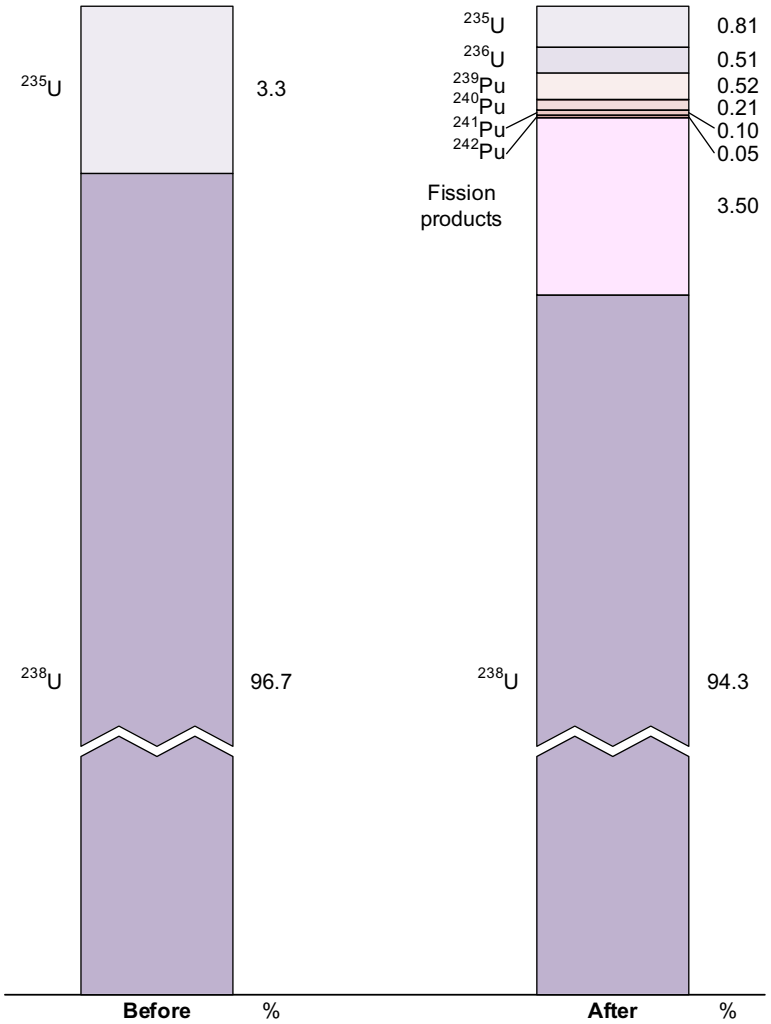

FIG. 23.3

Representative composition of fresh nuclear fuel and after a 33,000-MWD/MTU burnup.

Data from Cohen, B.L., 1977. High-level radioactive waste from light-water reactors. Rev. Mod. Phys. 49 (1), 1–20; Murray, R.L., 2003. Understanding Radioactive Waste, fifth ed. Battelle Press, Columbus, OH. An elementary survey intended to answer typical questions by the student or the public.

with seven PWR assemblies, the cask weighs up to 64,000 kg (70 short tons). The casks contain boron tubes to prevent criticality, heavy metal to shield against gamma rays, and water as needed to keep the fuel cool and to provide additional shielding. A portable air-cooling system can also be attached when the cask is loaded on a railroad car. The cask is designed to withstand normal conditions related to

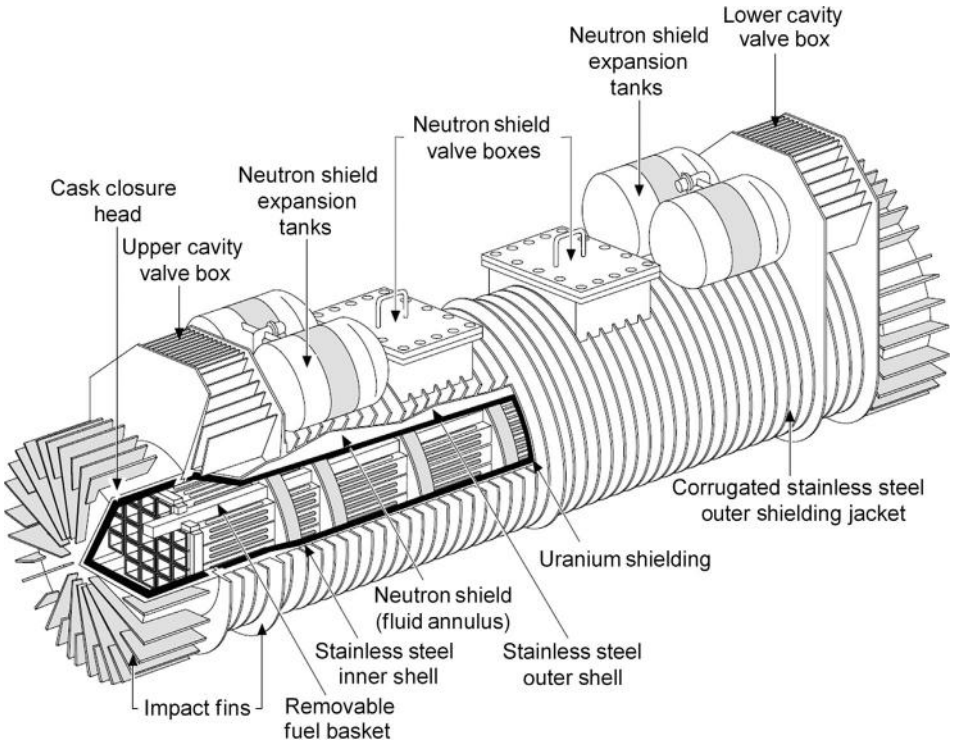

FIG. 23.4

Spent fuel shipping cask.

Courtesy of General Electric Company.

temperature, wetting, vibration, and shocks. In addition, the cask is designed to meet performance specifications (10CFR71.73) that simulate real conditions in road accidents. The cask must withstand a 9 m (30 ft) free fall onto an unyielding surface, a 1 m (40 in.) fall to strike a 15 cm (6 in.) diameter pin, a 30-min exposure to a fire at temperature 800°C (1475°F), and complete immersion in water. Some extreme tests have been conducted to supplement the design specifications. In one test, a trailer rig carrying a cask was made to collide with a solid concrete wall at 135 km/h (84 mi/h) (Jefferson and Yoshimura, 1978). Only the cooling fins were damaged; the cask would not have leaked if radioactivity had been present.

Public concern has been expressed about the possibility of accident, severe damage, and a lack of response capability. The agencies responsible for regulation do not assume that accidents can be prevented but expect all containers to withstand an incident. In addition, efforts have been expended to ensure that police and fire departments are familiar with the practice of shipping radioactive materials and with resources available in the form of state radiological offices and emergency response programs with backup by national laboratories.

EXAMPLE 23.6

For a vehicle cab at the limit of 2 mrem/h (10CFR71.47), the driver would reach the maximum annual occupational exposure after

$$T = D/\dot{D} = (5000\text{mrem})/(2\text{mrem/h}) = 2500\text{h}$$

This equates to driving about 7 h every day of the calendar year.

23.5 REPROCESSING

The physical and chemical treatment of spent nuclear fuel to separate the components—uranium, fission products, and plutonium—is given the name *reprocessing*. The used fuel from the Hanford and Savannah River Plant weapons production reactors and the naval reactors has been reprocessed in the defense program at the US government national laboratories. Commercial experience with reprocessing in the United States has been limited. In the period 1966–72, Nuclear Fuel Services (NFS) operated a facility at West Valley, New York (Croff et al., 2008). General Electric finished a reprocessing plant at Morris, Illinois, but design and operational problems prevented it from opening. Another plant was nearly completed by Allied General Nuclear Service (AGNS) at Barnwell, South Carolina, but it never operated as a matter of national policy. To understand that political decision, it is necessary to review the technical aspects of reprocessing.

On receipt of a shipping cask of the type shown in Fig. 23.4, the spent fuel is unloaded and stored for further decay in a water pool. The assemblies are then fed into a mechanical shear that cuts them into pieces approximately 3 cm long to expose the fuel pellets. The pieces fall into baskets that are immersed in nitric acid to dissolve the uranium dioxide and leave Zircaloy hulls. The aqueous solution from this chop-leach operation then proceeds to a solvent extraction process. Visualize an analogous experiment. Add oil to a vessel containing salt water. Shake to mix. When the mixture settles and the liquids separate, some salt has gone with the oil (i.e., it has been extracted from the water). In the plutonium and uranium recovery by extraction (PUREX) process, the solvent is the organic compound tributyl phosphate (TBP) diluted with kerosene. Countercurrent flow of the aqueous and organic materials is maintained in a packed column, as shown in Fig. 23.5. Mechanical vibration assists contact.

A flow diagram of the separation of components of spent fuel is shown in Fig. 23.6. The amount of neptunium-239, half-life 2.355 d and parent of Pu-239, depends on how fresh the spent fuel is. After a month of holding, the isotope will be practically gone. The three nitrate solution streams contain uranium, plutonium, and an array of fission product chemical elements. The uranium has a U-235 content slightly higher than natural uranium. It can either be set aside or re-enriched in an isotope separation process. The plutonium is converted into an oxide that is suitable for combining with uranium oxide to form a mixed oxide (MOX) that can comprise part or all of the fuel of a reactor. Precautions are taken in the fuel fabrication plant to protect workers from exposure to plutonium due to its radiotoxicity.

In the reprocessing operations, special attention is given to certain radioactive gases. Among them are 8.04-d I-131, 10.76-y Kr-85, and 12.32-y H-3, which is the product of the occasional ternary fission into three fragments. The iodine concentration is greatly reduced by reasonable holding periods.

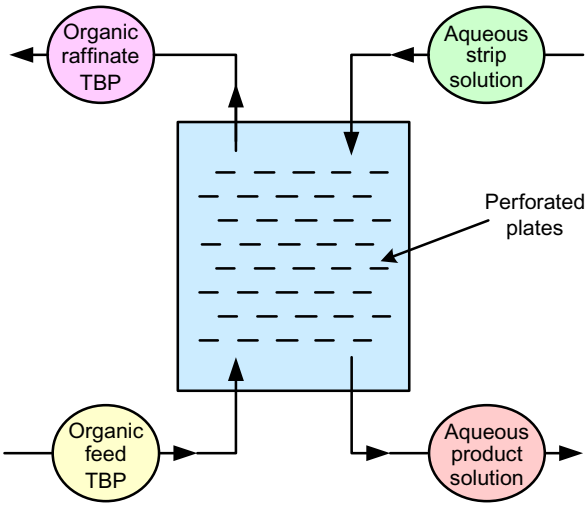

FIG. 23.5

Solvent extraction by the PUREX method.

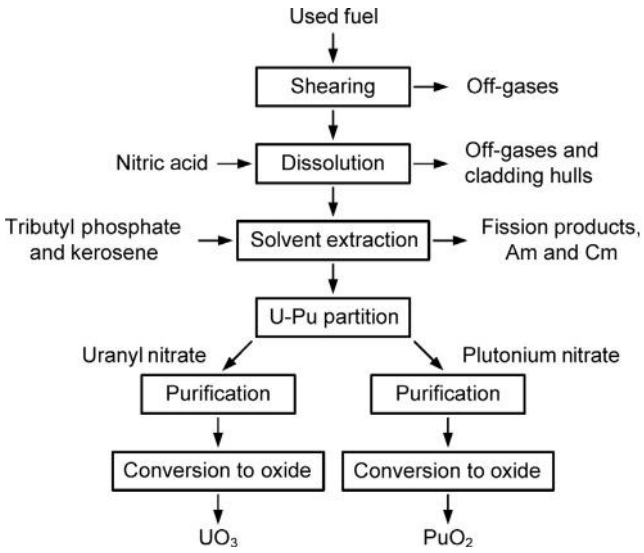

FIG. 23.6

Simplified flowchart of PUREX nuclear fuel reprocessing.

The long-lived krypton poses a problem because it is a noble gas that resists chemical combination for storage. It may be disposed of in two ways: (1) release to the atmosphere from tall stacks with subsequent dilution or (2) adsorption onto porous media such as charcoal maintained at very low temperatures. The hazard of tritium is relatively small, but water containing it behaves as ordinary water.

Reprocessing has merit in several ways other than making uranium and plutonium available for recycling:

1. The isolation of some of the long-lived transuranic materials (other than plutonium) would permit them to be irradiated with neutrons, achieving additional energy release and transmuting them into useful species or innocuous forms for purposes of waste disposal.
2. Numerous valuable fission products such as krypton-85, strontium-90, and cesium-137 have industrial applications or may be used as sources for food irradiation.
3. The removal of radionuclides with intermediate half-lives allows canisters of wastes to be placed closer together in the ground because the heat load is lower.
4. Several rare elements of economic and strategic national value can be reclaimed from fission products. Availability from reprocessing could avoid interruption of supply from abroad. Examples are rhodium, palladium, and ruthenium.
5. The volume of wastes to be disposed would be lower because the uranium has been extracted.
6. Even if it were not recycled, the recovered uranium could be saved for future use in breeder reactor blankets.

Several countries—France, the United Kingdom, Germany, Japan, and the former USSR—have working reprocessing facilities and benefit from some of the preceding virtues. Analyses by Bunn et al. (2005) indicate that uranium prices must significantly increase in order to economically justify reprocessing and recycling of plutonium.

An important aspect of reprocessing is that the plutonium made available for recycling can be visualized as a nuclear weapons material. Concern about international proliferation of nuclear weapons prompted US President Jimmy Carter in April 1977 to issue a ban on commercial reprocessing. It was believed that if the United States refrained from reprocessing, it would set an example to other countries. The action had no effect because the United States had made no real sacrifice, having abundant uranium and coal reserves, and countries lacking resources saw full utilization of uranium in their best interests. It was recognized that plutonium from high-burnup power reactor operation was undesirable for weapons because of the high content of Pu-240, which emits neutrons in spontaneous fission. In addition, it is possible to achieve weapons capability through the completely different route of isotope separation yielding highly enriched uranium. The ban prevented the AGNS plant from operating. US President Ronald Reagan lifted the ban in 1981, but industry was wary of attempting to adopt reprocessing because of uncertainty in government policy and lack of evidence that there was a significant immediate economic benefit.

EXAMPLE 23.7

The average annual electricity use by a US household is about 11,000 kWh. For a burnup of 33,000 MW d/tonne, Fig. 23.3 shows that the fission products account for 3.5% of the spent fuel mass. If 100% of the electric energy E_e were derived from nuclear power, each household would be responsible yearly for a fission product mass of

$$m_{FP} = \frac{0.035 E_e}{B\eta_{th}} = \frac{(0.035\,\text{g} - \text{FP/g} - \text{U})(11\,\text{MWh})(1\,\text{d}/24\,\text{h})}{(33,000\,\text{MW d/tonne} - \text{U})(0.33\,\text{MWe/MWt})\left(1\,\text{tonne}/10^6\,\text{g}\right)} = 1.5\,\text{g}$$

Alternative proliferation-resistant recycling methods, which should make plutonium less accessible to rogue nations or terrorists, are under development. As a substitute for the PUREX process, which

creates a pure plutonium product, the UREX+ process will include other actinides: neptunium, americium, and curium. The mixture of elements will be recycled to burn out wastes and obtain maximum energy.

23.6 HIGH-LEVEL WASTE DISPOSAL

The treatment given to wastes containing large amounts of fission products depends on the cycle chosen. If the fuel is reprocessed, as described in the previous section, the next step is to immobilize the radioactive residue. One popular method, called *vitrification*, is to mix the moist waste chemicals with pulverized glass similar to Pyrex, heat the mixture in a furnace to molten form, and pour the liquid into metal containers called canisters. The solidified waste form can be stored conveniently, shipped, and disposed. The glass waste is expected to resist leaching by water for hundreds of years.

If the fuel is not reprocessed, there are several choices. One is to enclose intact fuel assemblies within a canister. Another is to consolidate the rods (i.e., bundle them closely together in a container). A molten metal such as lead could be used as a filler if needed. What would be done subsequently with waste canisters has been the subject of a great deal of investigation concerning feasibility, economics, and social-environmental effects. Some of the concepts that have been proposed and studied are the following (DOE, 1980):

1. Send nuclear waste packages into space by shuttle and spacecraft. The weight of protection against vaporization in accidental reentry to the Earth's atmosphere would make costs prohibitive.
2. Place canisters on the Antarctic ice cap, either held in place or allowed to melt their way down to the base rock. Costs and environmental uncertainty rule out this method.
3. Deposit canisters in mile-deep holes in the Earth. With a lack of progress with a geological repository in the United States, deep borehole disposal has received renewed interest.
4. Drop canisters from a ship to penetrate the layer of sediment at the bottom of the ocean. Although considered as a backstop, there are evident environmental concerns.
5. Sink vertical shafts a few thousand feet deep, and excavate horizontal corridors radiating out. In the floors of these tunnels, drill holes in which to place the canisters, as shown in Fig. 23.7, or place waste packages on the floor of the corridor itself. The latter is the currently preferred technology in the US high-level waste disposal program.

The design of a repository for high-level radioactive waste or spent fuel uses a multibarrier approach. The first level of protection is the waste form, which may be glass waste or an artificial substance, or uranium oxide fuel, which itself inhibits diffusion of fission products and is resistant to chemical attack. The second level is the container, which can be chosen to be compatible with the surrounding materials. Choices of metal for the canister include steel, stainless steel, copper, and nickel alloys. The third level is a layer of clay or other packing that tends to prevent access of water to the canister. The fourth is a backfill of concrete or rock. The fifth and final level is the geological medium. It is chosen for its stability under heat as generated by the decaying fission products. The medium will have a pore structure and chemical properties that produce a small water flow rate and a strong filtering action.

The system must remain secure for thousands of years. It must be designed to prevent contamination of water supplies that would give significant doses of radiation to members of the public. Radioactivity in spent fuel originates from both fission and activation products. Fig. 23.8 shows the 14 principal

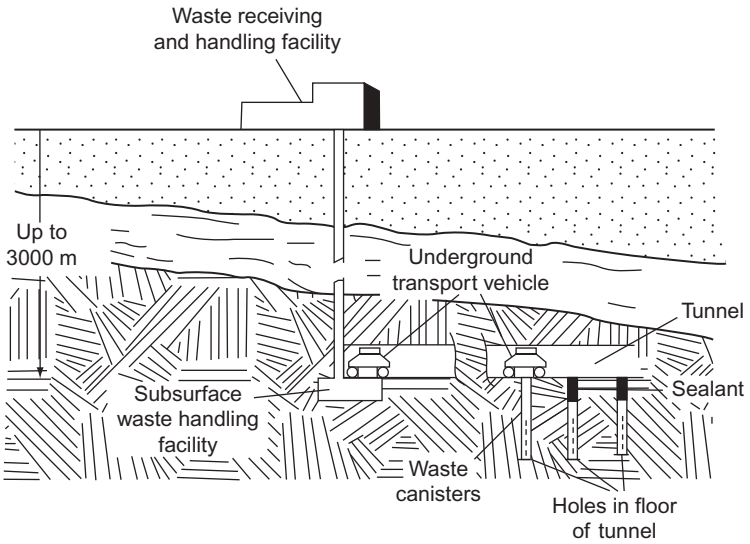

FIG. 23.7

Nuclear waste isolation by geologic emplacement.

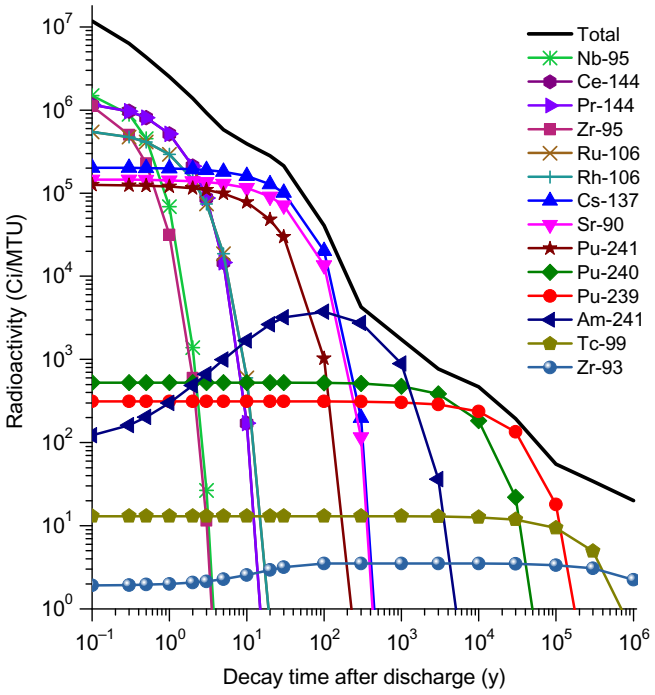

FIG. 23.8

Radioactivity of 3.2 w/o enrichment PWR spent fuel having a 33,000-MWD/MTU burnup after discharge from the reactor. Note: Ce-144 and Pr-144 overlay one another, as do Ru-106 and Rh-106.

Data from Croff, A.G., Liberman, M.S., Morrison, G.W., 1982. Graphical and tabular summaries of decay characteristics for once-through PWR, LMFBR, and FFTF fuel cycle materials. ORNL/TM-8061. Oak Ridge National Laboratory.

contributors to the activity. The radionuclides found in fission products can be divided into several classes, as follows:

- Nuclides of short half-life, up to about a month. Examples are Xe-133 (5.24 d) and I-131 (8.04 d). These would pose a problem in case of accident and give rise to heat and radiation that affect handling of fuel but are not important to waste disposal. The storage time for fuel is long enough that they decay to negligible levels.
- Materials of intermediate half-life, up to 50 y, which determine the heating in the disposal medium. Examples are Ce-144 (284.6 d), Ru-106 (1.020 y), Cs-134 (2.065 y), Pm-147 (2.62 y), Kr-85 (10.76 y), H-3 (12.32 y), Pu-241 (14.4 y), Sr-90 (29.1 y), and Cs-137 (30.1 y).
- Isotopes that are still present after many thousands of years and that ultimately determine the performance of the waste repository. Important examples are Ra-226 (1600 y), C-14 (5715 y), Se-79 (2.9×10^5 y), Tc-99 (2.13×10^5 y), Np-237 (2.14×10^6 y), Cs-135 (2.3×10^6 y), and I-129 (1.7×10^7 y). Radiological hazard is contributed by some of the daughter products of these isotopes; for example, Pb-210 (22.6 y) comes from Ra-226, which in turn came from almost-stable U-238.

Several candidate types of geologic media are found in various parts of the United States. One is rock salt, identified many years ago as a suitable medium because its very existence implies stability against water intrusion. It has the ability to self-seal through heat and pressure. Another is the dense volcanic rock basalt. Third is tuff, a compressed and fused volcanic dust. Extensive deposits of these three rocks as candidates for repositories are found in the states of Texas, Washington, and Nevada, respectively. Still another is crystalline rock, an example of which is granite as found in the eastern United States.

A simplified model of the effect of a repository is as follows. It is known that there is a small but continued flow of water past the emplaced waste. The container will be leached away in a few hundred years and the waste form released slowly over perhaps 1000 y. The chemicals migrate much more slowly than the water flows, making the effective time of transfer tens of thousands of years. All the short and intermediate half-life substances will have decayed by this time. The concentration of the long half-life radionuclides is greatly reduced by the filtering action of the geological medium. For additional details on the process of performance assessment, see SNL (2008).

A pair of Computer Exercises provides an introduction to the mathematical modeling of the behavior of radioactive waste in a repository or disposal facility. A simple moving pulse with decay is studied in 23.A, and the spreading of a pulse by dispersion is shown in 23.B.

The DOE's Office of Civilian Radioactive Waste Management (OCRWM) has responsibility for carrying out the NWPA, which involves management of the Waste Fund, repository site selection, and the design of a storage facility. Congress set a plan and a timetable for establishment of an HLW repository in the United States. The NWPA called for a search of the country for possible sites, the selection of a small number for further investigation, and characterization of one or more sites, taking account of geology, hydrology, chemistry, meteorology, earthquake potential, and accessibility.

A Nuclear Waste Fund provides financing for the waste disposal program being carried out by the federal government. The consumers of electricity generated by nuclear reactors pay a fee of 1/10 ¢/kWh collected by the power companies. This adds only approximately 2% to the cost of nuclear electric power. The Fund held assets exceeding $36 billion, when the collection was suspended in 2014. Concern has been expressed about the fact that Congress has used some of the Fund for other purposes.

EXAMPLE 23.8

For a single PWR fuel assembly of 480 kg-U achieving a burnup 45,000 MWD/MTU, the federal government would realize revenue of

$$\frac{(\$0.001/(\text{kWeh}))(45,000\text{MWD/MTU})(0.48\text{MTU})(0.33\text{kWe/kWt})}{(1\text{d}/24\text{h})(1\text{MW}/1000\text{kW})} = \$171,072$$

The NWPA called for a study of a monitored retrievable storage (MRS) system to serve as a staging center before disposal in a repository. Efforts to find a host were unsuccessful. Use of the Nevada weapons testing grounds as a storage area for spent fuel had been promoted as a stopgap. More recently, private entities have proposed establishing a consolidated interim storage facility in southeastern New Mexico or west Texas.

In 1987, Congress decreed that site studies in Texas and Washington State should cease and mandated that Nevada would be the host state. The location would be Yucca Mountain, near the Nevada Test Site for nuclear weapons. The project was delayed for several years by legal challenges from the state of Nevada, but characterization was begun in 1991, with cognizance by the DOE OCRWM. To test suitability of the site, an Exploratory Studies Facility was dug consisting of a corridor 10 m in diameter and 8 km (5 mi) long. Among features investigated were the effect of heating to 300°C and the flow of water down through the rock. As reported in the viability assessment document (DOE, 1998), the Yucca Mountain site is favorable because of the desert climate (only approximately 7 in. (18 cm) of water per year), the unsaturated zone with a 2000-ft (600-m) deep water table, the stability of the geological formation, and a very low population density nearby. The DOE issued a reference design document (RDD) (OCRWM, 2000). Some of the features cited are the following:

- 100 mi (160 km) northwest of Las Vegas, Nevada.
- 70,000 tonnes of spent fuel and other wastes in 10,200 packages.
- Underground horizontal tunnels (drifts).
- Diameter of drifts 18 ft (5.5 m); spacing 92 ft (28 m).
- Emplacement level approximately 1000 ft (305 m) below the surface.
- Waste packages hold 21 PWR or 44 BWR fuel assemblies.

Multiple engineered barriers include the solid waste form (UO_2), the metal fuel rod cladding, a container of special corrosion-resistant nickel alloy C-22,[1] a drip shield to deflect water, a V-shaped trough for support, and, underneath, the invert composed of stainless steel and volcanic rock to slow water flow. Fig. 23.9 shows the proposed design.

Dedicated trains to carry spent fuel and high-level waste to Yucca Mountain were proposed by the DOE. The choice as an alternative to trucks leads to fewer shipments, with 3500 estimated.

The project was brought under question by the revelation in March 2005 of some email messages in 1998 suggesting falsification of quality assurance data related to water infiltration. Investigations

[1]Nominal percentages in Hastelloy C-22: 56 Ni, 22 Cr, 13 Mo, 3 Fe, 2.5 Co, 3 W, 0.5 other.

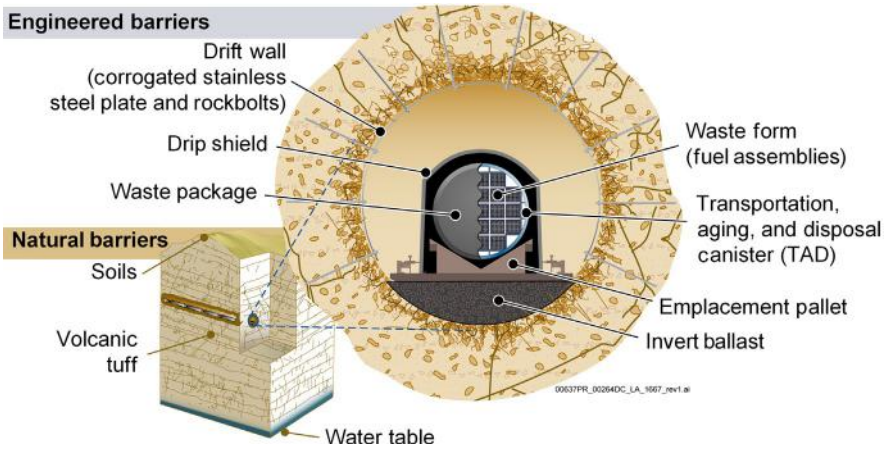

FIG. 23.9

Spent fuel at a geologic repository.

Courtesy: DOE Office of Civilian Radioactive Waste Management.

were made by Congress, the DOE, the US Geological Survey (USGS), and the Federal Bureau of Investigation (FBI), and certain measurements were repeated as a corrective action needed to verify repository safety. The investigations were completed in 2005 as described in *Nuclear News* (2006).

Safety standards developed by the Environmental Protection Agency (EPA) (40CFR197) are to be used in licensing and regulation by the NRC (10CFR60). The EPA placed limits on the maximum additional radiation dosage to members of the public because of the release of radioactive material. Two timeframes were established: (1) up to 10,000 y, with 15 mrem (0.15 mSv) per year, and (2) after 10,000 y to geologic stability, with 100 mrem (1 mSv) per year. The selection by the EPA of a time span of 10,000 y for protection against hazard from waste deposits was based on a logical analysis. A comparison was made between two radioactivities. The first was that of natural uranium as found in the ground, a figure that remains constant (see Exercise 23.1). The second was the declining activity of spent fuel, as the fission products and activation products decay. It was assumed that when the two figures are equal, the radiation dose caused by the waste is no greater than that caused by the original uranium. Calculations led to a time of approximately 1000 y, and a safety factor of 10 was applied; for further details, see Moghissi (2006). The longer timeframe was set on the basis that the highest radiation from waste may occur beyond the 10,000-y period.

The Yucca Mountain license application was delivered in 2008 by the DOE to the NRC. The DOE was to certify that the repository would meet standards set by the EPA. A plan would be prepared for transportation of spent fuel by rail from reactors to the final destination in Nevada. The legal cap in loading of the repository is 70,000 metric tonnes of heavy metal (MTHM). The projected date for the start of burial was 2020. According to the Nuclear Waste Policy Act, the DOE was required to accept spent fuel by 1998, but has not complied, to the concern of the nuclear industry.

EXAMPLE 23.9

The adequacy of the 70,000-MTHM capacity can be assessed for the present US power reactor capacity of 103 GWe. If the average fuel burnup is 45,000 MWD/MTU and a 90% capacity factor assumed, then sufficient room exists for a period of

$$T = \frac{(70,000\,\text{MT})(45,000\,\text{MWD/MT})(0.33\,\text{MWe/MWt})}{(103\times10^3\,\text{MWe})(0.90)(365\,\text{d/y})} = 30.7\,\text{y}$$

This result implies that the repository may already be fully booked. In fact, the GAO (2011) reported a current national inventory of 65,000 tonnes of spent fuel, increasing by 2000 tonne/y.

In 2010, US President Barack Obama proposed terminating funding for the repository at Yucca Mountain, and the DOE consequentially motioned to withdraw the license application with the NRC. As the GAO (2011) stated in a report, "DOE's decision to terminate the Yucca Mountain repository program was made for policy reasons, not technical or safety reasons." Presently, the political wrangling continues, but Yucca Mountain remains the sole legally designated high-level nuclear waste repository in the United States.

Subsequently, the Blue Ribbon Commission on America's Nuclear Future was tasked with reviewing the back end of the nuclear fuel cycle. Its report (BRC, 2012) made eight recommendations, including development of a consent-based approach to siting future waste management facilities and encouragement of prompt efforts to develop both geologic disposal and consolidated storage facilities. The former advice is intended to avoid NIMBY (not in my back yard) opposition.

With the federal government in breach of its legal duty to take possession of used fuel, utilities have successfully petitioned the federal courts for relief. So far, the courts have awarded utilities billions of dollars in compensation for expenses to store the spent fuel.

Progress in establishing the repository at Yucca Mountain has been consistently slow, and the completion date has been repeatedly extended. The difficulties and uncertainties of the project have already prompted consideration of alternatives. One is to irradiate certain radioisotopes in the spent fuel to destroy problem isotopes such as cesium-137 and strontium-90 that contribute to heating in the early period and neptunium-237, technetium-99, and iodine-129 that dominate the hazard at long times. These constitute only about 1% of the waste stream. If they are removed, the remaining waste needs to be secure for only approximately 100 y rather than the 10,000 y for spent fuel.

An R&D program titled Accelerator Transmutation of Wastes (ATW) was conducted over a number of years at Los Alamos National Laboratory (LANL). The concept first involves reprocessing spent fuel by pyroprocessing, which uses the Integral Fast Reactor technology (see Section 25.4). The key fission products, actinides, and possibly plutonium would then be irradiated in a subcritical system with an accelerator that causes spallation (see Section 9.7). A beam of protons of 100 MW was to be directed to a molten lead target. A surrounding liquid would contain the isotopes to be burned, with heat removed by liquid lead. Electricity would be produced. About 15 such burners were estimated to be able to handle US spent fuel. A roadmap for further development of the concept was prepared in 1999 (Van Tuyle et al., 2001). However, spallation research on ATW at LANL was suspended, and the ATW program was merged by the DOE with the program Accelerator Production of Tritium (APT; Section 27.6) and essentially abandoned. There is a current lack of interest in ATW, but it remains a possibility for the more distant future.

23.7 LOW-LEVEL WASTE GENERATION, TREATMENT, AND DISPOSAL

The nuclear fuel cycle, including nuclear power stations and fuel fabrication plants, produces approximately two-thirds of the annual volume of LLW (Holcomb, 1978). The rest comes from companies that use or supply isotopes and from institutions such as hospitals and research centers.

In this section, we look at the means by which low-level radioactive materials are produced, the physical and chemical processes that yield wastes, the amounts to be handled, the treatments that are given, and the methods of disposal.

In the primary circuit of the nuclear reactor, the flowing high-temperature coolant erodes and corrodes internal metal surfaces. The resultant suspended or dissolved materials are bombarded by neutrons in the core. Similarly, core metal structures absorb neutrons, and some of the surface is washed away. Activation products as listed in Table 23.2 are created, usually through an (n, γ) reaction. In addition, small amounts of fission products and transuranic elements appear in the water as the result of small leaks in cladding and the irradiation of uranium deposits left on fuel rods during fabrication. The isotopes involved are similar to those of concern for HLW.

Leaks of radioactive water from the primary coolant are inevitable and result in contamination of work areas. In addition, radioactive equipment must be removed for repair. For such reasons, workers are required to wear elaborate protective clothing and use a variety of materials to prevent spread of contamination. Much of it cannot be cleaned and reused. Contaminated dry trash includes paper, rags, plastics, rubber, wood, glass, and metal. These may be combustible or noncombustible, compactible or noncompactible. Avoidance of contamination of inert materials by radioactive materials is an important technique in waste reduction. The modern trend in nuclear plants is to try to reduce the volume of waste by whatever method is appropriate. Over the period 1980–98, by a combination of methods, the nuclear industry reduced the LLW volume by a factor of more than 15. Costs of disposal have not decreased proportionately, however, because capital costs tend to be independent of waste volume.

One popular technique is incineration, in which the flue gases are filtered, and the ash contains most of the radioactivity in a greatly reduced volume. Another method is compaction, with a large press to give a reduced volume and also to make the waste more stable against further disturbance after disposal. Supercompactors that reduce the volume greatly are popular. A third approach is grinding or shredding, then mixing the waste with a binder such as concrete or asphalt to form a stable solid.

Table 23.2 Activation Products in Reactor Coolant

Isotope	Half-Life (Years)	Radiation Emitted	Parent Isotope
C-14	5715	B	N-14[a]
Fe-55	2.73	X	Fe-54
Co-60	5.27	β, γ	Co-59
Ni-59	7.6×10^4	X	Ni-58
Ni-63	100	B	Ni-62
Nb-94	2.4×10^4	β, γ	Nb-93
Tc-99	2.13×10^5	B	Mo-98, Mo-99[b]

[a] *(n, p) reaction.*
[b] *Beta decay.*

Purification of the water in the plant, required for reuse or safe release to the environment, gives rise to a variety of wet wastes. They are in the form of solutions, emulsions, slurries, and sludges of both inorganic and organic materials. Two important physical processes that are used are filtration and evaporation. Filters are porous media that remove particles suspended in a liquid. The solid residue collects in the filter, which may be a disposable cartridge or may be reusable if backwashed. Fig. 23.10 shows

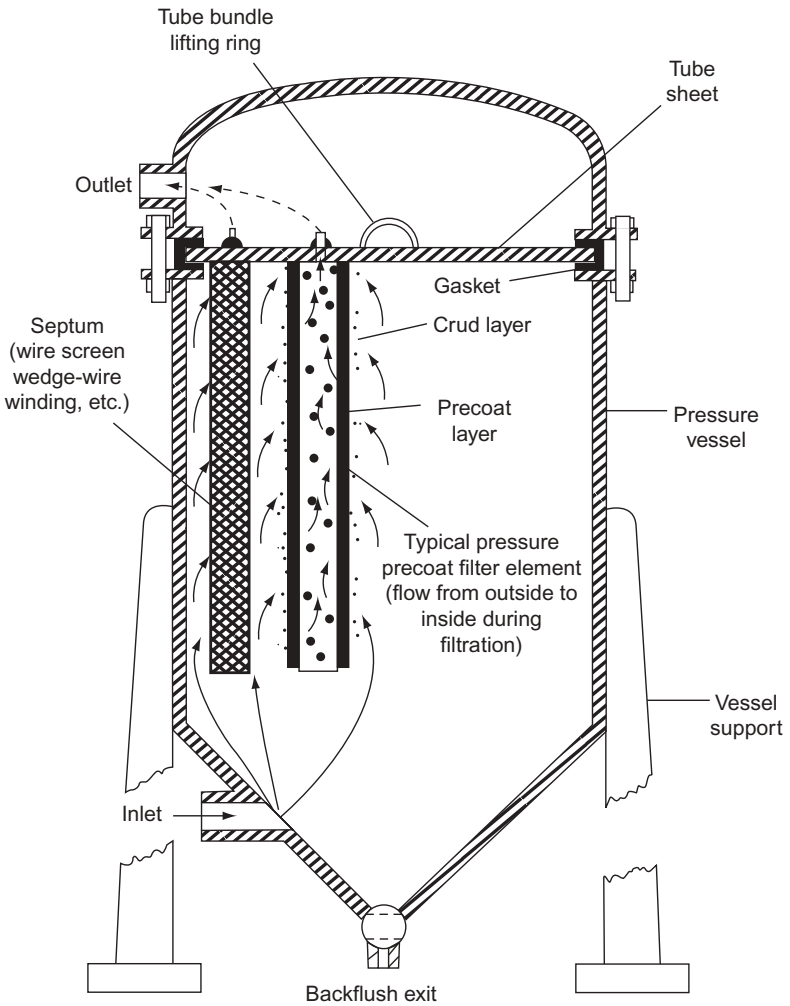

FIG. 23.10

Disposal-cartridge filter unit used to purify water and collect LLW.

From Kibbey, A.H., Godbee, H.W., 1978. The use of filtration to treat radioactive liquids in light-water-cooled nuclear reactor power plants. NUREG/CR-0141. Oak Ridge National Laboratory.

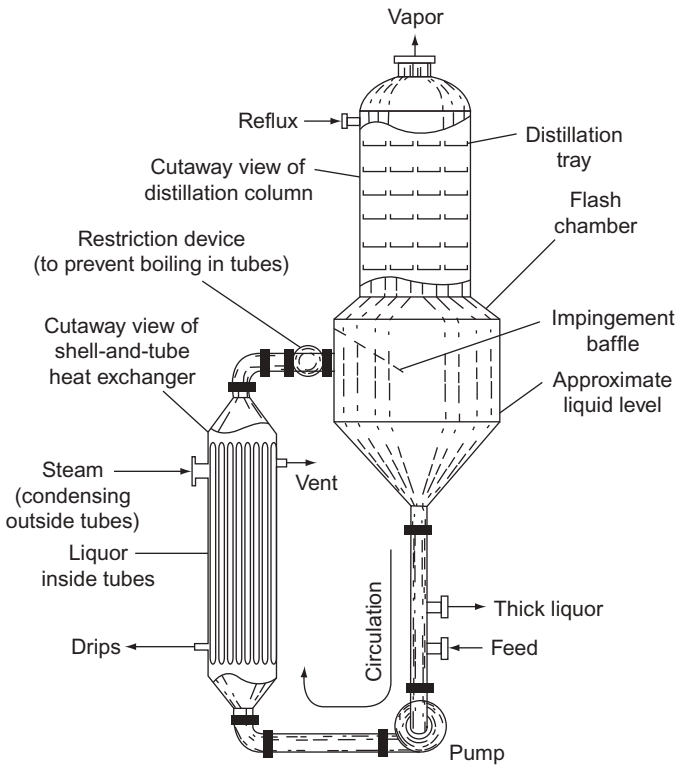

FIG. 23.11

Natural-circulation evaporator used to concentrate LLW.

From Godbee, H.W., Kibbey, A.H., 1978. The use of evaporation to treat radioactive liquids in light-water-cooled nuclear reactor power plants. NUREG/CR-0142. Oak Ridge National Laboratory.

the schematic arrangement of a filter in a nuclear plant. The evaporator is simply a vessel with a heated surface over which liquid flows. The vapor is drawn off, leaving a sludge in the bottom. Fig. 23.11 shows a typical evaporator arrangement.

The principal chemical treatment of wet LLW is ion exchange. A solution containing ions of waste products contacts a solid such as zeolite (aluminosilicate) or a synthetic organic polymer. In the mixed-bed system, the liquid flows down through mixed anion and cation resins. As discussed by Benedict et al. (1981), ions collected at the top move down until the whole resin bed is saturated, and some ions appear in the effluent, a situation called breakthrough. Decontamination factors may be as large as 10^5. The resin may be reused by application of an elution process, in which a solution of Na_2SO_4 is passed through the bed to extract the ions from the resin. The resulting waste solution will be smaller than before but will probably be larger than the exchanger. Whether to discard or elute depends on the cost of the ion-exchanger material.

The variety of types of LLW from institutions and industry is indicated in Table 23.3. The institutions include hospitals, medical schools, universities, and research centers. As discussed in Chapter 13, labeled pharmaceuticals and biochemicals are used in medicine for diagnosis and therapy

Table 23.3 Institutional and Industrial Low-Level Waste Streams

Fuel Fabrication Plant Trash Process wastes	Industrial Trash Source and special nuclear material[a]
Institutions Liquid scintillation vials Liquid wastes Biowastes	Special Isotope production facilities Tritium manufacturing Accelerator targets Sealed sources, such as radium

[a]*Special nuclear material (SNM) includes U-233, U-235, enriched uranium, and plutonium.*
Modified from U.S. Nuclear Regulatory Commission (NRC), 1982. Final environmental impact statement on 10 CFR Part 61: licensing requirements for land disposal of radioactive waste. NUREG-0945, vols. 1–3.

and in biological research to study the physiology of humans, other animals, and plants. Radioactive materials are used in schools for studies in physics, chemistry, biology, and engineering and are produced by research reactors and particle accelerators. Industries make various products: radiography sources; irradiation sources; radioisotope thermoelectric generators; radioactive gauges; self-illuminating dials, clocks, and signs; static eliminators; smoke detectors; and lightning rods. Radionuclides that often appear in LLW from manufacturing include carbon-14, tritium, radium-226, americium-241, polonium-210, californium-252, and cobalt-60. LLW disposal from the decommissioning of nuclear power reactors is of considerable future importance and is discussed separately in Section 23.9.

Although defined by exclusion, as noted in Section 23.2, low-level radioactive waste generally has low enough activity to be given near-surface disposal. There are a few examples of very small contaminations that can be disregarded for disposal purposes and some highly radioactive materials that cannot be given shallow-land burial.

The method of disposal of low-level radioactive wastes for many years was similar to a landfill practice. Wastes were transported to the disposal site in various containers such as cardboard or wooden boxes and 55-gallon drums and were placed in trenches and covered with earth without much attention to long-term stability.

A total of 6 commercial and 14 government sites around the United States operated for a number of years until leaks were discovered, and three sites were closed: West Valley, New York, Sheffield, Illinois, and Maxey Flats, Kentucky. One problem was subsidence, in which deterioration of the package and contents by entrance of water would cause local holes in the surface of the disposal site. These would fill with water and aggravate the situation. Another difficulty was the bathtub effect, in which water would enter a trench then, unable to drain sufficiently, cause the contents to float and be exposed.

Three remaining sites at Richland, Washington, Beatty, Nevada, and Barnwell, South Carolina, handled all the LLWs of the United States. These sites were more successful, in part, because trenches had been designed to allow ample drainage. Managers of the sites, however, became concerned with the waste generators' practices and attempted to reduce the amount of waste accepted. This situation prompted Congress to pass in 1980 the Low-Level Radioactive Waste Policy Act (LLRWPA), followed by the Low-Level Radioactive Waste Policy Amendments Act of 1985. These laws placed responsibility on states for wastes generated within their boundaries but recommended regional disposal.

Accordingly, a number of interstate compacts were formed, with several states remaining independent. Fig. 23.12 shows the division of the United States into states and compacts. The affiliation of states has tended to change over the years.

At the same time, the NRC developed a new rule governing LLW management. Title 10 of the Code of Federal Regulations Part 61 (10CFR61) calls for packaging of wastes by the generator according to isotope type and specific activity (Ci/m^3). Waste classes A, B, and C are defined in 10CFR61 and increasing levels of security prescribed. Wastes greater than Class C are unsuitable for near-surface disposal and are managed by the DOE as equivalent to high-level waste.

Computer Exercise 23.C describes an elementary expert system that determines the proper class of a given waste based on half-life and concentration.

The required degree of waste stability increases with the radioactive content. Limits are placed on the amount of liquid present with the waste, and the use of stronger and more resistant containers is recommended in the interest of protecting the public during the operating period and after closure of the facility.

Regulation 10CFR61 calls for a careful choice of the characteristics of the geology, hydrology, and meteorology of the site to reduce the potential radiation hazard to workers, the public, and the environment. Special efforts are to be made to prevent water from contacting the waste. Performance specifications include a limit of 25 mrem (0.25 mSv) per year whole-body dose of radiation to any member of the public. Monitoring is to be carried out over an institutional surveillance period of 100 y after closure. Measures are to be taken to protect the inadvertent intruder for an additional 500 y. This is a person who might build a house or dig a well on the land. One method is to bury the more highly radioactive material deep in the trench; another is to put a layer of concrete over the wastes.

The use of an alternative technology designed to improve confinement stems from one or more public viewpoints. First is the belief that the limiting dose should be nearer zero or even should be actually zero. Second is the concern that some unexpected event might change the system from the one analyzed. Third is the idea that the knowledge of underground flow is inadequate and not capable of being modeled to the accuracy needed. Fourth is the expectation that there may be human error in the analysis, design, construction, and operation of the facility. It is difficult to refute such opinions, and in some states and interstate compact regions, legislation on additional protection has been passed to make a waste disposal facility acceptable to the public. Some of the concepts considered as substitutes for shallow land burial are as follows (Bennett et al., 1984):

(a) *Belowground vault disposal* involves a barrier to migration in the form of a wall such as concrete. It has a drainage channel, a clay top layer and a concrete roof to keep water out, a porous backfill, and a drainage pad for the concrete structure.

(b) *Aboveground vault disposal* makes use of slopes on the roof and surrounding earth to assist runoff. The roof substitutes for an earthen cover.

(c) *Shaft disposal* uses concrete for a cap and walls and is a variant on the belowground vault that conceivably could be easier to build.

(d) *Modular concrete canister disposal* involves a double container, the outer one of concrete, with disposal in a shallow-land site.

(e) *Mined-cavity disposal* consists of a vertical shaft going deep in the ground, with radiating corridors at the bottom, similar to the planned disposal system for spent fuel and high-level wastes from reprocessing. It is only applicable to the most active LLWs.

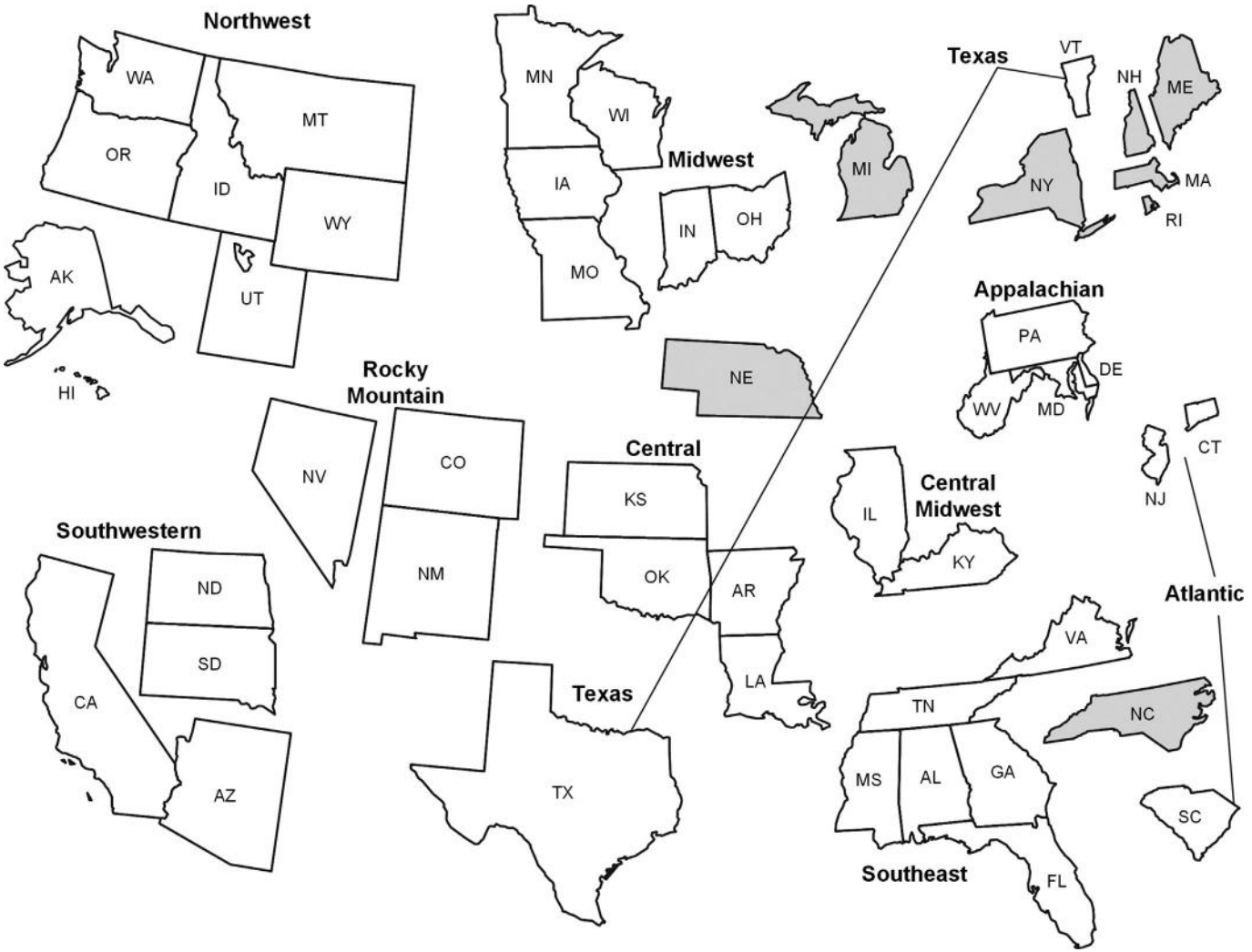

FIG. 23.12

United States interstate compacts for disposal of low-level radioactive wastes. States shaded are unaffiliated.

Data from U.S. Nuclear Regulatory Commission (NRC), 2017. 2017–2018 information digest. NUREG-1350, vol. 29.

(f) *Intermediate-depth disposal* is similar to shallow-land disposal except for the greater trench depth and thickness of cover.

(g) *Earth-mounded concrete bunker disposal*, used in France, combines several favorable features. In particular, wastes of higher activity are encased in concrete below grade and those of lower activity are placed in a mound with concrete and a clay cap, covered with rock or vegetation to prevent erosion by rainfall.

Each of the interstate compacts embarked on investigations in accord with LLRWPA and 10CFR61. These involved site selection processes, geological assessments, and designs of facilities. The nature of the facilities proposed depended on the location, with shallow-land burial deemed adequate for the California desert at Ward Valley, but additional barriers and containers planned for North Carolina in the humid southeastern United States. However, as the result of concerted opposition taking the form of protests, lawsuits, political action and inaction, and occasional violence, progress was very slow in establishing LLW disposal capability. Thus despite excellent planning and vigorous efforts, and the expenditure of millions of dollars in preparation, political and regulatory factors prevented most of the programs in the United States from coming to fruition. Presently, there are only four sites receiving low-level wastes in the United States.

23.8 ENVIRONMENTAL RESTORATION OF DEFENSE SITES

The legacy of World War II and the Cold War includes large amounts of radioactive waste and contamination of many defense sites. Priority was given to weapons production rather than environmental protection, leaving a cleanup task that will take several decades to carry out and cost many billions of dollars.

One of the most pressing problems to solve is the degraded condition of underground tanks at Hanford used to store the waste residue from reprocessing to extract plutonium. The single-wall tanks have leaked, and there is concern for the contamination of the nearby Columbia River. Some of the wastes have been processed to extract the valuable Cs-137 and Sr-90, and the contents of some tanks have been successfully stabilized to prevent hydrogen explosion. The hydrogen is produced by radiolysis of water and decomposition of organic solvents. Ideally, all the waste would be transferred to double-layered tanks or immobilized in glass. Similar tanks are located at the Savannah River Plant in South Carolina, where plutonium and tritium were produced.

Transuranic wastes (TRU) consist of materials and equipment contaminated by small amounts of plutonium. They have been stored or temporarily buried over the years, especially at Hanford, Idaho Falls, Los Alamos, Oak Ridge, and Savannah River. These wastes are scheduled to be buried in the Waste Isolation Pilot Plant (WIPP), a repository near Carlsbad, New Mexico, that opened in 1999. The geological medium is salt, which has several advantages: its presence demonstrates the absence of water and it is plastic, self-sealing under pressure. The TRU is packaged in 55-gallon drums and shipped to WIPP in a cylindrical cask, which contains multiple drums. The waste is buried approximately 2160 ft (658 m) below the surface. Construction of WIPP was under the supervision of the DOE, with advice by the National Research Council and regulation by the EPA. Sandia National Laboratories did performance assessment. For details of the roles of the various organizations, see National Research Council (1996).

The DOE is addressing the monumental challenge of environmental restoration of sites used in the US defense program. It has been recognized that it is not feasible to decontaminate the sites completely. Instead, cleanup to an extent practical is followed by "stewardship," involving isolation, monitoring, and maintenance of certain locations for a very long period. To achieve the goal of protection of the public and the environment, the DOE Environmental Management (EM) program has initiated research on new efficient technologies to handle radioactive materials.

23.9 NUCLEAR POWER PLANT DECOMMISSIONING

Decommissioning, a naval term meaning to remove from service (e.g., a ship), is applied to actions taken at the end of the useful life of a nuclear power plant. The process begins at shutdown of the reactor and ends with disposal of radioactive components in a way that protects the public. LLW disposal from dismantled reactors will be a significant issue in decades to come.

The first action is to remove and dispose of the spent nuclear fuel. Several choices of what to do with the remainder of the plant are available. The options as identified formally by the NRC (1996) are:

(a) SAFSTOR or mothballing, in which some decontamination is performed, the plant is closed and then monitored and guarded for a very long period, perhaps indefinitely.
(b) ENTOMB or entombment, in which concrete and steel protective barriers are placed around the most radioactive equipment, sealing it to prevent release of radioactivity, again with some surveillance.
(c) DECON or immediate dismantlement, in which decontamination is followed by destruction, with all material sent to an LLW disposal site.
(d) Delayed dismantlement, the same as the previous case, but with a time lapse of a number of years to reduce personnel exposure.

The distinction among these various options is blurred if it is assumed that the facility must eventually be disassembled. It becomes more a question of when. Aside from the aesthetic impact of an essentially abandoned facility, there is a potential environment problem related to the finite life of structural materials.

Operation of the reactor over a long period will have resulted in neutron activation, particularly of the reactor vessel and its stainless steel internal parts. Contamination of other equipment in the system will include the same isotopes that are of concern in LLW disposal. Various techniques are used to decontaminate: washing with chemicals, brushing, sand blasting, and ultrasonic vibration. To cut components down to manageable size, acetylene torches and plasma arcs are used. Because such operations involve radiation exposure to workers, a great deal of preplanning, special protective devices, and extra labor are required. A very large volume of waste is generated. Some of it may be too active to put into an LLW disposal site but will not qualify for disposal in a high-level waste repository. Cobalt-60 dominates for the first 50 y, after which the isotopes of concern are 76,000-y nickel-59 and 24,000-y niobium-94.

The NRC requires nuclear plant owners to provide a license termination plan and to set aside funds for decommissioning. A standardized cost-estimation procedure has been developed. Costs vary with units but are $300 million or more. This cost, a small fraction of the value of electricity generated over

the reactor life, is borne by the consumers of electrical power. The NRC (2017) provides data on reactors that have been decommissioned.

An option that has not yet been fully explored is "intact" decommissioning, in which the highly radioactive region of the system would be sealed off, making surveillance unnecessary. The virtues claimed are low cost and low exposure. Ultimately, renewal of the license after replacing all the worn-out components may be the best solution.

A number of reactors will need to be decommissioned in the first quarter of the 21st century. Factors that will determine action include the degree of success in reactor life extension, license renewal, and the general attitude of the public about the disposal of material from nuclear stations as low-level radioactive waste.

23.10 SUMMARY

Radioactive wastes arise from a great variety of sources, including the nuclear fuel cycle and from beneficial uses of isotopes and radiation by institutions.

Spent fuel contains uranium, plutonium, and highly radioactive fission products. In the United States, used fuel is accumulating, awaiting the development of a high-level waste repository. A multibarrier system involving packaging and geological media will provide protection of the public over the centuries the waste must be isolated. The favored method of disposal is in a mined cavity deep underground. In other countries, reprocessing the fuel assemblies permits recycling of materials and disposal of smaller volumes of solidified waste. Transportation of wastes is by casks and containers designed to withstand severe accidents.

LLWs come from research and medical procedures and from a variety of activation and fission sources at a reactor site. They generally can be given near-surface burial. Isotopes of special interest are cobalt-60 and cesium-137. Establishment of regional disposal sites by interstate compacts has generally been unsuccessful in the United States. Decommissioning of reactors in the future will contribute a great deal of low-level radioactive waste. Decontamination of defense sites will be long and costly. Transuranic wastes are being disposed of in the Waste Isolation Pilot Plant.

23.11 EXERCISES

23.1 (a) Compare the specific activities (Bq/g) of natural and depleted uranium and slightly enriched fuel, including the effect of uranium-234. Note the natural uranium density of 18.9 g/cm^3 and the half-lives and atom abundances in percent for the three isotopes in the table below.

Isotope	Half-Life (y)	Natural	Depleted	Enriched
U-235	7.038×10^8	0.7204	0.2026	3.0
U-238	4.468×10^9	99.2742	99.7938	96.964
U-234	2.455×10^5	0.0054	0.0036	0.036

(b) What fraction of the activity is due to uranium-234 in each case? (c) Which uranium blend is most radioactive?

23.2 With the following data, (a) calculate the power capacity of all US PWRs, BWRs, and the light-water reactor (LWR) total and (b) estimate the total annual amount of solid radioactive waste produced by US power reactors.

PWR			BWR		
No.	**Average Power (MWe)**	**Waste (m^3/(GWey))**	**No.**	**Average Power (MWe)**	**Waste (m^3/(GWey))**
69	949.33	23.2	35	929.31	91.5

23.3 A batch of radioactive waste from a processing plant contains the following isotopes:

Isotope	Half-Life	Fission Yield (%)
I-131	8.04 d	2.9
Ce-141	32.50 d	6.0
Ce-144	284.6 d	6.1
Cs-137	30.1 y	5.9
I-129	1.7×10^7 y	1.0

Form the products of the decay constants (in per s) and fission yields (in %) to serve as relative initial activities of the isotopes. Find the times when successive graphing of activity curves would intersect by use of equality of activities (e.g., $A_n = A_{n+1}$).

23.4 Traces of plutonium remain in certain waste solutions. If the initial concentration of Pu-239 in water were 100 parts per million (μg/g), find how much of the water would have to be evaporated to make the solution critical, neglecting neutron leakage as if the container were very large. Note: for H, $\sigma_a = 0.332$ b; for Pu, $\sigma_f = 752$ b, $\sigma_a = 1022$ b, $\nu = 2.88$.

23.5 If the maximum permissible concentration of Kr-85 in air is 1.5×10^{-9} μCi/cm^3, and the yearly reactor production rate is 5×10^5 Ci, what is a safe diluent air volume flow rate (in cm^3/s and ft^3/min) at the exit of the stack? Discuss the implications of these numbers in terms of protection of the public.

23.6 (a) Calculate the maximum decay heat from a single fuel assembly of the total of 180 in a 3000-MWt reactor at 1 d after shutdown of the reactor. (b) How much longer is required for the heat generation rate to decrease by an additional factor of 2?

23.7 The fission product percentage (3.5%) in Fig. 23.3 can be subdivided by source as: U-238, 0.16%; U-235, 1.98%; Pu-239, 1.21%; and Pu-241, 0.15%. (a) Calculate the percentages of total power caused by each fissionable isotope. (b) Assuming that one-third of the 180 fuel assemblies in the reactor are removed each year and that each originally contains 470 kg of U, find what mass of fission products the 60 assemblies contain. (c) What mass of fission products would be produced annually in the whole reactor if operated at its full rating of 3000 MWt, knowing that 1.11 g of fuel fissions per MWtd? (d) Deduce a capacity factor (actual energy divided by rated energy) from the results of (b) and (c).

23.8 Assume that high-level wastes should be secured for a time sufficient for decay to reduce the concentrations by a factor of 10^{10}. (a) How many half-lives does this require? (b) How long is this in years for strontium-90? For cesium-137? For plutonium-239?

23.9 A 55-gallon drum contains a 1-MeV gamma-ray emitting isotope, distributed uniformly with activity $100\,\mu Ci/cm^3$. For purposes of radiation protection planning, estimate the radiation flux at the surface, treating the container as a sphere of equal volume of water and neglecting buildup. (a) Show that the gamma flux at the surface, radius R, is given by $SRP_e/3$, where P_e is the escape probability and S is the source strength in Bq/cm^3. (b) With attenuation coefficient μ and $x=\mu R$, calculate the gamma flux at R using

$$P_e = \left[3/\left(8x^3\right)\right]\left[2x^2 - 1 + (1+2x)\exp(-2x)\right]$$

23.10 Using the results of Example 23.2, calculate the mass of Ra-226. How does the mass of Ra-226 compare to that of U-238 in the ore?

23.12 COMPUTER EXERCISES

23.A If buried radioactive waste is dissolved at a constant rate by water infiltration, it will be released as a square pulse (Murray, 1986). As the pulse migrates in an aquifer with some effective speed, the number of nuclei decreases because of decay. Program WASTEPULSE displays the motion in time. Load and run the program, trying a variety of combinations of distances, speeds, and half-lives.

23.B The transport of a waste radionuclide by groundwater involves the flow with retardation because of holdup in pores. A process called dispersion causes an initial square pulse to be rounded as it moves along (Murray, 1986). Computer program WTT gives numerical values of the contaminant concentration observed at a point in space for various times. Run the program with the default values, and then change individual parameters such as the dispersivities to observe effects.

23.C The NRC specifies in the *Code of Federal Regulations* 10 *Energy Part* 61 *Section* 55 (10CFR61.55) a classification scheme for low-level radioactive waste. The radionuclides present and their concentrations determine whether a shipment is Class A, B, or C. Computer program LLWES (LLW expert system) provides an easy way to classify a given waste. The program also illustrates an expert system that yields answers by a specialist to questions by a worker. Load and run the program, then learn about the NRC's rule from the printout. (a) Select some isotope and assign a specific activity value within the overall material to determine the classification. Note the effect of increasing or decreasing the concentration significantly. (b) Why is Cm-242 with half-life 162.8 d considered a long-lived radionuclide?

REFERENCES

Benedict, M., Pigford, T.H., Levi, H.W., 1981. Nuclear Chemical Engineering, second ed. McGraw-Hill, New York.

Bennett, R.D., Miller, W.O., Warriner, J.B., Malone, P.G., AcAneny, C.C., 1984. Alternative methods for disposal of low-level radioactive wastes. NUREG/CR-3774, U.S. Nuclear Regulatory Commission.

Blue Ribbon Commission on America's Nuclear Future (BRC), 2012. Report to the Secretary of Energy.

Bunn, M., Holdren, J.P., Fetter, S., Van Der Zwaan, B., 2005. The economics of reprocessing versus direct disposal of spent nuclear fuel. Nucl. Technol. 150 (3), 209–230.

Cohen, B.L., 1977. High-level radioactive waste from light-water reactors. Rev. Mod. Phys. 49 (1), 1–20.

Croff, A.G., Wymer, R.G., Tavlarides, L.L., Flack, J.H., Larson, H.G., 2008. Background, status, and issues related to the regulation of advanced spent nuclear fuel recycle facilities. NUREG-1909. U.S. Nuclear Regulatory Commission.

Holcomb, W.F., 1978. Summary of shallow land burial of radioactive wastes at commercial sites between 1962 and 1976, with projections. Nucl. Saf. 19 (1), 50–59.

Jefferson, R.M., Yoshimura, H.R., 1978. Crash testing of nuclear fuel shipping containers. SAND77-1462, Sandia Laboratories.

Moghissi, A.A., 2006. The origin of the EPA's 10,000-year time frame for the high-level waste repository. Nucl. News 49 (2), 41–42.

Murray, R.L., 1986. Radioactive waste storage and disposal. Proc. IEEE 74 (4), 552–579. A survey article that covers all aspects.

National Research Council, 1996. The Waste Isolation Pilot Plant. National Academies Press, Washington, DC. A review by a committee of the National Research Council.

Investigation closes on project's questionable QA records. 2006. Nucl. News 49 (7), 52–53.

Office of Civilian Radioactive Waste Management (OCRWM), 2000. Reference Design Description for a Geologic Repository, Revision 3. U.S. Department of Energy, Las Vegas.

Sandia National Laboratories (SNL), 2008. Total System Performance Assessment Model/Analysis for the License Application. vols. I–III. Las Vegas.

U.S. Department of Energy (DOE), 1980. Management of commercially generated radioactive waste. Final Environmental Impact Statement. DOE/EIS-0046F, vols. 1–3.

U.S. Department of Energy (DOE), 1998. Viability assessment of a repository at Yucca Mountain. DOE/RW-0508.

U.S. Government Accountability Office (GAO), 2011. Commercial nuclear waste: effects of a termination of the Yucca Mountain repository program and lessons learned. GAO-11-229.

U.S. Nuclear Regulatory Commission (NRC), 1996. Generic environmental impact statement for license renewal of nuclear plants: main report. NUREG-1437, vol. 1.

U.S. Nuclear Regulatory Commission (NRC), 2017. 2017–2018 Information Digest. NUREG-1350, vol. 29.

Van Tuyle, G., Hill, D., Beller, D., Bishop, W., Cotton, T., Finck, P., et al., 2001. A roadmap for developing ATW technology: system scenarios & integration. Progr. Nucl. Energy 38 (1–2), 3–23.

FURTHER READING

American Nuclear Society (ANS), Nuclear fuel cycle and waste management. http://www.new.ans.org/pi/ps/. ANS position statements and background information.

Bebbington, W., 1976. The reprocessing of nuclear fuels. Sci. Am. 235 (6), 30–41.

Berlin, R.E., Stanton, C.C., 1989. Radioactive Waste Management. Wiley, New York. Many tables, charts, and diagrams on all types of nuclear wastes.

Carleson, T.E., Chipman, N.A., Wai, C.M. (Eds.), 1995. Separation Techniques in Nuclear Waste Management. CRC Press, Boca Raton, FL. Describes many processes in various areas of the world.

Croff, A.G., Liberman, M.S., Morrison, G.W., 1982. Graphical and tabular summaries of decay characteristics for once-through PWR, LMFBR, and FFTF fuel cycle materials. ORNL/TM-8061. Oak Ridge National Laboratory.

Cochran, T.E., Tsoulfanidis, N., 1999. The Nuclear Fuel Cycle: Analysis and Management, second ed. American Nuclear Society, La Grange Park, IL.

Cohen, B.L., 1983. Before It's Too Late: A Scientist's Case for Nuclear Energy. Plenum Press, New York.

Godbee, H.W., Kibbey, A.H., 1978. The use of evaporation to treat radioactive liquids in light-water-cooled nuclear reactor power plants. NUREG/CR-0142, Oak Ridge National Laboratory.

International Atomic Energy Agency (IAEA), 1986. Methodology and technology of decommissioning nuclear facilities. IAEA Technical Reports Series, No. 267, Vienna.

Kittel, J.H. (Ed.), 1989. Near-Surface Land Disposal, Radioactive Waste Management Handbook. In: vol. 1. Harwood, Chur.

Kibbey, A.H., Godbee, H.W., 1978. The use of filtration to treat radioactive liquids in light-water-cooled nuclear reactor power plants. NUREG/CR-0141, Oak Ridge National Laboratory.

League of Women Voters Education Fund, 1993. The Nuclear Waste Primer. Lyons & Burford, New York. Brief and elementary information.

Moghissi, A.A., Godbee, H.W., Hobart, S.A. (Eds.), 1986. Radioactive Waste Technology. The American Society of Mechanical Engineers, New York. Sponsored by ASME and the American Nuclear Society.

Murray, R.L., 2003. Understanding Radioactive Waste, fifth ed. Battelle Press, Columbus, OH. An elementary survey intended to answer typical questions by the student or the public.

National Research Council, 1996. Nuclear Wastes: Technologies for Separation and Transmutation. National Academies Press, Washington, DC.

National Research Council, 2001. Improving Operations and Long-Term Safety of the Waste Isolation Pilot Plant. National Academies Press, Washington, DC.

National Research Council, 2006. Improving the Regulation and Management of Low-Activity Radioactive Wastes. National Academies Press, Washington, DC.

Noyes, R., 1995. Nuclear Waste Cleanup Technology and Opportunities. Noyes Publications, Park Ridge, NJ. Survey of the national problem and available technologies based on government reports.

Office of Civilian Radioactive Waste Management, http://archive.org/. http://www.ocrwm.doe.gov. Comprehensive discussion of Yucca Mountain Repository and waste transportation.

Platt, A.M., Robinson, J.V., Hill, O.F., 1985. The Nuclear Fact Book. Harwood Academic Publishers, New York. A large amount of useful data on wastes is included.

Resnikoff, M., 1983. The next nuclear gamble: transportation and storage of nuclear waste. Council on Economic Priorities, New York. Written by an opponent and critic of nuclear power.

Stewart, D.C., 1985. Data for Radioactive Waste Management and Nuclear Applications. Wiley, New York.

U.S. Department of Energy (DOE), Science at WIPP. http://www.wipp.energy.gov/science-at-wipp.asp. Physics and biology research underground.

U.S. Environmental Protection Agency (EPA), EPA's role at the waste isolation pilot plant. https://www.epa.gov/radiation/epas-role-waste-isolation-pilot-plant-wipp.

U.S. Nuclear Regulatory Commission (NRC), 1982a. Nuclear waste policy act as amended. http://www.nrc.gov/about-nrc/governing-laws.html. Various governing legislation.

U.S. Nuclear Regulatory Commission (NRC), 1982b. Final environmental impact statement on 10 CFR Part 61: licensing requirements for land disposal of radioactive waste. NUREG-0945, vols. 1–3.

U.S. Nuclear Regulatory Commission (NRC), 2002. Radioactive waste: production, storage, disposal. NUREG/BR-0216, Rev. 2. Mill tailings, low and high level waste.

U.S. Nuclear Regulatory Commission (NRC), 2003. Standard review plan for license termination. NUREG-1700, Rev. 1. NRC requirements for decommissioning.

U.S. Nuclear Regulatory Commission (NRC), Decommissioning of nuclear power plants. http://www.nrc.gov/reading-rm/doc-collections/fact-sheets/decommissioning.html. Regulations and history from NRC.

WM Symposia, Inc., Proceedings of the Symposium on Waste Management Phoenix, AZ. An annual event with a collection of papers on all aspects of radioactive waste around the world.

World Nuclear Association, 2017. The nuclear fuel cycle. http://world-nuclear.org/information-library/nuclear-fuel-cycle/introduction/nuclear-fuel-cycle-overview.aspx.

CHAPTER

NUCLEAR ENERGY FUTURE 24

CHAPTER OUTLINE

We have seen that nuclear energy primarily supplies electrical power, with the high capital cost of nuclear units making them more suited to base load generation. Renewables are experiencing increased use worldwide but for the most part are ill-equipped to provide dispatchable power, that is, to serve loads on demand, because the wind and sun are intermittent sources. The demand for electrical power is increasing worldwide, thus enhancing the role of nuclear energy. Besides electric power, reactors can serve in hydrogen production and desalination, as addressed later in this chapter.

Historically, overall energy needs were served by direct use of fuels, but increasingly electricity is the end use form of energy. Global electricity generation increased fourfold from 6131 TWh in 1973 to 24,255 TWh in 2015 (IEA, 2017a) while world population did not quite double (UN, 2017). The International Energy Agency (IEA, 2017b) World Energy Outlook 2017 states "electricity is the rising force among worldwide end uses of energy, making up 40% of the rise in final consumption to 2040."

Nuclear Energy. https://doi.org/10.1016/B978-0-12-812881-7.00024-1

Ultimately, decisions regarding fuel type are made based on economics. The brevity of this chapter will not give a full and detailed account of the complex and changing energy situation.

Future nuclear power may take several forms: converters, advanced converters, breeders, actinide burners, accelerators, and several types of fusion devices, along with the level of feasibility or practicality of each. For example, an advanced burner reactor would use fast neutrons to destroy transuranics by fission and transmutation. Breeder and fusion reactors are addressed in subsequent chapters.

24.1 WORLD ENERGY USE

The use of energy from the distant past to the present has changed dramatically. Primitive man burned wood to cook and keep warm. For most of the past several thousands of years of recorded history, the only other sources of energy were the muscles of men and animals, wind for sails and windmills, and waterpower. The Industrial Revolution of the 1800s brought in the use of coal for steam engines and locomotives. Electric power from hydroelectric and coal-burning plants was an innovation of the late 1800s. Oil and natural gas became major sources of energy only in the 20th century. Nuclear energy has been available for only approximately 50 y.

To think about the future, at a minimum it is necessary to understand the present. Table 24.1 gives world energy consumption by geographic region. Of special note is the disparity in per-capita consumption. Because productivity, personal income, and standard of living tend to follow energy consumption, the implications of these numbers for the human condition in much of the world is evident. The data on ratio of consumption and production confirm our knowledge that the Middle East is a major energy supplier through petroleum and shows that Europe is quite dependent on imported energy.

A breakdown of the electrical production according to primary energy source by region is given in Table 24.2. We see that there is minimal nuclear power in Africa or Central and South America. Of that in Asia, most is in Japan, South Korea, and China.

Table 24.1 World Primary Energy, 2015

Region	Consumption (10^{15} Btu)	Per Capita (10^{6} Btu)	Consumption/ Production
Africa	18.053	15.3	0.57
Asia and Oceania	216.794	53.5	1.27
Central and South America	29.624	58.5	0.91
Eurasia	42.592	146.8	0.58
Europe	79.089	128.8	1.87
Middle East	36.221	150.0	0.44
North America	119.369	246.9	1.03
World	541.742	73.5	0.99

Data from US Department of Energy (DOE), Energy Information Administration (EIA), 2018. International energy statistics. http://www.eia.gov/ies.

Table 24.2 World Total Net Electricity Generation (2015, billion kWh)

Region	Nuclear	Hydro	Others[a]	Fossil	Total[b]
Africa	11.0	120.2	16.2	593.6	739.9
Asia and Oceania	396.9	1535.2	539.5	7519.2	9982.4
Central and South America	20.4	659.5	105.1	455.5	1240.2
Eurasia	267.8	235.0	8.4	944.8	1454.5
Europe	837.3	612.5	640.1	1513.0	3590.2
Middle East	3.2	17.5	1.9	1023.5	1046.0
North America	904.0	657.0	381.7	3102.8	5040.2
World	2440.5	3836.9	1692.9	15152.4	23093.4

[a]*Nonhydro renewables: geothermal, wind, solar, tide, wave, fuel cell, biomass, and waste.*
[b]*This total includes a reduction due to hydroelectric pumped storage losses.*
Data from US Department of Energy (DOE), Energy Information Administration (EIA), 2018. International energy statistics. http://www.eia.gov/ies.

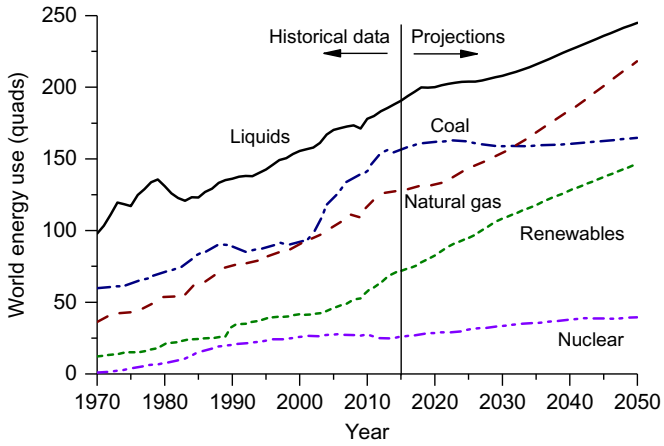

FIG. 24.1

World energy consumption 1970–2050.

Data from US Department of Energy (DOE), Energy Information Administration (EIA), 2005. International energy outlook 2005. DOE/EIA-0484(2005); US Department of Energy (DOE), Energy Information Administration (EIA), 2018. International energy statistics. http://www.eia.gov/ies.

Predictions have been made on world future energy consumption patterns. Fig. 24.1 shows that, except for coal, the use of all energy forms, including nuclear, continues to increase. The projection may not take enough account of eventual acceptance of the virtue of nuclear power in avoiding gaseous emissions. In addition, the curve for liquids does not take account of the large increase in oil prices. Finally, the rapid growth in renewables may be optimistic.

Table 24.3 World Population Data, 2015

Region	Millions of Inhabitants	Fertility Rate	Life Expectancy
Africa	1194	4.72	60.2
Northern America	356	1.85	79.2
Latin America and the Caribbean	632	2.14	74.7
Asia	4420	2.20	71.8
Europe	741	1.60	77.2
Oceania	40	2.41	77.9
World	7383	2.52	70.8

Data from United Nations (UN), 2017. World population prospects: the 2017 revision.

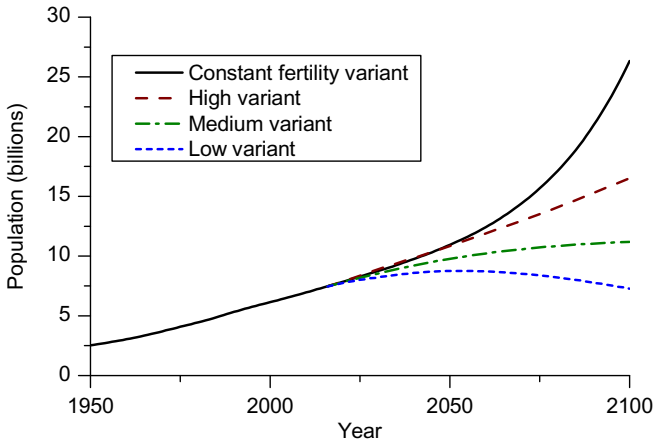

FIG. 24.2

Past and projected world population growth, 1950–2100, with four fertility scenarios.

Data from United Nations (UN), 2017. World population prospects: the 2017 revision.

Table 24.3 presents the most recent world population data. The fertility rate is defined as the number of children per woman. It is seen to be highest in less developed regions. The trend of population in the future depends crucially on that parameter, as shown in Fig. 24.2. The four growth projections involve fertility rates that vary with country and with time. The "high" case leads to a world population of almost 11 billion by the year 2050. The population in developed countries is expected to plateau.

A conclusion that seems inevitable is that every source of energy imaginable should be used in its appropriate niche in the scheme of things. The availability of diverse sources minimizes the disruption of life in the event of a transportation strike or international incident. Indeed, the availability of several sources that can be substituted for one another has the effect of reducing the possibility of conflict between nations. Included in the mix is extensive use of conservation measures.

Conservation provides a means for effectively increasing the supply of energy. Experience has shown that great savings in fuel in developed countries have resulted from changes in lifestyle and

improvements in technology. Successful examples are the use of lower room temperatures in winter, shifts to smaller automobiles with more efficient gasoline consumption, increased building insulation, energy-efficient home appliances and industrial motors, and electronically controlled manufacturing. Unfortunately, the move to larger vehicles in the United States was in the wrong direction. Hundreds of TWh consumed from standby power use by billions of network-enabled devices, such as smart televisions, could be avoided (IEA, 2014). There remains significant potential for additional saving, which has many benefits: conservation of resources, reduced emission of pollutants, and enhanced industrial competitiveness. However, there is limited applicability of the concept to less developed countries, in which more energy use is needed, not less.

Protection of the environment and of the health and safety of the public will continue to serve as constraints on the deployment of energy technologies. The environmental movement has emphasized the damage being done to the ecology of the rain forest in the interests of development; the harm to the atmosphere, waters, and land from industrial wastes; and the loss of habitats of endangered or valuable species of wildlife. Air pollution caused by emissions from vehicles and coal-fired power plants poses a problem in cities. Less well known is the release of radioactivity from coal plants, in amounts greater than those released from nuclear plants in normal operation (McBride et al., 1978). Although a core meltdown followed by failure of containment in a nuclear plant could result in many casualties, the probability of such a severe accident is extremely low. In contrast, there are frequent deaths resulting from coal mining, gas pipelines, and oil drilling. There is an unknown amount of life shortening associated with lung problems aggravated by emissions from burning coal and oil.

The oil embargo of 1973, in which limits were placed on shipments from producing countries to consuming countries, had a sobering effect on the world. It prompted a flurry of activity aimed at expanding the use of alternative energy sources such as solar, wind, biomass, and oil shale, along with conservation. Easing of the energy crisis reduced the pressure to find substitutes, and as oil prices fell, automobile travel increased. Use of energy in general is dominated by current economics. If prices are high, energy is used sparingly; if prices are low, it is used freely without concern for the future. Ultimately, however, when the resource becomes scarcer and expensive, its use must be curtailed to such an extent that social benefits are reduced. If no new sources are found, or if no renewable sources are available, the quality of existence regresses and civilization is brought back to an archaic condition.

The effects on the status of the world of various assumptions and actions related to energy can be examined by application of the program FUTURE in Computer Exercise 24.A.

24.2 NUCLEAR ENERGY AND SUSTAINABLE DEVELOPMENT

Throughout history, there has been little concern for the environment or human welfare. European countries systematically extracted valuable resources from Mexico, South America, and Africa, decimating cultures along the way. In the westward expansion in the United States, vast forests were razed to provide farmland. The passenger pigeon became extinct, and the bison nearly so. Slavery raged in the Americas until the latter half of the 19th century. Only after European countries lost their colonies after world wars did African nations and India regain autonomy.

The book *Silent Spring* by Rachel Carson (1962) stimulated the environmental movement of the 1960s. That overuse of resources could be harmful was revealed by Garrett Hardin's (1968) essay "The Tragedy of the Commons." Two centuries ago, Malthus (1798) predicted that exponential growth

of population would exceed linear growth of food supply, leading to widespread famine. The idea was revived by use of sophisticated computer models by Meadows et al. (1972) in *The Limits to Growth*, which predicted the collapse of civilization under various pressures associated with continued growth.

Finally, in the 1970s and 1980s the United Nations sponsored several international conferences on global problems and potential solutions. Out of these came the concept of *sustainable development*. The phrase gained great popularity among many organizations that were concerned with the state of the world. The original definition of the term was "… meets the needs of the present without compromising the ability of future generations to meet their own needs" (UN, 1987). As noted by Reid (1995), the phrase can be interpreted to support business as usual or to require drastic cutbacks. However, it generally implies conserving physical and biological resources, improving energy efficiency, and avoiding pollution while enhancing the living conditions of people in developing countries. Ideally, all goals can be met. The subject is broad in that it involves the interaction of many governments, cultures, and economic situations. Several conferences have been held under United Nations auspices to highlight the issues, obtain agreements, and map out strategies. One prominent conference was the Earth Summit held in Rio de Janeiro in 1992, which included Agenda 21, a list of 2000 suggestions for action. A follow-up appraisal of results was made in 1997. Progress since is monitored by a "watch" organization. Johannesburg hosted another Earth Summit in 2000, followed by a return to Rio in 2012 for a 20th anniversary meeting.

The objectives of sustainable development are furthered by nongovernmental organizations (NGOs). Unfortunately, implementation of goals has been frustrated by wars, the HIV/AIDS epidemic, drought, famine, and disease. One might be pessimistic and question whether there is any hope of achieving the desired improvements in light of failure over half a century. Alternatively, one might be optimistic that the concept can bring all parties together in a concerted effort and ultimate breakthrough.

A potential cure for a runaway population and continued misery is improved economic conditions. However, the gap between conditions in rich and poor countries persists, and no improvement is in sight. The problem has become more complex by the concerns about the environment related to the destruction of the rainforests in Central and South America. There are no easy solutions, but a few principles seem reasonable. Protection of the environment is vital, but it should not thwart the hopes of people in developing countries for a better life. It is obvious that simple sharing of the wealth would result in uniform mediocrity. The alternative is increased assistance by the developed countries in the form of capital investment and technological transfer. This must be done, recognizing the principle that the people of the country being helped should lead the program to improve.

Technology can be introduced in two ways: (1) supplying devices that are appropriate to the receiving country's urgent needs and that are compatible with existing skills to operate and maintain equipment or (2) supplying equipment, training, and supervision of sophisticated technology that will bring the country quickly to industrial status. Arguments for and against each approach can easily be found. It is possible that both should be followed to provide immediate relief and further the country's hopes for independence.

Technically advanced countries have applied restrictions to the transfer of nuclear technology to some developing nations in an attempt to prevent the achievement of nuclear weapons capability. Emerging countries resent such exclusion from the opportunity for nuclear power.

One major objective of sustainable development is the improvement of human health in developing countries. If nuclear medicine for diagnosis and treatment were expanded universally, it could make a

great difference to the health of people such as those in Africa. For countries that cannot afford to import coal, oil, and natural gas, the introduction of nuclear power for widespread supply of electricity could facilitate pollution-free industrial and commercial development while enhancing human comfort. Nuclear plants can be built to use the waste heat for desalination of seawater, providing safe water for human consumption. For such to be implemented, a reactor type is needed that avoids the high capital cost of conventional light-water reactors, requires little maintenance, and is passively safe.

The US nuclear power industry includes electric utilities that use reactors, equipment manufacturers and vendors, and service organizations. That industry is convinced that electricity from nuclear power will continue to be necessary to sustain economic growth. Leaders note that nuclear power does not contribute to pollution and potential climate change and helps provide energy security. The industry believes that energy conservation and the use of renewable sources of energy are highly desirable but not sufficient for long-term needs, especially in light of a growing population and the demand for environmental protection.

24.3 COMPONENTS OF ELECTRICAL POWER COST

Economics is the driving force behind choosing a given energy source. In terms of electricity generation, a variety of energy sources can be contemplated, including nuclear, coal, natural gas, hydropower, and so on. A review and forecast by the Department of Energy (DOE) of electrical generation covering the period 1950–2050 are shown in Fig. 24.3. In the United States, nuclear and coal-fired plants have traditionally supplied the base load. Coal plants are coming under increasing scrutiny due to CO_2 emissions, which are linked to global climate change. Hydraulic fracturing (fracking) and horizontal drilling are unleashing large deposits of natural gas and petroleum, which are

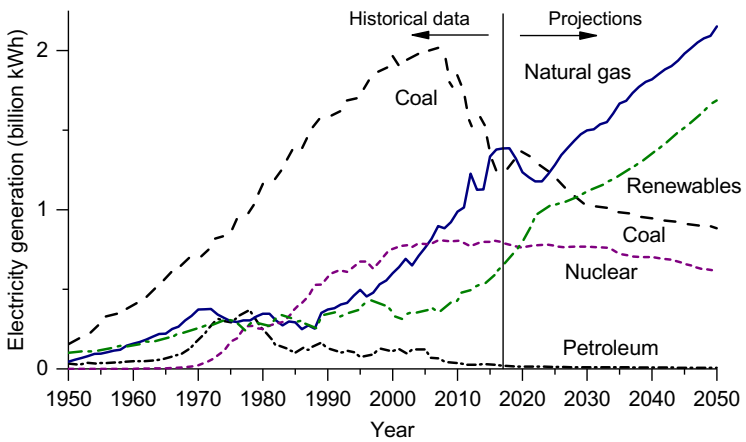

FIG. 24.3

US electricity generation by fuel, 1950–2050.

Data from US Department of Energy (DOE), Energy Information Administration (EIA), 2012. Annual energy review 2011. DOE/EIA-0384(2011); US Department of Energy (DOE), Energy Information Administration (EIA), 2017. Annual energy outlook with projections to 2050.

predicted to make the United States a net exporter of oil by 2030 (IEA, 2017a). The availability and price of natural gas along with its lower CO_2 emissions compared to coal are elevating it to the favored choice for new electric generation. Questions regarding possible groundwater contamination, radioactivity release, and induced seismic activity by fracking operations and eventual natural gas pricing when the export business is in full swing remain unanswered, as well as cost volatility. Renewable energy tax credits encourage growth in electricity generation from wind and photovoltaics (DOE, 2017a).

The consumer's interest lies in the unit cost of reliable electricity delivered to the home. In January 2018, the average residential cost of electricity in the United States was 12.2 ¢/kWh (DOE, 2018). The overall price can be broken into costs due to generation, transmission, and distribution. For a nominal cost of 10.3 ¢/kWh for all sectors (residential, commercial, industrial, and transportation), the average prices in 2016 for the three components were generation 5.9, transmission 1.1, and distribution 3.3 ¢/kWh (DOE, 2017a).

The comparison between costs of electricity generation from nuclear and natural gas varies in several ways. Generation costs are dominated by fuel costs for natural gas and by capital costs for nuclear (DOE, 2017b). Operating and maintenance (O&M) costs for nuclear plants are generally high because of the great complexity of the equipment and the stringent safety requirements of the regulators. Prices charged directly to the consumer do not include hidden external costs such as damage to the environment and detrimental effects on human health (Friedrich and Voss, 1993). The National Research Council (2010) reports that nuclear power and renewable sources have very small external costs in comparison to fossil fuels.

The capital costs of nuclear plants vary greatly, but the current figure is $5945 per installed kWe for a large plant, as detailed in Table 24.4. The overnight cost represents the funds required to construct the plant, excluding interest. Nuclear power has long been regarded as capital-intensive because equipment costs are high, whereas fuel costs are low. Typically, the main parts of the nuclear plant itself and percentages of the cost are the reactor and steam system (50%), the turbine generator (30%), and the remaining balance of plant (20%). Additional costs include land, site development, plant licensing and regulation, operator training, interest and taxes during construction, and an allowance for contingencies. Capital costs of both fossil and nuclear plants were high during the early 1970s to early 1980s due to high

Table 24.4 Estimates of Power Plant Capital and Operating Costs

Power Plant Technology	Nominal Capacity (MW)	Overnight Capital Cost ($/kWe)	Annual Fixed O&M Cost ($/kWe-y)	Variable O&M Cost ($/MWh)
Ultra supercritical coal with 30% carbon capture	650	5084	70	7.1
Advanced natural gas combined cycle	429	1104	10	2
Advanced nuclear	2234	5945	100.3	2.3
Biomass	50	4985	110	4.2
Onshore wind	100	1817	39.7	0
Photovoltaic-tracking	150	2534	21.8	0

The O&M costs do not include fuel costs.
Data from US Department of Energy (DOE), Energy Information Administration (EIA), 2016. Capital cost estimates for utility scale electricity generating plants.

Table 24.5 Construction Costs for Nuclear Units (in the United States)

Period[†]	Number of Units	Average Cost ($/kWe)
1968–71	11	161
1972–73	15	217
1974–75	19	404
1976–78	12	623
1979–84	17	1373
1985–86	15	2416
1987	7	4057
1988	5	3085

[†]*During which units entered commercial operation.*
Data from: U.S. Department of Energy (DOE), Energy Information Administration (EIA), 1989. Nuclear Power Plant Construction Activity 1988. DOE/EIA-0473(88). Washington, DC.

interest rates and high inflation, but the increase in cost was greater for nuclear plants because they are fundamentally more expensive and the construction time was prolonged. Table 24.5 gives the trend of plant costs for US reactors over various periods in which commercial operation began.

Further perspective is needed on the capital cost component. Utilities that are not affected by deregulation serve an assigned region without competition. In exchange, the price that they can charge for electricity is regulated by public commissions of state governments. When a utility decides to add a plant to its system, it raises capital by the sale of bonds, with a certain interest rate, and by the sale of stock, with a dividend payment to the investor. These payments can be combined with income tax and depreciation to give a charge rate that may be as high as 20%. The interest charge on the capital invested must be paid throughout the construction period. This is an important matter because the average total time required to put a plant into operation by 1985 was approximately 13 y in the United States, in contrast with a figure of less than 6 y in 1972. Fig. 24.4 shows trends in construction periods for the recent past. Several reasons have been advanced for the long time between receipt of a construction permit and commercial operation. In some cases, plants were well along when new regulations were imposed, requiring extensive modifications. Others have been involved in extended licensing delays resulting from intervention by public interest groups. Others suffered badly from lack of competent management.

EXAMPLE 24.1

The major costs of generating electricity from a nuclear power plant can be estimated using data from Table 24.4, which does not include fuel prices. Assuming a levelized annual fixed charge rate of 10% and a capacity factor of 95%, applying Eq. (18.3) gives a combined capital and nonfuel O&M cost of

$$e = \frac{F_B I + \text{O\&M}}{P_e CF(8760\text{h/y})} = \frac{(\$5945/\text{kWe})(0.1/\text{y}) + (\$100.3/\text{kWe/y})}{(0.95)(8760\text{h/y})} + \frac{\$2.3/\text{MWh}}{1000\text{kW/MW}}$$
$$= \$0.0858/\text{kWh}$$

According to Example 15.6, inclusion of fuel costs adds $0.0037/kWh, which is smaller than either the capital or O&M costs.

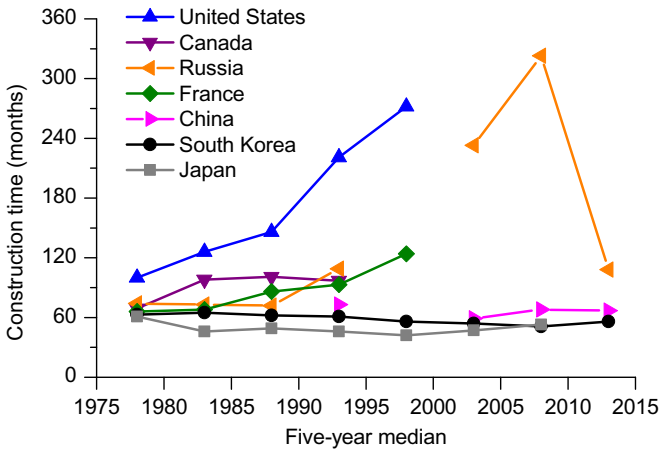

FIG. 24.4

Median construction periods for nuclear power plants.

Data from International Atomic Energy Agency (IAEA), 2012. Nuclear power reactors in the world; International Atomic Energy Agency (IAEA), 2017. Nuclear power reactors in the world.

24.4 NUCLEAR POWER STAGNATION

The demand for electrical power varies on a diurnal basis because of the activities of individuals, businesses, and factories. It also varies seasonally, showing peaks when either heating or air conditioning is used extensively. The utility must be prepared to meet the peak demand, avoiding the need for voltage reduction (i.e., a brownout) or rotating blackouts. The existing megawatt capacity must include a margin or reserve, prudently a figure such as 15%. Finally, the state of the national economy and the rate of development of new manufacturing determine the longer-range trends in electrical demand. Utilities must continually be looking ahead and predicting when new plants will be required to meet power demand or to replace older obsolete units.

Such forecasts must be made well into the future because of the long time required to build a new power plant. However, projections can readily turn out to be wrong because of unforeseen events or trends, including the interruption of energy supplies from abroad, shifts in the state of the economy, and major changes in the regulatory climate. If an estimate of power demand is too low and stations are not ready when needed, customers face the problem of shortages; but if the estimate is too high, and excessive capacity is built, customers and shareholders must bear the effects of added expense.

The history of nuclear growth and eventual stagnation over the last several decades of the 20th century serves well to illustrate this situation. It is not possible to identify any single cause for the situation, but we can indicate many of the factors that had an effect. Optimism about nuclear energy was based on the successful development of military applications and the belief that translation into peaceful uses was relatively easy and straightforward. After studying and testing several reactor concepts, the United States chose the light-water reactor. Hindsight indicates that safety might have been assured with far less complexity and resultant cost by adoption of heavy-water reactors or gas-cooled reactors (Cowan, 1990).

During the post-World War II economic boom, the demand for electric power was increasing by approximately 7% per year. New coal-fired plants satisfied most of the growth. In 1957, the first commercial power reactor was started at Shippingport, Pennsylvania, and new designs of larger units were developed by two concerns. Some of these were attractive to utilities because they were turnkey plants, priced very favorably (Burness et al., 1980). A large number of orders were placed in the 1960s to the four main vendors: Westinghouse, General Electric (GE), Babcock & Wilcox (B&W), and Combustion Engineering. These contracts were entered into based on sustained electric power demand growth well to the end of the century and an expected construction time of approximately 6 y.

Predictions were optimistic in that period. For example, in 1962 and later in 1967, the Atomic Energy Commission (AEC, 1962) predicted the following installed nuclear capacities:

Year	GWe
1970	10
1980	95
2000	734

The reasons for the optimism were expectations that the US economy would continue to expand, that electricity would substitute for other fuels, and that nuclear would fill a large fraction of the demand, reaching 56% by the year 2000. As it turned out, the level of 95 GWe was actually reached late in the 1980s, but the figure only reached 100 GWe after an additional decade.

What is the reason for the great discrepancy between forecasts and reality? The first is that it took longer and longer to build nuclear plants, adding large interest costs to the basic capital cost. Inflation in the 1970s drove costs of construction up dramatically, as we see in Table 24.5. The effect on nuclear plants was especially severe because of their complexity and the requirement of quality assurance at every stage from material selection to final testing.

The Middle East oil boycott of 1973 caused an increase in the cost of energy in general, accentuated a national recession, and prompted conservation practices by the public. The growth rate of electrical demand fell to 1% per year. Consequently, many orders for reactors were canceled; see Fig. 24.5. However, by this time, a large number of reactors were in various stages of completion—reactors that would not be needed for many years, if ever. Some that were approximately 80% completed were finished, but work on others of 50% or less was stopped completely. The hard fact was that it was cheaper to abandon a facility on which half a billion dollars had been invested rather than to complete it.

EXAMPLE 24.2

For a constant percentage growth rate of r, the time to double the quantity is

$$T_d = \ln(2)/(r/100\%) \tag{24.1}$$

In the post-World War II period, the doubling time for the 7% electricity growth rate was

$$T_d = \ln(2)/[(7\%/\text{y})/100\%) = 9.9\,\text{y}$$

The 1%/y rate subsequent to the oil boycott lengthened the doubling time to 69 y.

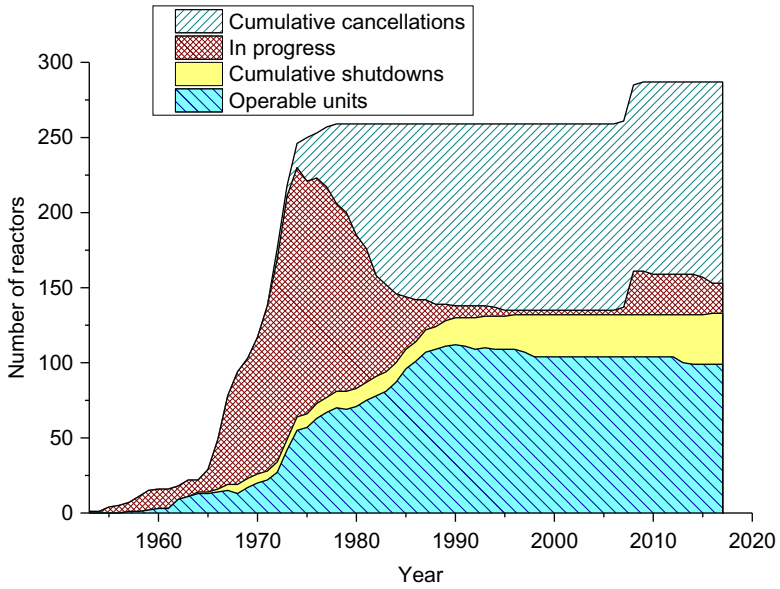

FIG. 24.5

Nuclear generating units in the United States.

Data from US Department of Energy (DOE), Energy Information Administration (EIA), 2005. Annual energy review 2005. DOE/EIA-0384(2005), and multiple volumes of NUREG-1350.

Nuclear power was barely getting started when the environmental movement began and consumers' interests became more vocal and influential. Opposition to nuclear power was composed of many elements. Early activists expressed themselves as opposed to the power of the entity called the military-industrial complex. Because nuclear energy is involved in both weapons and commercial power, it became a ready target for attack. Those philosophically inclined toward decentralized authority, the return to a simpler lifestyle, and the use of renewable energy were enlisted into the antinuclear cause. Those fearful of radiation hazards and those concerned about the growth of nuclear weapons were also willing recruits. Well-organized opposition forces set about to obstruct or delay reactor construction through intervention wherever possible in the licensing process. The Nuclear Regulatory Commission (NRC) had a liberal attitude toward interveners in the interests of fairness. The net effect in many cases was to delay construction and thus increase the cost. The high costs then served as an additional argument against nuclear power. The general public has tended to be swayed by statements of the organized opposition and to become doubtful or concerned. Traditional distrust of government was accentuated in the 1970s by the pains of the war in Vietnam. The aftermath of the Watergate affair was a loss in confidence in national leadership. The public was further sensitized by the revelation that industrial chemicals were affecting plant and animal life and that wastes had been mismanaged, as at Love Canal. Because of accompanying radiation, wastes from nuclear power were regarded as more dangerous than ordinary industrial wastes. Concerns were aggravated by the apparent inability of government and industry to deal effectively with nuclear wastes. Changes in policy and plans between national administrations based on differences in approach were ascribed to ignorance.

In the 1980s, the demand for electricity began to increase again, but by that time, other factors had developed that discouraged utility management from resuming a building program. In earlier years, the utilities in a state were regulated monopolies that could readily pass on costs to the consumers and could show continued decreases in the cost of electricity. When the recession occurred, costs increased, and customers adopted conservation measures, reducing income from the sale of electricity.

In the interests of improved protection of the public, the NRC increased the number and detail of its rules and guidelines, often requiring that changes in equipment be made or additional equipment be installed. Examples of mistakes in design, installation, testing, cost overruns, shoddy workmanship, and inept management received a great deal of media attention, further eroding confidence among investors and the general public.

During this period, the role of the public utilities commissions (PUCs) became more important. These state regulatory organizations are committed to protect the consumers' interests. They became alarmed at the rising costs of nuclear plants and were reluctant to allow utilities to pass costs on to consumers, thus reducing the margin of profit to the company and its stockholders. The practice of prudent review is applied to the construction of facilities after construction is complete. Questions are asked such as, "Would a reasonable person have incurred those costs, or canceled the project?" A related and useful test asks, "Were those facilities actually needed?" or "Should a cheaper power source have been built?" Expenditure by utilities was disallowed for many reasons. Some costs were unreasonable, such as cost overruns that could have been avoided with better project management. Others were in the category of errors in judgment but only in hindsight. An example is a decision to build a generating plant that turned out to be larger than necessary. In many cases, expenditures by the utility were excluded even though they were outside the control of the management. Because of unhappy experiences, utility executives became increasingly wary of any new large-scale long-term commitment. The prospect of fiscal disaster outweighed that of criticism for failing to anticipate and meet electricity needs.

On a very positive note, more than 100 reactors were in operation by the turn of the century, contributing approximately 20% of the total US electricity, with no harm to the public, and at a cost that was well below that of oil-fired units and many coal-burning plants. Realistically, however, it is a fact that the cost of nuclear plants has increased dramatically. Utilities found little sympathy for their requests for rate increases to meet costs of operation. For 30 years after 1978, there were no new orders for reactors in the United States.

The Three Mile Island (TMI) accident of 1979 (Section 21.6) dealt a severe blow to the nuclear power industry in the United States. Although releases of radioactivity were minimal and no one was hurt, the image of nuclear power was seriously tarnished. Media attention was disproportionate to the significance of the event and greatly increased the fears of local residents. The apparent confusion that existed immediately after the incident and the revelation of errors in design, construction, and operation caused nationwide concern over the safety of all reactors.

The Chernobyl disaster of 1986 (Section 21.8) commanded international attention. The effect on public opinion may have been greater in Europe than in the United States, in part because of the geographic proximity to the event. It is generally appreciated in the United States that the Chernobyl reactor was operated by the USSR without adequate precautions, was basically more unstable than light-water reactors (LWRs), and lacked a full containment. Nonetheless, the specter of Chernobyl remained over the nuclear industry.

In a scene reminiscent of TMI, the meltdowns at Fukushima Daiichi in 2011 (Section 21.9) occurred when the world economies were suffering a recession, just when a revival of nuclear power was beginning to take hold.

24.5 NUCLEAR POWER TODAY

The revival of interest in the United States in nuclear power in the early 21st century was initially characterized as a renaissance. The situation contrasted with the stagnant conditions of the previous two decades. A number of utilities applied for reactor license renewals, and construction began on four new power reactors, the first in more than 25 y. Specifically, two AP1000 units each were slated for commercial operation before 2020 at the Vogtle and Summer plants in the southeastern United States. Furthermore, the Tennessee Valley Authority resurrected the previously cancelled Watts Bar 2 unit, and brought it to commercial operation in October 2016. However, the nuclear power renaissance has been supplanted by the availability of low-cost natural gas made possible by hydraulic fracturing.

Efforts were underway for several years in the United States to develop a comprehensive energy program that would integrate the activities of the DOE, the NRC, the EPA, and other federal agencies, with contributions by the private sector. These initiatives culminated in the passage by Congress of the Energy Policy Act of 1992 (Public Law 102-486). It provided energy efficiency goals and standards, promoted alternative fuels, prescribed new R&D on electric vehicles, restructured the production of electricity, addressed radioactive waste disposal, established a uranium enrichment corporation, and simplified nuclear plant licensing. In essence, the law affirmed the nation's commitment to preserve and extend the nuclear option as part of a broad energy mix.

The Energy Policy Act of 2005 had a number of provisions related to nuclear energy. First is the Energy Loan Guarantee Fund, which is a sort of insurance that nuclear and other sources of sustainable energy can use. The guarantee is up to 80% of the cost of the project and long-term repayment is allowed. Second is a tax credit of 1.8 ¢/kWh produced on 6000 MW of new capacity for a period of 8 y. For example, if there is an allocation of 750 MW to a 1000-MW plant, it can claim (0.75)(1.8) = 1.35 ¢/kWh, with certain limitations. Third is the renewal for 20 y of the Price-Anderson Act, which provides insurance coverage in case of a nuclear accident. Plants are required to purchase $300 million of private insurance as primary coverage. Then they must pay a fee of $95.8 million per reactor. With more than 100 reactors in the United States, the total is more than $10 billion. Fourth is standby support for new plants if there is a delay caused by the NRC or from litigation. For the first two new plants, 100% coverage is up to $500 million each, with 50% for the next four plants. Fifth is a requirement on the NRC to take several actions in support of counterterrorism. Sixth is authorization of approximately $3 billion for nuclear R&D and hydrogen projects, including the establishment of a Next Generation Nuclear Power Plant Project for production of electricity and hydrogen (see Section 18.8).

Light-water reactors of the pressurized water reactor (PWR) and boiling water reactor (BWR) types have performed very well over several decades. However, without any action being taken, a number of reactors in the United States would come to the end of their license period and be shut down. Many believe that it is in the best interests of society to continue the nuclear option as a part of an energy mix. To do so, nuclear power must be acceptable to the public, the utilities, the regulatory agencies, and the financial community. This implies the need for confidence in reactor safety and economy.

The life of a nuclear reactor system was set by Congress on antitrust and economic grounds as 40 y, with prior termination for marginal safety and excessive outage for maintenance and repair. In view of the high capital cost of a reactor, it pays to stretch the life beyond the 40-y mark.

The NRC can grant 20-y extensions of an operating license. Special attention in the licensing must be given to the potential effects of aging of components and systems, with information on ways to mitigate the effects. The objective is to determine whether the plant can operate safely in the extended period. A number of plants have applied for and been granted license renewal. In January 2018, the NRC received the first *subsequent license renewals* for operation beyond 60 y. In addition, several plants have made equipment modifications to achieve power uprates of up to 20%. From 1977 to 2017, the NRC has approved almost 8000 MWe of power uprates, equivalent to constructing about seven new power reactors.

Nuclear energy itself may very well follow a sequential pattern of implementation. Converter reactors, with their heat energy coming from the burning of uranium-235, use uranium inefficiently because they require enrichment of fuel and disposal of spent fuel. Breeder reactors, in contrast, have the potential of making use of most of the uranium, thus increasing the effective supply by a large factor. Sources of lower uranium content can be exploited, including very low-grade ores and the dissolved uranium in seawater, as almost all the contained energy is recovered. To maintain an ample supply of uranium, storage of spent fuel accumulated from converter reactor operations should be considered instead of permanent disposal by burial as waste. Conventional arguments that reprocessing is uneconomical are not as important when reprocessing is needed as a step in the planned deployment of breeder reactors. Costs for storage of spent fuel should be examined in terms of the value of uranium in a later era in which fossil fuels are very expensive to secure. Eventually, fusion that uses deuterium and tritium as fuel may be practical, and fusion reactors would supplant fission reactors as the latter's useful lives end.

24.6 GREENHOUSE EFFECT AND GLOBAL CLIMATE CHANGE

The greenhouse effect is one of the processes by which the Earth is warmed. Sunlight of short wavelength can readily pass through water vapor and gases such as carbon dioxide in the atmosphere. Energy is absorbed by the Earth's surface, which emits long wavelength infrared radiation that is stopped by the vapor and gases. The effect accounts for an increase in natural temperature of approximately 30°C. Fig. 24.6 shows the energy flows for the effect.

There is good evidence that the carbon dioxide content of the air has increased from a preindustrial level of 280 ppm to the present value of 400 ppm (Blunden, 2014). Less certain is the amount of temperature change over that period because of natural fluctuations related to sun activity, volcanic dust, and shifting ocean currents.

Greenhouse gases are the collection of natural and manmade substances including water vapor (H_2O), carbon dioxide (CO_2), methane (CH_4), nitrous oxide (N_2O), and chlorofluorocarbons (e.g., Freon). Each of these has been increasing in concert with industrialization and increased biomass burning. Estimates have been made of a possible increase of 1–4°C in global surface temperature by the end of the 21st century if action is not taken (IPCC, 2014). The consequences of such global warming that have been proposed are more severe weather, including droughts, storms, and floods; higher incidence of tropical disease; and a melting of ice near the poles that would cause a rise in ocean level that would inundate coastal cities.

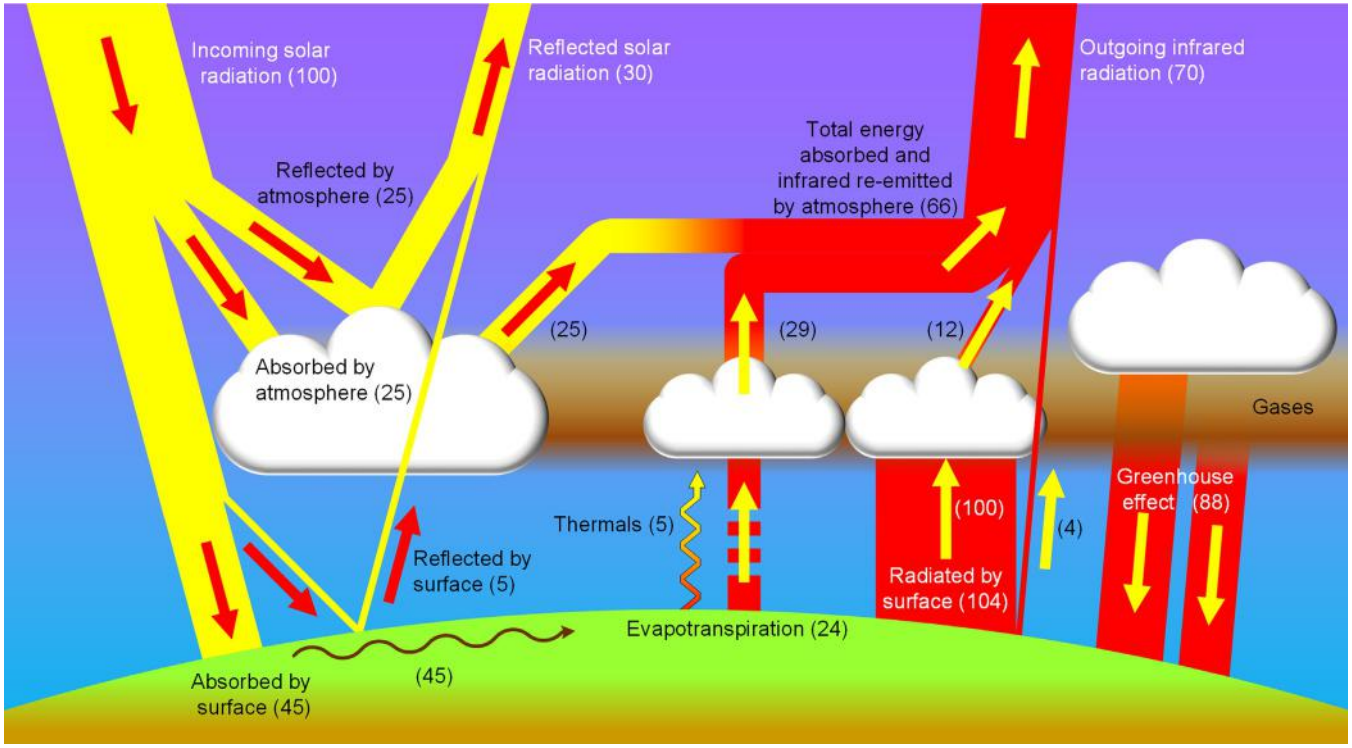

FIG. 24.6

Earth's radiation energy balance in relation to the greenhouse effect. Numbers are percentages of incoming sunlight.

Based on Schneider, S.H., 1992. Introduction to climate modeling. In: Trenbeth, K.E. (Ed.), Climate System Modeling. Cambridge University Press, New York.

International concern led to the Kyoto Protocol of December 1997, which calls for a reduction in carbon emission by all countries, with different percentages for each. If the United States were to ratify the treaty, it would be expected to reduce 7% from 1990 levels. Presently, there are 192 parties to the Kyoto Protocol.

Representatives of European Green Parties deliberately excluded nuclear power from the Kyoto protocol. This omission was criticized in a report of the Nuclear Energy Agency (OECD NEA, 2002). That report notes that current nuclear electric plants worldwide are reducing CO_2 emissions by approximately 17%.

Scientists from more than 100 countries have contributed to the study and evaluation of recent trends in observations, research, and modeling results related to global warming. Their work is for the Intergovernmental Panel on Climate Change (IPCC), which is sponsored by the World Meteorological Organization (WMO) and the United Nations Environment Programme (UNEP). The mission of IPCC is to assess all information on causes, impacts, and options for adaptation and mitigation.

A committee of the IPCC has highlighted in multiple voluminous reports on the science of climate change that there is a serious potential world problem. A key finding is the conviction that the main source of global warming is human activity. Estimates are made of the magnitude of temperature increases and the amount of rise in sea levels that would force migration of millions of people in low-lying countries. Predictions are made on the loss of arctic ice and increases in heat waves and tropical storms. Impacts are described for various parts of the world in several categories: water, ecosystems, food, coasts, and health. Adaptations and mitigations are suggested. The most obvious solution is the reduction of CO_2 emissions. In time, increases by developing countries are expected, whereas developed countries resist limitations. Improvements in efficiency of energy use, especially in vehicles, are desired. Capture and sequestration of carbon is under consideration. Nuclear power as an alternate source of electricity is mentioned in the report but not emphasized. The fifth assessment report was released by the IPCC during 2013 and 2014.

The subject of climate change is controversial for several reasons. Some believe the potential consequences are so severe that it is urgent to take immediate action. Waiting for additional confirmation through research is considered too late. Others are concerned about the worldwide economic disruption that might be caused by a drastic reduction of energy production to meet the Kyoto goals. Opposition to action has been expressed in the United States about the low limits on emission by developing countries. The US Congress has refused to ratify the Protocol on the grounds that it is unfair and if implemented could seriously affect the economy. From a scientific viewpoint, some believe that there is no real correlation between CO_2 increase and global temperature, that the modeling of trends is inadequate because it does not take proper account of the role of clouds or the absorption of carbon in the ocean, and that the computer models have not been able to reproduce past history correctly.

The nuclear industry calls attention to the fact that nuclear reactors provide electric power with the lowest life-cycle emission of carbon dioxide or other greenhouse gases, as shown in Fig. 24.7. This gives a rationale for the continued operation of nuclear power plants, for extending life through relicensing, and for building new plants. The World Nuclear Association estimates that nuclear power generation avoids 2600 million tonnes annually compared to burning coal (WNA, 2012). Besides reducing greenhouse gas emissions, "global nuclear power has prevented an average of 1.84 million air pollution-related deaths," Kharecha and Hansen (2013) conclude, deaths that would have otherwise occurred due to fossil fuel combustion.

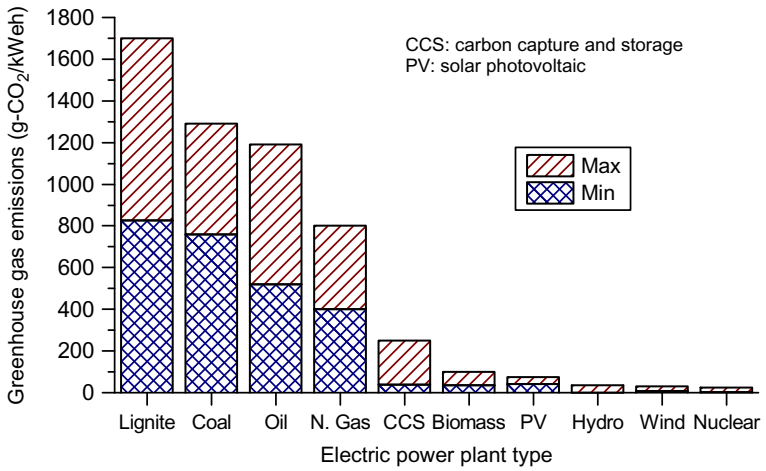

FIG. 24.7

Life-cycle greenhouse gas (CO_2 equivalent) emissions for selected power plants.

Data from Weisser, D., 2007. A guide to life-cycle greenhouse gas (GHG) emissions from electric supply technologies. Energy 32 (9), 1543–1559.

A number of reports, books, and web pages provide ample reading material on the subject of climate change (see Further Reading at the end of this chapter).

EXAMPLE 24.3

Approximate characteristics of bituminous coal include a heating value of 27,330 kJ/kg (Table 24.6) and a carbon content of 65%. For a 1000-MWe coal-fired power plant with a 40% thermal efficiency, the annual fuel requirement is

$$\dot{m}_F = \frac{P_e}{\eta_{th} HV} = \frac{(1000 \times 10^3 \text{ kW})(3.1558 \times 10^7 \text{ s/y})}{(0.40)(27,330 \text{ kJ/kg})(10^3 \text{ kg/tonne})} = 2.89 \times 10^6 \text{ tonne/y}$$

The combustion of 12 kg of C yields 44 kg of CO_2 such that carbon dioxide emissions are

$$\dot{m}_{CO_2} = \omega_C \dot{m}_F \frac{M_{CO_2}}{M_C} = \left(\frac{0.65 \text{ tonne-C}}{\text{tonne-coal}}\right)\left(\frac{2.89 \times 10^6 \text{ tonne-coal}}{\text{year}}\right)\left(\frac{44 \text{ tonne-CO}_2}{12 \text{ tonne-C}}\right) = 6.88 \times 10^6 \text{ tonne-CO}_2/\text{y}$$

Compare this 7 *million* tonne/y, which does not include other emissions such as sulfur dioxide (SO_2), nitrous oxides (NO_x), and ash, to the spent fuel mass of 28 tonne/y for a 1000-MWe nuclear unit (Exercise 24.4).

Table 24.6 Standard US Fuel Energy Values

Fossil Fuel	Higher Heating Value
Bituminous coal	27,330 kJ/kg = 11,750 Btu/lbm
Crude oil	42,100 kJ/kg = 5.8×10^6 Btu/barrel
Dry natural gas	57,450 kJ/kg = 1021 Btu/ft^3

Data from Culp, A.W., 1991. Principles of Energy Conversion, second ed. McGraw-Hill.

24.7 INTERNATIONAL NUCLEAR POWER

Although the United States spearheaded research and development of nuclear power, its use in other parts of the world has expanded greatly. There are two reasons: (1) many nations do not have natural energy sources of coal and oil, and (2) some nations such as France have state-owned or strongly state-supported nuclear power systems. On the other hand, the distribution of the use of nuclear power throughout the world is quite uneven.

A review of the status of nuclear power in nations around the world is provided in Table 24.7, which should be treated as a snapshot of a status subject to change. Several observations can be made about the table. The United States has almost one-fourth of the reactors of the world. France, with its population approximately a fifth that of the United States, has by far the largest per capita use of nuclear power. The continent of Africa is represented solely by a small nuclear program in South Africa; in South America, only Argentina and Brazil have nuclear power reactors.

Table 24.7 World Nuclear Power as of December 31, 2017

Nation	Units Operating		Units Forthcoming	
	No.	MWe	No.	MWe
Argentina	3	1632	1	25
Armenia	1	375	0	0
Bangladesh	0	0	2	2400
Belarus	0	0	2	2218
Belgium	7	5913	0	0
Brazil	2	1884	1	1245
Bulgaria	2	1926	0	0
Canada	19	13,554	0	0
China	37	33,364	28	28,720
Czech Republic	6	3930	0	0
Egypt	0	0	4	4760
Finland	4	2764	2	2800
France	58	63,130	1	1600
Germany	7	9515	0	0
Hungary	4	1889	2	2400
India	22	6225	8	5187
Iran	1	915	2	2000
Japan	42	39,752	2	2650
Mexico	2	1552	0	0
Netherlands	1	482	0	0
Pakistan	5	1320	3	3028
Romania	2	1300	2	1440
Russia	35	26,111	9	6718

Continued

Table 24.7 World Nuclear Power as of December 31, 2017 *Continued*

Nation	Units Operating		Units Forthcoming	
	No.	MWe	No.	MWe
Slovakia	4	1814	2	880
Slovenia	1	688	0	0
South Africa	2	1860	0	0
South Korea	24	22,493	5	6760
Spain	7	7121	0	0
Sweden	8	8629	0	0
Switzerland	5	3333	0	0
Taiwan	6	5052	2	2600
Turkey	0	0	4	4800
Ukraine	15	13,107	3	3020
United Arab Emirates	0	0	4	5380
United Kingdom	15	8883	2	3200
United States	99	102,127	6	7100
Total	446	392,640	97	100,931

*Data from: American Nuclear Society (ANS), 2018. 20th Annual Reference Issue **61** (3), 61.*

Another perspective of the world's nuclear activities is provided in Fig. 24.8, giving the percentage of the various nations' electricity that is supplied by nuclear power. The distributions of Table 24.7 and Fig. 24.8 tend to reflect the status of technological development, with variations dependent on available natural resources and public acceptance.

Table 24.7 also reveals that several nations, specifically Bangladesh, Belarus, Egypt, Turkey, and the United Arab Emirates, are constructing their first power reactors. Other nations initiating nuclear power programs include Jordan, Poland, and Saudi Arabia as well as reengagement by Lithuania, which shut down its RBMK units. The strongest growth in nuclear power is expected in China, India, Russia, and South Korea, as seen in Fig. 24.9. The People's Republic of China, with its vast population, has embarked on an ambitious power program with 37 operating reactors (33 GWe) and 28 additional units (29 GWe) forthcoming.

Nuclear programs of selected nations of several continents are reviewed briefly. For newer information, the reader is referred to the World Nuclear Association (WNA) website (see references).

24.7.1 WESTERN EUROPE

The leading user of nuclear power in Europe is France. Lacking fossil fuel resources and responding to the 1973 oil crisis, France focused on energy security through the production and use of nuclear power. Almost 80% of its electricity comes from its 58 reactors. Power is supplied by one company, Electricité de France (EdF), which is making a profit and reducing its debt despite a very large growth in facilities. EdF sells low-cost electricity to other countries, including the United Kingdom, by use of a cable under

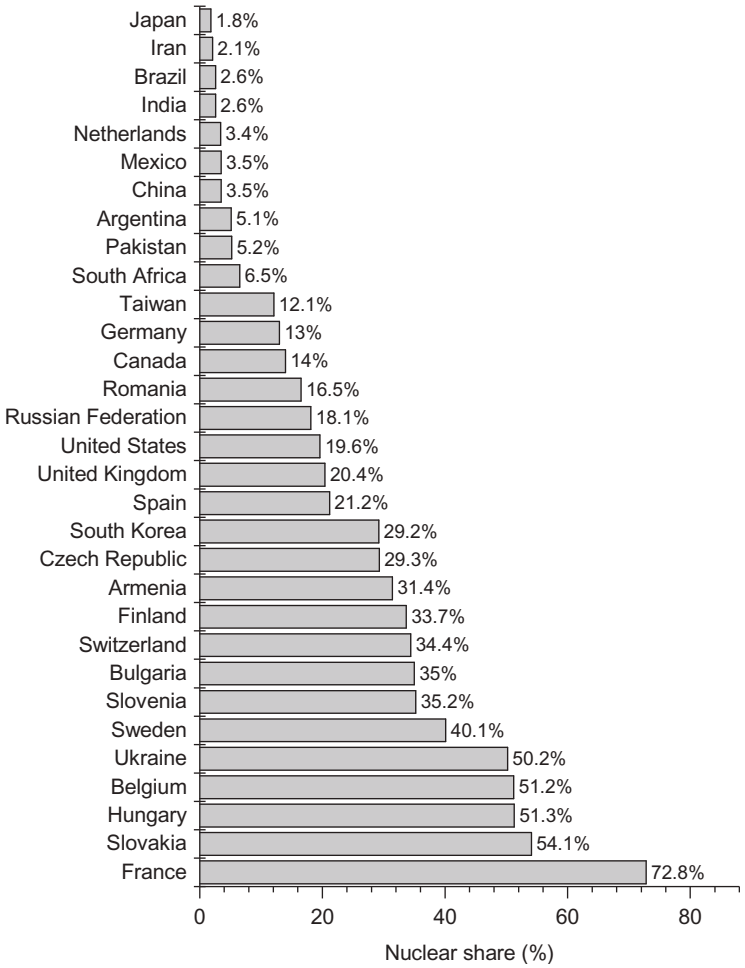

FIG. 24.8

Nuclear share of electricity generation 2016.

Data from International Atomic Energy Agency (IAEA), 2017. Energy, Electricity and Nuclear Power Estimates for the Period up to 2050.

the English Channel. All support for the French power system is provided by one company, Areva (formerly Framatome), for reactor design and construction, and for fuel supply and waste management, including reprocessing at La Hague. The Ecole Polytechnique provides the education of all of the operators and managers, and thus the common training is transferable between units. Safety in reactor operation is thus enhanced. Because reactors are standardized and the system is state owned, France is able to avoid the licensing and construction problems of the United States. Fig. 24.4 shows that the French were able to build a nuclear power station in 6 y or less. Historically, there was little opposition to nuclear power in France, in part because the state had provided attractive amenities to local

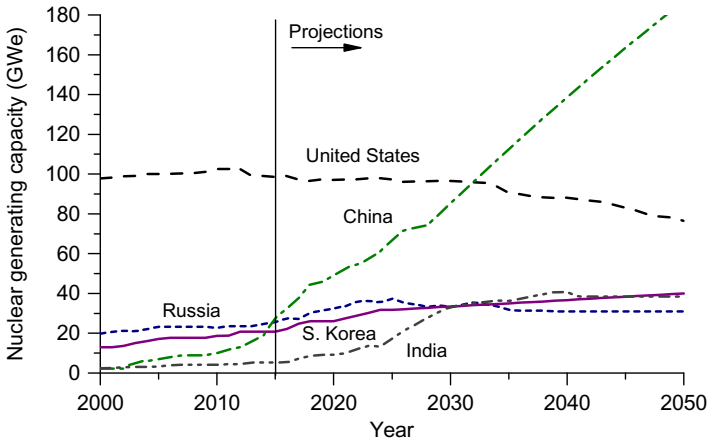

FIG. 24.9

Nuclear electricity generation capacity.

Data from US Department of Energy (DOE), Energy Information Administration (EIA), 2017. International energy outlook 2017; US Department of Energy (DOE), Energy Information Administration (EIA), 2018. Electric power monthly with data for January 2018.

communities while emphasizing the necessity of the power source for the nation's economy. In 2007, construction began on a 1600-MWe European Power Reactor (EPR) at Flamanville but it has been beset by delays in completion.

With the unification of Germany in 1990, the nuclear power program of the former East Germany was suspended in the interests of safety. Operation of the remaining plants was very successful, with high-capacity factors. Some electricity was available for export. However, there has been active opposition by antinuclear political parties. In response to Fukushima, eight reactors were retired permanently in August 2011. Presently, the remaining seven units are to be phased out by December 2022. In addition to challenges to the electric grid, the adoption of wind power is incurring skepticism by industry due to power quality issues and opposition in some locales due to noise and aesthetics.

For years in the United Kingdom, the cooperation of a state agency and a commercial organization worked well. In 1990, the nuclear industry was privatized, with British Energy buying facilities. The Sizewell B 1200-MWe PWR was put into operation in 1995. It features a highly modern computer management system. The older Magnox reactors are being phased out after several decades of operation. The other plants are gas-cooled reactors. Britain maintains reprocessing facilities at Sellafield, serving Japan. There is favorable government support for new nuclear capacity to avoid carbon emissions and to provide energy security. Plans call for two EPRs to be built at Hinkley Point.

24.7.2 EASTERN EUROPE AND THE FORMER SOVIET UNION

In the late 1980s, the former Soviet Union embarked on a nuclear power expansion program aimed at increasing electricity approximately 10% per year, with a long-range goal of approximately 100,000 MWe. It was expected that the use of centralized factories making standardized designs

and the use of specialist teams would permit construction times of less than 5 y. With the advent of the Chernobyl accident and related adverse public reaction and the economic stresses associated with the political changes in Eastern Europe, the planned program lost momentum and did not recover until around 2000. Several PWRs are being planned, are under construction, or are going into operation. Russia has a firm commitment to expand nuclear power. Russia has in operation 15 graphite-moderated light water-cooled reactors, including nearly a dozen RBMK-1000 units. A larger amount of power comes from VVERs (Voda Voda Energo Reactors), and several newer reactors are coming online. Besides domestic construction, Russia is actively engaged in the nuclear export business to nations such as Egypt and Turkey.

The breakup of the Soviet Union in 1991 and the creation of the Commonwealth of Independent States (CIS) resulted in a new national distribution of reactors. Several countries formerly allied with the Soviet Union were dependent on it for designs and technical assistance. Those that have VVER reactors are Armenia, Bulgaria, the Czech Republic, Hungary, Slovakia, and Ukraine while Romania has CANDU reactors.

24.7.3 EAST AND SOUTHEAST ASIA

Prior to March 2011, Japan was the principal user of nuclear power in this region. Government and industry had been committed to a successful nuclear program. Starting with a nuclear capacity of 33 GWe in 1991, Japan had hoped to reach 50 GWe by 2000 and 72.5 GWe by 2010. These goals were not quite reached, even though reactor construction times are low, slightly over 4 y. Japan's national goal of becoming essentially energy independent was to be met by use of facilities for enrichment, fabrication, reprocessing, and waste disposal. Reprocessing was justified on grounds of assuring a stable fuel supply rather than on economics. In recovering plutonium and burning it in LWRs or preferably fast breeders, Japan avoids large stockpiles of plutonium. The events at Fukushima (see Section 21.9) led to a mass shutdown of Japanese power reactors, mandatory inspections before resuming plant operations, and a national debate on the future role of nuclear power. There is considerable ambivalence about the future. Several prior nuclear accidents in Japan had already dampened enthusiasm for nuclear power expansion. A sodium leak occurred in the fast breeder MONJU, and there was a fire and explosion in a reprocessing plant. In 1999, a criticality accident happened at Tokaimura when operators put too much enriched uranium in a vessel. Fears of contamination of the vicinity were unfounded, but two workers died from radiation exposure.

South Korea has achieved very large growth in productivity over recent decades. Because it must import all its oil and gas, it is expanding its nuclear power program. Four of the reactors are CANDU reactors, the rest PWRs from Westinghouse, ABB-CE, and Framatome. Newer reactors (APR-1400) are being designed and built with Korean technology, which is being exported to the United Arab Emirates.

China's situation is different from that of many countries. It has a tremendous need for electric power. China's principal energy source is coal, creating serious environmental problems. Expansion of nuclear power with the help of foreign firms is underway, but the added power will be minimal in terms of the large population and energy demand. The 300-MWe Qinshan-1 PWR is of indigenous design and construction. Canada, France, Russia and the United States provided others. With two dozen

more units under construction, China is expected to surpass the US nuclear power generation before 2030. China's goal is a closed nuclear fuel cycle, and it has actively entered the export business.

24.7.4 OTHER COUNTRIES

Canada has 21 pressurized heavy-water power reactors that came online from the early 1970s through the early 1990s. Their CANDU units (see Section 18.5) have been exported to several nations, including Argentina, China, India, Romania, and South Korea.

India has two BWRs and several pressurized heavy water reactors of approximately 200-MWe capacity, with others under construction. India's fast reactor experimental facility is fueled by Pu-U carbide with a thorium blanket, intended to test the use of the large indigenous reserves of thorium.

The rate at which nuclear power is being adopted varies greatly throughout the world because each nation has a unique situation. In some countries, public opinion is a dominant factor; in others, it is limited capital; in still others, especially developing countries, it is a lack of technological base. For several Latin American countries, large national debts are limiting. Despite problems, the amount of nuclear power abroad continues to grow gradually.

24.8 DESALINATION

Scattered throughout the world are regions that badly need fresh water for drinking and industrial use. Remarkably, many are located next to the sea. Inland sites with brackish groundwater would also benefit from desalination facilities. Removal of salt by application of nuclear heat is a promising solution. Experience with nuclear desalination has been gained in more than 100 reactor-years in Kazakhstan by use of a fast reactor and in Japan by use of light-water reactors. Shut down after many years of operation, Kazakhstan's reactor at Aktau was unique in that it was a fast breeder reactor and used its waste heat for desalination of water.

Two modes of reactor application are (1) heat only and (2) electricity and waste heat. The first of these is simpler in that less equipment and maintenance are needed. The second has the benefit of providing a source of electric power.

In either mode, the contribution to the desalination process is the steam from a heat exchanger. There are two general technologies in which the heat can be used by desalination equipment. The first is distillation, in which the water evaporates on contact with a steam-heated surface and is separated from the salt. There are two versions of this technology: multistage flash distillation (MSF), and multieffect distillation (MED). The second is reverse osmosis (RO) in which a porous membrane with a pressure difference separates water from salt. Two subsets of the RO approach have been tested. To protect the membrane, considerable pretreatment is required.

Fig. 24.10 shows a nuclear desalination plant with three of the MED stages shown. Condenser waste heat, which would otherwise be dissipated to the environment, vaporizes water in an intermediate loop. This low-pressure steam, in turn, vaporizes the seawater, thereby separating pure water from the brine. This process continues in succeeding effects, except that the condensation of the vaporized fresh water provides the heat source for the subsequent stages, which are at successively lower pressure.

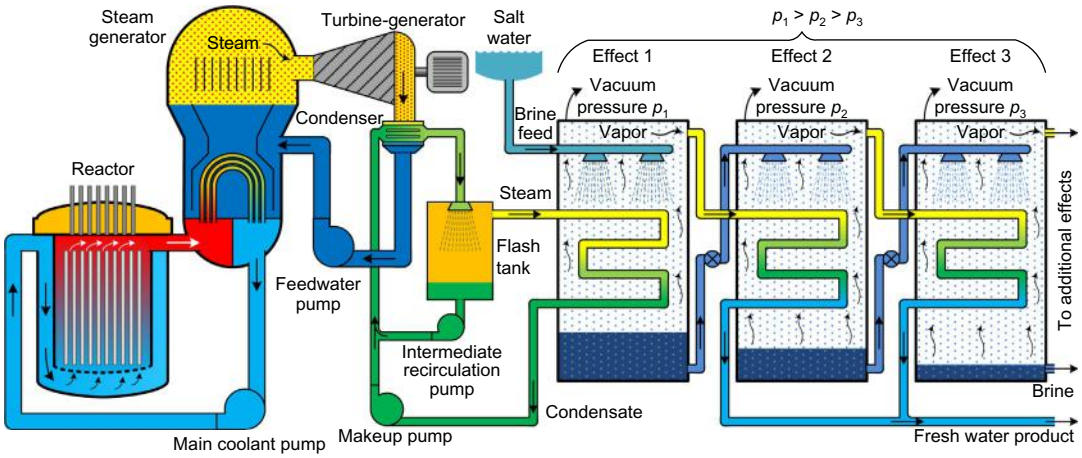

FIG. 24.10

Nuclear power plant with multieffect distillation.

EXAMPLE 24.4

A key parameter of performance of a desalination system is the fresh water volume produced per unit of heat power, V/Q. The maximum value, assuming no heat losses, is calculated from conservation of energy, considering the water temperature rise from 20°C to 100°C along with the heat required for vaporization

$$Q = m\left(c_p \Delta T + h_{fg}\right) = \rho V\left(c_p \Delta T + h_{fg}\right)$$

$$V/Q = 1/\left[\rho\left(c_p \Delta T + h_{fg}\right)\right]$$

$$= 1/\left\{\left(1\,\mathrm{g/cm^3}\right)\left[(4.186\,\mathrm{J/(g°C)})(100 - 20°\mathrm{C}) + 2258\,\mathrm{J/g}\right]\right\}$$

$$= 3.86 \times 10^{-4}\,\mathrm{cm^3/J} = 3.86 \times 10^{-10}\,\mathrm{m^3/J}$$

For a 1000-MWe nuclear reactor with 2000-MW waste heat, the maximum daily yield is

$$\dot{V} = \dot{Q}_{cond}(V/Q) = \left(2000 \times 10^6\,\mathrm{J/s}\right)\left(3.86 \times 10^{-10}\,\mathrm{m^3/J}\right)(86,400\,\mathrm{s/d}) = 6.67 \times 10^4\,\mathrm{m^3/d}$$

According to the IAEA (2000), approximately 23 million m^3/d of desalinated water is produced in the world by 12,500 plants, an average of 1840 m^3/d. To double the global water production would require a minimum of $(2.3 \times 10^7\,\mathrm{m^3/d})/(6.67 \times 10^4\,\mathrm{m^3/d}) = 345$ reactors.

The International Atomic Energy Agency (IAEA) is actively promoting the concept of nuclear desalination in several countries. It has published a guidebook to aid member states in making decisions and implementing projects (IAEA, 2002). The IAEA has developed the computer code DEEP to analyze the economics of an installation. It provides descriptions of the concepts MSF, MED, and RO. A comprehensive journal article by Megahed (2003) gives the history and future possibilities for nuclear desalination, along with a description of activities in Canada, China, Egypt, India, South Korea, and Russia.

24.9 WATER-ENERGY NEXUS

Energy and water are inextricably linked. Water treatment processes such as desalination and purification as well as pumping and distribution operations for water supply systems, both municipal and irrigation, require energy input. Conversely, hydropower and most thermal power stations, including biomass, coal, nuclear, geothermal and combined cycle, need substantial quantities of water.

Utilization of water for cooling thermoelectric power plants is receiving increasing attention and scrutiny. According to the US Geological Survey (USGS), 45% of all water withdrawals in the United States during 2010 were for thermoelectric power and 99% of those withdrawals were from surface water sources (Maupin et al., 2014). While the *withdrawal* of water is that diverted from a surface water source or removed from the ground for use, water *consumption* permanently withdraws water from its source, for example, due to evaporation. The estimated consumptive use of water for thermoelectric power in 1995 was about 2% of the withdrawals (Solley et al., 1998).

EXAMPLE 24.5

In 2010, a total of 161 billion gallons of water was withdrawn per day in the United States, resulting in the generation of 3130 billion kWh of electricity from thermal power plants that year. The corresponding average water withdrawal for net electricity production in 2010 was

$$\frac{V}{E}=\frac{(161\times10^9\,\text{gal/d})(365\,\text{d/y})}{3130\times10^9\,\text{kWh/y}}=18.8\,\text{gal/(kWh)}=71\,\text{L/(kWh)}$$

Factors such as use of recirculation and dry cooling and increased thermal efficiency have caused a decline from the 2005 value of 23 gal/(kWh).

24.10 THE HYDROGEN ECONOMY

The potential connection between nuclear power and hydrogen as a fuel was discussed as early as 1973 in an article in *Science* (Winsche et al., 1973). Hydrogen, which is storable and portable, is viewed as an alternative to electricity. Recently, there has been interest in the use of hydrogen gas instead of oil, natural gas, or coal. This is prompted by several concerns: (1) the uncertain supply of foreign oil and natural gas; (2) the health and environmental impact of polluting combustion gases; and (3) the potential for climate change from the increasing emission of carbon dioxide. A virtue of H_2 is that it burns with only water as a product.

Hydrogen is useful in the enhancement of low-grade sources of oil, but its greatest application would be in fuel cells, where chemical reactions yield electricity. To avoid the problem of excessive weight of containers to withstand high pressure, hydrogen could be held as a metal hydride, with density of H_2 comparable to that as a liquid. Gas is released on heating to approximately 300°C. Studies are in progress on the storage of hydrogen on special surfaces or nanostructures.

Of major importance is the means by which hydrogen is generated. At present, it is obtained by treatment of natural gas. It could be derived from coal as well. Both sources give rise to undesired products such as CO_2. If the carbon dioxide could be successfully sequestered, this problem would be eliminated.

There are two ways in which nuclear reactors could provide the hydrogen as an energy carrier (not as a source in itself). The obvious technique is electrolysis of water, which uses the electricity from a nuclear power plant. Alternately, the heat from a high-temperature gas-cooled reactor is sufficient to initiate thermochemical reactions that have higher efficiency. Of many possible reactions, the leading candidate is the following set. The temperature at which they take place is indicated (Forsberg et al., 2003).

$$\begin{aligned} &2H_2SO_4 \rightarrow 2SO_2 + 2H_2O + O_2 (800°C) \\ &2HI \rightarrow I_2 + H_2 (450°C) \\ &I_2 + SO_2 + 2H_2O \rightarrow 2HI + H_2SO_4 (120°C) \end{aligned} \tag{24.2}$$

Because the sulfur and iodine are recycled, the net reaction is

$$2H_2O \rightarrow 2H_2 + O_2 \tag{24.3}$$

The energy required is merely the heat of combustion of hydrogen.

Fission of uranium in the reactor as the primary source of energy does not yield carbon dioxide or other gases and provides a more continuous and reliable supply of heat or electricity than wind or solar power. The Next-Generation Nuclear Plant was originally envisioned to produce hydrogen and electricity (see Section 18.8). There is an obvious need for an infrastructure for large-scale commercial application of hydrogen fuel, especially for vehicle transportation.

Hydrogen can be used for transportation in two ways: by burning in an internal combustion engine and by serving as a source for fuel cells. A fuel cell is an energy conversion device that produces electricity by the reaction of hydrogen and oxygen to produce water, the reverse of electrolysis. A set of fuel cells can power electric motors that drive an automobile or truck. The most likely type to be used is the polymer exchange membrane fuel cell (PEMFC). Its components are anode, cathode, membrane, and catalyst.

To be successful technically, onboard storage of hydrogen sufficient for a 300-mile (500-km) vehicle range is required. Tanks with compressed gas at very low temperature would probably be heavy, expensive, and complicated to use. Research is under way on alternatives. One possibility is an ultrathin metal alloy film in which there are unusual quantum effects. Lightweight materials such as magnesium are promising candidates. Hydrides and carbon nanostructures are being considered as well. To be successful commercially, it would be necessary to provide refueling capability at ordinary gas stations.

Further information on what is now called the hydrogen economy is available in the literature and on the Internet. A committee of the National Research Council (2004) developed a 256-page book. Three articles in *Nuclear News* provide technical details and calculations on the nuclear power requirements (Forsberg and Peddicord, 2001; Forsberg et al., 2003; Forsberg, 2005).

EXAMPLE 24.6

We can estimate the impact of reactors producing hydrogen gas for use as fuel for transportation in place of gasoline. Consider one reactor of power 600 MWt with 50% efficiency of H_2 generation, such that the available thermal power is

$$\dot{Q}_{\text{th}} = \varepsilon \dot{Q}_{Rx} = (0.5)(600\text{MW}) = 300\text{MW}$$

As noted in Eqs. (24.2) and (24.3), the sulfur-iodine process causes the dissociation of water into component gases. By use of the heat of combustion ΔH_C of 142 MJ/kg with hydrogen density 0.09 kg/m^3, we find the production rate is

$$\dot{V}_{\text{H}} = \frac{\dot{Q}_{\text{th}}}{\Delta H_C \rho_{\text{H}}} = \frac{(300\text{MJ/s})(86,400\text{s/d})}{(142\text{MJ/kg})(0.09\text{kg/m}^3)} = 2.03 \times 10^6 \text{m}^3/\text{d}$$

If that hydrogen is burned in place of gasoline with a heat of combustion of 45 MJ/kg and density of 730 kg/m^3, the equivalent volume of gasoline is

$$\dot{V}_{\text{gas}} = \frac{\dot{Q}_{\text{th}}}{\Delta H_C \rho_{\text{gas}}} = \frac{(300\,\text{MJ/s})(86,400\,\text{s/d})}{(45\,\text{MJ/kg})(730\,\text{kg/m}^3)(3.7854\times10^{-3}\,\text{m}^3/\text{gal})} = 2.08\times10^5\,\text{gal/d}$$

The value of the H_2 product then depends on the price of gasoline.

24.11 SUMMARY

A single chapter cannot do justice to the dimensions of the world's energy situation. The energy future of the world is not clear because both optimistic and pessimistic predictions have been made. The population growth of the world remains excessive, with growth rates in less developed countries being highest. Increasing electricity use will concomitantly increase the need for large-scale generation such as nuclear. Nuclear power may play an important role in achieving sustainable development and in easing international energy tensions. Applications for the future include desalination with nuclear power, and the production of hydrogen for transportation to help prevent climate change. The decline in US reactors planned and under construction over the years is balanced by the rise in reactors in other countries. Ultimately, economics drives the selection of energy sources utilized for electricity generation; however, long-term costs due to climate change are not accounted for presently.

24.12 EXERCISES

24.1 The volume of the oceans of the Earth is $1.37\times10^{18}\,\text{m}^3$ (AAE, 1980). If the deuterium content of the hydrogen in the water is 1 part in 6400, how many kilograms of deuterium are there? With the heat available from deuterium, 5.72×10^{14} J/kg (see Exercise 26.4) and assuming a constant world annual energy consumption of approximately 300 EJ, how long would the deuterium last?

24.2 A plan is advanced to normalize the standard of living of all countries of the world to those of North America by the year 2050. A requisite would be a significant increase in the per-capita supply of energy to other countries besides the United States and Canada. (a) Assume that the medium growth case of Fig. 24.2 is applicable, resulting in a growth from 7.4 billion to 9.8 billion people. By what factor must world energy production increase? If the electricity fraction of energy remained constant, how many additional 1000-MWe reactors operating at 90% capacity factor (or equivalent coal-fired power plants) would be needed to meet the demand? Repeat these calculations for the (b) low growth case and the (c) high growth case in which the global population increases to 8.8 and 10.8 billion, respectively.

24.3 Many different energy units are found in the literature. Some of the useful equivalences are:

$$1\,\text{bbl (oil)} = 5.8\times10^6\,\text{Btu}$$

$$1\,\text{quad} = 10^{15}\,\text{Btu}$$

$$1\,\mathrm{Q} = 10^{18}\,\mathrm{Btu}$$

$$1\,\text{exajoule (EJ)} = 10^{18}\,\mathrm{J}$$

(a) Find out how many barrels (bbl) of oil per day it takes to yield 1 GW of heat power. (b) Show that the quad and the EJ are almost the same. (c) How many quads and Q correspond to the world annual energy consumption of approximately 500 EJ? (d) How many decays of nuclei yielding 1 MeV would be needed to produce 1 EJ?

24.4 Calculate the mass of used fuel generated annually from a 1000-MWe nuclear unit having (a) a 33% thermal efficiency and fuel burnup of 45 GW d/tonne, and (b) a 40% thermal efficiency and burnup of 50 GW d/tonne.

24.5 Use Table 24.6 data to determine the ratio of energy in (a) 1 tonne of coal, (b) 1 barrel of oil, and (c) 1000 ft^3 of natural gas to the energy content from fissioning every atom in 1 kg of natural uranium.

24.6 Derive the doubling time formula, Eq. (24.1), while considering the growth process being akin to radioactive decay in reverse.

24.7 Compute the doubling time (a) before the Great Recession of 2008, when the annual electricity growth rate in the United States was 2%, and (b) for 2015–40 projections of 0.8% yearly.

24.8 Using Table 24.4 and an assumed capacity factor of 95% and levelized annual fixed charge rate of 10%, calculate combined capital and O&M costs for (a) coal-fired with carbon capture, (b) natural gas combined cycle, and (c) biomass power plants.

24.9 If the cost of gasoline is $4 per gallon, compute the annual gross value of the H_2 product from a 1000-MWt reactor with a 45% efficiency for hydrogen generation.

24.10 Compute the water usage per kWh in the United States in 2010 for (a) once-through versus (b) recirculation cooling which withdrew 151 and 9.99 billion gallons per day, respectively, for annual electricity generation of 1460 and 1660 billion kWh.

24.11 Calculate the annual CO_2 emissions from a 600-MWe natural gas combined cycle plant having a capacity factor of 85% and thermal efficiency of 52%. Assume that the dry natural gas fuel consists of pure methane (CH_4).

24.13 COMPUTER EXERCISE

24.A Computer program FUTURE considers global regions and levels of development, mixes of source technology, energy efficiency, resource limitations, population, pollution, and other factors. Some of the methods and data of Goldemberg (1996) are used. Explore the menus, make choices or insert numbers, and observe responses.

REFERENCES

Academic American Encyclopedia (AAE), 1980. The Academic American Encyclopedia. vol. 14 Arete Publication, Princeton, NJ, p. 326.

Blunden, J., 2014. 2013 State of Climate: Carbon dioxide tops 400 ppm. National Oceanic and Atmospheric Administration, www.climate.gov.

Burness, H.S., Montgomery, W.D., Quirk, J.P., 1980. The turnkey era in nuclear power. Land Econ. 56 (2), 188–202.

Carson, R., 1962. Silent Spring. Houghton Mifflin Company, Boston.

Cowan, R., 1990. Nuclear power reactors: a study in technological lock-in. J. Econ. Hist. 50 (3), 541–567.

Forsberg, C.W., 2005. What is the initial market for hydrogen from nuclear energy? Nucl. News 48 (1), 24–26.

Forsberg, C.W., Peddicord, K.L., 2001. Hydrogen production as a major nuclear energy application. Nucl. News 44 (10), 41–44.

Forsberg, C.W., Pickard, P.L., Peterson, P., 2003. The advanced high temperature reactor for production of hydrogen or electricity. Nucl. News 46 (2), 30.

Friedrich, R., Voss, A., 1993. External costs of electricity generation. Ener. Policy 21 (2), 114–122.

Goldemberg, J., 1996. Energy, Environment and Development. Earthscan Publications, London.

Hardin, G., 1968. The tragedy of the commons. Science 162 (3859), 1243–1248.

Intergovernmental Panel on Climate Change (IPCC), 2014. Climate Change 2014: Synthesis Report. Contribution of Working Groups I, II and III to the Fifth Assessment Report of the IPCC. Geneva, Switzerland, p. 151. http://www.ipcc.ch.

International Atomic Energy Agency (IAEA), 2000. Introduction of Nuclear Desalination: A Guidebook. Technical Reports Series No. 400. Vienna, Austria.

International Atomic Energy Agency (IAEA), 2002. Status of design concepts of nuclear desalination plants. IAEA-TECDOC-1326.

International Energy Agency (IEA), 2014. More Data, Less Energy: Making Network Standby More Efficient in Billions of Connected Devices. IEA, Paris.

International Energy Agency (IEA), 2017a. Key World Energy Statistics 2017. IEA, Paris.

International Energy Agency (IEA), 2017b. World Energy Outlook 2017 Executive Summary. IEA, Paris.

Kharecha, P.A., Hansen, J.E., 2013. Prevented mortality and greenhouse gas emissions from historical and projected nuclear power. Environ. Sci. Technol. 47 (9), 4889–4895.

Malthus, T.R., 1798. An Essay on the Principle of Population. Johnson, London.

Maupin, M.A., Kenny, J.F., Hutson, S.S., Lovelace, J.K., Barber, N.L., Linsey, K.S., 2014. Estimated use of water in the United States in 2010. US Geol. Surv. Circular 1405.

McBride, J.P., Moore, R.E., Witherspoon, J.P., Blanco, R.E., 1978. Radiological impact of airborne effluents of coal and nuclear plants. Science 202 (4372), 1045–1050.

Meadows, D.H., Meadows, D.L., Randers, J., Behrens III, W.W., 1972. The Limits to Growth: A Report for The Club of Rome's Project on the Predicament of Mankind. Universe Books, New York.

Megahed, M.M., 2003. An overview of nuclear desalination: history and challenges. Int. J. Nucl. Desalin. 1 (1), 2–18.

National Research Council, 2004. Committee on Alternatives and Strategies for Future Hydrogen Production and Use, The Hydrogen Economy: Opportunities, Costs, Barriers, and R&D Needs. National Academies Press, Washington, DC.

National Research Council, 2010. Hidden Costs of Energy: Unpriced Consequences of Energy Production and Use. National Academies Press, Washington, DC.

Organisation for Economic Co-operation and Development (OECD), Nuclear Energy Agency (NEA), 2002. Nuclear Energy and the Kyoto Protocol. www.nea.fr/html/ndd/reports/2002/nea3808.html.

Reid, D., 1995. Sustainable Development: An Introductory Guide. Earthscan Publishers, London.
Solley, W.B., Pierce, R.R., Perlman, H.A., 1998. Estimated use of water in the United States in 1995. US Geol. Surv. Circular 1200.
United Nations (UN), 1987. Report of the World Commission on Environment and Development: Our Common Future, General Assembly Resolution 42/187. December 11.
United Nations (UN), 2017. World population prospects: the 2017 revision.
US Atomic Energy Commission (AEC), 1962. Civilian nuclear power—a report to the President (1967 supplement).
US Department of Energy (DOE), Energy Information Administration (EIA), 2017a. Annual energy outlook with projections to 2050.
US Department of Energy (DOE), Energy Information Administration (EIA), 2017b. Levelized cost and levelized avoided cost of new generation resources in the annual energy outlook 2017.
US Department of Energy (DOE), Energy Information Administration (EIA), 2018. Electric power monthly with data for January 2018.
Winsche, W.E., Hoffman, K.C., Salzano, F.J., 1973. Hydrogen: its future role in the nation's energy economy. Science 180 (4093), 1325–1332.
World Nuclear Association (WNA), 2012. Uranium, electricity and climate change. http://world-nuclear.org/info/Energy-and-Environment/Uranium,-Electricity-and-Climate-Change/.

FURTHER READING

American Nuclear Society (ANS), 2018. 20th Annual Reference Issue. vol. 61, no. 3, p. 61.
Balzhiser, R.E., Gobert, C., Guertin, D.L., Dircks, W.J., Dunkerley, J.C., Pettibone, S.P., 1999. An Appropriate Role for Nuclear Power in Meeting Global Energy Needs. Atlantic Council, http://www.acus.org.
Bodansky, D., 2003. Nuclear Energy: Principles, Practices, and Prospects, second ed. Springer/AIP Press, New York.
Carbon, M.W., 1997. Nuclear Power: Villain or Victim? Our Most Misunderstood Source of Electricity. Pebble Beach Publishers, Madison, WI.
Cravens, G., 2007. Power to Save the World: The Truth About Nuclear Energy. Alfred A Knopf, New York. A former skeptic embraces nuclear power.
Culp, A.W., 1991. Principles of Energy Conversion, second ed. McGraw-Hill, New York.
Gore, A., 2007. An Inconvenient Truth: The Crisis of Global Warming. Viking, New York.
Herbst, A.M., Hopley, G.W., 2007. Nuclear Energy Now: Why the Time Has Come for the World's Most Misunderstood Energy Source. Wiley, Hoboken, NJ.
Hoffmann, T., Johnson, B., 1981. The World Energy Triangle: A Strategy for Cooperation. Ballinger, Cambridge. A thoughtful investigation of the energy needs of the developing world and assessment of ways developed countries can help to their own benefit.
International Atomic Energy Agency (IAEA), 2012. Nuclear power reactors in the world.
International Atomic Energy Agency (IAEA), 2017a. Nuclear power reactors in the world.
International Atomic Energy Agency (IAEA), 2017b. Energy, Electricity and Nuclear Power Estimates for the Period up to 2050.
International Energy Agency (IAEA), Power Reactor Information System (PRIS). http://www.iaea.org/pris/. (select "country name, plant").
International Energy Agency (IEA), 2013. Redrawing the energy climate map.
Kahn, H., Brown, W., Martel, L., 1976. The Next 200 Years: A Scenario for America and the World. Morrow, New York. Contrast of pessimism and optimism.

National Research Council, Energy Engineering Board, Committee on Future Nuclear Power Development, 1992. Nuclear Power: Technical and Institutional Options for the Future. National Academies Press, Washington, DC.

Nuclear Energy Agency (NEA), http://www.oecd-nea.org/. Nuclear arm of the Organisation for Economic Co-operation and Development (OECD), based in Paris, with 28 member countries, mainly in Europe, North America, and the Far East.

Nuclear Energy Institute (NEI), 1997. Source Book on Soviet-Designed Nuclear Power Plants, fifth ed. http://www.nei.org/Master-Document-Folder/Backgrounders/Reports-And-Studies/Source-Book-Soviet-Designed-Nuclear-Power-Plants.

Nuclear Engineering International (NEI), 2012. World Nuclear Industry Handbook.

Nuclear Engineering International (NEI), http://www.neimagazine.com. Dedicated to nuclear matters around the world.

Nuclear Power Corporation of India, Ltd., http://www.npcil.nic.in. Performance data for all plants.

Ott, K.O., Spinrad, B.I., 1985. Nuclear Energy: A Sensible Alternative. Plenum Press, New York. Titles of sections: Energy and Society, Economics of Nuclear Power, Recycling and Proliferation, Risk Assessment, and Special Nuclear Issues Past and Present.

Pearce, D., 1998. Economics and Environment: Essays on Ecological Economics and Sustainable Development. Edward Elgar, Cheltenham.

Putnam, P.C., 1953. Energy in the Future. Van Nostrand, New York. A classic early study of plausible world demands for energy over the subsequent 50 to 100 years, sponsored by the US Atomic Energy Commission; includes a large amount of data and makes projections that were reasonable at the time; written before the development of commercial nuclear power and before the environmental movement got under way, the book is quite out of date but is worth reading for the thoughtful analysis.

Reynolds, A.B., 1996. Bluebells and Nuclear Energy. Cogito Books, Madison, WI.

Rhodes, R., 1993. Nuclear Renewal: Common Sense About Energy. Penguin Books, New York.

Schneider, S.H., 1992. Introduction to climate modeling. In: Trenbeth, K.E. (Ed.), Climate System Modeling. Cambridge University Press, New York.

Schneider, M., Froggatt, A., 2013. World Nuclear Industry Status Report.

Singer, S.F., 1998. Hot Talk Cold Science: Global Warming's Unfinished Business. Independent Institute, Oakland, CA.

Singer, S.F., 1999. Global Warming's Unfinished Debate. Independent Institute, Oakland, CA.

United Nations (UN), 1992. Earth summit in Rio de Janeiro, 1992. http://www.un.org/geninfo/bp/enviro.html. Agenda 21 adopted.

United Nations (UN), 1997. Earth Summit+5. http://www.un.org/esa/earthsummit. Special Session of the General Assembly to review and appraise the implementation of Agenda 21.

United Nations (UN), 2002. Earth Summit 2002. http://earthsummit2002.org. Johannesburg (Rio + 10).

US Department of Energy (DOE), Energy Information Administration (EIA), 2005. International energy outlook 2005. DOE/EIA-0484(2005).

US Department of Energy (DOE), Energy Information Administration (EIA), 2005. Annual energy review 2005. DOE/EIA-0384(2005).

US Department of Energy (DOE), Energy Information Administration (EIA), 2012. Annual energy review 2011. DOE/EIA-0384(2011).

US Department of Energy (DOE), Energy Information Administration (EIA), 2016. Capital cost estimates for utility scale electricity generating plants.

US Department of Energy (DOE), Energy Information Administration (EIA), 2017. International energy outlook 2017.

US Department of Energy (DOE), Energy Information Administration (EIA), 2018. International energy statistics. http://www.eia.gov/ies.

US Department of Energy (DOE), Hydrogen and fuel cells program. www.hydrogen.energy.gov. Links to subjects of production, delivery, storage, manufacturing, etc.

Waltar, A.E., 1995. America the Powerless: Facing Our Nuclear Energy Dilemma. Cogito Books, Madison, WI.
Weinberg, A.M., 1985. Continuing the Nuclear Dialogue: Selected Essays. American Nuclear Society, La Grange Park, IL.
Weisser, D., 2007. A guide to life-cycle greenhouse gas (GHG) emissions from electric supply technologies. Energy 32 (9), 1543–1559.
Worldwatch Institute, 2008. State of the world 2008: innovations for a sustainable economy. http://www.worldwatch.org.
World Nuclear Association (WNA), Information library: country profiles. http://www.world-nuclear.org.
Wuebbles, D.J., Edmonds, J., 1991. Primer on Greenhouse Gases. Lewis Publishers, Chelsea, MI.

CHAPTER

BREEDER REACTORS

25

CHAPTER OUTLINE

The most important feature of the fission process is, of course, the enormous energy release from each reaction. Another significant fact, however, is that for each neutron absorbed in a fuel such as U-235, more than two neutrons are released. To maintain the chain reaction, only one is needed. Any extra neutrons available can thus be used to produce other fissile materials such as Pu-239 and U-233 from the *fertile* materials, U-238 and Th-232, respectively. The nuclear reactions yielding the new isotopes were detailed in Section 6.3. If losses of neutrons can be reduced enough, the possibility exists for new fuel to be generated in quantities as large, or even larger than, the amount consumed, a condition called *breeding*. Several fuel cycles exist that are distinguished by the amount of recycling. In the once-through cycle, all spent fuel is discarded as waste. Partial recycling makes use of separated plutonium, which can be combined with low-enrichment uranium to form mixed oxide fuel. In the ultimate and ideal breeder cycle, all materials are recycled. There is continued interest in some level of recycling to help reduce radioactive waste and to use all fuel energy content.

In this chapter, we shall (1) examine the relationship between the reproduction factor and breeding, (2) describe the physical features of the LMFBR, and (3) look into the compatibility of uranium fuel resources and requirements.

Nuclear Energy. https://doi.org/10.1016/B978-0-12-812881-7.00025-3

25.1 THE CONCEPT OF BREEDING

The ability to convert significant quantities of fertile materials into useful fissile materials depends crucially on the magnitude of the reproduction factor, η, which is the number of neutrons produced per neutron absorbed in fuel. If ν neutrons are produced per fission, and the ratio of fission to absorption in fuel is σ_f/σ_a, then the number of neutrons per absorption is

$$\eta = \nu \frac{\sigma_f}{\sigma_a} = \frac{\nu\sigma_f}{\sigma_f + \sigma_\gamma} = \frac{\nu}{1+\alpha} \tag{25.1}$$

in which α is the capture-to-fission ratio, σ_γ/σ_f. The greater the reproduction factor excess above 2, the more likely is breeding. Fig. 25.1 graphs the average number of neutrons emitted $\overline{\nu}$ as a function of the energy of the neutron inducing the fission. It is found that both ν and the ratio σ_f/σ_a increase with neutron energy and thus η is larger for fast reactors than for thermal reactors. Table 25.1 compares values of η for the main fissile isotopes in the two widely differing neutron energy ranges designated as thermal and fast. Inspection of the table reveals that it is more difficult to achieve breeding with U-235 and Pu-239 in a thermal reactor, because the 0.07 or 0.11 neutrons are very likely to be lost by absorption in structural materials, moderator, and fission-product poisons.

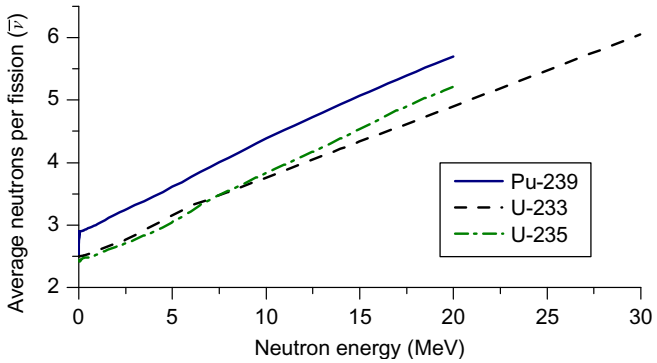

FIG. 25.1

Average number of neutrons produced per fission, nu-bar ($\overline{\nu}$).

Data from Chadwick, M.B., Herman, M., Obložinský, P., Dunn, M.E., Danon, Y., Kahler, A.C., et al., 2011. ENDF/B-VII.1 Nuclear data for science and technology: cross-sections, covariances, fission product yields and decay data. Nucl. Data Sheets 112 (12), 2887–2996.

Table 25.1 Values of Reproduction Factor η

	Neutron Energy	
Isotope	**Thermal**	**Fast**
U-235	2.07	2.3
Pu-239	2.11	2.7
U-233	2.30	2.45

A thermal reactor that uses U-233 is a good prospect, but the fast reactor that uses Pu-239 is the most promising candidate for breeding. Absorption of neutrons in Pu-239 consists of both fission and capture, the latter resulting in the isotope Pu-240. If the Pu-240 captures a neutron, the fissile isotope Pu-241 is produced.

The ability to convert fertile isotopes into fissile isotopes can be measured by the *conversion ratio* (CR), which is defined as

$$\mathrm{CR} = \frac{\text{Fertile atoms converted}}{\text{Fissile atoms consumed}} = \frac{\text{Fissile atoms produced}}{\text{Fissile atoms consumed}} \tag{25.2}$$

The fissile atoms are produced by neutron capture in fertile atoms; the consumption includes fission and capture.

We can compare CR values for various systems. First is a *burner* fueled only with U-235. With no fertile material present, CR = 0. Second is a decidedly thermal reactor with negligible resonance capture, in which fuel as natural uranium, 99.27% U-238 and 0.72% U-235, is continuously supplied and consumed. Pu-239 is removed as soon as it is created. Here CR is the ratio of absorption in U-238 and U-235, and because they experience the same flux, CR is simply the ratio of macroscopic cross-sections, $\Sigma_a^{238}/\Sigma_a^{235}$.

EXAMPLE 25.1

Using cross-sections from Table 4.2 and the atomic abundances for natural uranium (ignoring U-234), the CR for this second reactor is

$$CR = \frac{\Sigma_a^{238}}{\Sigma_a^{235}} = \frac{\gamma_{238} N_U \sigma_a^{238}}{\gamma_{235} N_U \sigma_a^{235}} = \frac{(0.9927)(2.68\,\mathrm{b})}{(0.00720)(98.3 + 582.6\,\mathrm{b})} = 0.543$$

Third, we ask: what CR is needed to completely consume both U isotopes in natural U as well as the Pu-239 produced? It is easy to show (Exercise 25.6) that CR is equal to the isotopic fraction of U-238 (namely, 0.9927).

Fourth, we can derive a more general relationship from the neutron cycle of Fig. 16.5. The diagram shows that for each neutron born, there are $\varepsilon\, \mathcal{L}_f\, (1 - \wp)$ neutrons captured by resonance absorption. For a given flux ϕ, the birth rate of neutrons per unit volume is $\nu\, \Sigma_f\, \phi$. The ratio of total absorption rate in U-238 to absorption rate in U-235 is thus

$$\mathrm{CR} = \frac{\Sigma_a^{238}\phi + \nu_{235}\Sigma_f^{235}\phi\varepsilon\mathcal{L}_f(1-\wp)}{\Sigma_a^{235}\phi} \tag{25.3}$$

Simplifying, the result for initial operation of a critical reactor, before any Pu is produced, is

$$\mathrm{CR} = \frac{\Sigma_a^{238}}{\Sigma_a^{235}} + \eta_{235}\varepsilon\mathcal{L}_f(1-\wp) \tag{25.4}$$

where η_{235} is the value for pure U-235 (i.e., 2.07).

EXAMPLE 25.2

For the last case with a natural U reactor with $\mathcal{L}_f = 0.95$, $\wp = 0.9$, and $\varepsilon = 1.03$, we find

$$\mathrm{CR} = \frac{\Sigma_a^{238}}{\Sigma_a^{235}} + \eta_{235}\varepsilon\mathcal{L}_f(1-\wp) = 0.543 + (2.07)(1.03)(0.95)(1-0.9) = 0.746$$

It is clear that reducing fast neutron leakage and enhancing resonance capture are favorable to the conversion process. An alternative simple formula, obtained by considerable manipulation as in Exercise 25.7, is

$$\mathrm{CR} = \eta_{235}\varepsilon - 1 - \mathcal{L} \tag{25.5}$$

where $\mathcal{L}$ is the total amount of neutron loss by leakage and by nonfuel (parasitic) absorption, per absorption in U-235. For U-235 fueled thermal reactors, CR $\approx$ 0.6 for light water reactors and CR $\approx$ 0.8 for heavy water and gas-cooled reactors (Judd, 1981).

If unlimited supplies of uranium were available at very small cost, there would be no particular advantage in seeking to improve CRs. One would merely burn out the U-235 in a thermal reactor and discard the remaining U-238. Because the cost of uranium goes up as the accessible reserves decline, it is desirable to use the U-238 as well as the U-235. Similarly, the exploitation of thorium reserves is worthwhile.

When the CR is larger than 1, as in a fast breeder reactor, it is instead called the *breeding ratio* (BR), and the *breeding gain* (BG) represents the extra plutonium produced per atom consumed

$$\mathrm{BG} = \mathrm{BR} - 1 \tag{25.6}$$

The *doubling time* (DT) is the length of time required to accumulate a mass of plutonium equal to the initial fissile fuel mass needed in a reactor system, and thus provide fuel for a new breeder. The smaller the inventory of plutonium in the cycle and the larger the BG, the quicker doubling will be accomplished. The technical term *specific inventory* is introduced, as the ratio of plutonium mass in the system to the electrical power output. Values of this quantity of 2.5 kg/MWe are sought. At the same time, a very long fuel exposure is desirable (e.g., 100,000 MW d/tonne) to reduce fuel fabrication costs. BG of 0.4 would be regarded as excellent, but a gain of only 0.2 would be very acceptable.

25.2 ISOTOPE PRODUCTION AND CONSUMPTION

The performance of a breeder reactor involves many isotopes of fertile and fissionable materials. In addition to the U-235 and U-238, there is short-lived neptunium-239 (2.356 d), Pu-239 (2.411×10^4 y), Pu-240 (6561 y), Pu-241 (14.325 y), and Pu-242 (3.75×10^5 y) as well as americium and curium isotopes resulting from multiple neutron capture. The idea of a chain of reactions is evident, as diagrammed in Fig. 25.2. To find the amount of any of these nuclides present at a given time, it is necessary to solve a set of connected equations, each of the general type

$$\text{Rate of change} = \text{Generation rate} - \text{Removal rate} \tag{25.7}$$

which is similar to Eq. (3.15) in Section 3.4 except that "removal" is more general than "decay" in that absorption (consumption or burnup) is included.

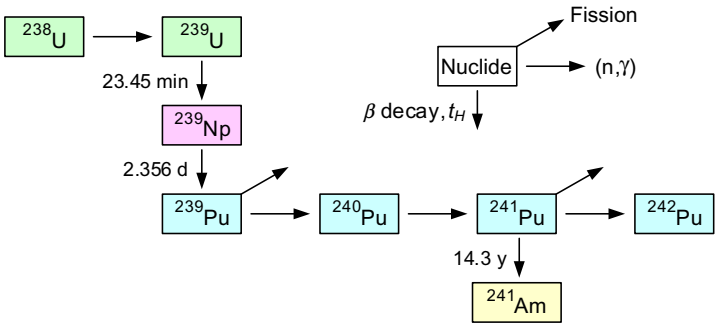

FIG. 25.2

Generation of plutonium isotopes from capture and decay reactions.

We can illustrate the approach to solving the balance equations as differential equations. Consider a simplified three-component system of nuclides: U-235, U-238, and Pu-239. Because all their radioactive half-lives are long in comparison with the time of irradiation in a reactor, radioactive decay can be ignored. However, it can be convenient to draw an analogy between decay and burnup. The depletion equation for U-235 is

$$\frac{dN_{235}}{dt} = -\phi N_{235}\sigma_a^{235} \tag{25.8}$$

If we assume constant flux ϕ, the solution of the differential equation is

$$N_{235}(t) = N_{235}(0)\exp\left(-\phi\sigma_a^{235}t\right) \tag{25.9}$$

A similar equation and solution may be written for U-238,

$$N_{238}(t) = N_{238}(0)\exp\left(-\phi\sigma_a^{238}t\right) \tag{25.10}$$

Neglecting the decay times of U-239 and Np-239, the growth equation for Pu-239 is

$$\frac{dN_{239}}{dt} = \phi N_{238}\sigma_\gamma^{238} - \phi N_{239}\sigma_a^{239} \tag{25.11}$$

where only the capture in U-238 gives rise to Pu-239, not the fission. Assuming that there is already some plutonium present when the fuel is loaded in the reactor, in amount $N_{239}(0)$, the solution is

$$N_{239}(t) = N_{239}(0)\exp\left(-\phi\sigma_a^{239}t\right) + \frac{N_{238}(0)\sigma_\gamma^{238}\left[\exp\left(-\phi\sigma_a^{239}t\right) - \exp\left(-\phi\sigma_a^{238}t\right)\right]}{\sigma_a^{238} - \sigma_a^{239}} \tag{25.12}$$

The first term on the right describes the burnup of initial Pu-239; the second term represents the net of production and consumption. Note the similarity in the form of these equations to those in Section 3.4 related to parent-daughter radioactivity processes.

It is straightforward to calculate the numbers of nuclei, but time-consuming and tedious if one wishes to vary parameters such as the reactor power and neutron flux level or the initial proportions of the different nuclides. To make such calculations easier, refer to Computer Exercise 25.A, in which the program BREEDER is applied.

A one-neutron group model is not adequate to analyze the processes in a fast breeder reactor, where cross-sections vary rapidly with energy. The accurate calculation of multiplication requires the use of several neutron energy groups, with neutrons supplied to the groups by fission and removed by slowing and absorption. In Computer Exercise 25.B, the computation is performed with 16 groups and the program FASTRX analyzes a simple fast reactor.

25.3 THE FAST BREEDER REACTOR

Liquid metal fast breeder reactors (LMFBRs) have been operated successfully throughout the world. In the United States, the Experimental Breeder Reactor-I at Idaho Falls was the first power reactor to generate electricity in 1951. Its successor, EBR-II, was used from 1963–94 to test equipment and materials. An important feature was its closed fuel cycle in which used fuel was removed, chemically processed, and refabricated. To accomplish these operations under conditions of high radioactivity, unique handling equipment was devised. In September 1969, the power reached its design value of 62.5 MWt (Stevenson, 1987).

The 200 MWt Fermi I reactor built near Detroit was the first LMFBR intended for commercial application. It was started in 1963 but was damaged by blockage of coolant flow passages and only operated briefly after being repaired.

The 400 MWt Fast Flux Test Facility (FFTF) at Richland, Washington, (now shut down) did not generate electricity but provided valuable data on the performance of fuel, structural materials, and coolant. After a number of years of design work and construction, the US government canceled the demonstration fast power reactor called Clinch River Breeder Reactor Project (CRBRP). There was a great deal of debate in the United States before CRBRP was abandoned. One argument for stopping the project was that increased prices of fuel, being only approximately one-fifth of the cost of producing electricity, would not cause converter reactors to shut down or warrant switching to the newer technology except on a long-term basis. This political decision shifted the leadership for breeder development from the United States to other countries.

France took the initiative in the development of the breeder for the production of commercial electric power in cooperation with other European countries. The 1200-MWe Superphénix was a full-scale pool-type breeder constructed with partial backing by Italy, West Germany, the Netherlands, and Belgium (Vendreyes, 1977). Because of sodium leaks and great public opposition, the reactor was shut down permanently in 1998. Its predecessor, the 233-MWe Phénix, operated from 1974 to 2009 as a research platform.

With the suspension of operation of Superphénix, the lead in breeder reactor development again shifted, this time to Japan, which placed its 280-MWe loop-type sodium-cooled MONJU into operation in 1993. It was part of Japan's long-range plan to construct a number of breeders starting around 2020. In 1995, the reactor suffered a sodium leak and was shut down. Renewed interest in breeding prompted a brief restart of MONJU in 2010 before a decision was made to decommission the unit permanently.

Presently, the only two operating LMFBRs in the world are at the Beloyarsk plant in Russia. Supplying electricity since 1981, the 560 MWe BN-600 has operated more successfully than any other

Table 25.2 Liquid Metal Fast Breeder Reactors, Beloyarsk Nuclear Power Station, Russia

Reactor	Unit 3	Unit 4
Model	BN-600	BN-800
Thermal power (MWt)	1470	2100
Electric power, gross/net (MWe)	600/560	885/789
Sodium coolant temperatures, reactor inlet/outlet (°C)	377/550	354/547
Sodium coolant pressure (kg/cm^2)	8.8	9.2
Coolant flow rate (tonne/h)	25,000	32,000
Active core height, diameter (m)	1.03, 2.05	0.88, 2.56
Vessel height, diameter (m)	12.6, 12.86	16.41, 12.9
Fuel and enrichment (w/o)	UO_2 (17, 21, 26)	UO_2/PuO_2 (19.5, 22.1, 24.7)
Pin outside diameter (mm)	6.9	6.6
Cladding	Stainless steel	Stainless steel
Clad thickness (mm)	0.4	0.4
Assembly pitch (cm)	9.82	10
Rods per assembly	127	127
Number of assemblies	369	565
Number of B_4C rods	27	27
Core power density, average/peak (kWt/L)	413/705	650/765
Cycle length (months)	5.3	5–7

Data from Nuclear Engineering International (NEI), 2012. 2012 World Nuclear Industry Handbook.; International Atomic Energy Agency (IAEA), 2018. Nuclear Power Reactors in the World. Vienna.

reactor in that country. Beloyarsk Unit 4, which is a larger 789 MWe BN-800 model, became operational in 2016. Some of their pertinent features are listed in Table 25.2.

The use of liquid sodium as coolant ensures that there is little neutron moderation in the fast reactor. Nonetheless, the sodium presence reduces the average neutron energy, thus shifting (or softening) the neutron spectrum to lower energy. The element sodium melts at 98°C (208°F), boils at 881°C (1618°F), and has excellent heat transfer properties (Foust, 1972). With such a high melting point, pipes containing sodium must be heated electrically and thermally insulated to prevent freezing. Alternatively, a sodium-potassium (NaK) alloy, which is a liquid at ambient temperatures for potassium compositions between 46 and 89 w/o, can be employed. The coolant becomes radioactive by neutron absorption in Na-23, producing the 15-h Na-24

$$^{23}_{11}\mathrm{Na} + {}^{1}_{0}\mathrm{n} \rightarrow {}^{24}_{11}\mathrm{Na} \tag{25.13}$$

Great care must be taken to prevent contact between sodium and water or air, which would result in a serious fire, accompanied by the spread of radioactivity. To avoid such an event, an intermediate heat exchanger is used in which heat is transferred from radioactive primary sodium to nonradioactive secondary sodium.

EXAMPLE 25.3

Although sodium is not intended as a moderator, using Eqs. (4.48) and (4.49) shows that, on the average, upon scattering with sodium ($A = 23$) the energy of a 2 MeV neutron reduces to

$$\alpha = \frac{(A-1)^2}{(A+1)^2} = \frac{(23-1)^2}{(23+1)^2} = 0.840$$

$$E_{\text{avg}} = E_0\,(1+\alpha)/2 = (2\text{MeV})(1+0.84)/2 = 1.84\text{MeV}$$

Additional scattering further decreases the neutron energy. Thus, if sodium coolant were removed from a region of the reactor core, the average energy of the neutron spectrum would increase (harden). This behavior gives rise to defining a sodium void coefficient of reactivity.

Two physical arrangements of the reactor core, pumps, and heat exchanger are possible. The loop type of Fig. 25.3 is similar to the thermal reactor system, whereas in the pool type of Fig. 25.4 all the components are immersed in a tank of liquid sodium. There are advantages and disadvantages to each concept (Campbell, 1973), but both are practical. For instance, the pool design boasts greater heat capacity due to the larger sodium mass, whereas the loop configuration reduces the neutron shielding needed to avoid secondary sodium activation.

To obtain maximum BRs in the production of new fissile material, more than one fuel zone is needed. The neutron-multiplying core of the breeder reactor is composed of mixed oxide (MOX) fuel as a mixture of U and Pu. Surrounding the core is a natural or depleted uranium oxide *blanket* or breeding blanket. In early designs, the blanket acted as a reflector for a homogeneous core, but modern

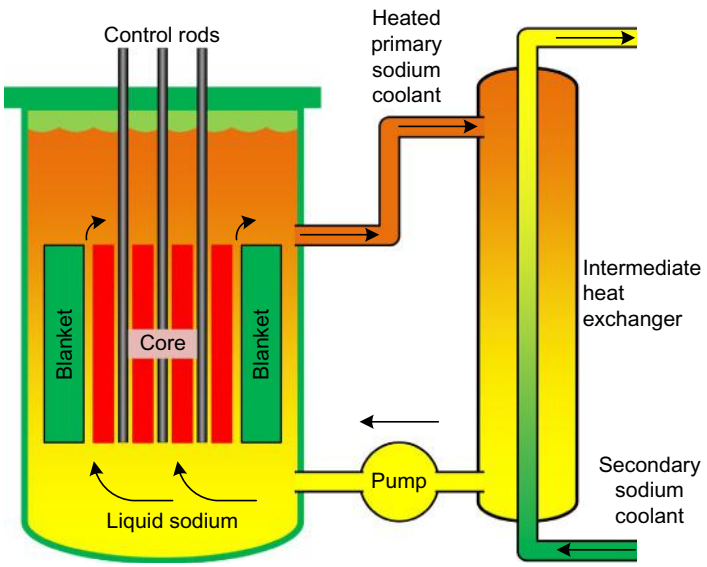

FIG. 25.3

Loop system for LMFBR.

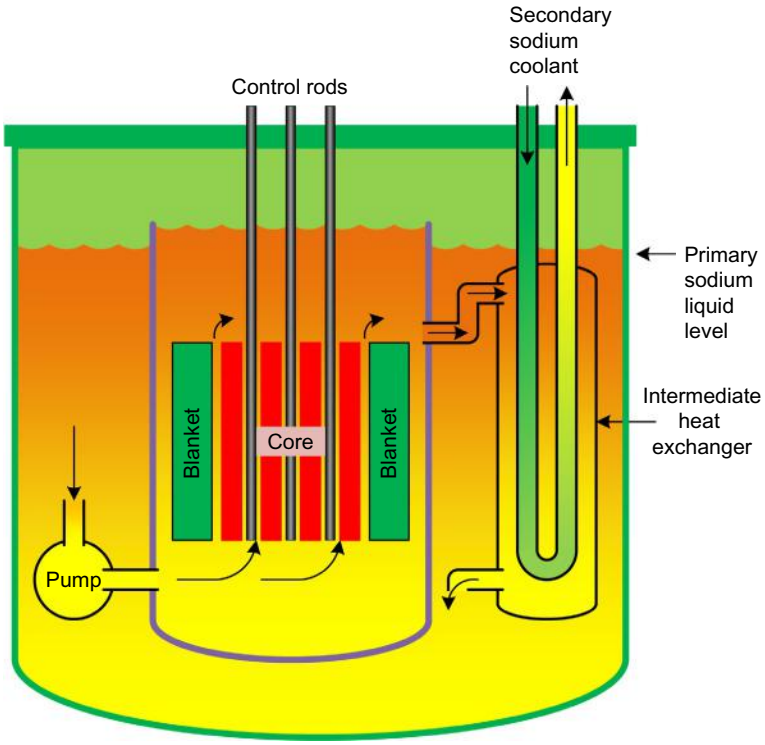

FIG. 25.4

Pool system for LMFBR.

designs involve blanket rings both inside and outside the core, rendering the system heterogeneous. The new arrangement is predicted to have enhanced safety as well.

Deployment of breeder reactors demands recycling of the plutonium. This in turn requires reprocessing, which involves physical and chemical treatment of irradiated fuel to separate uranium, plutonium, and fission products. Used nuclear fuel reprocessing was addressed in Section 23.5 in connection with waste disposal. The United States abandoned commercial reprocessing due to concerns about the diversion of plutonium and is unlikely to resume the practice for the present generation of power reactors. An alternative approach that does not require reprocessing is the traveling wave (breed and burn) reactor being developed by TerraPower (Hejzlar et al., 2013).

25.4 INTEGRAL FAST REACTOR

After the CRBRP was canceled, the United States continued development of breeder reactors. The success of the Experimental Breeder Reactor-II prompted an extension called the Integral Fast Reactor (IFR). It was a fast breeder reactor coupled with a pyrometallurgical process that allowed all fuels and products to remain in the system. The fuel cycle included fuel fabrication, power generation,

reprocessing, and waste treatment. Through the isolation of plutonium in a highly radioactive environment, the problem of weapons proliferation was eliminated. The reactor burned all actinides—elements 89–103. No additional fuel was introduced and the predicted lifetime was 60 y.

Fuel in the IFR was metal, as an alloy of U, Pu, and Zr, with a much higher thermal conductivity than ceramic uranium oxide. Thus, in operation, the centers of fuel rods were cooler than in conventional reactors at the same power. Coolant in the reactor was liquid sodium that operates at atmospheric pressure and is not corrosive. With the reactor located within a pool, the problem of loss of coolant is eliminated, there being adequate natural convection cooling.

The reactor was found to be inherently safe, as was proved by experiments with EBR-II. In one test, the power to cooling systems was cut off when the reactor was at full power. The core temperature rose slightly as convective cooling in the pool-type vessel took over. The reactor went subcritical and shut itself down.

Use of the IFR with its closed fuel cycle and consumption of plutonium would have eliminated the concern about the spent fuel repositories being "plutonium mines," with reactor grade plutonium available at some future date for some low-yield explosions (Till et al., 1997). As such, the IFR was highly proliferation-resistant. The use of uranium was essentially complete, in contrast with the few percent consumed in conventional power plants.

By the recycling of transuranic elements, the waste consisted only of fission products, which would need to be stored for a relatively short time. The need for extra waste repositories would vanish if IFR-type reactors were deployed. The reactor system was expected to be less expensive to build because of its simplicity. Most of the complex systems of water-cooled reactors are not needed, and the cost of basic fuel is essentially zero because of the large inventory of U-238 in the depleted uranium from years of operation of isotope separation plants.

The reactor serves as a source of experience and data, and as a starting point for the proposed Advanced Fast Reactor of the 21st century. Finally, it shares the virtue of all nuclear reactors in not releasing greenhouse gases that could contribute to climate change.

Even though there were many potential benefits to the continuation of R&D on the IFR, Congress chose not to provide funds in 1994. In a Q&A session by George Stanford (2001), "Well-meaning but ill-informed people…convinced so many administrators and legislators that the IFR was a proliferation threat that the program was killed." There remains a possibility that the concept will be revived, in view of the extensive knowledge base that was developed and the promise that IFR holds to solve many of the perceived problems of nuclear energy.

A commercial outgrowth of the IFR was the Advanced Liquid Metal Reactor (ALMR) or PRISM, involving Argonne National Laboratory and General Electric. The PRISM (power reactor innovative small modular) is designed to close the fuel cycle.

Although the principal attention throughout the world has been given to the liquid metal-cooled fast breeder that uses U and Pu, other breeder reactor concepts might someday become commercially viable. The thermal breeder reactor, which uses thorium and uranium-233, has always been an attractive option. Favorable CR values are obtained with thorium as fertile material (Perry and Weinberg, 1972). Neutron bombardment of Th-232 in a thermal reactor yields fissile U-233 as noted in Section 6.3. However, there is a special radiation hazard involved. The ^{233}U(n, 2n) reaction yields 69-y half-life U-232 that decays into Tl-208, a 2.6 MeV gamma emitter. To demonstrate feasibility, the original Shippingport core was converted to a light-water breeder reactor using ^{232}Th-^{233}U and operated from 1977 to 1982 (Freeman et al., 1989). India, which has large reserves of thorium, is especially interested in a U-233 breeder cycle.

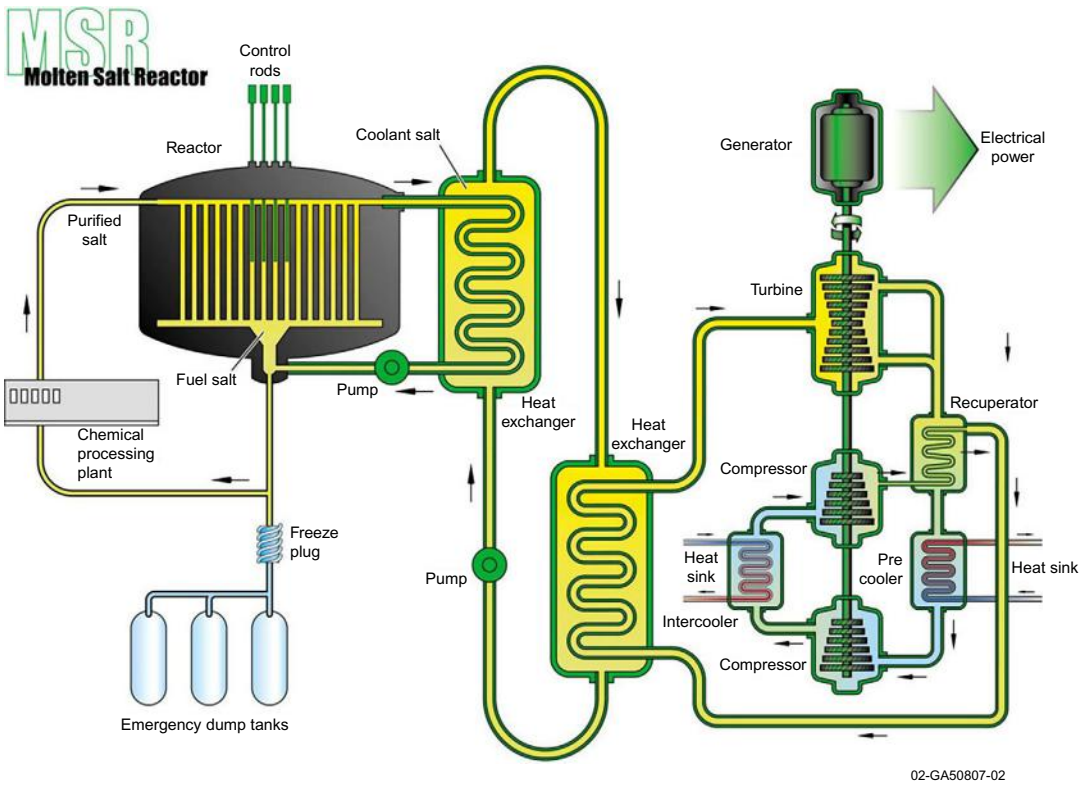

FIG. 25.5

Generation IV molten salt reactor.

Courtesy US Department of Energy (DOE), 2002. A technology roadmap for generation IV nuclear energy systems, GIF-002-00.

One extensive test of that type of reactor was the Molten-Salt Reactor Experiment at Oak Ridge, an outgrowth of the aircraft nuclear program of the 1960s (see Section 22.2). The reactor demonstrated the feasibility of the circulating fuel concept with salts of lithium, beryllium, and zirconium as solvent for uranium and thorium fluorides. Fig. 25.5 illustrates the Generation IV molten salt reactor that has a closed fuel cycle that burns Pu and minor actinides. When the mixture passes through the low neutron leakage core region, criticality is achieved. Other concepts are uranium and thorium fuel particles suspended in heavy water, and a high-temperature gas-cooled graphite-moderated reactor containing beryllium in which the (n, 2n) reaction enhances neutron multiplication. The intermediate sodium loop provides isolation between the radioactive primary sodium and the feedwater-steam because water and sodium undergo exothermic reactions of

$$\begin{aligned} 2\mathrm{Na} + \mathrm{H_2O} &\rightarrow \mathrm{Na_2O} + \mathrm{H_2} \\ 2\mathrm{Na} + 2\mathrm{H_2O} &\rightarrow 2\mathrm{NaOH} + \mathrm{H_2} \end{aligned} \tag{25.14}$$

These same reactions can occur between hot sodium and bare concrete (Waltar and Reynolds, 1981).

25.5 BREEDING AND URANIUM RESOURCES

From the standpoint of efficient use of uranium to produce power, it is clearly preferable to use a breeder reactor instead of a converter reactor. The breeder has the ability to use nearly all the uranium rather than a few percent. Its impact can be viewed in two different ways. First, the demand for natural uranium would be reduced by a factor of approximately 30, cutting down on fuel costs while reducing the environmental effect of uranium mining. Second, the supply of fuel would last longer by a factor of 30. For example, instead of a mere 80 y for use of inexpensive fuel, we would have 2400 y. It is less clear, however, as to when a well-tested version of the breeder would actually be needed. A simplistic answer is, "when uranium gets very expensive." Such a situation is not imminent because there has been an oversupply of uranium for a number of years, and all analyses show that breeders are more expensive to build and operate than converters. A reversal in trend is not expected until sometime well into the 21st century. The urgency to develop a commercial breeder has lessened as the result of slower adoption of nuclear power than anticipated, with the smaller rate of depletion of resources. Another key factor is the availability in the United States and the former USSR of large quantities of surplus weapons plutonium, which can be used as fuel in the form of MOX.

The International Atomic Energy Agency (IAEA) and OECD Nuclear Energy Agency (NEA) (2016) report uranium resource data as of January 2015 in the Red Book. Recoverable amounts of uranium are given for costs in $/kgU <40, <80, <130, and <260. Table 25.3 shows the sums by main country sources of two categories: reasonably assured resources (RAR) and inferred resources (IR). The world total identified resources (RAR plus IR) is 5,718,400 tonnes for <$130/kgU. The table also gives the annual uranium requirements by principal country users. The world total demand per year is 56,585 tonnes. Simple arithmetic tells us that these resources would last 101 y, assuming constant fuel requirements.

Table 25.3 Uranium Demand and Resources (in Thousands of Tonnes)

Country	Annual Demand (in 2014)	Country	Identified Resources (Recoverable) to $130/kg
United States	18.575	Australia	1664.1
France	8.000	Kazakhstan	745.3
Russia	4.400	Canada	509.0
Korea	4.200	Russia	507.8
China	4.200	South Africa	322.4
Ukraine	2.480	Niger	291.5
Germany	2.000	Brazil	276.8
Canada	1.800	China	272.5
United Kingdom	1.500	Namibia	267.0
Sweden	1.430	Mongolia	141.5
Spain	1.120	Uzbekistan	130.1
Belgium	0.870	Ukraine	115.8
India	0.850	Botswana	73.5

Table 25.3 Uranium Demand and Resources (in Thousands of Tonnes)—cont'd

Country	Annual Demand (in 2014)	Country	Identified Resources (Recoverable) to $130/kg
Czech Republic	0.680	United States	62.9
Finland	0.425	Tanzania	58.1
Brazil	0.400	Jordan	47.7
Japan	0.370	Peru	33.4
Slovak Republic	0.360	Central African Republic	32.0
Bulgaria	0.300	Zambia	24.6
South Africa	0.290	Argentina	18.5
Switzerland	0.250	Mauritania	16.4
Hungary	0.215	Slovak Republic	15.5
Romania	0.210	Mali	13.0
Mexico	0.190	Sweden	9.6
Iran	0.160	Slovenia	9.2
Slovenia	0.150	Indonesia	7.2
Argentina	0.120	Portugal	7.0
Pakistan	0.110	Turkey	6.6
Armenia	0.065	Romania	6.6
Netherlands	0.060	Japan	6.6
United Arab Emirates	0.0	Malawi	6.2
Belarus	0.0	Italy	6.1
		Gabon	4.8
		Iran	3.9
		Mexico	2.7
		Czech Republic	1.3
		Finland	1.2
Total	56.585	Total	5718.4

Data from International Atomic Energy Agency (IAEA)/OECD Nuclear Energy Agency (NEA), 2016. Uranium 2016: Resources, Production and Demand. IAEA/OECD NEA. (A biennial publication; the "Red Book".).

The use of global figures obscures the problem of distribution. Table 25.3 lists the top countries in the categories demand and resources. Some surprising disparities are seen. The leading potential uranium suppliers, Australia and Kazakhstan, are not on the list of users. On the other hand, the second highest user, France, has negligible U resources. Thus, there must be a great deal of import/export trade to meet fuel needs. Alternately, it means that to assure uninterrupted production of nuclear power, some countries are much more interested than others in seeing a breeder reactor developed. In 2017, the IAEA opened a Low Enriched Uranium (LEU) Bank to store up to 90 tonnes of fuel in Kazakhstan in order to ensure availability for Member States.

Table 25.4 US Domestic Uranium Industry

Attribute	2012	2016
Estimated reserves of U_3O_8 at <$30/lb and <$100/lb (million pounds)	51.8 and 304	59.9 and 339.2
Annual uranium mine production of U_3O_8 (million pounds)	4.335	2.545
Total mines and sources	12	9
Employment (person-years)	1196	560
Total expenditures (million $)	352.9	169.9
Average cost of uranium (U_3O_8) concentrate ($ per pound)	49.63	38.22

Data from US Department of Energy (DOE), Energy Information Administration (EIA) 2017. 2016 domestic uranium production report. DOE EIA.

Table 25.4 shows some data on US uranium production. Not included are byproducts of phosphate and copper mining, or the large stockpile of depleted uranium as tails from the uranium isotope separation processes. Such material is as valuable as natural uranium for use in a blanket to breed plutonium. The principal US deposits in order of size are in Wyoming, New Mexico, Colorado, Texas (coastal plain), and near the Oregon-Nevada border. The greatest concentrations of estimated additional resources are in Utah and Arizona. Most of the ores come from sandstone; approximately nine uranium mines were operating in 2016. Exploration by surface drilling has tapered off continually since the mid-1970s, when nuclear power was expected to grow rapidly.

There is considerable sentiment in the nuclear community for storing spent fuel from converter reactors rather than burying it as waste, in anticipation of an energy shortage in the future as fossil fuels become depleted. If such a policy were adopted, the plutonium contained in the spent fuel could be recovered in a leisurely manner. The plutonium would provide the initial loading of a new generation of fast breeder reactors, and the recovered uranium would serve as blanket material.

The energy content of uranium is so high that the cost of fuel for nuclear power plants is relatively small. In 2016, the average fuel cost incurred by US nuclear plants was 0.745 ¢/kWh (DOE, 2018). However, if shortages of inventory occur because of inadequacy of supply, the price may rise significantly.

Around 1980, a peak price of $46/lb ($101/kg) U_3O_8 was reached, but in subsequent decades dropped to a figure in 2001 of only $10/lb ($22/kg). The reason was the appearance of secondary sources such as depletion of inventories and released weapons uranium. Lesser amounts of secondary fuel can come from recycling, reenrichment of separation tails, and surplus plutonium. These alternatives are expected to decline in the coming years. As countries such as India, South Korea, and China expand their nuclear capabilities, the price of uranium may increase. Average prices paid in the United States rose from $10/lb in 2001 to peak at $56/lb ($123/kg) in 2011 but have declined to $42/lb ($93/kg) in 2016 (DOE, 2017).

Coupled with the increased demand for uranium will be a growth in exploration and mining, but this will be hampered by the lack of qualified personnel. There are said to be ample resources, but investment in retrieval may be slow in coming until a stable price structure is established. Finally, there is a large delay between discovery of new resources and the availability of nuclear fuel.

It is not possible to predict the rate of adoption of fast breeder reactors for several reasons. The capital costs and operating costs for full-scale commercial systems are not firmly established.

The existence of the satisfactory light water reactor (LWR) and the ability of a country to purchase slightly enriched uranium or MOX tend to delay the installation of breeders. It is conceivable, however, that breeders could replace the conventional converter reactors in the present century because of fuel resource limitations. It is possible that the breeder could buy the time needed to fully develop alternative sources such as nuclear fusion. In the next chapter, the prospects for fusion are considered.

25.6 RECYCLING AND BREEDING

The word "cycle" has come to mean the mode of management of nuclear fuels. There are several possibilities: *once-through*, the method currently used commercially in the United States, leading to used fuel being stored or buried; *recycle*, in which spent fuel is reprocessed and some of the products reused; *closed cycle*, with all materials retained in a system, involving nuclear and chemical treatment and burning out many undesired radioisotopes; and *breeding*, where as much or more fissile material is generated as was supplied initially. The equipment required for each mode of operation is distinctly different; there are different consequences in terms of safety and security and various associated costs of operation.

In the post-World War II period of 1945–70, when reactor R&D was underway, it was believed that the reserves of uranium were limited, especially in terms of an expected growth in nuclear power. Thus, it was thought necessary to use the U-238 by conversion into Pu-239 by means of reprocessing. The growth did not occur and there turned out to be much more uranium available. Reprocessing was stopped by US President Jimmy Carter and reinstated by US President Ronald Reagan, but in the meantime, the industry concluded that the process was too expensive.

Wilson (1999) gives a cogent discussion of reprocessing and breeding, stating that it may be 50–100 y before they are needed as a result of uranium ore costs becoming excessive. However, he proposes an alternative environmental reason for continuing to pursue reprocessing (namely, objection to underground disposal of high-level waste). The breeding cycle that requires reprocessing would reduce the volume of wastes and eliminate many of the long-lived radioisotopes that determine repository character.

One can visualize another important reason for continuing programs of research, development, testing, and deployment of the nuclear, physical, and chemical aspects of recycling and reprocessing. It is the need to maintain an information base that involves data, methodology, and people with technical knowledge and skills. This last aspect is especially significant in light of the continued retirement of nuclear scientists, engineers, and technicians who have accumulated vast experience over their professional careers. With these ideas in mind, we examine the activities identified as promising for the future.

In the Generation IV program, two of the concepts are the lead-cooled fast reactor (LFR) and the sodium-cooled fast reactor (SFR), as noted in Section 18.8. A variant of both that features recycling and breeding is the revival of the Integral Fast Reactor (IFR). At the time of its cancellation, the IFR was judged highly successful. It had the promise of full use of uranium instead of the low percentages attained by light-water reactors. The claim was made that such a reactor system has the potential of making nuclear power essentially inexhaustible and of satisfying humanity's long-term energy needs.

The IFR was a closed cycle with sodium coolant and metal fuel, with pyrometallurgical chemical processing. Because of the high levels of radioactivity in the fuel, diversion and proliferation were

virtually impossible. The system had the potential of burning the isotopes that dominate waste repository performance: plutonium, neptunium, americium, and curium. Wastes remaining would have a relatively short half-life and be of small volume, making a second repository in the United States unnecessary. Depending on the mode of operation, IFR/AFR-(advanced fast reactor) type systems could process surplus weapons plutonium, existing spent fuel, depleted uranium accumulated from isotope separation, and eventually natural uranium.

A powerful case for R&D on a fast reactor is found in an article by Hannum et al. (2005). There, a comparison is made among three cycles: once-through, plutonium recycle, and full recycle. The virtues of recycling are thoroughly discussed in testimony to Congress of Philip Finck (2005) of Argonne National Laboratory, and the need for the AFR as an extension of IFR is fully described in an article by Chang (2002). An article by Lightfoot et al. (2006) provides an analysis of nuclear fuel reserves and use. Finally, a position statement of the American Nuclear Society is titled, "Fast Reactor Technology: A Path to Long-Term Energy Sustainability" (ANS, 2005).

25.7 SUMMARY

If the value of the neutron reproduction factor η is larger than 2 and losses of neutrons are minimized, breeding can be achieved, with more fuel produced than is consumed. The CR measures the ability of a reactor system to transform a fertile isotope (e.g., U-238) into a fissile isotope (e.g., Pu-239). Complete conversion requires a CR value of nearly 1. Fast breeder reactors that use liquid sodium with BRs greater than 1 have been built and operated, but several development programs have been canceled. Two large-scale breeders presently operate in Russia. There is a great disparity between uranium resources and uranium use among the countries of the world. Application of the breeder could stretch the fission power option from a few decades to centuries.

25.8 EXERCISES

25.1 What are the largest conceivable values of the CR and the BG?

25.2 An "advanced converter" reactor is proposed that will use 50% of the natural uranium supplied to it. Assuming all the U-235 and Pu-239 are used, what must the CR be?

25.3 Explain why the use of a natural uranium blanket is an important feature of a breeder reactor.

25.4 Compute η and BG for a fast Pu-239 reactor if $\nu = 2.98$, $\sigma_f = 1.85\,\text{b}$, $\sigma_\gamma = 0.26\,\text{b}$, and $\mathcal{L} = 0.41$. (Note that the fast fission factor ε need not be included.)

25.5 With a BR = 1.20, how many kilograms of fuel will have to be burned in a fast breeder reactor operating only on plutonium to accumulate an extra 1260 kg of fissile material? If the power of the reactor is 1250 MWt, how long will it take in days and years, noting that it requires approximately 1.3 g of plutonium per MWt d?

25.6 (a) Show that $CR = \gamma_{238}$ is required to consume all the U-235, U-238, and Pu-239 in a uranium-fueled reactor. (b) Must the uranium be of natural enrichment for this to be true?

25.7 (a) By use of the neutron cycle, Fig. 16.5, find a formula for $\mathcal{L}$ as defined in Eq. (25.5); note that $\eta = \eta_{235}\Sigma_a^{235}/\Sigma_a^U$. (b) Calculate the value of $\mathcal{L}$ and verify that the alternative formula gives the same answer as in Example 25.2, $CR = 0.746$.

25.8 (a) Calculate the threshold reaction energy for ^{23}Na(n, γ). (b) What is the decay product of Na-24? (c) What are the energies of the gamma rays emitted from Na-24?

25.9 With the OECD estimate of 7.642 million tonnes of identified uranium resources at $260/kgU, how long can the world's 2014 demand be supplied?

25.10 The ^{23}Na(n,γ) reaction cross-section is 0.0008 b at fast energy levels. Compute the Na-24 production rate in a fast flux of 3.5×10^{15} n/(cm^2 s). Assume operational conditions such that the sodium is 550°C where the density is 0.820 g/cm^3.

25.11 Derive an alternative expression to Eq. (25.9) for the depletion of U-235 atoms as a function of time, assuming constant reactor power because nuclear power plants are base load facilities.

25.9 COMPUTER EXERCISES

25.A A breeder reactor is successful if it produces more fissionable material than it consumes. To test that possibility, apply computer program BREEDER, which allows the use of cross-sections for U-235, U-238, and Pu-239 as deduced from early critical experiments on weapons material assemblies, or more modern cross-sections appropriate to a power reactor design. (a) Run the program, varying parameters, to explore trends. (b) Use the following common input for both cross-section options: U-235 atom fraction 0.003 (depleted U), plutonium volume fraction 0.123, fast flux 4.46×10^{15}/(cm^2 s). (c) Discuss observations of trends and seek to explain in terms of assumed cross-section sets.

25.B Program FASTRX solves the neutron balance equations for a fast reactor with classic 16-group Hansen-Roach cross-sections prepared by Los Alamos. Those input numbers are found in the report ANL-5800 (ANL, 1963). Run the program with the menus, observing input data and calculated results. Compare results for the case of pure U-235 with those obtained in Computer Exercise 16.A, with program CRITICAL.

REFERENCES

American Nuclear Society (ANS), 2005. Fast reactor technology: a path to long-term energy sustainability. ANS Position Statement, ANS-74-2005.

Argonne National Laboratory (ANL), 1963. Reactor physics constants. ANL-5800, second ed., p. 568.

Campbell, R.H., 1973. Primary system design of sodium-cooled fast reactors. J. British Nucl. Energ. Soc. 12 (4), 357–365.

Chang, Y.I., 2002. Advanced fast reactor: a next-generation nuclear energy concept. Forum Phys. Soc. 31 (2), 3–6.
Finck, P.J., 2005. Hearing on nuclear fuel reprocessing before the house committee on science, Energy Subcommittee (June 16). http://www.gpo.gov/fdsys/pkg/CHRG-109hhrg21711.html.
Foust, O.J. (Ed.), 1972. Sodium-NaK Engineering Handbook, vol. I, Sodium chemistry and physical properties. Gordon and Breach, New York.
Freeman, L.B., Beaudoin, B.R., Frederickson, R.A., Hartfield, G.L., Hecker, H.C., Milani, S., Sarber, W.K., Schinck, W.C., 1989. Physics experiments and lifetime performance of the light water breeder reactor. Nucl. Sci. Eng. 102 (4), 341–364.
Hannum, W.H., Marsh, G.E., Stanford, G.S., 2005. Smarter use of nuclear waste. Sci. Am. 293 (6), 84–91.
Hejzlar, P., Petroski, R., Cheatham, J., Touran, N., Cohen, M., Truong, B., et al., 2013. TerraPower, LLC traveling wave reactor development program overview. Nucl. Eng. Technol. 45 (6), 731–744.
International Atomic Energy Agency (IAEA)/OECD Nuclear Energy Agency (NEA), 2016. Uranium 2016: Resources, Production and Demand. IAEA/OECD NEA. A biennial publication; the "Red Book".
Judd, A.M., 1981. Fast Breeder Reactors: An Engineering Introduction. Pergamon Press, Oxford.
Lightfoot, H.D., Manheimer, W., Meneley, D.A., Pendergast, D., Stanford, G.S., 2006. Nuclear fission fuel is inexhaustible. IEEE EIC Climate Change Technology, Ottawa.
Perry, A.M., Weinberg, A.M., 1972. Thermal breeder reactors. Annu. Rev. Nucl. Part. Sci. 22, 317–354.
Stanford, G.S., 2001. Integral fast reactors: source of safe, abundant, non-polluting power. National Center for Public Policy Research, http://www.nationalcenter.org/NPA378.html. AFR predecessor.
Stevenson, C.E., 1987. The EBR-II Fuel Cycle Story. American Nuclear Society, La Grange Park, IL.
Till, C.E., Chang, Y.I., Hannum, W.H., 1997. The integral fast reactor–an overview. Prog. Nucl. Energy 31 (1–2), 3–11.
US Department of Energy (DOE), Energy Information Administration (EIA), 2017. 2016 uranium marketing annual report; 2017. DOE EIA.
US Department of Energy (DOE), Energy Information Administration (EIA), 2018. Electric power annual 2016. DOE EIA.
Vendreyes, G.A., 1977. Superphenix: a full-scale breeder reactor. Sci. Am. 236 (3), 26–35.
Waltar, A.E., Reynolds, A.B., 1981. Fast Breeder Reactors. Pergamon Press, New York.
Wilson, R., 1999. The changing need for a breeder reactor. In: The Uranium Institute Twenty-Fourth Annual International Symposium. London.

FURTHER READING

Chadwick, M.B., Herman, M., Obložinský, P., Dunn, M.E., Danon, Y., Kahler, A.C., et al., 2011. ENDF/B-VII.1 Nuclear data for science and technology: cross-sections, covariances, fission product yields and decay data. Nucl. Data Sheets 112 (12), 2887–2996.
Cochran, T.B., 1974. The Liquid Metal Fast Breeder Reactor: An Environmental and Economic Critique. Resources for the Future Press, Baltimore, MD.
Fistedis, S.H. (Ed.), 1987. Nucl. Eng. Design 101 (1), 1–91. Special issue on EBR-II.
Hannum, W.H. (Ed.), 1997. The technology of the integral fast reactor and its associated fuel cycle. Prog. Nucl. Energ. 31 (1–2), 1–217.
International Atomic Energy Agency (IAEA), 1999. Status of liquid metal cooled fast reactor technology; 1999. IAEA-TECDOC-1083.
International Atomic Energy Agency (IAEA), 2018. Nuclear Power Reactors in the World. IAEA, Vienna.
Kang, J., von Hippel, F.N., 2001. U-232 and the proliferation-resistance of U-233 in spent fuel. Sci. Glob. Security 9 (1), 1–32.

Nuclear Engineering International (NEI), 2012. 2012 World Nuclear Industry Handbook. Nuclear Engineering International, London.

Serp, J., Allibert, M., Beneš, O., Delpech, S., Feynberg, O., Ghetta, V., et al., 2014. The molten salt reactor (MSR) in generation IV: overview and perspectives. Prog. Nucl. Energ. 77, 308–319.

US Department of Energy (DOE), 2002. A technology roadmap for generation IV nuclear energy systems. GIF-002-00.

US Department of Energy (DOE), Energy Information Administration (EIA), 2017. 2016 domestic uranium production report. DOE EIA.

US Department of Energy (DOE)/Argonne National Laboratory (ANL), Advanced Fast Reactor (AFR). http://www.ne.anl.gov/research/ardt/afr/index.html.

Wirtz, K., 1976. Lectures on Fast Reactors. American Nuclear Society, La Grange Park, IL.

World Information Service on Energy (WISE), Uranium project, world information service on energy. http://www.wise-uranium.org. Includes a Nuclear Fuel Supply Calculator and listings of organizations handling fuel.

Zaleski, C.P., 1985. Fast breeder reactor economics. In: Ott, K.O., Spinrad, B.I. (Eds.), Nuclear Energy: A Sensible Alternative. Plenum Press, New York/London.

CHAPTER

FUSION REACTORS

26

CHAPTER OUTLINE

A device that permits the controlled release of fusion energy is designated as a fusion reactor in contrast with one yielding fission energy, the fission reactor. As discussed in Chapter 7, the potentially available energy from the fusion process is enormous. The possibility of achieving controlled thermonuclear power on a practical basis has not yet been demonstrated, but progress in recent years gives encouragement that fusion reactors can be in operation in the 21st century. In this chapter, we will review the choices of nuclear reaction, study the requirements for feasibility and practicality, and describe the physical features of machines that have been tested.

26.1 COMPARISON OF FUSION REACTIONS

The main nuclear reactions that combine light isotopes to release energy, as described in Section 7.1, are the D-D, D-T, and D-^{3}He. There are advantages and disadvantages of each. The reaction involving only deuterium uses an abundant natural fuel available from water by isotope separation. However, the energy yields from the two equally likely reactions are low (4.03 and 3.27 MeV). In addition, the reaction rate as a function of particle energy is lower for the D-D case than for the D-T case, as shown in Fig. 26.1. As defined in Section 7.3, the *reactivity* $\overline{\sigma v}$, dependent on cross-section and particle speed, is a more meaningful variable than the cross-section alone.

Nuclear Energy. https://doi.org/10.1016/B978-0-12-812881-7.00026-5

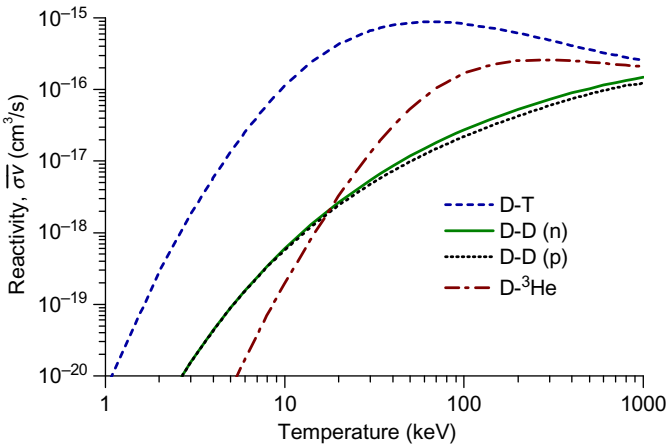

FIG. 26.1

Reaction rates for fusion reactions. The quantity $\overline{\sigma v}$, the average over a Maxwellian distribution of cross-section times speed, when multiplied by particle densities gives the fusion rate per unit volume.

Data from McNally Jr., J.R., Rothe, K.E., Sharp, R.D., 1979. Fusion reactivity graphs and tables for charged particle reactions. ORNL/TM-6914.

The D-T reaction yields a helium ion and a neutron with energies as indicated:

$$ {}_1^2\mathrm{H} + {}_1^3\mathrm{H} \rightarrow {}_2^4\mathrm{He}(3.5\,\mathrm{MeV}) + {}_0^1\mathrm{n}(14.1\,\mathrm{MeV}) \tag{26.1} $$

The D-T cross-section is large and the energy yield is favorable. The ideal ignition temperature for the D-T reaction is only 4.3 keV, in contrast with 48 keV for the D-D reaction (see Fig. 7.3), making the achievement of practical fusion with the former far easier. One drawback, however, is that the artificial isotope tritium is required. Tritium can be generated by neutron absorption in lithium, according to the two reactions

$$ \begin{aligned} {}_3^6\mathrm{Li} + {}_0^1\mathrm{n} &\rightarrow {}_1^3\mathrm{H} + {}_2^4\mathrm{He} + 4.8\,\mathrm{MeV} \\ {}_3^7\mathrm{Li} + {}_0^1\mathrm{n} &\rightarrow {}_1^3\mathrm{H} + {}_2^4\mathrm{He} + {}_0^1\mathrm{n} - 2.5\,\mathrm{MeV} \end{aligned} \tag{26.2} $$

The neutron can come from the D-T fusion process itself in a breeding cycle similar to that in fission reactors. Liquid lithium can thus be used concurrently as a coolant and a breeding blanket.

The fact that the D-T reaction gives a neutron as a byproduct is a partial disadvantage in a fusion machine. Wall materials are readily damaged by bombardment by 14.1 MeV neutrons, requiring frequent wall replacement. Also, materials of construction become radioactive as the result of neutron capture. These are engineering and operating difficulties, whereas the achievement of high enough energy to use neutron-free reactions would be a major scientific challenge.

In the end, use of the D-T reaction is limited by the availability of lithium, which is not as abundant as deuterium. All things considered, the D-T fusion reactor is the most likely to be operated first, and its success might lead to the development of a D-D reactor.

26.2 REQUIREMENTS FOR PRACTICAL FUSION REACTORS

The development of fusion as a new energy source involves several levels of accomplishment. The first is the performance of laboratory experiments to show that the process works on the scale of individual particles and to make measurements of cross-sections and yields. The second is to test various devices and systems intended to achieve an energy output that is at least as large as the input and to understand the scientific basis of the processes. The third is to build and operate a machine that will produce net power of the order of megawatts. The fourth is to refine the design and construction to make the power source economically competitive. The first of these levels was reached some time ago, and the second is in progress with considerable promise of success. The third and fourth steps remain for achievement in the 21st century.

The hydrogen bomb was the first application of fusion energy, and it is conceivable that deep underground thermonuclear explosions could provide heat sources for the generation of electricity (Johnson and Brown, 1958), but environmental concerns and international political aspects rule out that approach. Two methods involving machines have evolved. One consists of heating to ignition a plasma that is held together by electric and magnetic forces, the magnetic confinement fusion (MCF) method. The other consists of bombarding pellets of fuel with laser beams or charged-particle beams to compress and heat the material to ignition, the inertial confinement fusion (ICF) method. Certain conditions must be met for each of these approaches to be considered successful.

The first condition is achievement of the ideal ignition temperature of 4.3 keV for the D-T reaction. A second condition involves the fusion fuel particle number density n and a confinement time for the reaction, τ. It is called the *Lawson criterion* and is usually expressed as:

$$n\tau \geq \begin{cases} 10^{14}\,\mathrm{s/cm^3} & \text{D-T reaction} \\ 10^{16}\,\mathrm{s/cm^3} & \text{D-D reaction} \end{cases} \tag{26.3}$$

A formula of this type can be derived for MCF by looking at energy and power in the plasma. Suppose that the numbers of particles per cm^3 are n_D deuterons, n_T tritons, and n_e electrons. Furthermore, let the total number of heavy particles be $n = n_\mathrm{D} + n_\mathrm{T}$ with equal numbers of the reacting nuclei, $n_\mathrm{D} = n_\mathrm{T}$, and $n_\mathrm{e} = n$ for electrical neutrality. The reaction rate of the fusion fuel particles is written as $n_\mathrm{D} n_\mathrm{T} \sigma v$, and if E is the energy yield per reaction, the fusion power density is proportional to the square of the ion number density

$$p_\mathrm{f} = \left(n^2/4\right)\sigma v E \tag{26.4}$$

Now the power loss rate can be expressed as the quotient of the energy content $(n_\mathrm{e} + n_\mathrm{D} + n_\mathrm{T})\,(3kT/2)$ and the confinement time τ, that is,

$$p_\mathrm{l} = 3nkT/\tau \tag{26.5}$$

Equating the powers and solving (Gross, 1985),

$$n\tau = \frac{12kT}{\sigma v E} \tag{26.6}$$

EXAMPLE 26.1

For the D-T reaction, let σv be equal to the value of $\overline{\sigma v}$ from Fig. 26.1 of approximately 10^{-17} cm^3/s at the ideal ignition energy of $kT = 4.3$ keV. Substituting the fusion energy $E = 17.6$ MeV into Eq. (26.6) gives

$$n\tau = \frac{12kT}{\sigma v E} = \frac{(12)(4.3\text{keV})(10^{-3}\text{MeV/keV})}{(10^{-17}\text{cm}^3/\text{s})(17.6\text{MeV})} = 3 \times 10^{14}\,\text{s/cm}^3$$

This result is of the correct order of magnitude. The Lawson (1957) criterion, however, is only a rough rule of thumb to indicate fusion progress through research and development. Detailed analysis and experimental testing are needed to evaluate any actual system.

Similar conditions must be met for ICF. An adequate ion temperature must be attained. The Lawson criterion takes on a little different form, relating the density ρ and the radius r of the compressed fuel pellet (Duderstadt and Moses, 1982),

$$\rho r > \begin{cases} 3\,\text{g/cm}^2 & \text{D-Treaction} \\ 10\,\text{g/cm}^2 & \text{D-Dreaction} \end{cases} \tag{26.7}$$

The numerical value is set in part by the need for the radius to be larger than the range of alpha particles to take advantage of their heating effect.

EXAMPLE 26.2

Suppose that 1-mm radius spheres of a mixture of D and T in liquid form, density 0.18 g/cm^3, are compressed by a factor of $C = 2500$, where the compression ratio is defined as $C = \rho_{\text{final}}/\rho_{\text{initial}} = V_{\text{initial}}/V_{\text{final}}$ because the mass remains constant. Hence, the density is increased to

$$\rho_{\text{final}} = \rho_{\text{initial}} C = (0.18\,\text{g/cm}^3)(2500) = 450\,\text{g/cm}^3$$

Conversely, the radius is reduced to

$$C = \frac{V_{\text{initial}}}{V_{\text{final}}} = \frac{(4/3)\pi r_{\text{i}}^3}{(4/3)\pi r_{\text{f}}^3}$$

$$r_{\text{f}} = r_{\text{i}}/\sqrt[3]{C} = (1\text{mm})/\sqrt[3]{2500} = 0.0737\text{mm}$$

The final density and radius meet the objective, that is,

$$\rho r = (450\,\text{g/cm}^3)(0.00737\,\text{cm}) = 3.3\,\text{g/cm}^2 > 3\,\text{g/cm}^2$$

It is interesting to note that the factors that go into the products $n\,\tau$ are very different for the two types of fusion. For MCF typically $n = 10^{14}$/cm^3 and $\tau = 1$ s, whereas for ICF $n = 10^{24}$/cm^3 and $\tau = 10^{-10}$ s.

The analysis of fusion reactors involves many other parameters of physics and engineering. A useful collection of formulas and methods of calculating is discussed in Computer Exercise 26.A.

Progress toward practical fusion can be measured by the *amplification factor* Q, which is the ratio of energy output to energy input

$$Q = \frac{\text{Fusion energy generated}}{\text{External energy injected}} \tag{26.8}$$

Four stages of plasma can be identified. In the first, more energy must be supplied than is produced, $Q < 1$. In the second, the breakeven case, fusion power equals input power, $Q = 1$. In the third, for an operating fusion power plant, Q is considerably larger than 1 (e.g., 10). In the fourth, the burning plasma, which results from ignition, heats itself without external input, and Q is infinity.

26.3 MAGNETIC CONFINEMENT MACHINES

A number of complex MCF machines have been devised to generate a plasma and to provide the necessary electric and magnetic fields to achieve confinement of the discharge. We will examine a few of these to illustrate the variety of possible approaches.

First, however, consider a simple discharge tube consisting of a gas-filled glass cylinder with two electrodes, as in Fig. 26.2A. This is similar to the familiar fluorescent light bulb. Electrons accelerated by the potential difference cause excitation and ionization of atoms. The ion density and temperature of the plasma that is established are many orders of magnitude below that needed for fusion. To reduce the tendency for charges to diffuse to the walls and be lost, a current-carrying coil can be wrapped around the tube, as shown in Fig. 26.2B. This produces a magnetic field directed along the axis of the tube, and charges move in paths described by a helix, the shape of a stretched coil spring. The motion is quite similar to that of ions in the cyclotron (Section 9.4) or the mass spectrograph (Section 15.1). The radii in typical magnetic fields and plasma temperatures are the order of 0.1 mm for electrons and near 1 cm for heavy ions (see Exercise 26.1). To further improve charge density and stability, the current along the tube is increased to take advantage of the *pinch effect*, a phenomenon related to the electromagnetic attraction of two wires that carry current in the same direction. Each of the charges that moves along the length of the tube constitutes a tiny current, and the mutual attractions provide a constriction in the discharge.

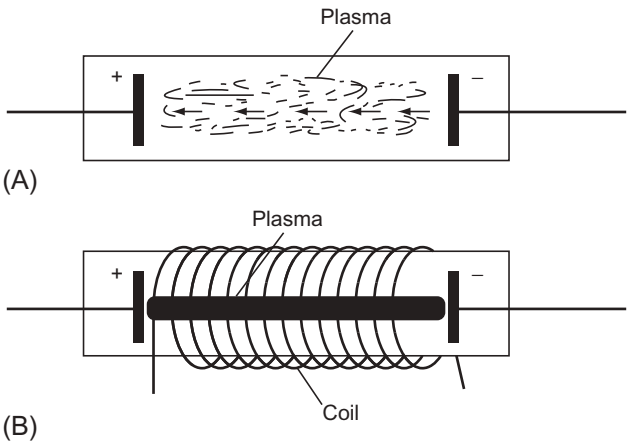

FIG. 26.2

Electrical discharges in gas-filled glass cylinders: (A) without and (B) with magnetic field.

Neither of the preceding magnetic effects prevents charges from moving freely along the discharge tube, and losses of both ions and electrons are experienced at the ends. Two solutions of this problem have been tested. One is to wrap extra current-carrying coils around the tube near the ends, increasing the magnetic field there. This causes charges to be forced back into the region of weak field (i.e., to be reflected). This *mirror machine* is not perfectly reflecting. Another approach is to create endless magnetic field lines by bending the vacuum chamber and the coils surrounding it. This arrangement, called a *stellarator*, is still being considered as a favorable system because it does not depend on internal currents for plasma confinement. It could operate continuously rather than in pulses.

A completely different solution to the problem of charge losses is to produce the discharge in a doughnut-shaped tube, a torus, as shown in Fig. 26.3. Scientists in the former Soviet Union developed the first successful ring-shaped fusion machine around 1955 (Azizov, 2012). They called it *tokamak*, an acronym in Russian for toroid-chamber-magnet-coil. Because the tube has no ends, the magnetic field lines produced by the coils are continuous. The free motion of charges along the circular lines does not result in losses. However, there is a variation in this toroidal magnetic field over the cross-section of the tube that causes a small particle migration toward the wall. To prevent such migration, a current is passed through the plasma, generating a poloidal magnetic field. The poloidal field lines are circles around the current and tend to cancel electric fields that cause migration. Toroidal magnetic fields are also used to stabilize the plasma. Together, the poloidal and toroidal fields form a helical shaped field.

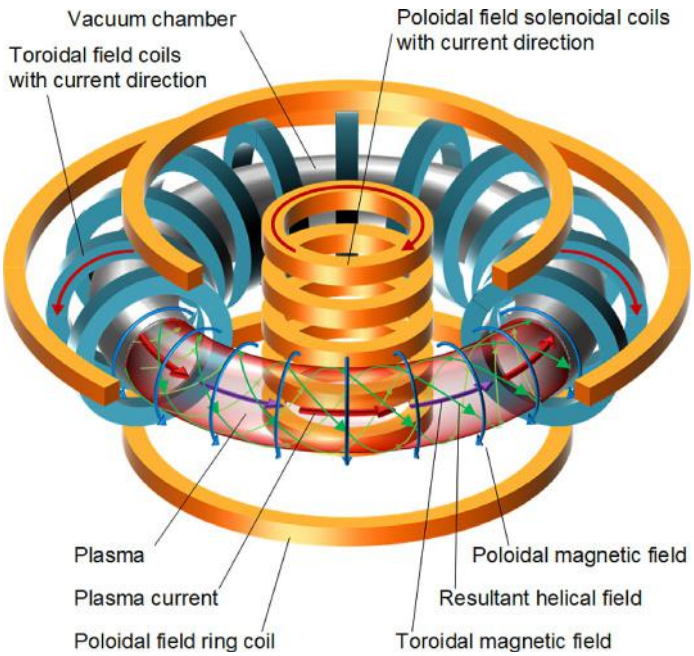

FIG. 26.3

Tokamak magnetic plasma confinement. The toroidal magnetic fields provide most of the plasma containment. The poloidal field coils induce a toroidal current through the plasma thereby creating a weaker poloidal magnetic field. A helical magnetic field results from the superposition of the two fields.

Plasmas of MCF machines must be heated to reach the necessary high temperature. Various methods have been devised to supply the thermal energy. The first method, used by the tokamak, is resistance (ohmic) heating. A changing current in the coils surrounding the torus induces a current in the plasma. The power associated with a current I through a resistance R is I^2R. The resistivity of a "clean" hydrogen plasma, one with no impurity atoms, is comparable to that of copper. Impurities increase the resistivity by a factor of four or more. There is a limit set by stability on the amount of ohmic heating possible.

The second method of heating is neutral particle injection. The sequence of events is as follows: (1) a gas composed of hydrogen isotopes is ionized by an electron stream; (2) the ions of hydrogen and deuterium produced in the source are accelerated to high speed through a vacuum chamber by a voltage of approximately 100 kV; (3) the ions pass through deuterium gas and by charge exchange are converted into directed neutral atoms; and (4) the residual slow ions are drawn off magnetically, whereas the neutralized ions cross the magnetic field lines freely to deliver energy to the plasma.

The third method uses microwaves in a manner similar to their application to cooking. The energy supply is a radiofrequency (RF) generator. It is connected by a transmission line to an antenna next to the plasma chamber. The waves enter the chamber and die out there, delivering energy to the charges. If the frequency is right, resonant coupling to natural circular motions of electrons or ions can be achieved. The phrase electron (or ion) cyclotron radiofrequency, ECRF (or ICRF), comes from the angular frequency of a charge q with mass m in a magnetic field B, proportional to qB/m, as discussed in Section 9.1.

Because the fusion reactions burn the deuterium-tritium fuel, new fuel must be introduced to the plasma as a puff of gas, as a stream of ions, or as particles of liquid or solid. The last method seems best, despite the tendency for the hot plasma to destroy the pellet before it gets far into the discharge. It seems that particles that come off the pellet surface form a protective cloud. Millimeter-sized cryogenic hydrogen pellets moving at several hundred meters per second are injected at a rate of about 30 per second (Combs and Baylor, 2018).

The mathematical theory of electromagnetism is used to deduce the magnetic field shape that gives a stable arrangement of electric charges. However, any disturbance can change the fields and in turn affect the charge motion, resulting in an instability that may disrupt the field configuration. The analysis of such behavior is more complicated than that of ordinary fluid flow because of the presence of charges. In a liquid or gas, the onset of turbulence occurs at a certain value of the Reynolds number. In a plasma with its electric and magnetic fields, many additional dimensionless numbers are needed, such as the ratio of plasma pressure to magnetic pressure (β) and ratios to the plasma size of the mean free path, the ion orbits, and the Debye length (a measure of electric field penetration into a cloud of charges). Several of the instabilities such as the "kink" and the "sausage" are well understood and can be corrected by assuring certain conditions.

Stability of the plasma is not sufficient to assure a practical fusion reactor because of various materials engineering problems. The lining of the vacuum chamber containing the plasma is subjected to radiation damage by the 14-MeV neutrons from the D-T reaction. Also, when the plasma is disrupted, the electric forces cause runaway electrons to bombard the chamber wall, generating large amounts of heat. Materials will be selected to minimize the effects on what are called plasma-facing components and reduce the replacement frequency. An example is a graphite fiber composite similar to those that were used to protect the surface of the space shuttle on reentry. Other possible wall materials are silicon carbide, beryllium, tungsten, and zirconium (with the latter metals possibly enriched in an isotope that

does not absorb neutrons). Some self-protection of the chamber lining is provided by vaporization of materials, with energy absorbed by a vapor shield.

The eventual practical fusion reactor will require a system to generate tritium. As an alternative to the use of liquid lithium in a breeding blanket, consideration is given to a molten salt—called *flibe*—composed of fluorine, lithium, and beryllium (Li_2BeF_4). The (n, 2n) reaction in Be would enhance the breeding of tritium. Another possibility is the use of the ceramic lithium oxide (Li_2O).

A number of tokamaks have been built at research facilities around the world. Prominent examples are:

(a) The Tokamak Fusion Test Reactor (TFTR) at Princeton, now shut down, which achieved very high plasma temperatures.

(b) The Joint European Torus (JET) at the Culham Centre for Fusion Energy at Abingdon, England, a cooperative venture of several countries that has used the D-T reaction. Fig. 26.4 shows the interior of JET with a person inside to provide scale. JET holds the world record for generating 16 MW of fusion power with a Q of 0.67.

(c) The Japan Torus-60 (JT-60 Upgrade) used to study plasma physics. The National Institute for Fusion Sciences also operates the Large Helical Device, a modern stellarator.

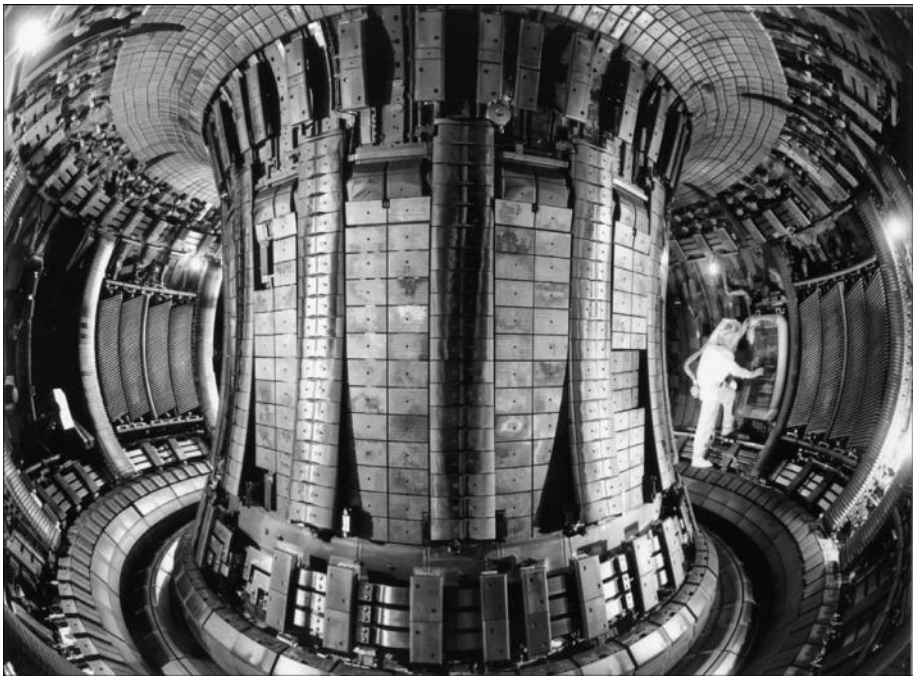

FIG. 26.4

Interior of tokamak fusion reactor Joint European Torus at Culham Centre for Fusion Energy.

Courtesy Joint European Torus.

(d) The DIII-D of General Atomic in San Diego is a modification of Doublet III. It involves science studies of turbulence, stability, and interactions, along with the role of the diverter, a magnetic method of removing debris from a fusion reaction.

(e) The Alcator C-Mod of the Massachusetts Institute of Technology (MIT), a compact machine with high general performance that shut down in 2016.

Concepts other than the tokamak have been studied. Princeton Plasma Physics Laboratory operates the National Spherical Torus Experiment Upgrade in which a hole passes through a spherical plasma. The National Compact Stellarator Experiment, in which the chamber is in the shape of a figure eight, was cancelled in 2008 by the Department of Energy. The Wendelstein 7-X, a large twisted-ring-shaped stellarator reactor at the Max Planck Institute in Germany, began operations in 2015.

26.4 INERTIAL CONFINEMENT MACHINES

Another approach to practical fusion is ICF, which uses very small pellets of a deuterium and tritium mixture as high-density gas or as ice. The pellets are heated by laser light or by high-speed particles. They act as miniature hydrogen bombs, exploding and delivering their energy to a wall and cooling medium. Fig. 26.5 shows a quarter coin with some of the spheres. Their diameter is approximately 0.3 mm. To cause the thermonuclear reaction, a large number of beams of laser light or ions are trained on a pellet from different directions. A pulse of energy of the order of a nanosecond is delivered by what is called the *driver*. The mechanism is believed to be as follows: the initial energy evaporates some material from the surface of the microsphere in a manner similar to the ablation of the surface of a spacecraft entering the Earth's atmosphere. The particles that are driven off form a plasma around the sphere that can absorb further energy. Electrons are conducted through the sphere to heat it and cause more ablation. As particles leave the surface, they impart a reaction momentum to the material inside the sphere, just as a space rocket is propelled by escaping gases. A shockwave moves inward, compressing the D-T mixture to many thousands of times normal density and temperature. At the center, a spark of energy of approximately 1 keV sets off the thermonuclear reaction. A burn front involving alpha particles moves outward, consuming the D-T fuel as it goes. Energy is shared by the neutrons, charged particles, and electromagnetic radiation, all of which will eventually be recovered as thermal energy. Consistent numbers are: 1 mg of D-T per pellet, 5 million joules driver energy, an energy gain (fusion to driver) of approximately 60, and a frequency of 10 bursts per second.

In an alternate indirect method of heating, laser lights or ions bombard the walls of a pellet cavity called a *hohlraum*, producing X-rays that drive the pellet target. One advantage besides high-energy efficiency is insensitivity to the focus of the illuminating radiation.

The energy released in the series of microexplosions is expected to be deposited in a layer of liquid such as lithium that is continuously circulated over the surface of the container and out to a heat exchanger. This isolation of the reaction from metal walls is expected to reduce the amount of material damage. Other candidate wall protectors are liquid lead and flibe. It may not be necessary to replace the walls frequently or to install special resistant coatings. Fig. 26.6 shows a schematic arrangement of a laser-fusion reactor.

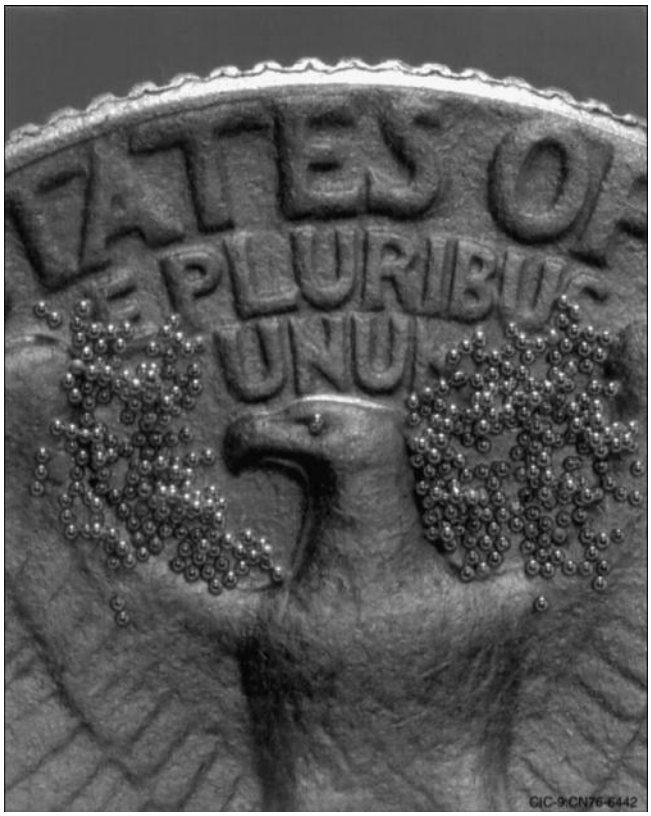

FIG. 26.5

Gold microshells containing high-pressure D-T gas for use in laser fusion.

Courtesy Los Alamos National Laboratory, No. CN 76-6442.

Research on ICF is carried out at several locations in the United States including:

(1) Lawrence Livermore National Laboratory (LLNL) operated Nova from 1985 to 1999. It used a neodymium-glass laser with 10 separate beams. Nova could deliver 40 kJ of 351-nm light in a 1-ns pulse. It was the first ICF machine to exceed the Lawson criterion. Experiments are discussed by Perry and Remington (1997). LLNL is also the site of the National Ignition Facility (NIF), which has a dual purpose. The first is to provide information on target physics for the US research program in ICF. The second is to simulate conditions in thermonuclear weapons as an alternative to underground testing of actual devices (also see Section 27.5). NIF focuses 192 beam lines on a target fuel capsule; see Fig. 26.7. The design permits either direct or indirect heating. One beam line called Beamlet was tested successfully, then transferred to Sandia National Laboratories.

(2) The University of Rochester's Laboratory for Laser Energetics (LLE) operates the facility OMEGA, which has had impressive success. Also, the effect on ICF of magnetic fields is being studied.

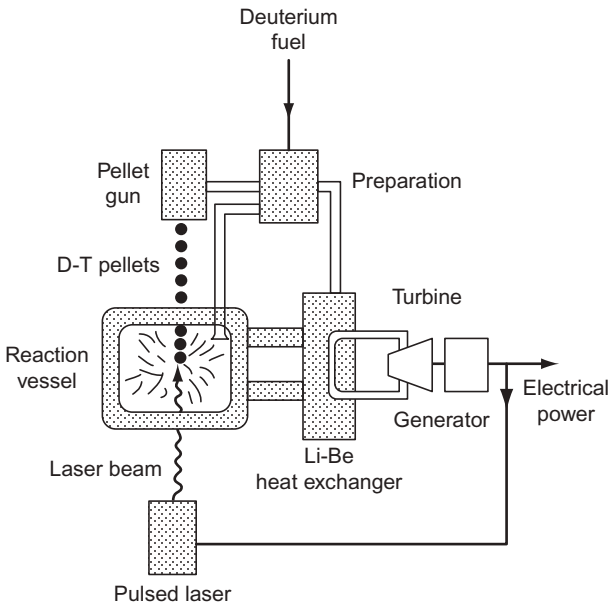

FIG. 26.6

Laser-fusion reactor.

(3) Sandia National Laboratories first demonstrated with its Particle Beam Fusion Accelerator (PBFA) that targets could be heated with a proton beam. The equipment was converted into the Z machine accelerator, which uses a pulse of current to create a powerful pinch effect (see Section 26.3). The energy from the electrical discharge goes into accelerating electrons that create X-rays that heat the D-T capsules. Power levels of over 300 trillion watts have been achieved (Jones et al., 2014).

A number of conceptual inertial fusion reactor designs have been developed by national laboratories, universities, and companies to highlight the need for research and development. These designs are intended to achieve power outputs comparable to those of fission reactors. They include both laser-driven and ion-driven devices. Examples are HIBALL-II (University of Wisconsin), HYLIFE-II and Cascade (Lawrence Livermore), Prometheus (McDonnell Douglas), and OSIRIS and SOMBRERO (W.J. Shafer). A considerable gap remains between performance required in these designs and that obtained in the laboratory to date.

26.5 OTHER FUSION CONCEPTS

Since 1950 when research on fusion was begun in earnest, there have been many ideas for processes and systems. One was the hybrid reactor with a fusion core producing 14-MeV neutrons that would be absorbed in a uranium or thorium blanket, producing new fissile material. It was proposed as a stepping stone to pure fusion, but seems unlikely to be considered.

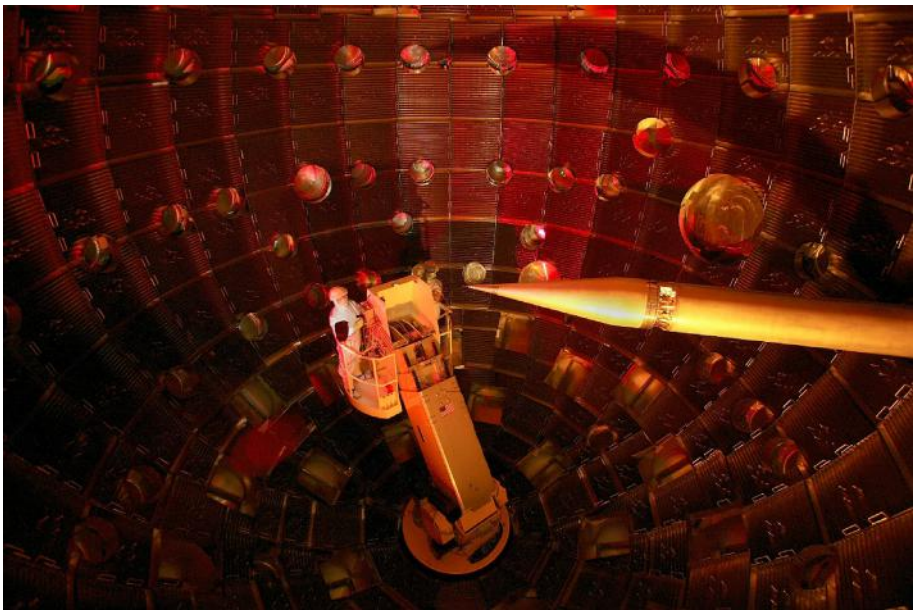

FIG. 26.7

Interior of the National Ignition Facility target chamber. The service module carrying technicians can be seen in the middle. The pencil-shaped target positioner is on the right.

Courtesy Lawrence Livermore National Laboratory.

Of the approximately 100 fusion reactions with light isotopes, some do not involve neutrons. If a neutron-free reaction could be harnessed, the problems of maintenance of activated equipment and disposal of radioactive waste could be eliminated. One example is proton bombardment of the abundant boron isotope, according to

$$ {}_1^1\mathrm{H} + {}_5^{11}\mathrm{B} \rightarrow 3{}_2^4\mathrm{He} + 8.68\,\mathrm{MeV} \tag{26.9} $$

Because $Z = 5$ for boron, the electrostatic repulsion of the reactants is five times as great as for the D-T reaction, resulting in a much lower cross-section. The temperature of the medium would have to be quite high. On the other hand, the elements are abundant and the B-11 isotope is the dominant one in boron.

EXAMPLE 26.3

The preceding reaction Q value is confirmed using Table A.5 data

$$ \begin{aligned} Q &= \Delta mc^2 = (m_{\mathrm{H}-1} + m_{\mathrm{B}-11} - 3m_{\mathrm{He}-4})c^2 \\ &= [1.007825 + 11.009305 - (3)(4.002603)](931.49) = 8.68\,\mathrm{MeV} \end{aligned} $$

The Coulombic threshold energy is

$$E_C = \frac{(1.2\text{MeV})Z_{H-1}Z_{B-11}}{A_{H-1}^{1/3} + A_{B-11}^{1/3}} = \frac{(1.2\text{MeV})(1)(5)}{(1)^{1/3} + (11)^{1/3}} = 1.86\text{MeV}$$

In comparison, Example 7.2 found an E_C of 0.44 MeV for the D-T reaction.

Another neutron-free reaction uses the rare isotope He-3,

$$^2_1\text{H} + ^3_2\text{He} \rightarrow ^4_2\text{He}(3.7\text{MeV}) + ^1_1\text{H}(14.7\text{MeV}) \tag{26.10}$$

The D-^{3}He electrostatic force is twice as great as the D-T force, but because the products of the reaction are both charged, energy recovery would be more favorable. The process might be operated in such a way that neutrons from the D-D reaction could be minimized. This would reduce neutron bombardment to the vacuum chamber walls. A D-^{3}He fusion reactor thus could use a permanent first wall, avoiding the need for frequent replacement and at the same time reducing greatly the radioactive waste production by neutron activation. Furthermore, advanced fuel cycles, such as those of D-^{3}He and p-^{11}B, rely upon naturally occurring isotopes.

The principal difficulty with use of the D-^{3}He reaction is the scarcity of ^{3}He. One source is the atmosphere, but helium is present only to 5 ppm by volume of air and the He-3 content is only two atoms per million of helium. Neutron bombardment of deuterium in a reactor is a preferable source. The decay of tritium in nuclear weapons could be a source of a few kilograms per year, but not enough to sustain an electrical power grid. Extraterrestrial sources are especially abundant but, of course, difficult to tap. Studies of moon rocks indicate that the lunar surface has a high ^{3}He content as the result of eons of bombardment by solar wind. Its ^{3}He concentration is 140 ppm in helium. It has been proposed that mining, refining, and isotope separation processes could be set up on the moon, with spacecraft transfer of equipment and product. The energy payback is estimated to be 250, and the total energy available is approximately 10^7 GWe y (Wittenberg et al., 1986). If affordable space travel is perfected, helium from the atmospheres of Jupiter and Saturn could be recovered in almost inexhaustible amounts.

A fusion process that is exotic physically but might be simple technically involves muons, negatively charged particles with mass 210 times that of the electron, and half-life 2.2 μs. Muons can substitute for electrons in the atoms of hydrogen but with orbits that are 210 times smaller than the normal 0.53×10^{-10} m (see Exercise 26.7). They can be produced by an accelerator and directed to a target consisting of a deuterium-tritium compound such as lithium hydride (LiH). The beam of muons interacts with deuterons and tritons, forming D-T molecules, with the muon, μ, playing the same role as an electron. However, the nuclei are now near enough together that some of them will fuse, releasing energy and allowing the muon to proceed to another molecule. Several hundred fusion events can take place before the muon decays. The system would appear not to need complicated electric and magnetic fields or large vacuum equipment. However, the muon-catalyzed fusion concept has not been tested sufficiently to be able to draw conclusions about its feasibility or practicality.

Fleischmann and Pons (1989) reported the startling news that they had achieved fusion at room temperature, a process termed *cold fusion*. The experiments received a great deal of media attention because if the phenomenon were real, practical fusion would be imminent. Their equipment consisted of a heavy water electrolytic cell with a cathode of metal palladium, which can absorb large amounts of hydrogen. They claimed that application of a voltage resulted in an enormous energy release. Attempts

by others to confirm the experiments failed, and cold fusion is not believed to exist. Under certain conditions, there may be a release of large amounts of stored chemical energy, and research on low-energy nuclear reactions is continuing.

A scientific breakthrough of which the effect is not yet determined is the discovery of materials that exhibit electrical superconductivity at relatively high temperatures, well above that of liquid helium. Fusion machines that use superconducting magnets will, at a minimum, be more energy efficient.

26.6 PROSPECTS FOR FUSION

Research on controlled thermonuclear processes has been underway for more than 50 years at several national laboratories, universities, and commercial organizations. The results of the studies include an improved understanding of the processes, the ability to calculate complex magnetic fields, the invention and testing of many devices and machines, and the collection of much experimental data. Over that period, there has been an approach to breakeven conditions, but progress has been painfully slow, spanning decades rather than years. Various reasons have been suggested for this. First, and probably most important, is the fact that fusion is an extremely complex process from both the scientific and engineering standpoints. Second are policy decisions (e.g., emphasis on fundamental plasma physics rather than building large machines to reveal the true dimensions of the problem). In the case of ICF, the US security classification related to weapons inhibited free international exchange of research information. Finally, funding allocations have been inconsistent.

Predictions have repeatedly been made that practical fusion was only 20 y away. Two events provide some encouragement that the elusive 20-y figure might be met. The first was the discovery of a new tokamak current. As noted earlier, current flow in the plasma is induced by the changing external magnetic field. Because that field cannot increase indefinitely, it would be necessary to shut down and start over. In 1971, it had been predicted that there was an additional current in a plasma, but not until 1989 was that verified in several tokamaks. That "bootstrap" current amounts to up to 80% of the total, such that its contribution would allow essentially continuous operation.

The second event was a breakthrough in late 1997 in fusion energy release. Most fusion research had been conducted with the D-D reaction rather than the D-T reaction, to avoid the complication of contamination of equipment by radioactive tritium. At the JET in England, tritium was injected as a neutral beam into a plasma. A series of records was set, ultimately giving 21 MJ of fusion energy, a peak power of 16 MW, and a ratio of fusion power to input power of 0.65. These results greatly exceeded those from D-D reactions.

In 1985, progress in tokamak performance over the years prompted planning for a large machine with the acronym ITER (originally denoting International Thermonuclear Experimental Reactor). Its objective is to demonstrate that fusion can be used to generate electrical power. Scientists will study conditions expected in a fusion power plant. Participants in the project are the European Union, Japan, China, India, South Korea, Russia, and the United States (which withdrew in 1999 but reentered in 2001). ITER is being built at Cadarache in the south of France, with leadership provided by Japan. On November 21, 2006, an agreement was signed that established the ITER International Organization.

The ITER D-T tokamak is expected to produce more power than it consumes, with a Q value greater than 10. Technologies being used include superconducting magnets, heat-resistant materials, remote

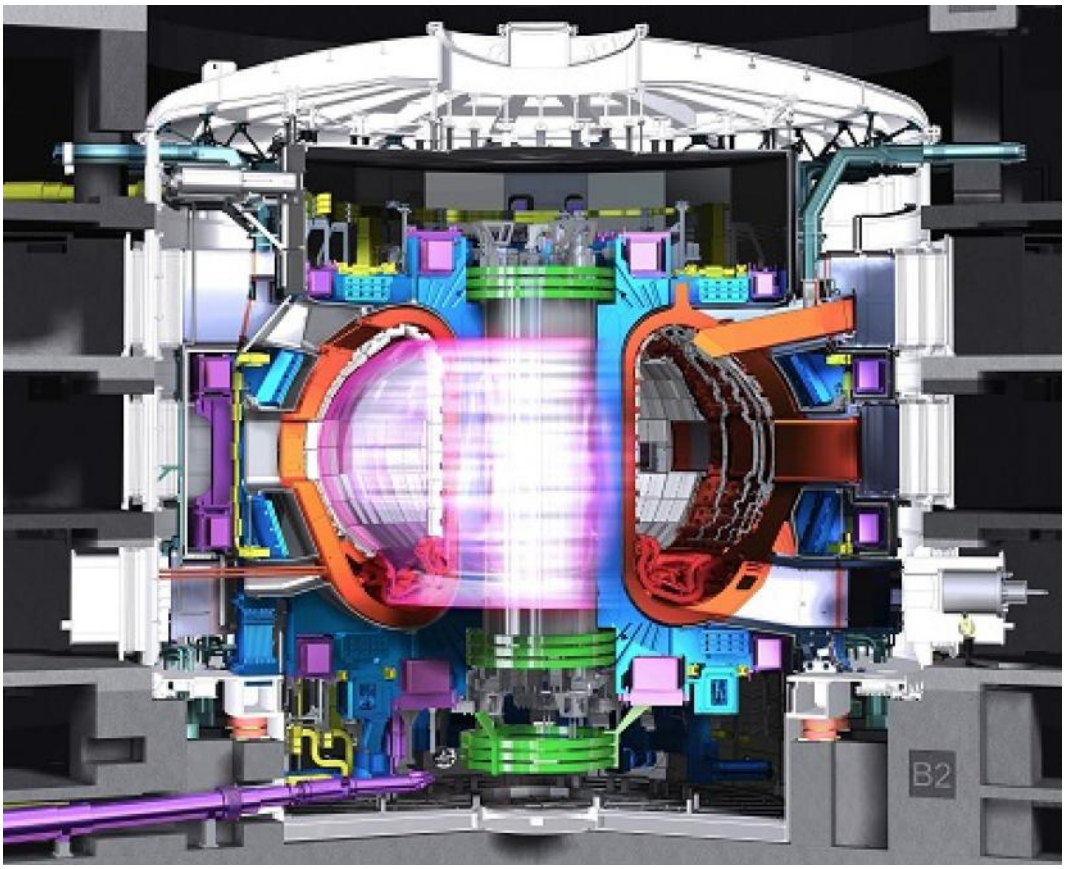

FIG. 26.8

ITER tokamak with its plasma.

Courtesy Credit © ITER Organization, http://www.iter.org/.

handling systems for radioactive components, and breeding of tritium from lithium. The design was completed in 2001; see Fig. 26.8. Some of the features are a large plasma volume of roughly elliptical shape, a blanket to absorb neutron energy, and a diverter to extract the energy of charged particles and the helium ash. Table 26.1 lists selected ITER parameters. The schedule calls for the first plasma by 2025 and an operating period for approximately 20 y. The construction cost is estimated to be 13 billion Euros (1 EUR ≅ 1.3 USD), with another 6 billion Euros over the 20 y.

DEMO is a proposed fusion power plant that follows ITER's expected success. It is intended to be comparable in output to current fission power plants, being able to make the tritium it needs.

Most of the R&D on magnetic fusion has been focused on the tokamak mode. There is a possibility that some magnetic confinement concept other than the tokamak will be used. The United States participates in and supports the ITER program but continues to explore other concepts. The Department of

Table 26.1 Selected ITER Design Specifications

Parameter	Value
Fusion power	500 MW
Burn time	≥400 s
Power gain (Q)	≥10
Plasma major and minor radii	6.2 and 2.0 m
Plasma current	15 MA
Toroidal magnetic field	5.3 T
Average 14-MeV neutron wall loading	≥0.5 MW/m^2

Data from Shimada, M., Campbell, D.J., Mukhovatov, V., Fujiwara, M., Kirneva, N., Lackner, K., et al., 2007. Chapter 1: Overview and summary. Nucl. Fusion 47 (6), S1–S17.

Energy's Fusion Energy Sciences Program provides research funds and receives recommendations from the Fusion Energy Sciences Advisory Committee (FESAC). Recently, various research teams have been pursuing approaches using compact fusion devices.

It seems that practical fusion reactors still will not be available soon unless there is an unanticipated breakthrough or a completely new idea arises that changes the prospects dramatically. There is yet much to understand about plasma processes and a great deal of time is required to carry out research, development, and testing of a system that will provide competitive electric power.

From time to time, the wisdom of pursuing a vigorous and expensive research program in controlled fusion has been questioned in light of the uncertainty of success in achieving affordable fusion power. An excellent answer is the statement attributed to Herman (1990), directed at the fusion pioneer Lyman Spitzer, "A fifty percent probability of getting a power source that would last a billion years is worth a great deal of enthusiasm."

26.7 SUMMARY

A fusion reactor, yet to be developed, would provide power that uses a controlled fusion reaction. Of the many possible nuclear reactions, the one that will probably be used first involves deuterium and tritium (produced by neutron absorption in lithium). A D-T reactor that yields net energy must exceed the ignition temperature of approximately 4.3 keV and have a product $n\tau$ above approximately 10^{14} s/cm^3, where n is the fuel particle number density and τ is the confinement time. Several experimental machines have been tested involving an electrical discharge (plasma) that is constrained by electric and magnetic fields. One promising fusion machine, the tokamak, achieves magnetic confinement in a doughnut-shaped structure. ITER is a large fusion facility being built in France by an international consortium. Research is also under way on inertial confinement in which laser beams or charged particle beams cause the explosion of miniature D-T pellets. Other possible concepts are a hybrid fission-fusion reactor and the use of neutron-free reactions.

26.8 EXERCISES

26.1 Noting that the radius of motion R of a particle of charge q and mass m in a magnetic field B is $R = mv/qB$ and that the kinetic energy of rotation in the x–y plane is $(1/2)mv^2 = kT$, find the radii of motion of electrons and deuterons if B is $10\,\text{Wb/m}^2$ and kT is 100 keV.

26.2 Show that the effective nuclear reaction for a fusion reactor that uses deuterium, tritium, and lithium-6 is

$$^{2}_{1}\text{H} + ^{6}_{3}\text{Li} \rightarrow 2\,^{4}_{2}\text{He} + 22.4\,\text{MeV}$$

26.3 Verify the statement that in the D-T reaction the ^{4}He particle will have 1/5 of the energy.

26.4 (a) Assuming that in the D-D fusion reaction the fuel consumption is 0.151 g/(MWt d) (Exercise 7.3), find the energy release in J/kg. By what factor is the value larger or smaller than that for fission? (b) If heavy water costs \$100/kg, what is the cost of deuterium per kilogram? (c) Noting $1\,\text{kWh} = 3.6 \times 10^6\,\text{J}$, find from (a) and (b) the thermal energy cost in ¢/kWh.

26.5 Confirm the Q value of -2.5 MeV for the ^{7}Li(n,nt) reaction.

26.6 For the D-^{3}He reaction, (a) calculate the overall threshold energy. Note that $Q = 18.35$ MeV from Eq. (7.4). (b) Compute the kinetic energies of the reaction products (see Example 4.3).

26.7 (a) With the formula for the radius of the smallest electron orbit in hydrogen,

$$R_1 = \frac{h^2 \varepsilon_0}{\pi m_e Z e^2} \tag{26.11}$$

and the basic constants in Table A.2, verify that R_1 is 0.529×10^{-10} m. (b) Show that the rest energy of the muon, 105.66 MeV, is approximately 207 times the rest energy of the electron. (c) What is the radius of the orbit of the muon about hydrogen in the muonium atom? (d) The lengths of the chemical bonds in H_2 and in other compounds formed from hydrogen isotopes are all approximately 0.74×10^{-10} m. Estimate the bond in molecules where the muon replaces the electron. (e) How does the distance in (d) compare with the radii of the nuclei of D and T (see Section 2.6)?

26.9 COMPUTER EXERCISE

26.A Computer program FUSION describes a collection of small modules that calculates certain parameters and functions required in the analysis of a plasma and a fusion reactor. Among the properties considered are the theoretical fusion reaction cross-sections, the Maxwellian distribution and characteristic velocities, the impact parameter for 90-degrees ion scattering, the Debye length, cyclotron and plasma frequencies, magnetic field parameters, and electrical and thermal conductivities. The filenames of the modules are MAXWELL, VELOCITY, DEBYE, IMPACT, RADIUS, MEANPATH, TRANSIT, and CROSSECT. Explore the modules with the menus provided and the sample input numbers.

REFERENCES

Azizov, E.A., 2012. Tokamaks: from A D Sakharov to the present (the 60-year history of tokamaks). Physics-Uspekhi 55 (2), 190–203.

Combs, S.K., Baylor, L.R., 2018. Pellet-injector technology—brief history and key developments in the last 25 years. Fusion Sci. Technol. 73 (4), 493–518.

Duderstadt, J.J., Moses, G.A., 1982. Inertial Confinement Fusion. Wiley, New York.

Fleischmann, M., Pons, S., 1989. Elecrtochemically induced nuclear fusion of deuterium. J. Electroanal. Chem. 261 (2), 301–308.

Gross, R.A., 1985. Fusion Energy. Wiley, New York.

Herman, R., 1990. Fusion: The Search for Endless Energy. Cambridge University Press, New York.

Johnson, G.W., Brown, H., 1958. Non-military uses of nuclear explosives. Sci. Am. 199 (6), 29–35.

Jones, M.C., Ampleford, D.J., Cuneo, M.E., Hohlfelder, R., Jennings, C.A., Johnson, D.W., et al., 2014. X-ray power and yield measurements at the refurbished Z machine. Rev. Sci. Instrum. 85(8)083501.

Lawson, J.D., 1957. Some criteria for a power producing thermonuclear reactor. Proc. Phys. Soc. B 70 (1), 6–10.

Perry, T., Remington, B., September 1997. Nova laser experiments and stockpile stewardship. Sci. Technol. Rev., 4–13. Lawrence Livermore National Laboratory.

Wittenberg, L.J., Santarius, J.F., Kulcinski, G.L., 1986. Lunar source of ^{3}He for commercial fusion power. Fusion Technol. 10 (2), 167–178.

FURTHER READING

El-Guebaly, L.A., 2009. History and evolution of fusion power plant studies: past, present, and future prospects. In: Aasen, A., Olsson, P. (Eds.), Nuclear Reactors, Nuclear Fusion and Fusion Engineering. Nova Science Publishers Inc., New York.

Fowler, T.K., 1997. The Fusion Quest. Johns Hopkins University Press, Baltimore, MD.

Greenspan, E., 1984. Fusion-fission hybrid reactors. Adv. Nucl. Sci. Technol. 16, 289–515.

Harms, A.A., Schoepf, K.F., Miley, G.H., Kingdon, D.R., 2000. Principles of Fusion Energy. World Scientific Co., Singapore.

International Thermonuclear Experimental Reactor (ITER), www.iter.org. Full description of the project and the device.

Joint European Torus (JET), www.euro-fusion.org/devices/jet/. Located in the UK.

Lawrence Livermore National Laboratory (LLNL), National ignition facility project. https://lasers.llnl.gov. Photos, videos, and explanations.

Lawrence Livermore National Laboratory (LLNL), Nova laser experiments and stockpile stewardship. https://www.llnl.gov/str/Remington.html. Relationship of NIF to weapons tests.

Lindl, J.D., 1998. Inertial Confinement Fusion: The Quest for Ignition and Energy Gain Using Indirect Drive. AIP Press, Springer-Verlag, New York.

McNally Jr., J.R., Rothe, K.E., Sharp, R.D., 1979. Fusion reactivity graphs and tables for charged particle reactions. ORNL/TM-6914.

National Compact Stellarator Experiment (NCSX), http://ncsx.pppl.gov.

National Spherical Torus Experiment Upgrade (NSTX-U), http://nstx-u.pppl.gov/.

Niu, K., 1989. Nuclear Fusion. Cambridge University Press, Cambridge.

Pfalzner, S., 2006. An Introduction to Inertial Confinement Fusion. Taylor & Francis and CRC Press, New York.

Raeder, J., Bunde, R., Danner, W., Klingelhofer, R., Lengyel, L., Leuterer, F., et al., 1986. Controlled Nuclear Fusion: Fundamentals of its Utilization for Energy Supply. Wiley, Chichester.

Sandia National Laboratories (SNL), Pulsed power technology. http://www.sandia.gov/pulsedpower.
Shimada, M., Campbell, D.J., Mukhovatov, V., Fujiwara, M., Kirneva, N., Lackner, K., et al., 2007. Chapter 1: Overview and summary. Nucl. Fusion 47 (6), S1–S17.
Stacey, W.M., 1984. Fusion: An Introduction to the Physics and Technology of Magnetic Confinement Fusion. Wiley, New York.
US Department of Energy (DOE), Office of science, fusion energy sciences. http://science.energy.gov/fes/.
Wesson, J., 2011. Tokamaks, fourth ed. Oxford University Press, Oxford.

CHAPTER

NUCLEAR WEAPONS 27

CHAPTER OUTLINE

The primary purpose of this book is to describe the peaceful and beneficial applications of nuclear energy. To attempt a discussion of the military uses is risky because of the emotional nature of the subject and the impossibility of doing justice to the complex problems involved. To neglect the subject, however, would be misleading, as if we wished to suggest that nuclear energy is entirely benign. Thus, we will review some important facts and ideas about nuclear explosions and their uses, with three objectives:

(1) Distinguish between nuclear power and nuclear weapons.
(2) Identify the technical aspects and strategic issues involved in the military use of nuclear processes.
(3) Indicate the continued need for control of nuclear materials.

We will describe nuclear explosions, nuclear weapons proliferation and safeguards, disarmament, and options for disposal of weapons material.

27.1 NUCLEAR POWER VERSUS NUCLEAR WEAPONS

In the minds of many people, there is no distinction between reactors and bombs, resulting in an inordinate fear of nuclear power. Others believe that the development of commercial nuclear power in countries abroad will lead to their achievement of nuclear weapons capability. Because of

Nuclear Energy. https://doi.org/10.1016/B978-0-12-812881-7.00027-7

these opinions, some even favor dismantling the domestic nuclear industry and prohibiting US commercial participation abroad.

Recalling some World War II history will help clarify the situation. The first nuclear reactor, built by Enrico Fermi's team in 1942, was intended to verify that a self-sustaining chain reaction was possible and also to test an apparatus that might generate plutonium for a powerful weapon (Smyth, 1945). The experiment served as a basis for the construction of plutonium *production reactors* at Hanford, Washington. These supplied material for the first atom bomb (Trinity) test at Alamogordo, New Mexico, and later for the bomb dropped on Nagasaki, Japan. Those water-cooled, graphite-moderated reactors generated heat but no electric power and were designed to favor the production of Pu-239. Later, heavy-water reactors at the Savannah River Plant in South Carolina produced plutonium for weapons.

Isotope separation production facilities at Oak Ridge during World War II yielded uranium enriched to approximately 93% U-235. The material, called oralloy, was fabricated into the bomb used at Hiroshima. Subsequently, enrichment facilities have been used to give the 3%–5% ^{235}U fuel for light-water *power reactors*. Such low-enrichment fuel can be made critical when formed into rods and moderated properly with water, but it cannot be used for construction of a nuclear weapon (OTA, 1977). If the fuel is inadequately cooled while in a reactor, fission heat can cause cladding damage and, under the worst conditions, fuel melting. The resultant chemical reaction with water bears no resemblance to a nuclear explosion. Therefore, it can be stated positively that a reactor cannot explode like a nuclear bomb.

The spent fuel in a reactor contains a great deal of U-238 as well as some U-235, Pu-239, Pu-240, and Pu-241, along with fission products (see Fig. 23.3). If this reactor-grade plutonium is chemically separated and made into a weapon, the presence of neutrons from the spontaneous fission of Pu-240 will encourage premature detonation and an inefficient explosion. For this reason, high-burnup spent fuel is a poor source of bomb material. A much more likely avenue to obtain weapons-grade plutonium is the dedicated research reactor, with low levels of neutron exposure to prevent Pu-240 buildup. Ahlswede and Kalinowski (2012) cite examples of this route being taken by India, Israel, North Korea, and Pakistan. Another favorable means is a specially designed isotope separation method to obtain nearly pure U-235.

Nevertheless, the nuclear fuel cycle utilizes technological approaches that can be employed similarly to produce nuclear weapon materials. Referring to Fig. 23.1, enrichment facilities may be configured to produce ^{235}U enrichments of greater than 5%, and purified plutonium could be diverted during the reprocessing step. While nuclear power reactors used for commercial electricity generation in the United States are legally prohibited (42 USC 2077), the Hanford N-reactor, which operated from 1963 to 1987, was a dual-purpose production-electricity generation facility. In addition, the Magnox reactors at Calder Hall in the United Kingdom produced both Pu and electricity.

27.2 NUCLEAR EXPLOSIVES

Security of information on the detailed construction of modern nuclear weapons has been maintained, and only a qualitative description is available to the public. We will draw on unclassified sources (Glasstone and Dolan, 1977; Rhodes, 1986; Serber, 1992) for the following discussion of the earliest versions.

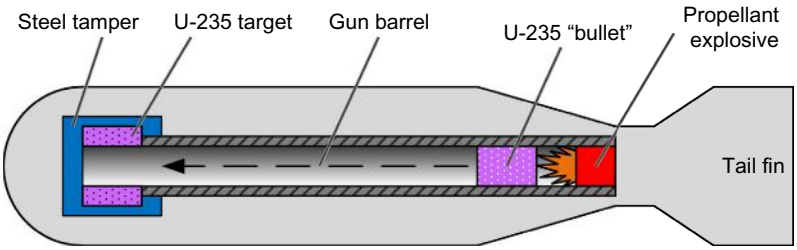

FIG. 27.1

Little Boy, gun-type uranium fission nuclear weapon.

First, we note that two types of devices have been used: (1) the fission explosive (atom bomb) that uses plutonium or highly enriched uranium, and (2) the fusion or thermonuclear explosive (hydrogen bomb). The reactions described in earlier chapters are involved. Next, it is possible to create an explosive fission chain reaction by two different procedures: either by the gun technique or by implosion. Fig. 27.1 simplifies the gun system, in which a plug of highly enriched uranium (HEU) is fired into a cylinder of uranium to produce a supercritical mass. A *tamper* holds the combined materials together momentarily. The first gun-type atom bomb, given the name Little Boy, was about 10.5 ft long (3.2 m) and 2.4 ft (73 cm) in diameter, and weighed 9700 lb (4400 kg) (Cox, 1999). The gun technique is not feasible for a weapon that uses plutonium. Spontaneous fission of Pu-240 would release neutrons that would trigger a premature ineffective explosion. Fig. 27.2 shows the alternative, the implosion method, in which chemical high explosives in the form of lenses compress a plutonium metal sphere to supercriticality. A tamper of heavy material is used. The first version of this weapon type used in war was called Fat Man.

In either of these devices, an initial supply of neutrons is required. One possibility is the polonium-beryllium source, with the (α, n) reaction, analogous to Rutherford's experiment (Section 4.1)

$$\begin{aligned} {}^{210}_{84}\mathrm{Po} &\xrightarrow{138.4\,\mathrm{d}} {}^{206}_{82}\mathrm{Pb} + {}^{4}_{2}\alpha \\ {}^{4}_{2}\alpha + {}^{9}_{4}\mathrm{Be} &\rightarrow {}^{12}_{6}\mathrm{C} + {}^{1}_{0}\mathrm{n} \end{aligned} \tag{27.1}$$

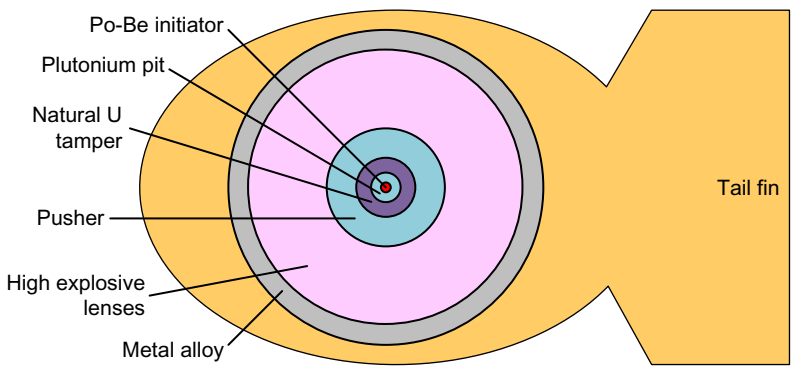

FIG. 27.2

Fat Man, implosion-type plutonium fission nuclear weapon.

The excess reactivity of the supercritical masses causes a rapid increase in power and the accumulated energy blows the material apart, a process labeled *disassembly*. In the case of implosion, when the fissile material is compressed, there is an increase in ratio of surface to volume that results in larger neutron leakage but a decrease in mean free path that reduces leakage. The latter effect dominates, giving a net positive increase of multiplication.

According to report ANL-5800 (ANL, 1963), an unreflected spherical plutonium assembly has a critical mass of approximately 16 kg, whereas that of a highly enriched (93.5%) uranium sphere is approximately 49 kg. By adding a 2.54-cm layer of natural uranium as a reflector, the critical masses drop to 10 kg and 31 kg, respectively. The critical mass of uranium with full reflector varies rapidly with the U-235 enrichment, as shown in Table 27.1. It is noted that the total mass of a device composed of less than 10% U-235 is impractically large for a weapon.

An appreciation of the effect on critical mass of an implosion that increases uranium density can be gained by the study of Computer Exercise 27.A.

Details of the compact and versatile modern thermonuclear weapons are not available, but we can describe the processes involved in the first hydrogen bomb explosion, the Ivy/Mike shot in the South Pacific in 1952. It included heavy hydrogen as fusion fuel, involving the two reactions also to be used in fusion reactors,

$$\begin{aligned} {}^{2}_{1}\mathrm{H} + {}^{2}_{1}\mathrm{H} &\rightarrow {}^{3}_{1}\mathrm{H} + {}^{1}_{1}\mathrm{H} \quad \text{or} \quad {}^{3}_{2}\mathrm{He} + {}^{1}_{0}\mathrm{n} \\ {}^{2}_{1}\mathrm{H} + {}^{3}_{1}\mathrm{H} &\rightarrow {}^{4}_{2}\mathrm{He} + {}^{1}_{0}\mathrm{n} \end{aligned} \tag{27.2}$$

The following description is an abbreviation of that found in the book *Dark Sun* (Rhodes, 1995). As shown in Fig. 27.3, the unit called Sausage was a hollow steel cylinder 20 ft (6 m) long and 6 ft 8 in. (2 m) diameter. The cavity was lined with lead. At one end of the cavity was a *primary* sphere of plutonium and enriched uranium that would be caused to fission by implosion. In the middle of the cavity was a cylindrical container of liquid deuterium, much like a large Thermos bottle. Along its axis was a stick of Pu called the sparkplug, which served as a *secondary* fission source. The deuterium container was surrounded by a natural U pusher. Finally, the inside of the casing was lined with polyethylene.

The sequence of events was as follows. An electrical discharge to detonators set off the high-explosive shell of the primary. A uranium tamper and shell vaporized and compressed the central plutonium ball while setting off a Po-Be source inside, releasing neutrons. X-rays from the resulting supercritical fireball heated the polyethylene to a plasma that reradiated X-rays to heat the U pusher. Neutrons and energetic alpha particles were released in the heated deuterium and fission took place in the sparkplug. Some tritium was formed, which contributed to the fusion reaction. Additional energy and radiation came from fast neutron fission in the U-238 in the tamper. The resultant explosion created a crater 200 ft (60 m) deep and 1 mile (1.6 km) across.

Table 27.1 Fully Reflected Critical Masses of U-235 and U Versus Enrichment

% U-235	U-235 (kg)	U (kg)
100	15	15
50	25	50
20	50	250
10	130	1300

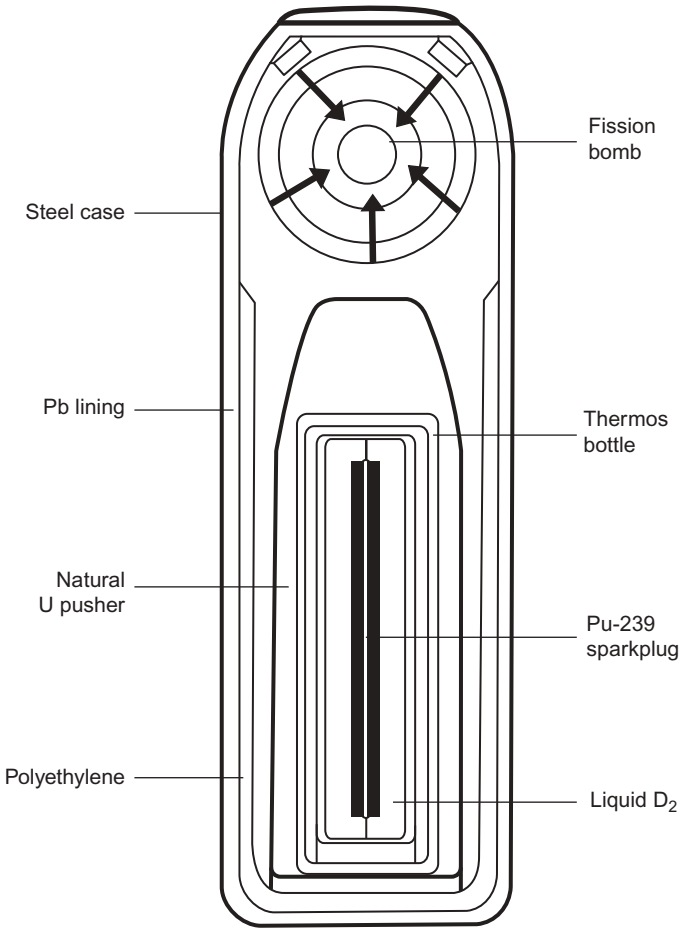

FIG. 27.3

Thermonuclear weapon.

Modified from Rhodes, R., 1995. Dark Sun: The Making of the Hydrogen Bomb. Simon & Schuster, New York. Highly readable political and technical aspects; role of espionage; diagrams of H-bomb explosion on p. 506.

In later weapon versions, the fusion component was composed of lithium deuteride (LiD). Neutrons from fission interact with the Li-6 according to

$$^{6}_{3}\mathrm{Li} + ^{1}_{0}\mathrm{n} \rightarrow ^{3}_{1}\mathrm{H} + ^{4}_{2}\mathrm{He} + 4.8\,\mathrm{MeV} \tag{27.3}$$

The tritium produced allows for the D-T reaction to occur. Other thermonuclear devices used tritium as the principal explosive material. To increase the yield from the primary, a technique called boosting may be employed to inject a D-T gas mixture.

Special designs of devices have been mentioned in the literature. Included is the *neutron bomb*, a small thermonuclear warhead for missiles and artillery shells (Kaplan, 1978). Used as a battlefield weapon, it would have little blast effect but would provide lethal neutron doses. The development and deployment of this enhanced radiation weapon was controversial.

By special arrangements of material in the fusion bomb, certain types of radiation can be accentuated and directed toward a chosen target. Examples of third-generation nuclear weapons could yield large quantities of lethal gamma rays or electromagnetic pulses (EMP) that disrupt solid-state electronic circuits. More detailed diagrams and descriptions of fission and fusion bombs are found in the book by Hansen (1988).

27.3 NUCLEAR WEAPON EFFECTS

Nuclear explosives release their energy in several ways. First is the blast effect, in which a shockwave moves outward in air, water, or rock, depending on where the event occurs. Second is the thermal radiation from the heated surrounding material, at temperatures of typically 6000°C. Finally, there is the nuclear radiation, consisting mainly of neutrons and gamma rays. The approximate distribution of the energy that goes into these three modes are, respectively, 50%, 35%, and 15% for the air burst of a fission weapon at an altitude below 40,000 ft (12,000 m) (Glasstone and Dolan, 1977). The initial and residual nuclear radiation comprise about 5% and 10% of the device's total energy output.

The device yield is based upon the initial energy release. The energy yield of a weapon is measured in equivalent tons of chemical explosive. By convention, 1 tonne of TNT (trinitrotoluene) corresponds to 10^9 calories of energy. Detonated on July 16, 1945, the first atom bomb, Trinity, had a strength of 21,000 tonnes (Loeber, 2005). A smaller device of 3.1 kilotonnes (kt) was exploded 1184 ft (361 m) underground in the Gnome test (Lawson, 1963). A large cavity was created, as shown in Fig. 27.4. The Ivy/Mike explosion gave 10.4 megatonnes. Tests of 50-megatonne devices have been reported. The energy of explosion is released in a very short time, on the order of a microsecond.

EXAMPLE 27.1

Determine the net number of neutrons and gammas emitted from a nuclear device with a 10-kt yield. Because the yield is based on prompt energy release of 180 MeV/fission, the detonation of ^{235}U requires

$$R_f = \frac{(10^4\,\text{tonne})(10^9\,\text{cal/tonne})(4.184\,\text{J/cal})}{(180\,\text{MeV/fission})(1.602\times10^{-13}\,\text{J/MeV})} = 1.45\times10^{24}\,\text{fissions}$$

Each fission releases ν neutrons but one of these is required to promote the chain reaction, and according to Section 6.3, about seven 1-MeV prompt gamma rays are released per fission event.

The use of weapons of mass destruction inflicts a substantial human toll, as shown in Table 27.2. Casualties are due to thermal (burns), mechanical (blast), and ionizing radiation effects. Roughly half the Japanese fatalities were due to burns. As seen in Fig. 27.5, dark colored fabric tended to transmit the thermal radiation, whereas light colored clothing provided a degree of protection by reflection of the radiant heat. The United Nations (UN, 1980) defines weapons of mass destruction (WMDs) as "atomic

FIG. 27.4

Underground cavity created by the Project Gnome fusion explosion, part of the Plowshare program. Note the person standing near the center.

Courtesy US Department of Energy.

Table 27.2 Fission Bombs Used in Wartime

Bomb Name	Little Boy	Fat Man
Device type	U-235 gun	Pu-239 implosion
Yield[a]	16 kt	21 kt
Target	Hiroshima	Nagasaki
Date of explosion	August 6, 1945	August 9, 1945
Civilian population[b]	256,300	173,800
Civilian casualties[b]		
Dead	68,000	38,000
Injured	76,000	21,000

[a]*Data source: Kerr et al. (2005)*
[b]*Data source: Glasstone and Dolan (1977).*

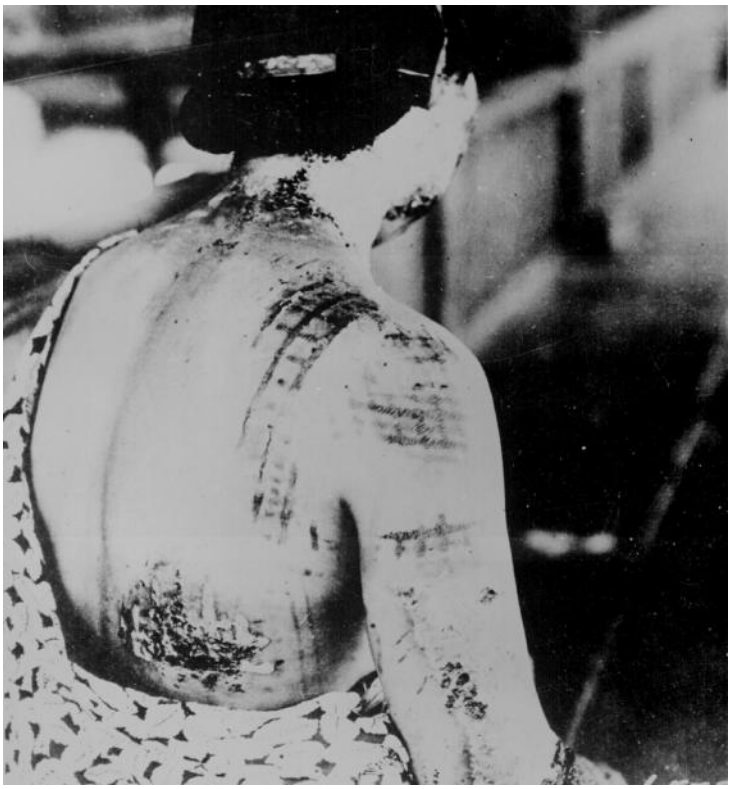

FIG. 27.5

An atomic bomb survivor's skin is burned in a pattern corresponding to the dark portions of a kimono worn at the time of the explosion.

Courtesy National Archives 77-MDH-6.55b.

explosive weapons, radioactive material weapons, lethal chemical and biological weapons and any weapons developed in the future which might have characteristics comparable in destructive effect to those of atomic bomb or other weapons mentioned above."

The immediate radiation effect of a nuclear explosion is extremely severe at distances up to a few kilometers. Table 27.3 shows the distances at which a neutron dose of 500 rem (5 Sv) is received for different yields. In addition to the initial X-rays, gamma rays, and neutrons, there is a great deal of radioactive fallout contamination (residual radiation) from fission products and neutron-induced activation products. Besides the early casualties, ionizing radiation has the potential to cause both deterministic and stochastic long-term effects. The late effects include cataracts, leukemia, and other cancers. The Radiation Effects Research Foundation studies health effects on the Japanese atomic bomb survivors (Cullings, 2014).

Table 27.3 Distance-Yield Conditions for 500 rem Exposure From a Nuclear Explosion

Yield (tonnes)	Radius (m)
1	120
100	450
10,000	1050
1,000,000	2000

EXAMPLE 27.2

Estimate the prompt gamma-ray fluence 1 km from a ground-level 10-kt explosion. If air attenuation is ignored, the simple point source model of Eq. (11.6) gives

$$\Phi_\gamma = \frac{S}{4\pi r^2} = \frac{(7\gamma/\text{fission})(1.45\times10^{24}\,\text{fissions})}{4\pi(10^5\,\text{cm})^2} = 8.1\times10^{13}\,\gamma/\text{cm}^2$$

Inclusion of air attenuation (Exercise 27.6) reduces the fluence to $3.8\times10^{10}\,\gamma/\text{cm}^2$. Glasstone and Dolan (1977) note that the secondary gamma rays produced by neutron interactions in air and the gamma rays from fission products deliver the bulk of the initial dose at such a distance.

A consequence of a major exchange of nuclear missiles near the Earth's surface would be an increase in the particles suspended in air. Part would be dust created by the blast; part would be smoke from fires in forests and other combustibles ignited by the heat. As a result, the amount of sunlight reaching the ground would be reduced, causing cooling of the atmosphere (National Research Council, 1985). The condition has been called *nuclear winter* by some investigators, who predict serious modification of the climate with a reduction in agricultural production. Such an effect occurred in the early 1800s primarily as the result of the volcanic eruption of Mount Tambora. The subject of atmospheric cooling has been studied a great deal, but scientists disagree as to the magnitude of the effect. The original theory was criticized for failure to take proper account of self-correcting processes, including increased precipitation that would tend to dispel dust and smoke.

27.4 THE PREVENTION OF NUCLEAR WAR

The nuclear arms race between the United States and the former USSR (Union of Soviet Socialist Republics) that began after World War II was stimulated by mutual suspicion and fear and by technological advances in nuclear weapons. Each of the superpowers sought to match and to exceed the other's military capability.

As of 1945, the United States clearly had nuclear weapons superiority, but by 1949, the USSR had acquired its own atom bomb. After considerable controversy, the United States undertook to develop the hydrogen bomb (Super bomb, or Super) by use of thermonuclear fusion and by 1952 had restored the advantage. By 1953, the Soviets had again caught up. In the ensuing years, each country produced

very large numbers of nuclear weapons. If deployed by both sides in an all-out war, with both military and civilian targets, hundreds of millions of people would die.

The policy adopted by the two powers to prevent such a tragedy was deterrence, which means that each country maintains sufficient strength to retaliate and ruin the country that might start a nuclear war. The resultant stalemate is given the term mutual assured destruction (MAD, a fitting acronym). This balance of terror could be maintained unless one country developed an excessive number of very accurate missiles and chose to make a first strike that disables all retaliatory capability.

The methods by which nuclear warheads can be delivered are: (1) carried by bombers, such as the US B-2 and B-52; (2) intercontinental ballistic missiles (ICBMs) launched from land bases; and (3) missiles launched from submarines.

The ICBM is propelled by rocket but experiences free flight under the force of gravity in the upper atmosphere. The nuclear warhead is carried by a reentry vehicle. The ICBM may carry several warheads (MIRV, multiple independently targetable reentry vehicles), each with a different destination.

An alternative is the cruise missile, an unmanned jet aircraft. It can hug the ground, guided by observations along the way and by comparison with built-in maps and GPS (global positioning satellite) telemetry, and maintain altitude by computer control (Tsipis, 1977).

There are two uses of nuclear weapons. One is *tactical*, whereby limited and specific military targets are bombed. The other is *strategic*, involving large-scale bombing of both cities and industrial sites with intent both to destroy and to demoralize. Most people fear that any tactical use would escalate into strategic use.

Thousands of nuclear warheads have been available to the superpowers for many years, with the number of megatonnes of equivalent TNT per weapon ranging from 0.02 to 20. The area that could be destroyed by all these weapons is approximately 750,000 km^2, disrupting each country's functions such as manufacturing, transportation, food production, and healthcare. A civil defense program would reduce the hazard but is viewed by some as tending to invite attack.

The international aspect of nuclear weapons first appeared in World War II when the Allies believed that Germany was well on its way to producing an atomic bomb. The use of two weapons by the United States to destroy the cities of Hiroshima and Nagasaki in 1945 alerted the world to the consequences of nuclear warfare. Many years have been devoted to seeking bilateral or international agreements or treaties that seek to reduce the potential hazard to humanity. The increase in fallout from nuclear weapons testing prompted the Limited Test Ban Treaty (LTBT), first signed by the United States, the USSR, and the United Kingdom in 1963. The LTBT forbade nuclear tests in the atmosphere, underwater, or outer space, and the parties thereafter conducted all testing underground. However, this treaty did not control the expansion in nuclear arms.

In 1968, an international agreement, referred to as the Nonproliferation Treaty (NPT), was developed at Geneva. Taking effect in 1970, the NPT's goals included stopping the spread of nuclear weapons while permitting the transfer of peaceful nuclear energy technologies. The treaty is somewhat controversial in that it recognized as nuclear weapon states (NWS) the existing five nations (China, France, Russia, the United Kingdom, and the United States) which had prior to 1967 tested nuclear devices while the remaining countries were termed non-NWS (NNWS). The main articles of the treaty require that each of the latter would agree (1) to refrain from acquiring nuclear weapons or from producing them and (2) to accept safeguards set by the International Atomic Energy Agency (IAEA) based in Vienna. The treaty involves an intimate relationship between technology and politics on a global scale and a degree of cooperation hitherto not realized. There are certain ambiguities in the treaty.

No mention is made of military uses of nuclear processes as in submarine propulsion or of the use of nuclear explosives for engineering projects. Penalties to be imposed for noncompliance are not specified, and finally the authority of the IAEA is not clear. The treaty has been signed by the five NWS and almost 200 NNWS. Notable holdouts to signing include India, Israel, and Pakistan, who are all known or believed to have nuclear weapons. In 1995, the NPT was extended indefinitely. North Korea was a signatory, but withdrew in 2003 as the first nation to ever do so.

The NWS can withhold information and facilities from the NNWS and thus slow or deter proliferation. To do so, however, implies a lack of trust of the potential recipient. The NNWS can easily cite examples to show how unreliable the NWS are. For instance, the NPT calls for complete nuclear disarmament.

We have already discussed in Section 23.5 the attempt by US President Jimmy Carter to inhibit proliferation. By banning commercial spent fuel reprocessing in the United States, he had hoped to discourage its use abroad. Export controls restrict the sale to foreign countries of sensitive equipment and materials, so-called dual-use technologies that are adaptable for manufacture of nuclear weapons. If the regulations are extended to the transfer of legitimate nuclear power technology, however, such prohibitions can be counterproductive for several reasons. International relations suffer, and the United States loses any influence it might have on nuclear programs. Perceived inequity may strengthen a country's determination to achieve weapons capability and to seek alternative alliances that further that goal.

Negotiations between the United States and USSR began in 1969 on Strategic Arms Limitation Talks (SALT) and an accord was signed in 1972. SALT I led to a ceiling on strategic nuclear weapons and thus tended to achieve equality in strength. However, it said nothing about continued improvements in missiles. It restricted the deployment of antiballistic missile (ABM) defense systems, with each nation allowed to defend its capital and one other location.

The SALT II agreement between leaders of the two nations in 1979 dealt with detailed limits on types of launchers and missiles, including the MIRV type. It placed emphasis on preserving the ability of both sides to verify compliance. The US Congress never ratified the treaty, and talks were not resumed.

In 1983, US President Ronald Reagan initiated a program of detection and interception of nuclear missiles. This research and development effort was called the Strategic Defense Initiative (SDI) but soon became known popularly as "Star Wars" because of its space implications. In this multibillion dollar project, various devices were proposed and studied, including Earth satellite weapons platforms, X-ray laser beams, small tactical nuclear bombs, and smart pebbles, small high-speed objects that could destroy incoming missiles. The SDI program was controversial for technical reasons having to do with feasibility and political reasons related to the wisdom of mounting the program. Some believe, however, that it had a favorable influence on the achievement of an end to the Cold War in 1991.

Negotiations continued over the years, leading to the Intermediate-Range Nuclear Force Treaty (INF) of 1988, in which a number of missiles were destroyed in the United States and the USSR, with inspection teams from the other country functioning smoothly. Two new sets of bilateral accords called Strategic Arms Reduction Talks (START) were developed in the Reagan-Bush era. The use of the word "reduction" instead of "limitation" is significant. By 2001 the START I treaty reduced the number of nuclear warheads from 10,000 to 6000 in each country. The START II, which dealt with intercontinental missiles and MIRVs, called for the reduction of strategic warheads, but the treaty never entered into force. Further progress in disarmament was made in 2003 with the ratification by Russia and the

United States of the Strategic Offensive Reduction Treaty (SORT), which called for a level of 1700–2200 warheads by the end of 2012. New START, ratified in 2011, required the number of warheads to be reduced to 1550 by February 2018.

With progress in arms reduction, the Star Wars program became less relevant and was greatly scaled down. The elimination of thousands of warheads was an important step in terms of world safety, but there still remain enough weapons for mutual destruction. The breakup of the Soviet Union left ICBMs in the independent states of Ukraine, Belarus, and Kazakhstan, but agreement was reached to transfer the weapons to Russia. Internal economic, political, and ethnic tensions make control difficult. Concern has also been expressed that weapons scientists and engineers of the former USSR may be induced for economic reasons to emigrate to nations seeking nuclear capability (e.g., Iran and North Korea).

US legislation called Cooperative Threat Reduction (CTR) provided funding and expertise to help Russia control nuclear weapons. Also known as the Nunn-Lugar-Domenici Act, after the senators who authored it, the program was designed to account for weapons, to secure them, and to arrange for disposition. Of special importance was provision for the employment elsewhere of thousands of former weapons experts. Accomplishments included deactivation of some 7610 warheads and the elimination of about 300 tonnes of highly enriched uranium.

Another byproduct of the international political changes was the purchase by the United States from Russia of highly enriched uranium (HEU) from dismantled nuclear weapons to be converted by blending into low-enriched uranium (LEU) for use in power reactors. The program, called "megatons to megawatts," transferred a total of 500 metric tons of HEU. The LEU at 4.5% enrichment was sent by the Russian firm TENEX and received by the United States Enrichment Corporation. The project was completed in December 2013 with about 20,000 warheads having been eliminated permanently. Several virtues accrued: financial benefit to Russia, diversion of weapons grade material to peaceful purposes, and relief from the necessity by the United States to expand isotope separation capability.

The program also included downblending of part of the US stockpile of HEU. A large quantity of the high-enriched uranium (160 tonnes) from the US weapons is slated to be diverted to naval ship reactors. Another 20 tonnes is to be blended with natural uranium to a concentration appropriate for commercial power reactors. An additional 20 tonnes will be held for space and research reactor fueling. All these actions under the Department of Energy (DOE) National Nuclear Safety Administration (NNSA) will render the HEU less accessible to terrorists. The NNSA also partners internationally to remove or dispose of excess HEU and separated plutonium, for instance, the conversion of research reactors using HEU fuel to low enrichment uranium.

EXAMPLE 27.3

Consider the downblending of 10 tonnes of oralloy with 0.2 w/o uranium enrichment tails to form 5 w/o reactor grade uranium. We can determine the input tails needed and output product masses using a material balance similar to that of Section 15.4. The HEU m_o and tails m_t masses must equal the product mass

$$m_p = m_o + m_t$$

and likewise the U-235 input and output masses are equivalent

$$x_p m_p = x_o m_o + x_t m_t$$

where x is the mass fraction of U-235 in the particular material flow.

Substituting numerical values into the preceding expressions gives

$$m_p = 10\,\text{tonne} + m_t$$

$$0.05\,m_p = 0.93\,(10\,\text{tonne}) + 0.002\,m_t$$

Solving these simultaneous equations reveals that m_t and m_p are 183 and 193 tonnes, respectively. Thus, a significant amount of reactor fuel can be manufactured from downblending weapons grade material. Computer Exercise 27.B considers not only the arithmetic of the process by which HEU is diluted into reactor grade uranium, but also investigates cost aspects of a purchase from Russia by the United States.

An agreement between the United States and Russia was reached in 2006 for each to convert 34 metric tons of excess weapons-grade plutonium into unusable forms. The United States is constructing a mixed oxide (MOX) fuel fabrication facility at the Savannah River Site to produce fuel for power reactors. The MOX fuel is to be approximately 5% PuO_2 and 95% depleted UO_2. Although the construction is more than half finished, cost overruns seem to have doomed completion of the facility. Alternatively, the plutonium can be diluted and disposed of in the Waste Isolation Pilot Plant. Russia plans to use the breeder reactors at Beloyarsk (see Section 25.3) for plutonium disposal.

Although treaties aid in the reduction of possible nuclear war, inevitably human decisions weigh heavily. The conduct of Stanislav Petrov in 1983 epitomizes the impact that a sole human can have. As a Soviet lieutenant colonel, he judged correctly that the nuclear early-warning system had issued a false alarm (Mattern, 2007). This event earned him recognition as "the man who saved the world."

27.5 NONPROLIFERATION AND SAFEGUARDS

We now discuss proliferation of nuclear weapons and the search for means to prevent it. Reducing the spread of nuclear materials has become more important as the result of increases in political instability and acts of violence throughout the world. Kristensen and Norris (2017) estimated that there are nearly 15,000 nuclear weapons worldwide.

To prevent proliferation, we can visualize a great variety of technical modifications of the way nuclear materials are handled, but it is certain that a country that is determined to have a weapon can do so. We also can visualize the establishment of many political institutions such as treaties, agreements, central facilities, and inspection systems, but each of these is subject to circumvention or abrogation. It must be concluded that nonproliferation measures can merely reduce the chance of spread.

We now turn to the matter of employment of nuclear materials by organizations with revolutionary or criminal intent. One can define a spectrum of such, starting with a large well-organized political unit that seeks to overthrow the existing system. To use a weapon for destruction might alienate people from their cause, but a threat to do so might bring about some of the changes it demands. Others include terrorists groups, criminals, and psychopaths who may have little to lose and thus are more apt to use a weapon. Fortunately, such organizations tend to have fewer financial and technical resources. Nonetheless, thwarting nuclear terrorism by nonstate actors has received considerable interest in recent years.

Notwithstanding difficulties in preventing proliferation, it is widely held that strong efforts should be made to reduce the risk of nuclear explosions. We thus consider what means are available in Fig. 27.6, a schematic outline.

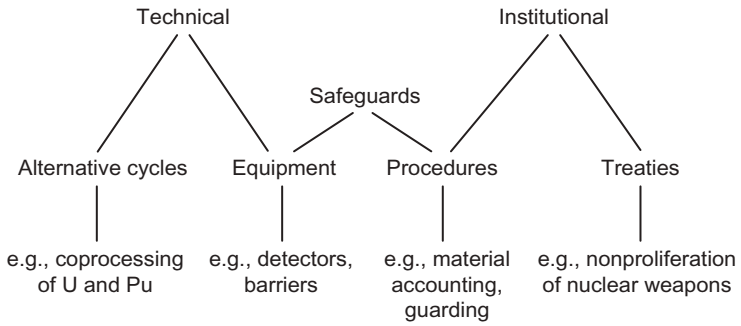

FIG. 27.6

Nonproliferation measures.

Protection against diversion of nuclear materials involves many analogs to protection against the crimes of embezzlement, robbery, and hijacking. Consider first the extraction of small amounts of fissile material such as enriched uranium or plutonium by a subverted employee in a nuclear facility. The maintenance of accurate records is a preventive measure. One identifies a material balance in selected process steps (e.g., a spent-fuel dissolver tank or a storage area). To an initial inventory, the input is added and the output subtracted. The difference between this result and the final inventory is the material unaccounted for (MUF)

$$\text{MUF} = \frac{\text{Beginning}}{\text{Inventory}} - \frac{\text{Ending}}{\text{Inventory}} + \frac{\text{Input}}{\text{Transfers}} - \frac{\text{Output}}{\text{Transfers}} \tag{27.4}$$

Any significant value of MUF prompts an investigation. Ideally, the system of accountability would keep track of all materials at all times, but such detail is probably impossible. Inspection of the consistency of records and reports is coupled with independent measurements on materials present.

Restricting the number of persons who have access to the material and careful selection for good character and reliability is a common practice. Similarly, limiting the number of people who have access to records is desirable. It is easy to see how falsification of records can cover up a diversion of plutonium. A discrepancy of only 10 kg of plutonium would allow for material for one weapon to be diverted. Various personnel identification techniques are available, such as picture badges, access passwords, signatures, fingerprints, voiceprints, and retinal scans.

Protection against intruders can be achieved by the usual devices such as ample lighting of areas, use of a guard force, burglar alarms, video surveillance, and barriers to access. More exotic schemes to delay, immobilize, or repel attackers have been considered, including dispersal of certain gases that reduce efficiency or of smoke to reduce visibility, and the use of disorienting lights or unbearable sound levels.

Illegal motion of nuclear materials can be revealed by the detection of characteristic radiation, in rough analogy to metal detection at airports. A gamma-ray emitter is easy to find, of course. The presence of fissile materials can be detected by observing delayed neutrons resulting from brief neutron irradiation—a technique known as *active interrogation*.

In the transportation of strategic nuclear materials, armored cars or trucks are used, along with escorts or convoys and remote monitoring. Automatic disabling of vehicles in the event of hijacking is a possibility.

27.6 IAEA INSPECTIONS

Shortly after the Nonproliferation Treaty of 1968 was signed, the IAEA set up a worldwide safeguards system. It applied to all source materials (uranium and thorium) and special fissionable materials (plutonium and uranium-233). The primary purpose of IAEA inspections has been to detect the diversion of significant quantities of nuclear material from peaceful to military purposes. Since 1970, large numbers of portable instruments for nondestructive testing have been developed to carry out the surveillance. Gamma-ray and neutron detectors are used to determine the enrichment of uranium and the content of plutonium in spent fuel. The IAEA considers either 25 kg of high enriched uranium or 8 kg of plutonium to be sufficient to construct one nuclear weapon, as detailed in Table 27.4, which categorizes fissionable materials in terms of whether they can be directly employed in a nuclear device.

The role of the IAEA was highlighted in the 1991 investigation of the nuclear weapons program of Iraq under Saddam Hussein, under the auspices of the United Nations Security Council. Large amounts of uranium had been imported from other countries without being reported. Orders were placed abroad for equipment that could have a dual purpose. As revealed by IAEA inspectors, such equipment was channeled into the construction of modern versions of electromagnetic uranium isotope separators (Section 15.1), to centrifuges, and to reactors and reprocessing equipment for plutonium weapons production. In support of the field investigations after the end of the Gulf War, laboratory studies at the IAEA's laboratories in Austria were conducted. Samples taken by inspectors were found to contain as high as 6% enrichment in U-235 (Donohue and Zeisler, 1992). A particle spectral measurement confirmed the presence of polonium-210, which is a component of an initiator for an implosion-type nuclear weapon. Much of Iraq's nuclear capability was destroyed in the 1991 Gulf War and afterward in response to sanctions by the United Nations. The assumption by the United States that Iraq still had weapons of mass destruction (i.e., biological, chemical, and nuclear) led to the invasion of 2003.

On a long-range basis, the IAEA is concerned about the possibility that a repository for spent fuel, intended to isolate the waste from the biosphere, may in the future become a "plutonium mine" from which Pu is extracted, possibly as source of fissile material for nuclear explosives (Semenov and Oi, 1993; Lyman and Feiveson, 1998).

Various other countries are known or suspected of having or have at one time had nuclear weapon programs. Prominent among the lists given by Jones and McDonough (1998) and by Morrison and Tsipis (1998) are Israel, India, Pakistan, North Korea, Iran, Iraq, and South Africa. India termed its 1974 detonation of a nuclear device as a "peaceful nuclear explosion."

Table 27.4 IAEA Significant Quantities

Usage	Material	Significant Quantity
Direct use material	Pu (<80% Pu-238)	8 kg Pu
	U-233	8 kg U-233
	HEU (≥20% U-235)	25 kg U-235
Indirect use material	U (<20% U-235) including low enriched, natural and depleted uranium	75 kg U-235 (or 10 tonne natural U or 20 tonne depleted U)
	Th	20 tonne Th

From International Atomic Energy Agency (IAEA), 2002. IAEA Safeguards Glossary, 2001 ed. Vienna.

More than 2000 nuclear weapon test detonations have been carried out globally (Norris and Arkin, 1998). The Comprehensive Test Ban Treaty (CTBT) of 1996 seeks international agreement not to "carry out any nuclear weapon test explosion or any other nuclear explosion." This means underground tests as well as those in the air, on water, or in space, even those for peaceful purposes. Excluded are explosions by inertial fusion devices or the destruction of any terrorist weapon. The treaty also calls for a system of monitoring and inspection to verify compliance. Ratification is required by the 44 countries that either helped draft the document or have power reactors or research reactors. Many countries have signed, but not all have ratified. The treaty seems to have public support in the United States, but some claim that acceptance by the United States would hamstring defense while some nations would violate the treaty. In 1999, the US Senate narrowly rejected the CTBT.

27.7 PRODUCTION OF TRITIUM

Over the many years of the Cold War (1947–91), the DOE and its predecessors had maintained a stockpile of weapons material, especially tritium and plutonium. The isotope H-3, tritium, as one of the ingredients of the hydrogen bomb, was produced in heavy water reactors at the Savannah River Plant. Because of safety concerns, the reactors were shut down in 1988. A program of refurbishing the old reactors was undertaken, and as supporting capacity to produce a continuing supply of tritium, a development program called the New Production Reactor was started. Two types of reactors were designed: a heavy water reactor and a high temperature gas-cooled reactor. With the reduction in international tension, the United States determined that tritium supplies would be adequate for two decades and in 1992 suspended design of the new reactors. The amount of tritium needed depends on the level of weapons capability that is maintained. In a scenario with a smaller number of warheads, recycling of tritium from dismantled weapons would provide an adequate source. Subsequently, however, it was decided that an alternative supply was needed to maintain the stockpile because tritium has a half-life of 12.3 y, corresponding to a loss of 5.5% per year (Exercise 27.7). Consequently, the DOE sponsored two studies of production techniques either with a power reactor or with a particle accelerator.

Research was performed at Los Alamos on the alternative source of tritium in the program called Accelerator Production of Tritium (APT). It involved use of a 1000-ft (300-m) linear accelerator to bring protons to 1 GeV. These bombarded a tungsten target to yield spallation neutrons, which would be absorbed in helium-3 to give tritium. In 1998, the DOE decided in favor of the commercial light-water reactor (CLWR) route.

Power production in a conventional reactor by neutron bombardment involves burnable poison rods. Auxiliary to the main control, these poison rods contain an isotope of large thermal neutron cross-section such as boron-10, which burns out quickly and allows a larger initial fuel loading (see Section 20.6). It was proposed by the DOE to replace the boron rods with an appropriate number containing lithium-6. These target rods consist of concentric cylinders of Zircaloy, lithium aluminate ($LiAlO_2$), and stainless steel. Absorption of a neutron in Li-6, with thermal cross-section 940 barns, yields tritium and an alpha particle; see Eq. (4.8). Tests at the Tennessee Valley Authority reactors indicated that production of tritium would be adequate and that the reactor would operate safely. In 2003, TVA's Watts Bar 1 reactor started producing the first US tritium in more than 15 y. Irradiated tritium-producing burnable absorber rods (TPBARs) were shipped in 2005 to the Savannah River Site

for storage and extraction in a new facility. TVA operates commercial power reactors, but as a quasigovernmental institution, it is obligated to permit this practice. Understandably, this comingling of nuclear power and material for nuclear weapons has been criticized.

27.8 MANAGEMENT OF WEAPONS URANIUM AND PLUTONIUM

During the Cold War, both the United States and the USSR accumulated large amounts of highly enriched uranium and weapons-grade plutonium. The START treaties brought about a program of dismantlement. An excess of the materials over that needed for continued nuclear deterrence was to be disposed of in some way. It had been estimated that a total of 100 tonnes of Pu and 2000 tonnes of HEU, roughly in equal amounts, remained in the two countries. Enriched uranium can be readily diluted with natural or depleted uranium to produce a low-enrichment fuel, helping meet the demand of current and future power reactors. Plutonium is not as easy to handle because there are no Pu isotopes to serve as a diluent. Thus, stockpiles of Pu are vulnerable to diversion to nations or groups who might use, or threaten to use, the material to gain their ends.

The plutonium of principal concern is in pure form, in contrast with that present in spent fuel. The latter would require special equipment to extract the Pu, and the product would be less suitable for a weapon because of the presence of Pu-240.

Plutonium is far from being "the most dangerous substance known to man," as claimed by some, but it is highly radiotoxic and requires special precautions in all handling. Use of Pu increases the chance of radioactive contamination as was experienced at various DOE sites, especially at Rocky Flats, Colorado.

There are several possibilities for managing plutonium. Some believe that it should be stored in anticipation of a need for its energy values sometime later this century. One could visualize a storage facility like Fort Knox where gold and silver are secured. Storage over a long period would require protection against chemical degradation and accidental criticality as well as from theft.

A National Academy of Sciences (NAS) panel composed of prominent knowledgeable people identified three principal options (NAS, 1994):

1. Vitrification of the Pu with a highly radioactive contaminant to deter diversion and processing. This would result in glass logs that could be treated as spent fuel and put in an underground repository. Future mining of the Pu would be very unattractive.
2. Blending the plutonium as the oxide with a suitable amount of uranium oxide to form MOX that could serve as fuel for power reactors. This would eliminate the plutonium and have the advantage of a beneficial use. The disadvantage is the cost of processing and fabrication, which is significantly higher than that for uranium because of the hazard of ingesting the radioactive material. This approach requires the development of a suitable fuel fabrication plant. Several countries, notably France, England, Belgium, and Japan, are in a position to prepare and use the MOX, whereas the United States has little experience or inclination to use it, having abandoned the option of reprocessing spent fuel.
3. Placing the Pu in a deep drilled hole in the ground. Although this is feasible, there is no strong support for the idea.

The NAS panel also examined the option of the use of an accelerator-driven subcritical system to burn the plutonium, but concluded that there were too many uncertainties, including the possible need for reprocessing. The NAS recommended carrying along options (1) and (2) in parallel, a strategy that was adopted by the DOE. The surplus weapons plutonium is stored at several DOE sites, with the bulk at Savannah River and Hanford. Most is in the form of *pits*, the spherical weapons cores, but there are some 12-ft (3.7-m) long rods at Hanford. Eventually, all will be stored at one location to improve security and reduce storage costs.

For disposal of Pu by immobilization and burial, a criterion called the spent fuel standard is applied (i.e., the Pu should be as inaccessible for weapons use as that in spent fuel from commercial reactors).

It is expected that the burning option would consist of a once-through fuel cycle. To use up the 50 tonnes of excess Pu in a reasonable period would require relatively few commercial reactors. It is straightforward arithmetic to determine the combination of time and number of reactors to perform the task; see Exercise 27.3.

Whatever method of disposal is finally adopted, meticulous procedures and records must be maintained and special rigorous precautions taken to prevent the material from getting into unscrupulous hands. The NAS report urged that agreements be reached between the United States and Russia and mechanisms established through the IAEA that would assure that each nation fulfilled its commitments. This would reduce mutual concerns that one party might retrieve Pu and rearm nuclear weapons.

When one realizes the enormous damage that nuclear explosions can create, it is clear that all possible steps must be taken to prevent them from occurring. In addition to continued efforts to reduce the stockpile of armaments, to secure workable treaties, and to use technology to provide protection, there is an urgent need to eliminate the unfavorable conditions—social, economic, and cultural—that prompt conflict in the world.

27.9 SUMMARY

Although spent fuel from power reactors contains plutonium, it is not the same grade material as that in a nuclear weapon. The original atom bombs used U-235 and Pu, but the much more powerful modern weapons are based on the fusion of hydrogen isotopes. Intercontinental ballistic missiles from land and missiles from submarines make up the bulk of the arsenals of the United States and the former USSR. Continual efforts are made to prevent further proliferation of nuclear weapons. For the good of the international community, the use of nuclear weapons should be avoided.

27.10 EXERCISES

27.1 The critical mass of a uranium-235 metal assembly varies inversely with the density of the system. If the critical mass of a sphere at normal density $18.5\,g/cm^3$ is 50 kg, how much reduction in radius by compression is needed to make a 40-kg assembly go critical?

27.2 A proposal is advanced to explode fusion weapons deep underground, to pipe to the surface the heat from the cavity produced, and to generate and distribute electricity. If no energy were lost, how frequently would a 100-kt device have to be fired to obtain 3000 MW of thermal power? Alternately, how many weapons per year would be consumed?

27.3 Find out how many commercial reactors would be needed to consume 50 tonnes of Pu in 30 y, assuming the following data: reactor power, 1200 MWe; efficiency, 0.33; capacity factor, 0.85; 60 assemblies removed and new ones installed per year, 3-y irradiation to fuel burnup 45,000 MW d/tonne, one-third of new fuel containing MOX at 2.5% Pu.

27.4 Assuming an annual need for 4% U-235 fuel of 50 tonnes per power reactor, how many reactor-years of operation can be achieved with 20 tonnes of 90% U-235, when down-blended with (a) 0.7% natural U and (b) tails of 0.3% U-235?

27.5 A 22-kt nuclear weapon is exploded at an altitude of 500 m. Assuming each fission yields 8 fission gammas of 1 MeV and 3 prompt neutrons of 2 MeV, estimate both the gamma and neutron fluence at 1500 m horizontally from ground zero, which is directly below the blast. Neglect the attenuating effect of air.

27.6 Compute the gamma fluence for the conditions of Example 27.2, but include the effect of air attenuation (but with no buildup).

27.7 Verify that the decay of tritium results in an annual loss of 5.5% of the material.

27.8 Calculate the neutron emission rate from 1 μg of ^{210}Po-Be.

27.9 With the assistance of Fig. 23.3, determine the average mass of Pu produced annually in a 1000-MWe power plant for a capacity factor of 90%.

27.10 (a) Use Table 6.3 data to show that about 90% of the energy from fission is prompt (device yield). (b) Also show that the prompt and delayed nuclear radiation energies are roughly 5% and 10%, respectively.

27.11 Calculate the mass of material fissioned to produce the yield of the (a) Little Boy and (b) Fat Man bombs.

27.11 COMPUTER EXERCISES

27.A The implosion of a mass of fissionable material can be studied by use of the computer program FASTRX, introduced in Chapter 25. It is a neutron multigroup method for calculating criticality in a pure U-235 metal assembly. (a) Calculate the critical size and mass for several values of the uranium density, including higher densities than normal as would be achieved by implosion of a nuclear warhead. Suggested values of the parameter UN besides 0.048 are 0.036 and 0.060. (b) From the results of (a), deduce a good value of x in a formula for critical mass as a function of metal density of the form

$$M = M_0 \, (\rho/\rho_0)^x$$

where M_0 is the critical mass at ordinary density ρ_0.

27.B Arrangements are made for the purchase by the United States of Russian uranium at enrichment 94 w/o to be blended with natural U to create 3 w/o fuel for power reactors. With computer program ENRICH (Chapter 15), estimate a fair price to pay per kilogram of HEU

if the blending is done (a) in Russia, or (b) in the United States. If importation amounts to 10 tonne/y for 5 y followed by 30 tonne/y for 15 y, which would take about half the stockpile, what is the total worth in each case? What additional information would be useful to arrive at a proper figure?

REFERENCES

Ahlswede, J., Kalinowski, M.B., 2012. Global plutonium production capabilities with civilian research reactors. Sci. Glob. Security 20 (2–3), 69–96.

Argonne National Laboratory (ANL), 1963. Reactor physics constants. ANL-5800, second ed., Section 7.2.1.

Cox, C., 1999. Report of the select committee on U.S. national security and military/commercial concerns with the People's Republic of China. Report 105-851. U.S. House of Representatives.

Cullings, H.M., 2014. Impact on the Japanese atomic bomb survivors of radiation received from the bombs. Health Phys. 106 (2), 281–293.

Donohue, D.L., Zeisler, R., 1992. Behind the scenes: scientific analysis of samples from nuclear inspections in Iraq. IAEA Bull. 34 (1), 25–32.

Glasstone, S., Dolan, P.J. (Eds.), 1977. The Effects of Nuclear Weapons, third ed. U.S. Department of Defense (DOD) and U.S. Department of Energy (DOE), U.S Government Printing Office, Washington, DC.

Hansen, C., 1988. United States Nuclear Weapons: The Secret History. Aerofax, Arlington, TX. Very detailed descriptions with many photos of all weapons and tests; diagram of H-bomb explosion on p. 22.

Jones, R.W., McDonough, M.G., 1998. Tracking Nuclear Proliferation: A Guide in Maps and Charts. Carnegie Endowment for International Peace, Washington, DC.

Kaplan, F.M., 1978. Enhanced-radiation weapons. Sci. Am. 238 (5), 44–51.

Kerr, G.D., Young, R.W., Cullings, H.M., Christy, R.F., 2005. Bomb parameters. In: Reassessment of the Atomic Bomb Radiation Dosimetry for Hiroshima and Nagasaki, Dosimetry System 2002. vol. 1. Radiation Effects Research Foundation, Hiroshima, pp. 42–61.

Kristensen, H.M., Norris, R.S., 2017. Worldwide deployments of nuclear weapons, 2017. Bull. At. Sci. 73 (5), 289–297.

Lawson, D.E., 1963. Review and summary of some project Gnome results. Trans. Am. Geophys. Union 44 (1), 129–135.

Loeber, C.R., 2005. Building the Bombs: A History of the Nuclear Weapons Complex, second ed. Sandia National Laboratories, Albuquerque SAND2005-5648P.

Lyman, E.S., Feiveson, H.A., 1998. The proliferation risks of plutonium mines. Sci. Glob. Security 7 (1), 119–128.

Mattern, D., 2007. Beyond nuclear terrorism. Peace Rev. 19 (4), 563–569.

Morrison, P., Tsipis, K., 1998. Reason Enough to Hope: America and the World of the Twenty-First Century. MIT Press, Cambridge.

National Academy of Sciences (NAS), 1994. Management and Disposition of Excess Weapons Plutonium: Reactor-Related Options. National Academies Press, Washington, DC.

National Research Council, Committee on the Atmospheric Effects of Nuclear Explosions, 1985. The Effects on the Atmosphere of a Major Nuclear Exchange. National Academies Press, Washington, DC.

Norris, R.S., Arkin, W.M., 1998. Known nuclear tests worldwide, 1945–98. Bull. At. Sci. 54 (6), 65–67.

Office of Technology Assessment (OTA), 1977. Nuclear Proliferation and Safeguards. United States Congress, Washington, DC.

Rhodes, R., 1986. The Making of the Atomic Bomb. Simon & Schuster, New York. Thorough, readable, and authoritative; this is regarded as the best book on the Manhattan Project.

Rhodes, R., 1995. Dark Sun: The Making of the Hydrogen Bomb. Simon & Schuster, New York. Highly readable political and technical aspects; role of espionage; diagrams of H-bomb explosion on p. 506.
Semenov, B.A., Oi, N., 1993. Nuclear fuel cycles: adjusting to new realities. IAEA Bull. 35 (3), 2–7.
Serber, R., 1992. The Los Alamos Primer. University of California Press, Berkeley. A set of five lectures on the early (1943) state of knowledge on the possibility of an atom bomb, with extensive explanatory annotations; included are history, nuclear physics, and chain reactions.
Smyth, H.D., 1945. Atomic energy for military purposes. Rev. Mod. Phys. 17 (4), 351–471.
Tsipis, K., 1977. Cruise missiles. Sci. Am. 236 (2), 20–29.
United Nations (UN), 1980. Yearbook of the United Nations 1977. vol. 31. UN, New York, p. 41.

FURTHER READING

Bernstein, J., 2007. Nuclear Weapons: What You Need to Know. Cambridge University Press, New York.
Cochran, T.B., Arkin, W.M., Hoenig, M.M., 1988. Nuclear Weapons Databook, vol. I: U.S. Nuclear Forces and Capability. Ballinger Publishing Co., Cambridge, MA.
CTBTO, Preparatory commission, Comprehensive test Ban treaty. http://www.ctbto.org/.
Domenici, P., 2004. A Brighter Tomorrow: Fulfilling the Promise of Nuclear Energy. Rowman & Littlefield, New York.
Federation of American Scientists, WMD Resources. http://www.fas.org/nuke. Weapons of mass destruction.
Garwin, R.L., Charpak, G., 2001. Megawatts and Megatons: A Turning Point in the Nuclear Age. Random House, New York.
Hewlett, R.G., Holl, J.M., 1989. Atoms for Peace and War 1953–1961, Eisenhower and the Atomic Energy Commission. University of California Press, Berkeley.
International Atomic Energy Agency (IAEA), 2002. IAEA Safeguards Glossary. 2001 ed. IAEA, Vienna.
Kelly, C.C. (Ed.), 2007. The Manhattan Project: The Birth of the Atomic Bomb in the Words of its Creators, Eyewitnesses, and Historians. Black Dog & Leventhal Publishers, Inc., New York.
Messenger, G.C., Ash, M.S., 1992. The Effects of Radiation on Electronic Systems, second ed. Van Nostrand Reinhold, New York.
Nolan, J.E., Wheelon, A.D., 1990. Third world ballistic missiles. Sci. Am. 263 (2), 34–40.
Pillay, K.K.S., 1996. Plutonium: requiem or reprieve. Radwaste Mag. 4 (3), 59–65.
Scheinman, L., 1985. The Nonproliferation Role of the International Atomic Energy Agency: A Critical Assessment. Resources for the Future, Washington, DC.
Scheinman, L., 1987. The International Atomic Energy Agency and World Nuclear Order. Resources for the Future, Washington, DC.
Schroeer, D., 1984. Science, Technology, and the Nuclear Arms Race. Wiley, New York.
Schwartz, S. (Ed.), 1998. Atomic Audit: The Costs and Consequences of U.S. Nuclear Weapons Since 1940. Brookings Institute Press, Washington, DC.
Thaul, S., O'Maonaigh, H. (Eds.), 1999. Potential Radiation Exposure in Military Operations. National Academies Press, Washington, DC.
Walker, G., 2005. Trinity atomic web site. www.abomb1.org.
World Nuclear Association (WNA), 2017. Safeguards to prevent nuclear proliferation. http://www.world-nuclear.org/information-library.aspx.
Yadav, M.S., 2007. Nuclear Weapons and Explosions: Environmental Impacts and Other Effects. SDS, New Delhi.

APPENDIX

REFERENCE INFORMATION AND DATA

A

(See Tables A.1–A.6)

Table A.1 Greek Alphabet

A	α	Alpha	N	ν	Nu
B	β	Beta	Ξ	ξ	Xi
Γ	γ	Gamma	O	ο	Omicron
Δ	δ	Delta	Π	π	Pi
E	ε	Epsilon	P	ρ	Rho
Z	ζ	Zeta	Σ	σ	Sigma
H	η	Eta	T	τ	Tau
Θ	θ	Theta	Υ	υ	Upsilon
I	ι	Iota	Φ	ϕ	Phi
K	κ	Kappa	X	χ	Chi
Λ	λ	Lambda	Ψ	ψ	Psi
M	μ	Mu	Ω	ω	Omega

This table provides the Greek uppercase and lowercase letters for reference.

Table A.2 Values of Fundamental Physical Constants

Speed of light in vacuum (c)	299,792,458 m/s
Elementary charge (e)	$1.6021766208 \times 10^{-19}$ C
Electronvolt (eV)	$1.6021766208 \times 10^{-19}$ J
Planck constant (h)	$6.626070040 \times 10^{-34}$ J s $= 4.135667662 \times 10^{-15}$ eV s
Avogadro constant (N_A)	$6.022140857 \times 10^{23}$/mol
Molar gas constant (R)	8.3144598 J/(mol K)
Boltzmann constant ($k = R/N_A$)	$1.38064852 \times 10^{-23}$ J/K $= 8.6173303 \times 10^{-5}$ eV/K
Electron rest mass (m_e)	$9.10938356 \times 10^{-31}$ kg or 0.5109989461 MeV/c^2
Proton rest mass (m_p)	$1.672621898 \times 10^{-27}$ kg or 938.2720813 MeV/c^2
Neutron rest mass (m_n)	$1.674927471 \times 10^{-27}$ kg or 939.5654133 MeV/c^2
Deuteron rest mass (m_d)	$3.343583719 \times 10^{-27}$ kg or 1875.612928 MeV/c^2
Triton rest mass (m_t)	$5.007356665 \times 10^{-27}$ kg or 2808.921112 MeV/c^2
Helion rest mass (m_h)	$5.006412700 \times 10^{-27}$ kg or 2808.391586 MeV/c^2

Continued

Table A.2 Values of Fundamental Physical Constants—cont'd

Alpha rest mass (m_α)	$6.644657230 \times 10^{-27}$ kg or 3727.379378 MeV/c^2
Atomic mass unit ($u = m_{C\text{-}12}/12$)	$1.660539040 \times 10^{-27}$ kg or 931.4940954 MeV/c^2
Magnetic constant (μ_0)	$4\pi \times 10^{-7}$ N/A^2 = 12.566370614… $\times 10^{-7}$ N/A^2
Electric constant ($\varepsilon_0 = 1/(\mu_0 c^2)$)	$8.854187817\ldots \times 10^{-12}$ F/m
Gravitational constant (G)	6.67408×10^{-11} m^3/(kg s^2)
Stefan-Boltzmann constant (σ)	5.670367×10^{-8} W/(m^2 K^4)

Data from Mohr, P.J., Newell, D.B., Taylor, B.N., 2015. CODATA Recommended Values of the Fundamental Physical Constants: 2014. arXiv:1507.07956v1 [physics.atom-ph]. Available from the National Institute of Science and Technology (NIST), http://physics.nist.gov/constants.

Table A.3 Conversion Factors

Original System	Multiplication Factor	SI
Acre (43,560 ft^2)	4046.9	Square meter (m^2)
Ångström (Å)	0.1	Nanometer (nm)
Atmosphere	1.013×10^5	Pascal (Pa)
Bar	100	Kilopascal (kPa)
Barn	10^{-28}	Square meter (m^2)
Barrel (42 gal for petroleum)	0.1590	Cubic meter (m^3)
British thermal unit (Btu)	1055	Joule (J)
Thermal conductivity (Btu/(h ft))	1.7307	W/(m °C)
Specific heat (Btu/(lbm °F))	4.1868	kJ/(kg °C)
Calorie, thermochemical (cal)	4.184	Joule (J)
Centipoise (cP)	0.001	Pascal second (Pa s)
Curie (Ci)	3.700×10^{10}	Decay per second (dps)
Day (d)	8.640×10^4	Second (s)
Degree (angle)	0.0174533	Radian
Degree Fahrenheit (°F)	°C = (°F − 32)/1.8	Degree Celsius (°C)
Electronvolt (eV)	1.6022×10^{-19}	Joule (J)
Foot (ft)	0.3048	Meter (m)
Square foot (ft^2)	0.092903	Square meter (m^2)
Cubic foot (ft^3)	0.028317	Cubic meter (m^3)
Cubic foot per minute (ft^3/min)	4.7195×10^{-4}	Cubic meter per second (m^3/s)
Gallon (gal) US liquid (231 in^3)	3.7854×10^{-3}	Cubic meter (m^3)
Gauss	10^{-4}	Tesla (T)
Horsepower (hp) (550 ft lbf/s)	745.7	Watt (W)
Inch (in)	0.0254	Meter (m)
Square inch (in^2)	6.4516×10^{-4}	Square meter (m^2)
Cubic inch (in^3)	1.6387×10^{-5}	Cubic meter (m^3)

Table A.3 Conversion Factors—cont'd

Original System	Multiplication Factor	SI
Kilowatt hour (kWh)	3.600×10^6	Joule (J)
Kilogram-force (kgf)	9.80665	Newton (N)
Liter (L)	0.001	Cubic meter (m^3)
Micron (μ)	10^{-6}	Meter (m)
Mil (0.001 in.)	0.0254	Millimeter (mm)
Mile (mi)	1609	Meter (m)
Miles per hour (mi/h)	0.44704	Meters per second (m/s)
Square mile (mi^2)	2.590×10^6	Square meter (m^2)
Pound, avoirdupois (lb)	0.4536	Kilogram (kg)
Pound-force (lbf)	4.4482	Newton (N)
Pound-force per square inch (psi)	6895	Pascal (Pa)
Rad	0.01	Gray (Gy)
Rem	0.01	Sievert (Sv)
Roentgen (R)	2.580×10^{-4}	Coulomb per kilogram (C/kg)
Ton (short, 2000 lb)	907.2	Kilogram (kg)
Tonne (metric)	1000	Kilogram (kg)
Watthour (Wh)	3600	Joule (J)
Year, sidereal (y)	3.1558×10^7	Second (s)

To convert from numbers given in the British or other system of units to numbers in SI units, multiply by the factors in this table. For example, multiply the energy of thermal neutrons of 0.0253 eV by 1.6022×10^{-19} to obtain the energy as 4.0535×10^{-21} J. Note that some conversion factors are rounded off.
Based on IEEE, 2011. IEEE/ASTM SI 10-2010 American National Standard for Metric Practice, IEEE.

Table A.4 Atomic Weights and Densities of the Elements

Z	Element Name	Symbol	Atomic Weight	Density (g/cm^3)
1	Hydrogen	H	1.008	8.375×10^{-5}
2	Helium	He	4.002602	1.663×10^{-4}
3	Lithium	Li	6.94	0.534
4	Beryllium	Be	9.0121831	1.848
5	Boron	B	10.81	2.37
6	Carbon	C	12.011	1.70 [graphite]
7	Nitrogen	N	14.007	1.165×10^{-3}
8	Oxygen	O	15.999	1.332×10^{-3}
9	Fluorine	F	18.998403163	1.58×10^{-3}
10	Neon	Ne	20.1797	8.385×10^{-4}
11	Sodium	Na	22.98976928	0.971
12	Magnesium	Mg	24.305	1.74

Continued

Table A.4 Atomic Weights and Densities of the Elements—cont'd

Z	Element Name	Symbol	Atomic Weight	Density (g/cm^3)
13	Aluminum	Al	26.9815385	2.699
14	Silicon	Si	28.085	2.33
15	Phosphorus	P	30.973761998	2.20
16	Sulfur	S	32.06	2.00
17	Chlorine	Cl	35.45	2.995×10^{-3}
18	Argon	Ar	39.948	1.662×10^{-3}
19	Potassium	K	39.0983	0.862
20	Calcium	Ca	40.078	1.55
21	Scandium	Sc	44.955908	2.989
22	Titanium	Ti	47.867	4.54
23	Vanadium	V	50.9415	6.11
24	Chromium	Cr	51.9961	7.18
25	Manganese	Mn	54.938044	7.44
26	Iron	Fe	55.845	7.874
27	Cobalt	Co	58.933194	8.90
28	Nickel	Ni	58.6934	8.902
29	Copper	Cu	63.546	8.96
30	Zinc	Zn	65.38	7.133
31	Gallium	Ga	69.723	5.904
32	Germanium	Ge	72.630	5.323
33	Arsenic	As	74.921595	5.73
34	Selenium	Se	78.971	4.50
35	Bromine	Br	79.904	7.072×10^{-3}
36	Krypton	Kr	83.798	3.478×10^{-3}
37	Rubidium	Rb	85.4678	1.532
38	Strontium	Sr	87.62	2.54
39	Yttrium	Y	88.90584	4.469
40	Zirconium	Zr	91.224	6.506
41	Niobium	Nb	92.90637	8.57
42	Molybdenum	Mo	95.95	10.22
43	Technetium	Tc	(97)	11.5
44	Ruthenium	Ru	101.07	12.41
45	Rhodium	Rh	102.90550	12.41
46	Palladium	Pd	106.42	12.02
47	Silver	Ag	107.8682	10.5
48	Cadmium	Cd	112.414	8.65
49	Indium	In	114.818	7.31
50	Tin	Sn	118.710	7.31

Table A.4 Atomic Weights and Densities of the Elements—cont'd

Z	Element Name	Symbol	Atomic Weight	Density (g/cm^3)
51	Antimony	Sb	121.760	6.691
52	Tellurium	Te	127.60	6.24
53	Iodine	I	126.90447	4.93
54	Xenon	Xe	131.293	5.485×10^{-3}
55	Cesium	Cs	132.90545196	1.873
56	Barium	Ba	137.327	3.50
57	Lanthanum	La	138.90547	6.154
58	Cerium	Ce	140.116	6.657
59	Praseodymium	Pr	140.90766	6.71
60	Neodymium	Nd	144.242	6.90
61	Promethium	Pm	(145)	7.22
62	Samarium	Sm	150.36	7.46
63	Europium	Eu	151.964	5.243
64	Gadolinium	Gd	157.25	7.90
65	Terbium	Tb	158.92535	8.229
66	Dysprosium	Dy	162.500	8.55
67	Holmium	Ho	164.93033	8.795
68	Erbium	Er	167.259	9.066
69	Thulium	Tm	168.93422	9.321
70	Ytterbium	Yb	173.045	6.73
71	Lutetium	Lu	174.9668	9.84
72	Hafnium	Hf	178.49	13.31
73	Tantalum	Ta	180.94788	16.65
74	Tungsten	W	183.84	19.3
75	Rhenium	Re	186.207	21.02
76	Osmium	Os	190.23	22.57
77	Iridium	Ir	192.217	22.42
78	Platinum	Pt	195.084	21.45
79	Gold	Au	196.966569	19.32
80	Mercury	Hg	200.592	13.55
81	Thallium	Tl	204.38	11.72
82	Lead	Pb	207.2	11.35
83	Bismuth	Bi	208.98040	9.747
84	Polonium	Po	(209)	9.32
85	Astatine	At	(210)	10.0
86	Radon	Rn	(222)	9.066×10^{-3}
87	Francium	Fr	(223)	10.0
88	Radium	Ra	(226)	5.0

Continued

Table A.4 Atomic Weights and Densities of the Elements—cont'd

Z	Element Name	Symbol	Atomic Weight	Density (g/cm^3)
89	Actinium	Ac	(227)	10.07
90	Thorium	Th	232.0377	11.72
91	Protactinium	Pa	231.03588	15.37
92	Uranium	U	238.02891	18.95
93	Neptunium	Np	(237)	
94	Plutonium	Pu	(244)	
95	Americium	Am	(243)	
96	Curium	Cm	(247)	
97	Berkelium	Bk	(247)	
98	Californium	Cf	(251)	
99	Einsteinium	Es	(252)	
100	Fermium	Fm	(257)	
101	Mendelevium	Md	(258)	
102	Nobelium	No	(259)	
103	Lawrencium	Lr	(262)	
104	Rutherfordium	Rf	(267)	
105	Dubnium	Db	(270)	
106	Seaborgium	Sg	(269)	
107	Bohrium	Bh	(270)	
108	Hassium	Hs	(270)	
109	Meitnerium	Mt	(278)	
110	Darmstadtium	Ds	(281)	
111	Roentgenium	Rg	(281)	
112	Copernicium	Cn	(285)	
113	Nihonium	Nh	(286)	
114	Flerovium	Fl	(289)	
115	Moscovium	Mc	(289)	
116	Livermorium	Lv	(293)	
117	Tennessine	Ts	(293)	
118	Oganesson	Og	(294)	

Atomic weights data from Commission on Isotopic Abundances and Atomic Weights (CIAAW) of the International Union of Pure and Applied Chemistry (IUPAC) (http://www.chem.qmul.ac.uk/iupac/AtWt/). Meija, J., et al., 2016. Atomic weights of the elements 2013, Pure Appl. Chem. 88(3), 265–291, March. The 2013 data are listed except for the elements H, Li, B, C, N, O, Mg, Si, S, Cl, Br, and Tl that have a range of weights because the single conventional value is more convenient for working examples and exercises. For some elements that have no stable nuclide, the mass number of the isotope with the longest half-life is listed. Density data from Hubbell, J.H., Seltzer, S.M., 2004. Tables of X-Ray Mass Attenuation Coefficients and Mass Energy-Absorption Coefficients. National Institute of Standards and Technology (NIST). http://physics.nist.gov/xaamdi.

Table A.5 Selected Atomic Masses and Isotopic Abundances

Particle/Isotope	Atomic Mass (u)	Isotopic Abundance
Electron (e^-)	0.000548579909070	
Proton (p)	1.007276466879	
Deuteron (d)	2.013553212745	
Triton (t)	3.01550071632	
Alpha (α)	4.001506179127	
Neutron (n)	1.00866491585	
H-1	1.00782503223	0.99984426
H-2 (D)	2.01410177812	0.00015574
H-3 (T)	3.01604927791	
He-3	3.01602932008	0.000002
He-4	4.00260325413	0.999998
Li-6	6.01512288742	0.07589
Li-7	7.01600343659	0.92411
Be-9	9.012183065	1
B-10	10.012936949	0.1982
B-11	11.009305355	0.8018
C-12	12.0000000	0.988922
C-13	13.00335483507	0.011078
C-14	14.00324198843	
N-13	13.005738609	
N-14	14.00307400443	0.996337
N-15	15.00010889888	0.003663
N-16	16.006101925	
N-17	17.008448873	
O-16	15.99491461957	0.9976206
O-17	16.99913175650	0.0003790
O-18	17.99915961286	0.0020004
F-19	18.99840316273	1
Na-23	22.98976928196	1
Na-24	23.990962950	
Al-27	26.981538531	1
P-31	30.97376199842	1
Cl-35	34.968852682	0.757647
Cl-37	36.965902602	0.242353
Ar-40	39.96238312372	0.9960350
K-40	39.963998166	0.000117
Sc-45	44.955908275	1
Mn-55	54.938043910	1
Co-59	58.933194288	1
Co-60	60.932476620	

Continued

Table A.5 Selected Atomic Masses and Isotopic Abundances—cont'd

Particle/Isotope	Atomic Mass (u)	Isotopic Abundance
As-75	74.921594567	1
Y-89	88.905840348	1
Kr-90	89.919527931	
Sr-90	89.907730037	
Zr-90	89.904697659	
Kr-92	91.926173094	
Rb-92	91.919728389	
Nb-93	92.906373004	1
Sr-94	93.915355602	
Zr-103	102.927190678	
Rh-103	102.905497993	1
I-127	126.904471853	1
Cs-133	132.905451961	1
Xe-134	133.905394664	
Xe-137	136.911557781	
Cs-137	136.907089231	
Xe-140	139.921645817	
Cs-140	139.917283063	
Ba-141	140.914403333	
Pr-141	140.907657568	1
Ba-144	143.922954866	
Tb-159	158.925354710	1
Ho-165	164.930328835	1
Tm-169	168.934217889	1
Au-197	196.966568786	1
Pb-206	205.974465683	0.241
Bi-209	208.980399068	1
Po-210	209.982874076	
Po-218	218.008973546	
Rn-222	222.017578246	
Ra-226	226.025410330	
Th-232	232.038055760	1
Th-233	233.041582278	
U-232	232.037156297	
U-233	233.039635525	
U-234	234.040952306	0.000054
U-235	235.043930131	0.007204
U-236	236.045568210	
U-238	238.050788423	0.992742
Pu-238	238.049560111	

Table A.5 Selected Atomic Masses and Isotopic Abundances—cont'd

Particle/Isotope	Atomic Mass (u)	Isotopic Abundance
Pu-239	239.052163591	
Pu-240	240.053813750	
Pu-241	241.056851661	
Pu-242	242.058742809	

Atomic mass data from (1) Audi, G., Wang, M., Wapstra, A.H., Kondev, F.G., MacCormick, M., Xu, X., Pfeiffer, B., 2012. The AME2012 atomic mass evaluation (I): evaluation of input data, adjustment procedures. Chinese Phys. C 36(12), 1287–1602; and (2) Wang, M., Audi, G., Wapstra, A.H., Kondev, F.G., MacCormick, M., Xu, X., Pfeiffer, B., 2012. The AME2012 Atomic mass evaluation (II): tables, graphs and references. Chinese Phys. C 36(12), 1603–2014. Complete data available at http://amdc.impcas.ac.cn/ or https://www-nds.iaea.org/amdc/. Isotopic abundance data from Meija, J., et al., 2016. Isotopic compositions of the elements 2013 (IUPAC Technical Report). Pure Appl. Chem. 88 (3), 293–306.

Table A.6 Photon Mass Attenuation and Mass Energy-Absorption Coefficients (cm^2/g)

Energy (MeV)	Dry Air		Water		Concrete	Iron	Lead
	μ/ρ	μ_{en}/ρ	μ/ρ	μ_{en}/ρ	μ/ρ	μ/ρ	μ/ρ
0.001	3606	3599	4078	4065	3466	9085	5210
0.0015	1191	1188	1376	1372	1227	3399	2356
0.002	527.9	526.2	617.3	615.2	1368	1626	1285
0.003	162.5	161.4	192.9	191.7	464.6	557.6	1965
0.004	77.88	76.36	82.78	81.91	218.8	256.7	1251
0.005	40.27	39.31	42.58	41.88	140.1	139.8	730.4
0.006	23.41	22.70	24.64	24.05	84.01	84.84	467.2
0.008	9.921	9.446	10.37	9.915	38.78	305.6	228.7
0.01	5.120	4.742	5.329	4.944	20.45	170.6	130.6
0.015	1.614	1.334	1.673	1.374	6.351	57.08	111.6
0.02	0.7779	0.5389	0.8096	0.5503	2.806	25.68	86.36
0.03	0.3538	0.1537	0.3756	0.1557	0.9601	8.176	30.32
0.04	0.2485	0.06833	0.2683	0.06947	0.5058	3.629	14.36
0.05	0.2080	0.04098	0.2269	0.04223	0.3412	1.958	8.041
0.06	0.1875	0.03041	0.2059	0.03190	0.2660	1.205	5.021
0.08	0.1662	0.02407	0.1837	0.02597	0.2014	0.5952	2.419
0.1	0.1541	0.02325	0.1707	0.02546	0.1738	0.3717	5.549
0.15	0.1356	0.02496	0.1505	0.02764	0.1436	0.1964	2.014
0.2	0.1233	0.02672	0.1370	0.02967	0.1282	0.1460	0.9985
0.3	0.1067	0.02872	0.1186	0.03192	0.1097	0.1099	0.4031
0.4	0.09549	0.02949	0.1061	0.03279	0.09783	0.0940	0.2323
0.5	0.08712	0.02966	0.09687	0.03299	0.08915	0.08414	0.1614
0.6	0.08055	0.02953	0.08956	0.03284	0.08236	0.07704	0.1248
0.8	0.07074	0.02882	0.07865	0.03206	0.07227	0.06699	0.08870

Continued

Table A.6 Photon Mass Attenuation and Mass Energy-Absorption Coefficients (cm^2/g)—cont'd

Energy (MeV)	Dry Air		Water		Concrete	Iron	Lead
	μ/ρ	μ_{en}/ρ	μ/ρ	μ_{en}/ρ	μ/ρ	μ/ρ	μ/ρ
1	0.06358	0.02789	0.07072	0.03103	0.06495	0.05995	0.07102
1.25	0.05687	0.02666	0.06323	0.02965	0.05807	0.05350	0.05876
1.5	0.05175	0.02547	0.05754	0.02833	0.05288	0.04883	0.05222
2	0.04447	0.02345	0.04942	0.02608	0.04557	0.04265	0.04606
3	0.03581	0.02057	0.03969	0.02281	0.03701	0.03621	0.04234
4	0.03079	0.01870	0.03403	0.02066	0.03217	0.03312	0.04197
5	0.02751	0.01740	0.03031	0.01915	0.02908	0.03146	0.04272
6	0.02522	0.01647	0.02770	0.01806	0.02697	0.03057	0.04391
8	0.02225	0.01525	0.02429	0.01658	0.02432	0.02991	0.04675
10	0.02045	0.01450	0.02219	0.01566	0.02278	0.02994	0.04972
15	0.01810	0.01353	0.01941	0.01441	0.02096	0.03092	0.05658
20	0.01705	0.01311	0.01813	0.01382	0.02030	0.03224	0.06206

Material densities (ρ): dry air, 0.001205 g/cm^3; water, 1.00 g/cm^3; ordinary concrete, 2.30 g/cm^3; iron, 7.874 g/cm^3; lead, 11.35 g/cm^3. Data from Hubbell, J.H., Seltzer, S.M., 2004. Tables of X-Ray Mass Attenuation Coefficients and Mass Energy-Absorption Coefficients. National Institute of Standards and Technology (NIST). http://physics.nist.gov/xaamdi.

APPENDIX

TEXTBOOK-SPECIFIC INFORMATION

B

B.1 HOW TO USE THIS BOOK EFFECTIVELY

This textbook is comprised of enough material for a yearlong course. Therefore, instructors utilizing the book for a single semester will have ample material from which to select those topics germane to the particular course. The remaining material can provide precocious students with further breadth and depth into the subject of nuclear energy. For faculty who use the text in an academic course, instructor support materials, including PowerPoint slides and solutions to exercises, are available by registering at http://textbooks.elsevier.com.

The abundance of chapters facilitates customization of the reading material. An example syllabus for a one-semester course, not including examinations, is given in the following table.

Week	Coverage
1	Chapter 1; Sections 2.1–2.4
2	Sections 2.5–2.8; Sections 3.1–3.2
3	Sections 3.3–3.6
4	Sections 4.1–4.4
5	Sections 4.5–4.8
6	Chapter 5
7	Chapter 6
8	Chapter 10; Sections 11.1–11.3
9	Chapter 16
10	Chapter 17
11	Chapter 18
12	Sections 20.1–20.3; Sections 21.1–21.4
13	Sections 21.5–21.11
14	Chapter 23

B.2 COMPUTER PROGRAMS

Following is a list of titles of the MATLAB and Excel programs, the Computer Exercise number in which they are used, and a brief indication of function. The computer programs can be downloaded from http://booksite.elsevier.com/.

Title	Computer Exercises	Function
ALBERT	1.A	Relativistic properties of particles
ALBERT	2.A	Properties of the 1-MeV electron, proton, and neutron
BINDING	2.B	Semiempirical mass formula for B and M
DECAY	3.A	Radioactive decay, activity, graph
RADIOGEN	3.C	Parent-daughter radioactivity
MONTEPI	6.A	Monte Carlo estimate of pi (π)
ALBERT	9.A–B	High-velocity particles in accelerators
EXPOSO	11.A	Gamma attenuation, buildup factors
NEUTSHLD	11.B	Fast neutron shielding by water
EXPOSO	11.C	Array of sources in an irradiator
RADIOGEN	11.D	Radon activity in closed room
STAT	12.A–C	Binomial, Poisson, Gauss distributions
EXPOIS	12.D	Simulates counting data
COMPDIST	12.E	Graphically compare Gaussian distributions
RADIOGEN	13.A	Mo-Tc radionuclide generator
EXPOSO	13.B	Fixed gauge source measuring tank level
PREDPREY	14.A	Predator-prey simulation (requires LOTKAVOLT)
ERADIC	14.B	Application of sterile male technique
ENRICH	15.A–B	Material flows in isotope separator
CRITICAL	16.A	Critical conditions U and Pu assemblies
SLOWINGS	16.B	Scattering, absorption, and leakage
CONDUCT	17.A	Integral of thermal conductivity
TEMPPLOT	17.B	Temperature distribution in fuel pin
MPDQ	19.A	Criticality with space dependence
OGRE, OGREFUN	20.A	One-delayed-group reactor transient
KINETICS	20.B	Time-dependent behavior of reactor
RTF, RTFFUN	20.C	Reactor transient with feedback
XETR, XETRFUN	20.D	Xenon-135 reactivity transient
ORBIT	22.A	Trajectory of spacecraft from Earth
ALBERT	22.B	Mass increase of space ship
WASTEPULSE	23.A	Displays motion of waste pulse
WTT	23.B	Dispersion in waste transport
LLWES	23.C	Expert system, waste classification
FUTURE	24.A	Global energy analysis
BREEDER	25.A	Breeder reactor with cross-section data choice
FASTRX	25.B	Fast reactor criticality, Hansen-Roach
FUSION	26.A	Fusion parameters and functions
MAXWELL	26.A	Calculates and plots a distribution
VELOCITY	26.A	Four characteristic speeds
DEBYE	26.A	Debye length of fusion plasma
IMPACT	26.A	Parameters for ionic collision
RADIUS	26.A	Cyclotron radius and other quantities
MEANPATH	26.A	Mean free path of charged particles
TRANSIT	26.A	Fusion plasma parameters
CROSSECT	26.A	Fusion cross-section and reactivity
FASTRX	27.A	Critical mass as it depends on density
ENRICH	27.B	Blending Russian HEU material

B.3 ANSWERS TO SELECTED EXERCISES

This edition includes answers to most, but not all, exercises to provide instructors the option of assigning homework problems without answers. When multiple similar parts are specified, often only the answer to part (a) is given. As a cautionary note to students and instructors alike, because some constants have been updated, technical material expanded, and errors corrected, the solutions to some problems have changed and hence answers in older editions are not necessarily the same. A full solution manual is available from the publisher for instructors adopting this textbook.

1.1. 2400 J
1.2. (a) 20°C, (b) 260°C, (c) −459°F, (d) 1832° F
1.3. 22.5 kJ
1.4. 511 m/s
1.5. 149 kW, 596 kWh
1.6. (a) 2×10^{20} Hz
1.7. (a) (Proof), (b) 2.22×10^{-9} g
1.8. 3.04×10^{-11} J
1.9. 3.38×10^{-28} kg
1.10. 3.51×10^{-8} J
1.11. 8.67×10^{-4}
1.12. (Proof)
1.13. (a) 938.6 MeV
1.14. 931.49 MeV
1.15. (a) (Proof), (b) 0.140, 0.417, 0.866
1.16. (a) 6.16×10^{4} Btu/lb, (b) 1.43×10^{5} J/g, (c) 3.0 eV
1.17. (Derivation)
1.18. (Graph)

2.1. (a) 8.18×10^{22}/cm^3
2.2. 1.59×10^{-8} cm, 1.70×10^{-23} cm^3
2.3. (a) 2200 m/s
2.4. (Proof)
2.5. 3.116 kJ/(kg K)
2.6. (a) 4.43 eV
2.7. 3.29×10^{15} Hz
2.8. −1.51 eV, 4.77×10^{-8} cm, 12.1 eV, 2.9×10^{15} Hz
2.9. (Sketch)
2.10. (Proof)
2.11. 7.75×10^{-13} cm, 1.9×10^{-24} cm^2
2.12. 9.54×10^{-14}
2.13. (a) 0.030377 amu, 28.3 MeV
2.14. (a) 1784 MeV
2.15. 1.47×10^{17} kg/m^3, 9.9×10^{12} kg/m^3, 1.89×10^{4} kg/m^3
2.16. (Proof)
2.17. 1.21×10^{14} Hz, 2.48×10^{-4} cm
2.18. 2.4×10^{15} Hz, 1.25×10^{-7} m
2.19. (a) $M_{O-16} = 15.998$
2.20. (Graph)
2.21. (Graph)
2.22. (a) $M_{Li} = 6.9400$
2.23. −13.60 eV
2.24. (a) 10.2 eV, 0.121 μm
2.25. (a) 7.25 MeV
2.26. (a) 15.96 MeV

3.1. 7.30×10^{-10} /s, 2.19×10^{10} Bq, 0.592 Ci
3.2. 3.66×10^{10} Bq vs 3.7×10^{10} Bq
3.3. 1.65 μg
3.4. 3.21×10^{14} Bq, 8.68×10^{3} Ci, 1.06×10^{14} Bq, 2.86×10^{3} Ci
3.5. (Diagram)
3.6. (Graph)
3.7. 2.52×10^{20} atoms, 1.76×10^{-17} /s, 4440 dps and Bq, 0.12 μCi
3.8. (Derivation)
3.9. (Derivation)
3.10. (a) (Graph), (b) 1.78 h, argon-41
3.11. 1616 y, radium-226
3.12. (a) 3.56×10^{14} Bq/g
3.13. (Proof)
3.14. (a) Sec., no, sec., sec., trans., sec., sec., no.
3.15. (a) 187 ky

4.1. (Proof)
4.2. (a) $^{14}_{6}$C, (b) $^{10}_{5}$B
4.3. 4.2 MeV
4.4. 4.78 MeV
4.5. 3.95×10^{-30} kg, 3.55×10^{5} m/s, 1.3×10^{-3} MeV
4.6. 1.90×10^{7} m/s, 2.39×10^{7} m/s, 7.5 MeV, 11.8 MeV
4.7. 1.20 MeV
4.8. 1.46/cm, 0.68 cm
4.9. 1.70×10^{7} m/s, 4.12×10^{4}/cm^3
4.10. 6×10^{13}/(cm^2 s), 0.02/cm, 1.2×10^{12}/(cm^3 s)
4.11. 0.207, 0.074, 88, 0.4 cm
4.12. (a) (Proof), (b) 1932 barns
4.13. 2.74×10^{12}/(cm^3 s), 1.48×10^{12}/(cm^3 s)
4.14. 4.59×10^{-7}, 0.459
4.15. 0.1852 barns
4.16. 0.504/cm, 0.099 cm, 4.9%
4.17. 1.9%
4.18. 18.8 g/cm^3, 0.0482×10^{24}/cm^3, 0.0795/cm, 0.328/cm, 3.05 cm, 1.02 cm, 3.58 cm
4.19. $\mathbf{v}_1 \cong -\mathbf{u}_1$, $\mathbf{v}_2 \cong 0$, particle rebounds with original speed
4.20. (Proof), $\alpha = 0.98333$, $\xi = 0.00838$
4.21. (Proof)
4.22. (Proofs)
4.23. (a) -1.19 MeV, endothermic
4.24. Same answer as Example 4.7
4.25. (a) 84
4.26. (a) 5.304 MeV

5.1. 0.0233, 42.8
5.2. 1.45×10^{21} Hz, 2.07×10^{-13} m
5.3. (a) (Proof), (b) 0.245 MeV, (c) (proof), (d) $E' = E_0/2$
5.4. 0.62 MeV
5.5. 0.0011 cm
5.6. (a) 3.299×10^{22}/cm^3, (b) 0.482/cm
5.7. (a) 0.285 cm
5.8. 0.39 cm, 1.81×10^{-5} C/cm^3, 6.15×10^{-4} J/g
5.9. 0.00218 MeV, 2206
5.10. 8.16×10^{-14} J, 5.91×10^{9} K
5.11. (a) 85.5%
5.12. 41.8 keV, 50 keV
5.13. 1.9%, 95.1%
5.14. (a) 0.075, 0.078, (b) 0.249, 0.256
5.15. (Proof)
5.16. (a) 0.00256 MeV
5.17. (Proof)
5.18. 0.06268 cm^2/g
5.19. (a) 0.538 cm
5.20. (a) 3.96 cm
5.21. (Proof)

6.1. 6.53 MeV
6.2. $^{100}_{38}$Sr
6.3. (a) 66.4 MeV, 99.6 MeV, (b) 140, 93, (c) 0.96×10^{7} m/s, 1.44×10^{7} m/s
6.4. (a) 168.5 MeV
6.5. (a) 2.299
6.6. 1.0% U-235
6.7. 0.0057 g/d
6.8. 8.09×10^{6} kg/d, 5.89×10^{6} kg/d, 5.18×10^{6} kg/d
6.9. (a) 1.22 n/(g s)
6.10. (a) 1.19 g/(MWt d)
6.11. (Proof)
6.12. (a) ^{144}Ba->^{144}La->^{144}Ce->^{144}Pr->^{144}Nd
6.13. 0.0309
6.14. (a) 10.99 MeV, 2.82 MeV

7.1. 0.0265 amu, 24.7 MeV
7.2. (Verification)
7.3. 0.453 kg/d, 13,000 kg/d
7.4. (a) 3.10×10^{6} m/s, (b) 2.7×10^{17}/cm^3
7.5. 9.3×10^{5} K
7.6. 0.305 MeV
7.7. (a) 0.476 MeV
7.8. 3.4×10^{9} K
7.9. (a) 11.3 MeV, 0.42 MeV
7.10. 2.45 MeV
7.11. (Proof)
7.12. (a) 49 keV

8.1. (Sample)
8.2. (Activity)

8.3. $Q = 5.70\,\text{MeV}$, $E_C = 2.62\,\text{MeV}$
8.4. (a) 4.45/cm
8.5. (a) 1.92×10^{-6}
8.6. Example: Incredible Hulk (gamma rays)

9.1. (a) 0.114 V
9.2. (a) 4.70 MV
9.3. (a) 2.5 MHz
9.4. (a) 0.131 μs
9.5. $E = (qBR)^2/(2m)$
9.6. (a) $0.183\,\text{Wb/m}^2$
9.7. (a) 1.96 MeV/rev, (b) = 299,791,633 m/s, (c) 1.33 tesla
9.8. (a) 214.158, 0.999989
9.9. 746 mA, 373 MW
9.10. (Proof), 5.2×10^{-11}
9.11. 20.958 μs, 9 picoseconds
9.12. (a) $\Delta E\ (\text{keV}) \cong [88.46/R\ (\text{m})][E\ (\text{GeV})]^4$, (b) 8.8×10^{-14}, (c) $P \cong ae^2/(6\pi\,\varepsilon_0 c^3)$
9.13. (Proof)
9.14. (Graph)
9.15. +1 = +1
9.16. (Graph)
9.17. (a) $1.96 \times 10^6\,\text{m/s}$

10.1. $5.88 \times 10^{10}\,\text{ip/(cm}^3\,\text{s)}$, $2.2 \times 10^{-9}/\text{s}$
10.2. 200
10.3. 1.67 mrad, 3.34 mrem, 6.7×10^{-4}
10.4. 0.8%
10.5. 400 mrem, 4 mSv
10.6. $1/(1 + t_H/t_B)$, 1/3
10.7. (a) 240 mrem/y, (b) 1000 mrad/y
10.8. $2.55/mrem
10.9. (Proof)
10.10. (a) 14, 5
10.11. 0.00096°C
10.12. (a) $1.6022 \times 10^{-8}\,\text{rad/(MeV/g)}$
10.13. (a) Two
10.14. (a) $7.50 \times 10^{14} - 9.52 \times 10^{14}\,\text{Hz}$; $3.10 - 3.94\,\text{eV}$

11.1. (a) 834 mrem/y, 199 mrem/y
11.2. 45.3 μCi
11.3. (a) $5 \times 10^{-4}\,\mu\text{Ci/cm}^3$
11.4. Boron
11.5. $257/(\text{cm}^2\,\text{s})$
11.6. 0.33, 0.1, 1.7, 3.3, 0.05
11.7. (in μCi/mL): 2.96×10^{-7}, 2.81×10^{-7}, 3.15×10^{-7}
11.8. 7.60 d, 94.6 d, 69.6 d
11.9. $3.35 \times 10^{-6}\,\mu\text{Ci/g}$
11.10. (a) 0.19 mrem/y
11.11. 0.085
11.12. (a) 0.017 Bq/mL
11.13. (a) $0.24/(\text{cm}^2\,\text{s})$
11.14. (Discussion)
11.15. $0.084\,\text{mSv m}^2/(\text{GBq h})$
11.16. 1.69 m
11.17. (Graph)
11.18. 5.28 MeV

12.1. (a) $1.19 \times 10^{21}/\text{cm}^3$, (b) $2.66 \times 10^{19}/\text{cm}^3$
12.2. 0.0165
12.3. 6.0×10^5
12.4. 0.30
12.5. 10
12.6. (a) $n = 1$: $P(0) = 0.5$, $P(1) = 0.5$; $n = 2$: $P(0) = 0.25$, $P(1) = 0.50$, $P(2) = 0.25$; $n = 3$: $P(0) = 0.125$, $P(1) = 0.375$, $P(2) = 0.375$, $P(3) = 0.125$, (b) throw once: $P(0) = 5/6$, $P(1) = 1/6$, throw twice: $P(0) = 25/36$, $P(1) = 10/36$, $P(2) = 1/36$
12.7. $p = 1/6$; $n = 1$, $\bar{x} = 1/6$: $P(0) = 0.846$, $P(1) = 0.141$; $n = 2$, $\bar{x} = 1/3$: $P(0) = 0.717$, $P(1) = 0.239$, $P(2) = 0.040$
12.8. (a) 740 cps, 4.44×10^4 counts, (b) 211 counts, (c) 4×10^{-8}
12.9. (a) Proof, (b) 0.2907, (c) 0.2623
12.10. (Derivation)
12.11. (a) $\varepsilon_i = 0.948$
12.12. (a) $0.24/(\text{cm}^2\,\text{s})$, 8.0×10^{-5}, 2.5 cps, (b) 0.3 μrad/h
12.13. (a) 2.79 MeV
12.14. (Proof)
12.15. (a) 12%
12.16. 482 keV
12.17. 0.262 MeV
12.18. (a) 2.789 MeV
12.19. (a) $3.3 \times 10^{-12}\,\text{rad/s}$

13.1. Fe-59
13.2. ${}^{6}_{3}\mathrm{Li}+{}^{1}_{0}\mathrm{n}\rightarrow{}^{3}_{1}\mathrm{H}+{}^{4}_{2}\mathrm{He}$; ${}^{3}_{1}\mathrm{H}+{}^{16}_{8}\mathrm{O}\rightarrow{}^{18}_{9}\mathrm{F}+{}^{1}_{0}\mathrm{n}$
13.3. 0.63 mm
13.4. 3.0 s
13.5. 3.15×10^{8} y
13.6. 2358 y ago
13.7. 5.97×10^{-5}
13.8. $N_{\mathrm{Rb}}/N_{\mathrm{Sr}}=1/[\exp(\lambda t)-1]$
13.9. (Discussion)
13.10. (Discussion)
13.11. 11.97 d
13.12. 2.645 y
13.13. 4.33 μg, 0.00745 cm
13.14. Ir-192, Co-60, Cs-137
13.15. (a) 0.0871, (b) 0.1%
13.16. 2.4×10^{-4}
13.17. 14 cpm
13.18. 7.16 cm
13.19. Am-241 and Cs-137
13.20. (a) 477 keV
13.21. (a) 1060 γ/(cm^2 s)
13.22. (Nonlinear graph)
13.23. 19 d

14.1. 5 mCi
14.2. 241 rad
14.3. 89.8 kg
14.4. 19,500 Ci, 289 W
14.5. 3.46×10^{13}/(cm^2 s)
14.6. (Discussion)
14.7. 0.75 cm
14.8. 2.9 m/min
14.9. 4.5 kGy
14.10. (Proof)

15.1. (Proof)
15.2. 1.0030
15.3. (c) 0.0304, 0.0314
15.4. 9.59×10^{4} kg, 7.66×10^{4} kg-SWU
15.5. 0.71%
15.6. 195 kg/d
15.7. (a) 488
15.8. (Proof)
15.9. 1.0030
15.10. 0.422 kg/d, 0.578 kg/d
15.11. 238.028909; 99.283382, 0.711366, 0.005309
15.12. (a) $36.99 M, gain $25.9 M
15.13. (a) 90.3 A, (b) 4.5 MW, (c) no
15.14. (a) 2.5×10^{6} m/s^2, 2.55×10^{5}, (b) 1.146
15.15. (a) 75
15.16. 3.2%
15.17. (Discussion)
15.18. (a) 2.79 w/o

16.1. (a) 2.21
16.2. (a) 1.96×10^{10}/(cm^2 s)
16.3. (a) 1.171, 1.033, (b) 0.032
16.4. (a) 1.851, (b) 1.178, (c) 2.206
16.5. (a) 2.052, (b) yes
16.6. $\rho>0$, $\rho=0$, $\rho<0$
16.7. 0.0346
16.8. (a) 3.58 cm, (b) 0.0987/cm^2, (c) 0.441
16.9. (a) 13.59 cm^2, (b) 0.361
16.10. (a) 0.030/cm^2, 0.73
16.11. 0.43
16.12. (Proof)
16.13. (a) Fast: 3.06 cm $\gg$ thermal: 0.0319 cm
16.14. (a) 10.6 cm, 25%
16.15. (a) 0.22

17.1. (Proof)
17.2. (Discussion)
17.3. 150 W/cm^2, 3 W/(cm^2 °C)
17.4. (a) 303°C
17.5. 30°F
17.6. (a) 1830 MW, 1350 MW, (b) 26%
17.7. (a) 664 kg/s, (b) 2.6%
17.8. (a) 8.09×10^{6} m^2, (b) 8.26×10^{5} J/(m^2 h)
17.9. 20.5 million gal/d
17.10. (Proof)
17.11. (b) (Proof), (c) 0.76
17.12. (Proof)
17.13. 534°C
17.14. 284 W/cm^3
17.15. (Proofs)
17.16. (Proof)

18.1. (a) 10.2 MeV
18.2. (a) 10^{17}/s
18.3. (Discussion)
18.4. 10.6 ¢/kWh
18.5. 12.5 million barrels, $1.125 billion
18.6. (a) 8.64×10^6, (b) 89,700 kg, 2691 kg, (c) $91.9 M
18.7. (a) 28.8 m^3, 1.51 m, (b) 0.318
18.8. 34%
18.9. 93%
18.10. 1073 d
18.11. (a) 55,200
18.12. $8.24 \times 10^{20}/cm^3$
18.13. 17%
18.14. (a) 3.2×10^{13} n/(cm^2 s)
18.15. 1.2×10^6 n/s
18.16. (a) 1.39 cm

19.1. (Proof)
19.2. (Proof)
19.3. (Proof)
19.4. (Plot)
19.5. (Proof)
19.6. (a) 0.33
19.7. (Proof)
19.8. (a) 1.09×10^6 cm^3, 35.3 kg, (b) 8.78×10^5 cm^3, 28.4 kg
19.9. (a) 3.876
19.10. (a) $161/B^3$, (b) $148/B^3$
19.11. (a) 39.5 cm^2
19.12. (a) 0.9985
19.13. $0.564p$
19.14. (a) 55×55
19.15. (a) 8.4 cm, −1%

20.1. (a) 0.0065, 8.83 s
20.2. (a) 0.016, 2.40, (c) 7.7×10^{-4} s, (d) 63.8 s
20.3. 30.3 s
20.4. (a) 3.9×10^{-8} s, (b) 2.6×10^{-8} s
20.5. 40°C increase
20.6. −0.0208
20.7. (a) (Proof), (b) 2.1×10^{-5}/s, 0.039
20.8. 156 ft^3
20.9. 1.43 min
20.10. 117, 138, 150, 152, 153; yes
20.11. (a) 0.00052, 0.00013/cm, (b) 0.0195
20.12. (c) 9.0%
20.13. (a) 1.84 w/o, (b) 2.23 w/o
20.14. (c) 29,440 MW d/tonne
20.15. $B(3) = (3/2)B_1$, $B(4) = (8/5)B_1$
20.16. (Proof)
20.17. −78.6 s
20.18. (Proof)
20.19. (a) 121 s
20.20. 2.2 kg

21.1. (Discussion)
21.2. (Proof)
21.3. (Discussion)
21.4. (a), (b), (c), (e) active, (d) passive, (f) inherent
21.5. 0.90 s
21.6. (a) 0.0072
21.7. (b) 1.11×10^{-4}
21.8. 0.6 or 60%
21.9. (a) 600 kJ/kg, (b) some melting
21.10. 5.5 ms
21.11. (Graph)
21.12. (a) 340 GJ
21.13. 4.8
21.14. (a) 1.67×10^{14}/s
21.15. (b) 1.25×10^{-6}
21.16. 5770 s

22.1. (a) Proof, (b) 0.0721 g, 1.23 Ci
22.2. (a) Proof, (b) 7.81 km/s, (c) 22,284 mi, 35,855 km
22.3. 96%
22.4. (a) 0.71 W/g
22.5. (a) 36.3 kW
22.6. (a) 0.586 kW/m^2
22.7. 0.056
22.8. (a) 93,100 Ci
22.9. (a) 60.7 kg
22.10. 2.65×10^{20} atom

23.1. (a) 25,100 Bq/g, 95,900 Bq/g, (b) 49%, 85%
23.2. (a) PWR 65,500 MWe, BWR 32,500 MWe, Total 98,000 MWe, (b) 4496 m^3
23.3. 0–10 d I-131; 10–114 d Ce-141; 114 d–4.25 y Ce-144; 4.25–653 y Cs-137; >653 y I-129
23.4. 98.7%
23.5. 1.05×10^{13} cm^3/s, 2.22×10^{10} ft^3/min
23.6. (a) 0.120 MW, (b) 31 d
23.7. (a) 4.6%, 56.6%, 34.6%, 4.3%, (b) 987 kg, (c) 1215 kg, (d) 82%
23.8. (a) 33.219, (b) 956 y, 999 y, 801 ky
23.9. (a) Proof, (b) 1.215×10^7/(cm^2 s)
23.10. 14 mg

24.1. 4.78×10^{16} kg, 91 billion y
24.2. (a) 4.45, 10100
24.3. (a) 14,120, (c) 474 quads, 0.474 Q, (d) 6.24×10^{30}
24.4. (a) 28 tonne/y
24.5. (a) 0.337
24.6. (Proof)
24.7. (a) 34.7 y
24.8. (a) $0.077/kWh
24.9. $457 million
24.10. (a) 37.8 gal/kWh
24.11. 1.48×10^6 tonne/y

25.1. 1.7, 0.7
25.2. 0.986
25.3. (Discussion)
25.4. 2.61, 0.20
25.5. 6300 kg, 10.6 y
25.6. (a) (Proof), (b) no
25.7. (Proofs)
25.8. (a) 0, (b) Mg-24
25.9. 135 y
25.10. 6.0×10^{10}/(cm^3 s)
25.11. (Derivation)

26.1. 0.1 mm, 0.65 cm
26.2. (Proof)
26.3. (Proof)
26.4. 5.72×10^{14} J/kg, 0.116; $500/kg, 0.0003 ¢/kWh
26.5. (Proof)
26.6. (a) 0.888 MeV
26.7. (a), (b) Proofs, (c) 2.56×10^{-13} m, (d) 3.58×10^{-13} m, (e) 227 times, 199 times

27.1. 0.57 cm
27.2. Every 1.61 d, 227/y
27.3. 8 reactors
27.4. (a) 10.4 y
27.5. 8.2×10^{13} γ/cm^2, 2.0×10^{13} n/cm^2
27.6. 3.8×10^{10} γ/cm^2
27.7. (Proof)
27.8. 1.6×10^8 n/s
27.9. 266 kg
27.10. (Proofs)
27.11. (a) 905 g

Index

Note: Page numbers followed by *f* indicate figures, *t* indicate tables, and *b* indicate boxes.

D

E

F

G

H

N

O

P

Q

R

S

T

U

NUCLEAR ENERGY EIGHTH EDITION

An Introduction to the Concepts, Systems, and Applications of Nuclear Processes

RAYMOND L. MURRAY AND KEITH E. HOLBERT

The most popular introductory text on all aspects of nuclear science and technology, with a comprehensive view ranging from nuclear energy to nuclear health and safety

Murray and Holbert's ***Nuclear Energy: An Introduction to the Concepts, Systems, and Applications of Nuclear Processes***, first published in 1975, remains one of the most popular texts ever published on basic nuclear physics, systems, and applications of nuclear energy. The book is divided into three parts: Basic Concepts, Radiation and Its Uses, and Nuclear Power. This threefold structure is designed to provide students with a broad view of nuclear energy and science in an efficient and easily accessible manner. Updated with new content, this edition introduces important topics such as tritium-powered betavoltaic integrated circuit chips, photon-induced fission, estimation of ideal ignition temperature of fusion, lower limit of detection, complex radioactive decay paths, nucleon separation energy, and specific gamma-ray (dose) constant. Enhanced with more fundamental nuclear and radioactive decay data, ***Nuclear Energy*** is the essential resource for any first course on nuclear energy and systems.

KEY FEATURES

- Features coverage of such timely topics as alternative energy conversion methods for remote power applications; the water-energy nexus; radionuclide contaminant limits in drinking water; proton beam therapy; radiation effects of the atomic bombs; and more.
- Covers the industry response to the Fukushima nuclear disaster, including FLEX in the US.
- Includes more worked examples and end-of-chapter exercises.

ABOUT THE AUTHORS

Raymond L. Murray
Nuclear Engineering Department, North Carolina State University, USA

Keith E. Holbert
Associate Professor, School of Electrical, Computer and Energy Engineering, Arizona State University, USA

NUCLEAR ENGINEERING

ISBN 978-0-12-812881-7

9 780128 128817

ELSEVIER

Butterworth-Heinemann
An imprint of Elsevier
elsevier.com/books-and-journals